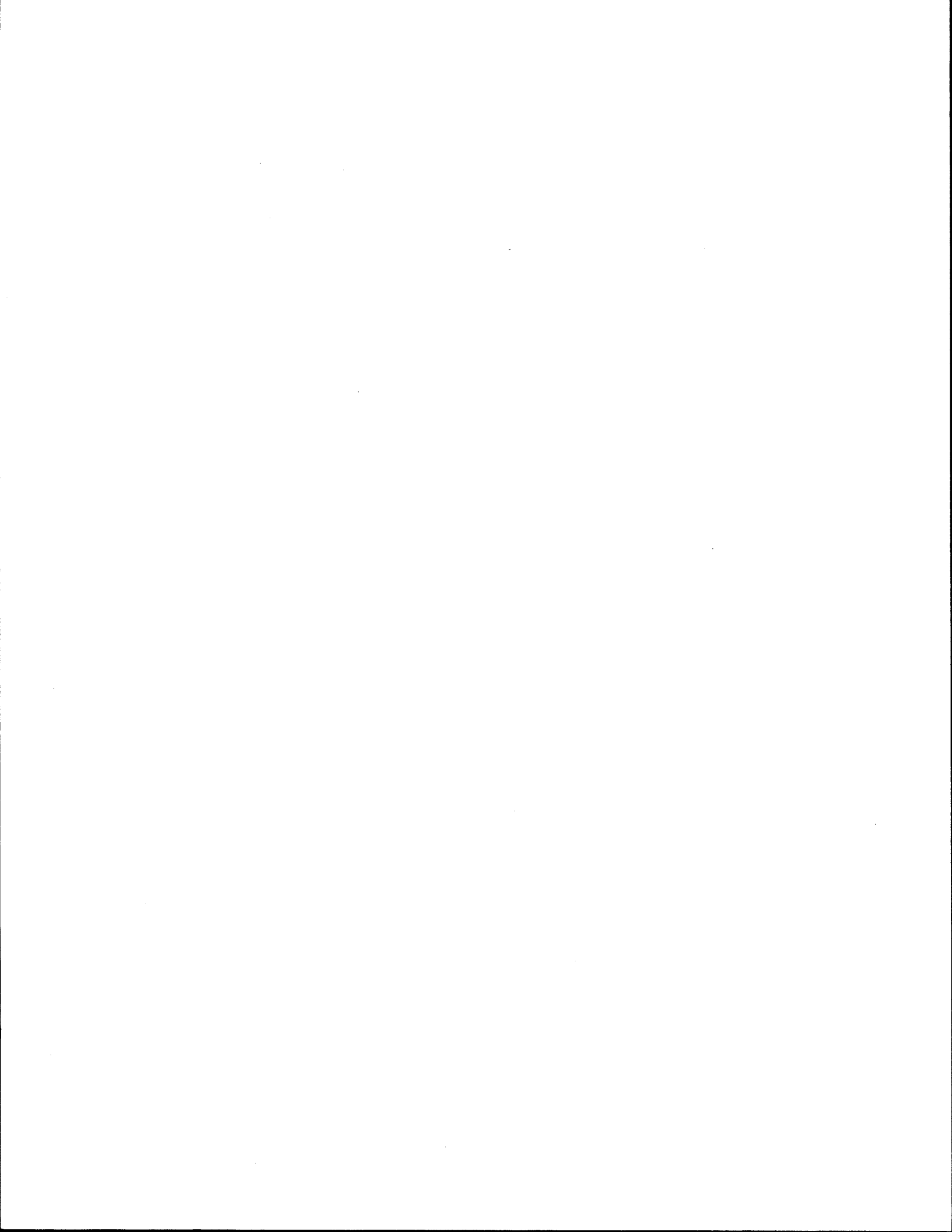


1. Report No. FHWA/TX-94/1287-2		2. Government Accession No.		3. Recipient's Catalog No.	
4. Title and Subtitle IDENTIFICATION OF THE STRUCTURAL BENEFITS OF BASE AND SUBGRADE STABILIZATION				5. Report Date November 1994; Revised: October 1995	
				6. Performing Organization Code	
7. Author(s) Dallas N. Little, Tom Scullion, Prakash B.V.S. Kota and Jasim Bhuiyan				8. Performing Organization Report No. Research Report 1287-2	
9. Performing Organization Name and Address Texas Transportation Institute The Texas A&M University System College Station, Texas 77843-3135				10. Work Unit No. (TRAIS)	
				11. Contract or Grant No. Study No. 0-1287	
12. Sponsoring Agency Name and Address Texas Department of Transportation Research and Technology Transfer Office P. O. Box 5080 Austin, Texas 78763-5080				13. Type of Report and Period Covered Interim: Sept. 91- Aug. 94	
				14. Sponsoring Agency Code	
15. Supplementary Notes Research performed in cooperation with the Texas Department of Transportation and the U.S. Department of Transportation, Federal Highway Administration. Research Study Title: Identify Structural Benefits of Stabilization and Updating TFPS to Accommodate Stabilized Layers					
16. Abstract <p>The Texas Department of Transportation uses stabilized subgrades and bases extensively. In fact subgrade stabilization is almost routine in many districts and especially in those with clay subgrades. A pressing need exists to determine the effectiveness of stabilization of subgrades and base courses, to evaluate the current mixtures and thickness design approaches and to suggest realistic structural properties associated with these stabilized pavement layers.</p> <p>Report 1287-2 considers both base course and subgrade stabilization. Stabilized bases are divided into three categories: heavily stabilized, moderately stabilized and lightly stabilized, depending on the amount of stabilizer used. Heavily stabilized bases perform as rigid structural layers. This report suggests modifications to currently used TxDOT mixture design and thickness design approaches to minimize structural damage within the stabilized base layer due to both non-load associated cracking and load associated fatigue cracking. Moderate and light levels of base stabilization significantly improve the structural contribution of the layer without, in most cases, producing a rigid structural layer. This type of stabilization is advantageous in many applications. Report 1287-2 suggests appropriate mixture design approaches and thickness design approaches employing current TxDOT testing and analytical tools for moderately and lightly stabilized bases.</p> <p>Lime stabilization of calcareous bases, caliche and limestone bases with low percentages of lime is addressed as a special topic. The mechanism of stabilization is explained, and expected engineering improvements in the calcareous bases are documented based on extensive laboratory testing and field measurements using the Falling Weight Deflectometer (FWD).</p> <p>The report investigates structural benefits derived from lime stabilization of subgrades based on laboratory testing and field testing using the FWD and the Dynamic Cone Penetrometer (DCP). The DCP is used to verify FWD measurements and, consequently, moduli backcalculations derived from FWD deflection data. This report suggests values of resilient moduli for design and analysis purposes for lime-stabilized subgrade soils.</p>					
17. Key Words Stabilization, Performance Pavements, Falling Weight Deflectometer, Dynamic Cone Penetrometer			18. Distribution Statement No restrictions. This document is available to the public through NTIS: National Technical Information Service 5285 Port Royal Road Springfield, Virginia 22161		
19. Security Classif.(of this report) Unclassified		20. Security Classif.(of this page) Unclassified		21. No. of Pages 442	22. Price



IDENTIFICATION OF THE STRUCTURAL BENEFITS OF BASE AND SUBGRADE STABILIZATION

by

Dallas N. Little
Research Engineer
Texas Transportation Institute

Tom Scullion
Associate Research Engineer
Texas Transportation Institute

Prakash B.V.S. Kota
Graduate Research Assistant
Texas Transportation Institute

and

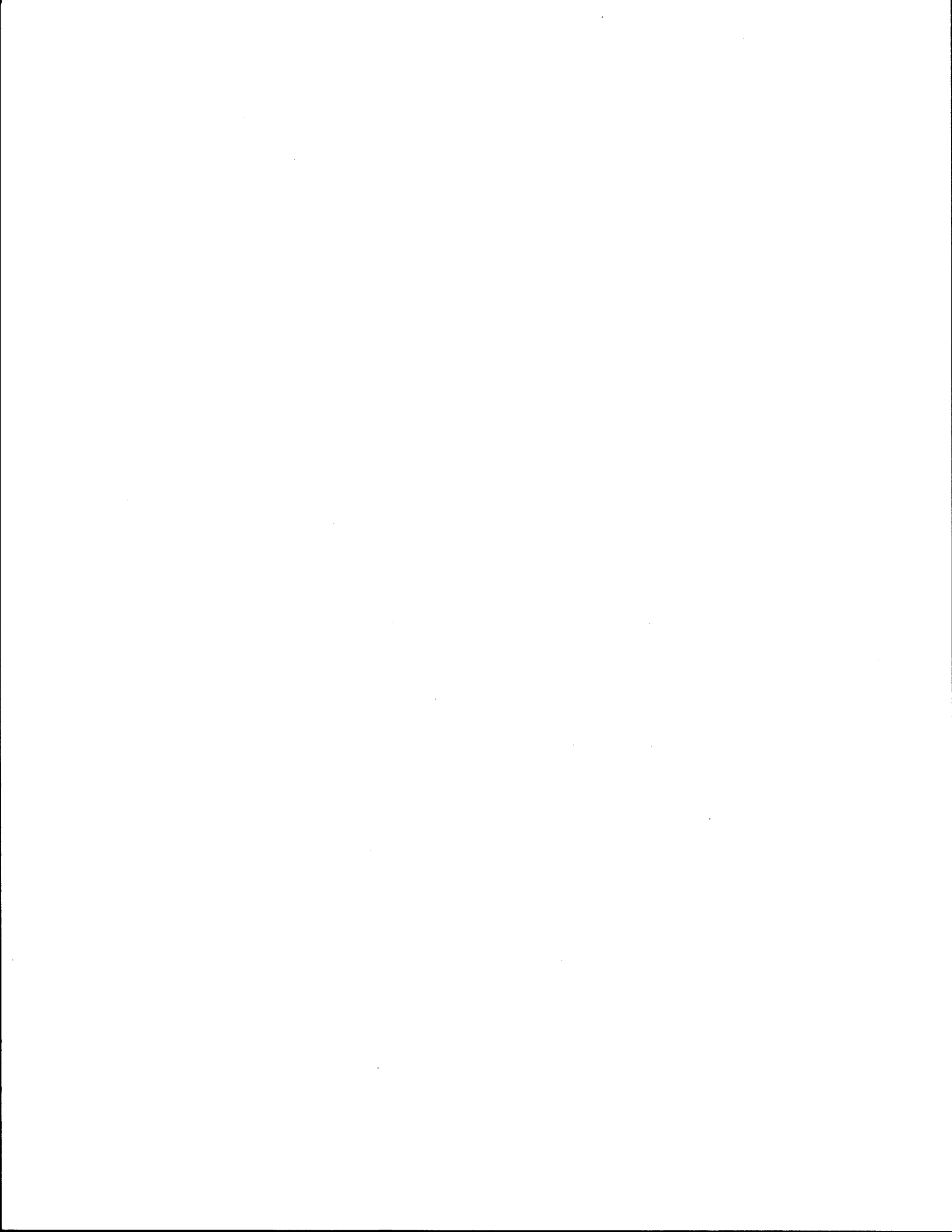
Jasim Bhuiyan
Graduate Research Assistant
Texas Transportation Institute

Research Report 1287-2
Research Study Number 0-1287
Research Study Title: Identify Structural Benefits of Stabilization
and Updating TFPS to Accommodate Stabilized Layers

Sponsored by the
Texas Department of Transportation
In Cooperation with
U.S. Department of Transportation
Federal Highway Administration

November 1994
Revised: October 1995

TEXAS TRANSPORTATION INSTITUTE
The Texas A&M University System
College Station, Texas 77843-3135



IMPLEMENTATION STATEMENT

The research in the Houston District with heavily stabilized bases demonstrates the importance of considering the effect of non-load associated cracking, such as shrinkage cracking, on the fatigue life of the bases. The research suggests using a simple stress ratio fatigue approach adjusted with a load transfer factor across shrinkage cracks of the type monitored in the Houston District. The rate of fatigue cracking is certainly accelerated due to diminished load transfer across shrinkage and reflection cracks. The computer program developed in project 1287 and presented in report 1287-2 is a reasonable approach in evaluating the life of heavily stabilized bases. This program should be evaluated in cooperation with the Houston District for implementation. Researchers on project 1287 should work with the Houston District on future design of heavily stabilized sections.

The research demonstrated that moderately and lightly stabilized bases provide excellent structural benefits for moderately and low trafficked pavements based on evaluations in the Atlanta, Bryan, Corpus Christi, Houston and Yoakum Districts. The researchers recommended treating these bases as flexible bases with enhanced structural properties due to stabilization. The relatively low level of stabilization prevents the development of a rigid matrix. The suggested mixture design and pavement design approach using existing testing (Texas Triaxial) and analytical (FPS-19) procedures should be evaluated for implementation with the help and cooperation of the Atlanta, Lufkin and Bryan Districts.

The researchers have documented the mechanism of stabilization of caliche and limestone bases with low levels of lime, one to two percent by weight of aggregate. The structural improvement due to this level and type of stabilization was documented through extensive laboratory and field testing. The structural improvement typically results in a 50 percent or better strength increase and a similar increase in resilient modulus. The base retains its flexible nature. The benefits of this type of stabilization should be implemented in pavement life cycle considerations. The TTI researches should work together with the Corpus Christi, Yoakum and Bryan Districts to evaluate the recommendation made in report 1287-2 for implementation.

The researches documented that well-designed lime-stabilized subgrades have a significant structural benefit due to improved support of the flexible aggregate base course and the hot mix

surface and due to the significant increase in in situ resilient modulus of the stabilized subgrade. The researchers in report 1287-2 recommend resilient moduli of lime-stabilized layers for design and analysis considerations. These recommendations should be considered for implementation. The researchers should work with the Bryan and Fort Worth Districts in this implementation.

DISCLAIMER

The contents of this report reflect the views of the authors who are responsible for the facts and the accuracy of the data presented herein. The contents do not necessarily reflect the official view or policies of the Texas Department of Transportation (TxDOT) or the Federal Highway Administration (FHWA). This report does not constitute a standard, specification, or regulation, nor is it intended for construction, bidding, or permit purposes. The engineer in charge of the project is Dallas N. Little, P.E. #40392.

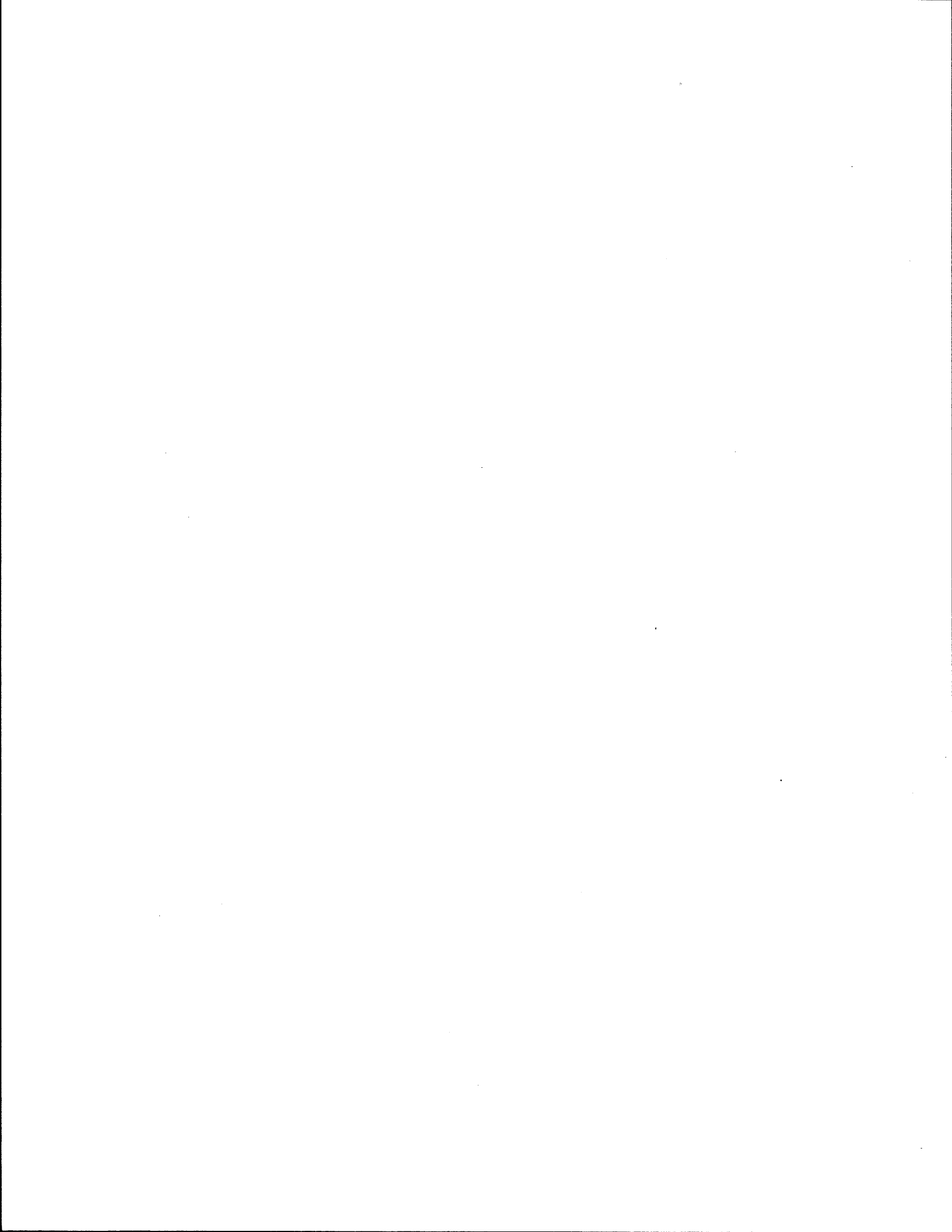


TABLE OF CONTENTS

LIST OF FIGURES	xiv
LIST OF TABLES	xix
SUMMARY	xxiii
CHAPTER 1 INTRODUCTION	1.1
1.1 STUDY PROBLEM STATEMENT	1.1
1.2 OBJECTIVES OF STUDY	1.1
1.3 SCOPE OF REPORT	1.2
CHAPTER 2 CONTRIBUTION OF STABILIZED LAYERS TO PAVEMENT PERFORMANCE BASED ON FINDINGS OF THIS STUDY AND REVIEW OF PERTINENT LITERATURE	2.1
2.1 CHARACTERIZATION AND PERFORMANCE EVALUATION OF LIME STABILIZED BASES AND SUBBASES	2.1
Mechanisms of Stabilization	2.1
Soil Modification	2.1
Soil Stabilization	2.2
Lime Stabilization in Base Courses	2.3
Material Characteristics Due to Stabilization	2.5
Influence of Material Improvements Through Lime Treatment on Pavement Performance	2.13
Mix Design Considerations	2.17
Recommended Structural Performance Algorithms	2.20
2.2 CHARACTERIZATION AND PERFORMANCE EVALUATION OF PORTLAND CEMENT STABILIZED SUBGRADES	2.24
Basic Reactions and Mechanisms of Stabilization	2.24
Material Characteristics Due to Stabilization	2.25
Mix Design Considerations	2.26
Influence of Material Improvements on Pavement Performance	2.26
Recommended Structural Performance Algorithms	2.27
2.3 CHARACTERIZATION AND PERFORMANCE EVALUATION OF LIME-FLY ASH AND CEMENT-FLY ASH STABILIZED BASES	2.29

TABLE OF CONTENTS (Continued)

Basic Reactions and Mechanisms of Stabilization	2.29
Material Characteristics Due to Stabilization	2.30
Influence of Material Improvements on Pavement Performance	2.32
Recommended Structural Performance Algorithms	2.32
Mix Design Considerations	2.36
2.4 CONCLUSIONS	2.38
Structural Role of Lime Stabilized Subgrades	2.39
Evaluation of the Structural Role of the Lime Stabilized Subgrade	2.40
Structural Role of Lime Stabilized Bases	2.41
Structural Role Portland Cement Stabilized Bases and Subgrades (Heavily-Stabilized Bases)	2.41
Structural Role of Fly Ash Stabilized Bases and Subgrades	2.42
Summary of Deliverables	2.42
Chapter 3 STABILIZED BASES	3.1
3.1 INTRODUCTION	3.1
3.2 FIELD TEST PROCEDURE	3.3
3.3 RESULTS FROM THE HOUSTON DISTRICT	3.9
3.4 FAILURE INVESTIGATION OF SH 36	3.16
3.5 ATLANTA DISTRICT BASE RESULTS	3.25
Field Testing	3.28
Discussion of Results	3.28
Conclusions	3.31
3.6 BRYAN DISTRICT	3.33
3.7 HISTORIC RECYCLING CASE	3.38
Waco, Texas	3.38
Yolo, California Recycling Project	3.39
Meridian Oil Company Runway	3.40
CHAPTER 4 EVALUATION OF LIGHTLY STABILIZED BASES	4.1
4.1 OVERVIEW	4.1
4.2 THE CARBONATION REACTION	4.3
4.3 EFFECTS OF CARBONATION ON ENGINEERING PROPERTIES	4.6
4.4 EFFECTS OF LIME TREATMENT ON CARBONATE CEMENTATION	4.7

TABLE OF CONTENTS (Continued)

4.5	MATERIALS AND TEST METHODS USED TO EVALUATE EFFECTS OF CARBONATE CEMENTATION ON CALCAREOUS BASES	4.13
	Aggregate	4.13
	Lime	4.13
4.6	SPECIMEN PREPARATION AND LABORATORY PROCEDURE	4.15
	Moisture-Density Relationships	4.15
	Texas Triaxial Test	4.16
	Resilient Modulus Test	4.17
	Atterberg Limit Tests	4.18
	Other Tests	4.18
	X-ray Diffraction Analysis	4.20
	Scanning Electron Microscopy	4.20
4.7	FIELD TESTS	4.21
	Selection of Pavement Sections	4.21
	Test Operation and Data Analysis	4.21
4.8	RESULTS AND DISCUSSION OF LABORATORY AND FIELD EVALUATIONS	4.22
	Mineralogical Analysis	4.22
	Atterberg Limits	4.25
	Texas Triaxial Strength	4.25
	SEM Examinations	4.27
	Resilient Modulus	4.34
	Field Data	4.34
4.9	STATISTICAL ANALYSIS	4.34
	Paired-Comparisons T Test	4.34
4.10	DISCUSSION	4.45
4.11	RECOMMENDATION AND DESIGN IMPLICATIONS	4.48
CHAPTER 5	STABILIZED SUBGRADES	5.1
5.1	INTRODUCTION	5.1

TABLE OF CONTENTS (Continued)

5.2	FIELD TEST PROCEDURES	5.2
	Results from the Bryan District	5.6
	TTI Test Track Project	5.14
	Results from the Atlanta District	5.15
	Results from the Fort Worth District	5.18
5.3	CONCLUSIONS	5.22
CHAPTER 6	RECOMMENDATIONS FOR MIX DESIGN AND THICKNESS DESIGN	6.1
6.1	MIX DESIGNS CONSIDERATIONS FOR BASES	6.1
	Heavily Stabilized Bases	6.1
	Moderately Stabilized Materials	6.3
	Lightly Stabilized Bases	6.3
6.2	THICKNESS DESIGN CONSIDERATIONS FOR BASES	6.4
	Heavily Stabilized Bases	6.4
	Moderately and Lightly Stabilized Bases	6.6
6.3	DESIGN ALGORITHM FOR HEAVILY STABILIZED BASES	6.7
	Effect of Wide Shrinkage Cracks	6.7
	Stabilized Base Thickness Design Program	6.9
	Users Guide to Stabilized Base Thickness Design Program	6.12
6.4	MIX DESIGN CONSIDERATIONS FOR LIME-STABILIZED SUBGRADES	6.14
	Current Approach	6.14
	Recommended Changes	6.14
6.5	STRUCTURAL CONSIDERATIONS FOR STABILIZED SUBGRADES	6.16
	General	6.16
	Procedure	6.16
	Estimation of Stabilized Subgrade Modulus	6.17
	Resistance of Lime-Stabilized Layers to Flexural Fatigue	6.19
	Example Calculation	6.24

TABLE OF CONTENTS (Continued)

REFERENCES 7.1

APPENDIX A.1

LIST OF FIGURES

Figure	Page
2.1. The Quantity of Lime Required to Produce Pozzolanic Reaction is Influenced by the Mineralogy of the Soil Being Stabilized (After Eades and Grimm, 1960) 1 psi + 6.9KPa)	2.8
2.2. Comparison of Strength after 7 Days at 43°C (110°F) with Strength Increases at 22°C (72°F) (After Alexander, 1978) (1 psi = 6.894 Pa)	2.10
2.3. The Resilient Modulus of the Tama B Soil is Significantly Influenced by Lime Stabilization Even After 10 Freeze-Thaw Cycles (After Thompson, 1985) (1 psi = 6.89KPa)	2.14
2.4. The Texas Method for Establishing an Optimum Lime Content is Based on the Binder Content (Passing No. 40 Sieve) and the Plasticity Index	2.18
2.5. The Thompson Mixture Design Flow Chart is Based on Soil-Lime Reactivity (After Little, et al., 1987)	2.21
2.6. Structural Layer Coefficient, a_2 , as Determined by Thompson as a Function of Compressive Strength for Lime Stabilized Layers (After Thompson, 1970)	2.23
2.7. Variation in a for Cement-Treated Bases with Base Strength Parameter (After AASHTO, 1986)	2.28
2.8. Typical Relationship of Stress Ratio to Traffic Conditions (ESALs - 18 kip Equivalent Single Axle Loads) (After Flexible Pavement Manual, 1990)	2.35
2.9. Typical PSM Thickness Design Chart (1 in = 25.4 mm, 1 psi = 6.89KPa)	2.37
3.1. Typical Monitor Site on FM-526, Houston, Section 1	3.4
3.2. Typical Crack Map of 160 m Long Test Section	3.6
3.3. Schematic of the Dynamic Cone Penetrometer	3.8
3.4. Schematic Diagram of the Number of Blows vs. Depth of Penetration with Depth	3.10

LIST OF FIGURES (Continued)

Figure	Page
3.5. Observed Relationship Between Base Modulus and Crack Spacing	3.17
3.6. Observed Relationship Between Base Modulus and Load Transfer Efficiency	3.18
3.7. Observed Relationship Between Unconfined Compressive Strength and Base Modulus	3.19
3.8. Observed Relationship Between Crack Spacing and Crack Opening	3.20
3.9. Observed Relationship Between Base Modulus and Crack Opening	3.21
3.10. Transverse Crack Pattern in the Pavement (Note: Y Shaped Crack Near Shoulder Paint Stripe)	3.23
3.11. Photographs of Core Obtained from Solid and Distressed Portions of the Pavement	3.24
3.12. Deterioration Cycle of CTB on SH-36	3.26
3.13. Typical Example Showing Effective Layer Thickness Being Less Than Actual Thickness	3.30
3.14. FM-2446 near Franklin, Testing of 2 Percent Lime Section	3.36
3.15. DCP Results from FM-2446	3.37
4.1. Strength Increase of Untreated Quartz/Calcite Sand Mixes as a Function of Mineralogical Composition and Time (after Graves, 1987)	4.9
4.2. Strength Increase of Quartz/Calcite Sand Mixes Treated with 1 Percent Ca(OH) ₂ as a Function of Mineralogical Composition and Time (after Graves, 1987)	4.10
4.3. Strength Increase of Untreated Cemented Coquina Materials as a Function of Mineralogical Composition and Time (after Graves, 1987)	4.11
4.4. Strength Increase of Cemented Coquina Materials Treated with 1 Percent Ca(OH) ₂ as a Function of Mineralogical Composition and Time (after Graves, 1987)	4.12

LIST OF FIGURES (Continued)

Figure	Page
4.5. Sieve Analysis of Limestone and Caliche Aggregates	4.14
4.6. Photo of Specimens in the Environmentally Controlled Chamber During the Curing Process	4.17
4.7. Photo of Specimens Subjected to Overnight Capillary Wetting	4.19
4.8. Photo of a Specimen Subjected to Texas Triaxial Compression Testing	4.19
4.9. Photo of a Specimen Subjected to Laboratory Resilient Modulus Testing	4.20
4.10. X-ray Diffraction Analysis of Natural Limestone	4.23
4.11. X-ray Diffraction Analysis of Natural Caliche	4.24
4.12. SEM Image of Unstabilized Limestone (X500)	4.31
4.13. SEM Image of Limestone Stabilized with 1 Percent Hydrated Lime (X500)	4.31
4.14. SEM Image of Limestone Stabilized with 2 Percent Hydrated Lime (X500)	4.32
4.15. SEM Image of Unstabilized Caliche (X500)	4.32
4.16. SEM Image of Caliche Stabilized with 1 Percent Hydrated Lime (X500)	4.33
4.17. SEM Image of Caliche Stabilized with 2 Percent Hydrated Lime (X500)	4.33
4.18. Resilient Modulus Versus Deviatoric Stress for Natural Limestone in Wet Condition	4.41
4.19. Resilient Modulus Versus Deviatoric Stress for Limestone Stabilized with 1 Percent Lime in Wet Condition	4.41
4.20. Resilient Modulus Versus Deviatoric Stress for Natural Caliche in Wet Condition	4.42
4.21. Resilient Modulus Versus Deviatoric Stress for Caliche Stabilized with 1 Percent Lime in Wet Condition	4.42

LIST OF FIGURES (Continued)

Figure	Page
4.22. Resilient Modulus Versus Deviatoric Stress for Limestone Stabilized with 1 Percent Lime in Dry Condition	4.43
4.23 Resilient Modulus Versus Deviatoric Stress for Limestone Stabilized with 2 Percent Lime in Dry Condition	4.43
5.1. Typical Example of Cumulative Number of Blows vs. Depth of Penetration Using Depth	5.4
5.2. Typical Example of Variation of CBR vs. Depth Using Depth	5.5
5.3. DCP Strength Profiles for Two Locations on FM-3478. At Station 125 the Stabilized Subbase is not Detected	5.10
5.4. DCP Penetration Data for FM-1179, Variable Stabilized Layer	5.12
5.5. FM 2818 DCP Data from FM-2818, a Well Stabilized Subbase is Clearly Seen	5.13
5.6. Cumulative Number of Blows vs. Depth of Penetration	5.17
5.7. Cumulative Number of Blows vs. Depth of Penetration Measured with DCP	5.21
6.1. Recommended Approach for Mixture Design for Lime-Stabilized Subgrades	6.15
6.2. Relationships Between Unconfined Compressive Strength and Moduli of Lime-Stabilized Soils	6.18
6.3. Selected Design Relationship between Unconfined Compressive Strength and Resilient Modulus for Lime-Stabilized Subgrade Pavement Layers	6.18
6.4. Relationship Between In Situ Modulus of the Natural Subgrade Soil as Determined by FWD Measurements and the Moduli Ratio (Lime-Stabilized Layer to Natural Subgrade Layer) as Determined by FWD Measurements	6.20
6.5. Stress Ratio Versus Cycles to Failure Fatigue Relationship (After Thompson and Figueroa (1989))	6.20

LIST OF FIGURES (Continued)

Figure	Page
6.6. Relationship Between Modulus of Lime-Soil Mixture and Radial Stress Induced in the Lime-Stabilized Layer and Flexural Strength for Soft Natural Subgrades (After Thompson and Figueroa (1989))	6.22
6.7. Relationship Between Modulus of Lime-Soil Mixtures and Radial Stress Induced in the Lime-Stabilized Layer and Flexural Strength for Medium Stiffness Natural Subgrades (After Thompson and Figueroa (1989))	6.22
6.8. Relationship Between Modulus of Lime-Soil Mixtures and Radial Stress Induced in the Lime-Stabilized Layer and Flexural Strength Stiff Natural Subgrades (After Thompson and Figueroa (1989))	6.23
6.9. Typical Resilient Modulus Versus Deviatoric Stress Relationships for Soft, Medium and Stiff Subgrades	6.23

LIST OF TABLES

Table	Page
2.1. Unconfined Compressive Strengths of Selected Soils	2.7
2.2. Resilient Moduli of Lime Stabilized Subgrade (LSSs) Backcalculated From Falling Weight Deflectometer (FWD) Data	2.11
2.3. Average Values of Bulk Stress, Θ , Within the Flexible Base (Aggregate Base) Layer as a Function of Hot Mix Asphalt Concrete Thickness and Subgrade Support (After AASHTO Guide, 1986)	2.16
2.4. Typical Variation in the Resilient Modulus of Flexible Base (Aggregate Base) as a Function of Moisture Condition and Stress States (After AASHTO Guide, 1986)	2.16
2.5. Summary of Octahedral Stress Ratios Developed within Hot Mix Asphalt Concrete Surfaces as a Function of the Supporting Modulus of the Flexible Base Course Layers	2.19
2.6. Recommended Physical and Chemical Requirements* for Fly Ash for Use in Pozzolanic Stabilized Mixtures (PSMs) (After Flexible Pavement Manual, 1990)	2.31
2.7. Suggested AASHTO Structural Layer Coefficient (a_2) for PSM Base Layers (After Flexible Pavement Manual, 1990)	2.38
3.1. Details of the Pavement Sections Investigated	3.11
3.2. Summary of the Average Backcalculated Moduli (Houston District)	3.12
3.3. Summary of FWD and Lab Test Results	3.13
3.4. Summary of LTE and Crack Length (Severe Type)	3.14
3.5. TxDOT Laboratory Compressive Strengths Obtained on SH8 Experimental Pavement near Douglasville. The Raw Material Strength was 245 KPa	3.29
3.6. Base Section In Situ Test Results from Atlanta District	3.32
3.7. Modulus 4.2 Output for US-19	3.34

LIST OF TABLES (Continued)

Table	Page
3.8. Backcalculated Base Moduli for FM-2446	3.35
4.1. Backcalculated Properties of Phoenix, Arizona, Granite Aggregate Base Coarse (ABC) with and without Lime Stabilization	4.3
4.2. Maximum Dry Densities and Optimum Moisture Contents of Stabilized and Unstabilized Limestone and Caliche	4.15
4.3. Particle Size Distribution and Calcite Content of Limestone and Caliche	4.25
4.4. Atterberg Limit Test Results for Limestone and Caliche with 0, 1, and 2 Percent Lime	4.25
4.5. Triaxial Test Data for Limestone after 28 Days of Curing	4.26
4.6. Triaxial Test Data for Limestone after 60 Days of Curing	4.26
4.7. Triaxial Test Data for Caliche after 28 Days of Curing	4.28
4.8. Triaxial Test Data for Caliche after 60 Days of Curing	4.28
4.9. Summary of Average Triaxial Strength and Other Calculated Parameters for Limestone after 28 Days of Curing	4.29
4.10. Summary of Average Triaxial Strength and Related Strength Parameters for Limestone after 60 Days of Curing	4.29
4.11. Summary of Average Triaxial Strength and Related Strength Parameters for Caliche after 28 Days of Curing	4.30
4.12. Summary of Average Triaxial Strength and Other Calculated Parameters for Caliche after 60 Days of Curing	4.30
4.13. Laboratory Data of Resilient Moduli for Unstabilized Limestone in Dry Condition	4.35
4.14. Laboratory Data of Resilient Moduli for Limestone with 1 Percent Lime in Dry Condition	4.35
4.15. Laboratory Data of Resilient Modulus for Limestone with 2 Percent Lime in Dry Condition	4.36

LIST OF TABLES (Continued)

Table	Page
4.16. Laboratory Data of Resilient Modulus for Unstabilized Caliche in Dry Condition	4.36
4.17. Laboratory Data of Resilient Modulus for Caliche with 1 Percent Lime in Dry Condition	4.37
4.18. Laboratory Data of Resilient Modulus for Caliche with 2 Percent Lime in Dry Condition	4.37
4.19. Laboratory Data of Resilient Modulus for Unstabilized Limestone in Wet Condition	4.38
4.20. Laboratory Data of Resilient Modulus for Limestone with 1 Percent Lime in Wet Condition	4.38
4.21. Laboratory Data of Resilient Modulus for Limestone with 2 Percent Lime in Wet Condition	4.39
4.22. Laboratory Data of Resilient Modulus for Unstabilized Caliche in Wet Condition	4.39
4.23. Laboratory Data of Resilient Modulus for Caliche with 1 Percent Lime in Wet Condition	4.40
4.24. Laboratory Data of Resilient Modulus for Caliche with 2 Percent Lime in Wet Condition	4.40
4.25. Backcalculated Moduli Values from FWD Data for Stabilized and Unstabilized Base Courses in Yoakum and Corpus Christi Districts of Texas	4.44
4.26. Summary of Paired-Comparisons T Test for Texas Triaxial Data	4.46
5.1. Details of the Monitor Sections in the Bryan District	5.7
5.2. Variability of Deflection Data on Stabilized Subgrade Sections in the Bryan District	5.7
5.3. Point Specific Comparison of Backcalculation Moduli vs. In situ CBR Value	5.8

LIST OF TABLES (Continued)

Table	Page
5.4. Layer Thickness Information from Stabilized Subgrade Sections in Atlanta	5.15
5.5. Average In situ Moduli Values and DCP Results from Stabilized Subgrades in Atlanta	5.16
5.6. Backcalculated Layer Moduli from Stabilized Subgrade Sections in Fort Worth	5.20
5.7. Summary of Backcalculated Moduli for Lime Stabilized Subgrades	5.23
6.1. TxDOT Strength Specifications for Item 276	6.1
6.2. Influence of Stabilizer Content of Base Modulus. BIF is Ratio of Backcalculated Modulus of the Moderately or Lightly Stabilized Layer to the Backcalculated Modulus for an Unstabilized Layer	6.6
6.3. Impact of Base Stabilization on Thicknesses Predicted Using FPS19	6.8

SUMMARY

Stabilized bases in Texas can effectively be divided into three categories: heavily, moderately and lightly stabilized. Heavily stabilized bases normally require six percent or more stabilizer, usually portland cement. These bases perform as rigid layers with very high stiffnesses based on laboratory and field calculations. The percentage of stabilizer required for these bases is based on a minimum level of unconfined compressive strength. These layers function very well as long as shrinkage cracking and fatigue cracking are held in check. Study 1287-2 suggests that bases can be too rigid, resulting in very low levels of load transfer across shrinkage cracks. This results in accelerated load-associated fatigue cracking and pavement failure. It is important to use no more stabilizer than that required to achieve the minimum required compressive strength. Furthermore, the severity of non-load associated cracking was found to be directly related to the compressive strength and the stiffness of the layers evaluated. A computer program was developed which predicts the rate of load associated fatigue damage for heavily stabilized bases. The rate of fatigue is associated with the level of load transfer across shrinkage cracks and reflection cracks within the stabilized layers. These load transfer factors were determined from extensive Falling Weight Deflectometer (FWD) testing in the Houston District. Six pavement sections with heavily stabilized bases were monitored, and the effects of seasonal variations were considered.

Moderately and lightly stabilized bases were monitored in the Atlanta, Bryan, Corpus Christi and Yoakum Districts. Moderately stabilized bases contain two to four percent stabilizer, and lightly stabilized bases contain less than three percent stabilizer. Moderately and lightly stabilized bases usually offer considerable structural improvement including 70 to 500 percent increases in strength and similar increases in resilient modulus. Moderately and lightly stabilized bases are attractive alternatives for moderate and low traffic areas. However, they may not be suitable for very heavily trafficked pavements. Report 1287-2 suggests mixture and thickness design approaches for moderately and lightly stabilized bases which employ currently used TxDOT testing procedures and analytical techniques. Moderately and lightly stabilized bases are not treated as rigid bases but as flexible bases with enhanced strength and stiffness.

The researchers evaluated lime-stabilized subgrades in the Houston, Bryan, Lufkin, Atlanta, Austin, Fort Worth, Corpus Christi and Yoakum Districts. Subgrades were evaluated in situ using the Falling Weight Deflectometer (FWD) and the Dynamic Cone Penetrometer (DCP). Both DCP and FWD testing demonstrated significant structural improvement in the majority of the subgrades evaluated. Certain cases were found where little or no structural improvement resulted. The lack of structural improvement is likely due to insufficient lime used in the construction process to assure pozzolanic reaction. The report suggests an improved mixture design approach using the Eades and Grim pH test, following with strength testing to help insure the use of adequate lime for pozzolanic reaction.

Backcalculated resilient moduli of lime-stabilized subgrades demonstrated a significant structural improvement with stiffness increases typically in the order of 5 to 10 over that of the natural, untreated subgrade. These values were verified in situ using the DCP.

The report evaluates the special topic of lime stabilization (with low percentages of lime) of caliche and limestone bases. The mechanism of stabilization is primarily carbonation and not pozzolanic cementation. The structural benefits are significant. As with the moderately stabilized bases, the bases with low levels of lime are not transformed into rigid bases but retain the nature of a flexible base with enhanced strength and stiffness. Stabilization of calcareous bases with one to two percent lime provides a significant increase in shear strength (50 percent or more) and a significant increase in stiffness (50 percent or more).

CHAPTER 1

INTRODUCTION

1.1 STUDY PROBLEM STATEMENT

Texas uses stabilized bases and subgrades extensively. Portland cement, lime and fly ash, typically in combination with lime or portland cement, are used. The current FPS design approach does not accommodate the use of stabilized bases or subgrades in pavement thickness design.

Various levels of stabilization occur when lime, portland cement and/or fly ash is added to soil or aggregate. In some instances, the intent is to increase interparticle binder matrix interaction. In some instances, the intent is to provide a stiff, cemented material to provide a rigid layer within the pavement structure. The current methodologies do not differentiate among the options in selecting materials and/or engineering properties to be used in design and/or analysis. In addition, current approaches do not address the change in stabilized layer properties which occur as a function of time (environmental damage) and traffic (load-related damage). This is a necessary part of a reliable, credible system.

Specifically, the following needs exist:

1. Determine realistic, in situ stiffness or moduli values (accounting for cracks and crack spacing) for portland cement and/or lime and fly ash stabilized bases.
2. Determine seasonal effects on in situ modulus or stiffness and whether or not a single (or perhaps weighted average) stiffness or modulus value is justified.
3. Determine realistic stiffness and structural contribution characteristics of lime treated subgrades.
4. Establish target design values, strength and stiffness for stabilized layers which should be strived for in mix design.

1.2 OBJECTIVES OF STUDY

Study objectives were to:

1. Determine realistic levels of strength and in situ moduli as a function of time (age) for characterization of stabilized layers accounting for the effects of shrinkage and load-

- induced cracking (frequency and severity),
2. Determine realistic strength and in situ stiffness or moduli values which can be used in thickness design for lime treated subgrades, and
 3. Identify the typical failure mechanisms of stabilized pavement layers and recommend design and construction approaches to prevent the occurrence of such failures.

1.3 SCOPE OF REPORT

This report addresses, in separate chapters, heavily and moderately stabilized bases, lightly stabilized bases and stabilized subgrades. This categorization of stabilized layers was selected as each was found to perform in a considerably different manner, and the performance of each is influenced by a different failure mechanism.

The report is divided into six chapters and four appendices. Chapter 1 is the introduction. Chapter 2 is a review of the pertinent literature on base and subgrade stabilization for the purpose of structural enhancement. Chapter 3 is a summary of a field evaluation of heavily and moderately stabilized bases. Chapter 4 is a summary of a laboratory and field evaluation of lightly stabilized bases. Chapter 5 is a summary of a laboratory and field evaluation of stabilized subgrades. Chapter 6 presents recommendations for mix design and thickness design for lightly, moderately and heavily stabilized bases and stabilized subgrades.

The appendices include details of the pavement sections evaluated, including Falling Weight Deflectometer (FWD) data, crack maps, site and core photos, Dynamic Cone Penetrometer (DCP) data and backcalculated moduli results.

CHAPTER 2
CONTRIBUTION OF STABILIZED LAYERS TO PAVEMENT
PERFORMANCE BASED ON FINDINGS OF THIS STUDY
AND REVIEW OF PERTINENT LITERATURE

2.1 CHARACTERIZATION AND PERFORMANCE EVALUATION OF LIME STABILIZED BASES AND SUBBASES

Mechanisms of Stabilization

Basic stabilization mechanisms in lime treated clay soils are (1) cation exchange, (2) flocculation and agglomeration, (3) pozzolanic reaction, and (4) carbonation. Little (1987) and Little (1994) explain these reactions in detail. This report will not attempt to review the mechanisms of lime stabilization in detail. However, it is pertinent to review the basic physical property changes that occur upon the addition of lime to soil.

Soil Modification

Upon the addition of lime to soils containing a significant clay fraction, approximately 10 percent or more, the rapidly occurring reactions of cation exchange, flocculation and agglomeration, and some rapidly occurring pozzolanic reactions lead to a significant reduction in plasticity and swell potential. These reactions have been shown to occur with virtually all fine-grained soils and can occur at relatively low lime contents.

As a result of the textural and plasticity changes that occur in the lime treated soils, shear strength increases, and a significant increase in stiffness or resilient modulus has also been documented. However, the effects of modification of the soil with lime need to be differentiated from the effects of stabilization of the soil with lime. Therefore, modification should be defined as the reduction of plasticity and/or swell potential to an acceptable level to meet design requirements. This modification usually also carries with it strength and stiffness improvements and a significant improvement in workability, constructability and textural changes.

Soil Stabilization

Soil stabilization is a permanent change in the properties of the lime treated soils. This stabilization reaction requires a significant level of pozzolanic reactivity. Little (1987) and Little (1994) discuss the pozzolanic reaction in detail. Succinctly stated, this reaction entails the development of a high pH environment in the soil-lime-water system through the addition of the appropriate level of lime to produce a high pH environment. The result of this high pH system is that the clay minerals (comprised of alternating layers of silicates and aluminates) are partially dissolved since the solubility of both silica and alumina is very high in high pH systems. When the optimum amount of lime is added to a soil-water system, the pH exceeds 12.4 at 25°C. This pH is well above the level required to dissolve clay silica and clay alumina.

The reaction among clay silica and clay alumina and calcium hydroxide (lime) and water results in products referred to as calcium-aluminate-hydrates and calcium-silicate-hydrates. The reaction is referred to as pozzolanic because it relies on pozzolans provided by the clay. These pozzolans are clay silica and clay alumina.

The pozzolanic products that form have been shown to be permanent reactions products by Little (1982), Kennedy and Tahmoressi (1987), and Eades and Grim (1960). The products formed at the surface of the clay mineral represent a change in mineralogy and result in a significant increase in stiffness (resilient modulus). The pozzolanic reaction continues with time, when proper conditions for the reaction are maintained, i.e., temperature above 4°C, time, and the presence of the reactants (calcium and pozzolans). The only way to insure the continuation of the reaction is to provide the appropriate level of lime to continue to keep the pH high and the supply of calcium adequate until an appreciable level of the pozzolanic product has been developed.

The pozzolanic product represents a permanent change in the clay mineral. Researchers have documented the permanency and durability of this product in a number of studies, i.e., McCallister and Petry (1991), Eades (1965), McDowell (1966), Kelly (1977), Little (1992), Gutchick (1985), etc. The key to permanency is that appropriate steps have been taken in the mixture design process to insure that an adequate lime content has been added to promote the pozzolanic reaction. If too little lime is added, it is possible to promote cation exchange without the development of pozzolanic products. The results can be improved workability, and reduced plasticity, and reduced swell. However, since these physical changes can be predominately the result of cation exchange, leaching

action can reverse this process. However, as McCallister and Petry (1991) have demonstrated the reversal of the pozzolanic reaction is very unlikely.

Therefore, lime stabilization as the result of pozzolanic reaction results in a pavement layer of substantial strength, stiffness and durability. This is required if the lime is to be used to produce a structural layer. Since the pozzolanic reaction is evident by the development of shear strength, shear strength tests have been used to measure pozzolanic reactivity and indirectly to evaluate the permanency of the reaction.

Lime Stabilization in Base Courses

Lime stabilization of base course materials has received increased attention during the last several years. Essentially, the same mechanisms of stabilization are involved as with lime stabilization of subgrade materials. In most cases where lime is used to stabilize base courses, the base material to be stabilized is comprised of a substantial amount of clay binder. The binder fraction of the base course is usually defined as the percentage of the gradation passing the number 40 sieve. When the plasticity index of this fraction exceeds 10 percent and the fines (fraction passing the number 200 sieve) is greater than about 25 percent, lime is a potential stabilizer (Little et al., 1987).

Lime has been successfully used to stabilize aggregate base courses with plastic binder (minus 40 sieve fraction). For example, Little (1990) documents the success encountered when an Arizona granite aggregate base course with plastic fines (PI ranging from 12 to 17) was stabilized with 1 percent lime by weight of the total aggregate base course. This level of stabilizer, of course, is in the order of 5 or 6 percent by weight of the binder fraction and is, therefore, typical of the amount generally required for the development of pozzolanic reactivity.

Little (1990) documented that engineering properties of the lime stabilized (1 percent by weight of the aggregate) base were, substantially and statistically, significantly superior to the unstabilized control sections. The engineering properties measured were the unconfined compressive strength and the in situ resilient modulus, determined from Falling Weight Deflectometer (FWD) deflection basins. The average resilient modulus of the control (unstabilized) aggregate base layers was approximately 140 MPa, while the average resilient modulus of the stabilized layers was approximately 1,575 MPa.

The level of resilient modulus achieved in the granite aggregate base course is in a good range

to provide excellent performance of a base course. The stiffness is high enough to provide good protection of underlying layers and good support of the hot mix asphalt concrete surface, yet the stiffness is not so high as to develop a brittle, rigid slab effect as is often the case when the layer is stabilized with higher percentages of stabilizers. The level of resilient modulus achieved in this case may be said to be highly compatible with the moduli of the other layers within the system. In this case, compatibility is based on the ratio of layer stiffnesses. A compatible layer is considered to be one that produces a favorable stress distribution within the flexible pavement without producing a rigid, brittle layer susceptible to cracking and shrinkage.

The unconfined compressive strengths of the Arizona lime stabilized aggregate base course were sufficiently high enough to produce durable material. The unconfined compressive strengths were in the range of 2,800 KPa.

Lime stabilization has been successfully used in Texas to alter the properties of bank run river gravel aggregate. Little (1994) documents the stabilization of a high fines content, high plasticity (PI of approximately 30) bank run Colorado River gravel using from 3 to 5 percent lime. The need for the high percentage of lime is due to the high binder content and the high plasticity of the fines. The addition of the lime increased the CBR of the aggregate from approximately 40 to approximately 100 and increased the unconfined compressive strength from approximately 350 KPa to approximately 840 KPa.

One of the most interesting uses of lime has been to enhance the properties of carbonate aggregate bases. The Yoakum, Corpus Christi, and Bryan Districts, among others, have successfully used lime to enhance the properties of limestone bases. In some cases, these limestones have had enough plastic fines to react with the lime pozzolanically. However, in many cases the limestone base has been virtually devoid of plastic, clay fines, even though the lime has still reacted with the carbonate base to produce improved compressive strengths and improved resilient moduli.

The explanation of the reaction of the lime with the carbonate aggregate was provided by Graves et al. (1990), who documented this reaction with limestone aggregates in Florida. Graves explained that the reaction is due to substantial development of calcium carbonate. It is well known that calcium carbonate develops when calcium hydroxide reacts with carbon dioxide from the atmosphere. This forms a cement. However, the reaction has traditionally been labeled as somewhat unreliable as it uses lime which could have reacted pozzolanically with clay. However, in the case

of carbonate material without clay, the development of a carbonate cementitious matrix represents a substantial improvement in mixture properties. It has also been established that carbonate aggregates without lime tend to "set up" through carbonation. Graves et al. (1990) explain that the addition of low percentages of lime "catalyzes" and enhances this reaction.

In addition, Graves et al. (1990) found that the interfacial bonding of lime treated aggregates was a key to strength development. Graves reported that strength development of all aggregates was a function of calcite to quartz ratios. Higher ratios result in greater strength due to the more complete development of carbonate bonding.

Graves et al. (1990) also reported that granite aggregates stabilized with portland cement produce high strengths but that the weak link in their strength is the interfacial bond. Microfractures in this bond developed during cyclic wetting and drying or freezing and thawing may result in reduced strength. However, when the granite aggregate was pretreated with Ca(OH)_2 the residual strength was significantly higher. Scanning electron microscopic (SEM) analysis showed that the lime treated aggregate developed a better interfacial bond between the cement paste and the aggregate than was developed without the lime pretreatment. Furthermore, SEM analysis documented the nature of the carbonate cement matrix in calcareous aggregates. The addition of relatively low levels of Ca(OH)_2 was shown to develop a much denser CaCO_3 cement matrix than that developed in this aggregate without lime.

The literature, primarily developed by Graves et al. (1990), supports the use of Ca(OH)_2 as an enhancement for calcareous bases. The beneficial results are expected to be strength increase and resilient modulus increase through carbonation reactions. The carbonate cement apparently bonds to and grows from calcareous surfaces. Thus one would expect a more beneficial reaction from lime when used with more pure calcareous materials. Chapter 4 will address this issue in detail.

Material Characteristics Due to Stabilization

When adequate lime is added to optimize the pozzolanic reaction with soils, substantial improvement in shear strength and resilient moduli can be realized. Table 2.1 illustrates typical improvement levels in strength and stability for various classifications of soils.

Table 2.1 demonstrates the strength levels achieved when testing five lime stabilized Texas soils with very different mineralogies. It is well known that the mineralogy and conditions of

soils with very different mineralogies. It is well known that the mineralogy and conditions of weathering substantially influence the reactivity of lime with soils (Thompson, 1970).

The soils in Table 2.1 are all reactive with lime. However, the Beaumont clay is the least reactive. This clay possesses what is referred to by soil scientists as non-specific acidity. This acidity refers to the presence of poorly structured aluminate layers interdispersed within the clay structure. As a result of the influence of the aluminate layers, the Beaumont clay requires more lime than most soils for stabilization, and a longer curing time is required for the pozzolanic reaction to develop. The slow reaction between lime and the Beaumont clay is probably partially due to the time required for the aluminate underlayers to react with lime so that the pozzolanic reaction can be fully developed.

Figure 2.1 further illustrates the variation among different soils in terms of lime reactivity. In this figure, it is apparent that some soils begin developing pozzolanic reaction with low levels of lime, i.e., the cologned clays. However, the montmorillonite soils require a substantial amount of lime prior to the development of strength. This indicates that a substantial amount of lime is necessary to satisfy cation exchange effects and cation or $\text{Ca}(\text{OH})_2$ molecule crowding effects prior to the development of pozzolanic reactivity. This would seem logical for the high surface area and highly negatively charged montmorillonite minerals.

The data presented in Table 2.1 provide similar results to those presented in Figure 2.1. The data from Table 2.1 also demonstrate (1) the variation in pozzolanic reactivity among different soil types, (2) the effect of different soil mineralogies on optimum lime content, and (3) the significant level of strength developed within each soil due to its pozzolanic reactivity. (Note the high level of reactivity in the Utah soil even though the clay content is relatively low compared to the CH soils in Table 2.1). Furthermore, the estimated optimum strength (approximated from strength testing following accelerated-high temperature curing) is often not a good approximation of longer term curing at ambient temperature. Lime-soil pozzolanic reactions are slow-forming compared to cementitious reactions (i.e., between portland cement and soil). These long-term reactions are often very beneficial due to the nature of the slow, long-term reaction. This long-term strength gain which can continue for years in soils with adequate lime contents can produce what is referred to as autogenous healing. This healing can result in rebonding over microcracks and reestablishment of the bonding matrix.

Table 2.1. Unconfined Compressive Strengths of Selected Soils.

Soil	Percent Lime	Accelerated Strength*, KPa	28-Day Strength**, KPa
Arlington Clay (CH)***	4	1,225	
	6	2,170	
	8	2,450	4,830
Beaumont Clay (CH)	4	490	
	6	490	
	8	700	1,540
Burleson Clay (CH)	4	630	
	6	1,400	
	8	1,750	2,310
Denver, Co. Sandy Clay (CL)	4	2,100	
	6	2,030	2,870
	8	1,750	
Victoria Clay (CH)	4	700	
	6	1,050	
	8	1,470	1,925
Utah Clay Silt (CL)	4	1,000	
	5	1,920	6,900
	6	4,100	
	7	4,000	
Orange Co., California (SC)	4	1,000	
	5	1,500	1,620
	6	1,400	

* 2 days at 35°C

** 28 days at 22°C

*** Unified classification

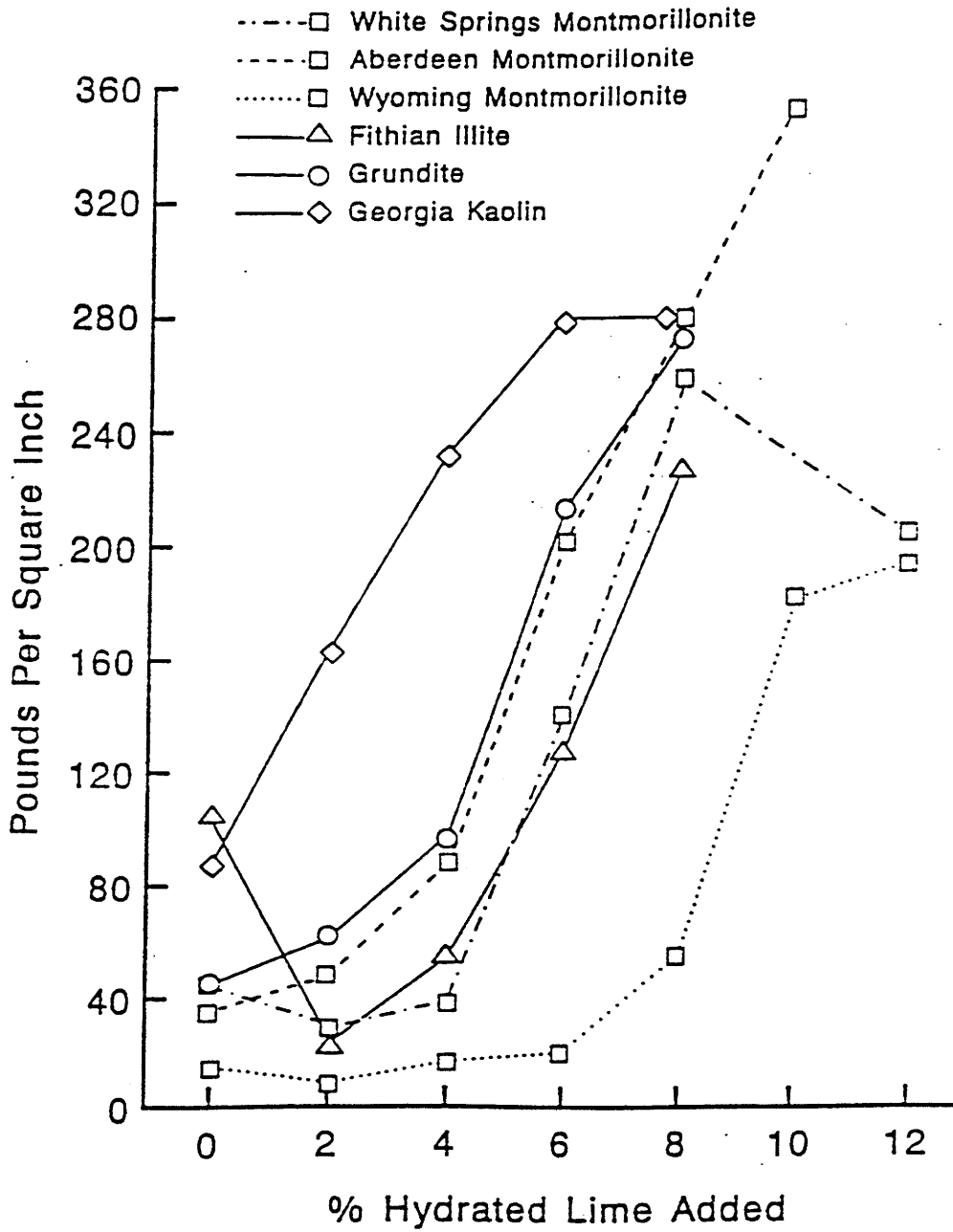


Figure 2.1. The Quantity of Lime Required to Produce Pozzolanic Reaction is Influenced by the Mineralogy of the Soil Being Stabilized (After Eades and Grimm, 1960). (1psi=6.98 KPa)

Figure 2.2 illustrates the long-term strength gain expected in lime stabilization. These data (from a CALTRANS study by Alexander and Doty, 1978) illustrate not only the long-term strength gain but also the effects of lime content. Additionally, it is confirmed that some soils, based on mineralogy, are very reactive pozzolanically (soils 12, 11, 10, 3, 2, 8, 5 and 9) and some are relatively low in reactivity (4 and 6). Of particular interest is that soils 11 and 9 have low PI's (below 15), yet they are very pozzolanically reactive. This apparently is due to the very highly reactive nature of the clay fraction within the soil. Even though the clay concentration may be low, the mineral is highly reactive resulting in significant strength gain.

Table 2.2 summarizes typical values of resilient moduli measured in situ for various Texas soils in this study. From this table the following conclusions may be drawn.

1. The range of resilient moduli values determined through in situ measurements is quite large, from about 175 MPa to about 6,510 MPa. However, in every case the resilient modulus determined represents a significant and substantial improvement over the native, unstabilized subgrade.
2. The average value of the in situ moduli are from four to twenty times the in situ moduli of the natural, unstabilized soil.
3. Lime stabilized subgrades produce moduli which are high enough to add structurally to the flexible pavement system, and this structural benefit should be considered in pavement design and pavement systems considerations.
4. Most of the LSS layers evaluated had been in place for over 10 years, which is indicative of the durability of the layer and the permanency of the reaction. The TTI research annex LSS layers were evaluated after 2 years of very wet (much higher than average rainfall) conditions without cover.

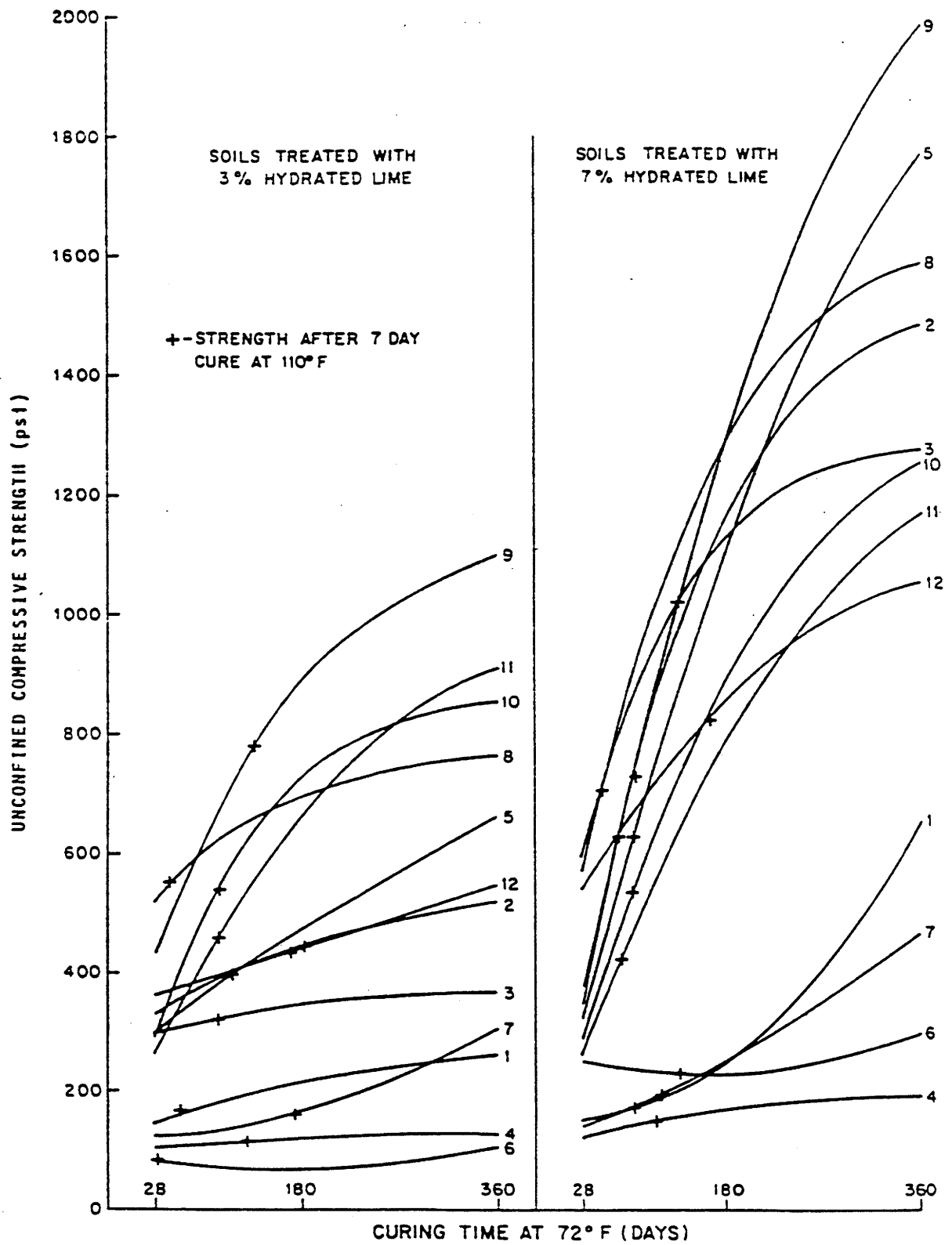


Figure 2.2. Comparison of Strength after 7 Days at 43°C (110°F) with Strength Increases at 22°C (72°F) (After Alexander, 1978) (1 psi = 6.894 KPa).

Table 2.2. Resilient Moduli of Lime Stabilized Subgrade (LSSs) Backcalculated From Falling Weight Deflectometer (FWD) Data.

Highway	Pavement Section	In Place Resilient Modulus, MPa	
		Natural Subgrade	Lime Treated Subgrade
IH40	254 mm HMAC 381 mm ABC 368 mm LSS Clay Sand	91	644
SH105	50 mm HMAC 244 mm ABC 165 mm LSS Clay Sand	133	1,820
US77	190 mm HMAC 305 mm ABC 152 mm LSS Silt	84	3,010
SH19	279 mm HMAC 152 mm ABC 293 mm LSS Sandy Clay	105	1,120
SH23	76 mm HMAC 457 mm ABC 203 mm LSS Clay Sand	126	770
SH21	216 mm HMAC 279 mm ABC 114 mm LSS Clay Sand	126	5,600
IH37	178 mm HMAC 254 mm ABC 152 mm LSS Sandy Clay	175	6,510
SH19	51 mm HMAC 279 mm ABC 229 mm LSS Sandy Clay	175	2,100

Table 2.2 Resilient Moduli of Lime Stabilized Subgrade (LSSs) Backcalculated from Falling Weight Deflectometer (FWD) Data. (Continued)

Highway	Pavement Section	In Place Resilient Modulus, MPa	
		Natural Subgrade	Lime Treated Subgrade
US83	254 mm HMAC 266 mm Soil-Aggregate 140 mm LSS Clay	91	1,995
US77	51 mm HMAC 279 mm ABC 178 mm LT-Sand Sand	105	98
US59	51 mm HMAC 203 mm ABC 229 mm LS Clay Sand	70	245
IH37	254 mm HMAC 432 mm Soil-Aggregate 152 mm LSS Sandy Clay	182	931
TTI Research Annex	152 mm LSS (before traffic)	7-28	238-546
	304 mm LSS (before traffic)	7-28	175-490
	304 mm LSS (after traffic)	7-28	231-280
Houston, Texas City Streets	152 mm (approx. 6 locations)	21-53	140-490

Influence of Material Improvements Through Lime Treatment on Pavement Performance

The improved shear strength and improved resilient modulus of lime stabilized subgrades can influence the structural performance of the flexible pavement system in the following ways.

1. The increased shear strength achieved through pozzolanic reaction reduces the potential of the stabilized layer to deform excessively under heavy wheel loads. This is particularly important in clay soils under wet conditions or in clayey soils which have been subjected to cyclic moisture effects such as freeze-thaw and/or wet-dry cycling. Figure 2.2 illustrates this situation for a Tama B soil from Illinois.
2. The increased stiffness or resilient modulus produced in a lime stabilized subgrade layer produces two additional effects on the pavement system:
 - a. Protection of the natural subgrade under the lime stabilized layer from being overstressed, which could lead to pavement roughness and/or deep layer rutting.
 - b. Better support of the overlying layers, including the flexible base layer and the hot mix asphalt concrete layer.

Little (1995) reports that the resilient moduli of clay soils can be improved much more substantially than is illustrated for the Tama B soil in Figure 2.3.

Superior support (offered by a high modulus subbase) of the granular, flexible base course layers results in improved performance of these layers. It has long been accepted that the resilient modulus response of aggregate base courses is stress and moisture dependent. This stress dependency of resilient modulus, M_R , is defined by the general law:

$$M_R = K\theta^n$$

where K and n are regression constants, and θ is the bulk stress invariant, defined as the sum of the principal stresses.

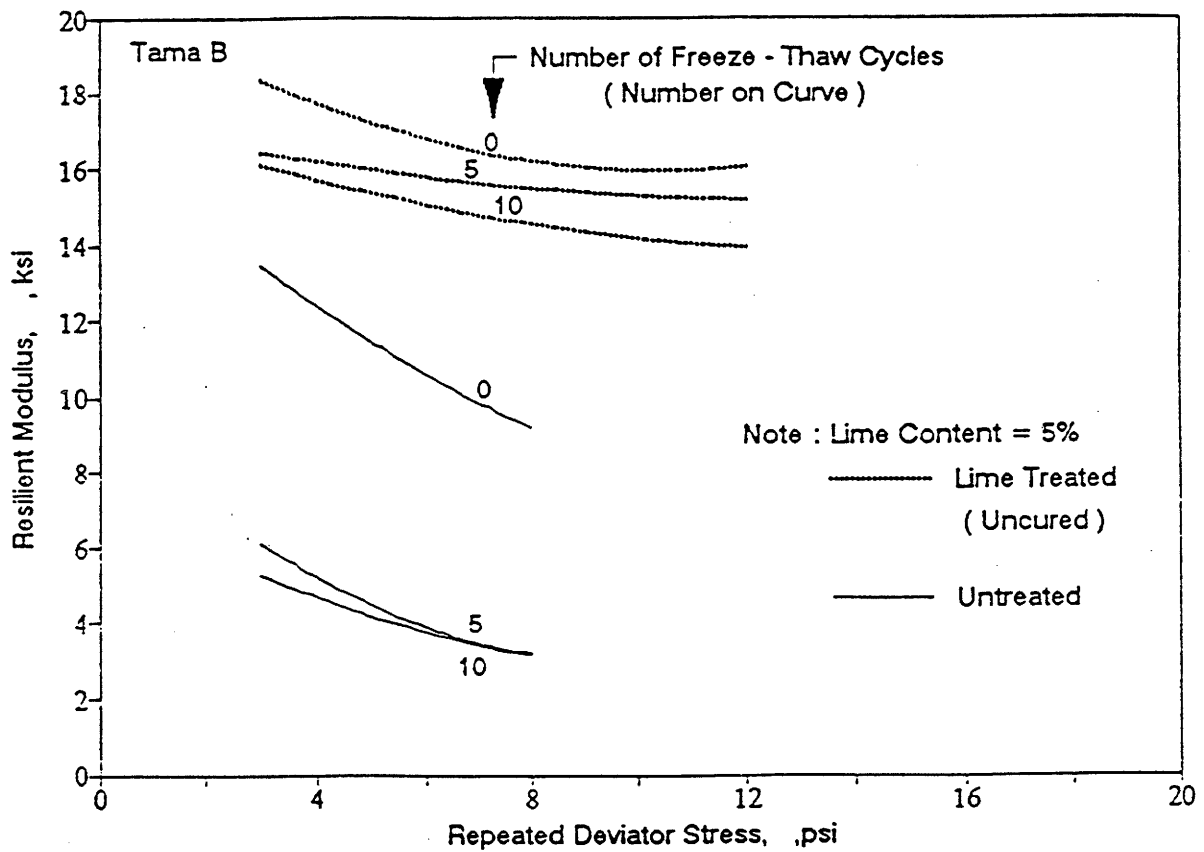


Figure 2.3. The Resilient Modulus of the Tama B Soil is Significantly Influenced by Lime Stabilization, Even After 10 Freeze-Thaw Cycles (After Thompson, 1985) (1 psi = 6.89 KPa).

The 1986 AASHTO pavement design guide illustrates that the supporting power of the subgrade substantially affects the average value of θ within the flexible base and hence substantially influences the value of the resilient modulus of the flexible base. Tables 2.3 and 2.4, taken directly from the 1986 design guide, illustrate this effect. Little (1994) used finite element elastic analysis to evaluate the effects of lime stabilization in enhancing the resilient modulus of the flexible base. Little's study illustrated the effect of lime stabilization on the Tama B soil, shown in Figure 2.2, after being subjected to 10 freezer thaw cycles. A pavement section consisting of an 89 mm hot mix asphalt concrete surface and a 305 mm flexible base was evaluated. Two cases were considered. In Case A, the flexible base rested directly on the unstabilized Tama B subgrade. In case B, the identical pavement structure was evaluated except that the top 203 mm of the Tama B subgrade was stabilized with lime. In each case the non-linear, stress sensitive resilient modulus of the flexible base was calculated. Under an 80 kN single axle load, the resilient modulus of the flexible base increased from 140 MPa when the flexible base rested directly on the unstabilized subgrade to 196 MPa when the stabilized subgrade lime stabilized layer supported the flexible base.

According to the 1986 AASHTO design guide, the structural layer coefficient, a_2 , is a function of the resilient modulus as (M_R , when M_R is expressed in psi).

$$a_2 = 0.249 \log M_R - 0.977$$

The increase in M_R of the flexible base in the example considering stabilization effects on the Tama B soil results in an increase in a_2 from 0.09 to 0.14 for the flexible base layer. This increase in the structural layer coefficient results in approximately a 100 percent increase in performance life, according to the 1986 AASHTO design equation.

Table 2.3. Average Values of Bulk Stress, θ , Within the Flexible Base (Aggregate Base) Layer as a Function of Hot Mix Asphalt Concrete Thickness and Subgrade Support (After AASHTO Guide, 1986).

Asphalt Concrete Thickness, mm	Roadbed Soil Resilient Modulus, KPa		
	21,000	52,500	105,000
Less than 50.8	140*	175	210
50.8 - 101.6	70	105	140
101.6 - 152.4	35	70	105
Greater than 152.4	35	35	35

* Value of bulk stress, θ

Table 2.4. Typical Variation in the Resilient Modulus of Flexible Base (Aggregate Base) as a Function of Moisture Condition and Stress States (After AASHTO Guide, 1986).

Moisture State	Stress State (MPa)			
	$\theta = 35$	$\theta = 70$	$\theta = 140$	$\theta = 210$
Dry	149	223	338	431
Damp	74	111	169	215
Wet	58	89	135	172

Little (1990) demonstrated that the level of shear stresses induced in hot mix asphalt concrete surfaces is substantially reduced when the modulus ratio between the hot mix surface and the flexible base is reduced. Little (1990) used the octahedral shear stress ratio as the factor associated with rutting or distortion potential in the hot mix surface. This ratio of induced shear stress within the surface layer to shear strength of the surface hot mix layer is an indicator of distortion or rutting potential within the layer. Little (1986) demonstrated that as this ratio approaches 0.70, rutting potential becomes high.

Table 2.5 summarizes moduli of the flexible base layers and the octahedral shear stress ratios developed within the Arizona pavements discussed earlier. Note that the ratio is above the 0.70 value for all of the unstabilized layers (low moduli of the flexible base or high surface to base modulus ratio). On the other hand, the stress ratio for the pavements with lime stabilized bases is much lower, below the 0.70 value in each case, as a result of the lower surface to base modulus ratios due to stabilization of the flexible base with lime. The same effect results when the response modulus of the flexible base is increased through the superior support offered by the stabilized subgrade layer. Verification of the influence of shear stress ratios on hot mix asphalt concrete surface layer performance is another important part of this study.

Mix Design Considerations

Currently, TxDOT selects the design lime content for lime-stabilized layers based on the percent binder-size material (minus 40 sieve-size) and the plasticity index (PI), Figure 2.4. The evaluation has been thought to be conservative, but research by Currin et al. (1976) and Haston and Wolhgemuth (1985) has shown that the percent lime selected from Figure 2.4 can be liberal and often does not predict the lime required to optimize strength, especially when high lime content is required.

The procedure suggests strength criteria of 690 KPa for base construction and 345 KPa for subbase construction.

Details of the procedure are presented in Tex-117-E of the Manual of Testing Procedures for TxDOT. A summary of the procedure follows.

1. Based on the grain size and PI data, the lime percentage is selected using Figure 2.4. The percentages in this figure should be substantiated by approved testing methods on any particular soil material. Use of the chart for materials with less than 10 percent No. 40 and cohesionless materials (PI of less than 3) is prohibited. A relatively high purity lime, usually 90 percent or more of Ca and Mg hydroxides, or both, and 85 percent or more of which passes the No. 200 sieve is required for stabilization. Percentages shown are for stabilizing subgrades and base courses where lasting effects are desired. Satisfactory temporary results are sometimes obtained by the use of as little as one-half

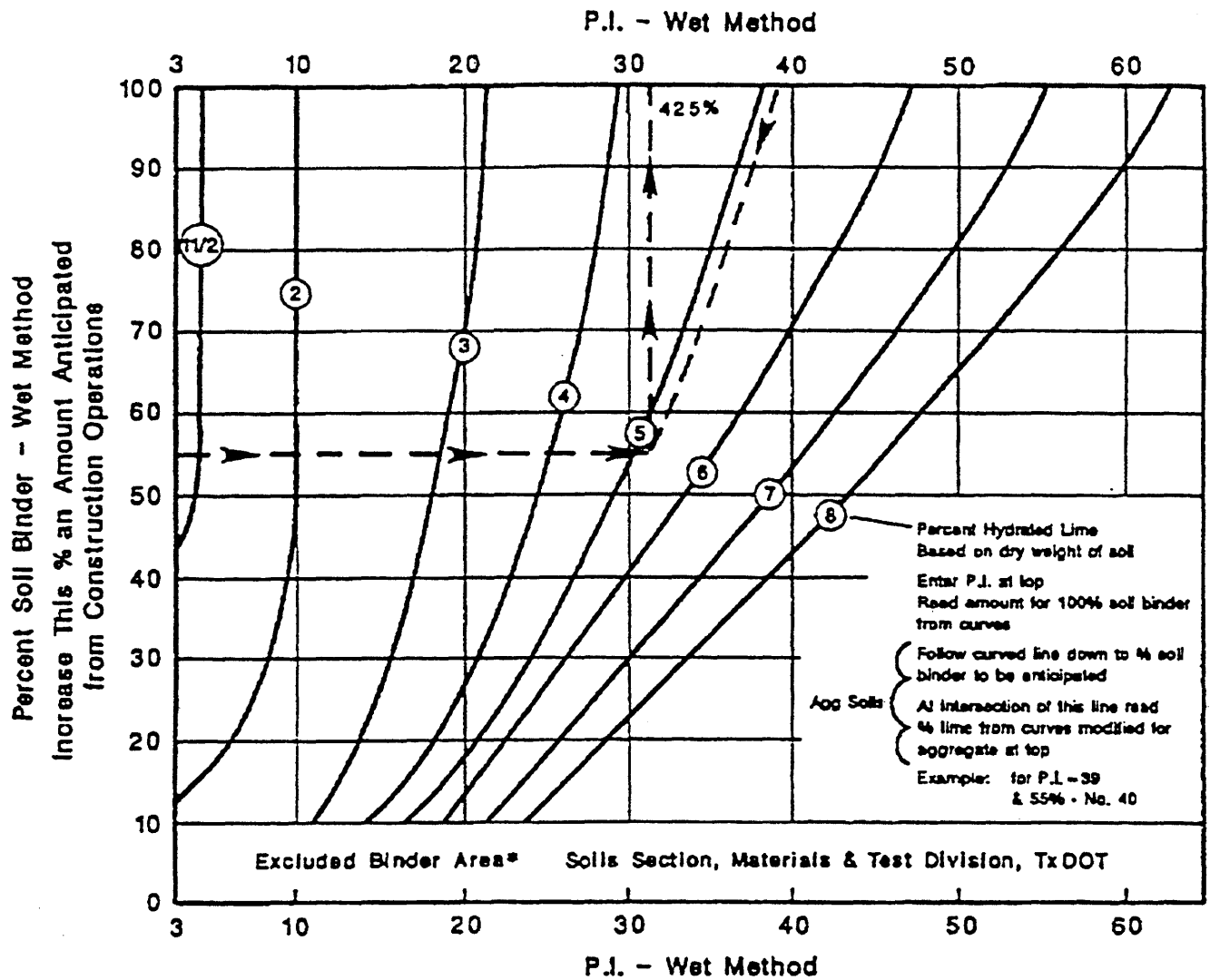


Figure 2.4. The Texas Method for Establishing an Optimum Lime Content is Based on the Binder Content (Passing No. 40 Sieve) and the Plasticity Index.

Table 2.5. Summary of Octahedral Stress Ratios Developed within Hot Mix Asphalt Concrete Surfaces as a Function of the Supporting Modulus of the Flexible Base Course Layers.

Pavement Section Identification	Resilient Modulus of Flexible Base, MPa	Stress Ratio, OSSR
Section 7 89 mm HMAC 254 mm flex. base	245	0.70
Section 8 (Same as section 7)	91	0.78
Section 9 (Same as section 7)	140	0.75
Section 1 89 mm HMAC 254 mm flex. base (1% lime stabilization)	378	0.65
Section 3 (Same as section 1)	1,568	0.50
Section 6 (Same as section 1)	2,849	0.45

of the aforementioned percentages.

2. Optimum moisture and maximum dry density of the mixture are determined in accordance with appropriate sections of Tex-113-E. The compactive effort is 50 blows of a 44.5 N hammer with 45.7 cm drop.
3. Test specimens 15.2 cm in diameter and 203 cm in height are compacted at optimum moisture content and maximum dry density.
4. The specimens are placed in a triaxial cell (Tex-121-E) and cured in the following manner:
 - a. Allow the specimen to cool to room temperature;
 - b. Remove cells and dry at a temperature not exceeding 60°C for about 6 hours or until one-third to one-half of the molding moisture has been removed;
 - c. Cool the specimens for at least 8-hours; and

- d. Subject the specimens to unconfined compression in accordance with AASHTO T-212 Sections 7 and 8 or Tex-117-E.

The results of the unconfined compression strength testing can be used for substantiation of optimum lime content.

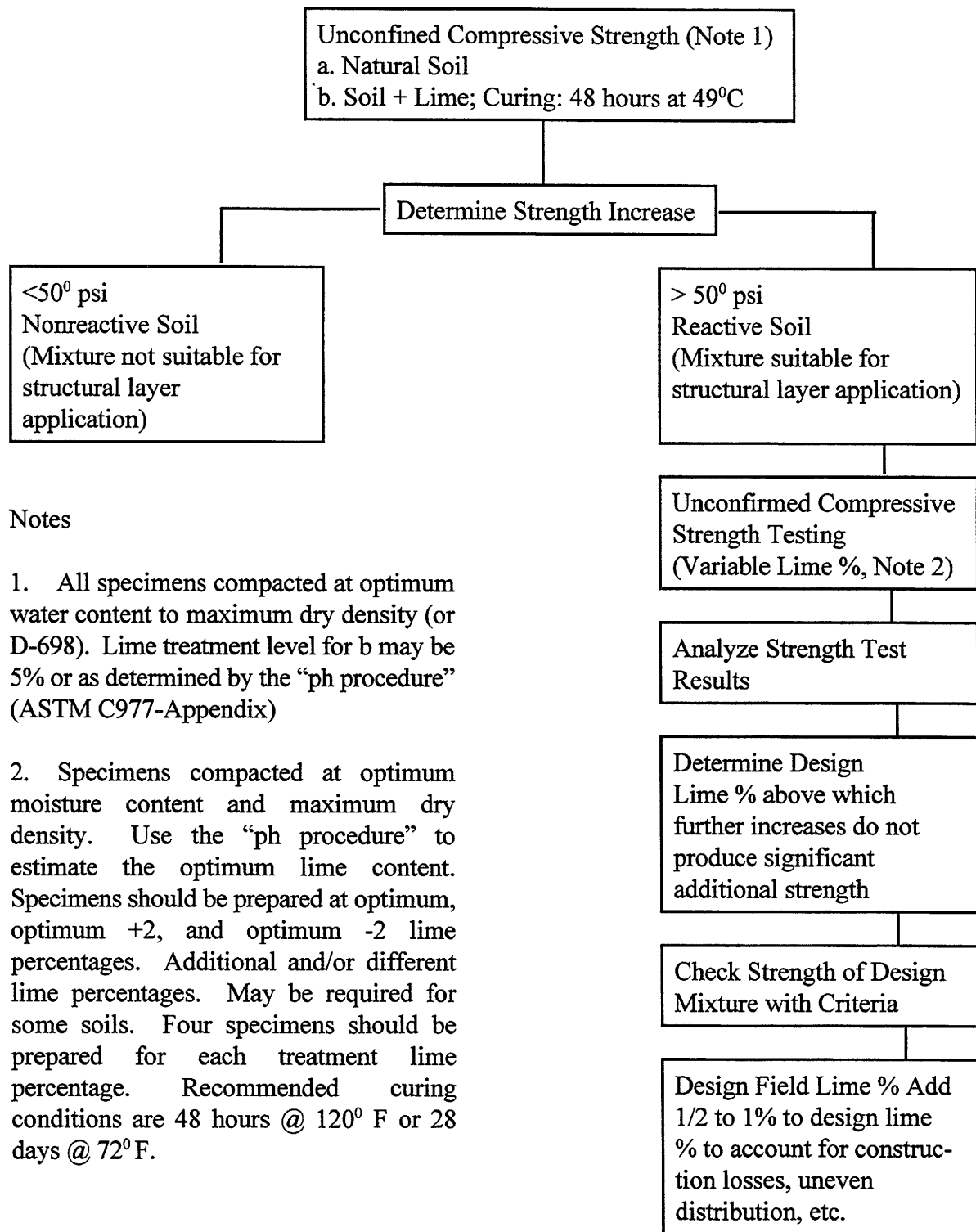
Eades and Grim (1960) and McCallister and Petry (1991) have shown that although lime-stabilization may not be permanent if too little lime is used, it should be a durable and permanent reaction if significant pozzolanic reaction is achieved. The McCallister and Petry study (1991) of Texas soils confirmed that some lime-treated soils subjected to extensive leaching suffered deleterious changes in physical properties when the lime treatment was in the range of 3 to 4 percent lime by weight of soil. However, when the stabilization level was increased to 5 to 7 percent lime, no significant changes in physical properties were noted, even after extensive leaching. The lime content, which produced optimum strength for the Texas soils studied, was in the 5 to 7 percent range for each soil.

Currently, approximately eight mix design approaches are used nationwide for lime-stabilized soil mixtures. Among these, Little et al. (1987) and Little (1995) recommend the Thompson procedure (1970) because it includes two approaches to insure that enough lime is used to promote pozzolanic reactivity: (1) the pH test and (2) confirmation by compressive strength facts. Figure 2.5 presents an outline of the Thompson procedure.

Recommended Structural Performance Algorithms

The primary function of the lime stabilized subgrade or lime stabilized base course layer in a flexible pavement system is to improve the shear strength of the stabilized layer, protect the underlying layers and native subgrade from being overstressed, enhance the response modulus generated by the flexible base layer due to the improved support of the lime stabilized subgrade and reduce shear stresses within the hot mix asphalt concrete surface as a result of the better support offered by the lime stabilized subgrade layer.

In the interim recommendations of Study 1287, Little et al. (1993) recommended accounting for the structural beneficiation of lime stabilized subgrades by assigning structural factors to the layers. As an example, a structural layer coefficient can be assigned to be used in accordance with



Notes

1. All specimens compacted at optimum water content to maximum dry density (or D-698). Lime treatment level for b may be 5% or as determined by the "ph procedure" (ASTM C977-Appendix)
2. Specimens compacted at optimum moisture content and maximum dry density. Use the "ph procedure" to estimate the optimum lime content. Specimens should be prepared at optimum, optimum +2, and optimum -2 lime percentages. Additional and/or different lime percentages. May be required for some soils. Four specimens should be prepared for each treatment lime percentage. Recommended curing conditions are 48 hours @ 120° F or 28 days @ 72° F.

Figure 2.5. The Thompson Mixture Design Flow Chart is Based on Soil-lime Reactivity (After Little, et al., 1987).

1 psi = 6.89 KPa
 72° F = 23° C
 120° F = 51° C

the AASHTO performance equation to determine pavement serviceability based on the unconfined compressive strength of the lime stabilized subgrade layer as defined by Thompson (1970). This procedure requires additional study and in situ verification and validation of resilient moduli of lime stabilized subgrades.

Presently, test method TEX-121-E requires that the unconfined compressive strength of lime stabilized material be determined using 152 mm diameter by 203 mm high samples tested in accordance with the Texas Triaxial testing method. The curing method in this test requires 7 days of moist curing followed by 6 hours of drying at 60°C. This relatively short-term curing may not be a satisfactory indication of the strength likely to develop in many lime-soil mixtures as the pozzolanic development in many of these mixtures is considerably slower than in portland cement stabilized or lime and fly ash stabilized materials. This is illustrated by Alexander (1978) in Figure 2.2. The long-term curing effects required for the Beaumont clay discussed in Table 2.1 is a good example of the requirement for long term evaluation of strength gain in some lime-soil mixtures.

In the interim report for Study 1287, Little et. al. (1993) recommended assigning a structural layer coefficient of 0.09 to 0.11 to lime stabilized layers according to Figure 2.6 (Thompson 1970) if the unconfined compressive strength of the mixture exceeds 700 KPa when tested in accordance with TEX 121-E.

In special cases where the lime stabilized layer comprises the major structural layer of the pavement, Little et al. (1993) recommended assigning a structural layer coefficient as discussed above followed by an evaluation of the ability of the stabilized layer to resist flexural fatigue as discussed by Thompson and Figueroa (1989).

In this special case, the lime stabilized layer must be stabilized and not modified. The pavement section is essentially a two layered system with the two layers consisting of a native subgrade and a composite structural layer of lime stabilized subgrade and a thin asphaltic surface treatment. The composite layer functions with a "slab-effect." The basic steps in this approach are to determine the compressive strength of the lime stabilized layer, determine or approximate the resilient modulus of the native soil, approximate the maximum induced flexural tensile stress within the lime stabilized layer by means of a regression model as discussed by Little et. al. (1993), and evaluate the fatigue damage potential within the stabilized layer according to the stress ratio concept

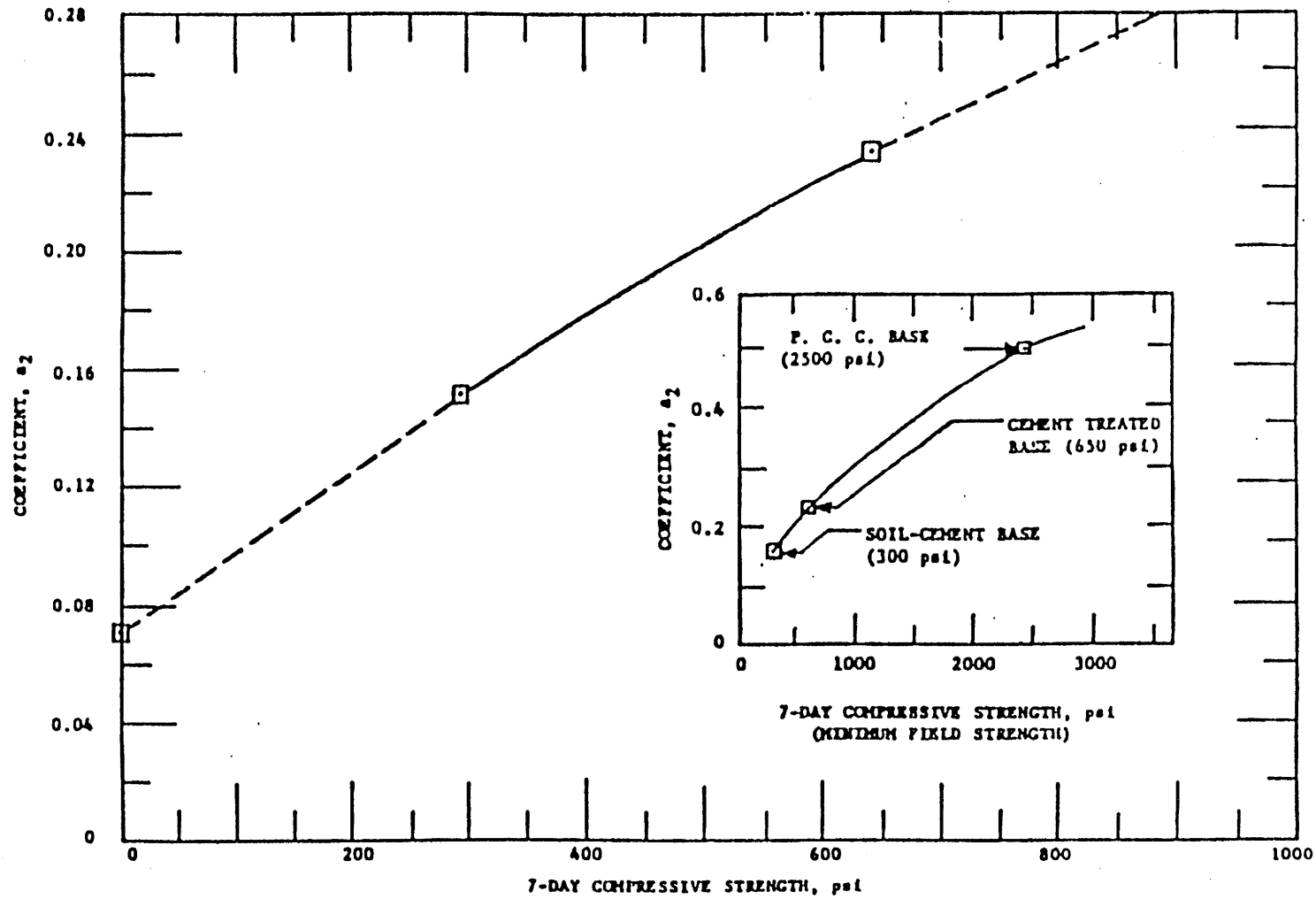


Figure 2.6. Structural Layer Coefficient, a_2 , as Determined by Thompson as a Function of Compressive Strength for Lime Stabilized Layers (After Thompson, 1970).

1 psi = 6.89 KPa

discussed by Little et al. (1993).

2.2 CHARACTERIZATION AND PERFORMANCE EVALUATION OF PORTLAND CEMENT STABILIZED SUBGRADES

Basic Reactions and Mechanisms of Stabilization

The basic reactions between portland cement and soil are: (1) cation exchange, (2) flocculation and agglomeration, (3) pozzolanic reaction between the available calcium in the portland cement and the soil, (4) cementitious reaction and (5) carbonation.

The reactions of cation exchange, flocculation and agglomeration, pozzolanic reaction and carbonation are the same reactions that occur during lime stabilization. These reactions are initiated and driven by the presence of available calcium. Although a chemical oxide analysis will indicate that portland cement is predominately calcium oxide (about 63 percent by weight), the great majority of the CaO is combined with aluminates and silicates and is not available for reaction with the soil. In the hydration process, the availability of the CaO increases markedly, but the practical aspects of a short mixing time may limit, to some extent, the potential for cation exchange, flocculation and agglomeration and pozzolanic reaction in highly plastic soils. It is important to conduct more field studies in Texas with focus on the ability of portland cement to stabilize plastic clays.

Lime is generally used with more plastic soils because of the availability of large amounts of free calcium (over an extended period of time) to trigger cation exchange and flocculation and agglomeration. These reactions result in plasticity reduction and a reduction in swell potential. The key to the success of lime in ameliorating the physical properties of plastic soils is not only the large quantities of available calcium but also the slow pozzolanic reaction time between lime and soil. This slow "strength-developing" reaction allows a long period of mixing during which the plastic soil can be broken down and mixed intimately with the lime. This mixing period can extend up to several days, including several mixing periods and intermediate mellowing periods, without detrimental effects on the final product.

Mixing with portland cement and compaction must occur within 4 to 8 hours. Otherwise, the hydration of the cementitious product within the portland cement will result in a rapid strength gain, which interferes with necessary compaction, and if this compaction is achieved, it may occur at the

expense of irreversibly destroying the cementitious product. Therefore, although portland cement can be used to stabilize plastic soils, it must be mixed intimately over a very short time frame, less than 4 to 8 hours in order to do so. Under certain conditions and with excellent mixing equipment, it may be possible to achieve adequate mixing of high PI soils with portland cement so that a durable pavement layer can be constructed.

The main component of portland cement stabilized soils is the cementitious reaction which can develop considerable compressive strengths within the stabilized soil. This cementitious reaction is due to the hydration of calcium silicate and calcium aluminate to form calcium silicate hydrates and calcium aluminate hydrates.

Material Characteristics Due to Stabilization

It is well known that cement stabilization can be used effectively over a wide range of soil types and classifications. Granular soils at optimum cement contents typically have 7-day unconfined compression strengths of 2,100-5,000 KPa and 28-day unconfined compression strengths of 2,800-10,000 KPa. Highly plastic, fine-grained soils may have 7-day strengths of 700-2,800 KPa and 28-day strengths of from 1,700-4,200 KPa (Bulletin 292, Highway Research Board, 1961) if they can be intimately mixed with the stabilizer during the 4 to 8 hour period before compaction is necessary.

Unlike lime stabilized soils, the strength gain in portland cement stabilized soils is rather rapid with as much as 50 percent of the 28-day compressive strength occurring within the first 7 days. Although strength gain can continue for very long periods of time, the great majority of strength gain usually occurs in the first 28 days or so of curing.

The high compressive strengths developed in portland cement stabilized soils lead to high stiffnesses or resilient moduli of the resulting pavement layers. In many cases the strengths are so high and the stiffnesses so great that the cement stabilized layer must be treated as a structural slab. This rapid strength gain, which occurs rather rapidly, can result in considerable shrinkage, which must be accommodated by a proper construction techniques.

Mix Design Considerations

Unlike lime, where a variety of mix design methods are used, most portland cement stabilized mixes are designed in accordance with the PCA method (PCA, 1969). This well-established and well-verified method allows the designer to select an appropriate range of trial stabilizer contents based on soil index properties (e.g. density, gradation properties and plasticity). However, ultimate stabilizer contents are based on unconfined compressive strength (sandy soils) or durability tests (silty and clayey soils).

The Texas method of mixture design for soils containing portland cement is presented in Tex-120-E. This method is similar to the PCA method and is in essence an adaptation of the PCA method. The design cement content is based on unconfined compressive strength.

Influence of Material Improvements on Pavement Performance

The 1972 AASHTO interim pavement design guide demonstrates the substantial level of structural improvement that a portland cement stabilized layer can add to the pavement system. Structural layer coefficients for cement treated bases can be considerably higher than the structural layer coefficients for unbound aggregate base courses. However, in order to achieve this considerable level of structural contribution, the 1972 and 1986 AASHTO design guides require that a high 7-day unconfined compressive strength be achieved in order to assure durability.

Recent work by South African and Australian researchers provides considerable insight into the mechanism of failure of cement stabilized bases and provides pertinent input to the level of strength required to achieve a certain level of structural contribution. The South African study (Jordaan, 1992) indicates that in situ moduli are considerably less than previously reported and vary considerably with depth. The failure mechanism postulated by the South Africans and the stiffness gradient within the stabilized layer identified by the South Africans were evaluated in this study.

Although the studies referenced above may cause some reassessment of the design approaches of cement treated bases and subbases, the considerable strength increases achieved in cement stabilized layers and the considerable stiffnesses, often in the range of 7,000 to 14,000 MPa, usually requires the designer to treat the layer as rigid slab. This is because the modulus ratio between the stabilized layer and the underlying native subgrade is often very high. This high modulus ratio results in high tensile flexural stresses being induced in the slab, which can result in flexural fatigue

cracking and the ultimate deterioration of the structural slab. Little et.al. (1993) present several design approaches based on the concept of preventing excessive flexural fatigue cracking within the portland cement stabilized layer.

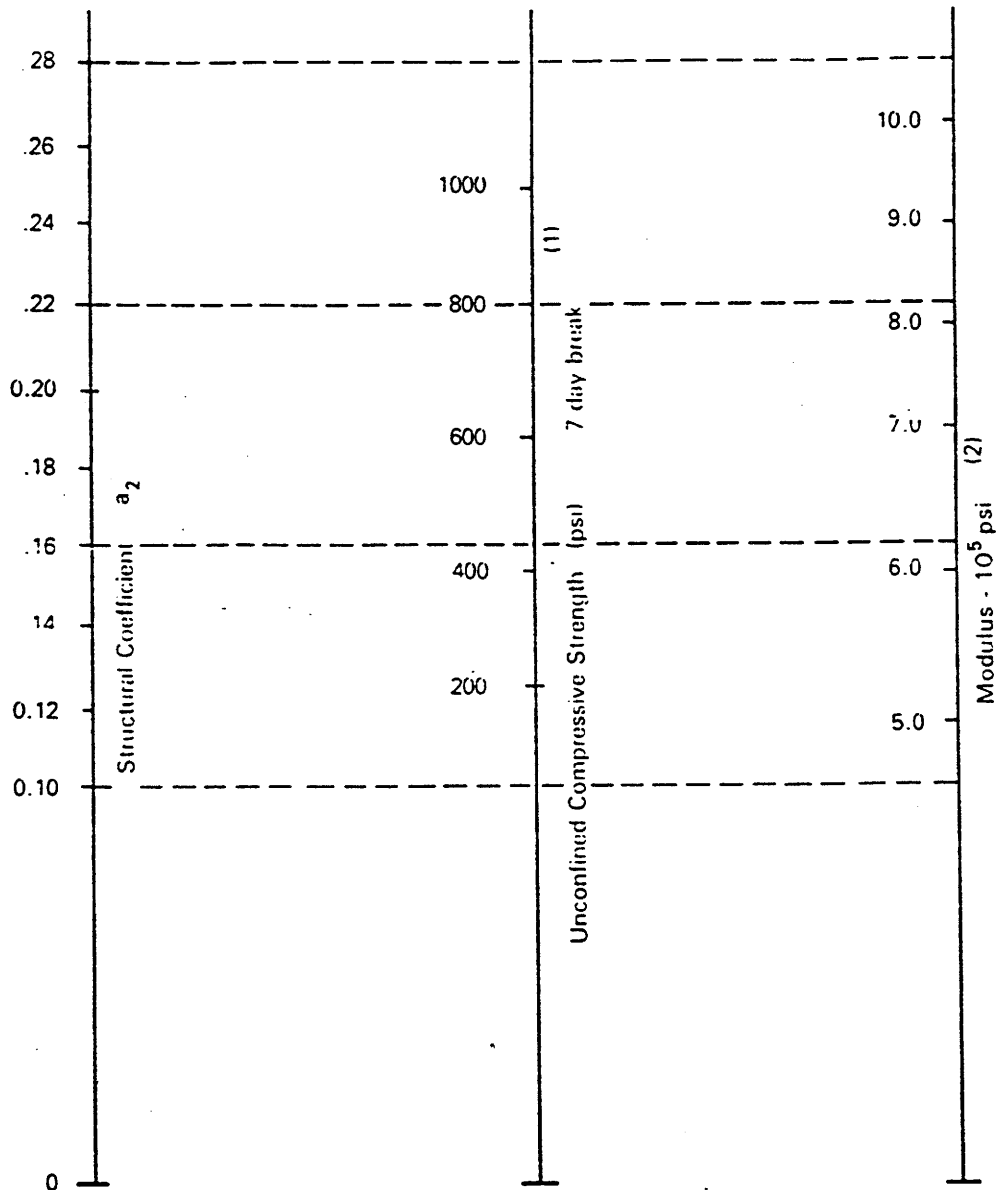
Recommended Structural Performance Algorithms

The Griffith model as modified by Raad (1977) offers a rather simple and realistic approach by which to evaluate the response of a portland cement stabilized layer under loading. The approach evaluates the susceptibility of the stabilized, slab-like layer to develop flexural fatigue based on the principles of crack propagation and fracture mechanics.

The Griffith approach as modified by Raad is attractive in that the only structural property required of the cement treated layer is the unconfined compressive strength. The major and minor principle stresses, σ_1 and σ_3 , respectively, are then determined to identify the stress state and the stress intensity field. Based on the material property of unconfined compressive strength and the stress conditions of major and minor principle stresses, the fatigue life of the portland cement stabilized layer is determined as discussed by Little et al. (1993).

Once the structural integrity of the slab is insured in terms of adequate resistance to flexural fatigue cracking according to the modified (by Raad) Griffith approach, the serviceability of the pavement section can be predicted using the 1986 AASHTO performance design guide by assigning the appropriate structural layer coefficient to the portland cement stabilized base in accordance with Figure 2.7.

Raad (1987) demonstrates that portland cement stabilized layers are bi-modular. This means that the tensile modulus is not equal to the compressive modulus. His research offers a relationship by which to characterize one from the other. It is imperative that when performing the structural analysis for fatigue potential, the appropriate flexural tensile modulus be used. It is important, therefore, to define the relationship between the appropriate modulus to be used in design (based on an approach such as Raad's) and the in situ determined modulus.



- (1) Scale derived by averaging correlations from Illinois, Louisiana and Texas.
 (2) Scale derived on NCHRP project (3).

Figure 2.7. Variation in a_2 for Cement-Treated Bases with Base Strength Parameter (After AASHTO, 1986).

1 psi = 6.89 KPa

It is imperative that research continue in the area of investigation of the mode of failure of portland cement stabilized bases in both flexible and rigid pavement systems. This vital and continuing research will determine whether the fatigue approach is sufficient or whether it is necessary to investigate different approaches of the evaluation of the structural performance of cement stabilized bases.

Little et.al. (1993) present a more complete survey of literature with regard to portland cement stabilized bases. Since structural characterization of portland cement stabilized bases is better defined in the literature (e.g., the AASHTO structural layer coefficient approach) than for lime-stabilized bases and subbases, this chapter has concentrated on lime stabilization.

2.3 CHARACTERIZATION AND PERFORMANCE EVALUATION OF LIME-FLY ASH AND CEMENT-FLY ASH STABILIZED BASES

Basic Reactions and Mechanisms of Stabilization

The basic reactions between fly ash and soil are very similar to those that occur between portland cement and soil. These reactions include: (1) cation exchange, (2) flocculation and agglomeration, (3) pozzolanic reaction, (4) cementitious reaction and (5) carbonation.

As with lime and portland cement, the immediate reactions that influence plasticity reduction and reduction in swell potential, i.e., cation exchange, flocculation and agglomeration, occur due to available lime. Available lime is defined as CaO that is not combined with other compounds and is available or "free" to react with the soil. Of course, some fly ashes have little or no CaO, type F, while others, type C ashes, contain an appreciable level of CaO, from 10 to 30 percent by weight. However, the vast majority of this CaO is combined with silicates and aluminates as in the case of portland cement. The combined CaO is not available for cation exchange and pezzolanic reaction except for a relatively short period of time during hydration of calcium silicates and calcium aluminates.

Type C fly ashes can be very reactive when moisture is added and a vigorous cementitious reaction can result. However, most ashes require the addition of an activator such as lime or portland cement to trigger the reaction of the fly ash. These activators react pozzolanically with the silicates and aluminates in the fly ash.

In order to successfully function as a pozzolan, fly ash should meet certain physical and chemical requirements summarized in Table 2.6. The chemical requirements of a minimum of 70 percent $\text{SiO}_2 + \text{Al}_2\text{O}_3 + \text{Fe}_2\text{O}_3$ for type F ash and a minimum of 50 percent for type C ash are based on the need for a plentiful supply of silicates and aluminates to develop a significant pozzolanic reaction with the activator.

Material Characteristics Due to Stabilization

Fly ash and lime fly ash stabilized soils develop the same type of improvement as discussed under the sections on lime and portland cement stabilization. These improvements include physical property changes of the soil, such as reduction in plasticity and reduction in swell potential. However, the main purpose of fly ash stabilization is to improve the shear strength and the resilient modulus or stiffness of the stabilized soil layer.

Soils suitable for fly ash stabilization include coarse-grained soils and fine-grained soils. However, when plastic clays are encountered, it is often necessary to add additional lime to reduce plasticity prior to fly ash mixing. The ability of the fly ash alone to react with the soil to reduce plasticity is dependent on the amount and reactivity of the CaO contained in the fly ash. Type F fly ashes without CaO should not be considered alone as a stabilizer of plastic or clayey soils.

For a more complete discussion on suitable soils for stabilization with fly ash, the reader should consult the "Flexible Pavement Manual," published by the American Coal Ash Association (1990) and Little et al. (1987).

The levels of shear strength and stiffness achieved by fly ash stabilization or stabilization with fly ash plus an activator can be considerable and can approach or equal those obtained due to stabilization with portland cement. Little and Alam (1984) used deflection data to evaluate in situ stiffnesses of fly ash and lime and fly ash stabilized pavement layers in 10 test sites throughout the State of Texas. As expected, the study demonstrated that a wide range of stiffnesses can be encountered, depending on the soil being stabilized and the percentages and combinations of each additive used. The study also demonstrated that the stiffnesses can be very high — well over 7,000 Mpa. Little and Alam (1984) determined that in 8 of the 10 sites evaluated, the use of lime as an activator considerably improved the reactivity of the fly ash as reflected by a higher back-calculated resilient modulus.

Table 2.6. Recommended Physical and Chemical Requirements* for Fly Ash for Use in Pozzolanic Stabilized Mixtures (PSMs) (After Flexible Pavement Manual, 1990).

A. Physical Requirements		
	Class of Fly Ash	
	F	C
Fineness — (amount retained on No. 325 sieve prior to dampening)	34% max	34% max
Strength index with portland cement — (percent of control at 28 days)	75% min	75% min
Strength index with lime — (compressive strength at 7 days)	5,600 KPa	--
B. Chemical Requirements		
	Class of Fly Ash	
	F	C
$\text{SiO}_2 + \text{Al}_2\text{O}_3 + \text{Fe}_2\text{O}_3$	70% min	50% min
SO_3	5% max	5% max
Loss on Ignition (LOI)	10% max	6% max

* The requirements of industry specifications ASTM C593 and ASTM C 618 have been applied in Table 2.6 to coal fly ash for PSM base layers for flexible pavement systems; however, sources of fly ash meeting various local standards for physical and chemical characteristics and related uniformity requirements have been used with highly satisfactory results. The physical and chemical characteristics shown in Table 2.6 can be determined for a given source of fly ash using standardized test methods which are found in ASTM C 311. Fly ash not conforming to the requirements of Table 2.6 may be proposed for use in a PSM, and such proposals should be supported by laboratory trials and/or field performance data demonstrating the suitability of PSMs containing the non-conforming fly ash.

Influence of Material Improvements on Pavement Performance

As previously discussed under the sections dealing with lime and portland cement stabilization, the shear strength enhancing and stiffening effect added to the pavement layer by means of fly ash or fly ash plus activator stabilization can be substantial. In summary, the stabilization of a pavement layer with fly ash or with fly ash plus an activator may influence pavement performance in the following ways:

1. Reduce the potential of the stabilized layer to deform under heavy loads (high shear stresses) by increasing the shear strength of the stabilized layer. This, of course, requires that proper mixture design be used to optimize the shear strength achieved for the soil and fly ash mixture.
2. Protect the layers underlying the fly ash stabilized layer from being overstressed by increasing the stiffness of the layer through stabilization with fly ash or with fly ash and activator. The increased stiffness or increased resilient modulus allows the stabilized layer to more efficiently spread the wheel induced loads and, hence, more effectively protect the underlying layers.
3. Provide better support of the surface hot mix asphalt concrete layer and, hence, reduce flexural stresses and shearing stresses within that layer. The net result of this effect is to reduce the potential for rutting, shoving or other forms of surface deformation.

Recommended Structural Performance Algorithms

Pozzolatically stabilized materials (PSMs) are expected to achieve very high stiffnesses with full curing. The American Coal Ash Association (1990) refers to the development of elastic moduli in excess of 14,000 MPa with full curing.

With elastic moduli of this level the PSM base behaves as a slab. The American Coal Ash Association (1990) states that plate-load tests have clearly shown a fully-cured PSM base layer behaves as a slab and its ultimate load-carrying capacity, under a single static load is greater by a significant amount than predicted by elastic slab theory.

PSM layers have also been shown to exhibit autogenous healing (Little et al., 1987) because of the effect of long-term pozzolanic reactions, which may continue for several years if the

temperature remains above 4°C.

Because of the high stiffnesses achieved by PSM layers, it is necessary to consider the slab effect of these layers in pavement design and pavement performance prediction. Also, because of the stiffness of the PSM layer and the slab effect, faulting of transverse pavement cracks may occur under extremely heavy traffic volumes. Sawed and sealed joints tend to moderate the faulting phenomenon (American Coal Ash Association, 1990).

The American Coal Ash Association (1990) recommends that the thickness of a PSM base layer for a flexible pavement system can be determined by one of three methods:

1. Method A — AASHTO flexible pavement design procedures, using structural layer coefficients,
2. Method B — Mechanistic pavement design procedures, using resilient modulus values for the pavement layers, and
3. Method C — A combination of Method A and Method B, using mechanistic design concepts for determining pavement layer coefficients.

The following paragraphs discuss the basic philosophies of these three design approaches. The detailed design approaches can be found on pages 23 through 41 of the American Coal Ash Association's Flexible Pavement Manual (1990).

In Method A, the AASHTO performance equation is used to predict pavement serviceability. The widely used and well established AASHTO performance equation as set forth in the 1986 design guide uses the structural number to account for the structural contribution of the pavement layers. The structural number is defined as:

$$SN = a_1D_1 + a_2D_2m_2 + a_3D_3m_3$$

where D represents the layer thicknesses, a_i represents the structural layer coefficients of the various layers, and m_i represents the drainage coefficients for the base and subbase layers. For a PSM base the drainage coefficient is 1.0.

According to the Flexible Pavement Manual (1990), the main factors influencing the variation in the structural layer coefficient are the unconfined compressive strength and the elastic modulus

of the layer. The field design strength, determined after 56 days of moist curing at 23°C (or other curing conditions required by individual agencies), is the compressive strength value used to determine the structural layer coefficient for PSMs.

According to the AASHTO design guide, a relationship exists between the modulus of elasticity (E_{psm}), the field design compressive strength (CS) and the structural layer coefficient. The relationship between E_{psm} and CS can be defined as:

$$E_{psm} = 500 + CS$$

where E_{psm} is in ksi and CS is in psi. The normal range of a_2 in the AASHTO design guide for PSM layers is from 0.20 to 0.28 with the 0.20 value being assigned to mixtures with a minimum compressive strength of 2,800 KPa.

In the mechanistic design approach (Method B), the required thickness of the PSM is based on the potential of the mixture to fatigue or fatigue consumption. Fatigue consumption is related to the number of load applications and the stress ratio, SR, which is calculated for the PSM layer as:

$$SR = (\text{PSM Design Flexural Stress})/(\text{PSM Flexural Strength}).$$

Figure 2.8 shows permissible SR values for various design reliabilities and traffic conditions (in terms of equivalent 80 KN axle loads, ESALs).

For a given wheel load, PSM strength and pavement thickness are the primary factors that control the PSM design flexural stress. The pavement thickness factor is quantified by the equivalent thickness, T_{EQ} , which is defined as:

$$T_{EQ} = 0.5T_{AC} + T_{PSM}$$

where T_{AC} is the asphalt wearing course thickness in inches and T_{PSM} is the thickness of the PSM base layer in inches.

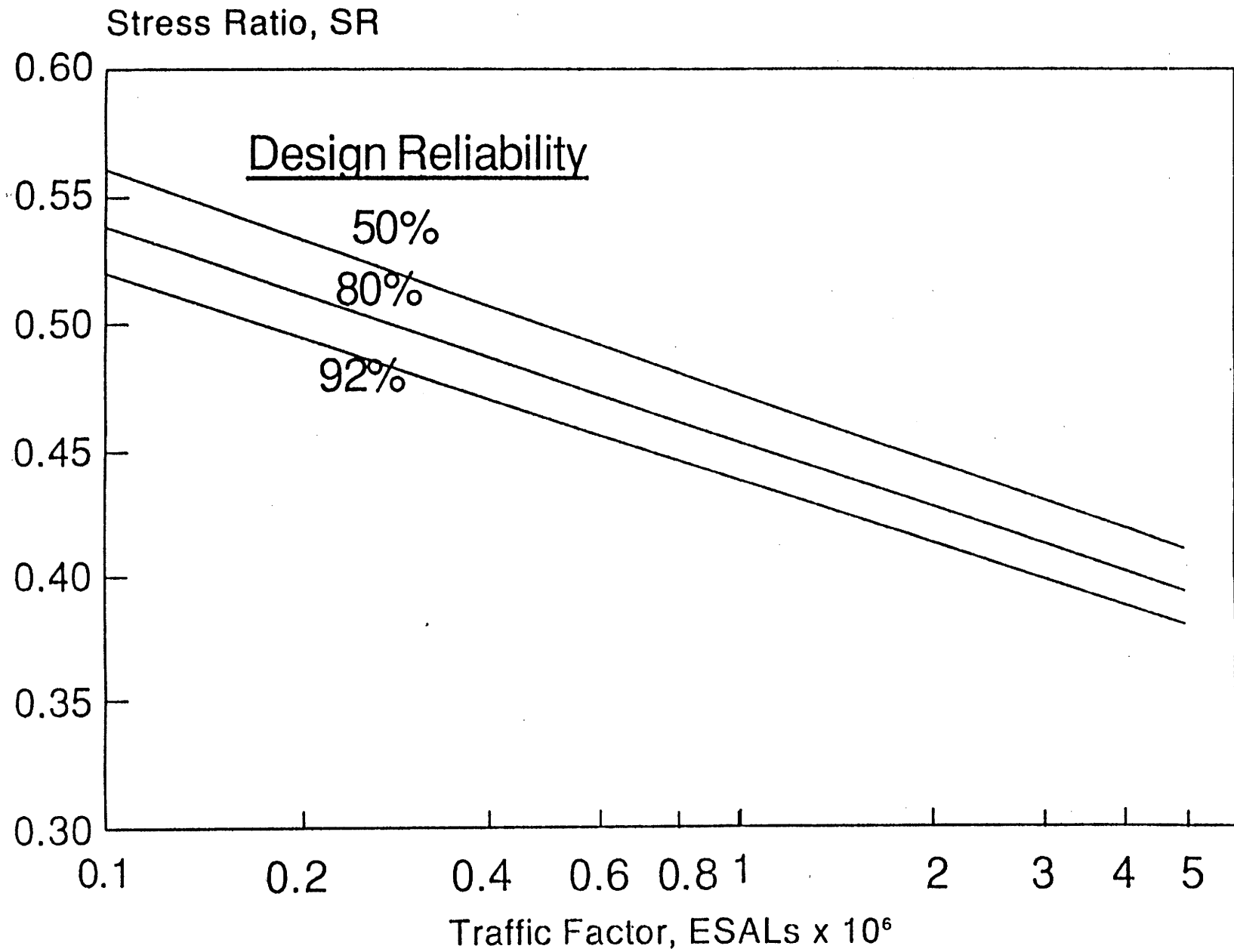


Figure 2.8. Typical Relationship of Stress Ratio to Traffic Conditions (ESALs - 18 kip Equivalent Single Axle Loads) (After Flexible Pavement Manual, 1990).

The Flexible Pavement Manual (1990) uses the relationship graphically presented in Figure 2.9 to determine the required T_{EQ} for routine pavement design. The use of Figure 2.9 requires values for the design SR and the "field design compressive strength" (CS). The maximum design SR that should be used is 0.65. The compressive strength which should be used is the compressive strength (CS) for curing conditions of 56 days at 23°C and 100 percent relative humidity.

Table 2.7 of the Flexible Pavement Manual (1990) presents recommended minimum asphalt concrete surface layer thicknesses, and the minimum PSM layer thickness is recommended to be 152 mm.

The AASHTO thickness design of flexible pavements using mechanistic concepts is the third method (Method C) presented in the Flexible Pavement Manual (1990).

In this method the required structural number (SN) is determined as in the normal AASHTO method. However, in this procedure the structural layer coefficient of the PSM base layer relates not only to the unconfined compressive strength of the layer but also to the base-layer thickness illustrated in Table 2.7.

For more details on Methods A, B or C, consult the Flexible Pavement Manual (1990).

Mix Design Considerations

The American Coal Ash Manual (1990) presents in detail the mixture design considerations required to produce PSMs. This comprehensive mixture design approach is suggested for use. The method assigns a fly ash content based on the amount required to achieve satisfactory density within the aggregate-fly ash mixture and then assures that the appropriate percentage of activator, if required, is added to produce pozzolanic strength to the required level.

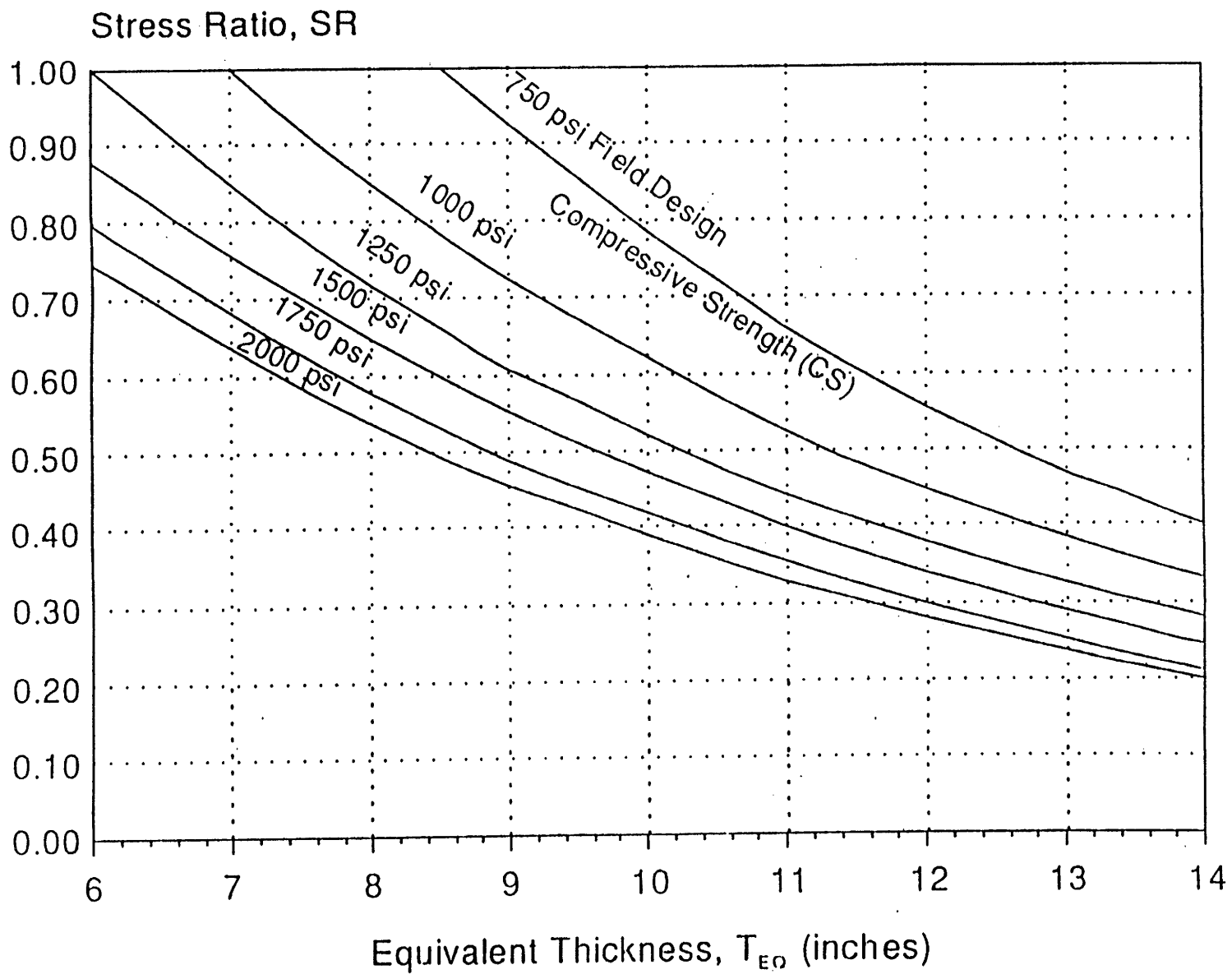


Figure 2.9. Typical PSM Thickness Design Chart (1 in = 25.4 mm, 1 psi = 6,894 Pa).

Table 2.7. Suggested AASHTO Structural Layer Coefficient (a_2) for PSM Base Layers (After Flexible Pavement Manual, 1990).

Field Design Compressive Strength (CS), KPa	Coefficient a_2 for PSM Base Layers				
	PSM Base Layer Thickness, mm				
	152	203	254	305	356
5,250	0.20	0.20	0.20	0.30	0.40
7,000	0.20	0.20	0.30	0.40	0.40
8,750	0.20	0.26	0.38	0.40	0.40
10,500	0.20	0.37	0.40	0.40	0.40
14,000	.30	.40	0.40	0.40	0.40

2.4 CONCLUSIONS

The literature provides the type of information necessary to formulate a design strategy for pavements, including stabilized layers. Two basic approaches are available for design and selection of appropriate pavement sections incorporating stabilized layers: (1) thickness design based on reliable measurements of strength or engineering properties of the various layers and specific conditions of climate and traffic with realistic engineering properties of the various layers; and (2) selection of the appropriate engineering properties that a stabilized layer must possess in order to function successfully in a specific environment (specific, climate, traffic condition and structural cross section).

Although this study addresses both of the approaches listed above, the latter is the focus of this effort. This study identifies the engineering properties of stabilized pavement layers that are necessary for the pavement to function properly. The approach is to identify the traffic, native subgrade, climatic and pavement structural cross-section to be employed and then to recommend the appropriate engineering properties of the stabilized layers necessary for the stabilized layer to function within the specific pavement system identified.

Pertinent modes of distress are considered: deep layer and surface deformation, fatigue cracking, thermal cracking and reflection cracking. Based on the consideration of these distress conditions, recommendations are made for the following structural layer properties:

1. Minimum resilient modulus and/or acceptable range of resilient moduli of the stabilized layer;
2. Minimum compressive strength and/or acceptable range of compressive strength of the stabilized layer; and
3. Minimum compressive strength of the stabilized layer to provide acceptable durability or resistance to moisture-induced damage.

Structural Role of Lime Stabilized Subgrades

The contribution of lime stabilization of the subgrade to the performance of the flexible pavement system is comprised of three components:

1. Reduction of the swell potential of the stabilized layer and concomitant improvement in textural and physical properties of this layer, which affect constructability;
2. A significant shear strength increase within the stabilized layer resulting in resistance of the layer to being overstressed; and
3. A significant stiffening of the stabilized layer resulting in
 - a. Protection of the underlying sublayers from being overstressed,
 - b. Better support of the flexible base course which may exist on top of the lime stabilized subgrade, resulting in an improved resilient modulus response of the flexible base due to a more favorable stress condition within the flexible base, and
 - c. Better support of the hot mix asphalt concrete surface, resulting in the reduction of flexural tensile stresses, which may lead to fatigue cracking, and shear stresses, which may lead to surface distortion, within the hot mix asphalt concrete surface layer.

Evaluation of the Structural Role of the Lime Stabilized Subgrade

The pavement performance algorithms suggested to model the lime stabilized layers address the contributions discussed in the preceding section. Probably the best way to insure that the stresses induced within the lime stabilized subgrade do not result in distortion of the layer is to insure that the compressive deviatoric stress induced within the lime stabilized layer is less than one-half of the unconfined compressive strength of the mixture, or that the compressive strain induced within the lime stabilized layer is less than one-half of the strain at failure in the unconfined compressive strength test (which is normally about 1 percent strain).

Induced strains within the lime stabilized layer kept at below one-half of the failure strain and induced deviatoric stresses that are kept below one-half of the unconfined compressive strength of the mixture remain, essentially, in the elastic region and do not result in permanent deformation. This is discussed by Holmquist and Little (1991) and by Zollinger (1990). At values above these levels, strain softening of the mixture or pavement layer begins to occur. Thus, a simple algorithm and either a layered elastic or finite element structural model could easily evaluate the potential of shear deformation based on this concept. This check should be made within the lime stabilized layer to evaluate distortion potential and within the underlying natural subgrade where a compressive strength and/or strain at failure could be assigned to the natural subgrade layer, depending on soil classification.

The level of the modulus developed within the lime stabilized layer is perhaps the most important contribution of the stabilized layer to the pavement system. The level of modulus developed in lime stabilized soils typically represents five to twenty-fold increase over the modulus of the native soil. In some cases it is lower, and in some cases it is substantially higher. Nevertheless, the modulus developed in the lime stabilized layer is generally substantially less than that produced in portland cement stabilized sands. In most cases the lime stabilized subgrade is probably not stiff enough to be concerned about designing for the "slab effect."

Since the ability of the lime stabilized layer to protect underlying layers and to support overlying layers is so heavily tied to the in situ modulus of the layer, emphasis was placed on field studies to identify the in situ moduli of these layers. In this investigation the effects of seasonal variation, soil type and mineralogy, and pavement structure were considered.

An important aspect of Study 1287 is in situ verification that higher stiffness subgrades

provide a superior resilient modulus response for flexible bases. In an effort to study this question, pavement sections were identified in which aggregate bases or flexible bases exist over both stabilized and unstabilized, or control, subgrades.

Structural Role of Lime Stabilized Bases

Lime stabilized bases consist of bases courses which use lime to upgrade properties of the base through pozzolanic reaction between the lime and the clay soil fraction or due to the development of and enhancement of carbonation as in limestone bases stabilized with low percentages of lime. Addition of the stabilizer has two important effects: improvement of the shear strength of the base layer and stiffening of the base or enhancement of the resilient modulus.

The measure of the performance of lime stabilized bases in a pavement system is most closely tied to the resilient modulus of the base layer. Since the structural layer coefficient of a flexible base is tied directly to the resilient modulus of the flexible base, it is logical that the structural coefficient of a lime stabilized base would be also. This is especially true since lime treatment of most bases typically does not stiffen the base to the point at which the layer acts as a rigid slab.

The resilient modulus of the stabilized base is the key to performance prediction. Therefore, the value of in situ stiffness of these layers must be determined with proper consideration given to the following variables: seasonal effects, layer thickness effects, base type and mineralogy, age of the base layer and traffic effects on the base layer.

In Study 1287, particular attention was placed on studies of limestone bases stabilized with low percentages of lime in the Corpus Christi and Yoakum Districts. This study evaluated the mechanism of stabilization and the level of stiffness and compressive strength that can be achieved in these layers through carbonation and pozzolanic reactions.

Structural Role of Portland Cement Stabilized Bases and Subgrades (Heavily-Stabilized Bases)

Since portland cement stabilized bases and subgrades often develop very high resilient moduli, the slab effect of these layers was evaluated. Most design and analysis philosophies call for a flexural fatigue analysis of the stabilized layer. This is discussed in some detail in Appendix A of Report 1287-1 (Little et al. 1993).

Recent studies by the South Africans and Australians (Jordaan 1992) and Caltabians and

Rawlings (1994) indicate that cement stabilized bases may fail in a different mode than flexural fatigue and that the modulus of the stabilized layers varies considerably with depth and is not nearly as high as generally considered in pavement design approaches.

Work in this study, especially in the Houston District, concentrated heavily on defining the mode of failure of stabilized subgrades and stabilized bases and in the determination of the composite moduli of the pavement layer and as a function of depth. The evaluation of performance of heavily-stabilized bases in the Houston District was based on an analysis of in situ modulus (stiffness), shrinkage (and reflection) cracking and load transfer across shrinkage and thermal cracks.

Structural Role of Fly Ash Stabilized Bases and Subgrades

The same general approach was taken to evaluate the performance of in situ fly ash stabilized bases as for portland cement stabilized bases. It is logical that the failure mechanism of fly ash stabilized bases and subgrades should be similar to portland cement stabilized bases. This is because the fly ash stabilized bases and subgrades tend to develop high strengths and slab action in a similar manner to the portland cement stabilized bases.

Field evaluations of the mode of failure and of in situ values of lime and fly ash stabilized subgrades and bases were performed in the Lufkin District.

Summary of Deliverables

Based on the literature survey and Task 1 research, the following were described necessary deliverables of this study.

Lime-Stabilized Subgrades

1. Appropriate range of resilient moduli and/or confined compressive strengths for acceptable performance for specific pavement types (i.e., specific structural cross sections, design traffic levels, climatic regions and native subgrade characteristics).
2. Recommended mixture design approach to help insure durability and permanency of reaction.

Lime-Stabilized Marginal Aggregates and Flexible Bases

The same items as required for lime-stabilized subgrades.

Portland Cement and Fly Ash Stabilized Bases

The same items required for the lime-stabilized layers will be required for portland cement and fly ash stabilized layers. However, in addition to recommendations for appropriate ranges in engineering properties, i.e., compressive strength and resilient modulus, the structural slab action of the stabilized layers was evaluated for susceptibility to deterioration based on flexural fatigue and to deterioration through other mechanisms.

CHAPTER 3

STABILIZED BASES

3.1 INTRODUCTION

The main study objective was to evaluate the field performance of stabilized base and subgrade layers in Texas pavements and to recommend how field strength and performance data can be incorporated into mix design and pavement design practices. This chapter presents field test results obtained from both heavily and moderately stabilized base sections. Chapter four presents laboratory and field results on bases modified with very low stabilizer contents. Chapter five presents the results from the field evaluation of stabilized subgrades.

A major objective of this project was to measure, with a Falling Weight Deflectometer (FWD), the insitu stiffness of stabilized bases so that this information could be used to improve the existing TxDOT thickness design procedures. Issues addressed included: 1) how does the strength of the layer vary with time and season? 2) what moduli values are appropriate for lightly and heavily stabilized materials? and 3) what level of stabilization gives the best overall long term pavement performance? All of these issues cannot be addressed in a single study given the diversity of materials, climates, and traffic level found in Texas. However Study 1287 should provide a significant data base for each of these areas and provide a foundation for further stabilization studies within TxDOT.

In Texas there are at least three philosophies concerning base stabilization. The first involves adding a low level of stabilizer, usually lime at around 1 to 3 percent, in an attempt to "kill" the plasticity of the binder (minus 40 sieve-size) fraction material. At this low stabilized content, no substantial long-term strength gain is anticipated. However, it is thought that the material may have improved performance characteristics primarily due to a reduced sensitivity to moisture fluctuation. Furthermore, with some aggregates, the addition of a small amount of stabilizer has been reported to yield noticeable strength gains. The Corpus Christi and Yoakum Districts are active in this area of stabilization. Chapter 4 discusses low level stabilization in calcareous aggregates from the Corpus Christi and Yoakum Districts.

The second philosophy, or rationale for stabilization, is to lightly or moderately stabilize the base. Here, the purpose is to improve the strength of a marginal material in an attempt to obtain

strength values similar to those obtained from Class 1 Texas Triaxial material. The lightly stabilized material will, hopefully, perform similar to a top quality flexible base but yet not become rigidly cemented and not exhibit significant thermal or shrinkage cracks. Typically, portland cement, lime or lime/fly ash combinations are used in relatively low percentages (2 to 3 percent to achieve this end). Lime or lime/fly ash stabilizers are more frequently used especially in the stabilization of bases with a significant clay content and where a slower reacting stabilizer is needed. This approach is frequently used in pavement rehabilitation where the existing base is still in reasonable condition but needs strengthening to carry the increased traffic loads. This material is classified as Item (262) in the Texas Standard Specification, 1993.

The third approach is heavy stabilization of bases in which substantial levels of stabilizer are added to produce a material approaching the strength of a low-strength concrete. This approach is frequently used for new construction in areas of poor subgrade, heavy rainfall and heavy traffic. In these instances the districts often feel that the traditional flexible bases do not perform adequately. This approach is also applied in areas of poor aggregates where haul distances are large, and where the highway carries substantial truck traffic. This is Item (276) in the Texas Standard Specifications, 1993. The stabilizer used is most often portland cement and the stabilizer content is determined either from a recipe (most often between 5 and 8 percent) or from unconfined compression tests where the required 7-day strength usually exceeds 4,550 KPa.

In this chapter, the results from monitor sites containing lightly and heavily stabilized bases are presented. In establishing monitor sites for this study, three districts were visited.

1. The Houston District, which for the past 8 to 10 years has extensively used heavily stabilized bases, typically using between 5 and 8 percent of cement.
2. The Atlanta District, which uses a combination of lime and lime/fly ash stabilizers and both lightly and heavily stabilized pavement sections.
3. The Bryan District, which has a few sections of cement stabilized bases but has recently begun a base upgrade program involving low levels of stabilizer, mixed in place, for its low volume Farm-to-Market system.

3.2 FIELD TEST PROCEDURE

Prior to visiting each district, the district nominated sections for inclusion in the study. Criteria for selection included age, traffic level, type and percentage of stabilizer. It was hoped to establish between 6 and 10 typical sections in each district. Once a final list was prepared, each selected section was monitored according to the following steps:

- 1) Select monitor site,
- 2) Map cracks,
- 3) Collect as-built data, traffic information, lab data (if available),
- 4) Measure deflections using Falling Weight Deflectometer (FWD),
- 5) Test using Dynamic Cone Penetrometer (DCP) testing (where possible), and
- 6) Core and test heavily stabilized materials in the lab.

Site Selection

Each pavement section was typically 3.2 to 16 km in length. From this section a 150 m monitor site was selected for testing. The entire section was driven, and the monitor site was chosen to provide a representative condition with regard to surface cracking and overall section geometrics. Once the monitor site was selected it was identified with paint marks at 30 m intervals on the shoulder. Figure 3.1 shows a typical site.

Crack Mapping

The prevalent distress in each section was surface cracking in the form of transverse (shrinkage) cracking and longitudinal cracking. The level of surface cracking varied widely from site to site. A few test sections had no visible cracking and a few showed a significant amount of severe cracking. Most exhibited moderate cracking. The first step in the evaluation was to sketch a crack map showing location and width of cracks. This was to be used in later evaluations where changes in crack severity levels could be computed. Measuring of crack widths was performed using feeler gauges. However, this is not a simple task, and it is not easy to interpret. For example, the crack width is measured at the surface of the pavement not in the base; however, it is reasonable to assume that wide cracks measured at the surface were caused by wide cracks in the base. Also, the crack

width varies as the crack meanders across the pavement. Typically the observed crack will be narrower in the wheel path than between the wheel paths.



Figure 3.1. Typical Monitor Site on FM-526, Houston, Section 1.

Figure 3.2 shows a typical crack map generated from this study. To summarize this information, the total lengths of slight, moderate and severe cracking were calculated for each section and for each visit. For the purposes of this study, all hairline cracks were classified as slight. With these cracks, it was impossible to insert the feeler gauge to make a width measurement. All cracks greater than 2.5 mm were classified as severe. Cracks in between the two extremes were classified as moderate. No other surface distresses were found on these sections, and the riding quality was high.

FWD Testing

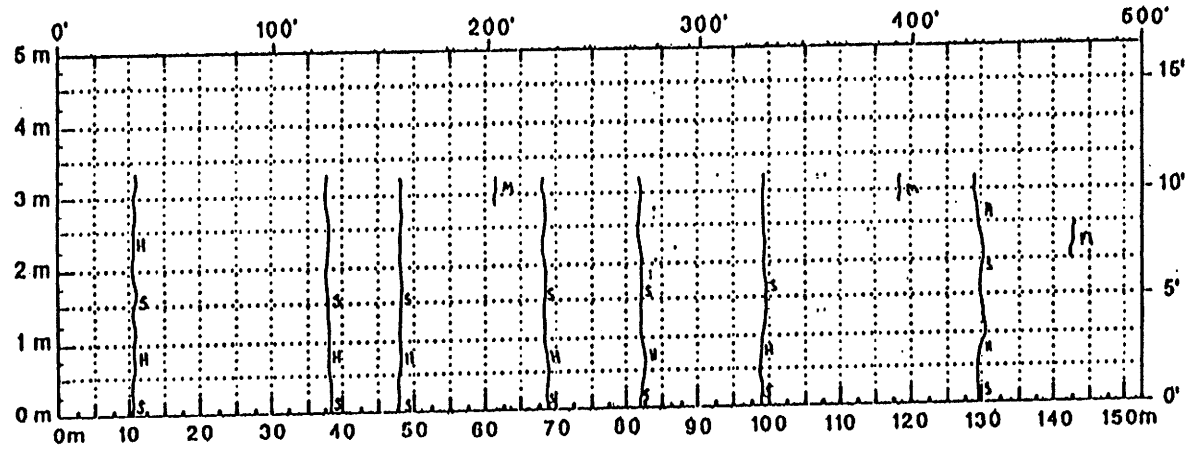
The principal method of determining layer moduli (a measure of in situ strength and load distribution potential) was the Falling Weight Deflectometer. Two sequences of FWD tests were

performed on each section. In the first, the FWD load plate was located on an intact (uncracked) area of the pavement, removed from any transverse cracks. These test results were used to determine an uncracked stiffness. In the second, the load plate was placed next to a transverse crack so that geophone 1 was on one side of the crack, and geophone 2 was on the other side. This approach was used to measure the load transfer across the crack and to determine the "cracked" strength (in terms of a resilient modulus response) of the section.

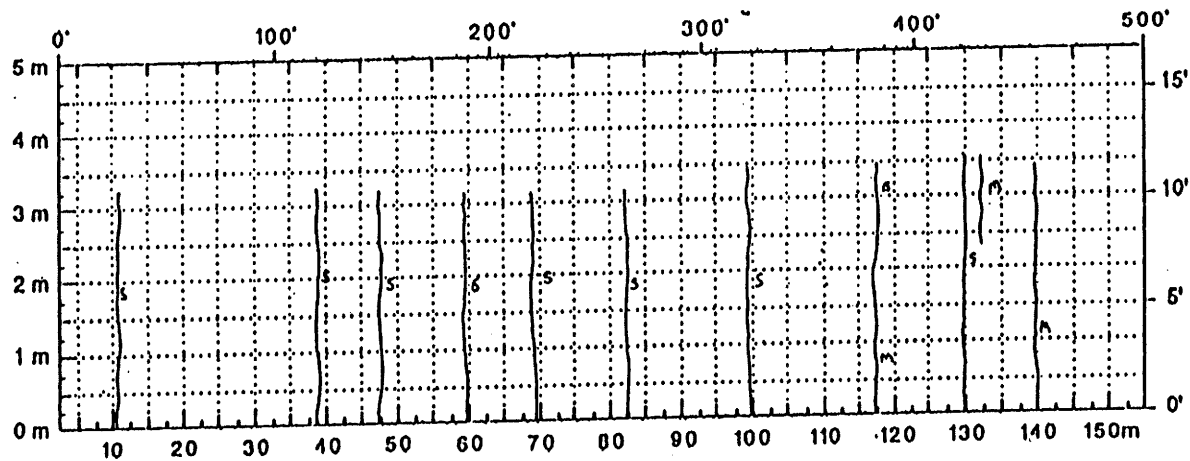
In all instances, the 7 FWD geophones were separated by a 300 mm spacing. Four different load levels were used, and the temperature of the asphalt was measured during testing. This temperature was recorded at a depth of approximately 25 mm below the surface. In a typical section, 8 to 10 locations were tested for both "cracked and uncracked" stiffness determination. In processing the data, the load transfer efficiency was simply calculated as geophone 2 deflection divided by geophone 1 deflection. To obtain layer moduli, the MODULUS 4.2 backcalculation program was used. In most cases, the thickness of the asphalt surfacing was thin, less than 76 mm. In these cases the modulus of the asphalt layer was kept as a constant during the backcalculation procedure. The backcalculation therefore focused on obtaining an in situ modulus for the stabilized base, subbase, and subgrade.

The deflections measured close to the existing cracks in the pavement were also used in a more sophisticated analysis described later in this chapter. The aim of this work was to evaluate the impact of the crack on the calculated stresses and strains induced by the wheel load at the bottom of the stabilized base. A finite element computer program ILLISLAB (Tabatabaie, 1977) was used to compute stresses and strains in the stabilized base. This analysis was performed to provide input to a thickness design procedure for heavily stabilized base layers. Thompson (1994) recommended this procedure, and it is based on the assumption that transverse thermal and shrinkage cracks are inevitable in heavily stabilized materials and that the pavement should be strong enough to prevent the formation of fatigue cracking in the wheel paths, which initiates at these transverse cracks. Chapter 6 will describe this work.

District Houston (Section 1)
 County Harris
 Highway FM 526



Comments: Crack Map for Summer 1993



Comments: Crack Map for Winter 1994

Figure 3.2. Typical Crack Map of 160 m Long Test Section.

Dynamic Cone Penetrometer Testing

The DCP, shown in Figure 3.3, was developed in South Africa in the 1960's by Van Vuuren (1969) and was used extensively by Kleyn et al. (1975). It has since gained considerable popularity worldwide with pavement engineers. The US Army Corps of Engineers (Webster et. al., 1992) have recommended the DCP as a replacement for the field CBR test. The test consists of driving a penetration cone through the pavement layers using a known weight dropped through a fixed (constant) height and thereby maintaining constant energy for each blow (drop of the weight). The basic philosophy is that stiffer (stronger) layers offer more resistance to cone penetration, so the average penetration per blow will be lower than for softer layers. The rate of penetration of the cone has been correlated with the California Bearing Ratio (CBR), and several researchers have attempted to correlate it with the ultimate shear strength of the layer material. However, frictional forces tend to complicate the calculation. The DCP is, however, an excellent tool for routine pavement evaluation and is the only test available that measures both layer thickness as well as relative layer strength. The DCP also is excellent at complementing FWD data collected from a test section. In instances where the engineer doing the backcalculation may not know the actual thicknesses or whether a stabilized subbase is present or not, the DCP can supply this information and provide more credibility for the backcalculated layer moduli.

Figure 3.4 shows a schematic of the number of blows versus depth of penetration. The slope of the line is used to estimate the layer CBR, and the intercept of the upper and lower layer slopes provides a measure of the layer thickness.

In this project, the DCP was used to test all lightly stabilized bases and subgrades. In the case of a heavily stabilized base, a 25 mm access hole was drilled through the CTB to permit testing of the subbase and subgrade. In all instances, the rate of penetration in mm/blow was converted into a CBR value using the correlation developed by Webster et al. (1992). Texas Class I bases have been determined through in situ testing to have a CBR of 85 or above. Very poor bases have a CBR of below 30.

Coring and Laboratory Testing

In the heavily stabilized bases, standard 101 mm cores were taken and returned to the laboratory for resilient modulus and unconfined compressive strength determination. In one instance, on SH

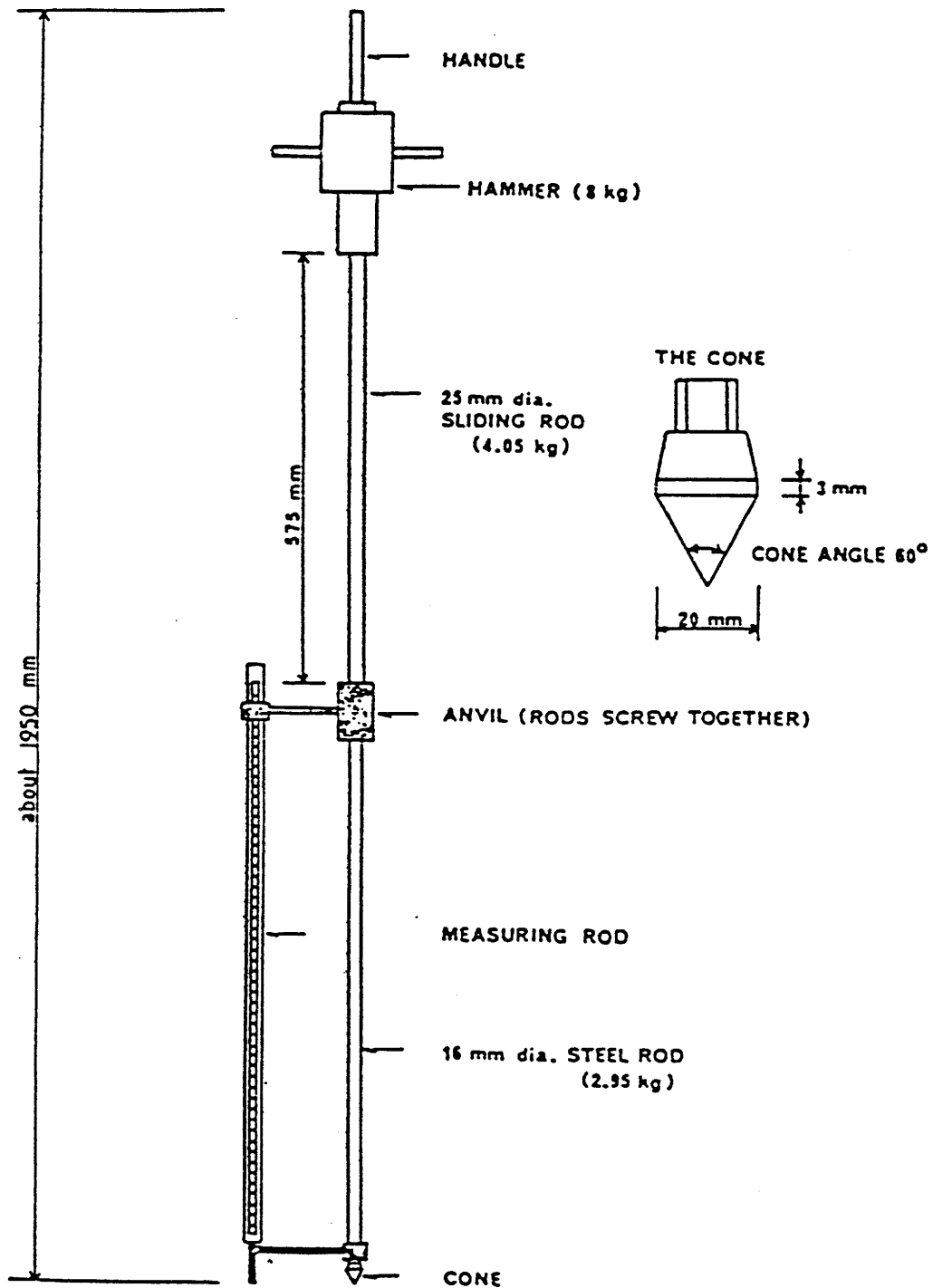


Figure 3.3. Schematic of the Dynamic Cone Penetrometer.

36 in Houston, specialized testing was performed in an attempt to identify the cause of premature pavement deterioration, which will be described later in this section.

3.3 RESULTS FROM THE HOUSTON DISTRICT

The Houston District currently incorporates portland cement stabilized bases in flexible pavement structures. A typical pavement structure consists of 150 mm of cement stabilized subbase (select material), 250 to 400 mm of good quality base material stabilized with 6 percent cement and a 75 to 100 mm asphalt surfacing. In total, 7 monitor sites were established in Houston. Details of the site data including the location of test section, the measured performance in terms of surface cracking, thicknesses and the type of materials used in layers of the pavement, summaries of the processed data collected from FWD and DCP tests and results of the laboratory testing are shown in Appendix A. In this section some of these collected data are graphically displayed.

Table 3.1 summarizes information about the pavement sections and includes a description of the layers and their thicknesses, type of aggregate in the stabilized base, type and amount of stabilizer and the age of the pavement. Table 3.2 presents a summary of the average back calculated moduli together with layer thicknesses. Table 3.3 shows a summary of the estimates of the moduli of the stabilized layers based on the FWD and Lab test results. Table 3.4 summarizes data from the more severe cracks evaluations and the Load Transfer Efficiency (LTE) across these cracks.

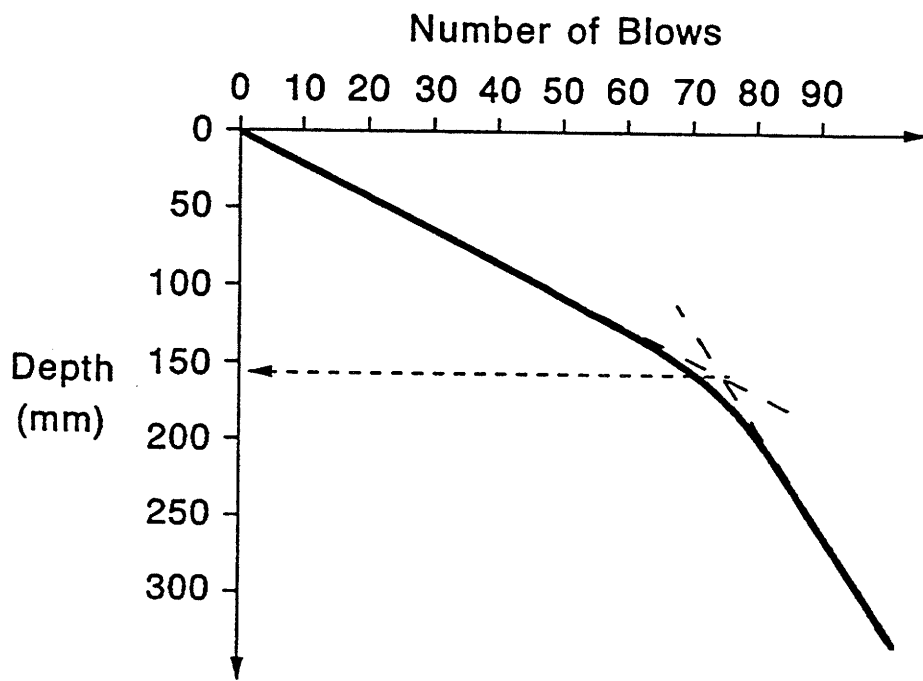


Figure 3.4. Schematic Diagram of the Number of Blows vs. Depth of Penetration with Depth.

Table 3.1. Details of the Pavement Sections Investigated.

Pavement Section	Description	Aggregate type	Type and Percent stabilizer	Age, years
1	75 mm HMAC 350 mm CTB 150 mm LTS	LS	C = 6	7
2	75 mm HMAC 225 mm LTB 175 mm LTS	REB	L < 4	7
3	75 mm HMAC 350 mm CTB 150 mm LTS	LS	C = 6	3
4	100 mm HMAC 275 mm CTB 150 mm LTS	REB	C = 6	3
5	75 mm HMAC 300 mm CTB 150 mm LTS	RG	C = 6	7
6	75 mm HMAC 300 mm CTB 150 mm LTS	LS	C = 6	4
7	75 mm HMAC 350 mm CTB 150 mm LTS	OS	C = 6	15*

* Recent Overlay (5 years old)

C = Cement

L = Lime

LS = Limestone

REB = Recycled Existing Base

RG = River Gravel

OS = Oyster shell

Table 3.2. Summary of the Average Backcalculated Moduli (Houston District).

SITE #	Layer	Moduli Range, MPa	Layer Moduli, MPa			
			Summer		Winter	
			Uncracked	Cracked	Uncracked	Cracked
1	Asphalt-76 mm	2411 / 4437	2411	2411	4437	4437
	CTB-356 mm	3445 - 34450	34450	16519	33084	7781
	LTS-152 mm	206 - 4134	2417	3546	1288	4001
	Subgrade	172	184	241	209	276
2	Asphalt-76 mm	1426 / 5670	1426	1426	5670	5670
	LTB-229 mm	206 - 6890	1574	502	3420	1012
	LTS-178 mm	35 - 2067	77	58	414	76
	Subgrade	69	92	71	108	91
3	Asphalt-76 mm	2239 / 2756	2239	2239	2756	2756
	CTB-356 mm	3445 - 34450	18653	7384	14648	4413
	LTS-152 mm	206 - 4134	1724	2314	2360	3165
	Subgrade	207	231	249	236	273
4	Asphalt-102 mm	1281 / 3190	1281	1281	3190	3190
	CTB-279 mm	3445 - 34450	31341	17873	20908	4040
	LTS-152 mm	206 - 4134	675	283	495	2106
	Subgrade	172	300	313	347	339
5	Asphalt-76 mm	4079 / 3445	4079	4079	3445	3445
	CTB-305 mm	3445 - 34450	23745	9869	26544	3445
	LTS-152 mm	206 - 4134	1193	449	1440	2671
	Subgrade	138	165	172	160	212
6	Asphalt-76 mm	1426 / 2935	1426	1426	2935	2935
	CTB-305 mm	3445 - 34450	32605	12961	28134	4443
	LTS-152 mm	206 - 4134	1768	2186	2257	1923
	Subgrade	138	133	143	145	187
7	Asphalt- 89 mm	1467	1467	N/A	N/A	N/A
	CTB-406 mm	3445 - 34450	5209			
	LTS-152 mm	206 - 4134	1475			
	Subgrade	138	220			

N/A Not Available

HMAC = Hot Mixed Asphalt Concrete Layer

CTB = Cement Treated (Stabilized) Base

LTB = Lime Treated (Stabilized) Base

LTS = Lime Treated Subgrade

Table 3.3. Summary of FWD and Lab Test Results.

Section #	Modulus of Uncracked Base, GPa			UCS of Cores, MPa
	Back-Calculated form FWD		From Lab Testing	
	Summer	Winter		
1	34.45	33.08	14.48	16.06
2	1.57	3.42	2.54	9.67
3	18.65	14.65	8.86	23.33
4	31.34	20.91	8.78	8.33
5	23.74	26.54	21.90	17.43
6	32.60	28.13	26.14	13.75
7	5.21	-	2.82	11.69

Table 3.4. Summary of LTE and Crack Length (Severe Type).

Section #	LTE, Percent						Crack length@, meters	
	Summer			Winter			Summer	Winter
	Min	Max	Avg	Min	Max	Avg		
1	47.9	94.1	73.5	35.5	70.2	56.8	16.5	22.9
2	-	-	-	81.1	81.1	81.1	-	1.5
3	67.5	95.9	80.3	53.0	88.6	76.9	15	18.9
4	73.7	91.5	87.0	66.4	88.3	75.4	5.8	15.5
5	68.7	97.6	89.6	48.8	77.5	64.2	76.3	77.0
6	63.2	91.6	83.3	36.9	90.7	60.1	30.5	30.5
7	-	-	-	-	-	-	-	-

@ Length of severe type cracks (crack width > 2.5 mm) in 150 meter long section

From the results presented in Tables 3.1 and 3.2 the following conclusions are drawn

1. The base and subbase moduli are extremely high for all the cement stabilized sections. The unconfined compressive strength of base layers in all of these sections far exceeded the required minimum 7-day Unconfined Compressive strength requirement of 4,550 KPa.
2. The best performing base in terms of surface cracking is the oyster shell base used in section 7. After over 15 years of service, the surface remains uncracked. The resurfacing applied in 1990 was for skid resistance purposes. One of the worst performers is the river gravel section (No. 5), which contained over 100 m of severe transverse and longitudinal cracking. The spacing between cracks was short, less than 6.71 m.
3. The difference in cracking performance is clearly a function of the aggregate used. The total length of the severe type cracks, the average spacing and width of the crack openings are important factors in pavement performance. For a given stabilized material, we generally prefer a section with closely spaced cracks (so that the crack opening will be reduced). However, Section 5 should not be considered to be a better performer since it has wide crack openings for such small crack spacings. The greater the total length of severe type cracks, the higher is the potential for damage to the pavement due to moisture infiltration. Similarly, water can seep through wider crack openings more easily than a tight held hairline crack.
4. The crack spacings on the Limestone sections (Nos. 1, 3 and 6) were fairly wide, 10 to 15 m. The wide crack spacings resulted in wider cracks with lower load transfer, particularly in the winter months. For example, on section 1 the crack spacing was approximately 15 m with an average load transfer was about 50 percent.
5. The low cost lightly lime stabilized base (section No. 2) deflects substantially more than the cement stabilized sections. Its initial cracking performance was good. However, some random cracking was monitored in the second inspection, but because the cracks are small, good load transfer was maintained.
6. The overall performance of the sections monitored is debatable. All of the sections had excellent riding quality, in the range 4.0 to 4.5. The major concern was the deterioration of the surface through cracking. As the crack maps show (Appendix B), the sections

continue to crack, and the crack widths are wide (> 2.5 mm). It was felt that these cracks should be sealed to prevent moisture from entering the structure. The district was considering sections 1, 2 and 5 for inclusion in the resurfacing program because of the extent and severity of the surface cracking. The sections were only 7 years old.

Figures 3.5 through 3.9 show observed relationships or trends between crack spacing, crack opening width, base modulus and average load transfer efficiency across the crack. These data demonstrate a general, logical and significant trend. This trend is that as the base becomes more rigidly cemented (e.g., modulus increases and strength increases) the average crack opening becomes larger and the road transfer efficiency across the cracks is significantly diminished. Chapter 6 will discuss these data which form the basis for a structural design approach for heavily cemented bases.

The Houston District changed from using unstabilized flexible base courses in the 1970's to stabilized bases because of the relatively poor performance of flexible bases. However, the life to first overlay of the heavily stabilized sections was not significantly improved over the flexible base section. Based on these findings, it is proposed that the district consider variations in either mix design and/or pavement design procedures. Use of 6 percent cement produces very strong and very stiff bases, which are prone to crack. Reducing the amount of stabilizer may lead to adequate strength and stiffness but with less cracking. Instead of widely spaced shrinkage cracks with wide openings that rapidly propagate through all surfacing and subsequent overlays, it is preferable to limit cracks to fine hairline cracks at closer spacings. These hairline cracks in the CTB may or may not propagate through the asphalt surfacing. In terms of pavement design philosophy, the district may wish to consider stabilizing the lower part of the base and leaving the upper half unstabilized. This would permit the stabilized layer to bridge the poor subgrade, but the unstabilized flexible base would minimize the amount of reflection cracking damage done to the asphalt surfacing. More work is needed in this area.

3.4 FAILURE INVESTIGATION OF SH-36

As part of the in situ evaluation, the researchers investigated the rapid failures of portions the cement treated base layer on SH-36 (section 6).

This highway was totally reconstructed in 1990. The existing pavement of asphalt surfacing

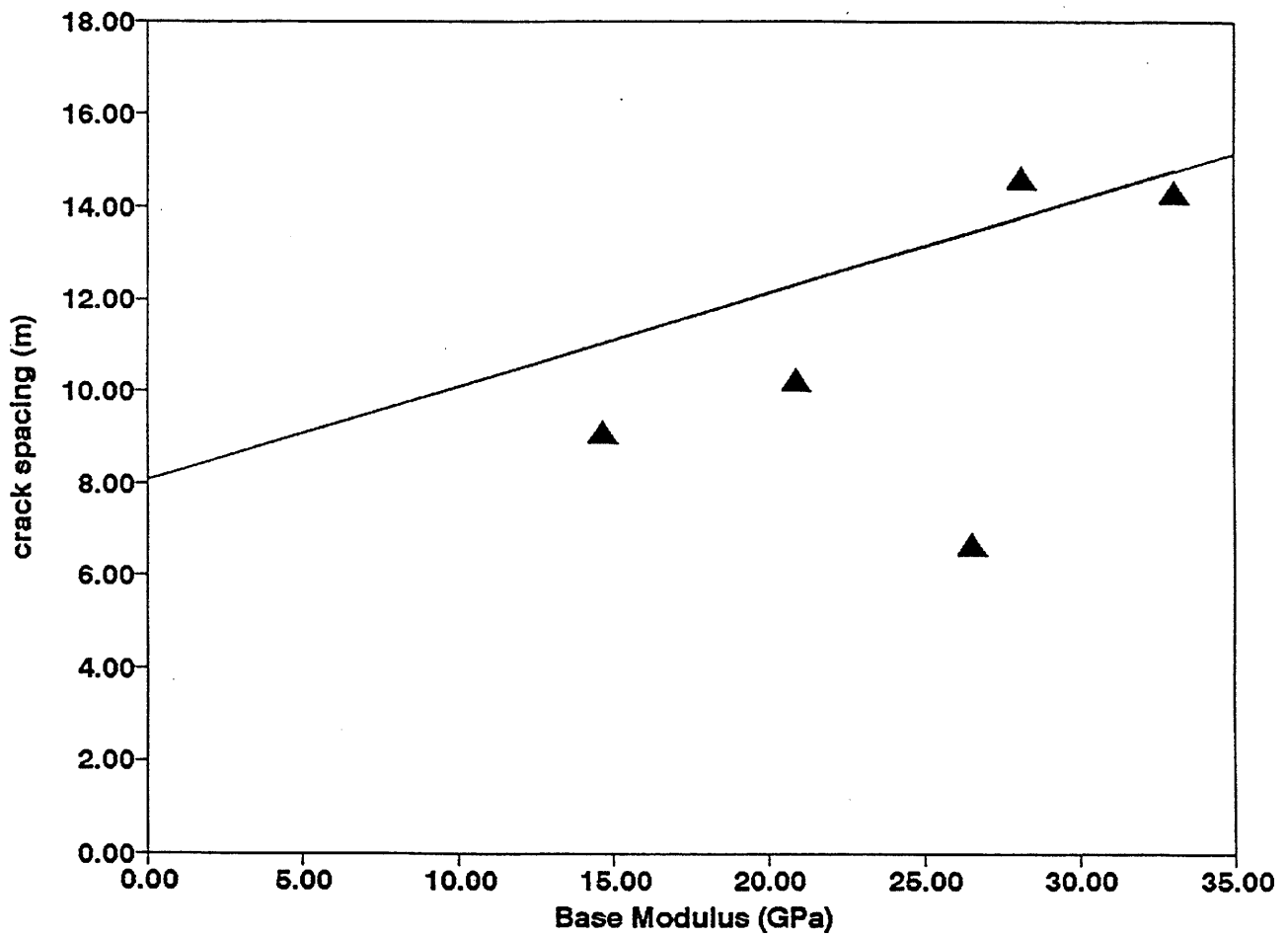


Figure 3.5. Observed Relationship Between Base Modulus and Crack Spacing.

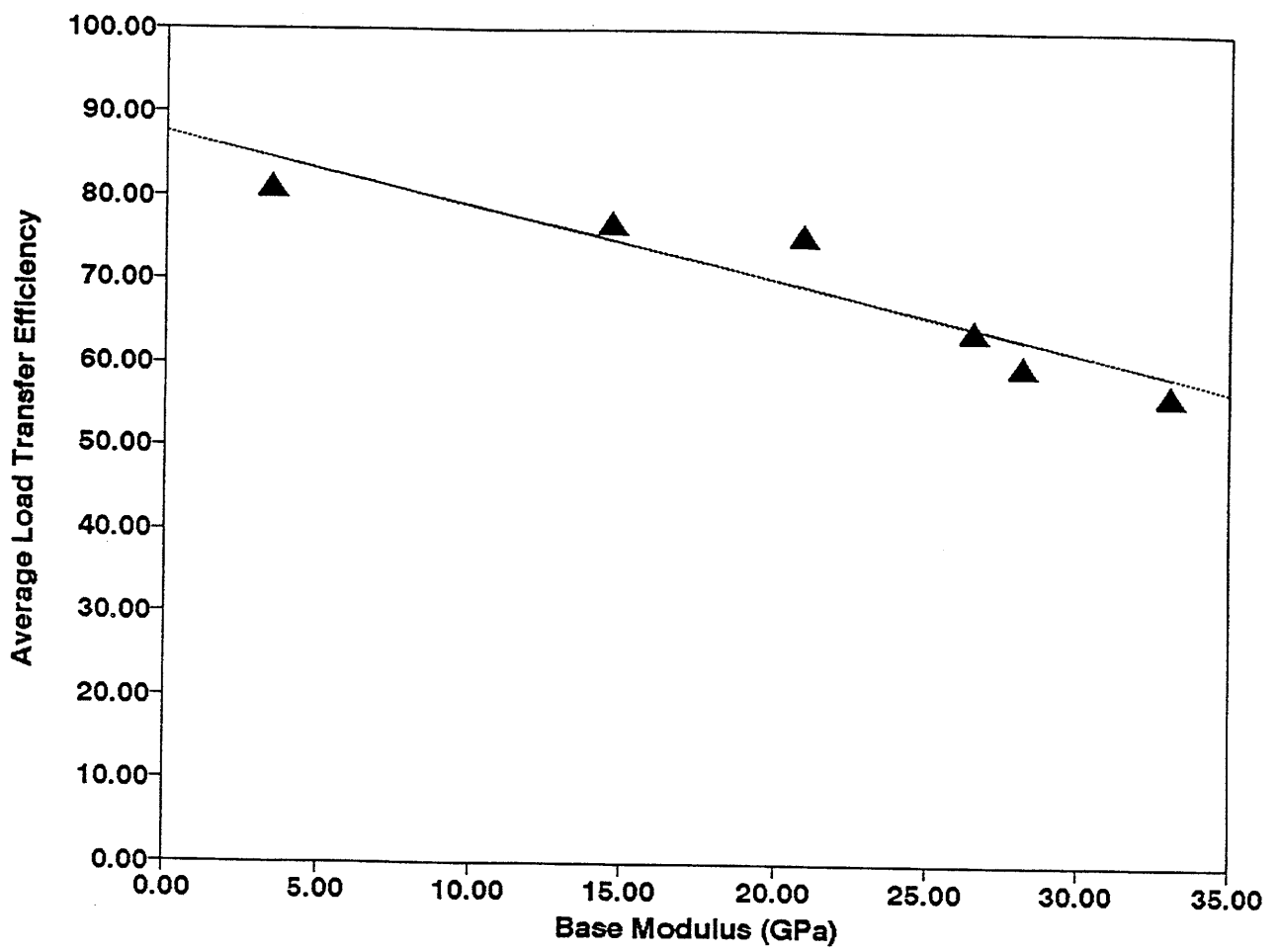


Figure 3.6. Observed Relationship Between Base Modulus and Load Transfer Efficiency.

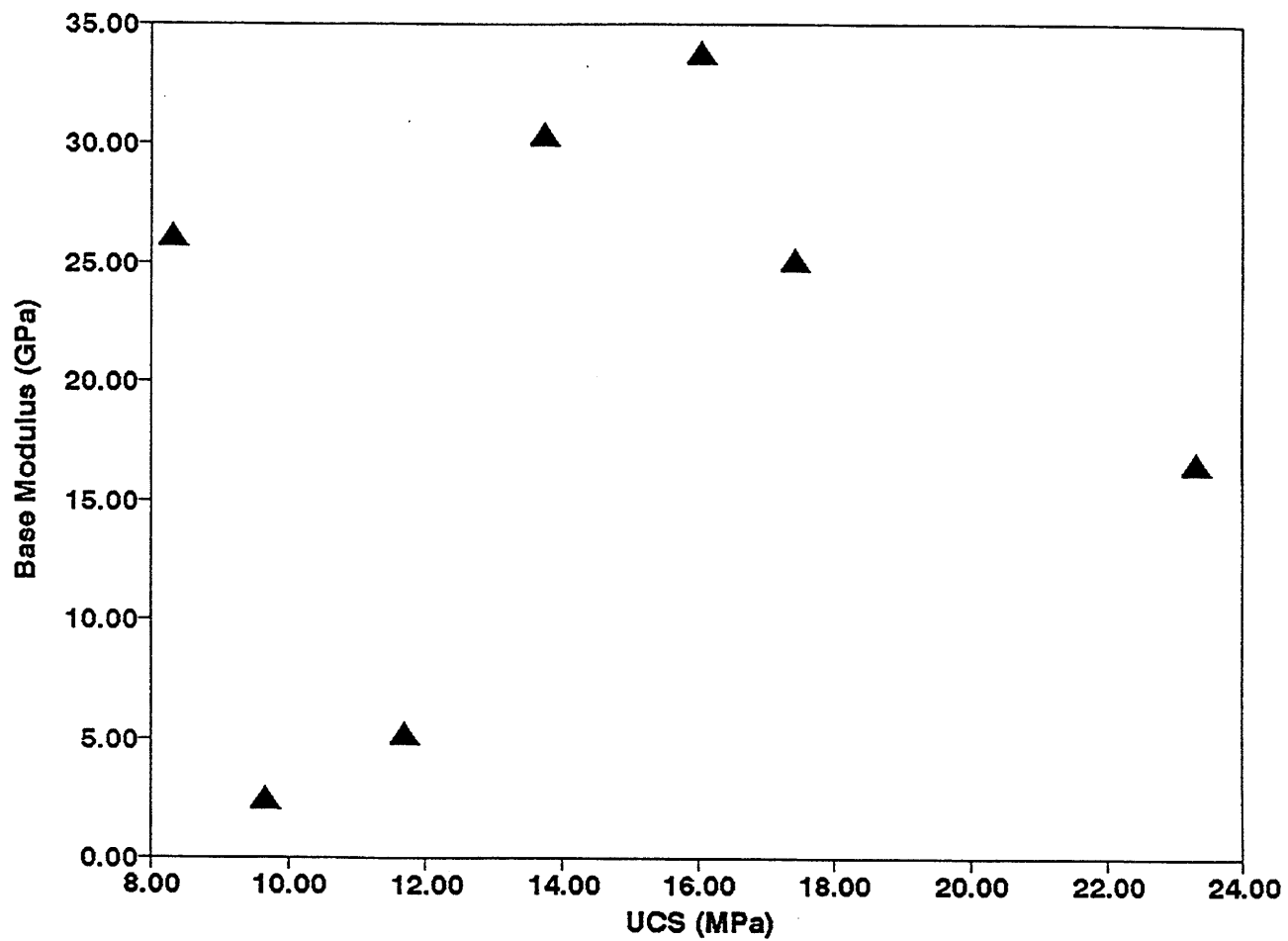


Figure 3.7. Observed Relationship Between Unconfined Compressive Strength and Base Modulus.

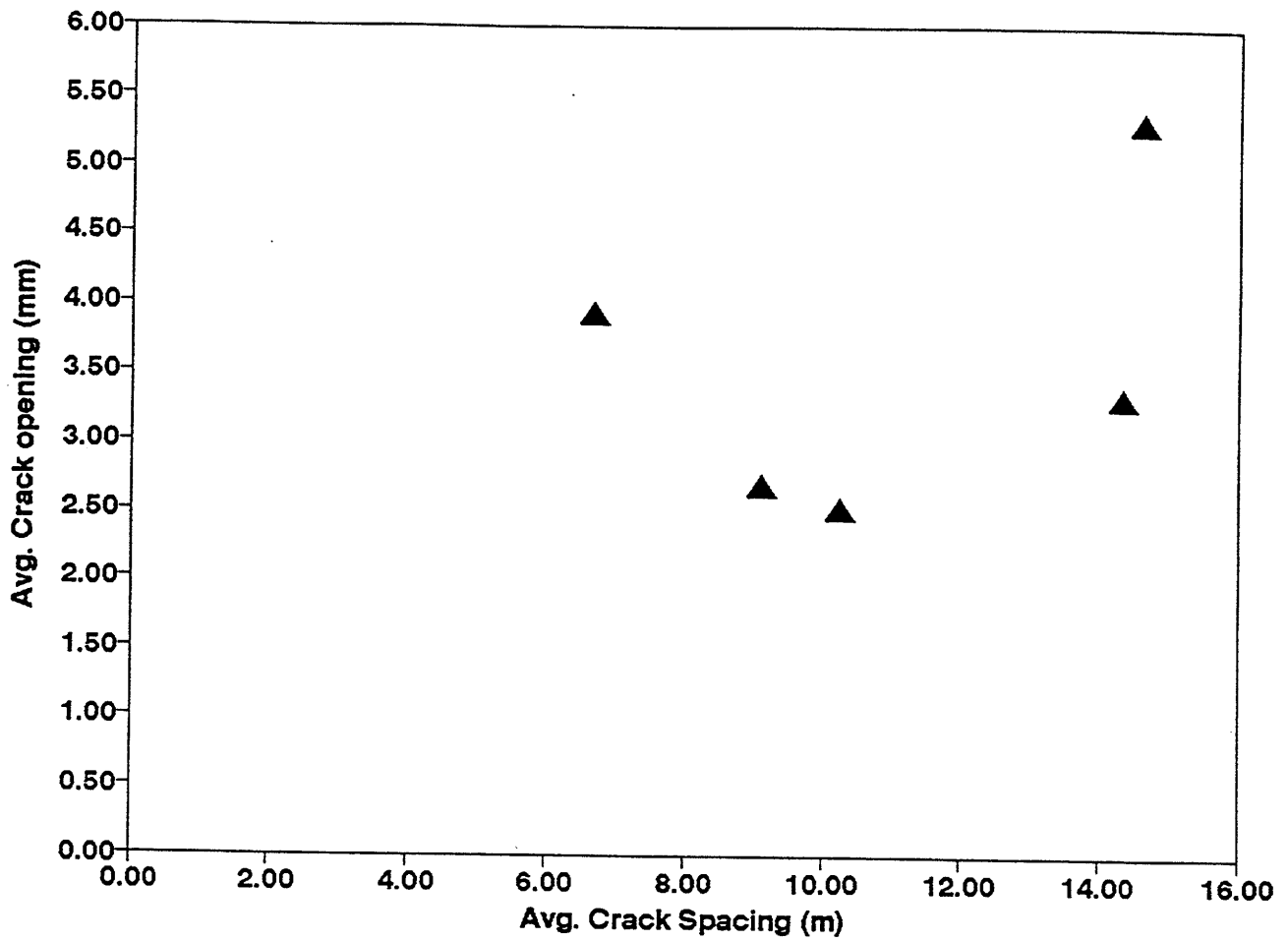


Figure 3.8. Observed Relationship Between Crack Spacing and Crack Opening.

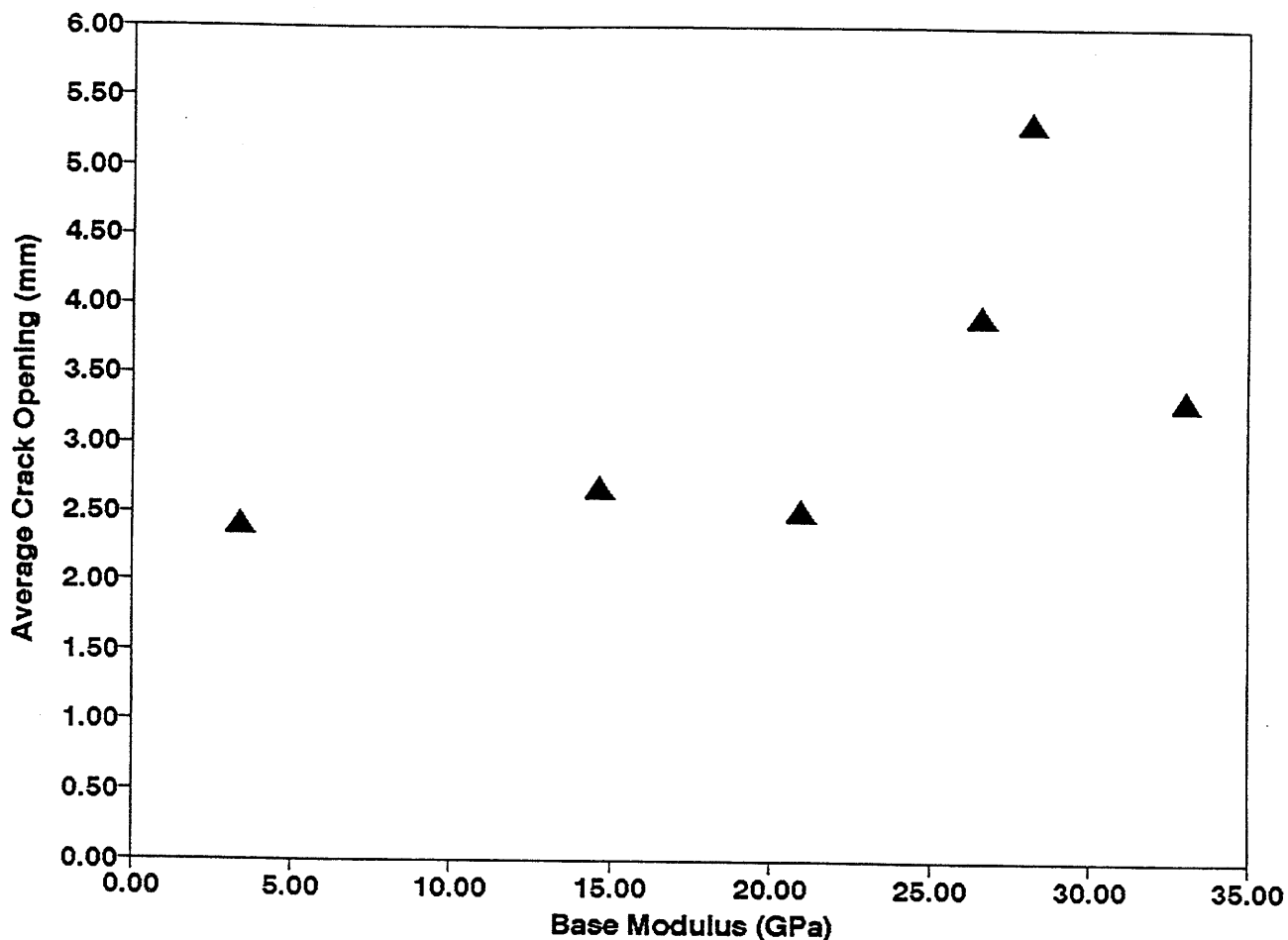


Figure 3.9. Observed Relationship Between Base Modulus and Crack Opening

over a gravel base was milled, stockpiled and stabilized with approximately 5 percent portland cement. The stabilization was performed at a central plant. This layer was placed over the entire section as a 150 mm thick base layer. An additional 150 mm base layer consisting of cement stabilized crushed limestone was added, giving a total CTB thickness of 300 mm. A 75 mm thick hot mix surfacing was placed over the entire section. The total width of pavement is typically 13.5 m. The traffic on the section is moderate. The ADT was reported to be 4,360 vehicles, and the design twenty year 80 kN was 3.4 million.

After two years of service, several sections on this highway were showing significant distress. The distress takes the form of transverse depressions in the wheel path, approximately 0.3 m wide.

In the worst areas the depressions are about 20 mm deep and at about 6 m spacings. The depressions were found initially in the wheel paths but eventually expanded to cover the entire lane. The depressions are centered around existing transverse reflection cracks, but they do not extend into the shoulder. The riding quality is noticeably reduced in these areas. The section rides like a faulted, jointed concrete pavement. Figure 3.10 shows the transverse cracking pattern in the pavement; note the unusual "Y" cracks developed in the wheel paths.

A forensic evaluation involving the Falling Weight Deflectometer, Ground Penetrating Radar, coring and laboratory testing was performed and submitted to the Houston District (Scullion, 1993). Figure 3.11 shows typical photographs of the stabilized base condition.

It is noted that in the failed areas, the top layer of heavily stabilized material had completely disintegrated. The conclusions from this investigation are as follows.

1. Visual evaluation of the cones indicated that the top CTB layer had completely disintegrated. The lower CTB had not disintegrated. The primary cause of the failure of this layer is moisture trapped within this layer. A likely deterioration cycle is as follows.
 - a. The two CTB layers have different shrinkage and thermal expansion properties. During curing and temperature cycling, these layers cracked and debonded. The transverse cracks in the two layers occur at different locations.
 - b. Water entering in the cracked top layer was trapped; it could not enter the lower layer or vent through the shoulder.
 - c. Under the action of traffic the hydraulic forces of pressurized water moving within the top layer caused erosion and loss of fines through pumping.
 - d. The top CTB layer completely disintegrated in the problem areas. The bottom CTB layer remained relatively intact. This deterioration cycle is sketched in Figure 3.12.
2. The severity of the disintegration suggests that there may also be a materials problem. Small quantities of clay were found in the disintegrated aggregates.
3. Under high rainfall conditions, it is anticipated that continued rapid deterioration of this highway will occur. At the time of evaluation, the condition was deemed critical, although only a small percentage of the section was showing significant problems. The

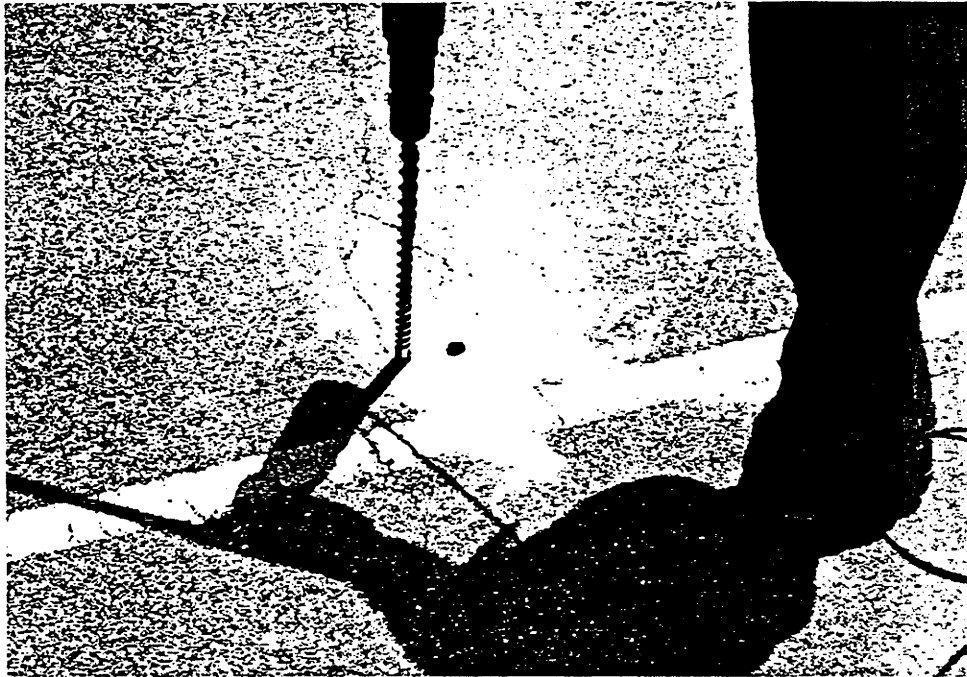


Figure 3.10. Transverse Crack Pattern in the Pavement (Note: Y Shaped Crack Near Shoulder Paint Stripe).

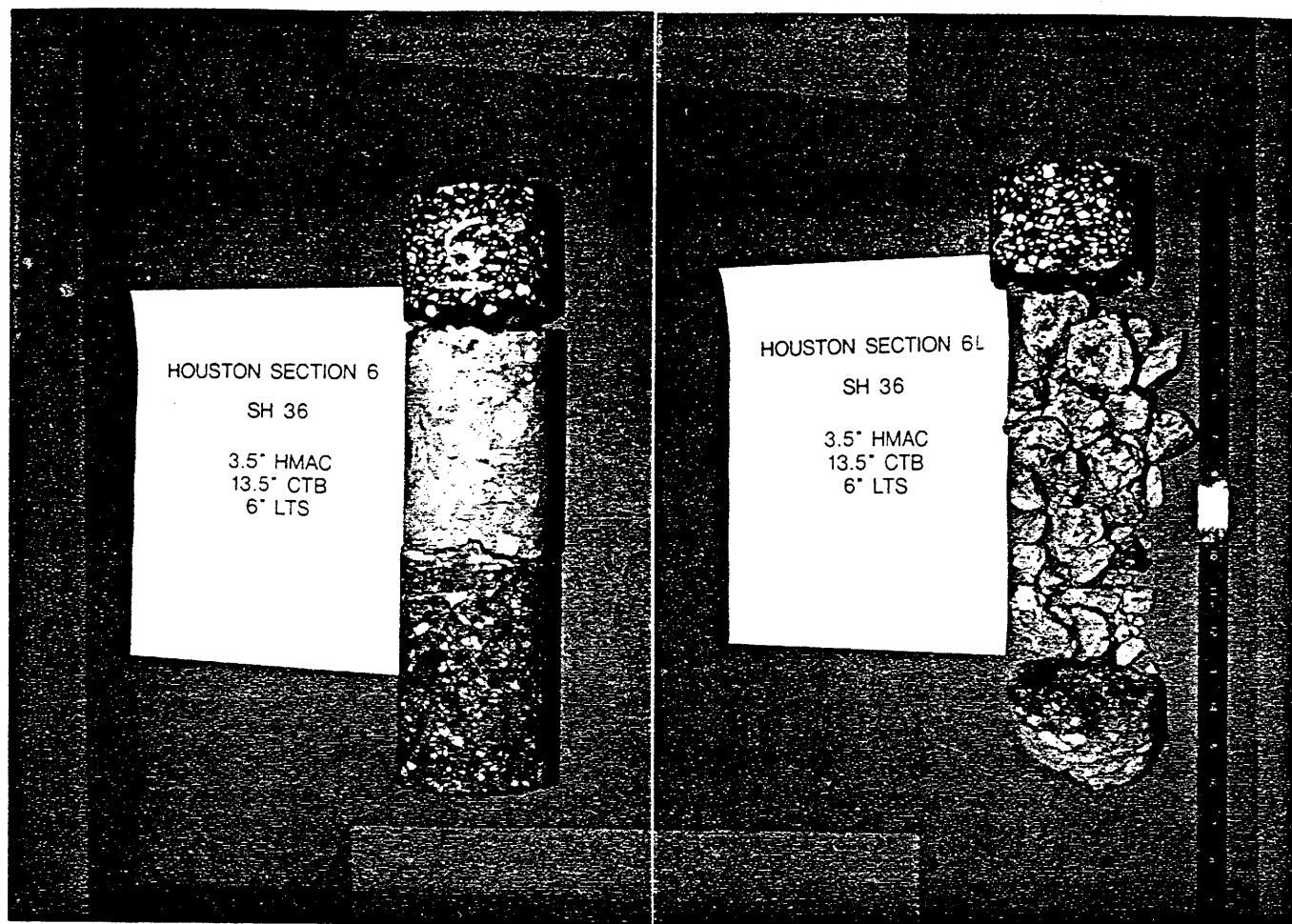


Figure 3.11. Photographs of Core Obtained from Solid and Distressed Portions of the Pavement.

damage accelerates rapidly if left untreated and eventually fails.

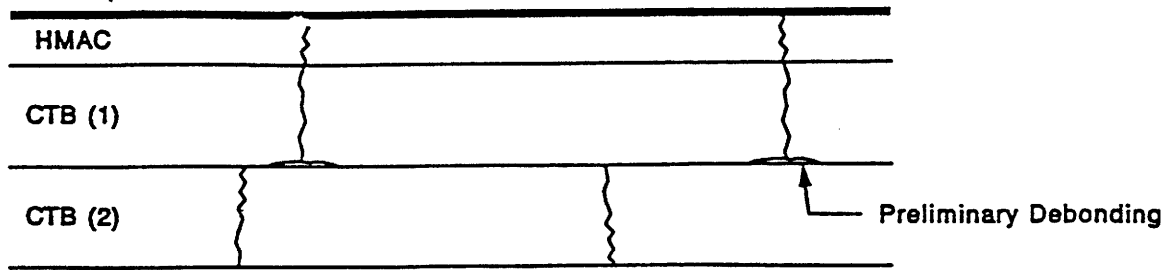
4. Laboratory testing showed that the thermal coefficient of linear expansion of the lower CTB layer is approximately twice that of the upper CTB layer (20 micrometers/meter per °C compared to 11.1 micrometers/meter per °C).
5. Ground Penetration Radar (GPR) evaluation indicated that: a) GPR can be used to distinguish between distressed and non-distressed areas and b) The dielectric measurements on the top CTB layer implied that the moisture content of the entire layer was high. It had rained significantly the day before GPR testing. This moisture appeared trapped in the top layer.
6. The aggregates used on this job had been successfully used on several other projects in the Houston District.

This case study points out the problems that can occur when thermal and shrinkage mismatches occur in pavements that permit moisture to become trapped between layers. No major problems were found with the materials or construction practices. The construction technique of using heavily stabilizing existing layers overlain with heavily stabilized materials from a different source needs further evaluation.

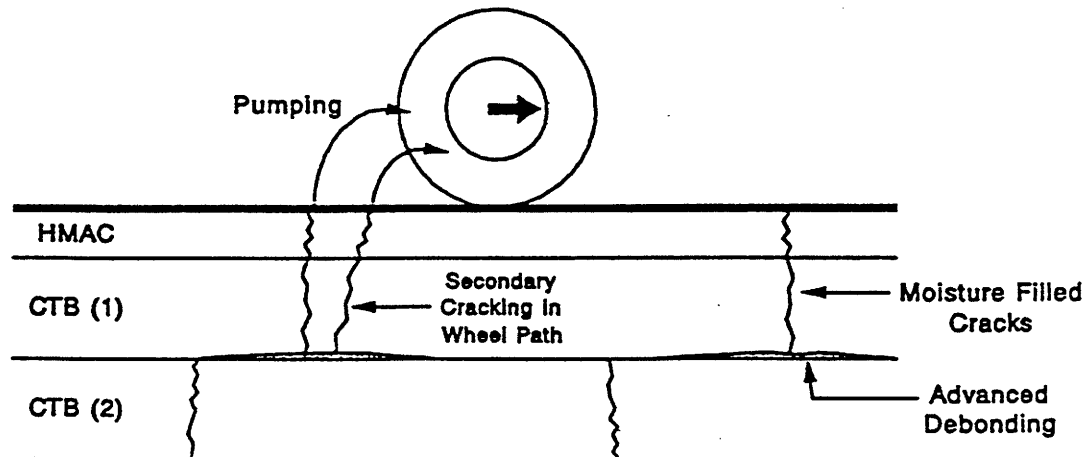
3.5 ATLANTA DISTRICT BASE RESULTS

The Atlanta District has many years experience in base stabilization. This area of Texas has relatively poor base material, most of which is iron-ore gravel. Stabilization is used in some new construction, but it is used extensively in pavement rehabilitation where a need exists to improve an existing base. In the 1960's the District started using cement as the stabilizing agent.

Phase 1 - Crack formation and initial debonding caused by differential shrinkage and thermal mismatch of CTB layer.



Phase 2 - Water ingress and deterioration under load.



Phase 3 - Final stages.

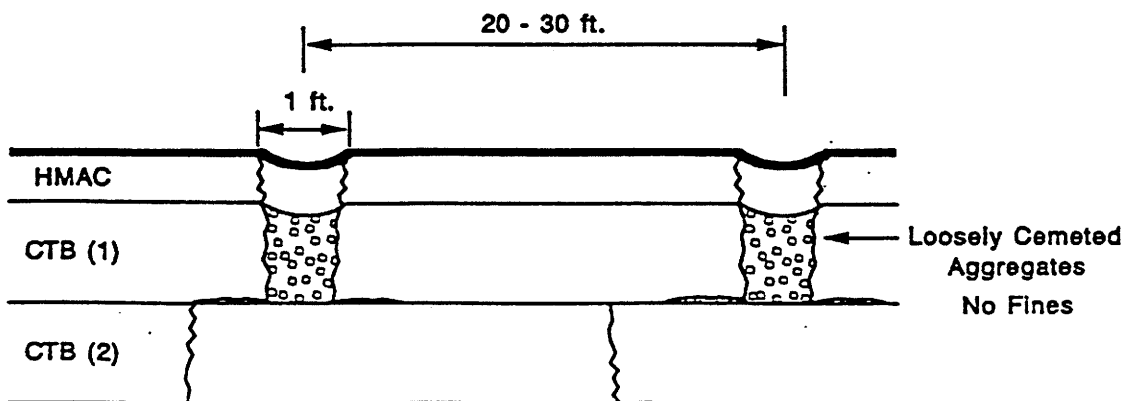


Figure 3.12. Deterioration Cycle of CTB on SH-36.

However, thermal and shrinkage cracking resulted, and the sections became maintenance headaches. Since then the use of cement has largely been replaced with lime and lime/fly ash blends. Lime/fly ash is also used to stabilize subgrades, and the results obtained on these subgrades will be presented in a later section of this report.

Within the District there has been a divergence of opinion as to what level of stabilizer works best. Efforts to meet the standard TxDOT strength specifications, in place in the 1980's (7-day minimum compressive strength of 4,550 KPa) resulted in stabilizer contents in the 5 to 6 percent range by weight. Other engineers promoted the use of very low levels of stabilizer, used only to "kill the PI of the base," and several sections with only 1 to 2 percent stabilizer were constructed. In recent years the move has been toward use of an intermediate level of stabilizer to upgrade the base to a "Class 1" material while still retaining the performance characteristics of a flexible base. The District staff is currently leaning toward use of intermediate levels. The concern with the use of lime/fly ash blends is the level of benefit achieved from the fly ash and calculating the optimum ratio of lime to fly ash. Currently a 1:2 lime to fly ash ratio is used, for example, 2 percent lime with 4 percent fly ash. The fly ash used in this district is classified a type F ash; it has a low calcium oxide content, typically less than 8 percent.

In an attempt to answer some of these questions, the District constructed a series of stabilization test sections on SH-8 near Douglasville. Six 614 m test sections were built with the following percent lime to percent fly ash combination: 1:1 (1 percent lime to 1 percent fly ash), 1:2, 2:2, 2:3 and 2:4. These six sections were included in the Project 1287 monitoring effort in this district. For each section, the laboratory strengths obtained using an unconfined Texas Triaxial Test are shown in Table 3.5. The strength of the unstabilized base material was, on average, 245 KPa.

In general, the Atlanta District's current method for selecting the required stabilizer content for a typical pavement rehabilitation job involves obtaining a triaxial compressive strength for the raw base material and then adding incremental percentages of lime/fly ash and measuring the resulting strengths. The samples are compacted at optimum moisture content. They are cured using a combination of 7 days of air curing and 10 days of moisture room curing (Thomas, 1994). The criteria applied calls for selecting the stabilizer content that gives between a two-fold and three-fold strength gain after 10 days of moist curing. These criteria generally result in a total stabilizer content of 2 to 3.5 percent.

Field Testing

In the Atlanta District, 11 monitor sections were set up. Included in this test program was the experimental section, section 8, containing the 6 different stabilized bases on SH-8. Some of the sections contained stabilized subgrades only. These are reported in Chapter 5 of this report. For each test pavement, the evaluation procedure established for the Houston pavements was followed, including crack mapping, FWD and, where possible, DCP testing. Appendix B gives the detail test results for each section.

Discussion of Results

Table 3.5 gives a summary of the backcalculated modulus results obtained from the Atlanta District. For each section, the average layer moduli backcalculated from the FWD data using MODULUS 4.2 is presented together with an assessment of the pavement performance in terms of surface cracking. In order to judge the strength gain associated with the stabilization, a Base Improvement Factor (BIF) was calculated as $E_{base}/(3 * E_{sg})$, where three times the calculated subgrade modulus (E_{sg}) is assumed to be a first order estimate of the anticipated modulus value for unstabilized granular base. Therefore, the BIF is intended to indicate what increase in modulus is associated with the stabilization compared with an unstabilized base. Therefore, the BIF is intended to indicate what increase in modulus is associated with the stabilization compared with an unstabilized base. As noted in Table 3.5, the BIF range is from 0.8 to 24. This is equated to no apparent impact of stabilization to over a 20 fold modulus gain. The major conclusions presented in this table are listed below.

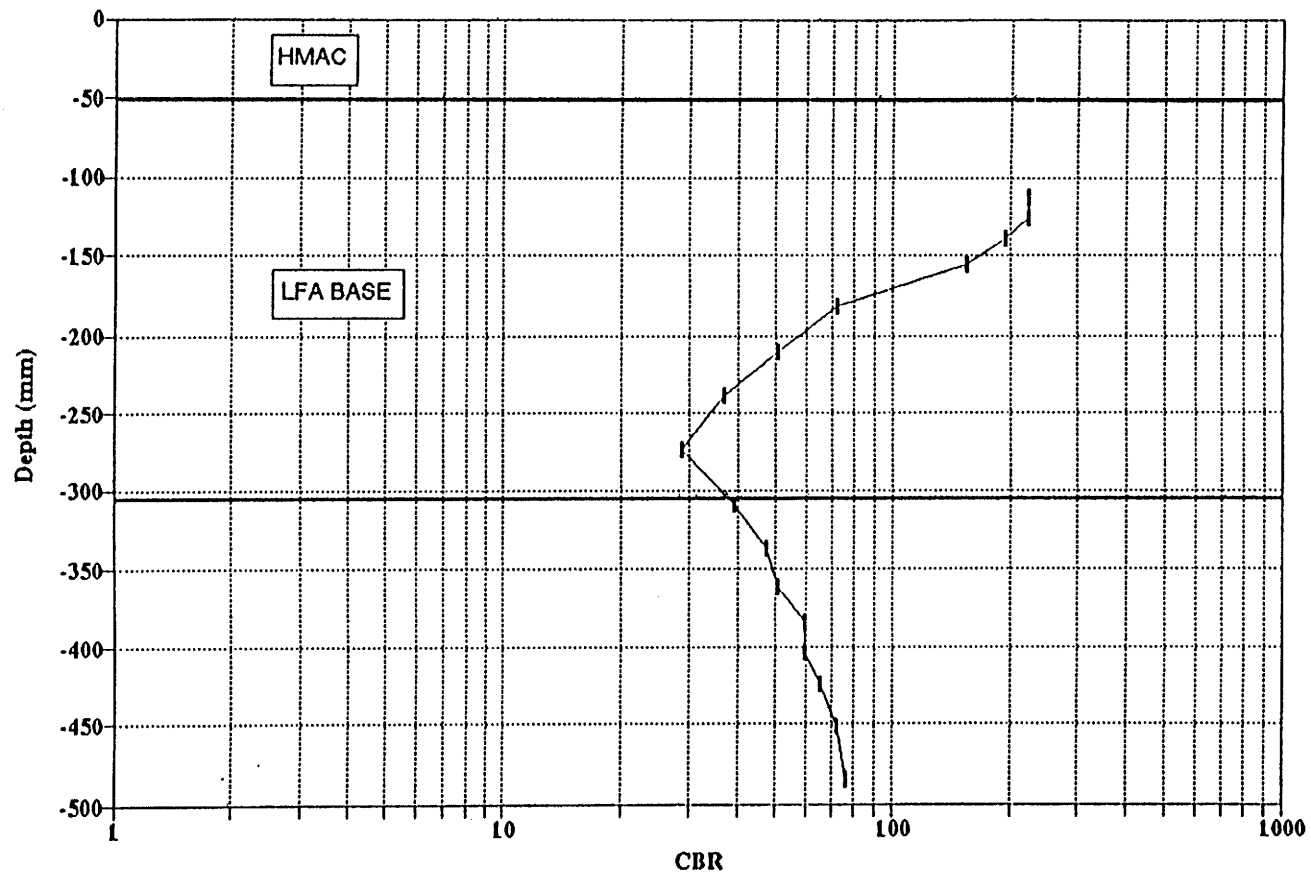
1. The worst performing sections are the heavily stabilized sections containing greater than 4.5 percent stabilizer; sections 1 and 10 fall into this category. Both have base moduli in excess of 7,000 MPa (BIF greater than 30) and relatively low variations in strength throughout the section; however, each has extensive surface cracking. Section 10 is a continuing problem for the District. The cracked base has pumped excessively, and the section has become rough due to deterioration around the initial transverse cracks. Section 1 is relatively new but has major cracking problems with between 12 and 14 moderate to severe transverse cracks per 30 m.

Table 3.5. TxDOT Laboratory Compressive Strengths Obtained on SH-8 Experimental Pavement near Douglasville. The Raw Material Strength was 245 KPa.

Section	% Lime	% F.A.	Compressive Strength, KPa		
			10 days	30 days	90 days
A	2	4	3,234	3,822	3,724
B	2	3	3,136	3,528	3,528
C	2	2	3,304	2,989	3,381
D	1	1	1,470	1,764	1,617
E	1	2	2,695	2,793	2,401
F	1	3	2,107	2,205	2,205

- The best performing sections are those stabilized with intermediate levels, between 2 to 4 percent total stabilizer. Sections 9, 11, and 8A, 8B and 8C are all performing very well, with minimal surface cracking and Base Improvement Factors of between 1.7 and 3.1. Section 9 is 15 years old and is performing exceptionally well with a 4 percent lime stabilized base. The traffic on these sections is relatively light in terms of average daily traffic, but each section carries very heavy individual truck loads, usually logging trucks. The average base moduli found backcalculated in these sections was between 630 and 1,225 MPa. However, the moduli values obtained within each section were quite variable. Section 11 had a low value of 231 MPa with a high of 1,869 MPa, for a mean of 930 MPa with a coefficient of variation of 60 percent. This variation is attributed to several factors, including natural variations in lightly stabilized layers, the variations in subgrade support and variations in the thickness of the stabilized layer. These thickness variations were also observed during the DCP testing. Most of the sections had a nominal thickness of 250 mm. However, as shown in Figure 3.13, the effective depth of the stabilizer was often less than the nominal thickness. In Figure 3.13 the plot of CBR versus depth is given for a specific location on SH-77. For the stabilized layer to be effective, the CBR value is expected to be above 80. The layer structure of section was 50 mm of asphalt and a nominal 250 mm base. However, from this figure the stabilized base appears to be

ATLANTA DISTRICT
SH-77 Site-4 Trial-2 Station @ 30'



3.30

Figure 3.13. Typical Example Showing That Effective Layer Thickness Is Less Than Actual Thickness Based on DCP Data.

only 125 to 150 mm thick. This loss of thickness could be attributed to either inadequate mixing of the stabilizer leaching of the stabilizer into the subgrade or loss of strength due to flexural fatigue damage.

3. The low levels of stabilizer (around 1 percent) did not produce any significant impact on layer resilient moduli for these materials. Neither the laboratory nor the field data showed any significant gain in strength. Sections 2, 8D, 8E and 8F had Base Improvement Factor ranging from 0.8 to 1.5. Given the natural variability of these materials, it is difficult to assign any strength gain to these materials.
4. The contribution of the fly ash alone to the overall layer strength is unclear. The results from SH-8, sections 8A to 8F do not show any significant impact of fly ash content. It may be that the levels of this low CaO ash may be insufficient to active stabilization without the use of lime or cement.
5. The laboratory compressive strengths shown in Table 3.6 correlate fairly well with the backcalculated moduli values. If little improvement was seen in the lab, then little or no strength gain was found in the field. For the 2 percent lime stabilization in the laboratory, a relative strength increase of between 170 and 200 percent was found over the raw material strengths. The field corresponding BIF factors were between 1.7 and 3.1.

Conclusions

The major conclusion from the Atlanta District data is that the best pavement performance in the Atlanta District was obtained with intermediate levels of stabilizers, between 2 and 4 percent total stabilizer content. The existing procedure for selecting levels of stabilization (2-3 times strength gain over raw materials) seems a reasonable approach. However, if the same techniques were to be applied to a range of different material, then it is probable that the two- to three-fold strength gain criteria would not identify the optimum stabilizer range. What is required is a more fundamental evaluation of the causes of shrinkage cracking. Caltabian (1992), in an Australian study, adopted a simple bar shrinkage test to predict the eventual cracking of the stabilized base. The Australians recommend permitting a maximum shrinkage of 250 microstrain after 20 days of moist curing. Preliminary tests were conducted on the iron ore base material found in District 19. It was found that after 10 days, the shrinkage was 100 microstrain with the material stabilized with 3 percent lime.

Table 3.6. Base Section In Situ Test Results from Atlanta District.

Section No.	Thick, mm	% Lime	% FA	Modulus ¹ , MPa			Age, years	ADT	Cracking
				Mean	C.O.V. %	BIF ²			
1	250	4.5	0	9,058	25	24	2	2,000	Extensive
2	250	1	2	168	32	0.8	3	2,900	None
4	250	3	6	1,057	47	4.1	6	1,650	Moderate
8A	250	2	4	644	26	1.7	3	2,500	Minor
8B	250	2	3	903	69	3.1	3	2,500	None
8C	250	2	2	658	100	2.7	3	2,500	None
8D	250	1	1	350	22	1.5	3	2,500	None
8E	250	1	2	301	21	1.0	3	2,500	None
8F	250	1	3	336	100	1.2	3	2,500	None
9	200	4	0	1,204	74	3.1	15 ³	2,300	Minor
10	250	4	8	9,219	37	23	14	2,000	Extensive ⁴
11	250	2.5	0	938	60	2.3	3	3,500	None

¹ Base Moduli Backcalculated Using Modulus 4.2 Software

² Modulus of Unstabilized Base Assumed to be 3 Time Subgrade
 BIF = Backcalculated Base Modulus/Calculate Base Modulus (3 Esg)

³ New Overlay 5 Years Old

⁴ Severe Pumping/Poor Ride

Based on field results in this study, 3 percent seems to be approaching the boundary between moderately and heavily stabilized materials, and, therefore, the Australian criteria seem reasonable. More work is required to evaluate the applicability of incorporating shrinkage criteria in the procedures for selecting optimum stabilizer content.

3.6 BRYAN DISTRICT

The Bryan District mostly uses subgrade stabilization, and those results will be presented in Chapter 5 of this report. Very little base stabilization is used. The only known section was a short section of US 190 on poor subgrade. In this section, a very thick, 450 mm heavily stabilized base was constructed. The base was high quality crushed limestone stabilized with 6 percent cement. The strength and stiffness values obtained from this section and the pavement cracking were very similar to those observed in the Houston District. Table 3.7 shows the results from the FWD backcalculation. The average base modulus was calculated to be 23 GPa with a Coefficient of Variation (COV) of 33 percent. The section also exhibited longitudinal and transverse cracking with crack widths ranked as moderate to severe. In recent years, the Bryan District has begun to use lime stabilization as a means of upgrading the base layers of existing low volume farm-to-market highways. The existing base and thin surfacing are crushed and blended; then a low percentage of lime is introduced. The section is then reshaped and compacted. To qualify for this stabilization, the existing base is tested to ensure that a minimum quality and thickness of material is present. If the existing base is less than 150 mm, then an alternative rehabilitation method would be recommended, which possibly includes stabilizing the existing highway and adding 150 to 250 mm of new unstabilized base on top. However, for those sections with adequate base, a remixing or recycling operation is recommended. The District feels that this low level stabilization is a cost effective way of upgrading its FM highways. However, two issues are under investigation within the District:

- a. Which is the best level of stabilizer to use?
- b. Should additional high quality rock be added to the layer?

Table 3.7. Modulus 4.2 Output for US-19.

TTI MODULUS ANALYSIS SYSTEM (SUMMARY REPORT)														(Version 5.0)
District:	0													
County:	190													
Highway/Road:		Thickness(in)							MODULI RANGE(psi)		Poisson Ratio Values			
		Pavement:	2.00		100,000		250,000		H1: % = 0.35					
		Base:	18.00		500,000		5,000,001		H2: % = 0.25					
		Subbase:	0.00		0		0		H3: % = 0.35					
		Subgrade:	280.00		25,000				H4: % = 0.40					
Station	Load (lbs)	Measured Deflection (mils):							Calculated Moduli values (ksi):				Absolute Dpth to	
		R1	R2	R3	R4	R5	R6	R7	SURF(E1)	BASE(E2)	SUBB(E3)	SUBG(E4)	ERR/Sens	Bedrock
62.000	10,141	4.02	2.58	2.30	1.94	1.61	1.37	1.12	118.	1970.5	0.0	23.4	0.70	300.00
76.000	10,097	3.37	2.41	2.19	1.85	1.59	1.36	1.15	198.	2227.0	0.0	23.3	0.62	300.00
95.000	10,185	3.64	2.40	2.17	1.83	1.58	1.33	1.12	135.	2400.5	0.0	23.4	0.37	300.00
106.000	10,141	3.19	2.70	2.39	2.01	1.69	1.36	1.16	250.	2090.6	0.0	22.0	4.20	300.00 *
117.000	10,157	3.19	2.57	2.27	1.94	1.68	1.39	1.17	250.	2159.5	0.0	22.3	2.00	300.00 *
137.000	10,105	2.83	2.24	2.09	1.76	1.52	1.34	1.17	250.	2921.9	0.0	22.2	2.08	300.00 *
151.000	10,145	2.87	1.96	1.84	1.57	1.39	1.21	1.04	176.	3737.6	0.0	23.8	0.77	300.00
168.000	10,141	3.12	1.96	1.80	1.59	1.43	1.16	1.01	127.	3990.3	0.0	23.4	1.18	300.00
187.000	10,085	2.83	1.81	1.67	1.47	1.28	1.16	1.03	143.	4588.9	0.0	24.2	0.98	300.00
200.000	10,089	2.39	1.68	1.56	1.36	1.20	1.08	0.96	222.	4692.1	0.0	26.1	0.93	300.00
211.000	10,026	2.85	1.74	1.62	1.44	1.31	1.12	1.02	129.	5000.0	0.0	23.8	0.72	300.00 *
227.000	10,105	2.94	1.97	1.82	1.61	1.43	1.28	1.13	153.	4396.2	0.0	21.5	0.63	300.00
263.000	10,089	3.20	2.19	2.03	1.76	1.56	1.35	1.17	156.	3370.0	0.0	21.1	0.36	300.00
Mean:		3.11	2.17	1.98	1.70	1.48	1.27	1.10	177.	3349.6	0.0	23.1	1.20	300.00
Std. Dev:		0.41	0.34	0.28	0.21	0.16	0.11	0.07	51.	1116.8	0.0	1.3	1.05	15.56
Var Coeff(%):		13.21	15.78	14.05	12.36	10.51	8.57	6.71	29.	33.3	0.0	5.7	87.93	5.19

3.34

To investigate these issues the district constructed three experimental sections as part of the rehabilitation of FM 2446 near Franklin, Texas. These sections were:

- Section 1 Existing Base stabilized with 2 percent Lime,
- Section 2 Existing Base with 50 mm new base, stabilized with 2 percent Lime, and
- Section 3 Existing Base with 50 mm new base stabilized with 3 percent Lime.

In each case the rehabilitated base was designed to be 200 mm thick. These sections were tested with the FWD and DCP after compaction but prior to the placement of the single surface treatment. Figure 3.14 presents photographs of Section 1 being tested with the FWD and the final pavement surface. The results obtained from the DCP testing are shown in Figure 3.15, and the moduli values backcalculated for each of the test sections and the existing base are given in Table 3.8. Conclusions from these data are as follows.

1. The DCP indicated that the top 100 mm of the existing pavement was very weak, with an average CBR of approximately 25 (poor base); the base treated with 2 percent lime had a CBR of approximately 35, whereas the two sections with added rock had CBR values of approximately 80. For reference, a top quality class 1 base would have a CBR value of 80 or above. It should be noted that DCP testing was done within a few days of lime treatment. Since lime treatment results in a slow pozzolanic strength gain, it should be expected that considerably higher strength will occur in the lime-treated bases with additional time of curing.
2. The strength of the layer was variable with depth, and the strength appears to decrease with depth throughout the layer. The layer was compacted as a single 200 mm layer; it is anticipated that a superior strength profile would be achieved if the layer was compacted in 2 lifts.

Table 3.8. Backcalculated Base Moduli for FM-2446.

Section	Modulus, KPa	C.O.V.	Life Predictions (Year) FPS 19
2% Lime	336	20%	9
2% Lime + Rock	483	17%	13
3% Lime + Rock	602	36%	15
Existing	140	43%	-



Figure 3.14. FM-2446 near Franklin, Testing of 2 Percent Lime Section.

VARIATION OF CBR WITH DEPTH
FM-2446 SECTION-1

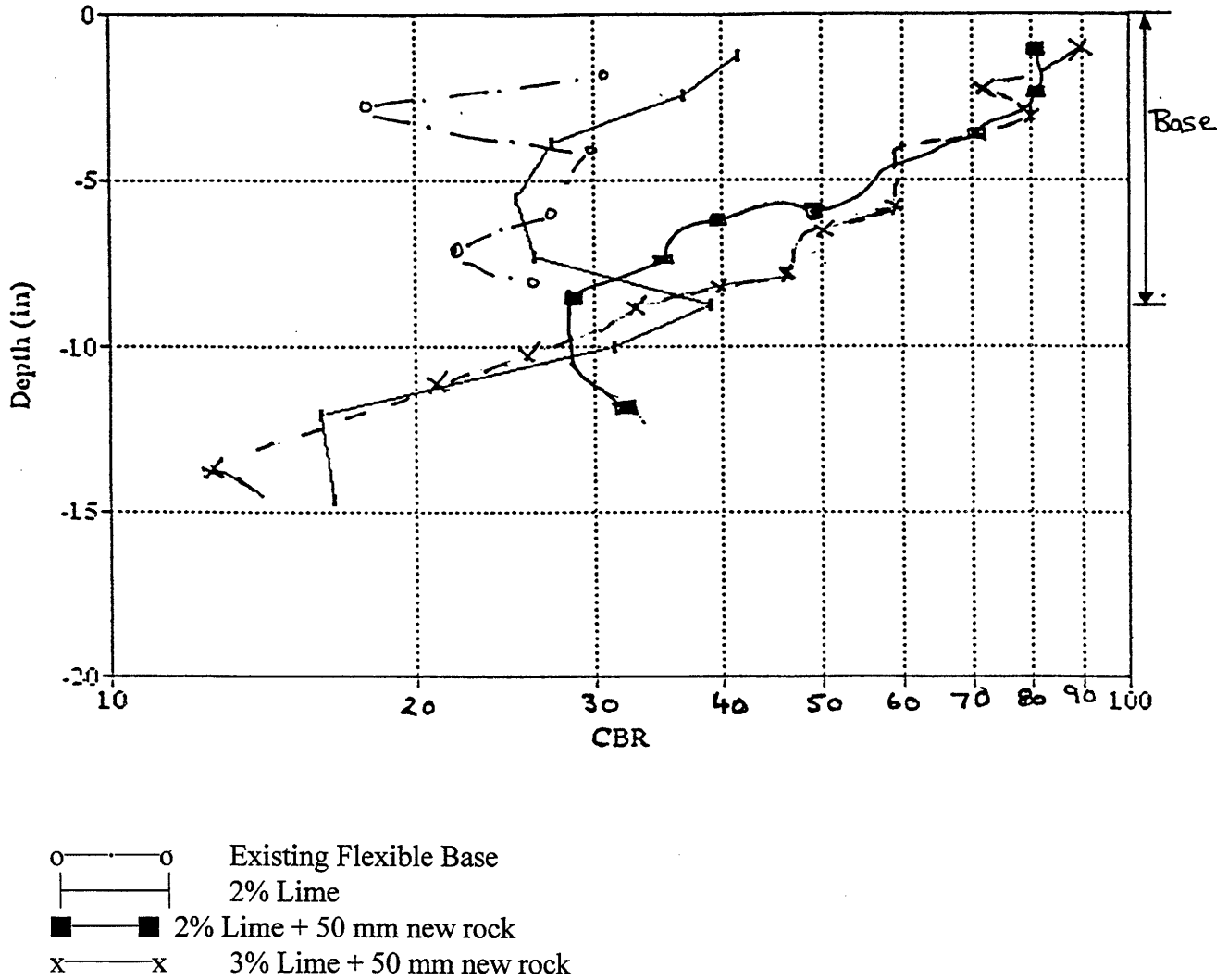


Figure 3.15. DCP Results from FM-2446.

3. The average backcalculated moduli values for this layer appear reasonable. Each showed a distinct improvement over the average modulus of the existing base, 180 MPa. The 3 percent Lime section with added base had an average moduli of 600 MPa.
4. In order to estimate the anticipated life, the Flexible Pavement System (FPS 19) was performed with an assumed 20 year traffic of 275,000 - 80 kN Equivalent Single Axle loads. The resulting performance lives were 9, 13 and 15 years for Sections 1, 2 and 3, respectively. It must be remembered that these moduli values were obtained shortly after construction, and neither the effect of age nor traffic was evaluated. However, the results presented from the Atlanta District demonstrate that it is possible to achieve base moduli values in the order of 700 to 800 MPa on highways stabilized with 2 to 3 percent lime after 7 years in service.

The base stabilization operation in the Bryan District is essentially a recycling operation. Little (1995) has evaluated a number of similar recycling operations using lime to upgrade marginal bases of clay-contaminated bases.

3.7 HISTORIC RECYCLING CASES

Waco, Texas

The city of Waco, Texas, like most cities, suffered from badly deteriorating residential streets. Their policy had been to reconstruct these streets by removing the worn out streets and rebuilding them with new material, a very costly process.

Waco city planners made a detailed study of the 227.5 km of residential streets to determine which would be good candidates for reconstruction. Selection was based on the availability of proper quality and quantity of existing gravel base material, the presence of sewer and water lines in satisfactory condition and the absence of drainage problems (Reinhardt, 1992).

After street selection, the next step was to adjust the manholes and water valves to a depth of 305 to 457 mm below existing grade. A grader-scarifier then scarified the old asphalt surface and base course to a depth of 204 and 254 mm, followed by pulverization and pre-mixing with a Bomag stabilizer. The material was then inspected to determine which soil stabilizer to use — hydrated lime or Portland cement of asphalt emulsion. Because of the abundance of plastic clay present in the base

material, lime was selected for nearly all reconstruction. During the initial pre-mixing operation, excess material was removed and stockpiled for future use. Following premixing, the material was shaped and recompacted lightly to permit traffic to use the street during the pre-stabilization period (Reinhardt, 1992).

The stabilization procedure included scarifying, adding lime in slurry form, mixing, compaction, shaping and curing. The slurry lime was prepared in a Portabatch lime slaker at about 32 percent solids. The lime was delivered and spread by slurry trucks handling 9.1 to 10.9 metric tons of lime solids. The lime was spread to the desired rate of 13.3 kg/m² for a depth of 204 mm (approximately a 4 percent application) (Reinhardt, 1992).

Once the proper gradation and water content were attained, the lime-stabilized gravel base was shaped and compacted with sheepsfoot, pneumatic and flat wheel rollers in succession until proper density was achieved. A prime coat of MS-1 emulsion and water mixed at a rate of 3.8 liters of emulsion to 10 liters of water was applied at 1 liter/m³. The stabilized base was cured for 1 to 2 weeks prior to paving with only light traffic permitted during the curing period (Reinhardt, 1992).

Waco city officials are satisfied with the performance of the recycled pavements. They believe that the added stiffness and strength provided by the lime-stabilized recycled base allows them to produce reconstructed pavements that can serve well over an expected life of 30 years and which are comparable or better than newly constructed pavements (Reinhardt, 1992).

The cost per linear meter of completed recycled street was estimated to be \$51.38 (\$15.81 per linear foot) as compared with \$162.50 (\$50 per linear foot) for undercutting and wasting old material and reconstructing with new material (Reinhardt, 1992).

The recycled pavements have provided excellent serviceability. The most noticeable distress of the streets prior to recycling and of other old residential streets which are in need of recycling is the substantial level of deep layer rutting due to the soft and low-stability gravel base contaminated with plastic clay. The recycled street with lime application to stabilize the existing gravel, clay and pulverized asphalt is much more rut resistant and has shown no signs of rutting distress.

Yolo, California, Recycling Project

From 1976 through 1979, Little (1979) made an extensive structural evaluation of recycled paving materials. One particularly impressive project was on Highway 45 near Yolo, California.

In this project an aggregate base that was contaminated with clay fines was recycled, and lime was added in the recycling process. The original pavement consisted of 102 mm of asphalt concrete surface and approximately 254 to 305 mm of aggregate base course with plastic clay fines. The recycled pavement consisted of 254 mm of the existing base course restabilized with hydrated lime. This recycled base was covered with 51 mm of new hot mix asphalt concrete.

Non-destructive testing of the pavement sections with the Dynaflect demonstrated that the recycled base vastly improved the load carrying potential of the recycled pavement as compared to the pavement section prior to recycling. Little (1979) states that, based on a dual parametric analysis of the maximum surface deflection and the shape of the deflection basin, the recycling operation improved the structural capacity of the pavement by approximately 400 percent.

Meridian Oil Company Runway

In 1984 a runway designed to carry light aircraft was rehabilitated to upgrade the structural capacity. The original section consisted of 300 mm of caliche base and a double bituminous surface treatments. Eighty percent of the runway was recycled through a remixing operation. Lime (4 percent) was added to a depth of 200 mm. The recycled caliche base and the original caliche base were evaluated during this study (in 1994) using the DCP. This evaluation revealed an average approximate CBR of 20 of the unstabilized caliche base. The recycled and stabilized caliche, on the other hand, responded with an approximate CBR of 110.

In 1994 the entire runway was recycled with lime and fly ash to a depth of 350 mm to accommodate still heavier aircraft. Prior to the 1994 recycling operation, the existing runway was proof-rolled by a 335 KN water truck to crudely evaluate the existing stability of the runway. The truck was well-supported by the recycled portion of the runway, but the truck caused catastrophic failure in the portion of the runway where recycling was not accomplished.

CHAPTER 4

EVALUATION OF LIGHTLY STABILIZED BASES

4.1 OVERVIEW

Aggregate base courses may be divided into two categories based on strength and stiffness: stabilized and flexible. Stabilized bases refer to those where a significant percentage of stabilizer has been used to form a substantial matrix bonding of aggregate particles together. Flexible bases are unbound; although they possess substantial strength and load-spreading capability, they derive strength primarily from interparticle friction and not from cementitious bonding among particles. Consequently, the flexible bases are not rigidly bound but can "flex" under load.

A mixture design approach widely used for stabilized bases has been to add enough "glue" to achieve a minimum strength level to ensure durability. These "high-strength" bases have functioned well in certain instances, yet they have caused problems due to their rigid nature and their tendency to crack during hydration reactions.

Rigidly stabilized bases are typically stabilized with portland cement, fly ash, or a combination of lime and fly ash or cement and fly ash. Rigidly stabilized or even moderately stabilized bases, discussed in Chapters 2 and 3, generally contain 6 percent or more of the stabilizer by dry weight of aggregate. Lime and fly ash combinations may require as much as 20 to 25 percent stabilizer by dry weight of aggregate.

In this chapter the term "lightly stabilized" refers to from 1 to 2 percent stabilizer added to bases with relatively low levels of plasticity (PI less than about 15). Lightly stabilized bases have been found to function well. The level of stabilization is usually too low to achieve a rigid cement matrix but is high enough to establish a marked improvement in shear strength and resilient modulus when compared to the unstabilized bases.

Little (1990) described a case history in which a low level of lime stabilization (1 percent by dry weight of aggregate) was used to upgrade a marginal granite base course. The granite base met gradation specifications for an aggregate base course (ABC) prescribed by the City of Phoenix, Arizona. However, the base possessed a high plasticity (PI = 10 to 14).

Little (1990) evaluated six pavement sections all with an identical pavement cross-section (87 mm of HMA and 250 mm of ABC over a decomposed granite subgrade). The HMA and ABC

in each pavement were identical except that in three sections, the ABC was stabilized with 1 percent hydrated lime.

Little (1990) evaluated approximately 80 FWD deflection basins from each of the six pavement sections. He found that the backcalculated resilient moduli of the stabilized ABC layers were significantly statistically different at a 95 percent confidence level from those of the unstabilized layers. The backcalculated moduli were evaluated using the computer model MODULUS.

Table 4.1 summarizes the backcalculated resilient moduli for the six pavement sections together with the calculated tensile flexural strain at the bottom of the HMA surface, the vertical compressive strain at the top of the subgrade and the octahedral shear stress ratio within the HMA. All calculations were made under a 20 kN wheel load.

From the data summarized in Table 4.1, it can be seen that the changes in resilient moduli are substantial from a standpoint of structural enhancement. The 1 percent lime treatment increased the ABC resilient modulus by a factor of between approximately 3 and approximately 30.

The effect of the increase in modulus is to reduce vertical compressive strain by an average of 62 percent, which substantially reduces the potential of the pavement to deform or become rough due to the accumulation of permanent strain within the granular layers. The modulus increase reduces flexural tensile strain within the HMA and thus reduces fatigue potential by as much as four orders of magnitude. Finally, the increased modulus of the ABC afforded by lime stabilization provides a better support for the HMA, which not only reduces the flexural tensile strain within the HMA but also reduces the critical shear stresses within the HMA. These stress can result in rutting. The octahedral shear stress ratio is used in Table 4.1 to evaluate a rutting potential within the HMA. Column 6 presents the ratio of octahedral shear strength to critical octahedral shear stress induced within the HMA. This ratio can be envisioned as a factor of safety against HMA rutting. As can be seen in column 6, this safety factor is substantially increased when a low level of stabilization is used. The conclusion of Little (1990) was that the low level of lime treatment of the granite ABC substantially improved the performance potential of the pavement.

The mechanism of the stabilization of the granite base was a pozzolanic reaction between the hydrated lime and the plastic clay fines within the ABC. Although the fine content was relatively

Table 4.1. Backcalculated Properties of Phoenix, Arizona, Granite Aggregate Base Coarse (ABC) with and without Lime Stabilization.

Pavement Section	Average Resilient Modulus, MPa	Tensile Flexural Strain in HMA,	Predicted Fatigue Life, ESALs	Subgrade Compressive Strain, mm/mm	Shear ¹ Stress Ratio in HMA
1 (2% Lime)	381	200 x 10 ⁻⁶	10 ⁶	290 x 10 ⁻⁶	1.53
3 (1% Lime)	1,569	60 x 10 ⁻⁶	2 x 10 ⁷	110 x 10 ⁻⁶	2.00
6 (1% Lime)	2,849	50 x 10 ⁻⁶	10 ⁸	125 x 10 ⁻⁶	2.22
7 (unstabilized)	244	280 x 10 ⁻⁶	7 x 10 ⁵	390 x 10 ⁻⁶	1.42
8 (unstabilized)	94	360 x 10 ⁻⁶	7 x 10 ⁴	370 x 10 ⁻⁶	1.25
9 (unstabilized)	139	320 x 10 ⁻⁶	9 x 10 ⁵	450 x 10 ⁻⁶	1.33

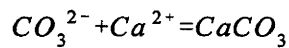
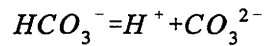
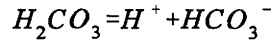
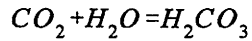
¹Stress Ratio is Ratio of Shear Strength to Critical Induced Shear within HMA.

low (17 percent minus 200 sieve material), the clay was reactive with lime. The stabilized fines formed an improved matrix within the aggregate but not a rigid matrix. Thus substantial strength and stiffness improvement was noted, yet flexibility was maintained.

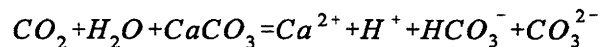
Another area where low levels of lime stabilization have been effectively used is in the upgrade of marginal calcareous bases. Here the mechanism of stabilization differs significantly when the calcareous bases possess little or no clay. The reaction has been determined to be primarily due to the formation of calcium carbonate cement rather than due to a pozzolanic reaction. This type of stabilization is used in south Texas, especially in the Corpus Christi and Yoakum Districts. This mode of base enhancement was deemed to be significant enough to warrant attention in this research study.

4.2 THE CARBONATION REACTION

Calcium carbonate is known to be a natural cement. Due to constant fluctuation of the chemical conditions in nature, calcium carbonate is dissolved and reprecipitated as a cementing agent. The reactions that take place during the natural carbonate cementation process as suggested by Miller (1952) are as follows:



Summarizing the above reactions:



The solubility of $CaCO_3$ as a function of CO_2 concentration depends on temperature and pressure of CO_2 in equilibrium with the water. At constant temperature, solubility of $CaCO_3$ increases with the increase of CO_2 pressure. Solubility of $CaCO_3$ increases with the decrease of temperature when CO_2 pressure remains the same. According to Boynton (1980), limestone is virtually insoluble in pure water, but the solubility increases with increasing partial pressures of CO_2 . The solubility of calcite at temperatures of 17 - 25° C, free of CO_2 , is 0.014 - 5 g/l, and at 100° C the value is about 0.03 - 4 g/l. The solubility of calcite is significantly increased by increasing increments of CO_2 pressure. But in the presence of CO_2 , the solubility of calcite decreases with increasing temperature (Bounton, 1980). Concentrations of carbon dioxide vary widely in nature. Through several processes in nature, the amount of CO_2 is either enriched or depleted in natural waters, which, in turn, increases or decreases the capacity of water as a solvent for $CaCO_3$ (Bounton, 1980). For example, rain water entrains and absorbs CO_2 in excess of its atmospheric quota. Using an atmospheric partial pressure of CO_2 (3.5×10^{-4} bars), Miller (1952) showed the calculation of how 3000 kilograms of $CaCO_3$ per square kilometer per mm of rain could be removed from a limestone area. CO_2 concentration in ground water in the upper vadose zone may also be high because of the presence of soil bacteria that provides CO_2 (Miller, 1952). According to Howard and David (1936), organic acids generated from

the decomposition of organic matter and carbonic acid formed from CO_2 dissolve carbonate in nature. An investigation of the solution kinetics of calcite by Weyl (1958) revealed that the water present in the pores of a limestone is always saturated with calcite under normal geological conditions. When the solubility of calcite changes due to changes in temperature, pressure, or chemical composition of the water, calcite dissolves and reprecipitates. In a laboratory experiment, Thorstenson et al. (1972) successfully demonstrated how CO_2 degassing of CaCO_3 - rich waters, initially saturated at one atmosphere CO_2 , produced cementation of carbonate skeletal sands. In their experiment, carbon dioxide charged water was allowed to leach through a source bed and to flow to a second carbonate sand unit, where the CO_2 was driven off and the dissolved carbonate was reprecipitated as cement.

Unlike calcium carbonate, the chemistry of quartz behavior is very simple. Quartz, in nature, tends to be very stable at normal surface and near surface conditions. Blatt et al. (1980) showed that quartz is only appreciably soluble at very high pH, and even then, it is only slightly soluble. Due to this difference in chemistry, calcite is more likely to contribute significantly as a cementing agent than quartz under normal surface conditions. According to Graves (1987), quartz particles might be an effective source of silica cement if very high pH conditions persisted for long periods of time. Materials including volcanic glass, clay minerals, and high temperature silicate minerals such as olivine and calcic feldspars are very unstable compared to quartz under surface conditions and might serve as sources for dissolved silica during weathering processes.

The strength of bonding reactions in stabilized soils depends on the density and concentration to which the cement surrounds the grains of soil, bonding properties of the cement to the grains, and roughness of the grain. It is the bonding properties of the cement to the grains as a function of cement-particle mineralogy that is of particular interest.

Dapples (1979) claims two structural varieties of mineral cements: compatible and incompatible. Compatible cement is compatible with the individual detrital grains and attaches itself to the crystals of the grains. Since compatible cement is mineralogically the same as the substrate, it nucleates at many points on the substrate and forms a mosaic of crystals in structural continuity with the substrate. Incompatible cements, on the other hand, form a crystallographical discordant boundary with the detrital grains. They normally form a sharp outline with the substrate and make it much easier to be recognized as incompatible cements (Dapples, 1979).

Another important factor in cement-particle interaction is surface energy. According to Wollast (1971), nucleation of cement is maximized when the surface energies of the precipitate and particles are the same. In the case of incompatible cementation, nuclei are not readily available on the grain surfaces for cement crystallization due to the fact that grains and cements have different mineralogical composition and, hence, different surface energies. This results in a slow and small amount of cementation in the pore spaces of incompatible systems (Wollast, 1971). Dapples (1979) claimed that crystallization occurs in interstitial openings and acts as a lithifying agent for surrounding detrital grains and is mainly responsible for the formation of incompatible cements.

Cement particle bonding strength is different in compatible and incompatible cementation due to the different mechanisms involved in them. Compatible cements normally result in stronger bonds than incompatible cements (Dapples, 1979). In compatible cementation, the cement nucleates on the particles and grows as part of the particle structure and is more likely to produce stronger bonds. Rupture of lithified rock is very common along the boundaries between incompatible cements and detrital grains (Dapples, 1979).

There are other factors than cement-particle composition that can influence the rates and amount of cementation developed. A study of quartz cementation conducted by Heald and Renton (1966) showed that sands of smaller grain size were cemented more rapidly due to the higher surface area. Similarly, angular particles with a corresponding higher surface area are cemented more rapidly than rounded particles. Cementation can also be influenced by the amount of cementing material available.

4.3 EFFECTS OF CARBONATION ON ENGINEERING PROPERTIES

Strength of soils has popularly been expressed by a simple equation as postulated by Mohr and Coulomb:

$$\tau = c + \sigma \tan\phi$$

where τ = shear strength,
 c = cohesion,
 σ = normal stress,
 ϕ = friction angle, and
 $\tan \phi$ = coefficient of friction.

Accordingly, strength has two components, "cohesion" and "friction". While the friction component is assumed to be directly proportional to normal stresses, the cohesion component is considered to be completely independent of normal stresses. The term "cohesionless" is used for granular materials such as sands and gravels where the strength of the material is regarded to be solely due to the frictional component. The frictional behavior of soil is attributed to the frictional resistance within the soil. Frictional resistance within the soil mass is directly proportional to the normal force acting on that point. Since the primary mechanism of soil deformation is relative movement, shear resistance at particle contacts controls the susceptibility of a soil mass to deformation.

Whether natural or artificial, cementation tends to develop a cohesive component of strength in cohesionless soils and increases the amount of cohesion in cohesive soils. The study on the effects of artificial cementation using portland cement conducted by Wissa and Ladd (1965) showed that the strength of quartz sands was increased due to a large increase in cohesion and a slight increase in friction. However, the cohesive resistance was at its maximum at lower strain levels and subsided at very high strains supposedly due to the breaking of cementation bonds. The study also showed that the cohesion component increased with an increase in cement content and curing time. In the same study, volume change (dilation) for cemented dense sands was less at low strains and unaffected at high strain levels, presumably due to breaking of cementation bonds as mentioned earlier.

Naturally cemented sands were carefully sampled and tested by Saxena and Lastrico (1978), and the results obtained were similar in nature. Here also, cohesion was the governing factor for strength gain at low strain levels, and frictional resistance was primarily responsible for strength gain at high strains due to breaking of cementation bonds. It was as if the soil was acting as an uncemented material at high strain levels, although at low strain levels the strength gain was very high.

4.4 EFFECTS OF LIME TREATMENT ON CARBONATE CEMENTATION

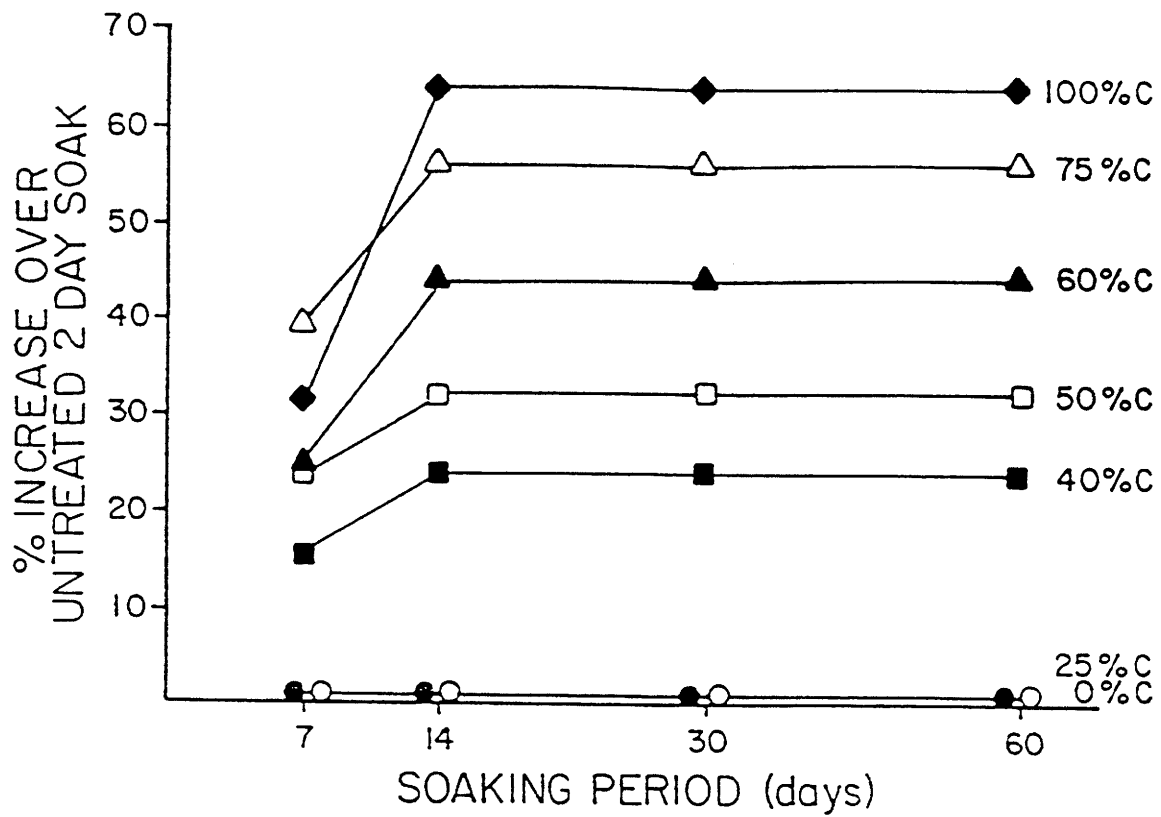
Graves (1987) showed that the natural tendency toward the carbonation reaction can be enhanced by adding lime to the system. In his experiments, the Limerock Bearing Ratio (LBR) was used to investigate strength increases resulting from carbonate cementation in both lime stabilized and unstabilized compacted sands of variable quartz/calcite compositions. The Florida Department of Transportation used the LBR to measure strength of various pavement materials. Pure quartz and

calcite sands were mixed in various proportions, compacted into LBR molds, soaked for time periods of from 2 days up to 60 days and tested to determine the strength increase with time. Another set of specimens were prepared by adding 1 percent hydrated lime with the same type of quartz/calcite mixtures. Cemented coquina materials were also mixed with 0 and 1 percent hydrated lime, compacted, soaked, and tested for LBR strengths in a similar fashion (Graves, 1987).

The LBR data for untreated specimens revealed that more strength developed as the calcium carbonate composition of the quartz/calcite sand mixes and cemented coquina samples was increased. Figures 4.1 and 4.2 show that the strength increases with soaking period for quartz/calcite mixes and cement coquina materials, respectively. The addition of lime to all samples enhanced carbonate cementation effects and promoted large strength increases. However, like untreated materials, the strength gain was much higher for materials having a higher percentage of calcite and a lower percentage of quartz. Lime treated high carbonate sands demonstrated strength increases of as high as 450 percent following a 60 day soaking period. Figures 4.3 and 4.4 show that the strength increased with soaking period for lime treated sand mixes and cemented coquina materials, respectively.

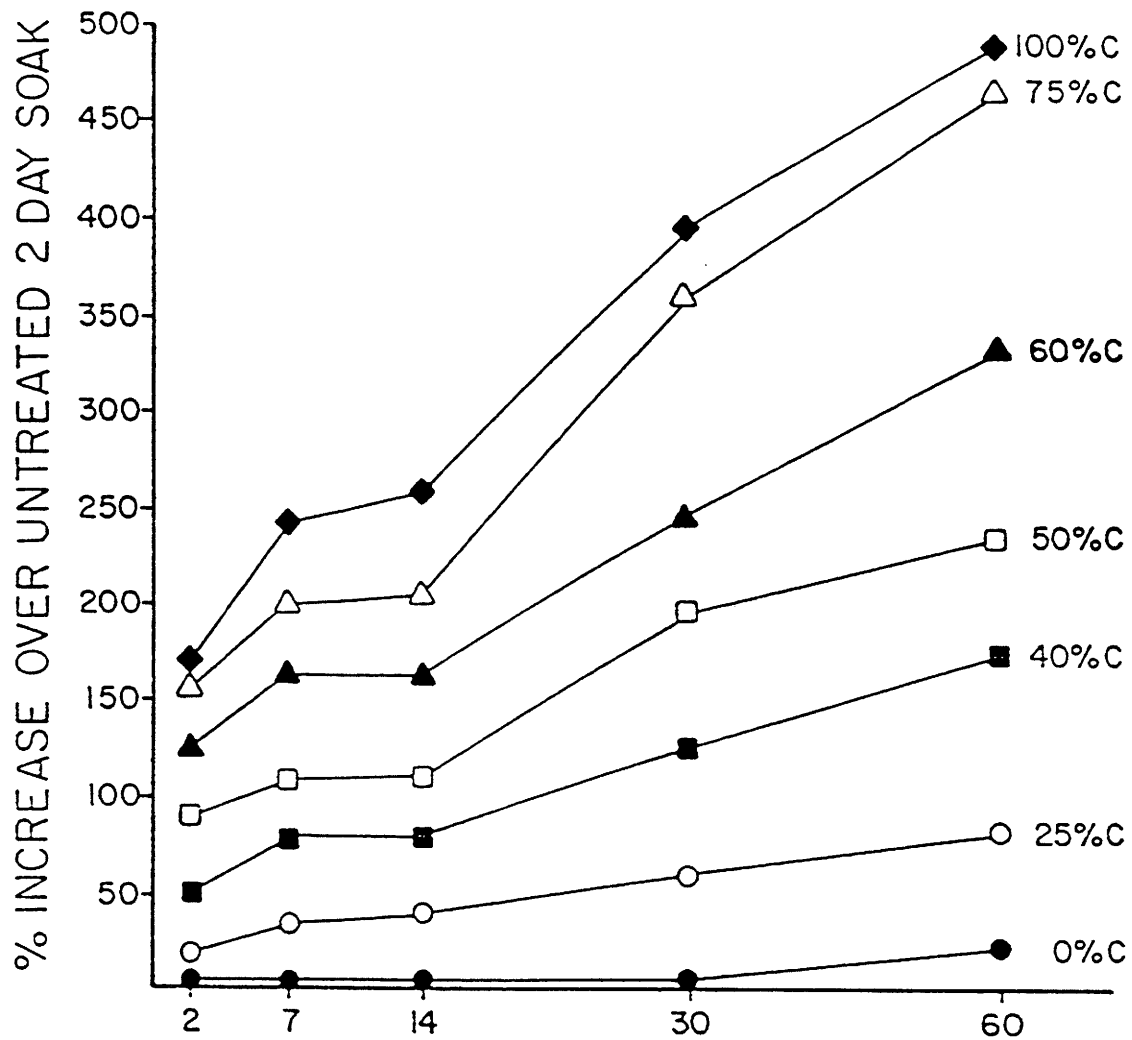
Using Scanning electron microscopy (SEM), Graves (1987) documented the presence of carbonate cement adhering to the carbonate particle surfaces. He further demonstrated the lack of bonding of the carbonate material with the quartz particles.

Graves (1987) conducted another experiment as a demonstration of the growth of calcite from a calcium hydroxide solution onto crystals of quartz and calcite. In this experiment, an SEM was used to examine quartz and calcite crystals after they were placed in covered petri dishes with a calcium hydroxide solution for two weeks and dried; results showed that the calcite precipitates nucleated on the calcite particle surfaces with an outward growth of crystals. On the other hand, the calcite precipitates did not nucleate onto the quartz crystals since the growth was not in contact with the quartz surface but rather nucleated from precipitation in the solution with small crystals growing downward and settling onto the quartz particle surface. Graves' experiment proved that the calcite cement formed during the carbonation reaction bonds to calcite particles but not to quartz particles.



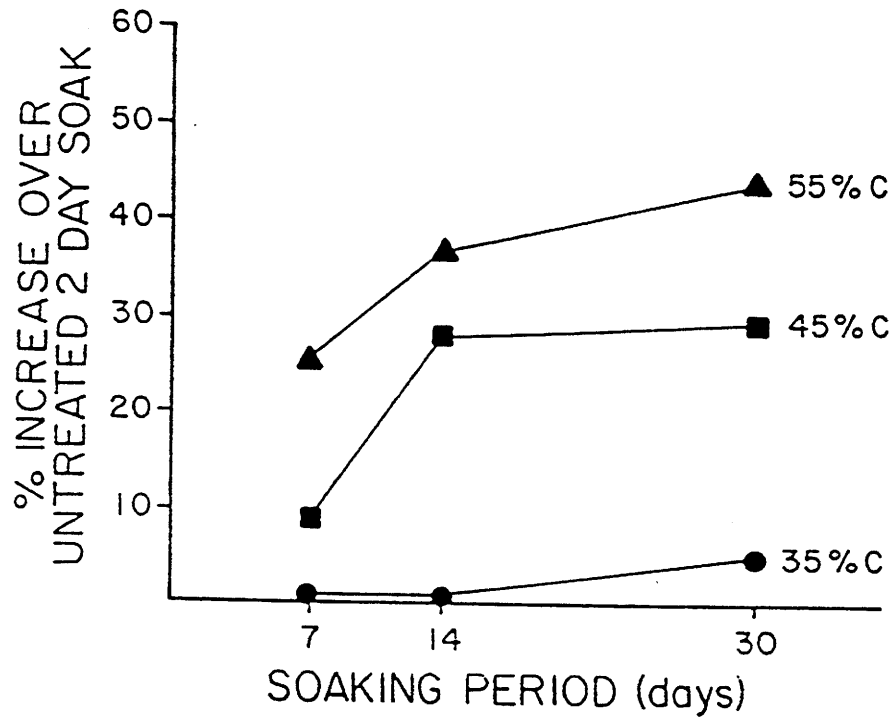
(C indicates calcite composition as a percentage of mineralogical make up)

Figure 4.1. Strength Increase of Untreated Quartz/Calcite Sand Mixes as a Function of Mineralogical Composition and Time (after Graves, 1987).



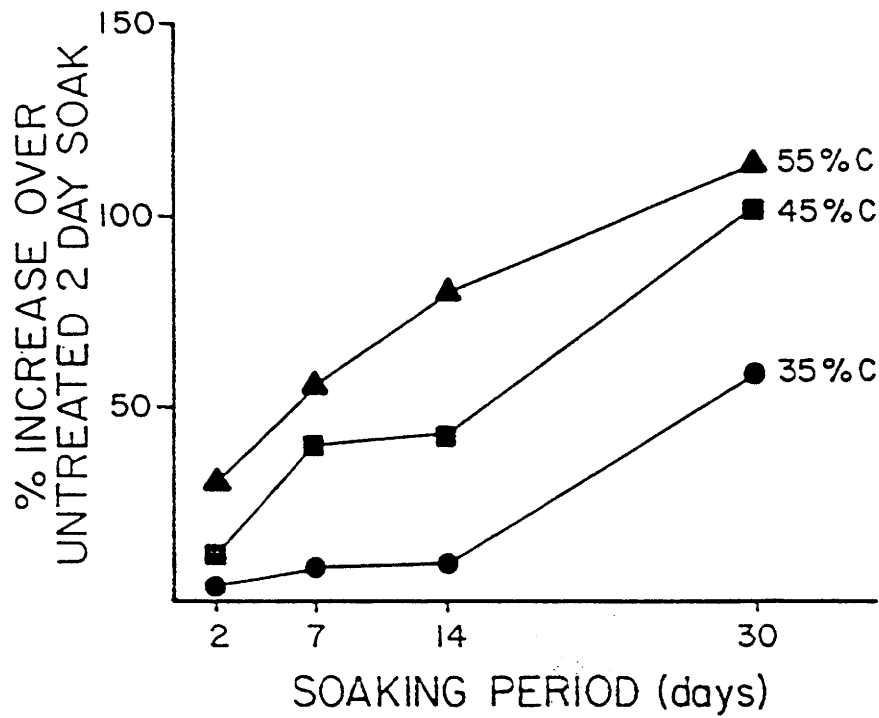
(C indicates calcite composition as a percentage of mineralogical make up)

Figure 4.2. Strength Increase of Quartz/Calcite Sand Mixes Treated with 1 Percent $\text{Ca}(\text{OH})_2$ as a Function of Mineralogical Composition and Time (after Graves, 1987).



(C indicates calcite composition as a percentage of mineralogical make up)

Figure 4.3. Strength Increase of Untreated Cemented Coquina Materials as a Function of Mineralogical Composition and Time (after Graves, 1987).



(C indicates calcite composition as a percentage of mineralogical make up)

Figure 4.4. Strength Increase of Cemented Coquina Materials Treated with 1 Percent $\text{Ca}(\text{OH})_2$ as a Function of Mineralogical Composition and Time (after Graves, 1987).

4.5 MATERIALS AND TEST METHODS USED TO EVALUATE EFFECTS OF CARBONATE CEMENTATION ON CALCAREOUS BASES

A study was planned to investigate the effects of adding low percentages of lime to calcareous base materials. The approach was to perform Texas triaxial tests on stabilized and unstabilized lab samples in order to evaluate strength change as a function of lime content and curing period. The laboratory resilient modulus test (AASHTO T274) was performed to investigate the effects of carbonate cementation on resilient modulus as a function of lime content and curing period. Evaluation of in situ resilient moduli was performed to evaluate the effects of carbonation on field properties and also to compare laboratory and field moduli values with and without stabilization.

Visual Characterization of the stabilized and unstabilized materials was performed in order to observe cementation characteristics which may aid in explaining strength and moduli variations. X-ray diffraction and other mineralogical analyses were performed in order to aid in explaining the mechanism of strength gain.

Aggregate

The two aggregates used in the study were limestone and caliche. Limestone is used in the base courses in both Yoakum and Corpus Christi Districts. Caliche is used in the Corpus Christi District. It was observed that approximately 1.5 percent lime was used with caliche aggregate in the base courses of the Corpus Christi District on a routine basis.

Limestone aggregate was collected from a stockpile in Hearne, Texas, with an original source of Kosse, Texas. Caliche was collected from Corpus Christi, Texas. The two materials were tested in both stabilized and unstabilized conditions.

Sieve analyses were performed on both limestone and caliche aggregates according to the ASTM D422-63 procedure, and the grain size distributions are graphically presented in Figure 4.5. It was observed that the caliche aggregate gradation was significantly coarser than the limestone aggregate gradation.

Lime

Commercially available hydrated lime was used as the stabilizer for both materials. Lime was added at rates of 0, 1, and 2 percent by weight to the aggregates in dry mixtures. An optimum

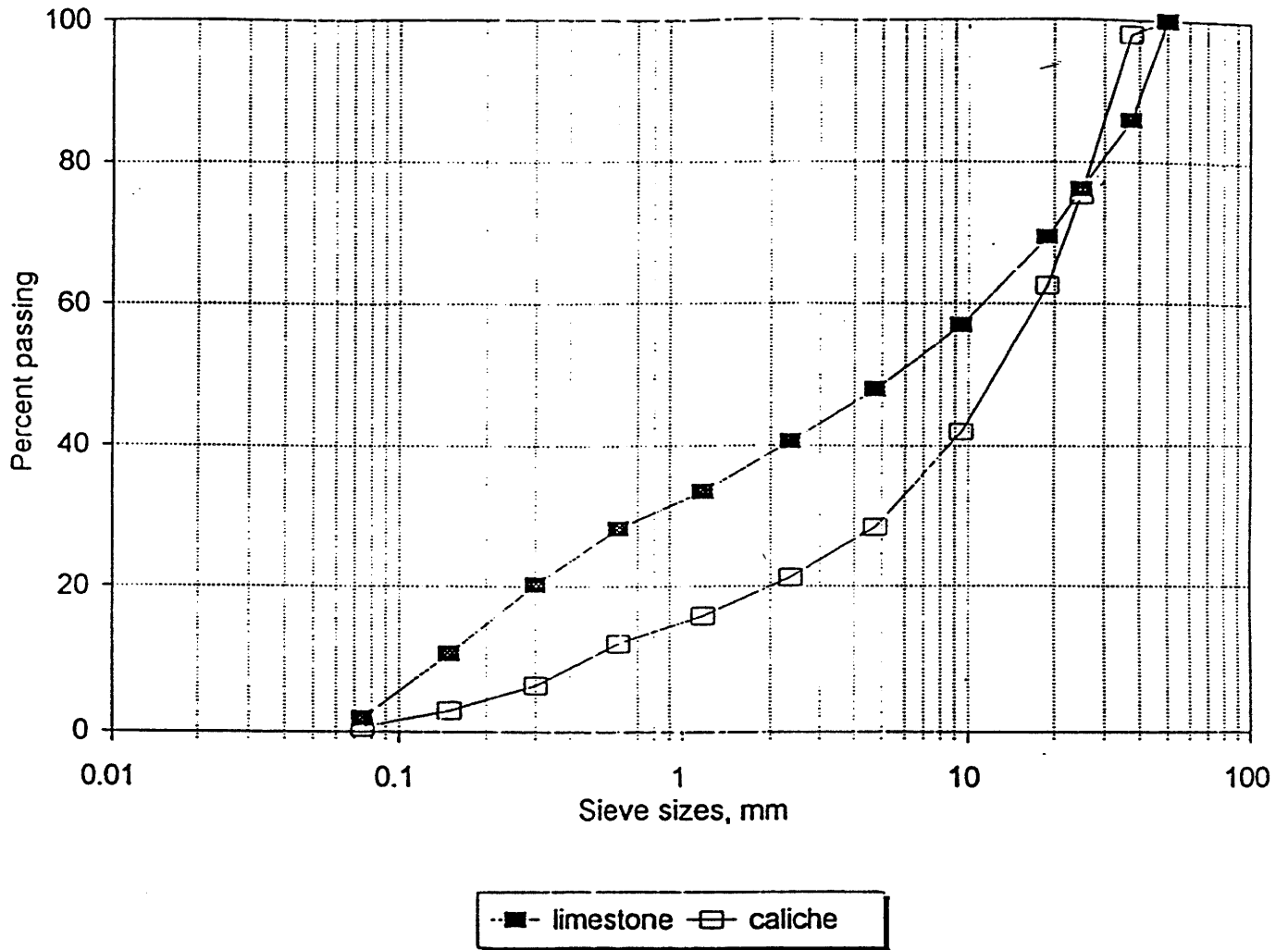


Figure 4.5. Sieve Analysis of Limestone and Caliche Aggregates.

amount of water was then added to the dry soil-lime mixtures. Optimum moisture contents for stabilized and unstabilized aggregates were determined in accordance with test method Tex 113-E.

4.6 SPECIMEN PREPARATION AND LABORATORY PROCEDURE

The laboratory procedure began with the processing of materials. Aggregates were oven-dried at 60°C for 24 hours. After the materials were taken out of the oven, they were allowed to cool and were then pulverized.

Moisture-Density Relationships

At first, moisture-density relationships were determined for limestone and caliche aggregate using test procedure Tex 113-E. Since it is known that the addition of lime immediately increases the optimum moisture content and decreases the dry density of the materials, moisture-density relationships were also established for limestone and caliche aggregate following the addition of 1 and 2 percent lime by weight. Lime was added to the dry materials and then mixed with water to determine the optimum moisture content of the mixture. An automatic compactor was used for compaction, and a hydraulic pump was used to extract the molds. Table 4.2 summarizes moisture-density data.

Table 4.2. Maximum Dry Densities and Optimum Moisture Contents of Stabilized and Unstabilized Limestone and Caliche.

Material Type	Percent Lime	Optimum Moisture Content (%)	Dry Density Kg/m ³
Limestone	0	8.0	2150
	1	9.5	2020
	2	11.0	1960
Caliche	0	11.5	1980
	1	13.0	1870
	2	13.5	1830

Texas Triaxial Test

The Texas triaxial compression test was performed to evaluate strength increase of limestone and caliche aggregate due to carbonate cementation.

Specimen Preparation

Test specimens were prepared at the optimum moisture content. Lime was mixed with the dry aggregate at rates of 0, 1 and 2 percent by dry weight, and then water was added slowly until the optimum moisture contents were reached for each aggregate lime mixture. After thorough mixing of the soil-lime mixtures with water, they were left in bowls covered with wet cloths for 2 hours. This was necessary so that the materials would not lose moisture and would be uniformly wetted. After a mellowing period of 2 hours, triaxial specimens were molded using an automatic compactor. A 4,540 gm hammer was dropped 50 times on each layer of four 50 mm thick layers to produce a 152 mm diameter and 216 mm high sample. The specimen heights were maintained as close to 216 mm as possible.

After compaction, each specimen was extruded from the mold with the help of a hydraulic pump. Extreme care was taken during the extraction process to make sure that the specimens remained intact with a consistent shape and size. Immediately after extraction, a latex rubber membrane was placed on each specimen keeping only the top of the specimen open to the atmosphere. This was done with the assumption that during and following construction, the carbonation reaction primarily occurs when CO₂ from the atmosphere diffuses into the lime stabilized layer through the top surface.

Curing of Specimens

The specimens were placed into an environmentally controlled chamber where a temperature of 25°C and a relative humidity of 80 percent were maintained throughout the entire curing period. Some specimens were cured for 28 days and some were cured for 60 days to observe the effect of curing time and also to evaluate the rate of the carbonation cementation reaction. Figure 4.6 is a photograph of some specimens in the environmentally controlled chamber during the curing process. The specimens were subjected to overnight capillary wetting and were then tested in compression. For capillary wetting, the specimens were placed on porous stones, and then filter papers were

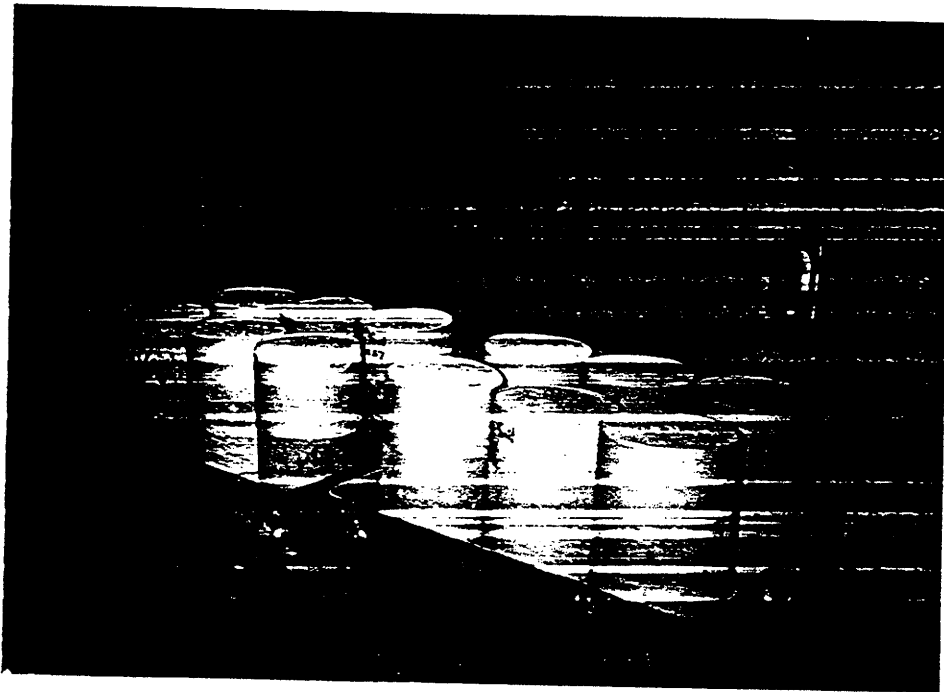


Figure 4.6. Photo of Specimens in the Environmentally Controlled Chamber During the Curing Process.

wrapped around the specimen. Water was poured into the pan, which contained the porous stones until the water level rose to approximately the middepth of the stones. Photographs of specimens subjected to overnight capillary wetting and a specimen under Texas triaxial testing are furnished in Figures 4.7 and 4.8 respectively.

Resilient Modulus Test

Test specimens were prepared in accordance with the AASHTO T274-82 procedure using the same optimum moisture contents, and the same compaction energies were used for the specimens prepared for triaxial strength testing. The samples were cured in the same manner as those samples used for triaxial testing. The specimens were subjected to overnight capillary wetting before the resilient modulus test was performed on a Materials Testing System (MTS) machine, with 200 repetitions applied at each deviatoric stress. A photograph of a specimen under resilient modulus

testing is shown in Figure 4.9.

Atterberg Limit Tests

Liquid limits and plastic limits were determined on all stabilized and unstabilized materials following ASTM D4318-84.

Other Tests

Particle size distribution analysis was performed at the Soil and Crop Science Department of Texas A&M University. In this analysis, bulk samples were dried in a forced-draft oven at 35°C and crushed between electric motor driven wooden rollers. The soil fines were passed through a 2-mm diameter sieve and mixed, and a representative sample was stored in a liter cardboard carton. Any significant quantities of coarse fragments were soaked overnight in water and washed upon a 2 mm sieve, collected, dried, weighed and related back to the quantity of total aggregate as a percentage by dry weight. Particle size distribution was determined in duplicate using the pipette method of Kilmer and Alexander (1949). Ten grams of samples in 400 ml of distilled water which contained 5 ml of 10 percent sodium hexametaphosphate were dispersed by shaking overnight on a horizontal oscillating shaker. Aliquots of 5 ml were taken at a 5 cm depth following a settling time as given by Stokes' equation. The percentages of calcite and dolomite were determined using the gasometric procedure of Dreimanis (1962).

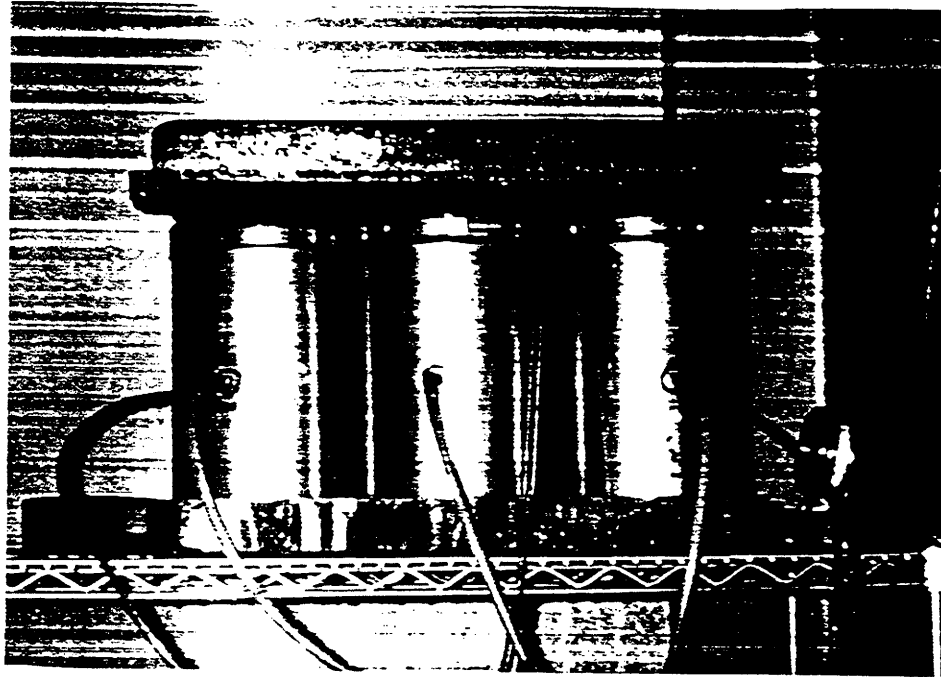


Figure 4.7. Photo of Specimens Subjected to Overnight Capillary Wetting.

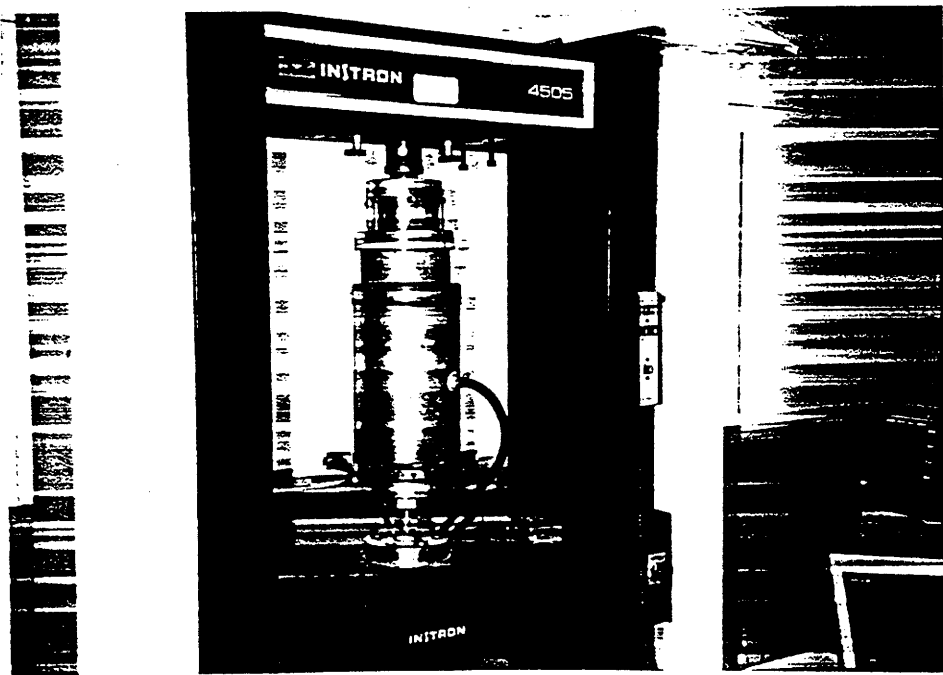


Figure 4.8. Photo of a Specimen Subjected to Texas Triaxial Compression Testing.

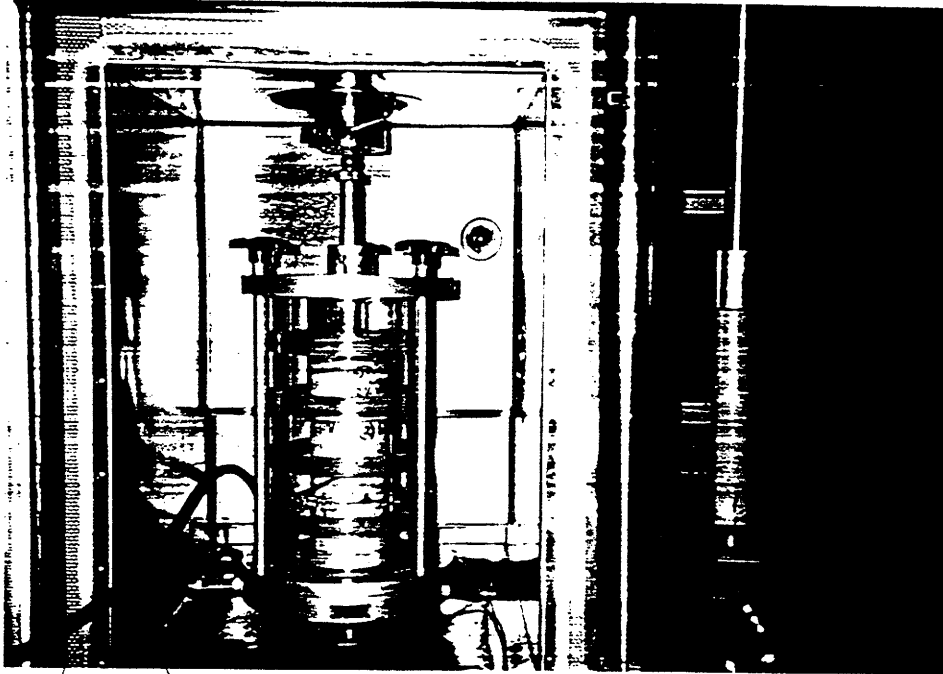


Figure 4.9. Photo of a Specimen Subjected to Laboratory Resilient Modulus Testing.

X-ray Diffraction Analysis

X-ray diffraction (XRD) analysis was performed at the Geology Department of Texas A&M University. Sample preparation included the grinding of material and fractionating into various size fractions. Approximately 1 gram of the clay size fraction was applied to a slide with acetone. The XRD spectrum was evaluated to determine the presence of minerals including calcite, quartz, and clay minerals. The characteristic X-ray peaks are presented in terms of diffraction angles (2θ). The intensities of calcite and quartz peaks at 29.449° and 26.6° , respectively, are the greatest.

Scanning Electron Microscopy

Visual characterization of both stabilized and unstabilized materials was done using scanning electron microscopy. A small amount of sample from each triaxial specimen was taken after they

were tested for triaxial strengths. The samples taken were then dried in an oven at 100°C and were taken to the SEM laboratory for viewing.

All SEM work was done at the Electron Microscopy Center of Texas A&M University using a JEOL JSM-6400 scanning electron microscope. The scope has a tungsten filament and a resolution of 3.5 nm, maximum magnification 300,000x. All work was done in the Secondary Electron Mode (SE). Sample preparation included mounting samples on carbon double-stick tape on aluminum stubs. A carbon glue was also used to improve adhesion and conductivity. The samples were coated with 300Å of gold/palladium using a Hummer I sputter coater.

4.7 FIELD TESTS

A field test was also carried out in this project to investigate the in situ resilient moduli of different pavement sections containing lime stabilized or unstabilized base courses. The field test was performed using a state-of-the-art deflection measuring device falling weight deflectometer (FWD). The FWD data was then backcalculated for pavement layer resilient moduli using a program called MODULUS.

Selection of Pavement Sections

Ten pavement sections in the Yoakum and Corpus Christi Districts were selected based on the preliminary survey of the available information on those pavement sections. Two pavements in the Yoakum District contained limestone base courses of which one was lime stabilized. One of the eight pavement sections in Corpus Christi District contained an unstabilized limestone base course. Each of the other pavement sections in Corpus Christi District contained lime stabilized caliche aggregate in the base course. Stabilized base courses were stabilized with either 1.5 or 2 percent lime.

Test Operation and Data Analysis

FWD testing was performed at three different sections on each of the selected highways. Each section was 150 meters long, and the test was run at 12.5 meter intervals. At each test point, four drops of loads of varying magnitude were applied. The magnitudes of the four load drops were in the neighborhood of 26.66 kN, 35.56 kN, 44.44 kN, and 62.22 kN. The tests were performed in the

wheel paths of the pavement sections.

The FWD deflection data for a load drop of 44.44 kN was chosen for backcalculation since that was the closest value to the standard 80 kN single axle load. Ranges of moduli values for the surface, base course, and subbase were assigned as input to the program while the subgrade layers were given fixed moduli values. Poisson's ratios for surface, base course, subbase layers were assumed to be 0.35, and the subgrade Poisson's ratio was assumed to be 0.40.

4.8 RESULTS AND DISCUSSION OF LABORATORY AND FIELD EVALUATIONS

Mineralogical Analysis

Since the objective of this research was to investigate the strength increase due to carbonate cementation, a mineralogical analysis was performed on representative samples to check for the presence of clay minerals. Particle size distribution revealed that both materials contained clay-sized particles (Table 4.3). However, x-ray diffraction analysis showed that both limestone and caliche materials contained primarily calcite and quartz and no apparent phyllosilicate (Figure 4.10 and 4.11). Absence of definable phyllosilicate indicates that there should be little if any, pozzolanic reactions between the lime and aggregates. A close evaluation of the x-ray diffraction spectra in Figures 4.10 and 4.11 reveals that evidence of clay minerals could be partially masked by the intense peaks of the highly crystalline minerals. However, if clay minerals are present, they are present at very low concentration levels (too low to significantly contribute to pozzolanic reactivity).

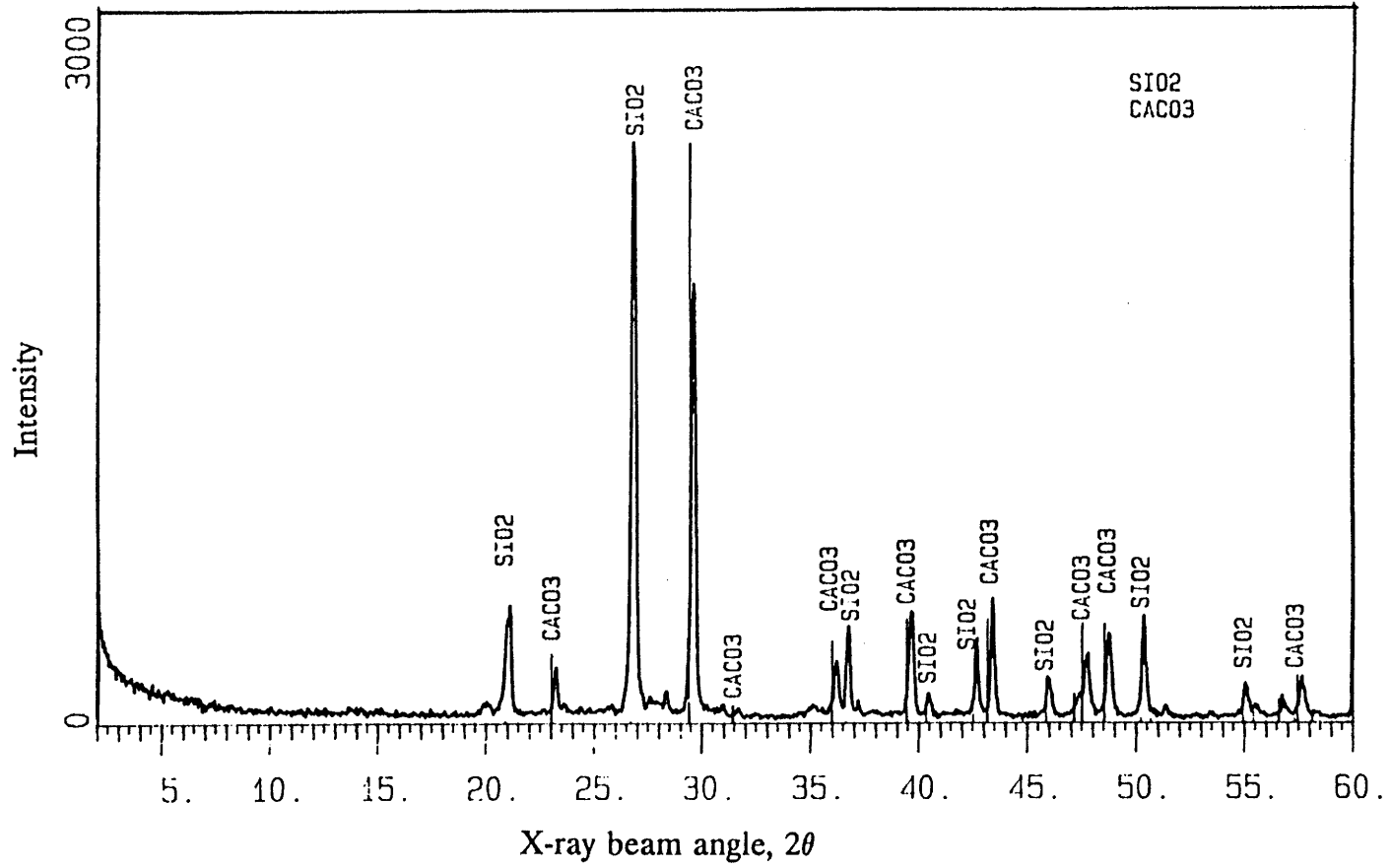


Figure 4.10. X-ray Diffraction Analysis of Natural Limestone.

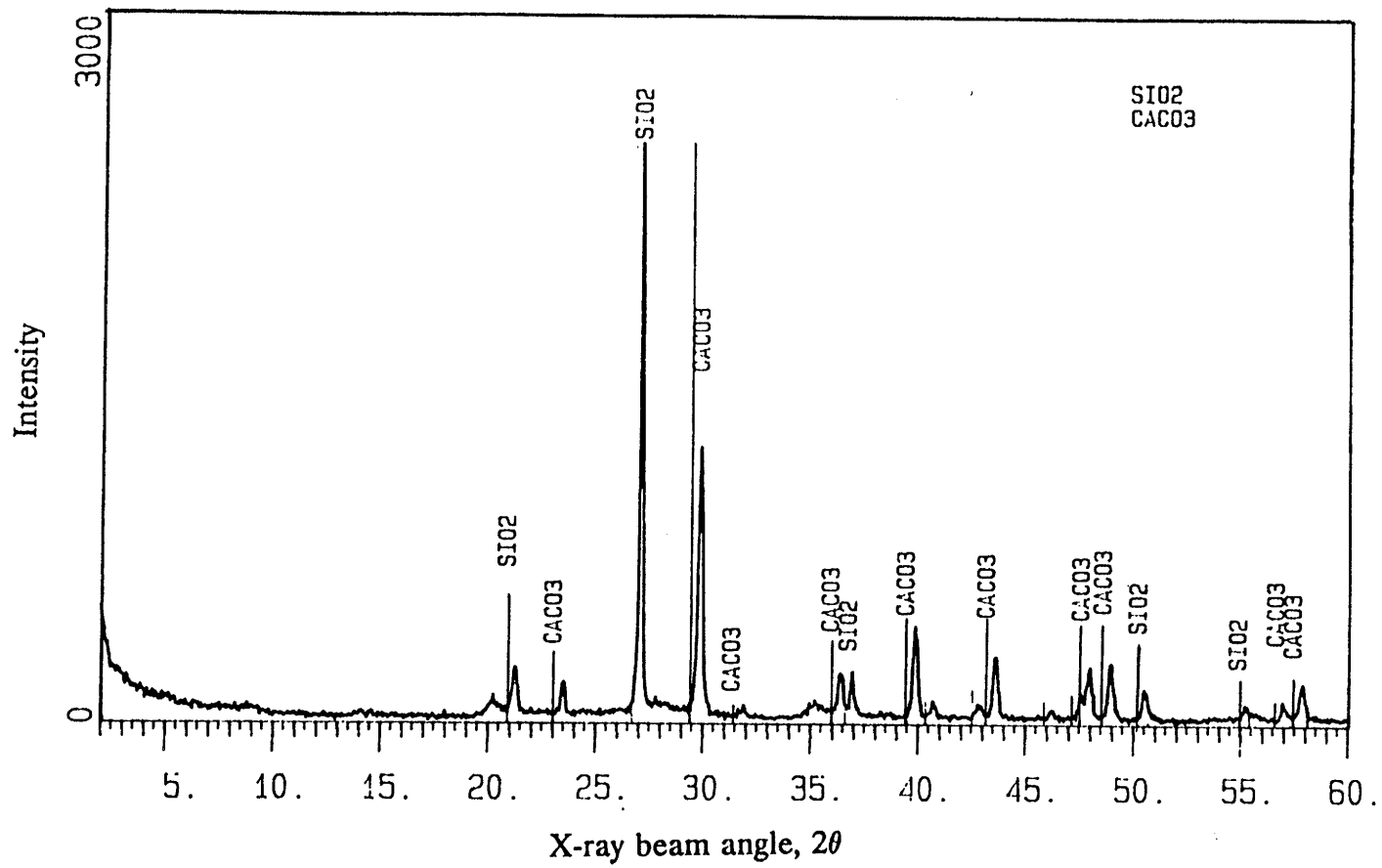


Figure 4.11. X-ray Diffraction Analysis of Natural Caliche.

Table 4.3. Particle Size Distribution and Calcite Content of Limestone and Caliche.

Material Type	Particle Size Distribution, mm			Calcite
	Sand (2-.05)	Silt (.05-.002)	Clay (<.002)	
Limestone	72.3	18.7	9.0	31.1
Caliche	55.5	15.7	16.9	23.2

Atterberg Limits

Atterberg limit test results are presented in Table 4.4. Liquid limits, plastic limits, and plasticity indices were determined for limestone and caliche soil treated with 0, 1, and 2 percent lime. Liquid limits and plastic limits both tended to increase with an increased percentage of lime, but plastic limits increased more than the liquid limits, resulting in a reduction in plasticity indices.

Texas Triaxial Strength

Texas triaxial strength data demonstrate substantial strength increases due to lime treatment. Triaxial strength data for limestone are furnished in Tables 4.5 and 4.6 while strength data for

Table 4.4. Atterberg Limit Test Results for Limestone and Caliche with 0, 1, and 2 Percent Lime.

Percent Lime	Limestone			Caliche		
	Liquid Limit	Plastic Limit	PI	Liquid Limit	Plastic Limit	PI
0	27.3	22.9	4.4	39.2	29.3	9.9
1	28.6	26.9	1.7	41.4	37.1	4.3
2	29.1	28.8	0.3	43.4	42.3	1.1

* PI = Plasticity Index

Table 4.5. Triaxial Test Data for Limestone after 28 Days of Curing.

Percent Lime	Confining Pressure, kPa	Sample #	Percent Moisture Content, %	Triaxial Strength, MPa
0	0	#1	8.2	0.60
		#2	8.3	0.70
	100	#1	7.5	1.20
		#2	6.7	1.12
1	0	#1	7.4	1.27
		#2	7.9	0.85
	100	#1	8.7	1.74
		#2	7.4	1.27
2	0	#1	9.6	0.74
		#2	9.3	0.86
	100	#1	8.3	1.98
		#2	9.0	1.62

Table 4.6. Triaxial Test Data for Limestone after 60 Days of Curing.

Percent Lime	Confining Pressure, kPa	Sample #	Percent Moisture Content, %	Triaxial Strength, MPa
0	0	#1	8.5	0.22
		#2	7.9	0.24
	100	#1	7.1	1.12
		#2	7.1	1.14
1	0	#1	9.2	0.96
		#2	7.7	1.24
	100	#1	8.7	2.18
		#2	7.8	1.94
2	0	#1	9.5	0.82
		#2	9.6	0.93
	100	#1	9.3	1.95
		#2	9.1	2.17

caliche are shown in Tables 4.7 and 4.8. The average strength in each case with the calculated cohesion and angle of friction for limestone and caliche bases are shown in Tables 4.9, 4.10, 4.11 and 4.12. According to the Tables 4.5, 4.6, 4.7, and 4.8, moisture contents of the samples were very close to the prescribed optimum for maximum density with the stabilized samples prepared and maintained at a slightly higher moisture content than the unstabilized samples. Therefore, the significant strength difference between stabilized and unstabilized samples are not likely due to moisture differences.

Cohesion and angle of friction values were determined by plotting a Mohr-circle diagram from triaxial data. The chart for classification of subgrade and flexible base material in the Texas triaxial test method is a family of failure envelopes. For a particular case, the failure envelope is drawn and transferred to the chart. Classification of the material can be achieved to the nearest one-tenth of a class. The critical point, or the weakest condition, is selected when the envelope of failure falls between class limits. The measurement of the vertical distance down from a boundary line to the point provides the classification. Significant increases in cohesion and slight increases in angle of internal friction were observed in all stabilized specimens. The cohesion and internal friction values determined in Texas triaxial testing are not "pure" values. This is because test peculiarities such as the stiffness of the membrane and the nature of confinement affect these parameters. However, the relative values can be effectively used to rank the performance of various materials.

SEM Examinations

Scanning electron microscopy images of materials taken from the triaxial samples also showed evidence of carbonate precipitates leading to bonding of particles in stabilized samples. Two samples for each test variable including material type, curing time, and percent lime, were scanned to evaluate differences. Figures 4.12 through 4.14 show representative images of unstabilized and stabilized limestone while Figures 4.15 through 4.17 show representative images of unstabilized and stabilized caliche soil. All images shown in Figures 4.12 through 4.17 were from samples extracted from triaxial test specimens which were tested at 100 kPa confining pressure. These images represent a typical and consistent visualization of the samples evaluated and not isolated situations.

Table 4.7. Triaxial Test Data for Caliche after 28 Days of Curing.

Percent Lime	Confining Pressure, kPa	Sample #	Percent Moisture Content, %	Triaxial Strength, MPa
0	0	#1	16.5	0.10
		#2	13.5	0.18
	100	#1	16.0	0.62
		#2	13.3	0.95
1	0	#1	15.3	0.40
		#2	14.0	0.56
	100	#1	15.9	1.08
		#2	15.4	1.14
2	0	#1	16.2	0.66
		#2	17.2	0.60
	100	#1	15.3	1.81
		#2	17.0	1.34

Table 4.8. Triaxial Test Data for Caliche after 60 Days of Curing.

Percent Lime	Confining Pressure, kPa	Sample #	Percent Moisture Content, %	Triaxial Strength, MPa
0	0	#1	13.7	0.22
		#2	13.5	0.20
	100	#1	13.5	0.79
		#2	13.2	0.82
1	0	#1	16.4	0.30
		#2	15.5	0.34
	100	#1	16.3	1.08
		#2	16.0	1.07
2	0	#1	16.6	0.67
		#2	15.7	0.62
	100	#1	16.4	1.52
		#2	15.0	1.63

Table 4.9. Summary of Average Triaxial Strength and Other Calculated Parameters for Limestone after 28 Days of Curing.

Percent Lime	Texas Triaxial Strength, MPa		Cohesion, c	Angle of Friction, ϕ	Triaxial Class
	Confining Pressure, 0 kPa	Confining Pressure, 100 kPa			
0	0.65	1.16	0.15	41.2	3.2
1	1.10	1.50	0.25	39.9	2.0
2	0.80	1.60	0.17	47.0	2.0

Table 4.10. Summary of Average Triaxial Strength and Related Strength Parameters for Limestone after 60 Days of Curing.

Percent Lime	Texas Triaxial Strength, MPa		Cohesion, c	Angle of Friction, ϕ	Triaxial Class
	Confining Pressure, 0 kPa	Confining Pressure, 100 KPa			
0	0.23	1.13	0.04	52.4	3.2
1	1.10	2.00	0.18	53.6	2.0
2	0.87	2.00	0.13	55.9	2.0

Table 4.11. Summary of Average Triaxial Strength and Related Strength Parameters for Caliche after 28 Days of Curing.

Percent Lime	Texas Triaxial Strength, MPa		Cohesion, c	Angle of Friction, ϕ	Triaxial Class
	Confining Pressure, 0 kPa	Confining Pressure, 100 kPa			
0	0.14	0.78	0.03	45.9	3.7
1	0.48	1.11	0.09	46.5	3.2
2	0.63	1.53	0.10	53.3	2.5

Table 4.12. Summary of Average Triaxial Strength and Other Calculated Parameters for Caliche after 60 Days of Curing.

Percent Lime	Texas Triaxial Strength, MPa		Cohesion, c	Angle of Friction, ϕ	Triaxial Class
	Confining Pressure, 0 kPa	Confining Pressure, 100 kPa			
0	0.21	0.81	0.04	44.7	3.7
1	0.32	1.07	0.06	48.6	3.2
2	0.64	1.57	0.10	53.3	2.5

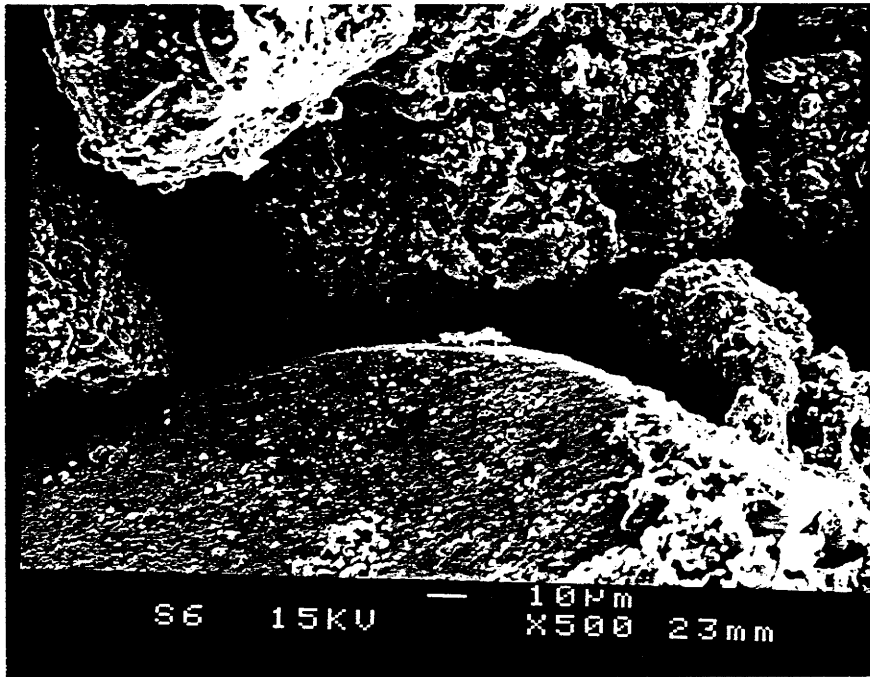


Figure 4.12. SEM Image of Unstabilized Limestone (X500).

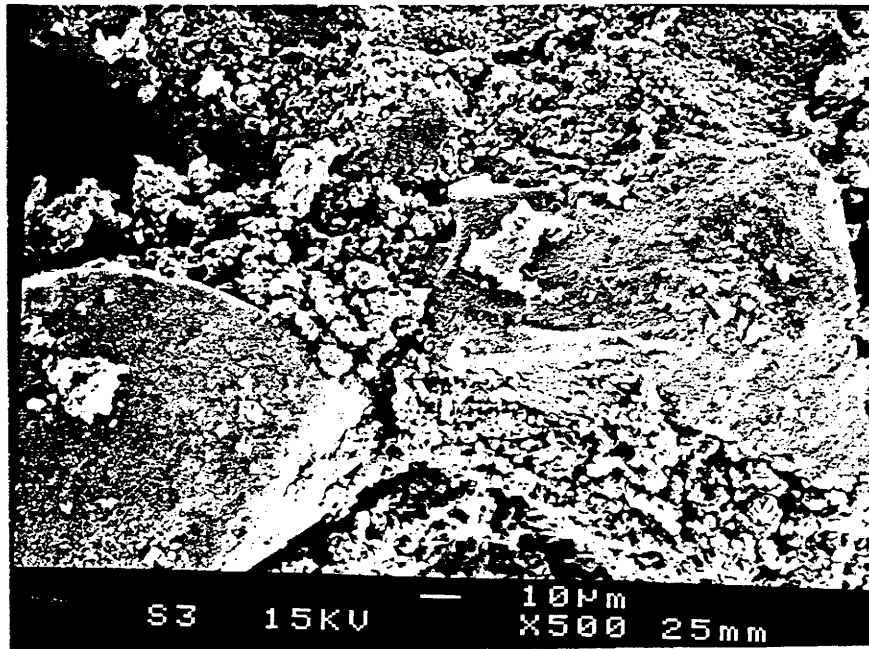


Figure 4.13. SEM Image of Limestone Stabilized with 1 Percent Hydrated Lime (X500).

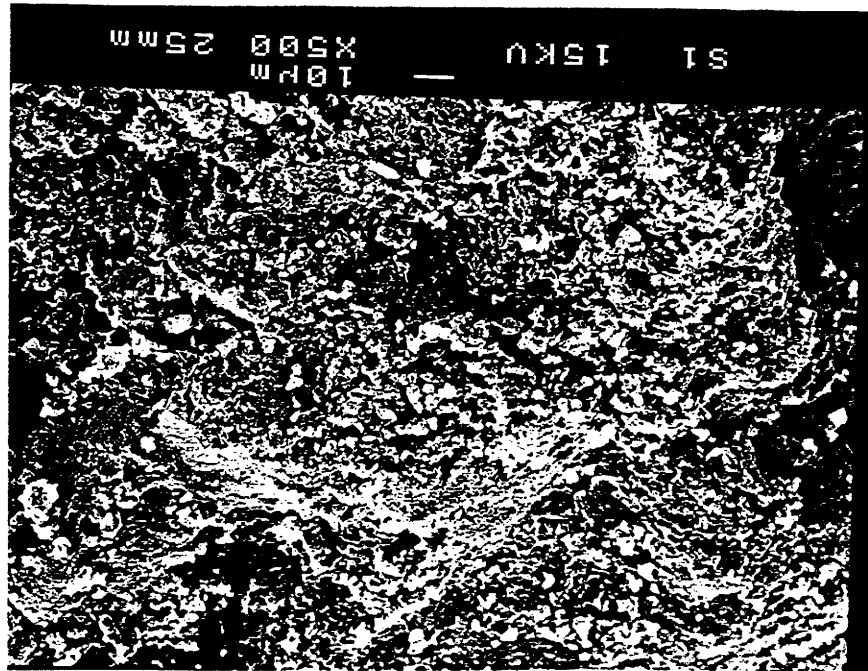


Figure 4.14. SEM Image of Limestone Stabilized with 2 Percent Hydrated Lime (X500).

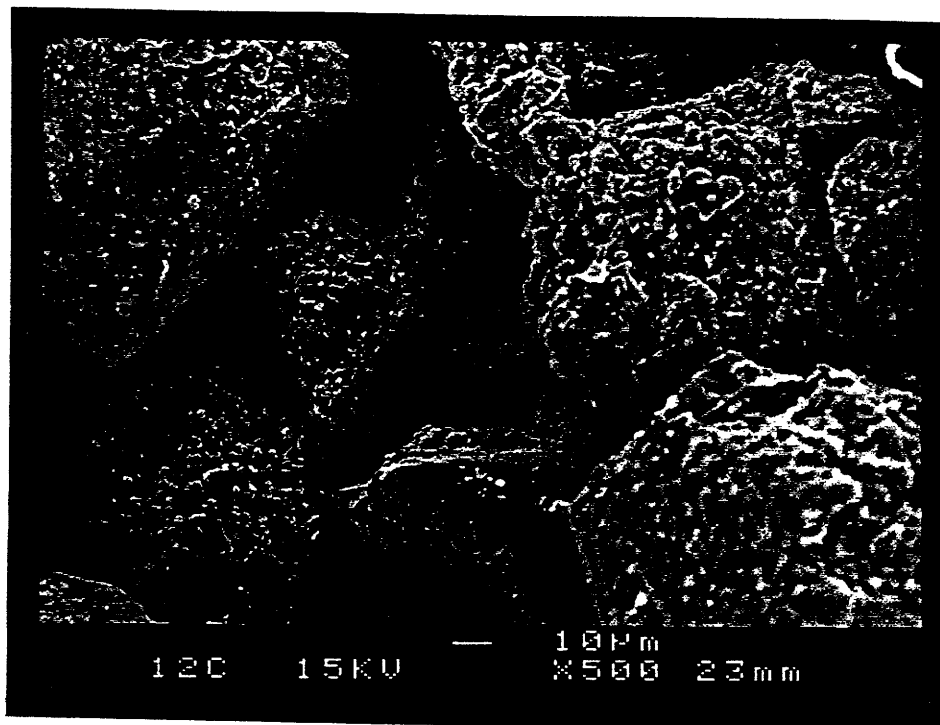


Figure 4.15. SEM Image of Unstabilized Caliche (X500).

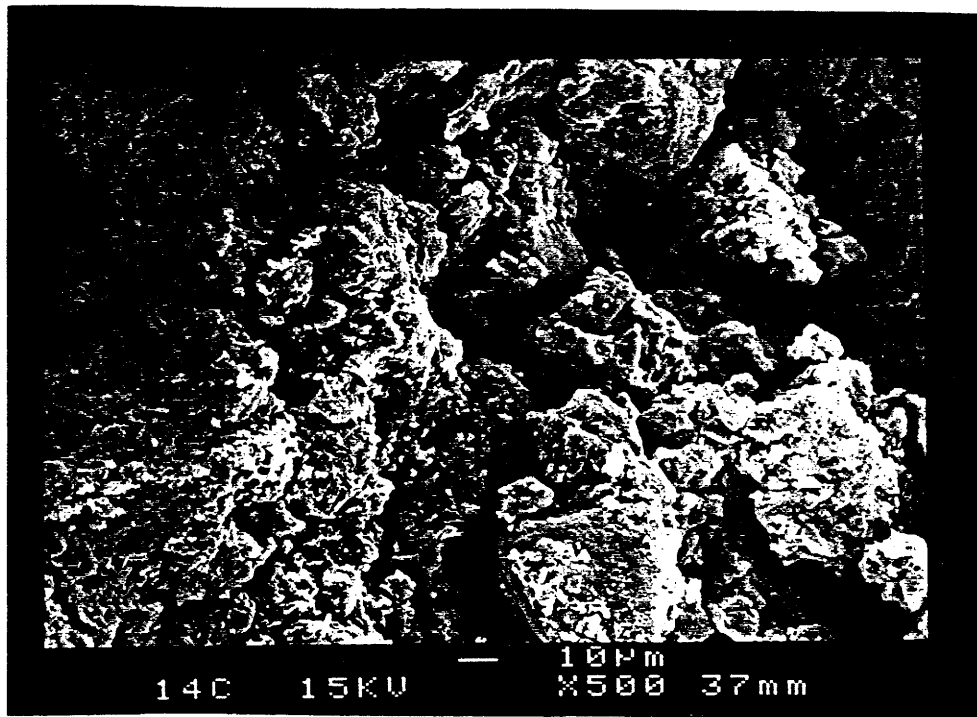


Figure 4.16. SEM Image of Caliche Stabilized with 1 Percent Hydrated Lime (X500).

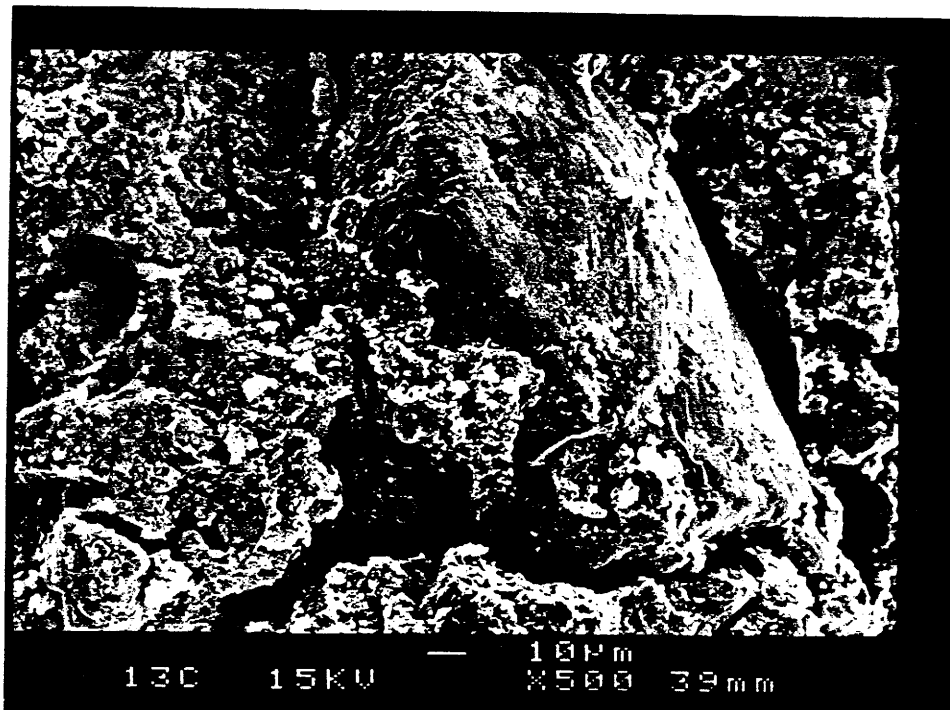


Figure 4.17. SEM Image of Caliche Stabilized with 2 Percent Hydrated Lime (X500).

Resilient Modulus

Resilient moduli values from lab tests are summarized in Tables 4.13 through 4.24. Tables 4.13 through 4.18 show the resilient moduli values of the samples that were tested in a dry condition which means the samples were tested immediately after they were taken out of the curing chamber. Tables 4.19 through 4.24, on the other hand, summarize the resilient moduli values of samples that were soaked overnight before being tested. Figures 4.18 and 4.21 show four typical plots of resilient moduli versus deviatoric stresses for limestone and caliche, respectively, with and without lime treatment. Plots showing the effect of change in deviatoric stress on resilient modulus have almost the same pattern for all specimens. Moduli values increased up to a certain level of deviatoric stress and then decreased. The effect of lime treatment on resilient modulus of limestone aggregate in the wet condition is graphically shown in Figures 4.18 and 4.19 while the same for caliche aggregate are shown in Figures 4.20 and 4.21. The differences in moduli values due to the variation in lime content for both limestone and caliche aggregate are graphically presented in Figures 4.22 and 4.23.

Field Data

Table 4.25 summarizes in situ resilient moduli backcalculated from FWD data from 10 pavement sections with either lime-stabilized caliche, lime-stabilized limestone or unstabilized limestone bases in the Yoakum and Corpus Christi Districts. Although the moduli values for all the layers of the pavements were back-calculated from the field data, only the base course moduli are shown in Table 4.25 as they are of primary interest. All of the caliche base courses have 200 mm of 4 percent lime stabilized natural soil supporting them. On the other hand, two of the limestone base courses have 150 mm of lime stabilized natural soil supporting them, while the third is only supported by natural subgrade.

4.9 STATISTICAL ANALYSIS

Paired-Comparisons T Test

In the test method, for paired comparisons, a variable related to the differences between the paired variables is created to test whether the mean difference is significantly different from zero. The steps that are followed in paired-comparisons t test are given below.

Table 4.13. Laboratory Data of Resilient Moduli for Unstabilized Limestone in Dry Condition.

Percent Lime	Confining Pressure, KPa	Resilient Modulus, MPA Deviatoric Stress (σ_d), KPa							
		7	14	35	70	100	140	170	200
0%	140	827	1285	1468	1665	1155	262	207	186
0%	100	758	1006	1364	1496	1114	214	172	165
0%	70	758	854	1337	1420	965	165	145	131
0%	35	792	944	1185	772	631	131	117	117
0%	7	661	937	924	717	396	126	117	90

*Moisture content of the sample during test = 3.5 percent

Table 4.14. Laboratory Data of Resilient Moduli for Limestone with 1 Percent Lime in Dry Condition.

Percent Lime	Confining Pressure, KPa	Resilient Modulus, MPA Deviatoric Stress (σ_d), KPa							
		7	14	35	70	100	140	170	200
1%	140	941	1233	1881	2956	3090	3286	1844	1333
1%	100	899	1016	1785	2707	2728	2610	1044	925
1%	70	859	965	1660	2290	2321	1948	1000	456
1%	35	789	916	1599	2029	2073	1211	666	336
1%	7	755	937	1357	1298	1352	1038	433	244

*Moisture content of the sample during test = 5.5 percent

Table 4.15. Laboratory Data of Resilient Modulus for Limestone with 2 Percent Lime in Dry Condition.

Percent Lime	Confining Pressure, KPa	Resilient Modulus, MPA Deviatoric Stress (σ_d), KPa							
		7	14	35	70	100	140	170	200
2%	140	1079	1189	1854	2687	3362	3637	3623	1888
2%	100	999	1130	1757	2508	3225	3203	2820	1764
2%	70	934	1096	1795	2377	2869	2631	2680	1275
2%	35	896	1026	1705	2276	2680	2402	1985	779
2%	7	896	1040	1423	2022	2035	1728	867	682

*Moisture content of the sample during test = 5.5 percent

Table 4.16. Laboratory Data of Resilient Modulus for Unstabilized Caliche in Dry Condition.

Percent Lime	Confining Pressure, KPa	Resilient Modulus, MPA Deviatoric Stress (σ_d), KPa							
		7	14	35	70	100	140	170	200
0%	140	458	592	995	462	262	227	172	138
0%	100	406	506	913	400	248	199	138	110
0%	70	382	516	930	441	245	193	138	110
0%	35	361	492	837	400	227	165	131	96
0%	7	348	392	744	455	214	152	124	110

*Moisture content of the sample during test = 9.5 percent

Table 4.17. Laboratory Data of Resilient Modulus for Caliche with 1 Percent Lime in Dry Condition.

Percent Lime	Confining Pressure, KPa	Resilient Modulus, MPA Deviatoric Stress (σ_d), KPa							
		7	14	35	70	100	140	170	200
1%	140	531	655	847	1371	1192	1089	961	927
1%	100	488	599	838	1197	655	475	386	338
1%	70	475	599	837	1185	682	475	379	338
1%	35	434	551	806	1082	717	510	386	331
1%	7	407	544	792	999	648	434	324	276

*Moisture content of the sample during test = 10 percent

Table 4.18. Laboratory Data of Resilient Modulus for Caliche with 2 Percent Lime in Dry Condition.

Percent Lime	Confining Pressure, KPa	Resilient Modulus, MPA Deviatoric Stress (σ_d), KPa							
		7	14	35	70	100	140	170	200
2%	140	710	1075	1399	2018	2511	2394	930	847
2%	100	700	1075	1381	1994	2483	2159	783	727
2%	70	685	992	1299	1912	2203	1075	558	407
2%	35	665	926	1233	1908	2152	941	551	420
2%	7	634	889	1223	1843	2086	885	448	358

*Moisture content of the sample during test = 10.5 percent

Table 4.19. Laboratory Data of Resilient Modulus for Unstabilized Limestone in Wet Condition.

Percent Lime	Confining Pressure, KPa	Resilient Modulus, MPA Deviatoric Stress (σ_d), KPa							
		7	14	35	70	100	140	170	200
0%	140	807	1040	1390	1630	972	200	159	138
0%	100	627	986	1250	1390	993	159	117	103
0%	70	786	876	1220	1280	345	124	97	90
0%	35	655	765	1070	579	110	90	69	76
0%	7	689	758	807	103	69	55	48	48

*Moisture content of the sample during test = 8 percent

Table 4.20. Laboratory Data of Resilient Modulus for Limestone with 1 Percent Lime in Wet Condition.

Percent Lime	Confining Pressure, KPa	Resilient Modulus, MPA Deviatoric Stress (σ_d), KPa							
		7	14	35	70	100	140	170	200
1%	140	827	1180	1760	2410	2490	2520	1770	558
1%	100	800	938	1740	2210	2300	1920	724	310
1%	70	724	841	1590	1750	1950	1280	359	221
1%	35	745	1070	1590	1500	1030	407	179	145
1%	7	689	910	1250	1140	303	186	117	117

*Moisture content of the sample during test = 11.5 percent

Table 4.21. Laboratory Data of Resilient Modulus for Limestone with 2 Percent Lime in Wet Condition.

Percent Lime	Confining Pressure, KPa	Resilient Modulus, MPA Deviatoric Stress (σ_d), KPa							
		7	14	35	70	100	140	170	200
2%	140	703	1080	1600	2670	2890	3590	3340	862
2%	100	958	1120	1790	2430	3210	2990	2480	1050
2%	70	945	1050	1700	2340	2780	2530	1980	738
2%	35	862	1070	1670	2270	2500	2220	1700	579
2%	7	883	993	1310	1870	1950	1570	545	414

*Moisture content of the sample during test = 11.5 percent

Table 4.22. Laboratory Data of Resilient Modulus for Unstabilized Caliche in Wet Condition.

Percent Lime	Confining Pressure, KPa	Resilient Modulus, MPA Deviatoric Stress (σ_d), KPa							
		7	14	35	70	100	140	170	200
0%	140	140	152	135	129	125	123	119	200
0%	100	133	145	137	127	116	100	93	90
0%	70	128	145	132	124	98	90	81	69
0%	35	125	140	131	119	95	75	53	49
0%	7	119	138	125	115	48	45	39	36

*Moisture content of the sample during test = 16 percent

Table 4.23. Laboratory Data of Resilient Modulus for Caliche with 1 Percent Lime in Wet Condition.

Percent Lime	Confining Pressure, KPa	Resilient Modulus, MPA Deviatoric Stress (σ_d), KPa							
		7	14	35	70	100	140	170	200
1%	140	152	200	276	331	290	145	129	125
1%	100	148	200	262	310	248	142	129	122
1%	70	131	172	255	310	200	136	102	98
1%	35	138	165	207	221	159	100	90	89
1%	7	124	165	186	200	150	99	87	82

*Moisture content of the sample during test = 18 percent

Table 4.24. Laboratory Data of Resilient Modulus for Caliche with 2 Percent Lime in Wet Condition.

Percent Lime	Confining Pressure, KPa	Resilient Modulus, MPA Deviatoric Stress (σ_d), KPa							
		7	14	35	70	100	140	170	200
2%	140	165	241	283	345	290	195	164	150
2%	100	152	200	303	317	256	190	151	139
2%	70	159	205	300	331	218	158	135	126
2%	35	159	193	255	234	160	140	110	103
2%	7	145	179	221	214	125	113	95	85

*Moisture content of the sample during test = 18 percent

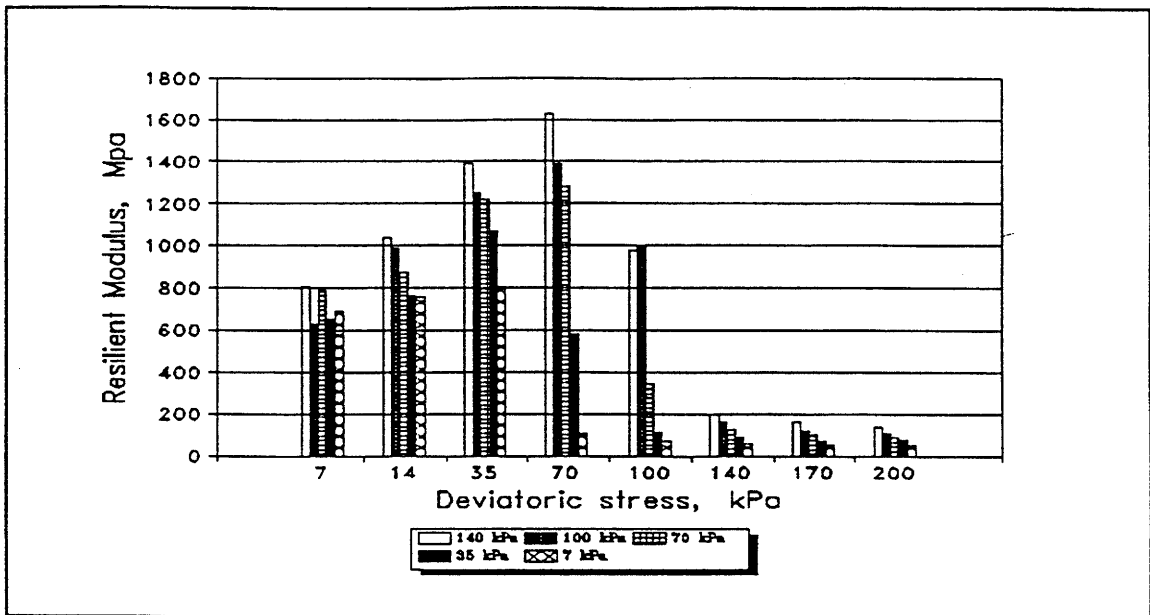


Figure 4.18. Resilient Modulus Versus Deviatoric Stress for Natural Limestone in Wet Condition.

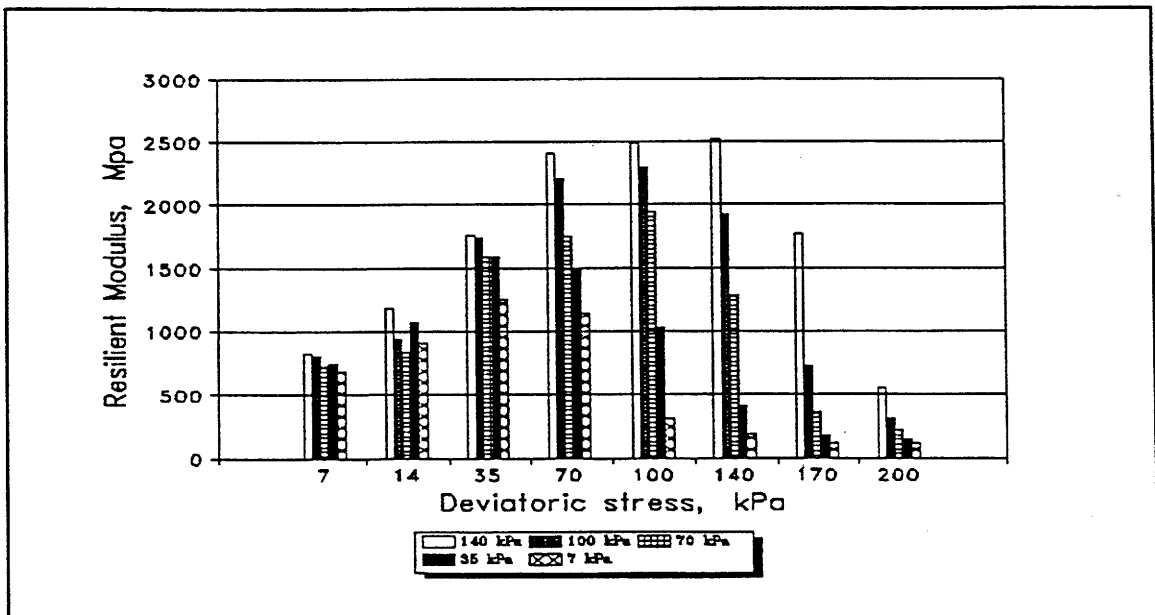


Figure 4.19. Resilient Modulus Versus Deviatoric Stress for Limestone Stabilized with 1 Percent Lime in Wet Condition.

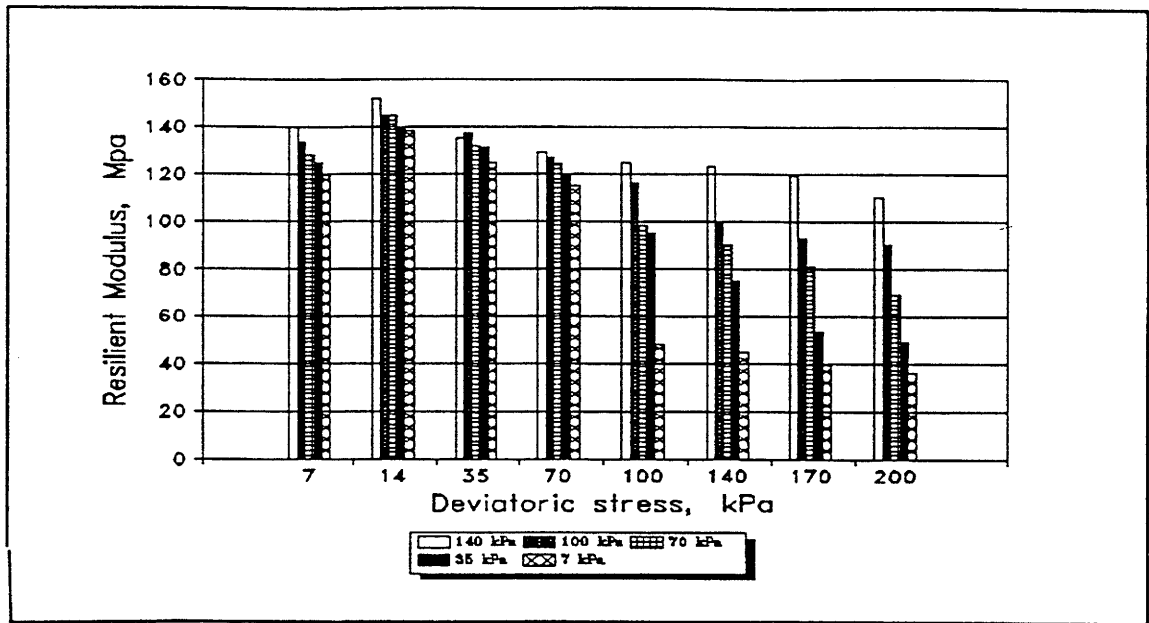


Figure 4.20. Resilient Modulus Versus Deviatoric Stress for Natural Caliche in Wet Condition.

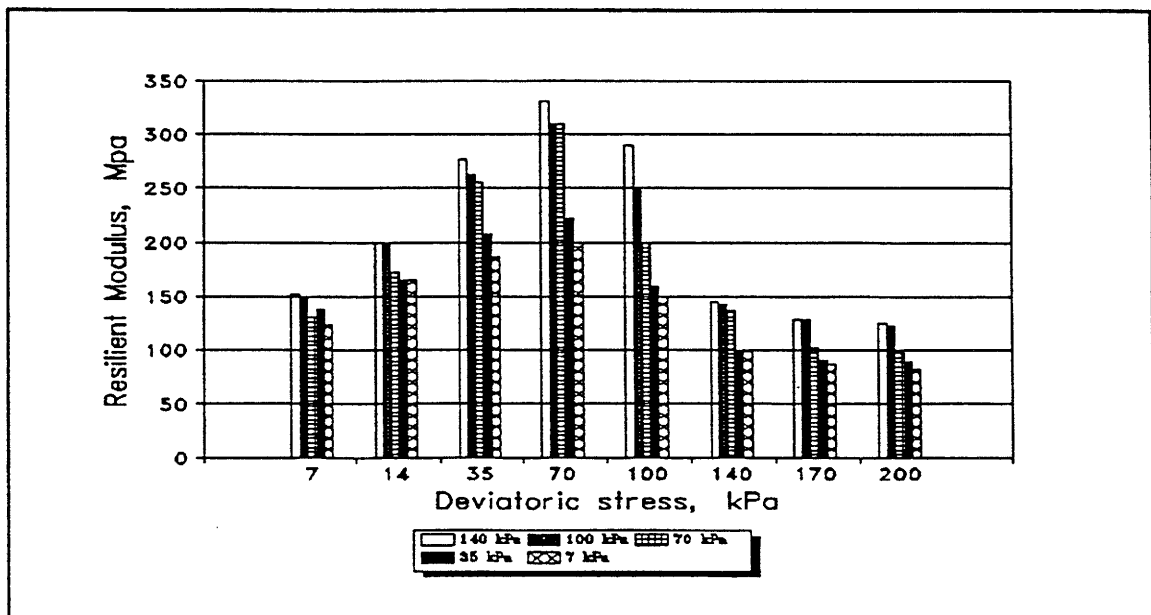


Figure 4.21. Resilient Modulus Versus Deviatoric Stress for Caliche Stabilized with 1 Percent Lime in Wet Condition.

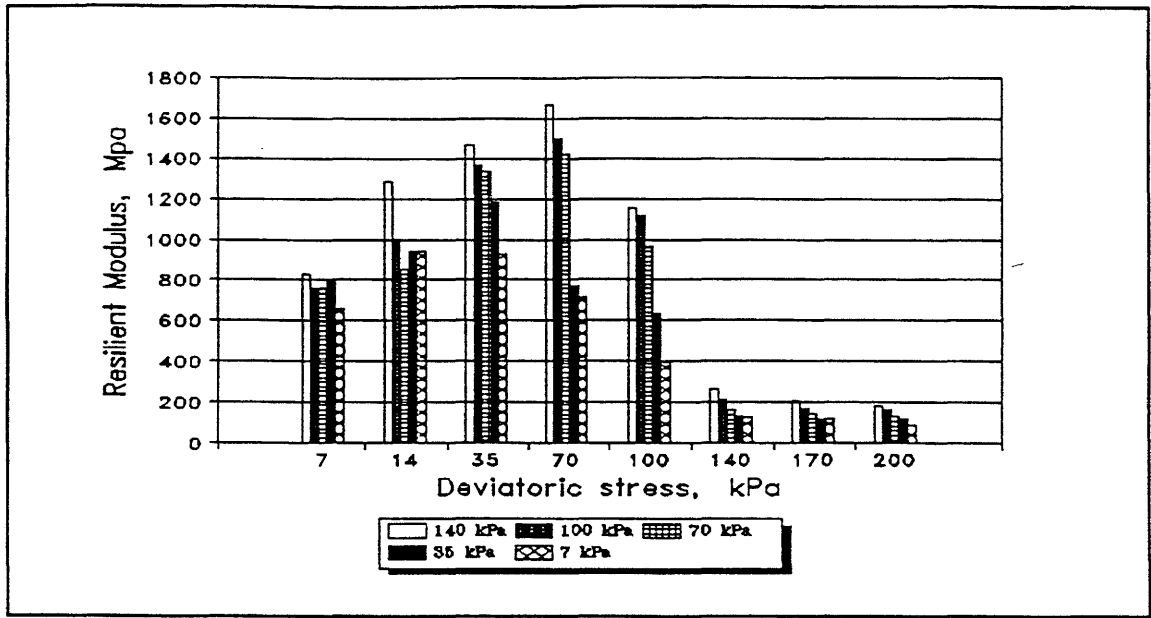


Figure 4.22. Resilient Modulus Versus Deviatoric Stress for Limestone Stabilized with 1 Percent Lime in Dry Condition.

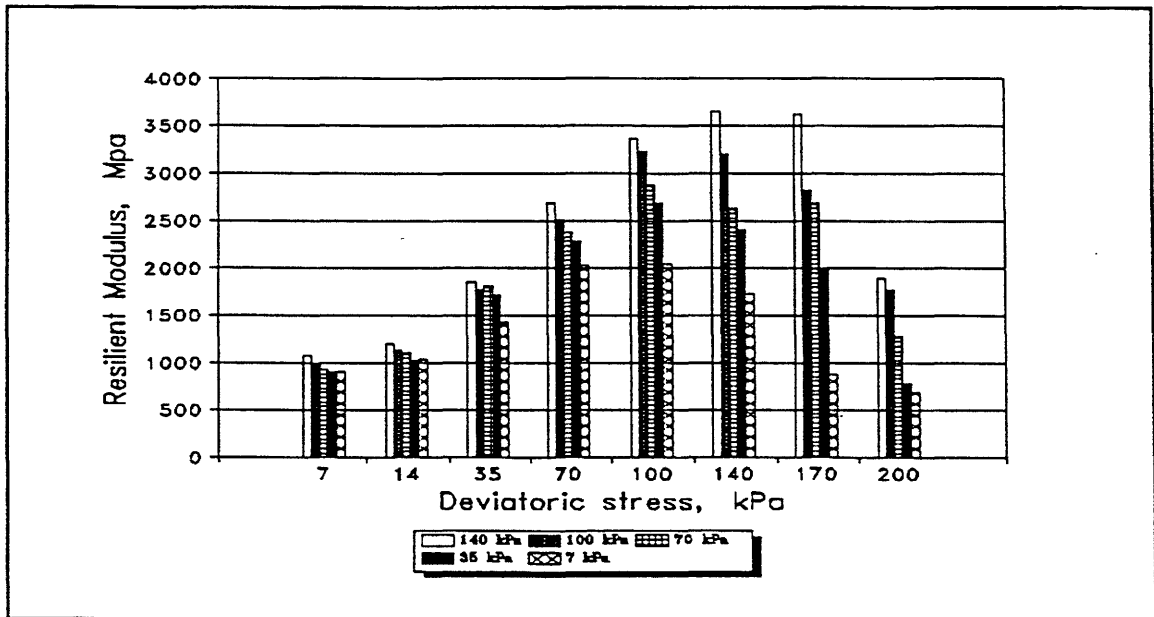


Figure 4.23. Resilient Modulus Versus Deviatoric Stress for Limestone Stabilized with 2 Percent Lime in Dry Condition.

Table 4.25. Backcalculated Moduli Values from FWD Data for Stabilized and Unstabilized Base Courses in Yoakum and Corpus Christi Districts of Texas.

County	Highway	Description of Base Courses	Number of Deflection Basins	Average Modulus Base Layers, MPa
Matagorda	FM1468	200 mm limestone with 2% lime	33	483
Fayette	SH71	150 mm limestone (unstabilized)	33	207
Nueces	SH286	660 mm limestone (unstabilized)	30	276
Refugio	FM136	150 mm caliche with 1.5% lime	30	1380
Jim Wells	US281	300 mm caliche with 1.5% lime	30	207
San Pat.	US77	150 mm caliche, 125 mm caliche (1.5% lime)	30	345
San Pat.	FM1069	200 mm caliche with 1.5% lime	30	8410
Nueces	BS-44C	250 mm caliche with 1.5% lime	30	828
Nueces	SH357	200 mm caliche with 1.5% lime	30	287
Nueces	FM24	300 mm caliche with 1.5% lime	24	414

If the computed value of t_{ts} (test statistic value) exceeds the critical value (tabular value), then the null hypothesis

$$H_0 : \mu_D = 0$$

is rejected in favor of the alternative hypothesis

$$H_a : \mu_D > 0$$

Test Statistic:

$$t_{ts} = (D_{\text{mean}} - \mu_D) / (S_D / \sqrt{(n-1)}),$$

n = the number of matched pairs of scores in the sample,

D = the difference between post and pre scores for each pair of scores in the sample,

D_{mean} = the mean of all the sample's difference scores,

S_D = the sample standard deviation of the difference scores and

μ_D = the mean of the difference scores for all possible pairs in the population.

The summary of the paired-comparisons t test is given in Table 4.26. Statistical analysis shows that there are significant differences between the triaxial strength of unstabilized and stabilized limestone and caliche aggregate.

4.10 DISCUSSION

Evidently, both the base course materials contain some very fine clay sized particles and hence possess some degree of plasticity, but as the x-ray diffraction analysis reveals, clay minerals were not present in sufficient quantity to be positively detected by this x-ray diffraction. This indicates that the base materials contain less than about five percent clay minerals. Therefore, the pozzolanic reaction is not likely to occur with either one of the materials. The limestone and caliche bases contains only 31.1 and 23.2 calcite percent respectively. According to the x-ray diffraction analysis both materials contain primarily of calcite and quartz minerals, and the percentage of quartz was much higher than calcite in both materials.

Carbonate cementation is substantially more effective with pure carbonate particles than with mixtures of calcite and quartz due to better bonding between carbonate precipitates and the carbonate cement (Graves, 1987). Even so, a significant strength increase was observed from Texas triaxial test

Table 4.26. Summary of Paired-Comparisons T Test for Texas Triaxial Data.

Material Type	Curing Time, days	Lateral Pressure	Compare Between	p-value	Comment
Limestone	28	0 kPa	0 and 1	0.3598	SD
			0 and 2	0.0424	SD
		100 kPa	0 and 1	0.3275	SD
			0 and 2	0.0145	SD
	60	0 kPa	0 and 1	0.0944	SD
			0 and 2	0.0443	SD
		100 kPa	0 and 1	0.0884	SD
			0 and 2	0.0682	SD
Caliche	28	0 kPa	0 and 1	0.0746	SD
			0 and 2	0.0903	SD
		100 kPa	0 and 1	0.2506	SD
			0 and 2	0.2984	SD
	60	0 kPa	0 and 1	0.1695	SD
			0 and 2	0.0219	SD
		100 kPa	0 and 1	0.0471	SD
			0 and 2	0.0330	SD

0, 1, 2 = 0, 1, 2 percent lime, SD = Significantly different

data for both the quartz-rich limestone and caliche aggregates tested in this study. It is obvious that the trend of strength increase for the stabilized limestone was a different trend than that of the caliche. For limestone, the strength gain was approximately equal for the 1 and 2 percent lime treatment levels, while the caliche soil continued to gain strength with the higher percentage of lime. None of the materials showed significant strength increases for a longer curing period, e.g., the 60 day curing period compared to the 28 day curing period, except that limestone showed a higher strength for the 60 day curing when lateral pressure was increased to 100 kPa. Statistical analysis performed using paired-comparisons t test indicated that there was significant difference between the pair of data for stabilized samples and the pair of data for unstabilized samples.

According to Wissa and Ladd (1965), artificial cementation increases strength of sand due to a large increase in cohesion and a slight increase in friction. This seems to be well supported by the calculated cohesion and angle of friction values from triaxial strength data of this experiment. Cohesion and angle of friction values for both the limestone and caliche aggregates were higher for the stabilized samples than the unstabilized ones. Determination of the Texas triaxial classification of the stabilized and the unstabilized materials showed that stabilization changed borderline base materials into fair base materials.

SEM images of the unstabilized limestone and caliche soil in Figures 4.12 and 4.15 show scattered quartz particles with some calcite on the surface. Voids around the quartz particles indicate a low level of cohesion and friction in those materials. Due to relatively low percentage of calcite, in these aggregate, the level of carbonate cementation is expected to be considerably lower than what would be expected in a more purely calcitic material. In Figures 4.13, 4.14, 4.16 and 4.17, however, the quartz particles are virtually covered with calcite deposits indicating a denser matrix. While some bonding might have occurred between the calcite particles and the calcite precipitate, cracks in the precipitate indicate loose deposits of calcite on the quartz particles. Thus, the increase in triaxial strength may have been dominated by the filling of the voids by the precipitate rather than cementing action. There was no evidence of the fiber like products of a pozzolanic reaction in any one of the images. This tends to confirm the strength increase by carbonate cementation only.

Lime stabilized samples demonstrated higher lab-determined moduli than the unstabilized samples in both dry and wet conditions, regardless of the material type. For all specimens tested for resilient modulus, the moduli values increased with deviatoric stress up to a certain point and then

decreased for higher stress levels. Moduli values were very low when the ratios of deviatoric stresses and confining pressures were high. This again, supports the work of Saxena and Lastrico (1978), where they showed that cohesion was the governing factor for strength gain at low strain level and frictional resistance was primarily responsible for strength gain at high strains due to breaking of cementation bonds. Therefore, at high deviatoric stresses and low confining pressures, increases in moduli were likely to be only due to friction rather than cohesion and friction. It was observed from the plots of moduli values of the stabilized and the unstabilized specimens that both stabilized limestone and stabilized caliche aggregate experienced significant increases in modulus at higher stress levels probably due to increases in the amount of friction. Moisture conditions did not seem to have much effect on modulus of limestone, as it showed little variation due to change in moisture content. Wet samples had only slightly lower moduli than the dry samples. Caliche samples on the other hand seemed to be very sensitive to moisture content. Dry samples demonstrated much higher moduli values than the wet samples.

Backcalculated field moduli of the lime stabilized limestone base course were higher than those of the two unstabilized base courses evaluated. Since there was no unstabilized caliche base tested, such a comparison was not possible, but the field data provided an idea of the range of moduli values for stabilized caliche base courses. The moduli values obtained were between 138 to 8,410 MPa.

4.11 RECOMMENDATION AND DESIGN IMPLICATIONS

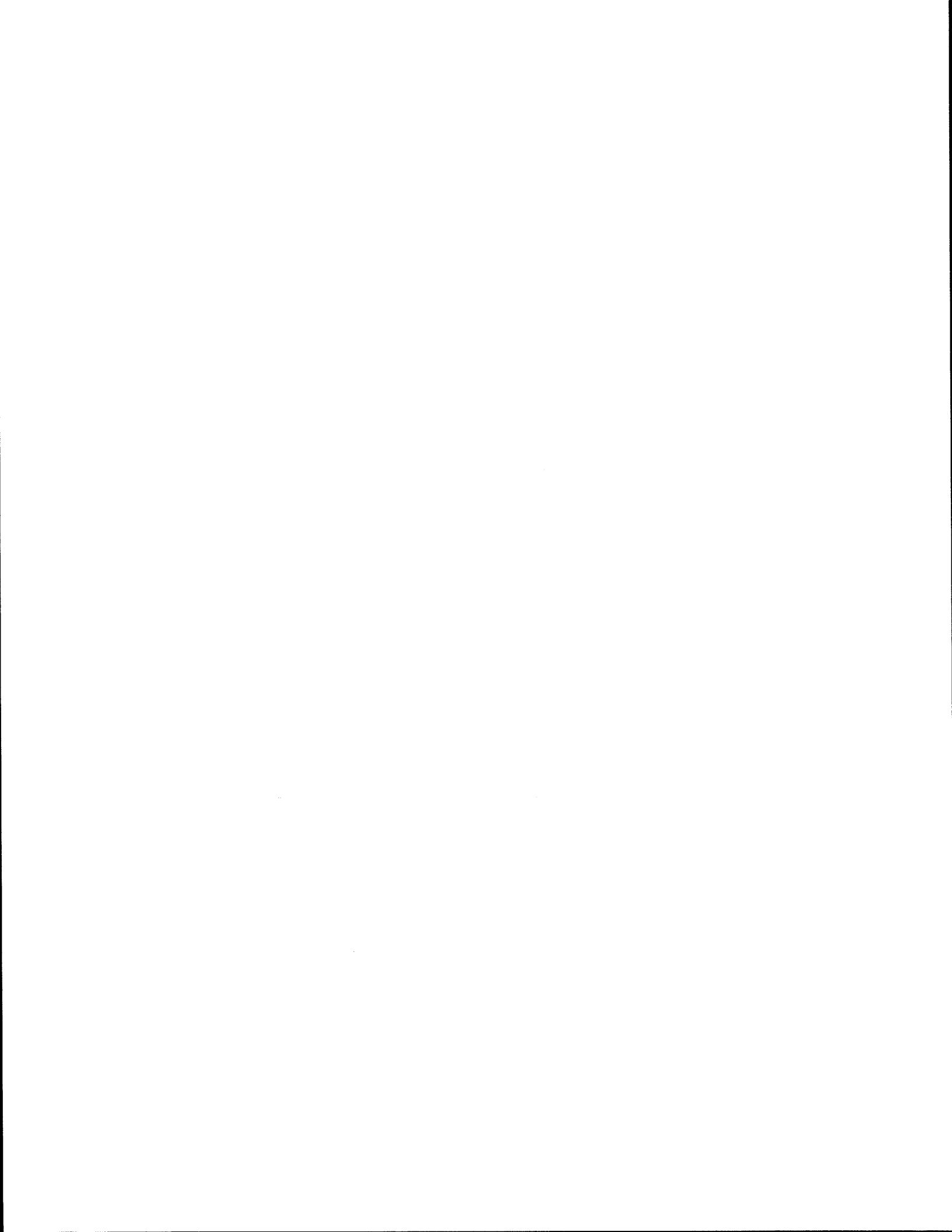
Texas Triaxial Strength testing demonstrates that 1 to 1.5 percent lime can improve shear strength of caliche and marginal quality limestone bases by 300 to 400 percent. This level of improvement can transform a low quality or even marginal quality base into a fair to good quality base.

The concomitant change in resilient modulus of calcareous bases upon low level lime treatment can be very substantial from a structural standpoint. Resilient moduli of wet calcareous bases can be improved by approximately 50 percent or more at deviatoric and bulk stress levels typically induced in flexible bases.

Low level lime treatment of calcareous aggregate bases, based on this research, does not transform the base into a rigid material, but the material is transformed by improved strength and stiffness while maintaining a flexible nature. Based on this research, the research of Graves (1987)

and the general literature, the researchers believe that the level of carbonate cementation increases as the purity of the calcareous base (calcite content) increases.

The Texas Triaxial method of base course evaluation Tex-117-E should be used to evaluate the structural beneficiation effect of low level lime treatment on calcareous aggregate bases.



CHAPTER 5

STABILIZED SUBGRADES

5.1 INTRODUCTION

Subgrade stabilization is used extensively throughout the State of Texas. Lime, lime/fly ash, cement and asphalt are commonly used in low strength subgrades. Lime is the most popular choice, particularly where the subgrade material often contains a substantial percentage of clay size materials. After stabilization, an unstabilized flexible base and thin surfacing are often placed over the stabilized subgrade. The percentage stabilizer selected is often based on practical experience with the soils. Most of the time little or no laboratory testing is conducted other than a soils classification. In low to medium volume highways, the in situ materials are typically stabilized to a depth of 150 to 200 mm, and the base course is laid and compacted directly on top of the stabilized subgrade. In some instances, on higher volume roadways, a stabilized subbase layer is used in which a local, lower quality aggregate is stabilized and placed between the subgrade and base layer. This chapter presents and discusses in-place strength and modulus values for stabilized subbases and stabilized subgrades.

As a result of Project 1287, the Design Division of TxDOT hopes to gain information in several specific areas.

1. Currently, treated or stabilized subgrades are not considered in the pavement design process. No increased strength is assigned to these layer, and no reduction in overall thickness is recommended. This is because the long term benefits of stabilization have not been sufficiently documented. A concern has been that chemical subgrade stabilization may not be permanent, and any support or confinement benefits will disappear after a few years.
2. The critical feature of the field testing is to determine whether subgrade stabilization is permanent or at least durable by evaluating it in a variety of existing, in service highways. If permanency is observed, it is important to document the impact of the stabilized layer on overall pavement response to load. Of particular interest is the effect of the stabilized subgrade support on the in situ moduli of granular base layers.

Furthermore, if long term benefits are observed, how can they best be accommodated in flexible pavement design?

3. Some districts do not stabilize subgrades for economic reasons, primarily because of the good local supply of top quality base. The argument is that the cost of a 150 mm lime stabilized subgrade is equivalent to between 50 and 75 mm of additional base. No one to date has demonstrated the long term cost benefits of subgrade stabilization as opposed to base thickening. A pressing need exists to generate defensible economic evaluations of the benefits of subgrade stabilization.
4. If permanency of subgrade stabilization is not achieved, it is important to document the cause of the problem and prepare guidelines on how to avoid this problem in the future.

In Project 1287, three Districts were visited to evaluate the performance of stabilized subgrades and subbases:

1. The Bryan District, which uses both cement and lime stabilization of subgrades;
2. The Atlanta District, which uses lime/fly ash stabilization of subgrades; and
3. The Fort Worth District, which has a variety of subgrade types but uses lime solely as the stabilizer.

To supplement the data from the Atlanta, Lufkin, and Ft. Worth Districts, additional data were collected from other districts throughout Texas. Included are the City of Houston and the Houston District, the City of Austin, the Corpus Christi District and the Abilene District.

5.2 FIELD TEST PROCEDURES

The test procedure described in Chapter 3 of this report for the stabilized bases was followed in the evaluation of the subgrades. The main focus of the investigation was the interpretation of the Falling Weight Deflectometer data to obtain layer moduli and the validation of these backcalculated strengths with the Dynamic Cone Penetrometer. It is well known that modulus backcalculation procedures can become precarious when encountering sections containing stabilized bases and/or

stabilized subgrades. When backcalculations are performed on 4 layer systems with one or more layers stabilized, the backcalculation procedures frequently cannot distinguish if the base or the subbase has the high modulus value. The only way to conclusively check if the backcalculated values are reasonable is by use of verification testing such as the Dynamic Cone Penetrometer. If a stabilized subbase is present, it will be seen clearly in the strength profile generated with the DCP. Indeed, if the layer is a heavily stabilized subbase, then it is likely that the DCP will not be able to penetrate this layer.

Figures 5.1 and 5.2 shows examples of typical DCP results. These examples are from US-287 in the Fort Worth District. This pavement structure consists of 25 mm of HMAC over an 275 mm flexible base with the top 350 mm of the clay subgrade stabilized with 6 percent lime. At the time of FWD testing, the section was almost 20 years old. In order to interpret the FWD deflection data, it is important to know if the stabilized layer is still active and to verify its thickness. This section was evaluated using the DCP. The first step was to drill a small 25 mm diameter access hole through the HMAC and granular base to a depth of 375 mm, the approximate location of the top of the stabilized subgrade. The DCP test was started at that depth. If the stabilization had been effective, the rate of penetration should have been low in the clay subgrade, and the calculated CBR should relatively high. Figure 5.1 shows the rate of penetration through the layer was low. It took 130 blows of the hammer to penetrate from 355 mm to 610 mm for an average penetration rate of 1.96 mm/blow. The U.S. Army Corp of Engineers DCP/CBR relationship converts the DCP data to a CBR value of 100+ (138). Below 635 mm, the rate of penetration increased substantially. It is concluded for this section that (a) the stabilized layer was permanently stabilized, (b) the effective thickness has remained constant throughout its 20 year life at 350 mm, (c) this layer should be included in the backcalculation process, and (d) a high backcalculated moduli value should be anticipated for this stabilized subgrade. The information shown in Figure 5.1 was converted into a CBR strength profile as shown in Figure 5.1. Although the strength values vary with depth, the average value in the stabilized subgrade is over 100. These DCP results illustrate a case where the stabilized layer is performing as anticipated by the designer. During the course of this study, this was not always the case. In some instances the stabilized layer could not be detected with the DCP or FWD.

FORT WORTH DISTRICT US-287 SITE-6

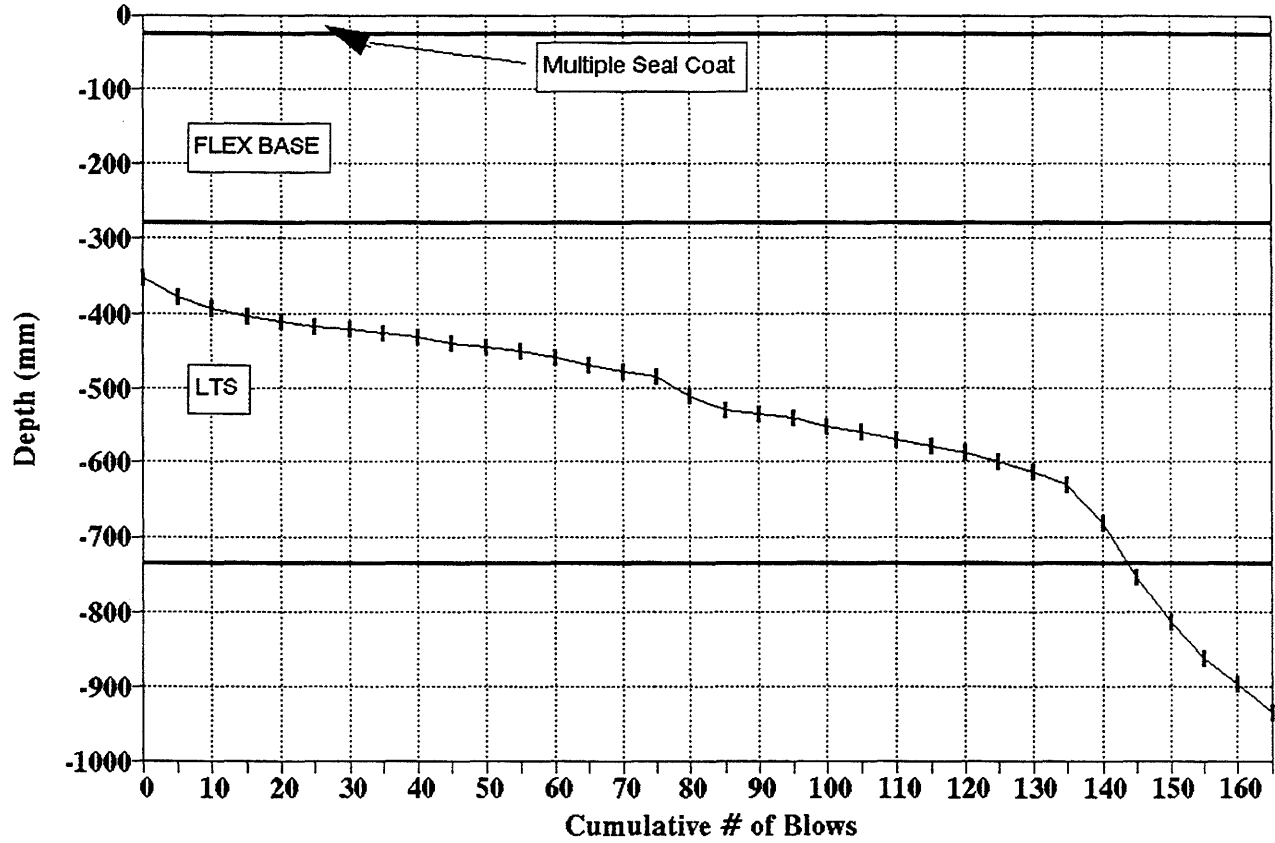


Figure 5.1. Typical Example of Cumulative Number of Blows vs. Depth of Penetration Using the DCP.

FORT WORTH DISTRICT
US-287 SITE-6

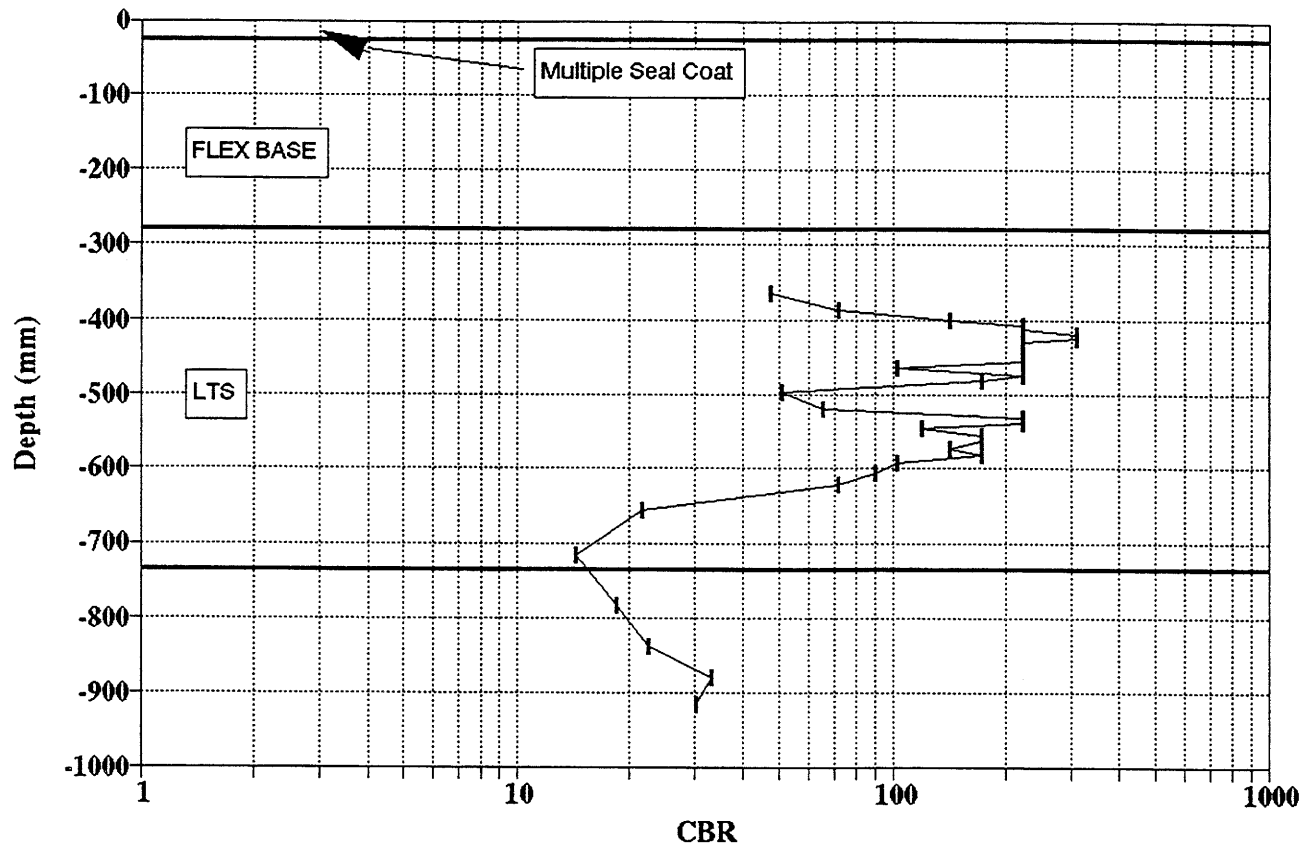


Figure 5.2. Typical Example of Variation of CBR vs. Depth Using DCP.

Results from the Bryan District

The Bryan District has a large variety of subgrade types to deal with ranging from fine sands to heavy clays. The decision to use stabilizers is made in a coordinated effort between the residencies and the head office. For low volume FM routes, the natural subgrade is stabilized with cement or more frequently lime. For higher volume highways, a lime treated subbase is frequently used, which may be plant mixed and generally contains marginal quality aggregates. When selecting the stabilizer content, the District frequently uses TxDOT method 121-E of the Material and Test Divisions test procedures manual.

In total, 6 sections were monitored within this district; Table 5.1 shows details of the layer thicknesses, stabilizer type and content. Three of the sections contained traditional subgrade stabilization where the in situ material was treated with between 3.5 and 4 percent stabilizer. Section 1 received cement stabilization as the top 150 mm of subgrade consists of a fine sandy material. Sections 2 and 4 are on clay subgrades, and both were stabilized with lime. Section 5 consisted of a lime treated subbase in which the imported materials were stabilized with approximately 5 percent lime. Sections 3 and 6 contained cement stabilized bases, and their moduli values were discussed in Chapter 3 of this report. The condition of these sections was good at the time of inspection. However, the traffic levels are light, and the sections are less than 6 years old. Section 4, which was 3 years old, had substantial meandering longitudinal cracking, which was not attributed to the stabilized layer, but probably to the expansive clay movements.

In general, the sections with the treated subgrades exhibited a considerable variation in deflection and layer strength. Appendix B presents details. Table 5.2 shows a summary of this variation. For section 1, the maximum deflection varied from 16 to 73 mils over the 150 m (500 ft) monitor site. This converted into a predictably large variability in the modulus of the stabilized subgrade. The stabilized subgrade modulus was calculated to vary from 35 to 3,450 MPa. If these predictions are correct, the stabilization has not worked as intended in certain portions of this section. A moduli of 35 MPa is typical of a very wet layer at the top of the subgrade. In order to validate these predictions, it was necessary to perform the DCP testing and compare the strength profile with that obtained from the FWD. A point-by-point comparison of FWD vs. DCP strength profile is shown in Table 5.3. The conclusions from Tables 5.2 and 5.3 are given below.

Table 5.1. Details of the Monitor Sections in the Bryan District.

Section	HMAC mm	Base		Stabilized Subgrade			Subgrade	Traffic ADT	Age (Years)
		mm	Type	mm	Type	% Stab			
1	37	200	CL	150	CTSG	4	Sandy/Loam	1000	2
2	10	175	CL	150	LTSG	4	Clay	100	6
3	50	460	CTB	-	-	-	Clay	3500	3
4	50	225	CL	200	LTSG	3.5	Clay	1000	3
5	50	250	CL	200	LTSB	5	Clay	1500	6
6	25	100	CTB	-	-	-	Sandy/Loam	250	15+

Base Type CL = Crushed Limestone
 CTB = Cement Treated Base
 Stabilized Subgrade CTSG = Cement Treated Subgrade
 LTSG = Lime Treated Subgrade
 LTSB (P) = Lime Treated Subbase

5.7

Table 5.2. Variability of Deflection Data on Stabilized Subgrade Sections in the Bryan District.

Section	FWD Deflection (mils)					Modulus of Stabilized Layer, KPa			
	Load Level, KN	Maximum	Minimum	Mean	COV %	Maximum	Minimum	Mean	COV %
1	68.8	73.4	16.49	37.3	47	3450	35	770	100
2	41.3	75.8	23.1	37.7	40	760	70	240	88
4	68.8	49.1	21.2	29.7	25	850	70	230	95
5	67.5	25.0	17.9	21.6	10	2070	135	1250	57

Table 5.3. Point Specific Comparison of Backcalculation Moduli vs. In situ CBR Value.

Section	Point	FWD Results			DCP Results					
		Moduli Values, MPa			Base		Stabilized Subgrade		Natural Subgrade	
		Base	Stabilized Subgrade	Natural Subgrade	mm/blow	CBR	mm/blow	CBR	mm/blow	CBR
1	1	460	572	96	3.0	85	1.8	150+	10.8	20
2	1	380	250	82	3.5	72	3.3	77	25.4	8
2	2	75	27	34	3.3	77	28	7	28.0	7
4	1	165	70	140	2.8	92	2.5 - 31	6-100	20.0	10
5	1	650	1863	82	-	-	1.0	250+	18.0	11

1. The comparison between DCP strength and backcalculated moduli for the stabilized subbase and subgrade layers is good. The two stabilized subbases with the high moduli values (sections 1 and 5) also were shown to have very high CBR values.
2. The results from section 2 (FM-3478) clearly show the benefits of stabilization and the consequences of not adding sufficient stabilizer to the natural subgrade. The two DCP test locations were 38 m apart. They were selected because of the large change in deflection between the two locations. At location 1 (Station 2) the maximum deflection was 23 mils, and at location 2 (Station 125) the deflection increased 3-fold to 75 mils. Figure 5.3 shows the DCP strength profiles for both locations. The penetration rate through the top 175 mm of flexible base is identical at both locations. The major difference is in the stabilized subgrade layer. At location 1 (Station 0), the lime treated layer is evident but at location 2 (Station 125), the stabilized layer was not detected. At Station 125, the strength decreased rapidly once entering the subgrade. At a depth of 400 mm, the top of the unstabilized subgrade, the CBR values at both locations were similar.

The contrast between the weak and strong stabilized layer has a distinct impact on the backcalculated moduli values, even though the DCP showed base properties to be similar between the two locations and natural subgrade properties to be similar between the two locations. In the areas of a strong stabilized layer, average backcalculated moduli for the base and subgrade were 380 and 82 MPa, respectively. In the location where subgrade stabilization was not evident, moduli values were 75 and 34 MPa for the base and subgrade, respectively. The stabilized subgrade is credited with providing better support for the base and for reducing the deviator stress in the subgrade; both of these effects cause an apparent increase in layer moduli. At location 125, the DCP data prove the base is no different than at Station 0 in terms of strength. However, backcalculated moduli from FWD deflections demonstrate the substantially higher flexible base resilient modulus due to superior subbase support. These findings have some significant implications for interpreting outputs of linear elastic backcalculation schemes. It is clear that the absolute moduli number is of much less significance than the modular ratio between

BRYAN DISTRICT
FM-3478 SITE-2

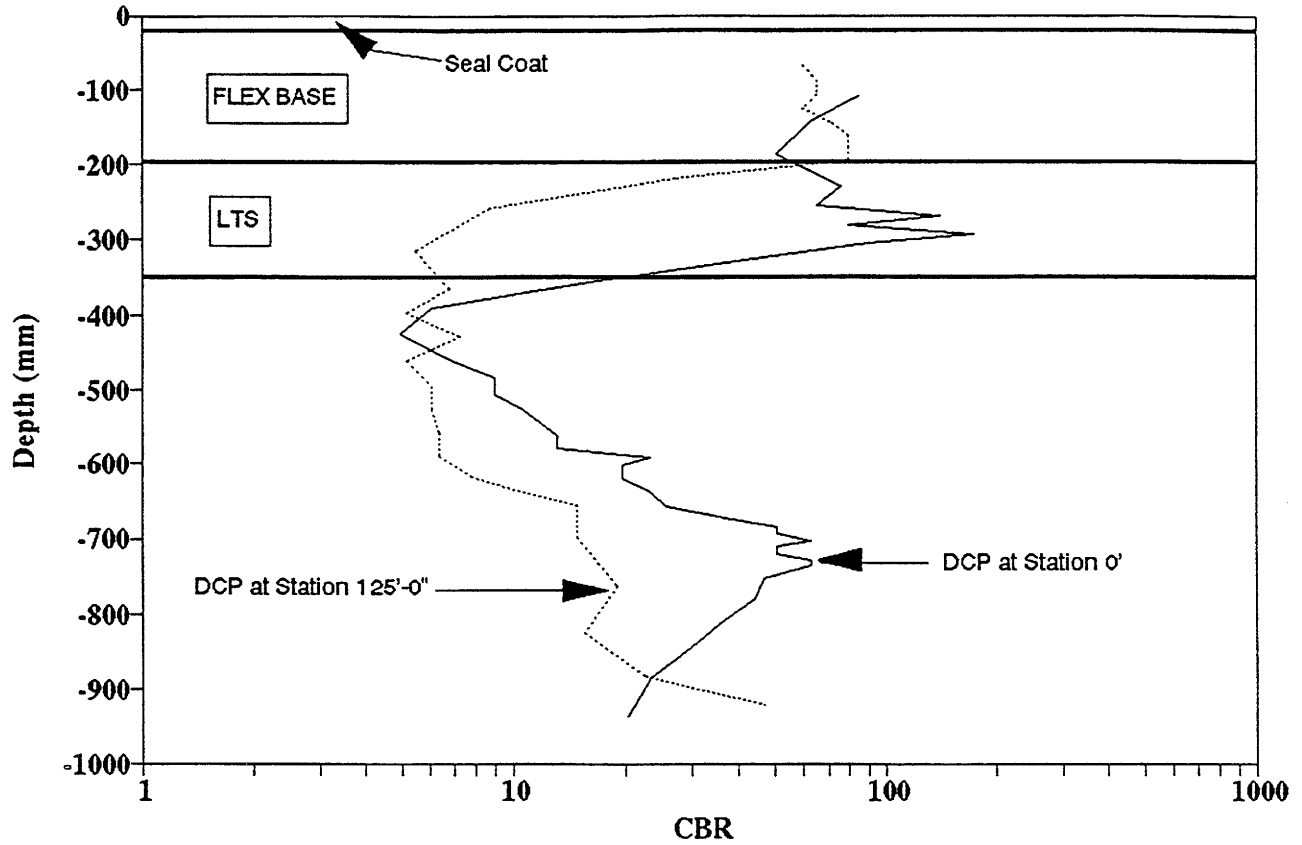


Figure 5.3. DCP Strength Profiles for Two Locations on FM-3478. At Station 125, the Stabilized Subbase is not Detected.

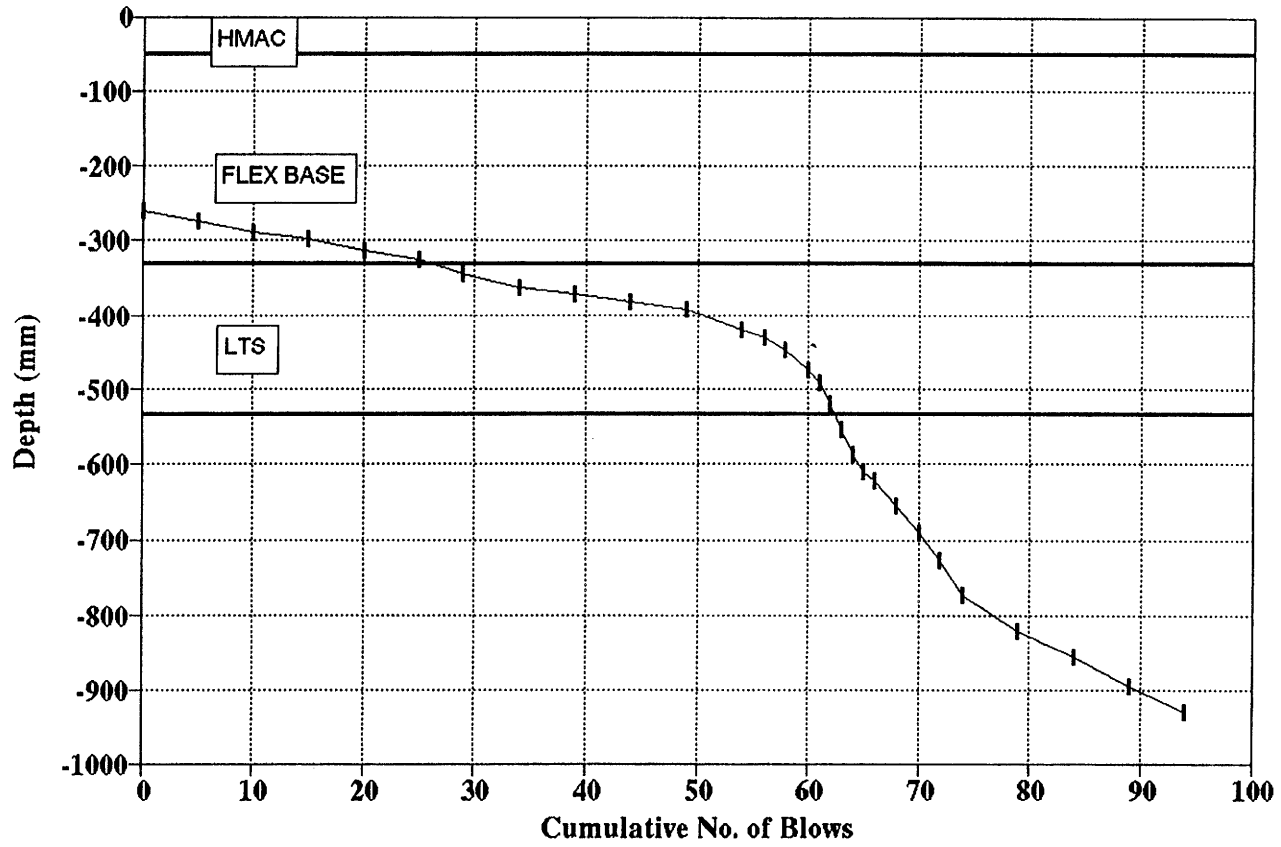
evaluation should be based upon modular ratio concepts rather than layer moduli.

3. The DCP penetration rate through base, subbase and subgrade layers in FM-1179 (Section 4) is shown in Figure 5.4. The strength of the 200 mm lime stabilized subgrade is variable. The top of the layer is stiff with a penetration rate of only 2.5 mm/blow. However, at about middepth, the rate becomes over 30 mm/blow. The resulting backcalculated moduli in the stabilized layer is relatively low. However, the mean value is approximately three times the natural subgrade modulus.
4. The lime stabilized subbase on FM-2818 (Section 6) is performing as intended. As shown in Figure 5.5, the rate of penetration is very low throughout the entire 200 mm. The high backcalculated modulus of 1,863 MPa is validated with the DCP which measured a penetration rate of only 1 mm/blow, which extrapolates to be a very high CBR value in excess of 200.

The four stabilized subgrades studied in the Bryan District reveal that chemical stabilization, in each case, improves the strength and modulus of the stabilized layer. However, the results from FM-1179 (Section No. 4) demonstrate that the lime stabilized layer, although strong and stiff at the top (upper-half) did not prove homogeneous, and little evidence of stabilization was apparent in the lower-half of the layer. FM-3478 (Section 2) demonstrated that lime stabilization was effective over the majority of the pavement (e.g., Station 0) but was not effective in selected areas (e.g., Station 125). The apparent lack of stabilization in the lower half of the layer in FM-1179 and in portions of FM-3478 could be due to a number of factors. The most logical explanations would appear to be related to either construction deficiencies (e.g., perhaps the lime was not appropriately mixed and compacted) or to mix design problems (e.g., perhaps the appropriate amount of lime was not used).

In Section 5, the lime-treated subgrade responded with a uniformly high CBR and uniformly high backcalculated resilient modulus. Although the backcalculated resilient modulus was variable (CV = 57 percent), even the minimum value backcalculated was approximately 2.5 times that of the natural subgrade modulus at that point, and the average backcalculated resilient modulus was about 15 times that of the average natural subgrade modulus.

**BRYAN DISTRICT
FM-1179 SITE-4**



5.12

Figure 5.4. DCP Penetration Data for FM-1179, Variable Stabilized Layer.

**BRYAN DISTRICT
FM-2818 SITE-5 (Final)**

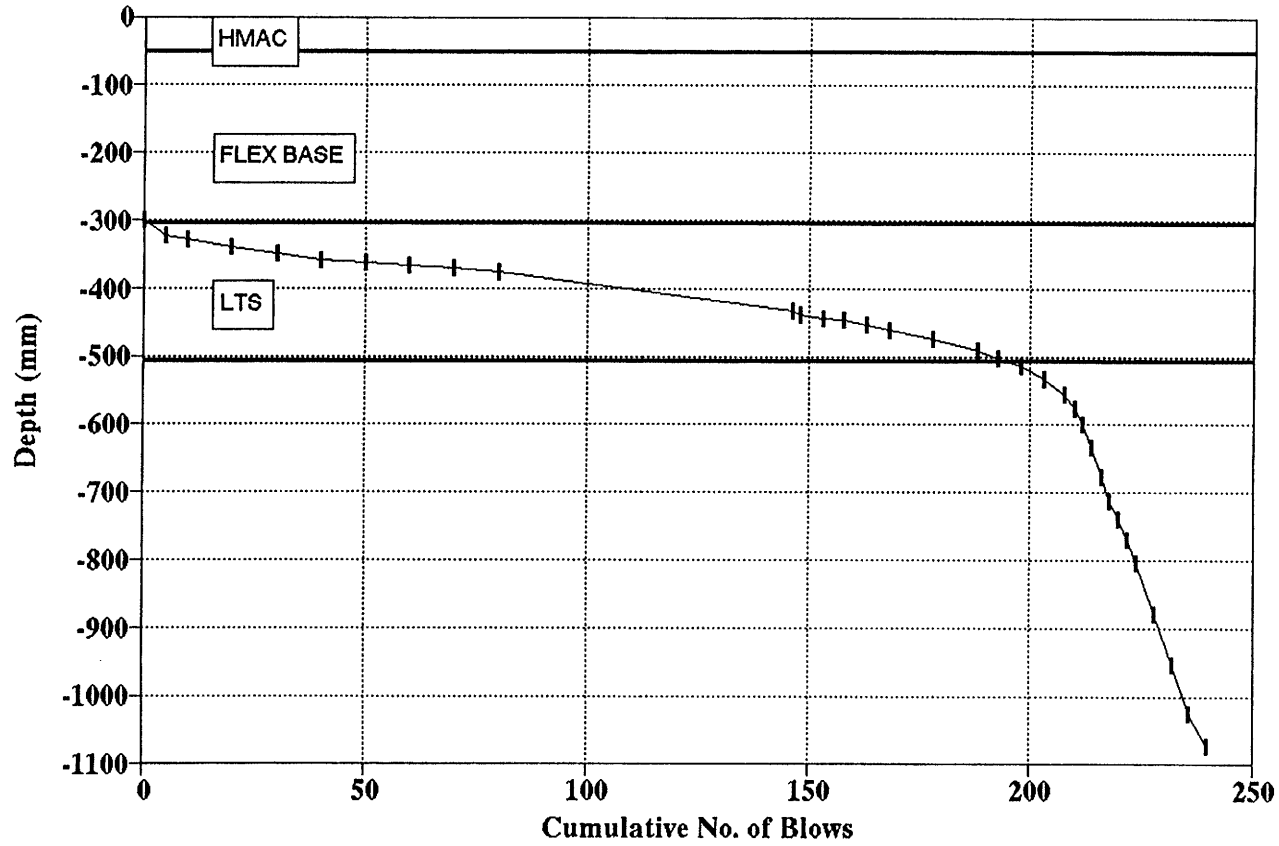


Figure 5.5. FM-2818 DCP Data from FM-2818, a Well Stabilized Subbase is Clearly Seen.

It is interesting to note that the lime content used in Sections 2 and 4 were 4 and 3.5 percent, respectively. The lime content in Section 5 was 5 percent. As discussed in Chapter 1, McCallister and Petry (1991) showed lime stabilization of some Texas soils to be partially reversible upon rigorous leaching when stabilized with 3 to 4 percent lime by weight, even though this lime content was effective in PI reduction for the Texas soils studied. However, when the same soils were stabilized with between 6 and 7 percent lime (within the optimum range based on strength for all soils) the stabilization was permanent and did not revert upon rigorous leaching.

It seems likely that the 3.5 and 4.0 percent stabilization rates on FM-1179 and FM-3478, respectively, are not an adequate level to assure permanency. This condition may be exacerbated when one considers that the actual lime content mixed into the soil during construction may be considerably less than the prescribed 3.5 or 4.0 percent, due to mixing inefficiencies. This is speculative, but Thompson (1970) recommended adding 0.5 to 1.0 percent more lime during construction than is actually required during mix design. More credibility is added to the hypothesis of inadequate lime content when one considers the success in the Ft. Worth District when a higher lime content is used. Still more credibility is added to this hypothesis when one considers the results of a TTI test track project discussed in the next section.

TTI Test Track Project

In 1990 a test track was constructed at the TTI Research Annex. The test track was built over the highly plastic Burleson clay which covers a considerable portion of the Bryan District. The test track evaluated the following sections of pavement:

- Section 1: 150 mm of Burleson clay stabilized with 6 percent hydrated lime,
- Section 2: 300 mm of Burleson clay stabilized with 6 percent hydrated lime, and
- Section 3: 300 mm of crushed limestone.

Each pavement section was placed directly over compacted native Burleson clay with no surface covering. Ten FWD deflection basis were measured within each pavement section at two points in time:

1. approximately four months after construction, and
2. approximately a year and a half after construction, and after the sections had been subjected to 5,000 application of a 80 KN axle load.

The results of the layer backcalculation of moduli demonstrate that 6 percent lime produces a durable and apparently permanent reaction. The modulus increase of the lime-treated layers are between 6 and 30 times the modulus of the native subgrade.

Results from the Atlanta District

The Atlanta District has used subgrade stabilization for several years as part of its new pavement design procedures. All of the sections evaluated in this study were stabilized with a lime/fly ash blend. The layer thicknesses and percentages of lime and fly ash used on the three subgrade monitor sites in this district are shown in Table 5.4.

Section 4 is located on US-59 and carries substantial truck traffic. The section at the time of inspection was 10 years old and exhibited longitudinal, transverse and alligator cracking. The subgrade of this section was heavily stabilized with a combination of 4 percent lime/8 percent fly ash. On top of the subgrade was 225 mm of asphalt stabilized base and asphalt surfacing. The initial cracking observed in this pavement was longitudinal and transverse. These were possibly reflection cracks from the heavily stabilized subgrade. Alligator cracking was documented in the wheel paths.

Table 5.4. Layer Thickness Information from Stabilized Subgrade Sections in Atlanta.

Section	Surface, Thick, mm	Base		Treated Subgrade			ADT	Age	Cracking
		Thick, mm	Type	Thick mm	Percent Lime	Percent Fly Ash			
4	37	225	ASB	400	4	8	7,500	10	Transverse + Alligator
6	12	300	CL	300	2.5	5	3,400	7	7 Minor
7	12	300	CL	300	5	10	3,400	7	7 Minor

Sections 6 and 7 were located on the same highway. The difference in the sections is in the percentage of stabilizer used in the subgrade. In section 6 the lime/fly ash percentages were 2.5 percent/5 percent, and in section 7, a 4 percent/8 percent application rate was used. The surfacing on these sections was a double surface treatment. The section carries substantial heavy truck traffic, and at the time of the evaluation it was 7 years old. The visible distress in the section was minor. Some hairline, widely spaced transverse cracking was found on both sections. The cause of the cracking could not be directly attributed to the stabilized subgrade. It may be thermal cracking of the thin surfacing. In any event, the cracking was minor.

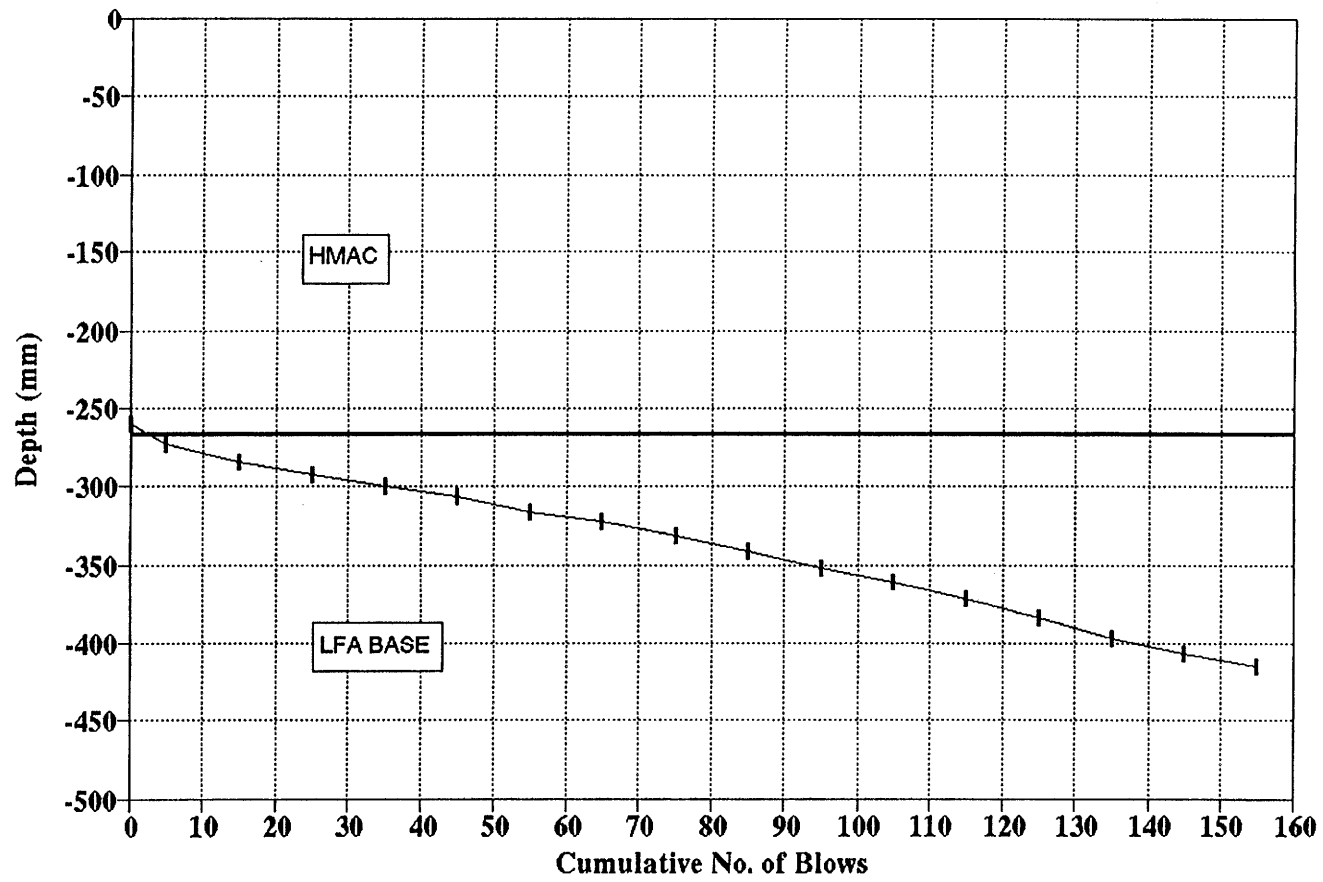
Table 5.5 shows the average backcalculated moduli values for these sections and the results of the DCP testing. From the results summarized in Table 5, the following conclusions are drawn:

Table 5.5. Average In situ Moduli Values and DCP Results from Stabilized Subgrades in Atlanta.

Section	Flexible Base Modulus, MPa				Stabilized Subgrade, MPa				Subgrade, MPa	Stabilized Layer	
	Mean	High	Low	COV %	Mean	High	Low	COV		mm/blow	CBR
4	-	-	-	-	4500	6900	1350	47	130	1.0	200+
6	310	365	41.6	11	2500	4750	550	68	175	4.6 (1)	47
7	415	495	44.7	15	4400	6300	2430	35	117	(2)	

1. The subgrades are permanently stabilized in all three sites and providing good support to the base layers. The structural beneficiation in these stabilized layers should be accounted for in the pavement design process.
2. High moduli values were predicted for each stabilized subgrade layer. These range from 4,750 MPa for the 2.5 percent lime/5 percent fly ash to 6,900 MPa for the 4 percent lime/8 percent fly ash. These high moduli were confirmed with the DCP testing. In section 4 the penetration rate was only 1 mm/blow, and in section 7

ATLANTA DISTRICT
US-59 SITE-5



5.17

Figure 5.6. Cumulative Number of Blows vs. Depth of Penetration.

the layer was too stiff to penetrate. Figure 5.6 shows the DCP data from section 4. Testing started at the top of the stabilized subgrade, and it took 150 blows of the hammer to penetrate approximately 150 mm, at which point testing was stopped. As can be seen from this figure, the rate of penetration is constant throughout this layer.

3. The sections containing 300 mm of flexible base on top of the heavily stabilized subbase are performing very well even under heavy truck loads.

Results from the Fort Worth District

The Fort Worth District has two major distinct soil groups. In the western and northwestern counties, fine loamy sand soil types predominate. In the southern and eastern counties, large quantities of high plasticity clays are found. Soil stabilization has been used for many years in most new flexible pavements. Over the years, the former district laboratory engineer (Mr. David Bass) developed a rationale for stabilization. Stabilization was recommended for all soils with a Plasticity Index above 10, and lime was recommended as the stabilizing agent. From experience, it was recommended that the best results were obtained with an application rate of 6 percent. For soils with a PI above 10 but below 30, a stabilization depth of 150 to 200 mm was recommended. For high PI (PI > 30) clays, a stabilization depth of between 300 and 400 mm was recommended.

In terms of flexible pavement design, the district felt it was getting good performance for light to moderate traffic levels with a stabilized subgrade, 200 to 300 mm of high quality crushed limestone base and a thin surfacing less than 75 mm. In this study, a total of 6 monitor sections were set up in this district.

A summary of field test results obtained in the Ft. Worth District are shown in Table 5.6. In all cases, 6 percent lime was used to stabilize the in situ materials. Included in this table are the following:

1. The layer thicknesses of the surface, base and stabilized subgrade layers,
2. The type of subgrade soil,
3. The average moduli backcalculated from the FWD data,
4. The DCP results of penetration per blow converted to a layer CBR value, and
5. The age of the section at the time of testing.

From the data presented in Table 5.6 the following observations are made:

1. The stabilized layer in each section is still present and performing as intended, even after 20 years in service.
2. The FWD indicated that the stabilized subgrade layers have backcalculated moduli values of between 2.8 and 9 times greater than the natural subgrade upon which it sits. This has two distinct benefits for the pavement structure. Firstly, the stabilized layer provides both support and confining for the granular base course. It is well known that granular materials are stress sensitive, and the more confinement applied to the materials, the higher is the measured modulus value. The granular bases in this study had backcalculated moduli in the range 386 to 945 MPa. These are very high values for lime stabilization. Normally, top quality granular materials resting on unstabilized subgrades have moduli in the 200 to 400 MPa range. The second benefit of these stiff stabilized subgrades is their load spreading capabilities in protecting the subgrade. Subgrade materials also exhibit non-linear characteristics. The measured modulus of fine subgrades is known to be strongly dependent upon the deviator stress applied. In the laboratory, high moduli values are obtained at low stress levels, and as the deviator stress increases, the measured modulus decreases. This non-linear effect is demonstrated in the relatively high backcalculated moduli values for the subgrades.
3. The DCP results confirm the backcalculated moduli results. In each case the stabilized layer was detected with the DCP. Figure 5.7 shows an example from site 1. The rate of penetration through the lime treated subbase is very slow. At the top of the natural subgrade at a depth of approximately 430 mm, the rate of penetration increased rapidly. The DCP is normally used on granular bases and subgrades where the calculated CBR values range from 2 to 100+. Using the DCP/CBR equation with the penetration rates measured on these stabilized subgrades, very high values CBR values were extrapolated. The absolute magnitude of these numbers is not too

Table 5.6. Backcalculated Layer Moduli from Stabilized Subgrade Sections in Fort Worth.

Section Number	Thicknesses, mm			Subgrade Material	Average Backcalculated Moduli, MPa			DCP Results		Age (Yrs)
	HMA C	Flex Base	Stab. Subg.		Base	Stabilized Subgrade	Subgrade	CBR Stab. Subgrade	CBR Subgrade	
1	50	250	150	Sandy/Loam	700	540	160	200+	10-20	0-5
2	100	150	150	Sandy/Loam	386	810	165	189	5-10	1.0
3	35	275	200	Sandy/Loam	945	790	276	-	-	13
4	225	-	150	Sandy/Loam	-	900	125	101	8-15	20+
5	25	250	200	Clay	580	580	160	63-200+	10-40	15+
6	25	275	350	Clay	475	1170	125	167	20-30	15+

FORT WORTH DISTRICT Section-1

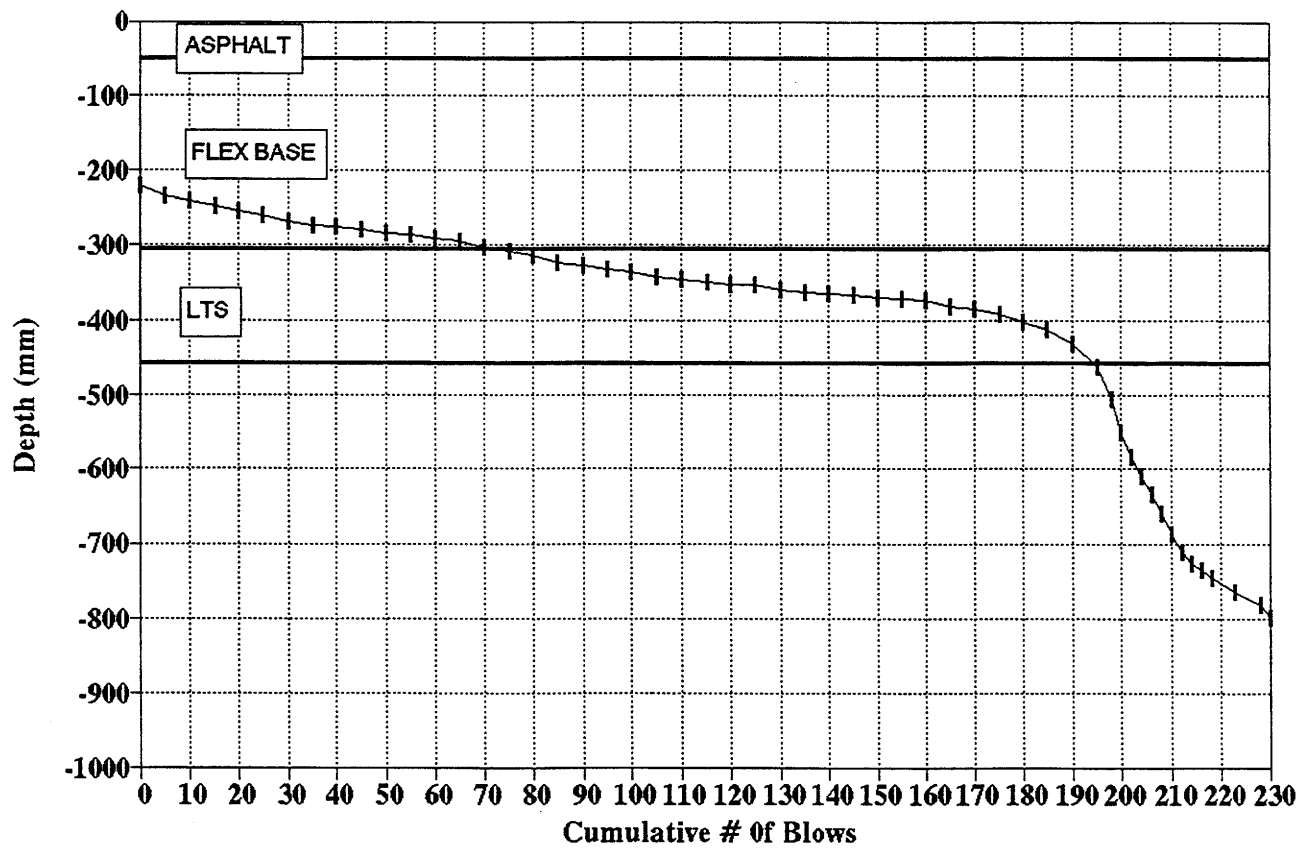


Figure 5.7. Cumulative Number of Blows vs. Depth of Penetration Measured with DCP.

important, but what is important is that these layers have significantly higher strengths than the natural subgrades.

4. Both the sandy/loam and heavy clay showed distinct moduli improvements with the 6 percent lime stabilization. This must mean that the sandy loam had enough clay and/or calcareous combinant to react with lime.

5.3 CONCLUSIONS

Lime treatment of soils improves the workability and compactability by reducing plasticity. However, substantial structural improvements can also occur. The degree to which these structural improvements occur and the durability of the lime treated layer depend on mixture design and whether or not the appropriate percentage of lime was used to insure pozzolanic strength development. In this study, a few field tests demonstrated that lime treatment was not evident after several years of service. On the vast majority of the cases studied, the effect of lime treatment was evident, and the effects of treatment indicate a significant structural improvement.

Table 5.7 summarizes the backcalculated resilient moduli for lime treated subgrades on 32 different sections evaluated in this study. In this table, the backcalculated modulus of the lime treated section is divided by the backcalculated resilient modulus of the natural subgrade to determine the modulus ratio between the lime treated subgrade and the natural soil. Backcalculation of moduli is a tedious task with considerable room for error. However, it is important to note that the backcalculations, presented in Table 5.7, were verified with DCP and other field measurements in 20 of the 32 sections presented in Table 5.7. Therefore, a high level of confidence is associated with the backcalculated moduli presented in this table.

Of the 30 backcalculated resilient moduli presented for the lime treated pavement layers in Table 5.7, all but one have a high enough modulus to equal or exceed that of a good quality aggregate base, approximately 200 MPa. Column 4 of Table 5.7 reveals that lime treatment increases the in situ modulus of the natural subgrade by a factor of from 0.98 to 44.4. Of the 30 lime treated layers in Table 5.7, 27 have modulus ratios above 3, which may be considered the minimum value needed if a structural improvement factor is to be assigned to the layer.

Table 5.7. Summary of Backcalculated Moduli for Lime Stabilized Subgrades.

Pavement Identification	Layer Structure	LSS or Base Modulus, MPa	Modulus Ratio, E_{LSS}/E_{sub}
Brodie Lane, Section 1 Austin District	115-mm HMA 275-mm Base 200-mm LSS CH clay	630 (LSS)	7.5
Brodie Lane, Section 2 Austin District	Same as section 1	357 (LSS)	5.1
Brodie Lane, Section 3 Austin District	100-mm HMA 560-mm Base CH clay	302 (Flex. Base)	1.5
Brodie Lane Section 3 Austin District	Same as section 3	279 (Flex. Base)	2.0
TTI Annex, Section 1	305-mm LSS	490 (LSS)	17.0
TTI Annex, Section 1 - After traffic	305-mm LSS	210 (LSS)	10.0
TTI Annex, Section 2	152-mm LSS	399 (LSS)	47.5
TTI Annex, Section 3	305-mm CLS	238 (CLS)	17.0
FM-3478, Section 1 Bryan District	37-mm HMA 200-mm CLS 152-mm LSS	770 (LSS)	7.9
FM-3478, Section 2 Bryan District	S.T. 175-mm CLS 150-mm LSS	240 (LSS)	3.7
FM-1179 Bryan District	50-mm HMA 275-mm CLS 200-mm LSS	230 (LSS)	1.7
US-59 Atlanta District	265-mm HMA 400-mm LSS	4,500 (LSS)	34.7

Pavement Identification	Layer Structure	LSS or Base Modulus, MPa	Modulus Ratio, E_{LSS}/E_{sub}
LP-436, Section 1, Atlanta District	S.T. 300-mm CLS 300-mm LSS	2,500 (LSS)	14.1
LP-436, Section 2, Atlanta District	S.T. 300-mm CLS 300-mm LSS	4,400 (LSS)	37.3
SH-199 Fort Worth District	50-mm HMA 250-mm CLS 150-mm LSS	540 (LSS)	3.4
FM-1709 Fort Worth District	100-mm HMA 150-mm CLS 150-mm LSS	810 (LSS)	4.7
SH-121 Fort Worth District	37-mm HMA 275-mm CLS 200-mm LSS	790 (LSS)	2.8
US-287, Section 1, Fort Worth District	225-mm HMA 150-mm LSS	900 (LSS)	7.2
US-287, Section 2, Fort Worth District	25-mm HMA 275-mm CLS 200-mm LSS	580 (LSS)	3.6
US-287, Section 3, Fort Worth District	25-mm HMA 275-mm CLS 350-mm LSS	1,170 (LSS)	9.4
IH-40	254-mm HMA 381-mm CLS 368-mm LSS	644 (LSS)	7.1
SH-105	50-mm HMA 244-mm CLS 165-mm LSS	1,820 (LSS)	13.7
US-77	190-mm HMA 305-mm CLS 152-mm LSS	3,010 (LSS)	35.8

Pavement Identification	Layer Structure	LSS or Base Modulus, MPa	Modulus Ratio, E_{LSS}/E_{sub}
SH-19	279-mm HMA 152-mm CLS 293-mm LSS	1,120 (LSS)	10.7
SH-23	76-mm HMA 457-mm CLS 203-mm LSS	770 (LSS)	6.1
SH-21	216-mm HMA 279-mm CLS 114-mm LSS	5,600 (LSS)	44.4
IH-37	178-mm HMA 254-mm CLS 152-mm LSS	6,510 (LSS)	37.2
SH-19	51-mm HMA 279-mm CLS 229-mm LSS	2,100 (LSS)	12.0
US-83	254-mm HMA 266-mm Soil Aggregate 140-mm LSS	1,995 (LSS)	21.9
US-77	51-mm HMA 279-mm CLS 178-mm LSS	98 (LSS)	0.95
US-59	51-mm HMA 203-mm CLS 229-mm LSS	245 (LSS)	3.5
US-37	254-mm HMA 432-mm Soil Aggregate 152-mm LSS	931 (LSS)	5.1
FM-526 Houston District, Site 1	76-mm HMA 356-mm CTB 152-mm LSS	2,417 (LSS - Summer) 1,288 (LSS - Winter)	13.1 (Summer) 6.2 (Winter)

Pavement Identification	Layer Structure	LSS or Base Modulus, MPa	Modulus Ratio, E_{LSS}/E_{sub}
FM-526 Houston District, Site 2	76-mm HMA 229-mm CTB 178-mm LSS	77 (LSS - Summer) 414 (LSS - Winter)	0.84 (Summer) 3.8 (Winter)
FM-2920 Houston District, Site 4	102-mm HMA 279-mm CTB 152-mm LSS	675 (LSS - Summer) 495 (LSS - Winter)	2.25 (Summer) 1.4 (Winter)
FM-1093 Houston District, Site 5	76-mm HMA 305-mm CTB 152-mm LTS	1,193 (LSS - Summer) 1,440 (LSS - Winter)	7.2 (Summer) 9.0 (Winter)
SH-36 Houston District, Site 6	76-mm HMA 305-mm CTB 152-mm LSS	1,768 (LSS - Summer) 2,257 (LSS - Winter)	13.3 (Summer) 15.6 (Winter)
FM-516 Houston District, Site 7	89-mm HMA 406-mm CTB 152-mm LSS	1,475 (LSS)	6.7

CHAPTER 6
RECOMMENDATIONS FOR MIX DESIGN
AND THICKNESS DESIGN

6.1 MIX DESIGNS CONSIDERATIONS FOR BASES

Heavily Stabilized Bases

The current basis for mix design of portland cement stabilized bases is the Minimum Design Compressive Strength as described in Item 276 of the TxDOT, 1993 Construction Specifications, the strength requirements are reproduced in Table 6.1.

Table 6.1. TxDOT Strength Specifications for Item 276.

Classification	Minimum Design Compressive Strength, Kpa	Allowable Cement Content Percent
L	5,250	4 - 9
M	3,500	3 - 9
N	Shown on plans	-
O	None	Shown on plans

Prior to these specifications, earlier approaches (1982 TxDOT Construction Specifications) were recipe type where the recommended levels of stabilizer were given for each aggregate type. No matter which specification is used, the percentage stabilizer is frequently in the range of 5 - 6 percent by weight.

The Houston District has made extensive use of these specifications and has constructed many miles of highways with heavily stabilized cement treated bases. In this study six sections were monitored with portland cement stabilized bases. Each of the sections provided good riding quality. The major difference in performance was the amount of non-load associated surface cracking, which ranged from none to extensive. The severity of cracking was directly related to the strength of the stabilized layer and was strongly dependent upon the type of aggregates used. The oyster shell base

had zero cracking after 15 years in service, whereas the river gravel base was extensively cracked.

The level of cracking was of concern to the district staff. In one instance the base was experiencing severe disintegration caused by trapped moisture. Three of the sections were scheduled for overlays after only 7 years in service. Performance of these bases could be improved considerably if more frequent fine cracks occur rather than wide cracks, which deteriorate rapidly over time. For new construction consideration should be given to:

1. Controlling the plasticity index and linear shrinkage of the fine portion of the base material. (Maximum values of 4 percent and 2.5 percent, respectively, were recommended by Caltabiano (1992)).
2. Introducing a Shrinkage Test in which shrinkage within a control beam of CTB should not exceed 250 microstrain after 20 days (Caltabiano, 1992).
3. Limiting the stabilizer content in order to reduce non-load associated cracking yet developing adequate compressive strength to maintain a significant structural contribution and maintain durability. The long term field strengths obtained with the current specifications are exceedingly high.

Backcalculation of resilient moduli from FWD data in the Houston District reveal that very high moduli of cement treated bases are clearly associated with wide shrinkage cracks and ultimately considerable non-load damage. For this reason, a realistic mixture design consideration is to add enough stabilizer to achieve the minimum strength requirement listed in Table 6.1, yet set an upper limit on the maximum allowable cement content. The Houston District study indicates that the minimum strength requirements set forth in Table 6.1 may be higher than required for optimal performance.

Heavily stabilizing marginal base materials with high levels of clay materials is not recommended. This, as shown in the Atlanta District, results in excessive cracking and durability problems.

Moderately Stabilized Materials

This classification was selected for stabilized bases in the Atlanta District where between 2 and 4 percent of total stabilizer was used. These correspond with Item 262 in the 1993 Texas Construction Specifications. Currently, no recommendations on the level of stabilizer to use are given in the Specification, other than "as shown on plans."

The work in the Atlanta District has concentrated on upgrading existing base materials. The procedure used in the Atlanta District is the unconfined Texas Triaxial Test procedure (Tex-117-E) with 7 KPa confining pressure. The raw materials are tested and compared with those treated with different levels of stabilizer. Curing of the stabilized material involves 7 days air curing, 2-3 hours in an oven at 60°C followed by 10 days of capillary rise. This approach is similar to the Tex-121-E method. The samples are tested after the 10 days of moist curing. The criteria is to identify the level of stabilizer that produces two- and three-fold in strength increase over that of the unstabilized aggregate.

The sections in the Atlanta District, which received the level of stabilization recommended by this procedure (2 - 4 percent), all performed very well. They were performing as flexible pavements and had not developed the crack patterns associated with heavily stabilized materials. The backcalculated moduli for these materials were between 2 and 4 times higher than would have been anticipated for an untreated flexible base.

The approach used in the Atlanta District is recommended; however, it is based on observations of the performance of the specific aggregates used in the Atlanta District, which are largely iron-ore gravels. A more thorough evaluation should be made of aggregates from other areas of the state. To supplement the strength tests used in the Atlanta District, it is recommended to include a linear shrinkage test such as that recommended by Caltabiano (1992). The objective of the mix design process should be to obtain a top quality "flexible" material without developing excessive shrinkage cracking.

Lightly Stabilized Bases

Calcareous bases in several districts have been stabilized with very low percentages of lime (1 to 4 percent, but typically 1 to 2 percent). Chapter 4 discusses this type of stabilization. It is a unique type of stabilization when calcareous bases with very little or no clay fraction are being

treated. This is because the cement matrix is chiefly carbonate in lieu of pozzolanic cement or hydrated calcium silicates or calcium aluminates.

Mixture design should be based on the Texas Triaxial test and should follow the general procedure outlined in Tex-121-E except that moist curing time should be extended to at least 14 days.

Data in Chapter 4 suggest that 1 to 2 percent lime in either caliche or limestone bases typically will increase compressive strength by 50 percent or more and resilient moduli by a similar amount. This level of strength and modulus increase represents a very significant structural upgrade.

6.2 THICKNESS DESIGN CONSIDERATIONS FOR BASES

Heavily Stabilized Bases

The principal thickness design procedure for flexible pavements in use within TxDOT is FPS 11. This procedure was developed primarily for "flexible" bases with either asphalt stabilized or unstabilized granular materials. The strength parameter used within FPS 11 is the stiffness coefficient parameter, which was backcalculated from Dynaflect deflection data using procedures developed by Scrivner (1968) in Study 32. For typical pavements the following stiffness coefficients are generally used:

- Asphalt Surfacing 0.95 - 1.0,
- Asphalt Stabilized Base 0.80 - 0.90, and
- Granular Materials 0.55 - 0.65.

Work in the Lufkin District based on observed field performance with cement treated bases indicated that a representative stiffness coefficient for Cement Treated Base (CTB) is 0.70. The use of this value in FPS 11 resulted in design thicknesses that the District thought were reasonable. In all cases a minimum layer thickness of 200 mm is recommended for semi-rigid layers.

The Pavement Design Section of TxDOT recognizes the limitations of this procedure. The FPS system is based on a criteria of limiting deflections (Surface Curvature Index) and the relationship between SCI and loss in Serviceability Index. While reasonable for "true flexible" pavements, this criteria is not suitable for heavily stabilized bases as the failure mechanisms for these two pavement

types are very different. The approach that is typically used for heavily stabilized bases involved limiting the tensile stress at the underside of these layer to a specified stress ratio ($SR = \text{actual stress} / \text{ultimate strength}$). Typically the thickness of the layer is increased until the stress ratio falls below 0.50.

The problems with this approach are:

1. Determining what value to use for the ultimate strength of the stabilized base since the semi rigid materials gain strength with time.
2. Calculating the actual stress under the design load, and determining what moduli value should be used for the stabilized layer (given the fact that the layer contains shrinkage cracks).

Thompson (1994) recommended a rationale approach to both of these issues. He proposed using, as the design ultimate strength, the strength achieved when the highway is first opened to traffic. He also stated that shrinkage/thermal cracks are inevitable in these materials and that they must be accounted for in the design process. The CTB should be thick enough to prevent secondary load associated cracks that initiate at the transverse shrinkage cracks. The presence of these transverse cracks causes an increase in tensile stress at the underside of the slab, and this is where fatigue cracking will initiate.

In the testing of the Houston pavements, FWD data were collected on cracked and uncracked sections in both summer and winter. Table 3.4 shows the load transfer efficiencies. In evaluating the impact of these variations in load transfer on induced stresses, the ILLISLAB finite element program was used. The aggregate interlock factor of the joints within the program were modified until a deflection bowl similar to that measured under the FWD was obtained. The increase in stress at the bottom of the slab was calculated and the ratio of stress at the crack to the stress in the uncracked section was calculated. In order to use this information within the pavement design process, a simple microcomputer based program was written to compute fatigue life. The user inputs the anticipated uncracked layer moduli and the average of the 10 heaviest wheel loads to be experienced by the pavement. Section 6.3 the algorithms used in this program.

Moderately and Lightly Stabilized Bases

In this study, lightly stabilized bases are defined as those bases containing between 1 and 2 percent stabilizer. Moderately stabilized bases contain between 2 and 4 percent stabilizer. In both cases the pavements primarily behave as flexible pavements in that the major forms of structural distress are wheel path rutting and cracking. They do not exhibit the longitudinal and transverse cracking associated with heavily stabilized materials. Consequently, it is proposed that the thickness of these layers be designed using the FPS 19 program. This program requires that an elastic modulus and poisson's ratio be input for each layer.

Table 6.2 records the modulus increase due to moderate or light levels of stabilization. The Base Improvement Factor (BIF), ratio of modulus of the stabilized layer to modulus of the unstabilized layer, is used as the criterion upon which to evaluate the effect of stabilization.

Table 6.2 shows that the modulus improvement for lightly stabilized sections is only 10 percent on average in the Atlanta District where the aggregate is iron one gravel (BIF = 1.1). This is insignificant. For these types of materials, no significant increase in modulus can be assigned,

Table 6.2 Influence of Stabilizer Content of Base Modulus. BIF is Ratio of Backcalculated Modulus of the Moderately or Lightly Stabilized Layer to the Backcalculated Modulus for an Unstabilized Layer.

Percent Stabilizer	Number of Sections	Base Improvement Factors	
		Range	Average
1 - 2	4 (Atlanta)	0.8 - 2.7	1.1
2 - 3	4 (Atlanta)	1.7 - 3.1	2.4
3 - 4	2 (Atlanta)	3.1 - 4.1	3.6
1 - 2	10 (Yoakum)	1.0 - 5.1	3.0

and the thickness should be designed as an unstabilized base. In the Yoakum District, the addition of 1 to 2 percent lime to calcareous bases results in a considerably high level of BIR. However, the base still retains a flexible nature and should be treated as a flexible base in thickness design.

For stabilizer contents greater than 2 percent, the increase in modulus for the base layer was both

substantial and permanent. For 2 - 3 percent stabilizer, the range of improvement was from 70 percent to 210 percent, with an average improvement of 140 percent. Therefore, for an unstabilized granular base which typically has a modulus of 200 MPa, the average modulus for the layer stabilized with 2 - 3 percent stabilizer would be 480 MPa.

Several runs of FPS-19 were made to evaluate the consequences of incorporating these base improvement factors. As a sensitivity evaluation a low BIF (1.7) and an average BIF (2.4) were evaluated. In all cases, the design thickness for the stabilized layer was compared with that obtained if untreated flexible base was used. Table 6.3 shows the results. Two Districts, Houston and Atlanta; three subgrade strengths ranging from very poor to very good; and two design traffic loadings, 1 and 2 million 80 KN axle equivalents, were considered. In all cases the pavement was designed to have a 37 mm thick hot mix surfacing. The stabilized layers were assigned higher moduli values and were predicted to require between 50 and 100 mm less base material for the same design life.

It is proposed that for design, the conservative Base Improvement factor of 1.7 be used until more field performance data are collected. When running FPS 19, the user should select option 1 for untreated base design. Based on the subgrade soils in that county, the program will recommend both a subgrade and flexible base moduli value. If the base is to be moderately stabilized, as described earlier, the unstabilized base modulus should be multiplied by 1.7 for thickness design purposes.

6.3 DESIGN ALGORITHM FOR HEAVILY STABILIZED BASES

Effect of Wide Shrinkage Cracks

Traditional layered elastic theory computer programs (like Chevron, BISAR and WESLEA etc.) predict the pavement response by assuming axi-symmetric loading which is equivalent to the interior loading. The critical stress to consider for stabilized base thickness design is the maximum flexural stress at the bottom of the stabilized base course. This approach is valid as long as the pavement is uncracked. But cementitious base materials typically shrink, forming transverse shrinkage cracks. Once a transverse crack forms, a different situation exists. Pretorius and Monismith (1972) described the critical stress condition for post-cracked stabilized bases. Increased stabilized base

Table 6.3. Impact of Base Stabilization on Thicknesses Predicted Using FPS19.

- Flex = Untreated Flexible Base
- $E_B * 1.7$ = Modulus Improvement Caused by Stabilization
- Design parameters
- HMA Thickness 37mm Time to First Overlay = 12 years
- Reliability Level = C
- ADT = 2500

District	Sub-grade		Design 80 KN applications, $X10^6$	Base Thickness (mm)		
	Description	E_s , MPa		Flex (E_B)	Stab. ($E_B * 1.7$)	Stab. ($E_B * 2.4$)
Houston	V. Poor	27.6	2	575	425	400
	Int.	55.2	2	450	375	325
	V. Good	138	2	350	250	200
Atlanta	V. Poor	27.6	2	625	450	425
	Int.	55.2	2	500	400	350
	V. Good	138	2	375	300	225
Houston	V. Poor	27.6	1	275	375	350
	Int.	55.2	1	375	325	275
	V. Good	138	1	250	150	150
Atlanta	V. Poor	27.6	1	500	400	400
	Int.	55.2	1	400	325	300
	V. Good	138	1	300	200	150

course tensile stresses must be anticipated due to the loss of continuity, and the critical loading is no longer interior loading. Depending on the width and the load transfer efficiency (LTE) across the crack, a critical loading condition equivalent to edge loading may result. The ILLI-SLAB program was used to predict the response of the cracked pavement since this program can directly model the cracks of different load transfer efficiencies by specifying different aggregate interlock factors. The maximum tensile stress occurs when the load is adjacent to the crack. This critical stress is at the bottom of the stabilized material layer and acts parallel to the crack. Researchers in this study recommend a multiplier of 2.0 to account for wide shrinkage cracks and their influence on the critical flexural tensile stress for interior loading. This multiplication factor can be reduced to as low as 1.0 depending on the Load Transfer Efficiency across the crack. Tight, hairline cracks have high LTE and in turn allow a low stress multiplication factor. Moderately stabilized bases in the Atlanta district are examples of pavements with good transfer efficiency, which justifies using a low value of stress multiplication factor (1.3 to 1.4). In the stabilized base thickness design program developed in this study, a conservative stress multiplication factor of 2.0 is used to insure that the heavily stabilized pavement sections, like those in the Houston District, are safe against fatigue-induced cracking.

Stabilized Base Thickness Design Program

In developing the microcomputer based thickness design procedure for CTB, the critical strains and stresses are calculated for specific traffic and pavement configurations. The following performance models are used to estimate repetitions of load to failure existing performance models:

1. Fatigue in the asphalt concrete surface based on tensile strain at the bottom of the asphalt layer is evaluated using the ARE fatigue equation (1975),
2. Rutting and roughness due to deep layer distress based on subgrade compressive strain are evaluated using the model developed by Luhr et. al. (1983),
3. Load-induced fatigue in the stabilized layer is evaluated using the American Coal Ash Association approach (1991).

The approach uses the WESLEA program to calculate strains due to 80 KN Equivalent Single

Axle Loads.

The program incorporates a pre-processing stage in which all the material properties and layer thicknesses are input, a processing stage in which induced stresses and strains are calculated together with the critical stresses and strains, and a post-processing stage. The post-processing stage, compares load-induced stresses and strains with critical strains calculated from the performance equations to evaluate the fatigue cracking and rutting potential in the asphalt, base and subgrade layers, respectively. The base layer thickness is incrementally increased until all criteria are met. A description of the input is given below.

Stage I

INPUT: In this stage the user inputs the following information:

1. Elastic moduli and poisson's ratio for all layers,
2. Thickness for all layers except stabilized layer,
3. Range of acceptable thicknesses for the stabilized base,
4. Initial Serviceability Index,
5. Terminal Serviceability Index, and
6. No. of 80 KN Equivalent Single Axle Loads.

Stage II

Processing Stage: The processing stage is in two phases.

Phase I:

Critical strains for resistance to fatigue of asphalt and stabilized base layers and subgrade rutting are calculated using the following performance models:

Asphalt Layer Fatigue:

ARE fatigue equation is

$$W_{18} = 9.73 * 10^{-15} (1/\epsilon_t)^{5.16}$$

where

W_{18} = Weighted 80 KN applications before class-2 cracking

ϵ_t = Critical tensile strain at the bottom of asphalt layer

Subgrade Rutting:

$$\text{Log}_{10}^{N_x} = 2.15122 - 597.662 (\epsilon_{SG}) - 1.32967 (\log_{10} \epsilon_{SG}) + \log_{10} [(PSI - TSI) / (4.2 - 1.5)]^{1/2}$$

where

$$\text{Log}_{10}^{N_x} = \text{Log}_{10} \text{ allowable applications of axle load } x$$

(In the general case axle load = 80 KN)

ϵ_{SG} = Subgrade Compressive strain due to axle load 'x'

PSI_x = Initial PSI of the pavement

TSI = Terminal Serviceability Index

Stabilized Base Fatigue:

The program checks for this criteria only when $E_{base} > 7,000$ MPa

The American Coal Ash Association equation is as follows:

$$\text{Stress Ratio} = 0.972 - 0.0825 \log_{10}^N$$

where

$$\log_{10}^N = \log_{10} \text{ allowable application of 80 KN axle loads}$$

Stage III

The WESLEA program calculates, for a pre-assumed thickness of stabilized base, strains and stresses at the top of the subgrade, bottom of bituminous surface layer and bottom of stabilized base. The tensile strain at the bottom of stabilized base is multiplied by a factor of 2.0 to account for poor load transfer across wide shrinkage cracks.

The WESLEA calculated induced stresses and strains are compared with the corresponding critical stresses and strains. The assumed thickness is considered sufficient when none of the calculated WESLEA stresses and strains exceed the corresponding critical stresses or strains from the applicable performance models. Otherwise, the thickness of the stabilized base is increased for the next trial. The process will be repeated (within the thickness range) until a suitable thickness is found which satisfies all requirements.

Users Guide to Stabilized Base Thickness Design Program

The design procedure described earlier has been programmed into a microcomputer program. The Program is supplied on diskette. To run the program type "DISPLAY" then type "STBC" to load

the input screen. It is assumed that the stabilized layer is Layer 2 of the structure. The user has to supply the following:

1. Design volume of traffic in 80 KN Equivalent Single Axle Loads (in millions),
2. Initial Serviceability Index of the Pavement (PSI),
3. Terminal Serviceability Index of the Pavement (TSI),
4. Thickness, modulus and poisson's ratio of the asphalt surface layer (in ins, ksi),
5. Range of thickness for stabilized base, modulus and poisson's ratio of the stabilized base (in ins, ksi),
6. Thickness, modulus and poisson's ratio of the subbase layer, if present (in ins, ksi), and
7. Depth to bed rock (if not known, leave for a default value by the program), modulus and poisson's ratio of the subgrade (in ins, ksi).

Note: Press "F1" to edit the first three fields.

Press "F2" to edit the thickness, modulus and poisson's ratio fields.

The program handles up to 4 layers (surface, Stabilized base, Subbase, Subgrade) above the bedrock. If no subbase is present, enter 0.0 for the subbase thickness. The thickness of layer 4 is the depth to a stiff layer as calculated by MODULUS program or assumed by the designer.

The program uses the WESLEA computer program as a subroutine to calculate induced tensile strain at the bottom of asphalt layer, the tensile strain at the bottom of stabilized base and the vertical strain at the top of the subgrade. This calculation is performed for the following three positions, (a) under the center of tire, (b) at the edge of the tire, and (c) between the tires. The results are then passed to the main thickness design program to compare with the critical strains calculated using performance models.

The user has to supply a practical possible range for the thickness (say, for example, 150 mm to 500 mm) of the stabilized base. The program tries to find a solution within the prescribed range. A message is displayed identifying whether or not the program succeeded. If a solution is not found, the program displays the message "Failed." In order to save computational time, it is advantageous to identify a narrow range of potential base thicknesses for design.

A final output showing the final thicknesses and modulus values for various layers of the

pavement is displayed. If the program fails to find the solution within the user input range, then the "failed" message will be displayed under all those layers where the criteria can't be met within the range of thicknesses. As an example, if the "failed" message is displayed under both asphalt and subgrade layers, then the user input range for stabilized base thickness is not sufficient to meet both asphalt layer fatigue and subgrade rutting criteria. In order to allow for an acceptable solution, it is advisable to increase the upper limit for the thickness of the stabilized base.

An extensive sensitivity analysis was performed using the design algorithm. This sensitivity analysis evaluated the following matrix:

1. HMA surface: 37.5 and 75 mm,
2. HMA modulus: 3,500 MPa,
3. Stabilized base modulus: 700; 1,400, 3,500, 7,000 and 14,000 MPa,
4. Subbase thickness: 0, 100 and 200 mm,
5. Subbase modulus: 140 MPa and 280 Mpa, and
6. Subgrade modulus: 3,500 and 7,000 KPa.

The thickness values of the stabilized base calculated were reasonable.

6.4 MIX DESIGN CONSIDERATIONS FOR LIME-STABILIZED SUBGRADES

Current Approach

Test method Tex-121-E presents the approach used by TxDOT to design lime-soil and lime-aggregate mixtures. In this method the recommended percentage of lime for stabilization is based on the percent binder (minus 40 sieve size fraction) and plasticity index (PI). A plot of the locus of these two index properties on a lime content design chart defines the trial lime content to be used in a lime-stabilized soil or base.

Tex-121-E requires samples to be fabricated in accordance with Tex-113-E at a compactive effort of 1.09 Joules per cubic centimeter (13.26 ft-lb per cu. in.). Samples are next moist cured at room temperature for 7 days, dry cured at a temperature not to exceed 60°C for 6 hours or until one-third to one-half of the molding moisture is removed. Finally, the sample is subjected to capillary rise for 10 days prior to triaxial compressive strength testing.

Unconfined triaxial compressive strength testing is performed in accordance with Tex-117-E. Tex-121-E recommends that a strength of 700 KPa is satisfactory for final course of base construction, and at least a 350 KPa unconfined compressive strength is required for subbase soils.

Recommended Changes

The recommended approach for mixture design is presented in Figure 6.1. The first step in this approach is to perform the pH test in accordance with ASTM C 977 appendix. This test defines the percentage of lime required to satisfy initial soil-lime reactions and still provide enough residual lime to drive the pozzolanic reaction. Verification of the pH test defined lime content is based on Tex-121-E strength testing.

The authors recommend modification of Tex-121-E to accommodate longer curing of lime-soil and/or lime-aggregate mixtures. The recommended approach is 14-day moist curing instead of 7-day moist curing. All other curing procedures remain the same as defined in Tex-121-E. The need for the longer period of moist curing is simply that pozzolanic reactions in lime-soil mixtures occur more slowly than cementitious hydration reactions. Furthermore, some lime-soil mixtures do not respond predictably to accelerated curing.

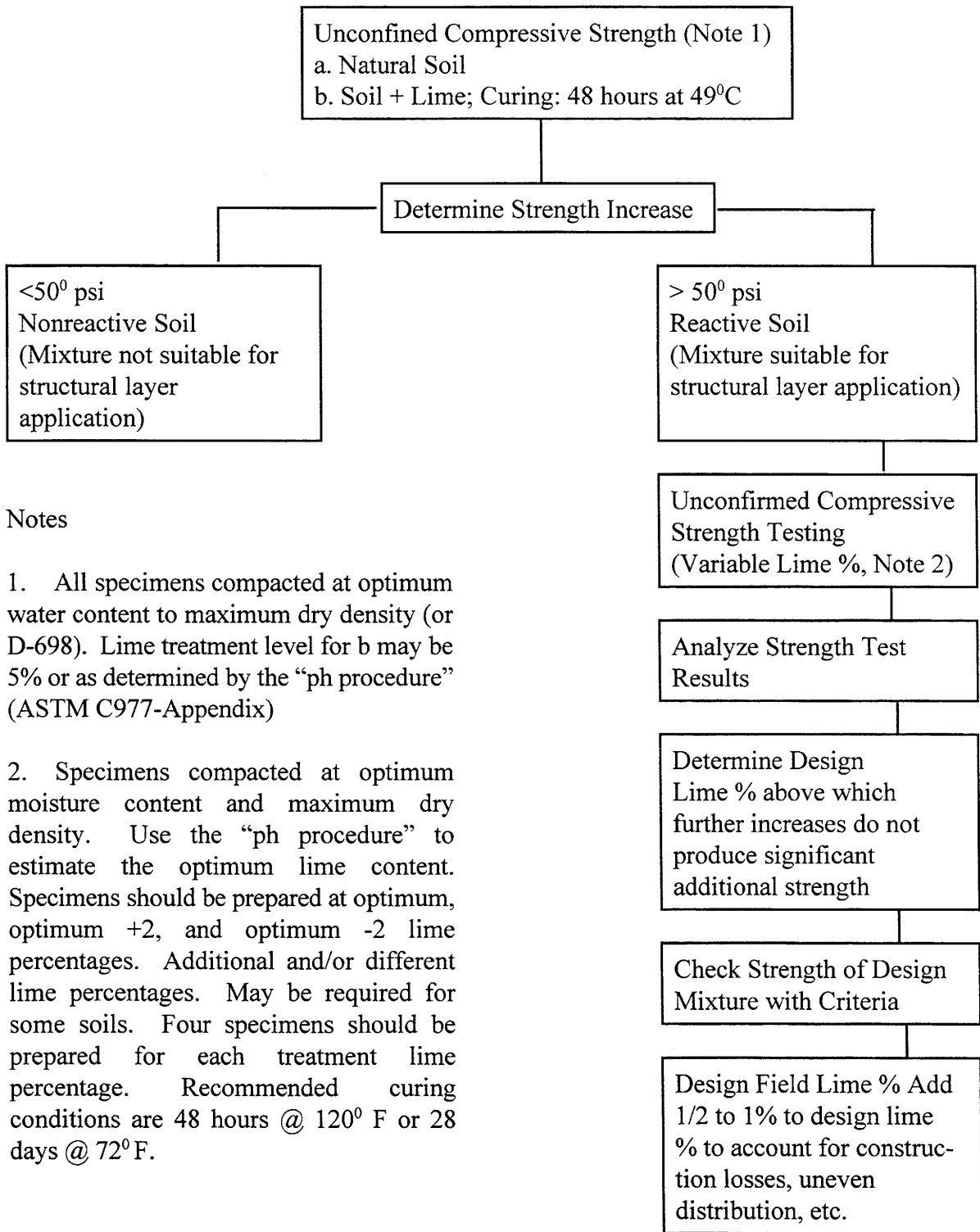


Figure 1. Recommended Approach for Mixture Design for Lime-Stabilized Subgrades.

6.5 STRUCTURAL CONSIDERATIONS FOR STABILIZED SUBGRADES

General

In order to be able to assign structural significance to a stabilized subgrade, the designer must be reasonably confident that the stabilization is permanent and that the structural contribution is significant. Although permanency or durability cannot be absolutely assured, it is possible to provide a high level of reliability by following the mixture design procedures established in section 6.4 of this chapter.

Procedure

The process for assigning structural significance to lime-stabilized subgrades in Texas is a two phase process. The first phase is to assign a realistic approximate resilient modulus to the stabilized layer. This approximation is based on laboratory testing and field FWD evaluations.

Assigning a realistic resilient modulus for design and analysis involves the following steps:

1. Estimate the average annual roadbed resilient modulus from FWD backcalculations based on the MODULUS program. A reasonable weighted average annual modulus can be calculated using the approach described in the 1986 AASHTO Pavement Design Guide.
2. Determine the unconfined compressive strength of the lime-stabilized mixture in accordance with Tex-121-E following a curing period of 28-days and cured at a temperature of 25°C.
3. Based on an average annual roadbed modulus and an average stabilized subgrade modulus to natural subgrade modulus ratio, determine a representative design modulus for the stabilized subgrade layer.

The second phase involves evaluation of the structural compatibility and capacity of the lime-stabilized subgrade with the pavement system. This phase involves the same three steps as listed above plus evaluation of the flexural fatigue damage potential within the stabilized subgrades.

Estimation of Stabilized Subgrade Modulus

A realistic and conservative estimate of the resilient modulus of a lime-stabilized subgrade can be determined based on the 28-day unconfined compressive strength determined in accordance with Tex-121-E at a test temperature of 25°C and an estimate of the average annual subgrade modulus

based on FWD data and MODULUS backcalculations.

A review of work by Thompson (1966), Suddath and Thompson (1975) and Thompson and Figueroa (1989) supplemented by testing in this study reveals a relationship between the unconfined compressive strength of the lime-soil mixture and the resilient modulus of the mixture.

Figure 6.2 presents a relationship between unconfined compressive strength and flexural modulus (based on data from Thompson and Figueroa (1989)), unconfined compressive strength and backcalculated field moduli (determined from FWD data from the 1287 study) and unconfined compressive strength and compressive moduli (based on data from Thompson and Figueroa (1989)). From this figure, it can be seen that the relationship between unconfined compressive strength and flexural modulus and between unconfined compressive strength and field (FWD backcalculated from Study 1287) modulus are in reasonable agreement. The compressive modulus approximated from unconfined compressive strength data appears to be a conservative approximation of the modulus of the lime-stabilized layer. Based on the findings summarized in Figure 6.2, a realistic and conservative approximate modulus for the lime-stabilized layer that can be used in design approximations is presented by the dashed line in Figure 6.2. For clarity, this relationship is replotted in Figure 6.3.

The researchers feel that it is reasonable that the resilient modulus of the stabilized subgrade should also be affected by the level of support provided by the natural subgrade. Figure 6.3 is a plot of subgrade resilient modulus versus the ratio of modulus of the lime-stabilized subgrade (from FWD backcalculations) to modulus of the natural subgrade (from FWD backcalculations). These data indicate that for natural subgrade moduli below about 50 MPa, the modulus ratio is typically 10 or above. For subgrade moduli between 50 MPa and 200 MPa, the modulus ratio is between 5 and 10, and for subgrade moduli exceeding 200 MPa, the modulus ratio is less than about 5.

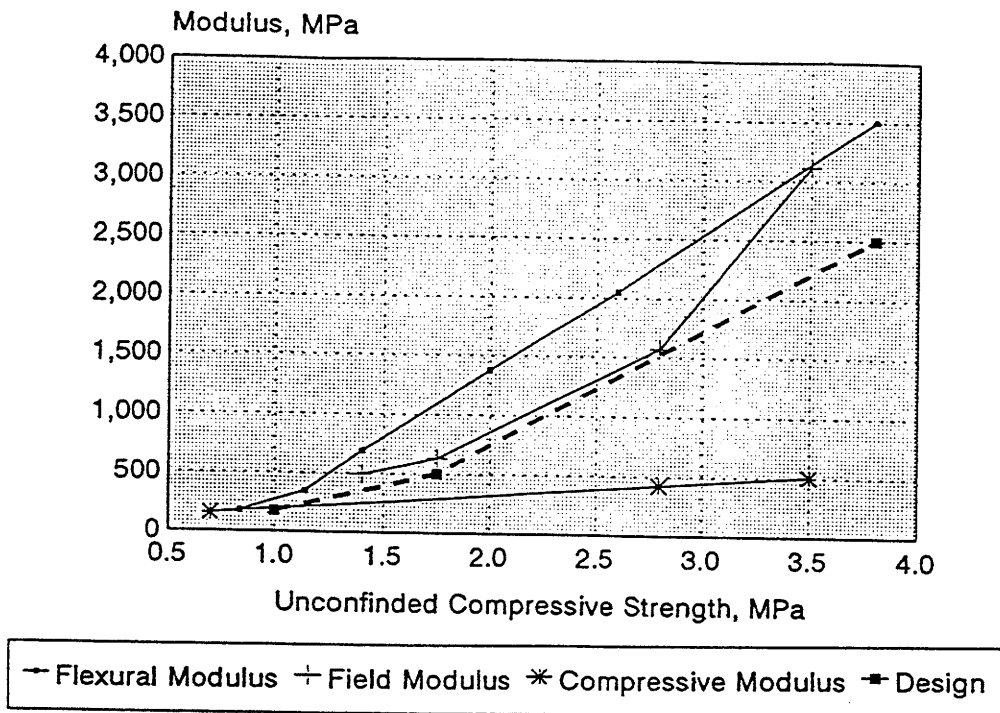


Figure 6.2. Relationships Between Unconfined Compressive Strength and Moduli of Lime-Stabilized Soils.

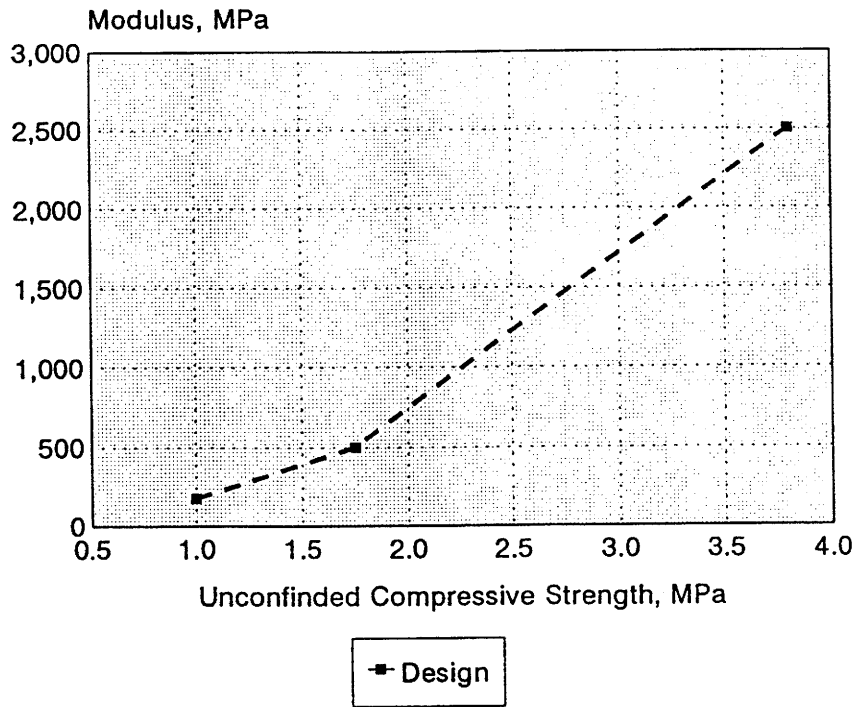


Figure 6.3. Selected Design Relationship Between Unconfined Compressive Strength and Resilient Modulus for Lime-Stabilized Subgrade Pavement Layers.

Based on the foregoing information, the approximate design modulus for the stabilized subgrade layer should be first approximated based on the 28-day, 25°C cured, unconfined compressive strength, Figure 6.3. This modulus should then be checked against a realistic value of the modulus ratio determined from the approximate average annual roadbed resilient modulus. Based on Figure 6.4, this ratio should, conservatively, not exceed 17 for subgrade moduli equal to or less than 50 MPa, 10 for subgrade moduli between 50 and 200 MPa, or 5 for subgrade moduli above 200 MPa.

Resistance of Lime-Stabilized Layers to Flexural Fatigue

Once the lime-stabilized soil mixture has been determined to be reactive, e.g., unconfined compressive strength of 1,000 KPa or greater and an increase in unconfined compressive strength of at least 350 KPa over that of the unstabilized soil, and the average annual roadbed modulus and stabilized layer moduli have been determined, the ability of the pavement structure to resist flexural fatigue should be evaluated.

This evaluation can be simply performed using any layered elastic computer model. This evaluation can easily be incorporated into computer models such as FPS-19 or the heavy stabilized CTB model presented in section 6.3. In the absence of a computer model, the ability of the stabilized layer to resist fatigue damage can be assessed by:

1. Determining the critical radial tensile stress developed under load within the lime-stabilized layer and
2. Comparing the flexural strength of the stabilized layer with the critical flexural tensile stress developed within the stabilized layer.

As shown in Figure 6.5, the stress ratio, ratio of induced tensile flexural stress to flexural strength, should be less than 0.50 to insure a long (10^7 axle applications or greater) life or a fatigue resistant layer. Since the flexural strength is approximately 0.25 times the unconfined compressive strength and since the ratio of tensile strength induced within the stabilized layer should be less than 0.50, the critical flexural stress within the stabilized layer should not exceed 12 percent of the compressive strength.

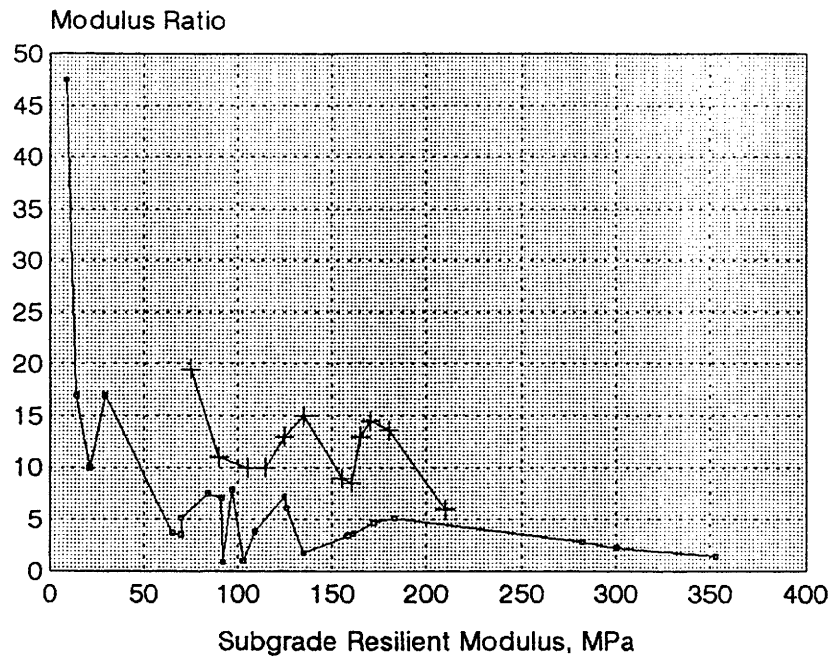
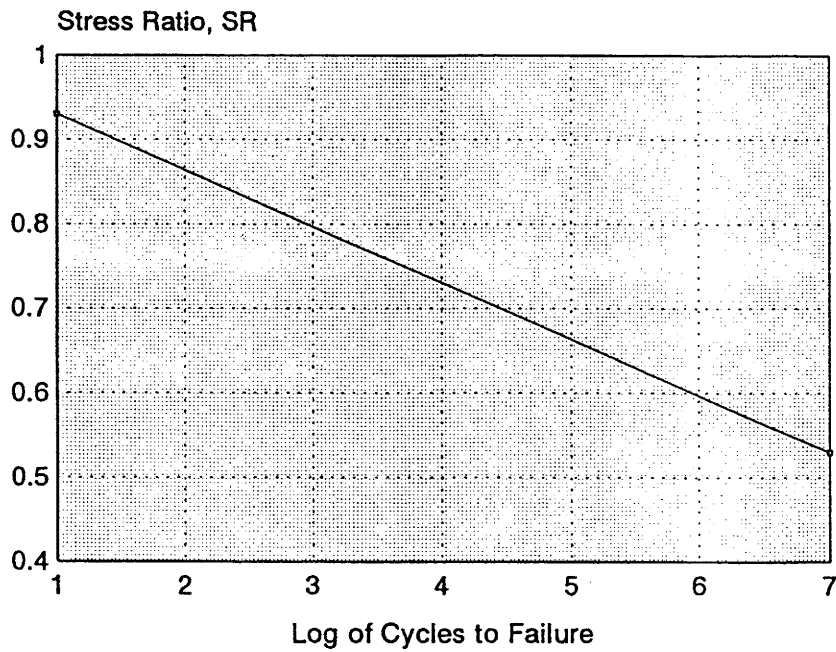


Figure 6.4. Relationship Between In Situ Modulus of the Natural Subgrade Soil as Determined by FWD Measurements and the Moduli Ratio (Lime-Stabilized Layer to Natural Subgrade Layer) as Determined by FWD Measurements.



$$S = 0.923 - 0.058 \log N$$

Figure 6.5. Stress Ratio Versus Cycles to Failure Fatigue Relationship (After Thompson and Figueroa (1989)).

Thompson and Figueroa (1989) calculated radial stresses in lime-stabilized subgrades of various moduli as a function of the layer thickness of the stabilized layer under a 80 KN axle load for stiff, medium and soft subgrades, Figures 6.6 through 6.9. In these figures, it is assumed that the surface layer is merely a surface treatment and does not contribute to the structural integrity of the pavement.

From the data in these figures, Thompson and Figueroa (1989) developed a regression model by which to calculate flexural tensile stress as a function of the thickness of the stabilized layer and the resilient modulus of the subgrade.

Although the model was developed for a two-layer system, it can be used in a multilayered structure by using Odemark's transformation to approximate the effect of the HMA and the unbound base layers. Applying the Odemark transformation and assuming realistic and conservative average annual moduli for the HMA and unbound base layers in Texas, the effective thickness of the pavement is calculated as follows:

$$T_{\text{eff}} = A T_{\text{HMA}} + B T_{\text{Flex.}} + T_{\text{LSS}}$$

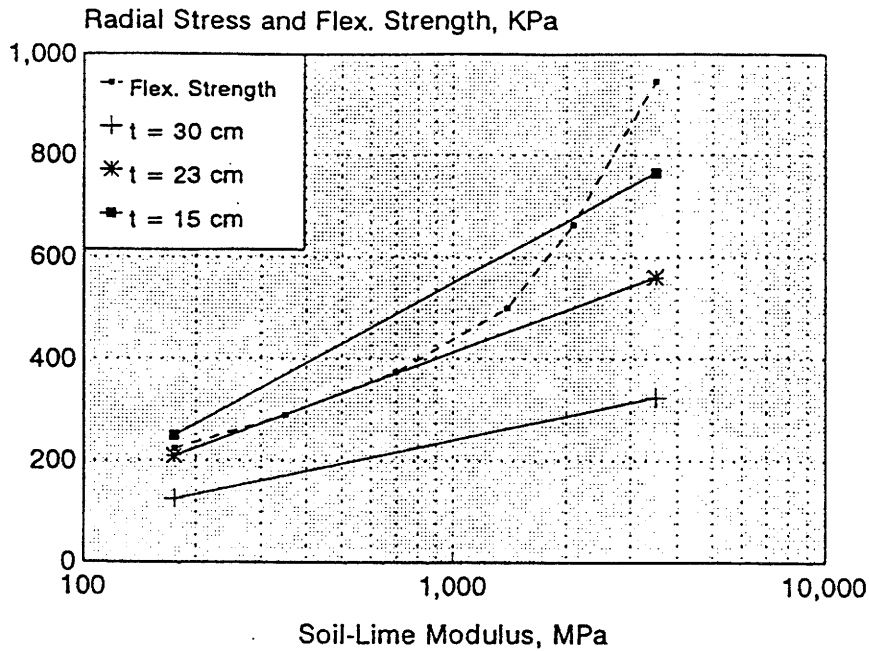
In this relationship A is calculated as the cube root of a representative the quotient of HMA modulus (2,590 MPa) and the lime-stabilized modulus (E_{LSS}):

$$A = (2,590 \text{ MPa}/E_{\text{LSS}} \text{ MPa})^{0.33}$$

B is the cube root of the quotient of a representative unbound base modulus and the modulus of the lime-stabilized subgrade:

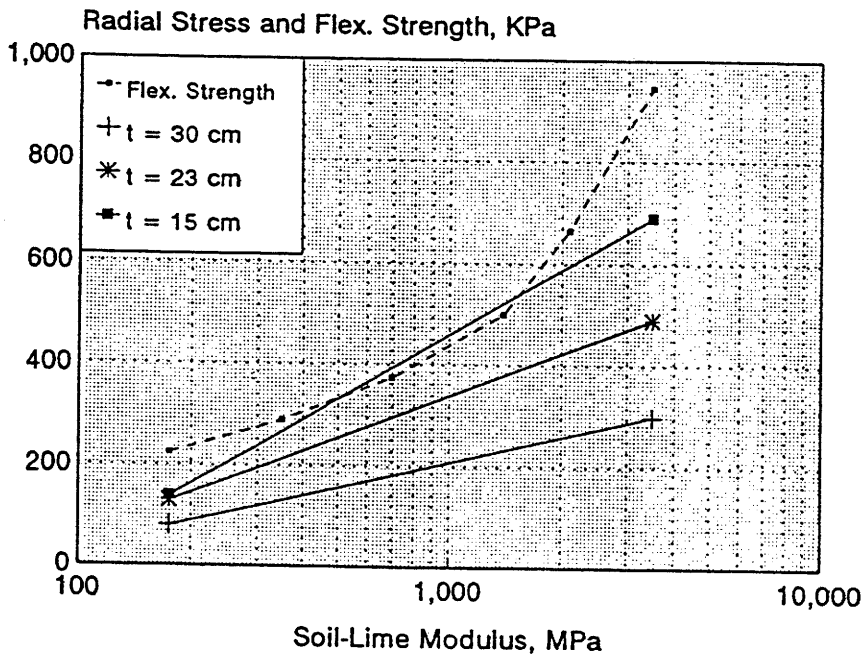
$$B = (245 \text{ MPa}/E_{\text{LSS}} \text{ MPa})^{0.33}$$

and T_{HMA} is the actual thickness of HMA, $T_{\text{Flex.}}$ is the actual thickness of the flexible base, and T_{LSS} is the actual thickness of the lime-stabilized layer.



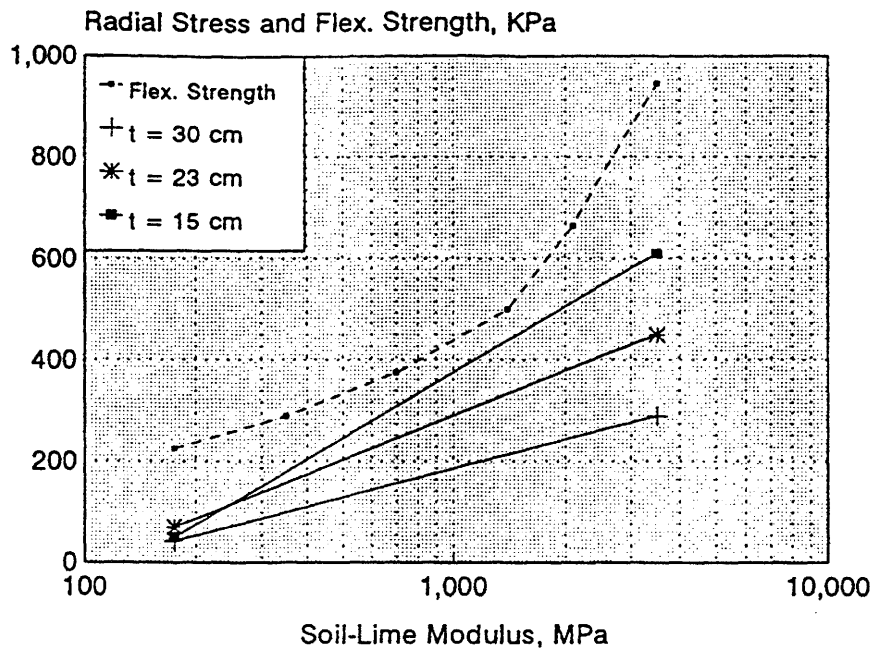
Soft Subgrade

Figure 6.6. Relationship Between Modulus of Lime-Soil Mixture and Radial Stress Induced in the Lime-Stabilized Layer and Flexural Strength for Soft Natural Subgrades (After Thompson and Figueroa (1989)).



Medium Subgrade

Figure 6.7. Relationship Between Modulus of Lime-Soil Mixtures and Radial Stress Induced in the Lime-Stabilized Layer and Flexural Strength for Medium Stiffness Natural Subgrades (After Thompson and Figueroa (1989)).



Stiff Subgrade

Figure 6.8. Relationship Between Modulus of Lime-Soil Mixtures and Radial Stress Induced in the Lime-Stabilized Layer and Flexural Strength Stiff Natural Subgrades (After Thompson and Figueroa (1989)).

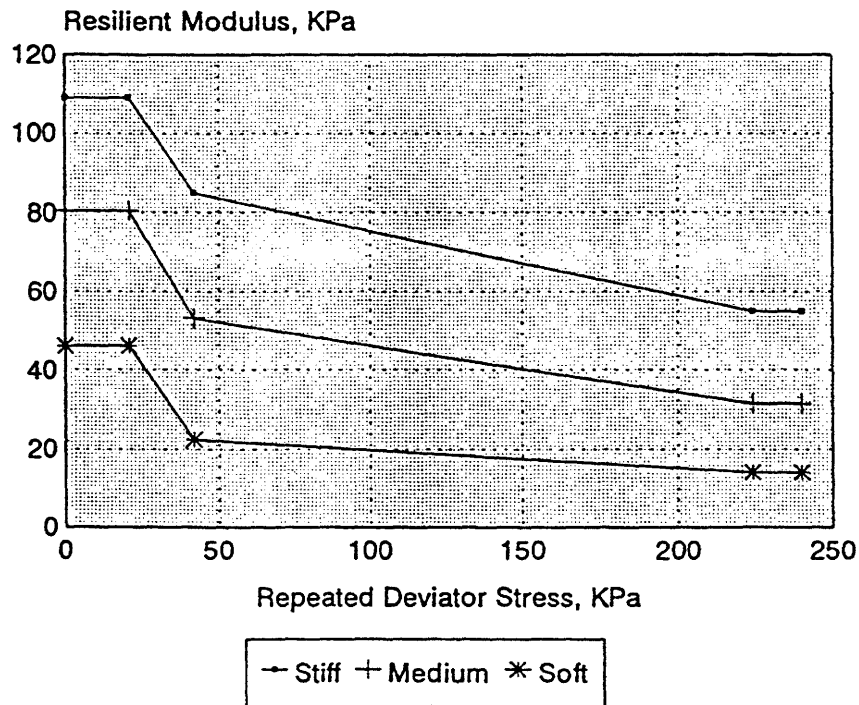


Figure 6.9. Typical Resilient Modulus Versus Deviatoric Stress Relationships for Soft, Medium and Stiff Subgrades.

Example Calculation

Assume a lime-stabilized layer where the mix was designed in accordance with the procedure set forth in section 6.4 has a compressive strength of 2,000 KPa. From Figure 6.3, the approximate resilient modulus is 800 MPa. The natural subgrade average annual modulus is 133 MPa, which is within the modulus ratio criteria, Figure 6.4.

The pavement structure is to consist of 75 mm of HMA, 305 mm of flexible base (crushed limestone) and 150-mm of LSS. The effective thickness in terms of the LSS is:

$$T_{\text{eff}} = (2,590/800)^{0.33} \times 75 + (245/800)^{0.33} \times 305 + 150 = 466 \text{ mm}$$

The flexural radial stress in the LSS is calculated from the Thompson and Figueroa (1989) regression equation:

$$\sigma_r = 23.22 - 4.66(T_{\text{eff}}) + 42.66 \log E_{\text{subg.}} - 29.11 \log E_{\text{LSS}}$$

where T_{eff} , $E_{\text{subg.}}$ and E_{LSS} are in inches, psi and psi, respectively.

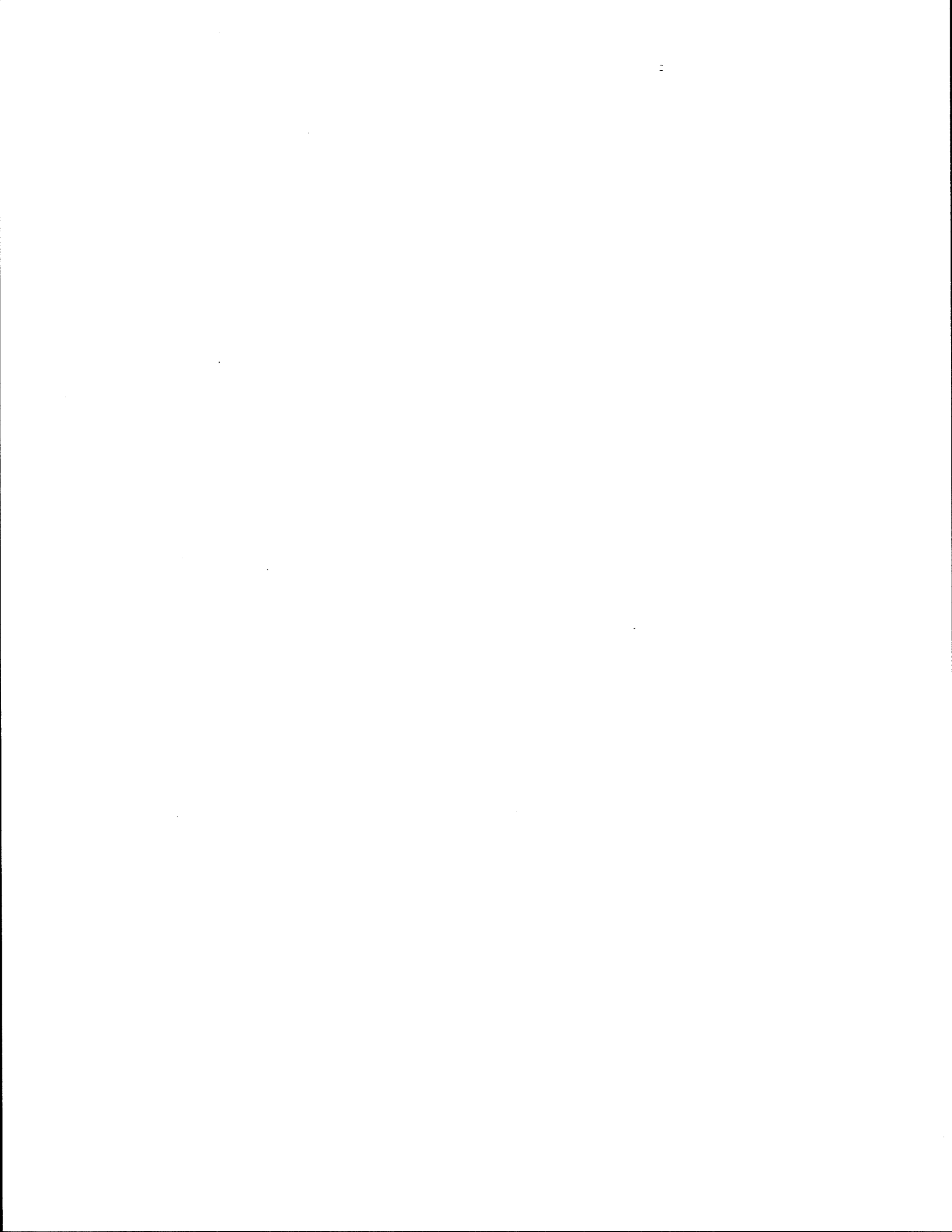
From this calculation, σ_r is -187.5 KPa, and the stress ratio, $SR = -187.5/0.5(2,000) = 0.187$, which is far less than 50 percent and is safe against fatigue.

Evaluation of flexural fatigue using the aforementioned approach should be made when either a thin HMA surface (less than 75 mm) or a surface treatment is placed directly over the lime-stabilized subgrade or over a thin aggregate base (less than 150 mm) and lime-stabilized subgrade. Otherwise, under typical highway wheel loads, significant flexural fatigue damage in the lime-stabilized layer is not a significant problem.

If fatigue damage is a potentially significant problem in flexible pavements due to heavy wheel loads, a layered elastic stress evaluation should be made using the subgrade and lime-treated subgrade moduli calculated as discussed in the preceding sections. The stress ratio fatigue evaluation explained in the preceding section should be used. The Thompson and Figueroa (1989) algorithm is only for an 80 KN axle load.

When flexural fatigue in the stabilized layer is not a consideration, the approximate modulus value of the lime stabilized layer may be appropriate for use in design algorithm. Such moduli

values can be derived as previously discussed.



REFERENCES

AASHTO *Interim Guide for Pavement Design*, 1973.

AASHTO *Pavement Design Guide*, 1986.

ACAA Flexible Pavement Manual - Recommended Practice - Coal Fly Ash in Pozzolanic Stabilized Mixtures for Flexible Pavement Systems, 1990. American Coal Ash Association, Washington, D. C.

Alexander, M. L. and Doty, R., 1978. "Determination of Strength Equivalency for Design of Lime-Stabilized Roadways," Report No. FHWA-CA-TL-78-37.

Amerigaznon, M. and Little, D. N., "Permanent Deformation Potential in Asphalt Concrete Overlays Over PCC Pavements," Research Report 452-3F, Texas Transportation Institute.

Caltabiano, M. A. and Rawlings, R. E., 1992. "Treatment of Reflection Cracking in Queensland," *7th International Conference on Asphalt Pavements*, Nottingham.

Currin, D. D., Allen, J. J. and Little, D. N., 1976. "Validation of Soil Stabilization Index System with Manual Development," Report FJSRL-TR-76-0006, Frank J. Seiler Research Laboratory, United States Air Force Academy, Colorado.

Design Coefficients for Lime-Soil Mixtures, 1970. Research Report IHR-28, Illinois Division of Highways, Bureau of Research and Development and U. S. Department of Transportation, Federal Highway Administration.

Eades, J. L. and Grim, R. E., 1960. "Reactions of Hydrated Lime with Pure Clay Minerals," *Highway Research Bulletin* No. 262.

Eades, J. L., Nichols, F. P., and Grim, R. E., 1962. "Formation of New Minerals with Lime Stabilization as Proven by Field Experiments in Virginia," *Highway Research Bulletin* No. 335.

Graves, R. E. and Eades, J. L., 1987. "Strength Developed from Carbonate Cementation in Silica/Carbonate Systems," Final Report, Department of Geology, University of Florida.

Graves, R. E., Eades, J. L. and Smith, L. L., 1990. "Calcium Hydroxide Treatment of Construction Aggregates for Improved Cementation Properties," *American Society of Testing and Materials*, Special Technical Publication, 1135.

Gutschick, K. S., 1985. "Canal Lining Stabilization Proves Successful," *Pit and Quarry*.

Haston, J. and Wohlgemuth, S. K., 1985. "Comparisons of Compressive Strengths of Lime-Soil Mixtures Based on Optimum Lime Contents Determined by Different Methods."

Jordaan, G. J., 1992. "Towards Improved Procedures for the Mechanistic Analysis of Cement Treated Layers in Pavements," *Proceedings of the 7th International Conference on Asphalt Pavements*.

Kelly, C. M., 1988. "A Long Range Durability Study of Lime Stabilized Bases at Military Posts in the Southwest," *National Lime Association, Bulletin 328*.

Kennedy, T. W. and Tahmoressi, M., 1987. "Lime and Cement Stabilization," *Updates and Applications in Construction*, National Lime Association, Issue No. 2, Waco, Texas.

Kleyn, E. G. and Savage, P. F., 1982. "The Application of the Pavement DCP to Determine the Bearing Properties and Performance of Road Pavements," *International Symposium on Bearing Capacity of Roads and Airfields*, Trondheim, Norway.

Little, D. N. and Alam, S., 1984. "Evaluation of Fly Ash Test Sites Using a Simplified Elastic Theory Model and Field Measurements," Research Report 240-2F, Texas Transportation Institute.

Little, D. N., 1986. "Basic Reactions of Soil-Lime Mixtures," *Bulletin 331*, National Lime Association.

Little, D. N., Thompson, M. R., Terrel, R. L., Epps, J. A. and Barenberg, E. J., 1987. "Soil Stabilization for Roadways and Airfields," Report ESL-TR-86-19, Air Force Services and Engineering Center, Tyndall Air Force Base, Florida.

Little, D. N., 1990. "Comparison of In-Situ Resilient Moduli of Aggregate Base Courses with and without Low Percentages of Lime Stabilization," *American Society of Testing and Materials, Special Technical Publication No. 1135*.

Little, D. N., Scullion, T. and Bhuydin, J., 1993. "Evaluation of Structural Properties of Stabilized Pavement Layers," Interim Report 1287, Prepared for the Texas Department of Transportation, Texas Transportation Institute.

Little, D. N. and Youseff, H., 1992. "Improved ACP Mixture Design: Development and Verification," Research Report FHWA/TX-92/1170-1F, Texas Transportation Institute.

Little, D. N., 1994. *Lime Stabilization Handbook*. Kenall Hunt Publishers, National Lime Association.

McCallister, L. D. and Petry, T. M., 1990. "Property Changes in Lime Treated Expansive Clays Under Continuous Leaching," Technical Report GL-90-17, University of Texas at Arlington.

McDowell, C., 1972. "Flexible Pavement Design Guide," Bulletin 327, National Lime Association, Arlington, Virginia.

Scrivner, F. H. and Moore, W. M., 1968. "An Empirical Equation for Predicting Pavement Deflections," Report No. 32-12, Texas Transportation Institute, Texas A&M University.

Raad, L., 1977. "Fatigue Behavior of Cement Treated Materials," *Transportation Research Record* 641.

Raad, L., 1985. "Behavior of Stabilized Layers Under Repeated Loads," *Transportation Research Record* 1022.

Scullion, T., 1993. "Forensic Evaluation of SH 36," Report Prepared for the Houston District of the Texas Department of Transportation.

Soil-Cement Laboratory Handbook, 1959. Portland Cement Association, Skokie, Illinois.

Soil-Cement Construction Handbook, 1969. Portland Cement Association, Skokie, Illinois.

Tabatabaie-Raissi, A. M., 1977. "Structural Analysis of Concrete Pavements Joints," Ph.D. Thesis, University of Illinois.

Thomas, D., 1994. Personal Communications with Atlanta District.

Thompson, M. R., 1970. "Soil Stabilization for Pavement Systems - State of the Art," Technical Report, Construction Engineering Laboratory, Champaign, Illinois.

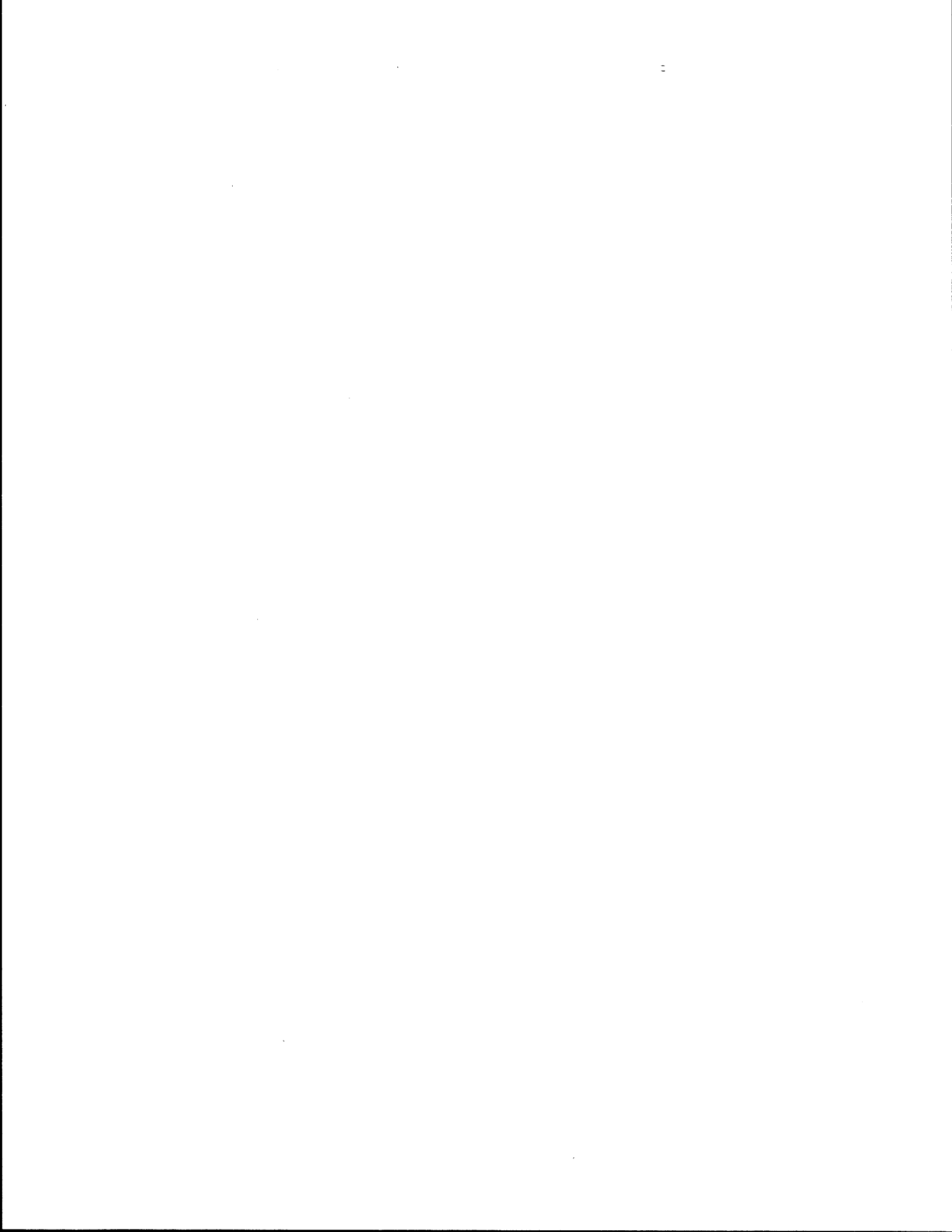
Thompson, M. R., 1985. "Mechanistic Thickness Design Concepts for PAM Pavements," *Proceedings - Seventh International Ash Stabilization Symposium*. U. S. Department of Energy, Report DOE-METC-85/6018, Vol. 2, Orlando.

Thompson, M. R. and Figueroa, J. L., 1989. "Mechanistic Thickness Design Procedure for Soil-Lime Layers," Paper Presented at the *Transportation Research Board*.

Thompson, M. R., 1994. "Design of Heavily Stabilized Bases," Paper Presented at the 1994 Meeting of the *Transportation Research Board*.

Van Vuuren, D. J., "Rapid Determination of CBR with the Portable DCP," *The Rhodesian Engineer*, Volume 7, No. 5.

APPENDIX



Section No.: 1 District: Houston County: Harris Highway: FM-526 (North)
Structure: Asphalt : 76 mm
CTB : 356 mm
LTS : 152 mm
Subgrade

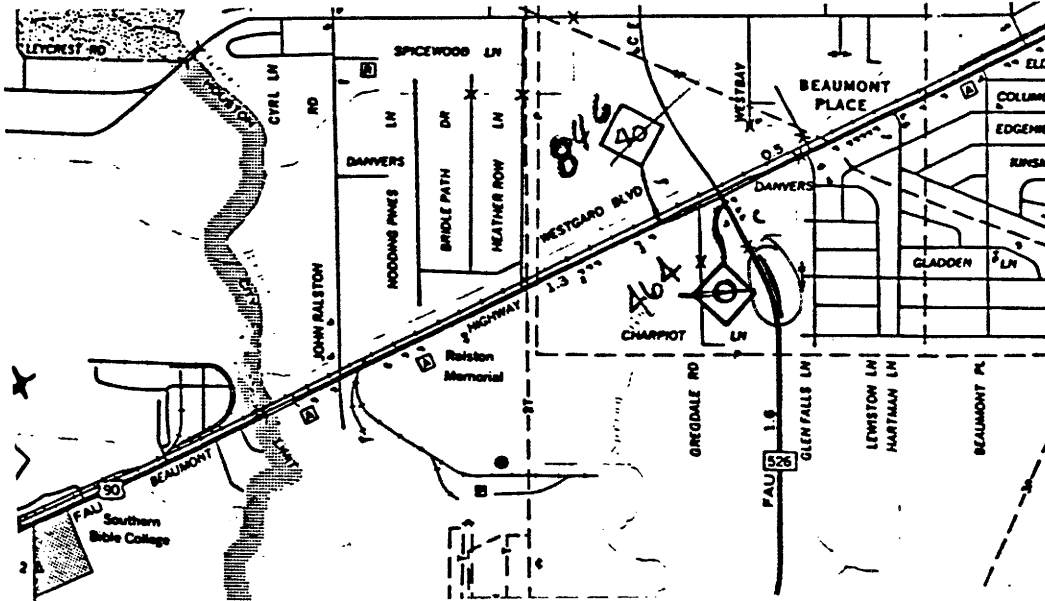
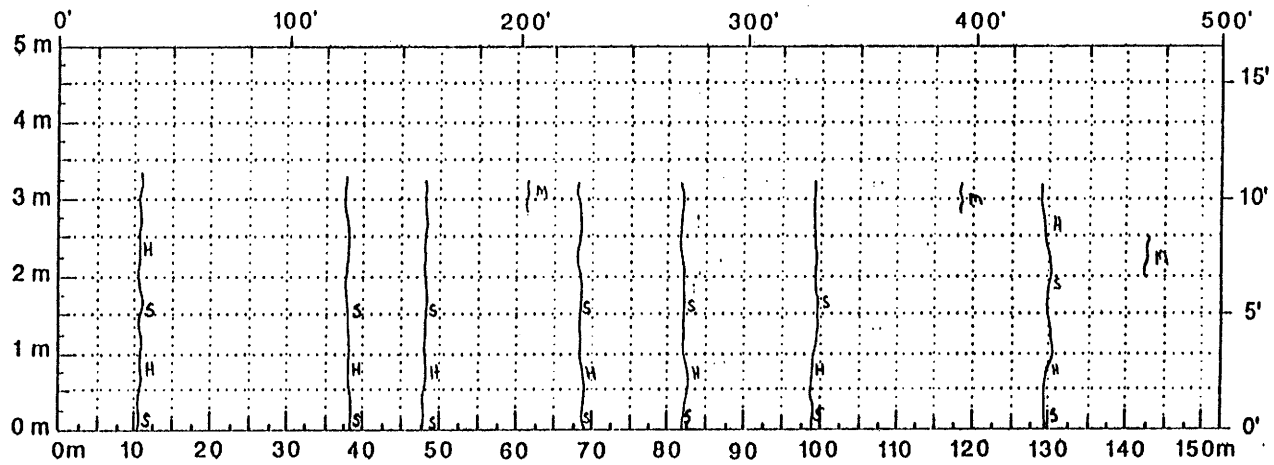
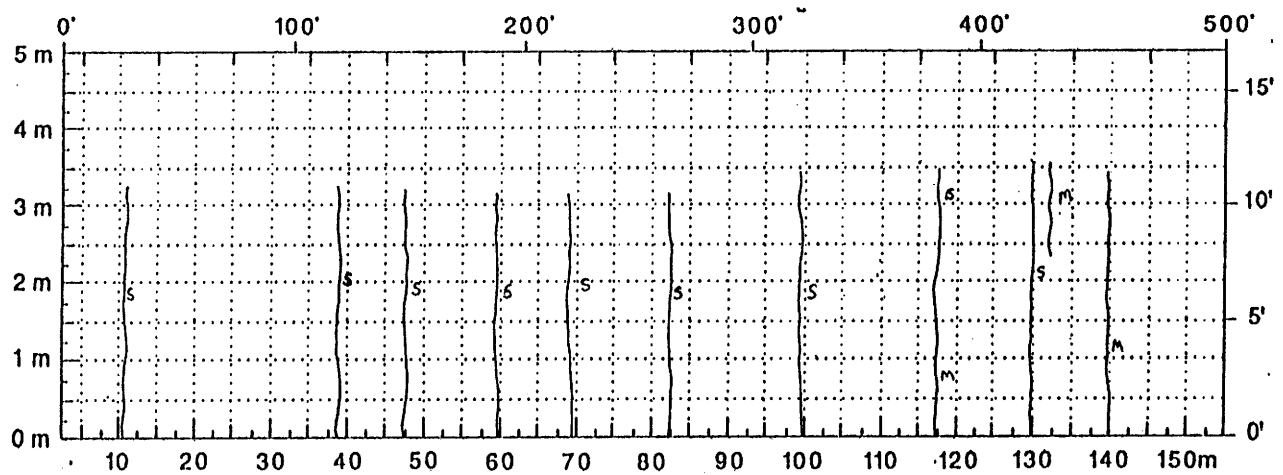


Figure A.1. Location and Details of Section-1 of Houston District.



Comments: Crack Map for Summer

A.4



Comments: Crack Map for Winter

Figure A.2. Crack map for Section-1 of Houston District.

TTI MODULUS ANALYSIS SYSTEM (SUMMARY REPORT)

(Version 4.2)

District:	12	MODULI RANGE(psi):		Poisson Ratio Values	
County:	102	Minimum	Maximum	H1: $\mu = 0.35$	
Highway/Road:	FM0526	349,965	350,035	H2: $\mu = 0.25$	
		500,000	5,000,001	H3: $\mu = 0.25$	
		30,000	600,000	H4: $\mu = 0.35$	
			25,000		

Station	Load (lbs)	Measured Deflection (mils):							Calculated Moduli values (ksi):				Absolute Dpth to	
		R1	R2	R3	R4	R5	R6	R7	SURF(E1)	BASE(E2)	SUBB(E3)	SUBG(E4)	ERR/Sens	Bedrock
1.000	10,927	2.63	2.14	1.96	1.79	1.59	1.43	1.26	350.	5000.0	577.8	25.5	3.58	300.00 *
2.000	10,911	2.46	2.10	1.92	1.79	1.59	1.39	1.22	350.	5000.0	320.2	27.5	6.04	300.00 *
3.000	10,935	2.79	2.18	2.00	1.79	1.63	1.47	1.31	350.	5000.0	563.0	24.8	2.70	300.00 *
4.000	10,847	2.46	1.97	1.81	1.63	1.38	1.22	1.06	350.	5000.0	337.0	30.6	3.67	300.00 *
5.000	10,863	2.34	1.76	1.65	1.55	1.47	1.30	1.22	350.	5000.0	62.3	35.8	9.80	300.00 *
6.000	10,959	2.83	1.93	1.81	1.55	1.55	1.43	1.26	350.	5000.0	260.9	29.0	6.57	300.00 *
7.000	10,903	2.46	1.97	1.81	1.67	1.55	1.43	1.26	350.	5000.0	127.5	30.1	7.96	300.00 *
8.000	10,879	2.95	2.52	2.38	2.23	2.04	1.92	1.80	350.	5000.0	455.5	19.6	6.35	300.00 *
9.000	10,927	3.23	2.68	2.42	2.19	2.20	2.04	1.80	350.	5000.0	451.7	17.9	6.34	300.00 *
Mean:		2.68	2.14	1.97	1.80	1.67	1.51	1.35	350.	5000.0	350.7	26.7	5.89	300.00
Std. Dev:		0.29	0.29	0.26	0.25	0.27	0.28	0.26	0.	0.0	180.3	5.6	2.26	0.00
Var Coeff(%):		10.81	13.69	13.33	14.01	16.22	18.27	19.33	0.	0.0	51.4	20.9	38.41	0.00

A.5

Figure A.3 FWD Back-Calculation Results for Uncracked Portion of Section-1 of Houston District in Summer.

FTI MODULUS ANALYSIS SYSTEM (SUMMARY REPORT)													(Version 4.2)	
District:	12								MODULI RANGE(psi)					
County:	102								Minimum	Maximum	Poisson Ratio Values			
Highway/Road:	FM0526		Pavement:	3.00			349,965	350,035	H1: $\nu = 0.35$					
			Base:	14.00			500,000	5,000,001	H2: $\nu = 0.25$					
			Subbase:	6.00			30,000	600,000	H3: $\nu = 0.25$					
			Subgrade:	277.00			25,000		H4: $\nu = 0.35$					
Station	Load (lbs)	Measured Deflection (mils):							Calculated Moduli values (ksi):				Absolute Dpth to Bedrock	
		R1	R2	R3	R4	R5	R6	R7	SURF(E1)	BASE(E2)	SUBB(E3)	SURG(E4)	ERR/Sens	Bedrock
1.000	10,911	4.40	1.80	1.65	1.51	1.34	1.18	1.06	350.	552.3	600.0	46.7	14.57	300.00 †
2.000	10,887	3.68	2.56	2.23	1.95	1.71	1.55	1.35	350.	2156.2	600.0	25.8	2.90	300.00 †
3.000	10,839	3.31	2.31	1.92	1.55	1.47	1.26	1.14	350.	1867.6	600.0	32.9	4.20	300.00 †
4.000	10,855	2.14	1.72	1.54	1.39	1.22	1.10	0.98	350.	5000.0	534.1	36.4	5.51	300.00 †
5.000	10,839	5.25	2.18	1.96	1.75	1.63	1.47	1.39	350.	500.0	600.0	36.7	14.14	300.00 †
6.000	10,831	2.34	1.76	1.62	1.47	1.34	1.22	1.10	350.	5000.0	69.0	37.0	7.11	300.00 †
7.000	10,839	3.80	2.35	2.08	1.83	1.63	1.51	1.35	350.	1707.2	600.0	28.9	6.18	300.00 †
Mean:		3.56	2.10	1.86	1.64	1.48	1.33	1.20	350.	2397.6	514.7	34.9	7.80	300.00
Std. Dev:		1.10	0.34	0.26	0.21	0.18	0.18	0.16	0.	1887.1	198.1	6.7	4.68	0.00
Var Coeff(%):		30.77	15.99	13.95	12.74	12.51	13.51	13.77	0.	78.7	38.5	19.3	59.97	0.00

Figure A.4 FWD Back-Calculation Results for Uncracked Portion of Section-1 of Houston District in Summer.

TTI MODULUS ANALYSIS SYSTEM (SUMMARY REPORT)

(Version 4.2)

District:	12	MODULI RANGE(ksi)		Poisson Ratio Values	
County:	102	Minimum	Maximum	H1: u = 0.35	
Highway/Road:	FM0526	643.936	644.064	H2: u = 0.25	
Pavement:	3.00	500.000	5,000.001	H3: u = 0.25	
Base:	14.00	30.000	600.000	H4: u = 0.35	
Subbase:	6.00				
Subgrade:	277.00	25.000			

Station	Load (lbs)	Measured Deflection (mils):							Calculated Moduli values (ksi):				Absolute Dpth to	
		R1	R2	R3	R4	R5	R6	R7	SURF(E1)	BASE(E2)	SUBB(E3)	SUBG(E4)	ERR/Sens	Bedrock
23,000	10,713	2.81	2.21	2.02	1.76	1.56	1.32	1.32	644.	3978.5	211.6	27.2	0.93	300.00
12,000	10,626	2.25	1.90	1.83	1.77	1.52	1.37	1.20	644.	5000.0	173.3	28.0	7.40	300.00 †
62,000	10,455	2.22	1.80	1.65	1.44	1.44	1.22	1.07	644.	5000.0	134.2	32.2	6.07	300.00 †
168,000	10,479	2.13	1.84	1.61	1.38	1.33	1.15	0.96	644.	5000.0	354.7	32.4	4.56	300.00 †
247,000	10,490	2.00	1.47	1.34	1.29	1.17	1.06	0.96	644.	5000.0	69.0	42.0	8.46	300.00 †
304,000	10,542	2.31	1.87	1.70	1.44	1.37	1.14	1.00	644.	5000.0	337.0	31.0	2.21	300.00 †
401,000	10,427	2.02	1.74	1.59	1.34	1.40	1.21	1.18	644.	5000.0	127.5	33.7	8.71	300.00 †
487,000	10,506	2.33	1.95	1.87	1.74	1.61	1.47	1.32	644.	5000.0	156.4	27.3	7.46	300.00 †
487,000	10,351	2.29	1.91	1.83	1.69	1.56	1.42	1.26	644.	5000.0	156.4	27.6	6.99	300.00 †
530,000	10,371	3.18	2.47	2.26	2.06	1.78	1.63	1.39	644.	4039.0	148.9	21.4	2.28	300.00
Mean:		2.35	1.92	1.77	1.59	1.47	1.30	1.17	644.	4801.7	186.9	30.3	5.51	300.00
Std. Dev:		0.37	0.27	0.25	0.25	0.17	0.18	0.16	0.	418.2	91.3	5.5	2.83	0.00
Var Coeff(%):		15.59	13.98	14.37	15.63	11.52	13.52	13.69	0.	8.7	48.8	18.0	51.38	0.00

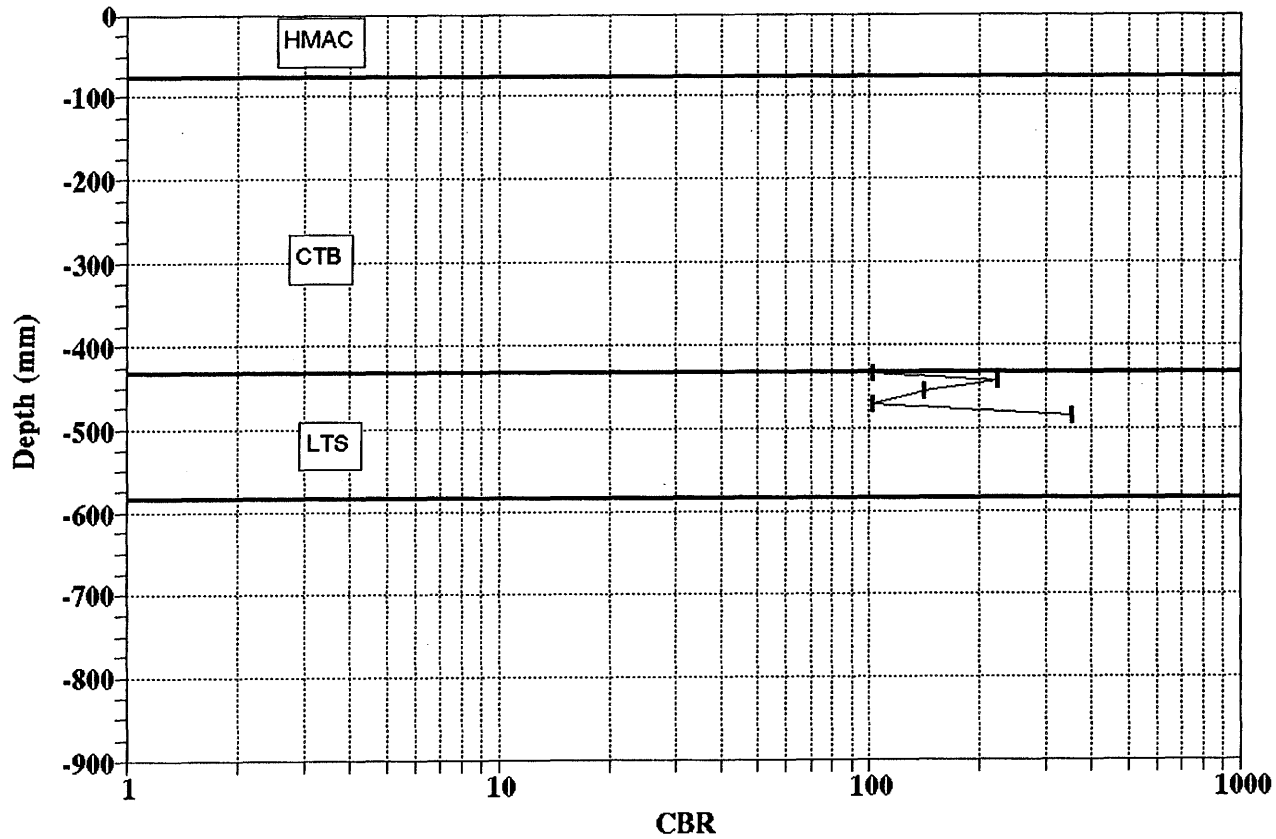
A.7

Figure A.5 FWD Back-Calculation Results for Uncracked Portion of Section-1 of Houston District in Winter.

TTI MODULUS ANALYSIS SYSTEM (SUMMARY REPORT)														(Version 4.2)	
District:	12													MODULI RANGE(ksi)	
County:	102			Thickness(in)					Minimum		Maximum		Poisson Ratio Values		
Highway/Road:	FM0526			Pavement:	3.00		643,936		644,064		H1: $\mu = 0.35$				
				Base:	14.00		500,000		5,000,001		H2: $\mu = 0.25$				
				Subbase:	6.00		30,000		600,000		H3: $\mu = 0.25$				
				Subgrade:	277.00				25,000		H4: $\mu = 0.35$				
Station	Load (lbs)	Measured Deflection (mils):							Calculated Moduli values (ksi):				Absolute Dpth to		
		R1	R2	R3	R4	R5	R6	R7	SURF(E1)	BASE(E2)	SUBB(E3)	SUBG(E4)	ERR/Sens	Bedrock	
125.000	10,296	3.88	1.80	1.57	1.36	1.20	1.03	0.87	644.	500.0	600.0	45.3	10.39	300.00 †	
151.000	10,228	3.84	1.85	1.65	1.43	1.19	1.04	0.88	644.	500.0	600.0	43.7	9.02	300.00 †	
223.000	10,260	2.70	1.63	1.48	1.33	1.17	1.06	0.91	644.	2097.7	600.0	39.4	7.23	300.00 †	
268.000	10,284	5.81	1.78	1.61	1.46	1.26	1.16	1.07	644.	500.0	600.0	39.6	17.49	300.00 †	
330.000	10,216	2.54	1.54	1.45	1.33	1.10	1.04	0.89	644.	2677.8	600.0	39.1	6.45	300.00 †	
427.000	10,244	5.63	2.41	1.93	1.72	1.41	1.35	1.08	644.	500.0	484.3	33.0	10.15	300.00 †	
Mean:		3.97	1.84	1.62	1.44	1.22	1.11	0.95	644.	1129.3	580.7	40.0	10.12	300.00	
Std. Dev:		1.28	0.30	0.17	0.15	0.11	0.13	0.10	0.	991.9	47.2	4.3	3.93	0.00	
Var Coeff(%):		32.27	16.60	10.65	10.29	8.65	11.27	10.29	0.	87.8	8.1	10.8	38.87	0.00	

Figure A.6 FWD Back-Calculation Results for Uncracked Portion of Section-1 of Houston District in Winter.

HOUSTON DISTRICT FM-526(North) SITE-1



A.9

Figure A.7. Variation of CBR Obtained from DCP Testing for Section-1 of Houston District.

UNIAXIAL RESILIENT MODULUS

Project 1287 Gage Length (in) 2
 Sample ID HOU1 Date of Test
 Height (in) 8 Temperature 77F

	Load lbs.	Def in.	Total Mr	Instant Mr
PEAK 1	474.43	3.657E-05	2064535	2418421
PEAK 2	474.34	3.561E-05	2119965	2303217
PEAK 3	474.49	3.602E-05	2096625	2137283
PEAK 4	474.07	3.676E-05	2052571	2155743
AVERAGE	474.33	3.624E-05	2083424	2253666

Failure Load (lbs) : 29300
 Correction Factor : 1
 Ultimate Stress (psi) : 2330.68

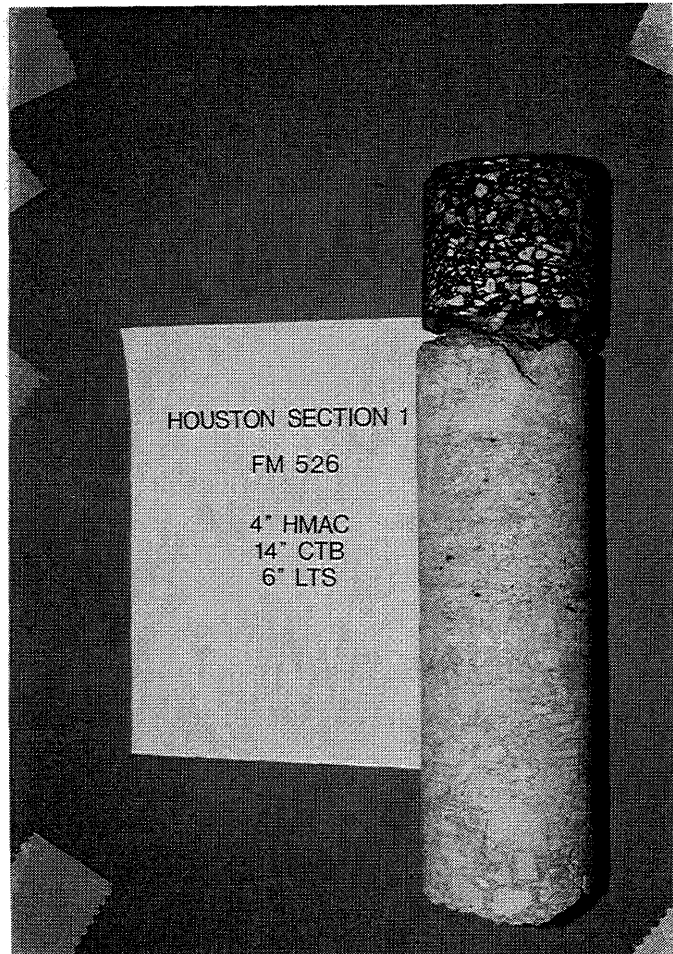


Figure A.8. Results of Laboratory Testing for Cores Obtained from Section-1 of Houston District.

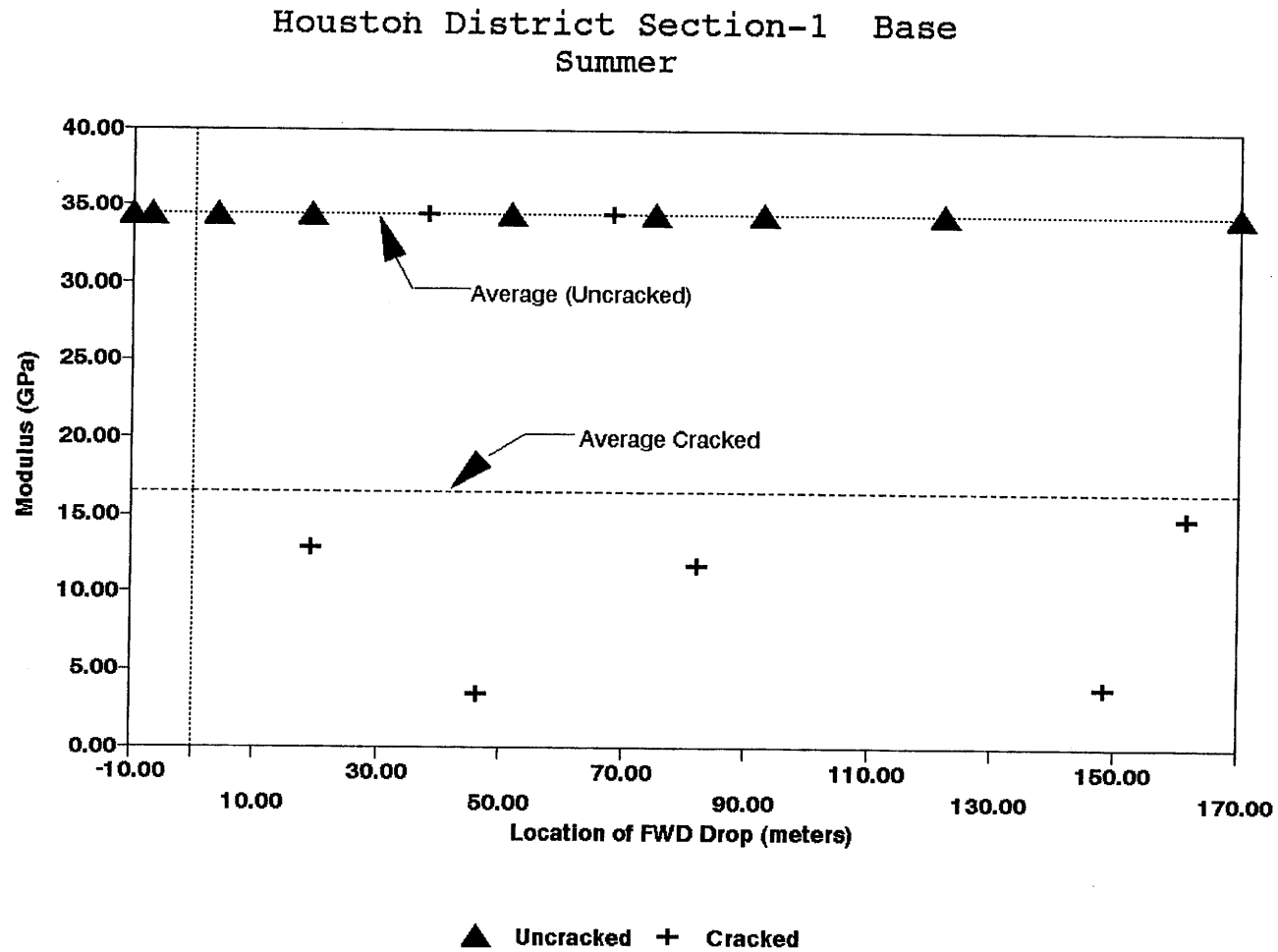


Figure A.9. Variation of Modulus of Stabilized Base within Test Section for Section-1 of Houston District in Summer.

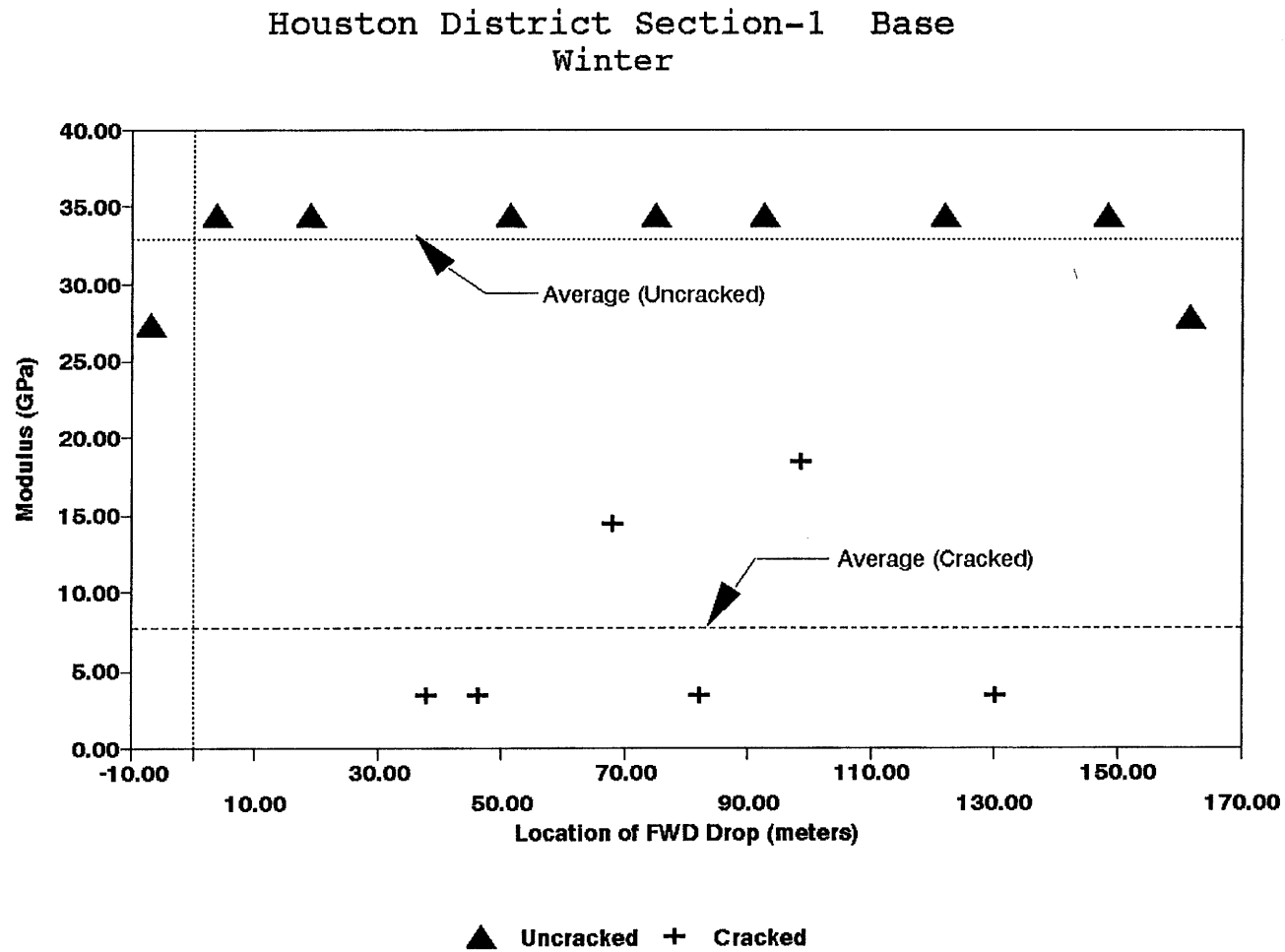


Figure A.10. Variation of Modulus of Stabilized Base within Test Section for Section-1 of Houston District in Winter.

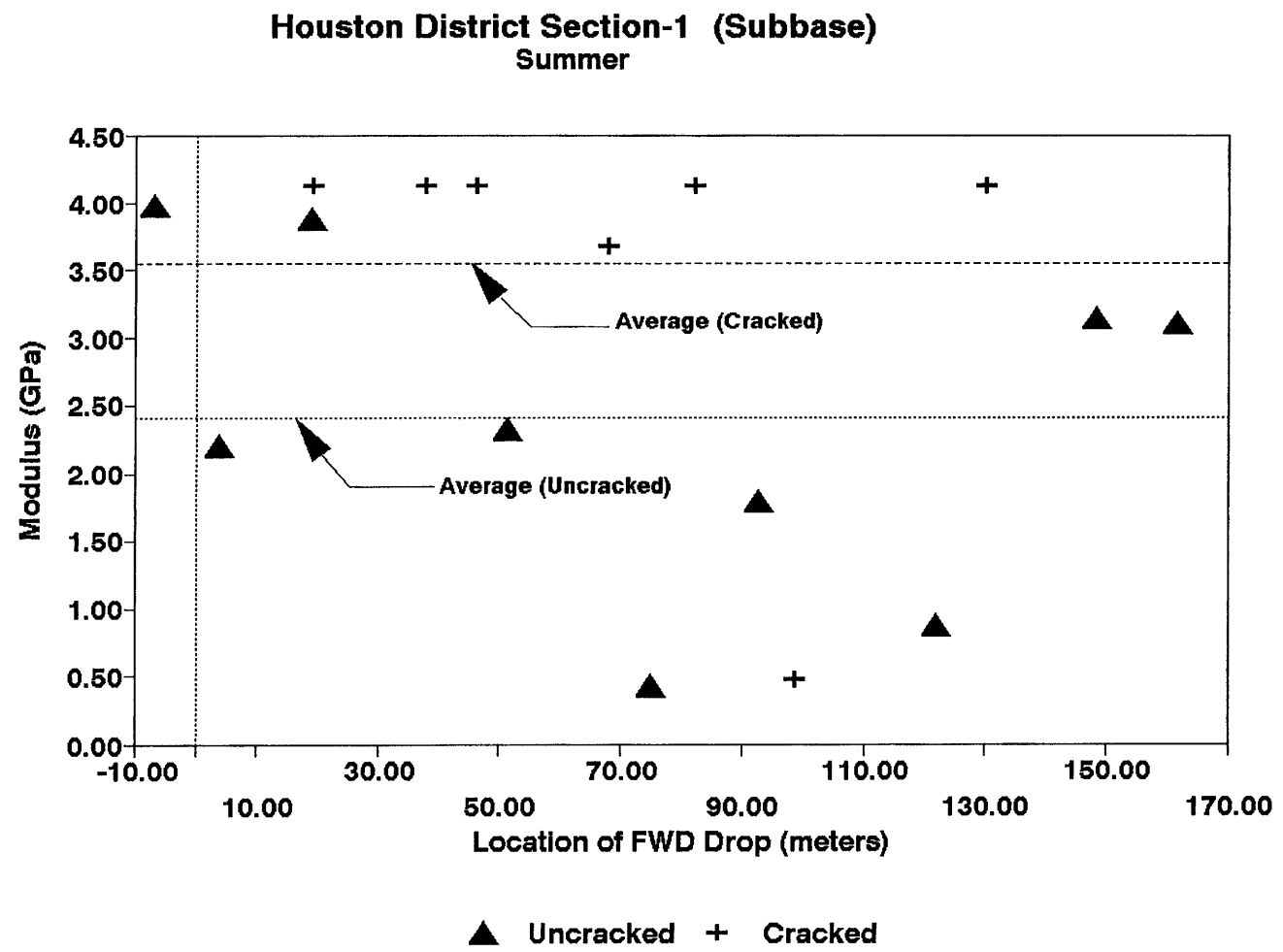


Figure A.11. Variation of Modulus of Stabilized Subbase within Test Section for Section-1 of Houston District in Summer.

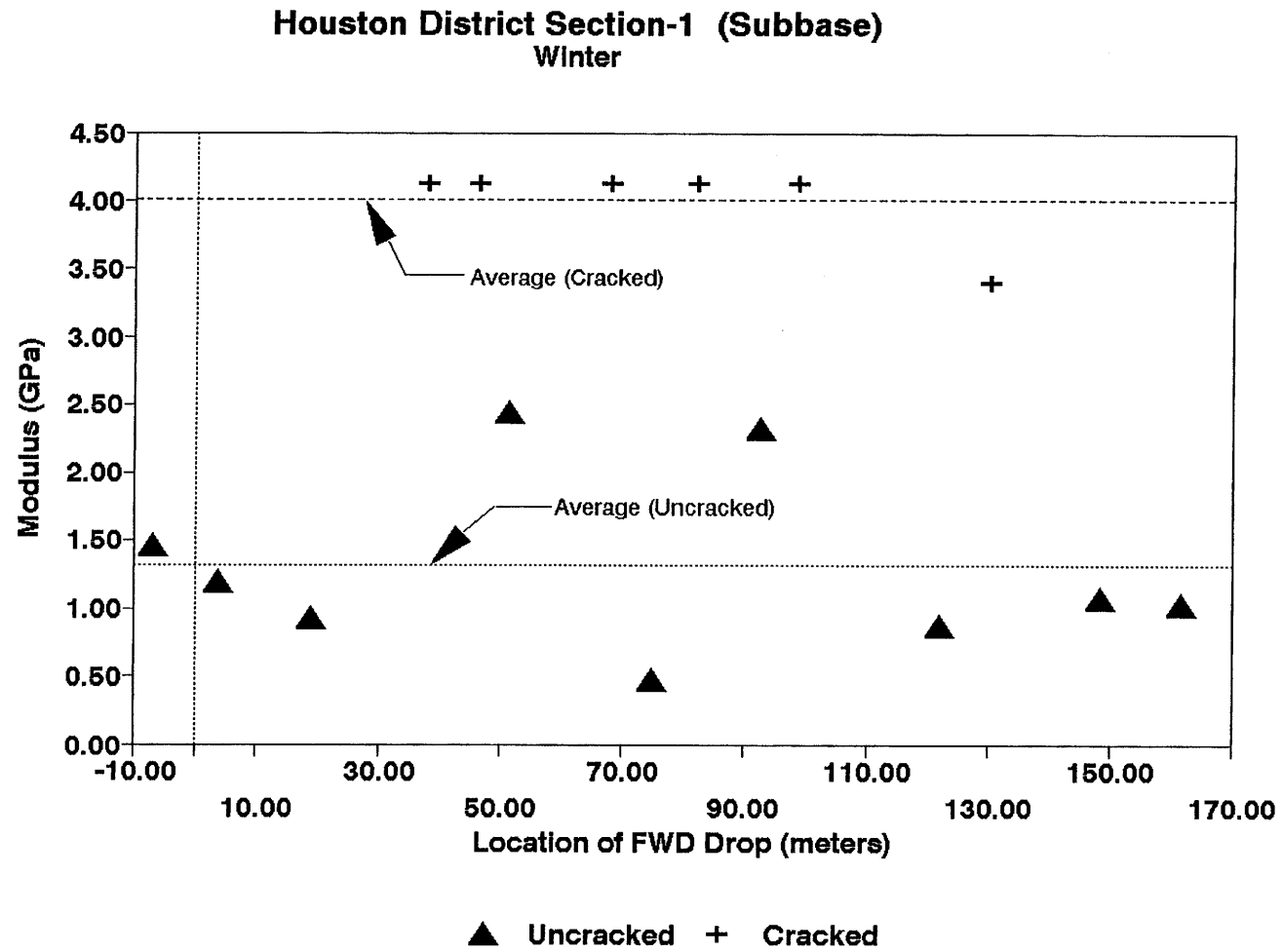


Figure A.12. Variation of Modulus of Stabilized Subbase within Test Section for Section-1 of Houston District in Winter.

Section No.: 2 District: Houston County: Harris Highway: FM-526 (South)
Structure: Asphalt : 76 mm
LTB : 229 mm
LTS : 178 mm
Subgrade

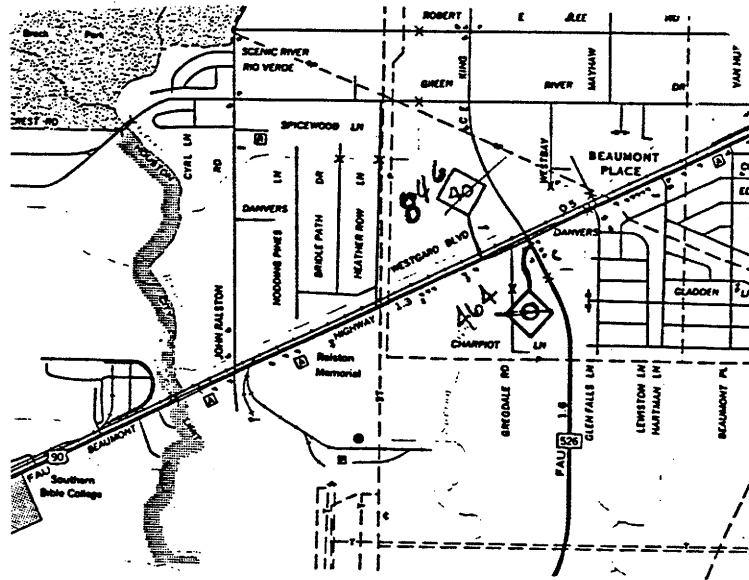
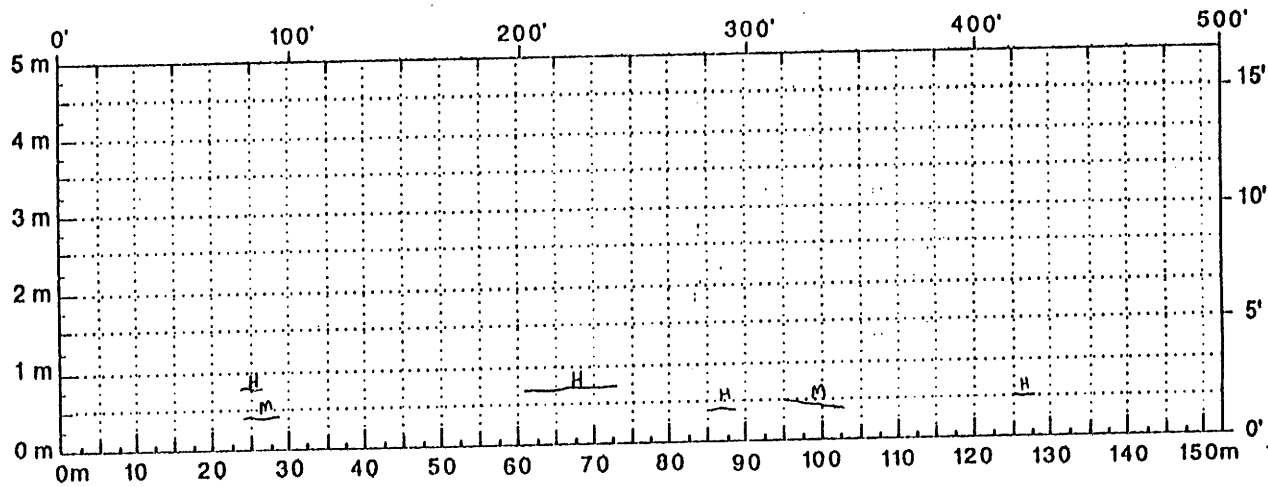
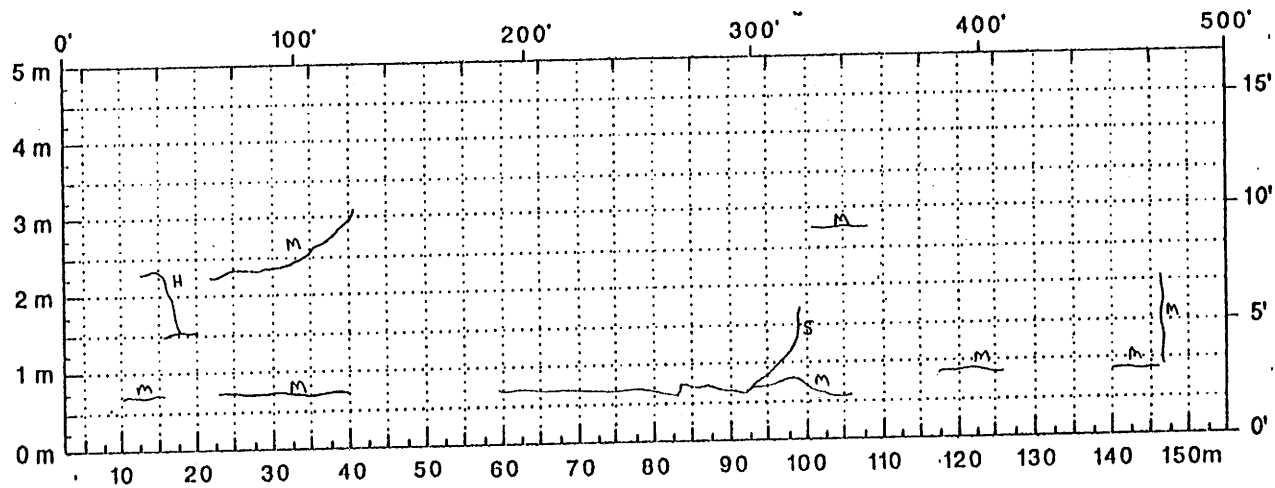


Figure A.13. Location and Details of Section-2 of Houston District.



Comments: Crack Map for Summer



Comments: Crack Map for Winter

Figure A.14. Crack Map for Section-2 of Houston District.

TTI MODULUS ANALYSIS SYSTEM (SUMMARY REPORT)

(Version 4.2)

District:	12	MODULI RANGE(psi)		Poisson Ratio Values	
County:	102	Minimum	Maximum	H1: $\nu = 0.35$	
Highway/Road:	FM0526	206,979	207,021	H2: $\nu = 0.25$	
		30,000	1,000,000	H3: $\nu = 0.25$	
		5,000	300,000	H4: $\nu = 0.35$	
		241.90	10,000		

Station	Load (lbs)	Measured Deflection (mils):							Calculated Moduli values (ksi):				Absolute Dist to	
		R1	R2	R3	R4	R5	R6	R7	SURF(E1)	BASE(E2)	SUBB(E3)	SUBG(E4)	ERR/Sens	Bedrock
1.000	10,727	20.72	14.26	8.85	5.62	3.50	2.40	1.88	207.	129.6	5.0	16.0	1.75	150.47 *
2.000	10,647	21.53	14.76	9.61	5.98	3.91	2.85	2.16	207.	129.7	5.0	14.1	2.47	195.97 *
3.000	10,535	22.34	14.17	8.54	5.34	3.38	2.36	1.84	207.	99.3	5.3	16.2	1.20	162.20
4.000	10,631	16.80	11.87	8.38	5.82	4.07	3.02	2.33	207.	224.8	11.8	12.8	0.93	300.00
5.000	10,639	14.18	10.61	7.61	5.34	3.75	2.77	2.24	207.	371.2	9.5	14.5	1.25	300.00
6.000	10,687	12.89	9.60	7.81	5.86	4.23	3.10	2.37	207.	664.4	10.1	12.8	1.54	300.00
7.000	10,535	22.30	14.47	9.69	6.69	4.64	3.38	2.53	207.	104.1	12.0	10.8	0.42	296.37
8.000	10,343	32.48	20.25	11.77	6.97	4.11	2.89	2.28	207.	45.5	5.0	11.4	4.67	121.73 *
9.000	10,615	12.56	8.97	7.19	5.38	3.87	2.89	2.24	207.	415.8	43.0	12.8	1.75	300.00
10.000	10,423	25.04	14.80	8.35	5.34	3.75	2.89	2.37	207.	58.7	11.2	13.2	3.00	300.00
11.000	10,591	14.66	10.94	8.00	5.74	3.99	2.97	2.37	207.	375.8	9.0	13.5	0.88	300.00
12.000	10,391	21.65	14.55	9.50	6.37	4.32	3.02	2.37	207.	123.7	6.4	12.4	0.52	223.61
Mean:		19.76	13.27	8.78	5.87	3.96	2.88	2.25	207.	228.5	11.1	13.4	1.70	260.98
Std. Dev:		5.84	3.08	1.24	0.55	0.35	0.28	0.20	0.	188.8	10.4	1.6	1.20	114.50
Var Coeff(%):		29.56	23.23	14.10	9.34	8.84	9.71	9.06	0.	82.6	93.9	12.2	70.71	43.87

A.17

Figure A.15. FWD Back-Calculation Results for Uncracked Portion of Section-2 of Houston District in Summer.

TTI MODULUS ANALYSIS SYSTEM (SUMMARY REPORT)													(Version 4.2)	
District:	12								MODULI RANGE(ksi)					
County:	102								Minimum	Maximum	Poisson Ratio Values			
Highway/Road:	FM0526	Pavement:		3.00			206,979	207,021	H1: u = 0.35					
		Base:		9.00			30,000	1,000,000	H2: u = 0.25					
		Subbase:		7.00			5,000	300,000	H3: u = 0.25					
		Subgrade:		145.60				10,000	H4: u = 0.35					
Station	Load (lbs)	Measured Deflection (mil):							Calculated Moduli values (ksi):				Absolute Dist to Bedrock	
		R1	R2	R3	R4	R5	R6	R7	SURF(E1)	BASE(E2)	SUBB(E3)	SUBG(E4)	ERR/Sens	Bedrock
1.000	10,591	26.22	16.02	10.11	6.41	4.07	2.85	2.20	207.	72.8	8.5	10.3	1.04	164.62
Mean:		26.22	16.02	10.11	6.41	4.07	2.85	2.20	207.	72.8	8.5	10.3	1.04	164.62
Std. Dev:		0.00	0.00	0.00	0.00	0.00	0.00	0.00	0.	0.0	0.0	0.0	0.00	0.00
Var Coeff(%):		0.00	0.00	0.00	0.00	0.00	0.00	0.00	0.	0.0	0.0	0.0	0.00	0.00

Figure A.16. FWD Back-Calculation Results for Cracked Portion of Section-2 of Houston District in Summer.

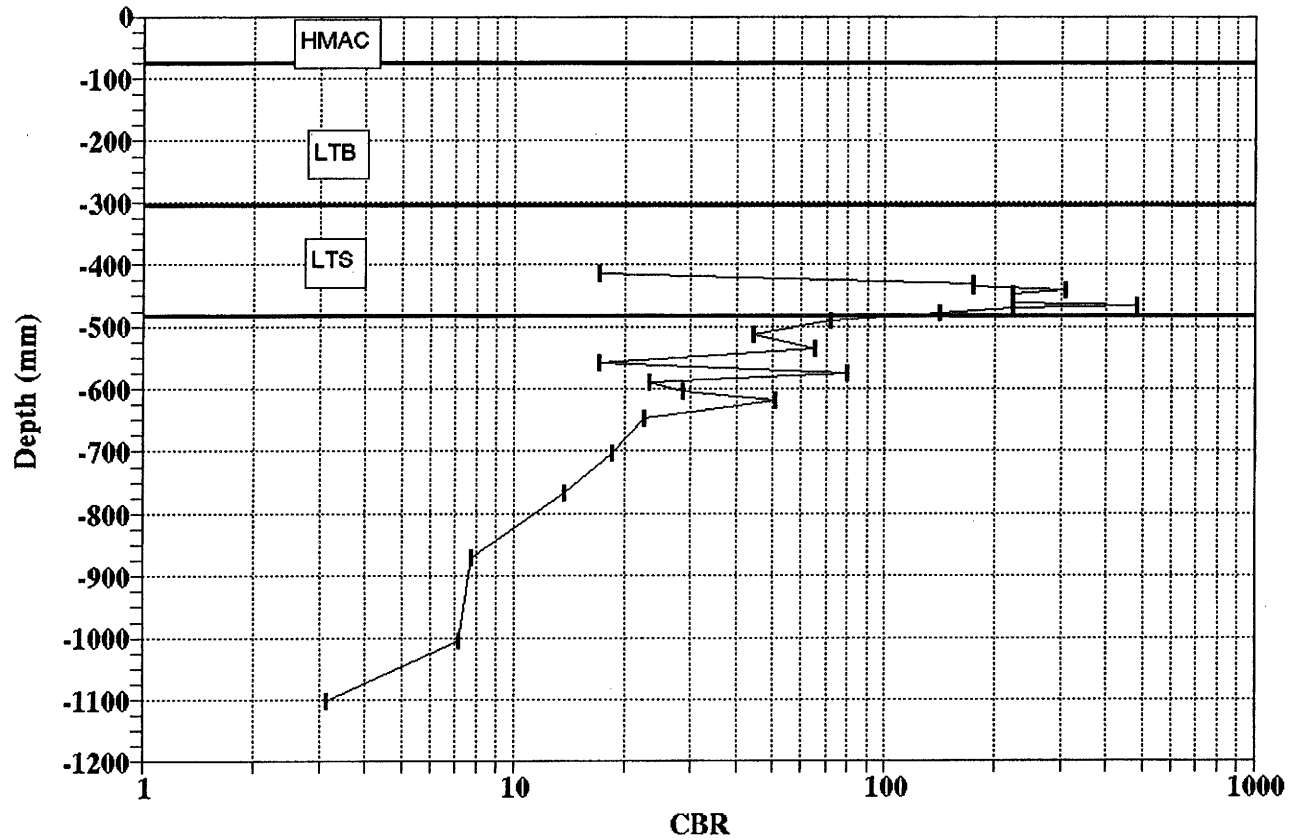
TTI MODULUS ANALYSIS SYSTEM (SUMMARY REPORT)													(Version 4.2)	
District:	12									MODULI RANGE(psi)				
County:	102		Thickness(in)							Minimum	Maximum	Poisson Ratio Values		
Highway/Road:	FM0526		Pavement:	3.00						822,918	823,082	H1: $\mu = 0.35$		
			Base:	9.00						30,000	1,000,000	H2: $\mu = 0.25$		
			Subbase:	7.00						5,000	300,000	H3: $\mu = 0.25$		
			Subgrade:	281.00							15,700	H4: $\mu = 0.35$		
Station	Load (lbs)	Measured Deflection (mils):							Calculated Moduli values (ksi):				Absolute Dpth to	
		R1	R2	R3	R4	R5	R6	R7	SURF(E1)	BASE(E2)	SUBB(E3)	SUBG(E4)	ERR/Sens	Bedrock
23,000	10,637	14.65	11.75	8.35	5.57	3.72	2.56	2.42	823.	191.2	5.0	16.0	4.28	206.59 *
12,000	10,602	15.28	11.77	7.79	5.00	3.38	2.30	1.84	823.	151.6	5.2	17.4	3.62	194.53 *
62,000	10,498	12.04	9.26	6.57	4.64	3.46	2.54	1.91	823.	267.9	9.0	16.7	1.29	300.00
168,000	10,590	6.36	5.46	4.59	3.73	3.06	2.35	1.99	823.	1000.0	201.5	16.0	2.05	300.00 *
246,000	10,498	12.38	9.46	7.23	5.50	4.19	3.15	2.35	823.	285.8	19.9	12.6	0.38	295.26
304,000	10,363	18.16	13.53	8.81	6.11	4.26	3.02	2.30	823.	121.5	5.0	13.5	1.14	245.36 *
400,000	10,427	6.50	5.59	4.72	3.81	3.02	2.38	1.90	823.	1000.0	142.3	15.9	1.92	300.00 *
487,000	10,363	10.10	8.15	6.19	4.76	3.72	2.80	2.48	823.	449.8	19.4	14.2	0.99	300.00
530,000	10,415	5.72	4.83	4.05	3.30	2.65	2.02	1.72	823.	1000.0	133.5	19.3	2.39	300.00 *
Mean:		11.24	8.87	6.48	4.71	3.50	2.57	2.10	823.	496.4	60.1	15.7	2.01	300.00
Std. Dev:		4.41	3.13	1.73	0.95	0.54	0.36	0.28	0.	389.2	76.7	2.1	1.27	128.82
Var Coeff(%):		39.25	35.25	26.67	20.09	15.38	14.12	13.56	0.	78.4	100.0	13.1	63.25	42.94

Figure A.17. FWD Back-Calculation Results for Uncracked Portion of Section-2 of Houston District in Winter.

TTI MODULUS ANALYSIS SYSTEM (SUMMARY REPORT)													(Version 4.2)	
District:	12								MODULI RANGE(psi)					
County:	102		Thickness(in)						Minimum	Maximum	Poisson Ratio Values			
Highway/Road:	FM0526		Pavement:	3.00				822.918	823.082	H1: $\mu = 0.35$				
			Base:	9.00				30,000	1,000,000	H2: $\mu = 0.25$				
			Subbase:	7.00				5,000	300,000	H3: $\mu = 0.25$				
			Subgrade:	276.30				10,000		H4: $\mu = 0.35$				
Station	Load (lbs)	Measured Deflection (mils):							Calculated Moduli values (ksi):				Absolute Dpth to	
		R1	R2	R3	R4	R5	R6	R7	SURF(E1)	BASE(E2)	SURB(E3)	SUBG(E4)	ERR/Sens	Bedrock
0.000	10,256	15.48	10.79	7.74	5.62	3.96	2.87	2.43	823.	146.8	11.0	13.1	1.26	295.35
Mean:		15.48	10.79	7.74	5.62	3.96	2.87	2.43	823.	146.8	11.0	13.1	1.26	295.35
Std. Dev:		0.00	0.00	0.00	0.00	0.00	0.00	0.00	0.	0.0	0.0	0.0	0.00	0.00
Var Coeff(%):		0.00	0.00	0.00	0.00	0.00	0.00	0.00	0.	0.0	0.0	0.0	0.00	0.00

Figure A.18. FWD Back-Calculation Results for Cracked Portion of Section-2 of Houston District in Winter.

**HOUSTON DISTRICT
FM-526(SOUTH) SITE-2**



A.21

Figure A.19. Variation of CBR Obtained from DCP Testing for Section-2 of Houston District.

UNIAXIAL RESILIENT MODULUS

Sample ID	HOU2A	Date of Test		
Height (in)	2.73	Temperature		
	Load lbs.	Def in.	Total Mr	Instant Mr
PEAK 1	480.47	0.0002305	331756	382349
PEAK 2	480.48	0.0002317	330092	362997
PEAK 3	480.50	0.0002328	328476	348842
PEAK 4	480.24	0.0002314	330324	348304
AVERAGE	480.43	0.0002316	330162	360623

Failure Load (lbs) : 20100
 Correction Factor : 0.878
 Ultimate Stress (psi) : 1403.8

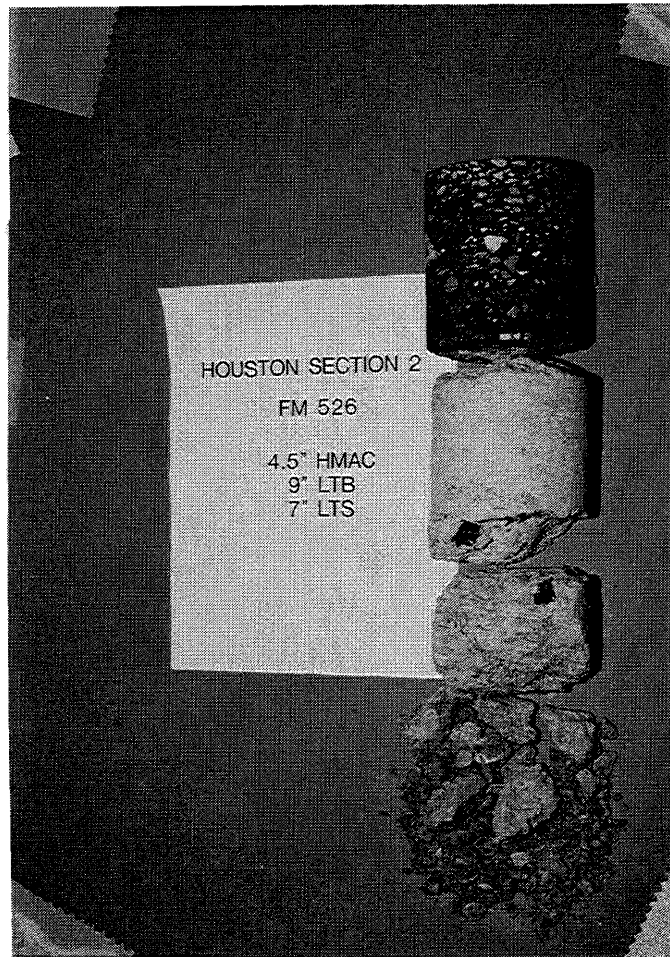


Figure A.20. Results of Laboratory Testing for Cores Obtained from Section-2 of Houston District.

Houston District Section-2 Base
Summer

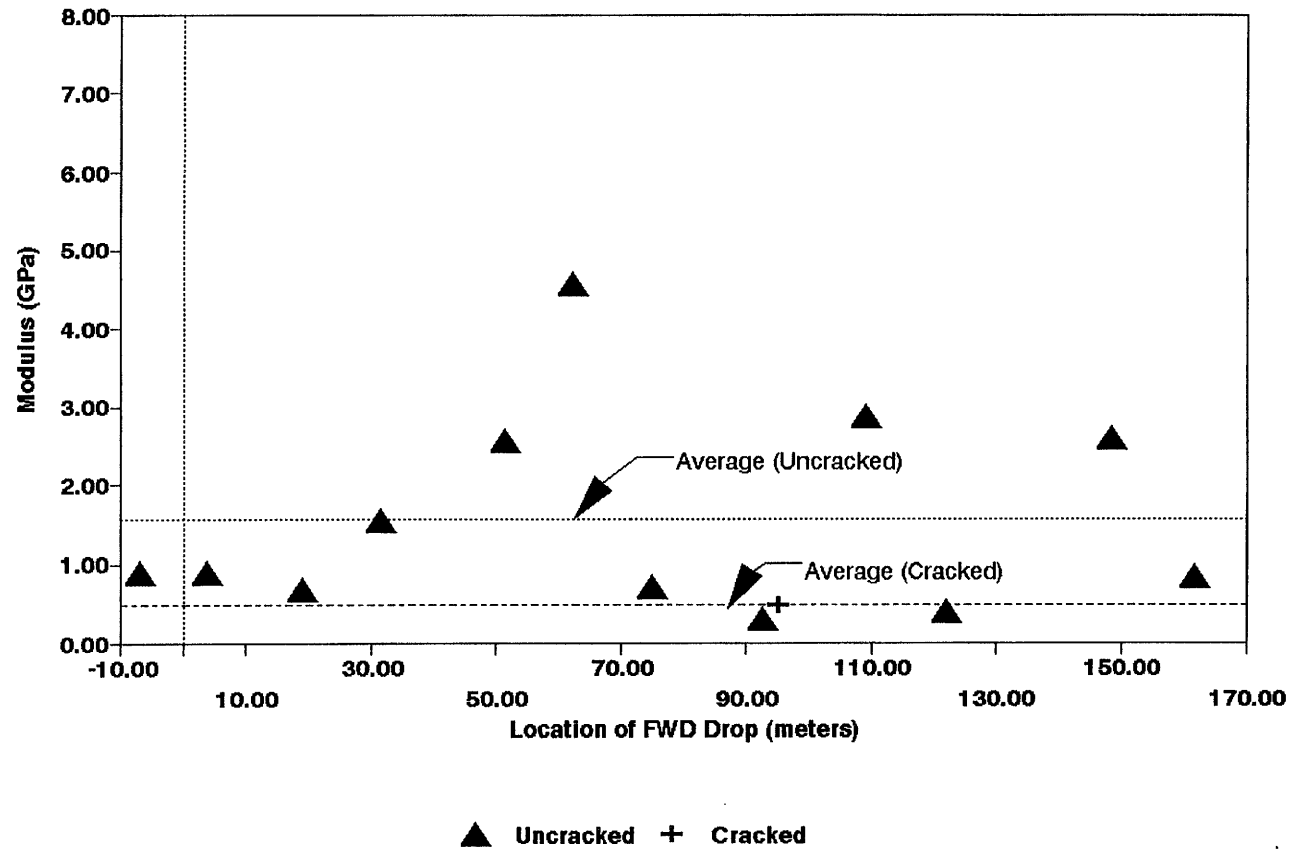
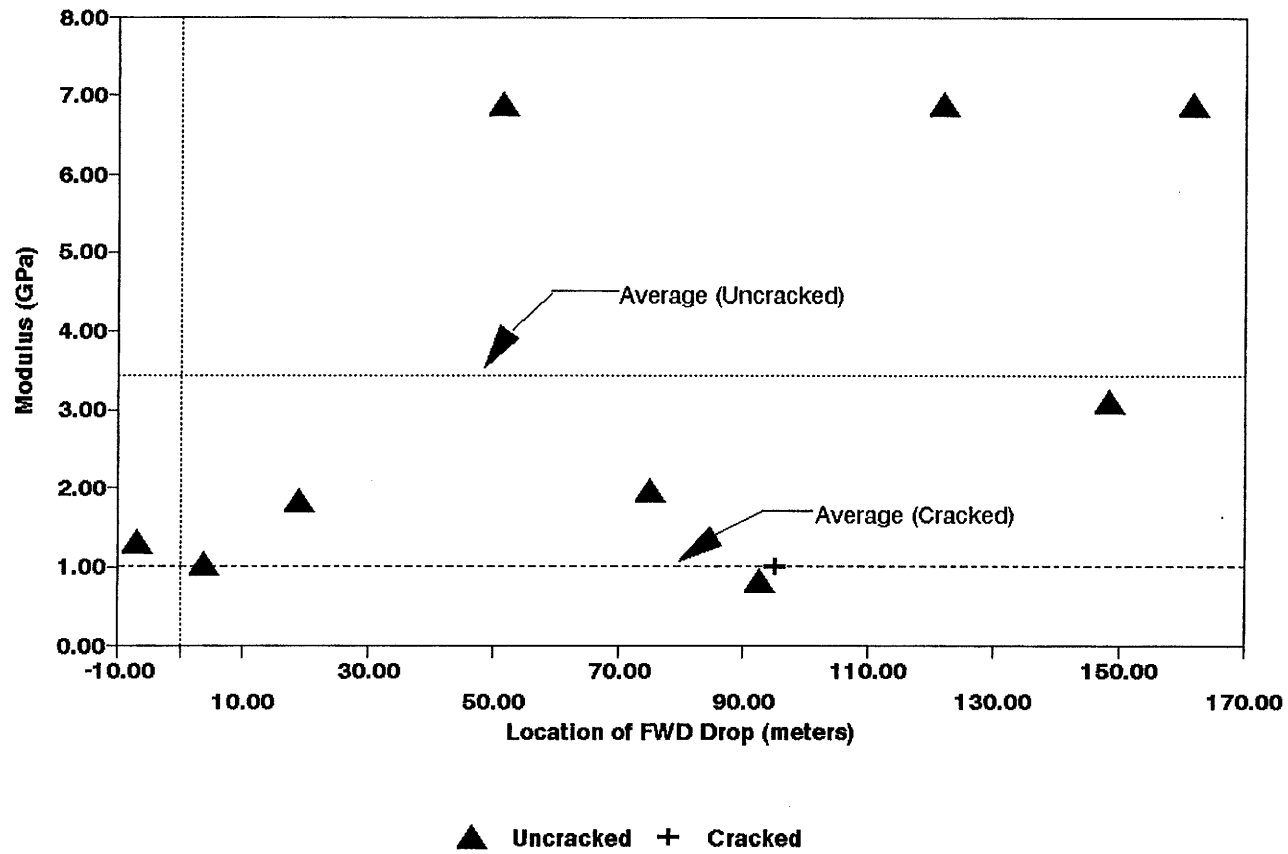


Figure A.21. Variation of Modulus of Stabilized Base within Test Section for Section-2 of Houston District in Summer.

Houston District Section-2 Base
Winter



A.24

Figure A.22. Variation of Modulus of Stabilized Base within Test Section for Section-2 of Houston District in Winter.

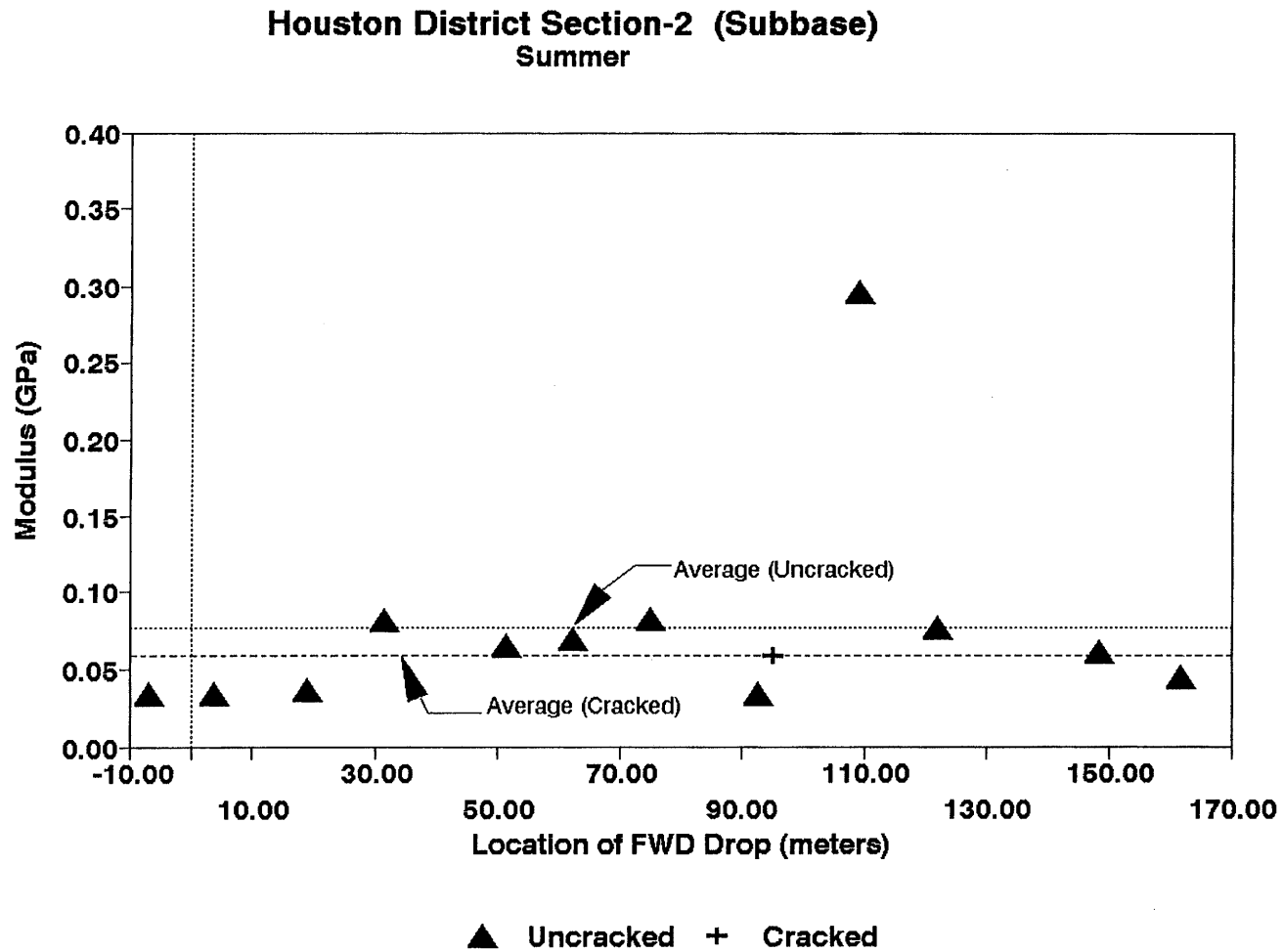


Figure A.23. Variation of Modulus of Stabilized Subbase within Test Section for Section-2 of Houston District in Summer.

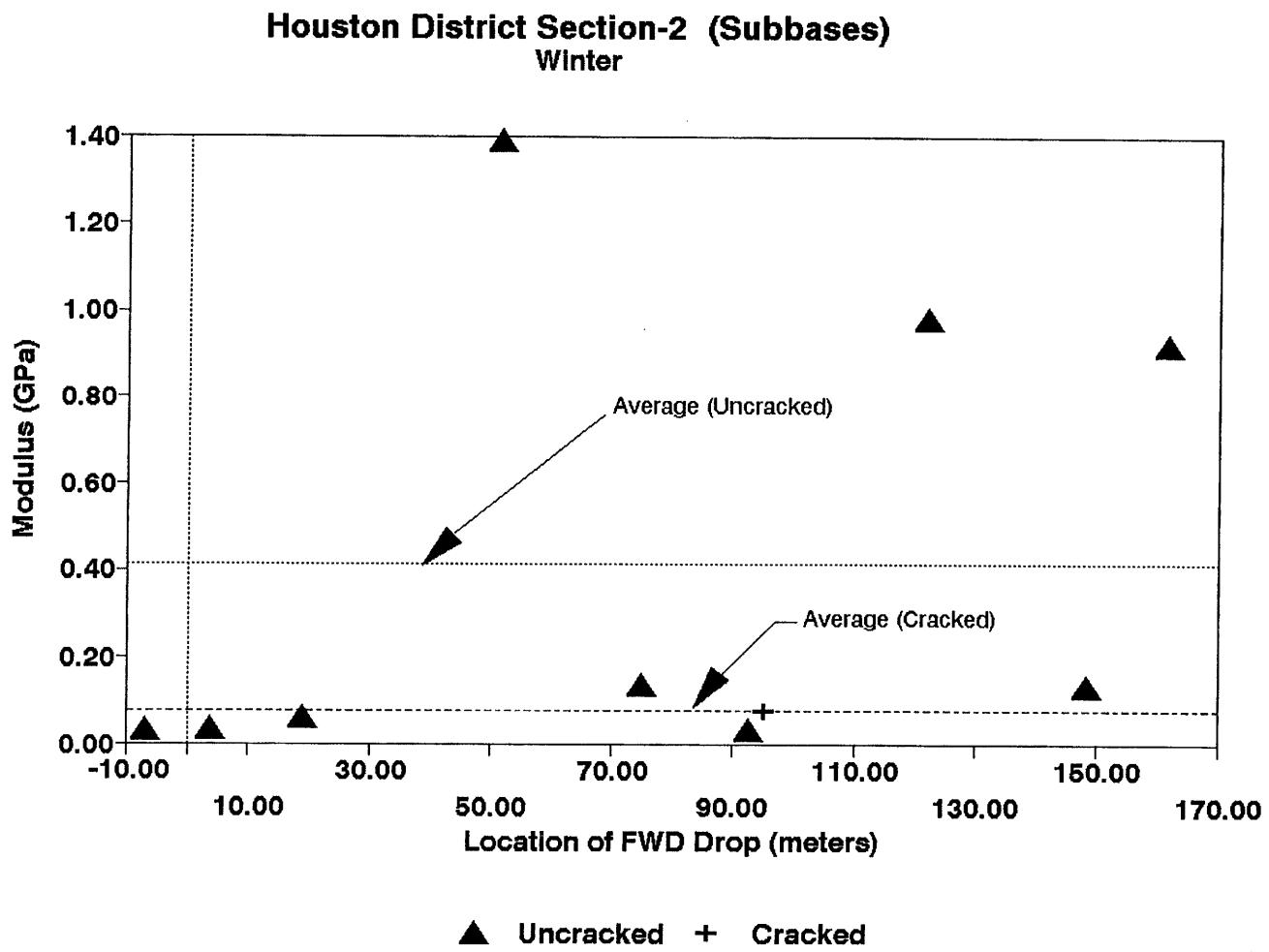


Figure A.24. Variation of Modulus of Stabilized Subbase within Test Section for Section-2 of Houston District in Winter.

Section No.: 3 District: Houston County: Harris Highway: FM-2920 (West)
Structure: Asphalt : 76 mm
CTB : 356 mm
LTS : 152 mm
Subgrade

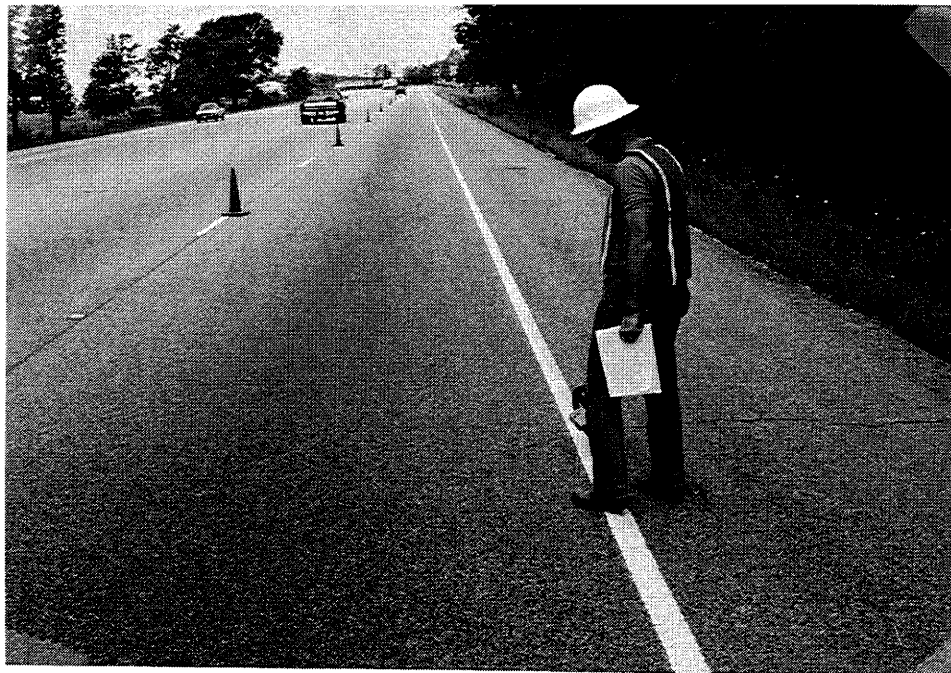
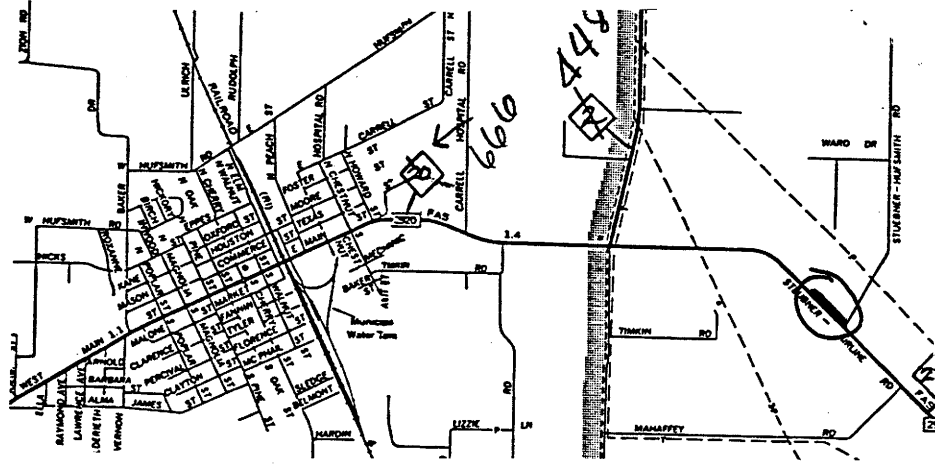
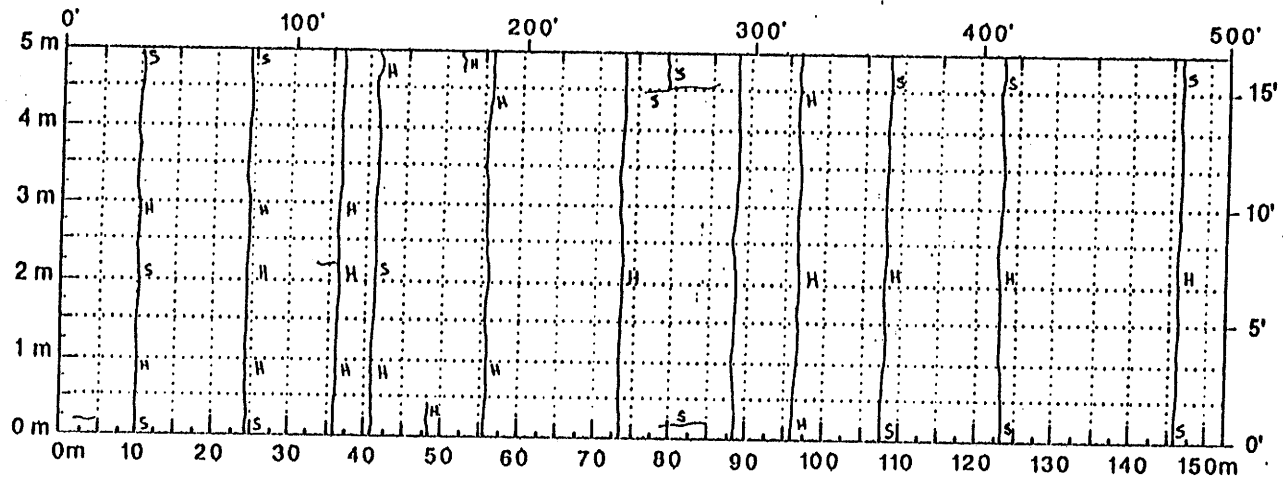
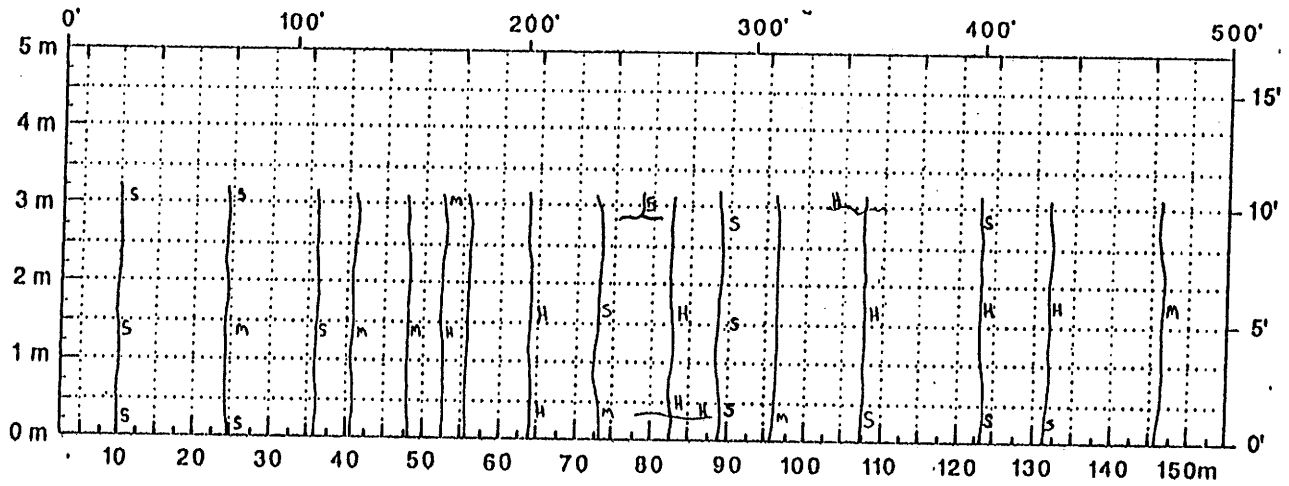


Figure A.25. Location and Details of Section-3 of Houston District.

A.28



Comments: Crack Map for Summer



Comments: Crack Map for Winter

Figure A.26. Crack Map for Section-3 of Houston District.

TTI MODULUS ANALYSIS SYSTEM (SUMMARY REPORT)													(Version 4.2)	
District:	12								MODULI RANGE(psi)					
County:	102								Minimum	Maximum	Poisson Ratio Values			
Highway/Road:	FM2920								325,367	325,433	H1: j = 0.35			
		Pavement:	3.00					500,000	5,000,001	H2: j = 0.25				
		Base:	14.00					30,000	600,000	H3: j = 0.25				
		Subbase:	6.00					25,000		H4: j = 0.35				
		Subgrade:	277.00											
Station	Load (lbs)	Measured Deflection (mils):							Calculated Moduli values (ksi):				Absolute Dpth to	
		R1	R2	R3	R4	R5	R6	R7	SURP(E1)	BASE(E2)	SUBB(E3)	SUBG(E4)	ERR/Sens	Bedrock
1.000	9,263	2.26	1.72	1.50	1.31	1.10	0.94	0.78	325.	4868.4	161.1	33.3	2.22	300.00
2.000	9,199	2.91	2.05	1.73	1.31	1.26	1.06	0.86	325.	1593.2	600.0	33.0	4.14	300.00 *
3.000	9,143	2.99	2.14	1.92	1.67	1.47	1.26	1.10	325.	3479.1	91.3	25.7	1.48	300.00
4.000	9,055	4.65	2.56	1.85	1.51	1.26	1.10	0.94	325.	500.0	165.8	36.1	6.66	300.00 *
5.000	9,127	4.56	2.52	1.73	1.39	1.22	1.06	0.86	325.	500.0	158.0	38.9	8.02	300.00 *
6.000	9,151	2.63	1.93	1.69	1.47	1.26	1.06	0.90	325.	3628.5	131.3	30.3	0.84	300.00
7.000	9,215	2.46	1.72	1.50	1.31	1.10	0.94	0.82	325.	3362.6	340.3	34.9	0.28	300.00
8.000	9,103	2.34	1.64	1.42	1.27	1.06	0.90	0.78	325.	3725.9	354.0	35.4	0.86	300.00
Mean:		3.10	2.04	1.67	1.40	1.22	1.04	0.88	325.	2707.2	250.2	33.5	3.06	300.00
Std. Dev:		0.96	0.36	0.18	0.14	0.13	0.12	0.10	0.	1628.6	170.8	4.0	2.91	90.22
Var Coeff(%):		31.08	17.50	10.70	9.74	10.84	11.07	11.90	0.	60.2	68.3	12.0	95.11	30.07

Figure A.27. FWD Back-Calculation Results for Uncracked Portion of Section-3 of Houston District in Summer.

A.30

TTI MODULUS ANALYSIS SYSTEM (SUMMARY REPORT)													(Version 4.2)	
District:	12								MODULI RANGE(psi)					
County:	102								Minimum	Maximum	Poisson Ratio Values			
Highway/Road:	FM2920	Pavement:	3.00					325,367	325,433	H1: J = 0.35				
		Base:	14.00					500,000	5,000,001	H2: J = 0.25				
		Subbase:	6.00					30,000	600,000	H3: J = 0.25				
		Subgrade:	277.00					25,000		H4: J = 0.35				
Station	Load (lbs)	Measured Deflection (mils):							Calculated Moduli values (ksi):				Absolute Dpth to	
		R1	R2	R3	R4	R5	R6	R7	SURF(E1)	BASE(E2)	SUBB(E3)	SUBG(E4)	ERR/Sens	Bedrock
0.000	9,135	4.04	2.35	1.77	1.51	1.26	1.10	0.94	325.	500.0	600.0	35.2	3.70	300.00 *
1.000	9,095	4.97	2.64	2.15	1.79	1.42	1.14	0.94	325.	500.0	179.4	31.5	4.55	300.00 *
2.000	9,119	2.59	1.89	1.54	1.35	1.06	0.86	0.73	325.	2604.9	42.6	40.9	2.28	300.00
3.000	9,103	3.47	2.43	2.00	1.71	1.38	1.14	0.98	325.	1219.0	257.0	29.8	0.78	300.00
4.000	9,111	3.68	1.89	1.58	1.35	1.06	0.90	0.73	325.	534.8	600.0	42.8	4.61	300.00 *
Mean:		3.75	2.24	1.81	1.54	1.24	1.03	0.86	325.	1071.7	335.8	36.1	3.19	300.00
Std. Dev:		0.87	0.34	0.26	0.20	0.17	0.14	0.12	0.	910.3	253.1	5.7	1.64	110.72
Var Coeff(%):		23.10	15.03	14.61	13.15	13.84	13.31	14.28	0.	84.9	75.4	15.7	51.51	36.91

Figure A.28. FWD Back-Calculation Results for Cracked Portion of Section-3 of Houston District in Summer.

TTI MODULUS ANALYSIS SYSTEM (SUMMARY REPORT)

(Version 4.2)

District:	12	MODULI RANGE(psi)		Poisson Ratio Values	
County:	102	Minimum	Maximum	H1: u = 0.35	
Highway/Road:	FM2920	399,960	400,040	H2: u = 0.25	
		500,000	5,000,001	H3: u = 0.25	
		30,000	600,000	H4: u = 0.35	
		30,000			

Station	Load (lbs)	Measured Deflection (mils):							Calculated Moduli values (ksi):				Absolute Dpth to	
		R1	R2	R3	R4	R5	R6	R7	SURF(E1)	BASE(E2)	SURR(E3)	SUBG(E4)	ERR/Sens	Bedrock
-25.000	10.316	2.73	1.89	1.72	1.49	1.27	1.07	0.91	400.	3725.0	106.5	34.9	1.16	300.00
0.000	10.089	3.62	2.50	2.20	1.89	1.45	1.28	1.04	400.	1221.0	431.9	29.4	2.25	300.00
57.000	9.974	3.05	2.20	2.04	1.75	1.50	1.27	1.04	400.	3352.7	80.5	28.0	1.20	300.00
197.000	10.002	3.54	2.15	1.82	1.53	1.30	1.09	0.91	400.	867.4	600.0	36.2	3.26	300.00 #
277.000	9.962	4.63	2.30	1.78	1.48	1.31	1.06	0.90	400.	500.0	445.3	38.7	7.55	300.00 #
334.000	10.010	3.21	2.10	1.90	1.61	1.37	1.12	0.94	400.	1485.8	600.0	32.6	1.69	300.00 #
419.000	10.018	2.72	1.92	1.69	1.44	1.24	1.04	0.85	400.	3195.6	111.6	35.7	1.32	300.00
467.000	9.962	2.57	1.77	1.61	1.30	1.13	0.93	0.74	400.	2659.4	364.0	38.9	1.62	300.00
Mean:		3.26	2.10	1.84	1.56	1.32	1.11	0.92	400.	2125.9	342.5	34.3	2.51	300.00
Std. Dev:		0.67	0.24	0.20	0.19	0.12	0.12	0.10	0.	1250.5	216.9	4.0	2.15	129.39
Var Coeff(%):		20.68	11.33	10.58	11.90	8.92	10.59	10.68	0.	58.8	63.3	11.7	85.97	43.13

A.31

Figure A.29. FWD Back-Calculation Results for Uncracked Portion of Section-3 of Houston District in Winter.

TTI MODULUS ANALYSIS SYSTEM (SUMMARY REPORT)													(Version 4.2)	
District:	12								MODULI RANGE(ksi)					
County:	102								Minimum	Maximum	Poisson Ratio Values			
Highway/Road:	FK2920								399,960	400,040	H1: u = 0.35			
		Pavement:	3.00					500,000	5,000,001	H2: u = 0.25				
		Base:	14.00					30,000	600,000	H3: u = 0.25				
		Subbase:	6.00							H4: u = 0.35				
		Subgrade:	277.00						39,700					
Station	Load (lbs)	Measured Deflection (mils):							Calculated Moduli values (ksi):				Absolute Dist to	
		R1	R2	R3	R4	R5	R6	R7	SURF(E1)	BASE(E2)	SUBB(E3)	SUBG(E4)	ERR/Sens	Bedrock
31.000	9,883	4.97	1.90	1.66	1.43	1.15	1.02	0.83	400.	500.0	466.9	42.2	10.57	300.00 †
81.000	9,815	6.09	3.89	2.47	1.94	1.50	1.27	0.99	400.	500.0	30.0	31.2	8.82	300.00 †
157.000	9,903	3.27	1.96	1.67	1.39	1.17	0.97	0.79	400.	938.1	600.0	40.1	2.91	300.00 †
315.000	9,934	3.65	2.28	1.95	1.57	1.31	1.09	0.89	400.	764.2	600.0	35.2	1.61	300.00 †
432.000	9,779	3.94	1.65	1.43	1.23	0.98	0.84	0.67	400.	500.0	600.0	50.0	8.31	300.00 †
Mean:		4.38	2.34	1.84	1.51	1.22	1.04	0.83	400.	640.5	459.4	39.7	6.44	300.00
Std. Dev:		1.14	0.90	0.40	0.27	0.19	0.16	0.12	0.	201.9	246.9	7.2	3.94	144.78
Var Coeff(%):		26.08	38.41	21.76	17.74	15.92	15.28	14.23	0.	31.5	53.7	18.1	61.08	48.26

Figure A.30. FWD Back-Calculation Results for Cracked Portion of Section-3 of Houston District in Winter.

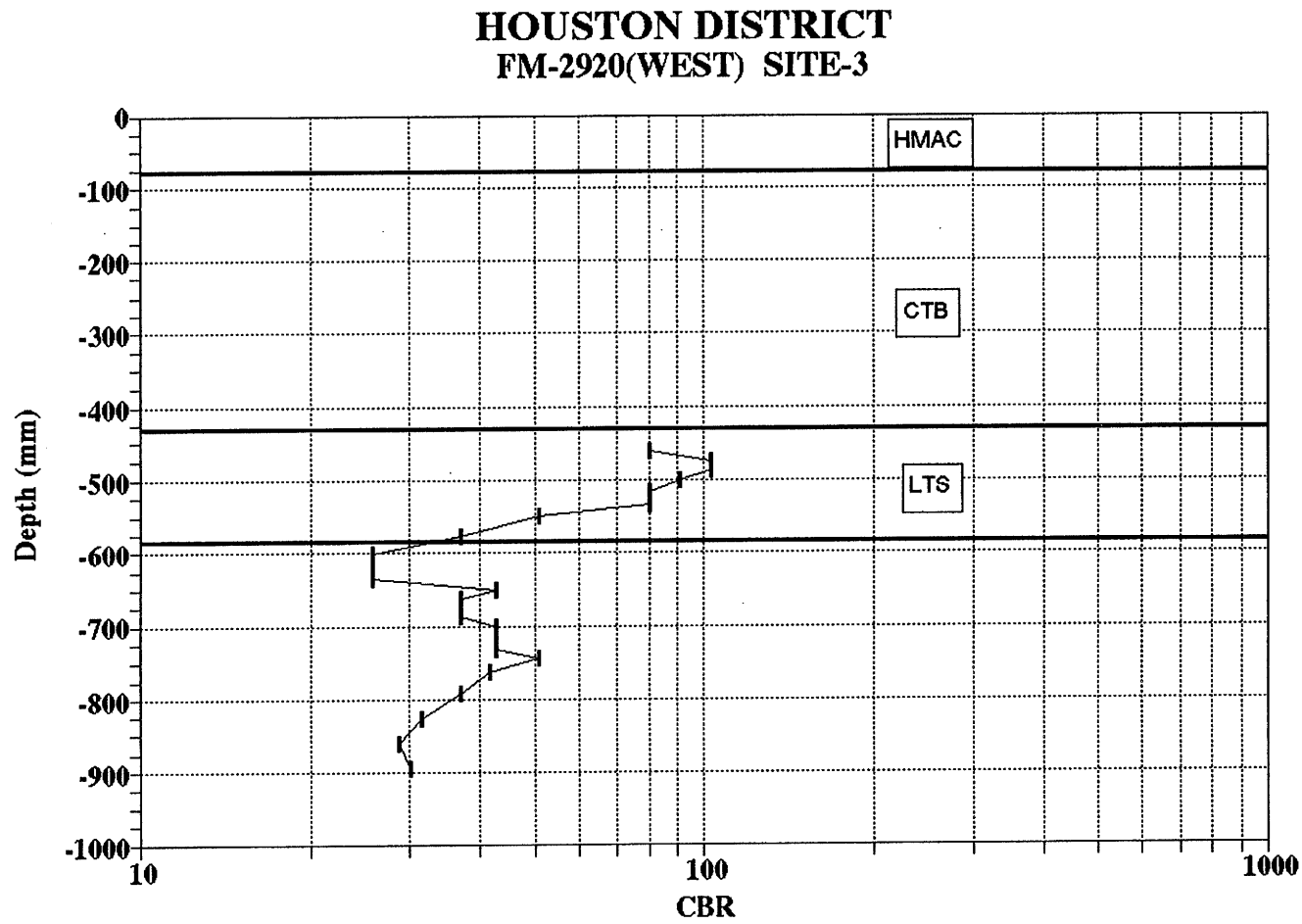


Figure A.31. Variation of CBR Obtained from DCP Testing for Section-3 of Houston District.

UNIAXIAL RESILIENT MODULUS

Project	1287	Gage Length (in)	2
Sample ID	HOU3	Date of Test	
Height (in)	3.15	Temperature	77F

	Load lbs.	Def in.	Total Mr	Instant Mr
PEAK 1	98.89	1.326E-05	1187055	1362061
PEAK 2	99.14	1.341E-05	1176848	1224201
PEAK 3	98.59	1.402E-05	1119367	1398307
PEAK 4	99.27	1.45E-05	1089637	1215360
AVERAGE	98.97	1.38E-05	1143227	1299982

Failure Load (lbs) : 48200
 Correction Factor : 0.883
 Ultimate Stress (psi) : 3385.5

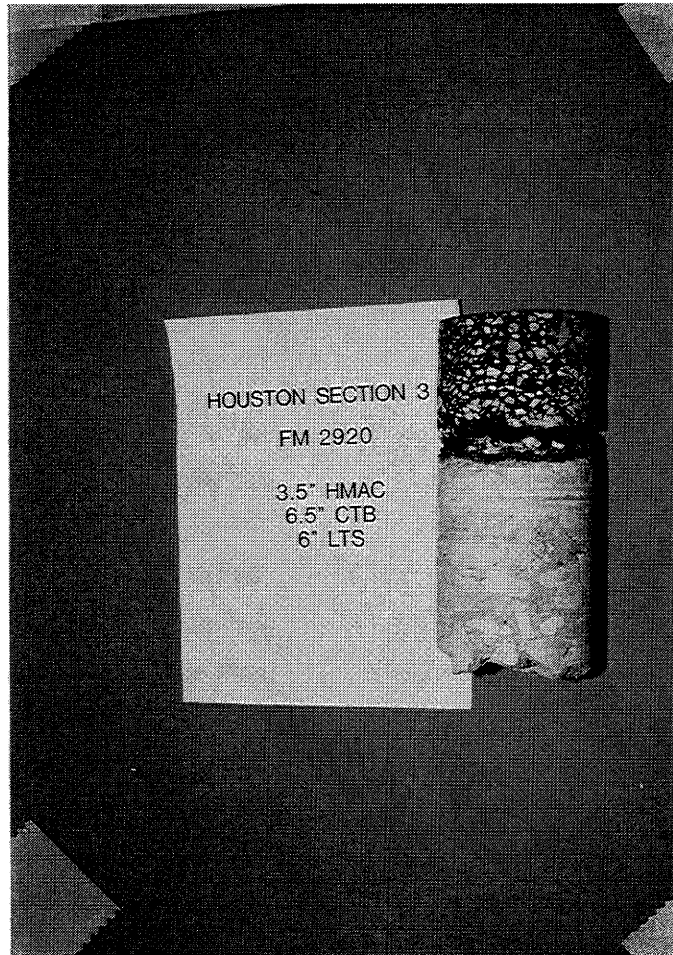
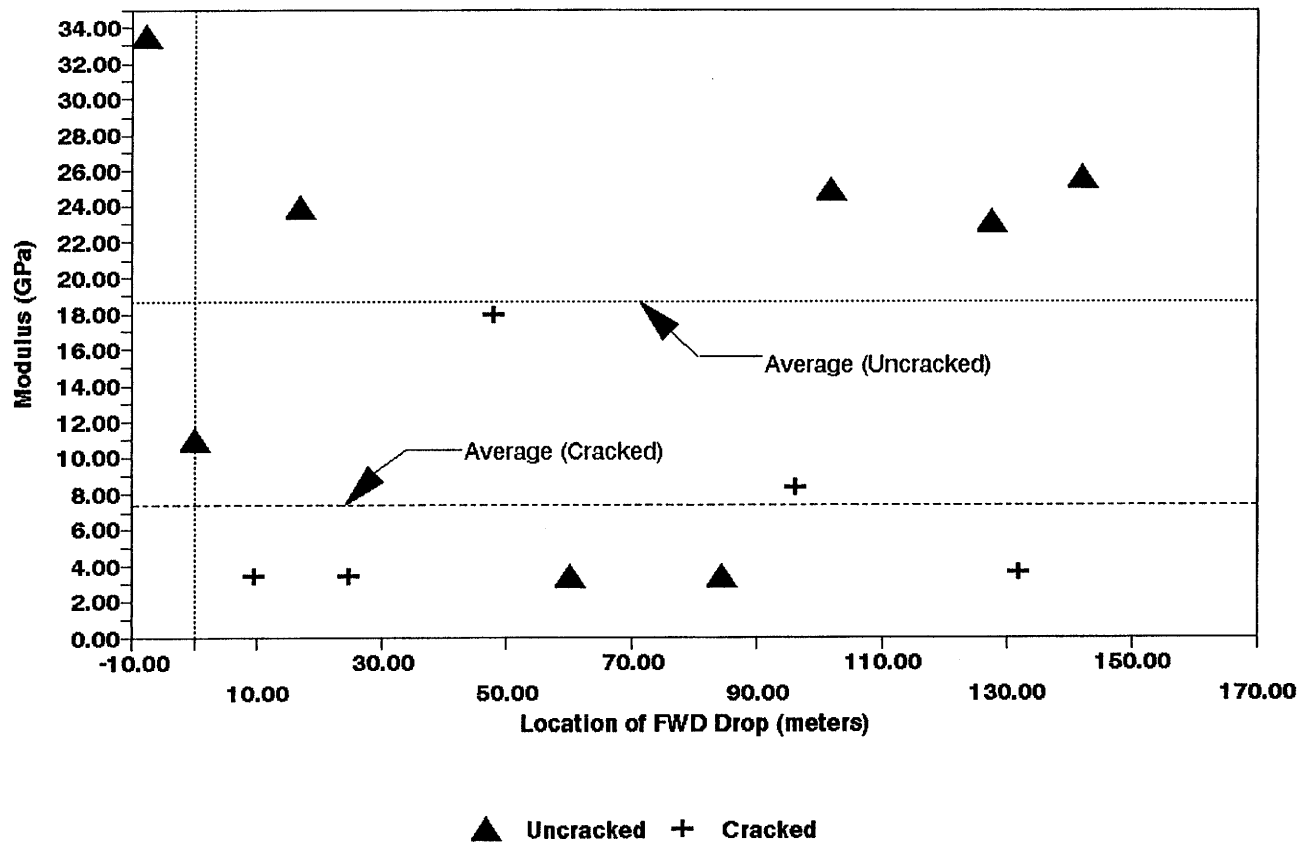


Figure A.32. Results of Laboratory Testing for Cores Obtained from Section-3 of Houston District.

Houston District Section-3 Base
Summer



A.35

Figure A.33. Variation of Modulus of Stabilized Base within Test Section for Section-3 of Houston District in Summer.

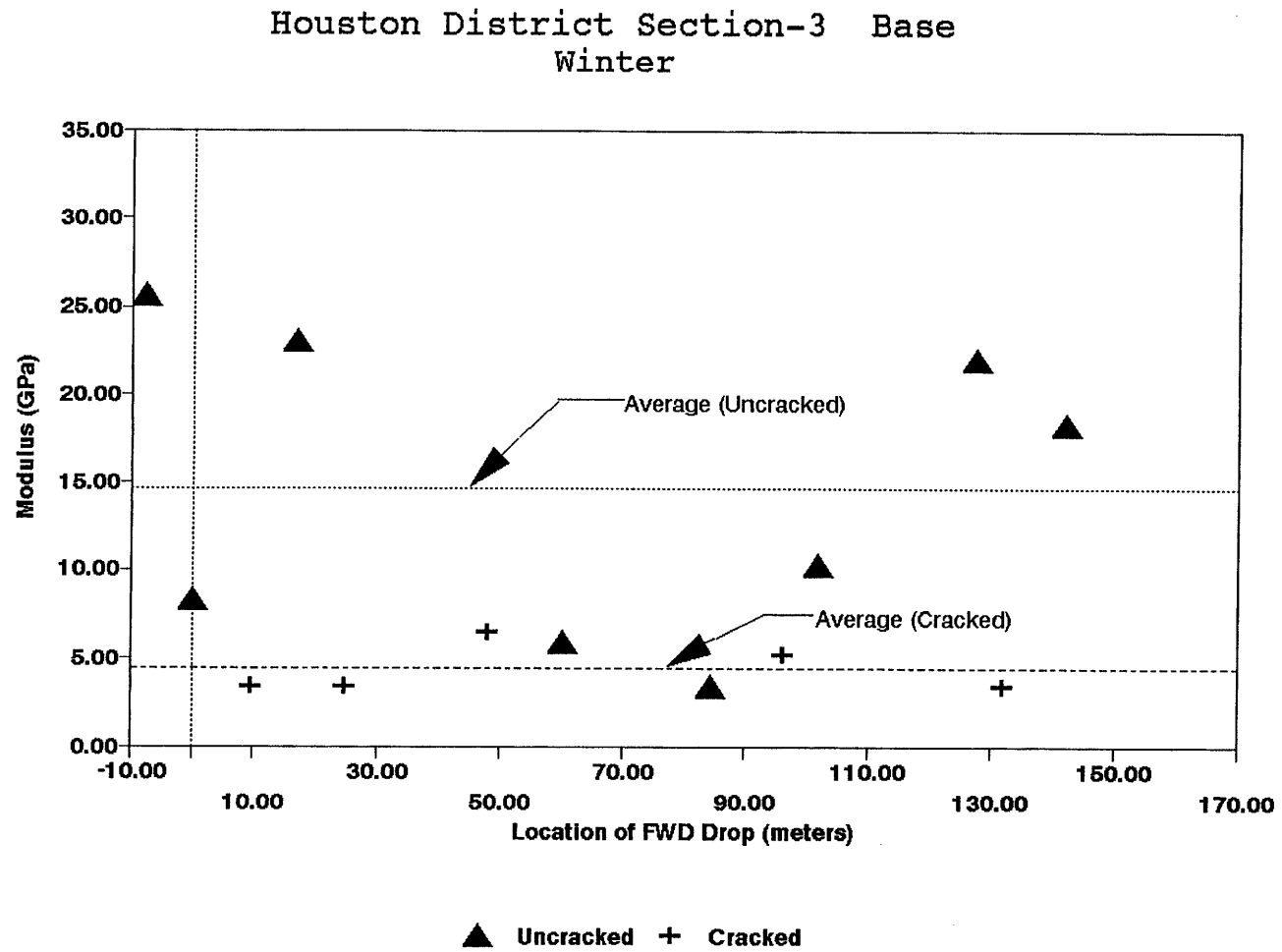


Figure A.34. Variation of Modulus of Stabilized Base within Test Section for Section-3 of Houston District in Winter.

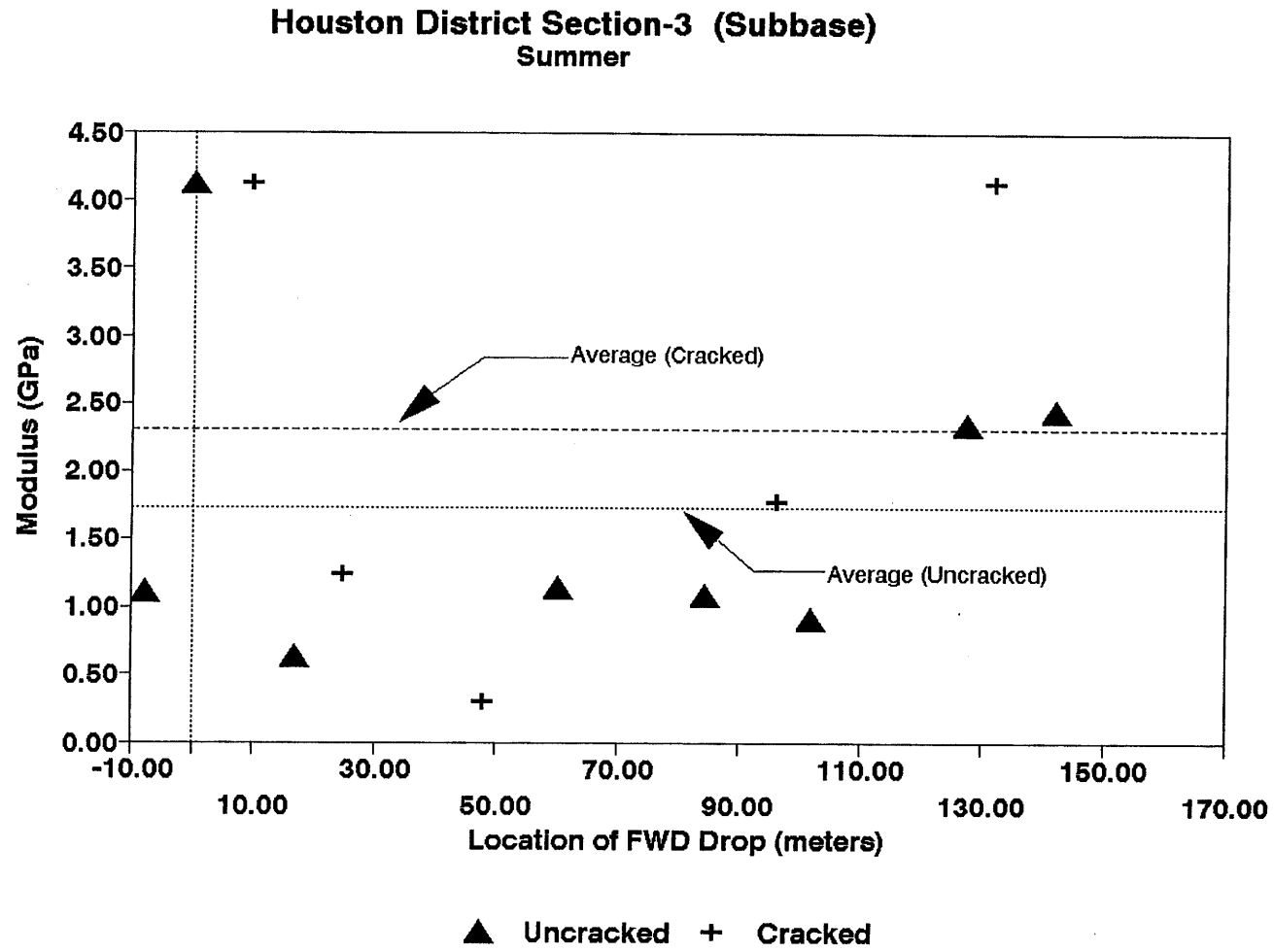


Figure A.35. Variation of Modulus of Stabilized Subbase within Test Section for Section-3 of Houston District in Summer.

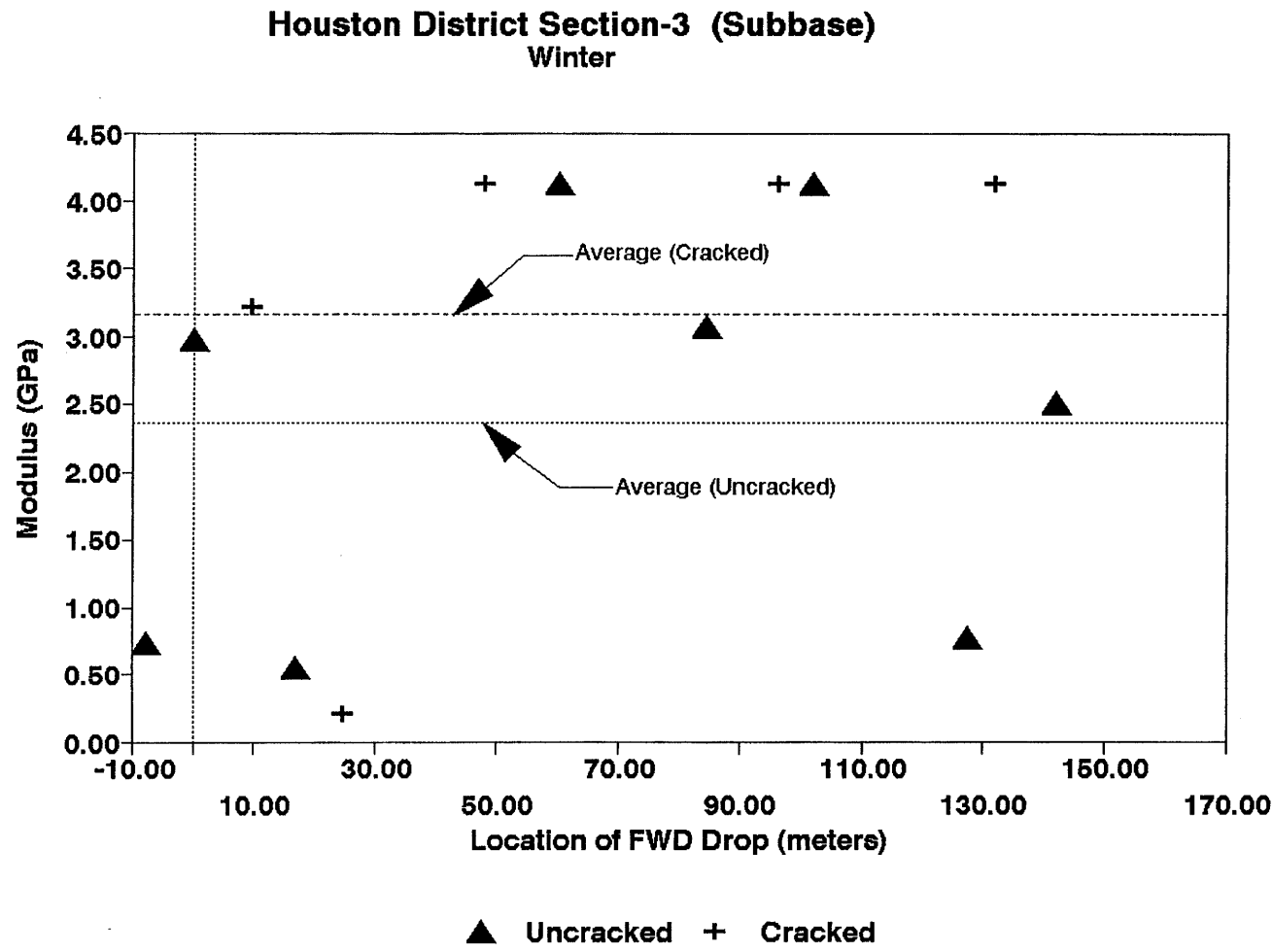


Figure A.36. Variation of Modulus of Stabilized Subbase within Test Section for Section-3 of Houston District in Winter.

Section No.: 4 District: Houston County: Harris Highway: FM-2920 (East)
Structure: Asphalt : 102 mm
CTB : 279 mm
LTS : 152 mm
Subgrade

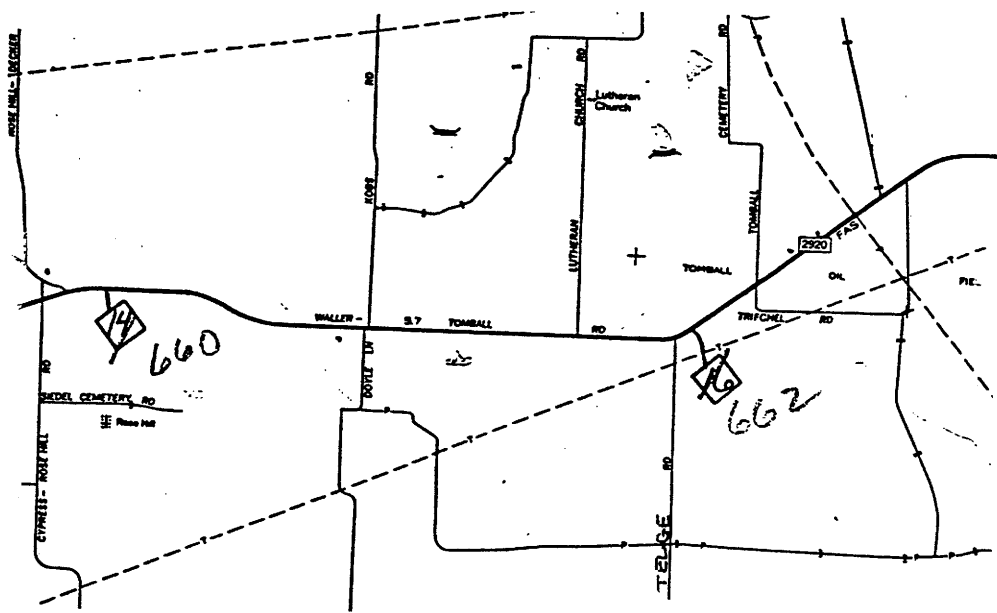
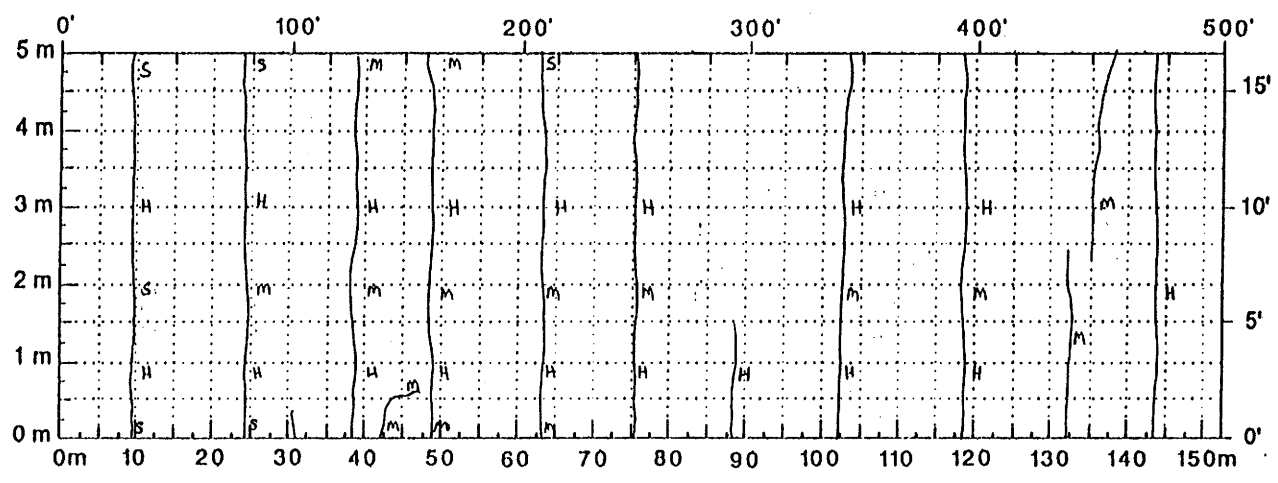
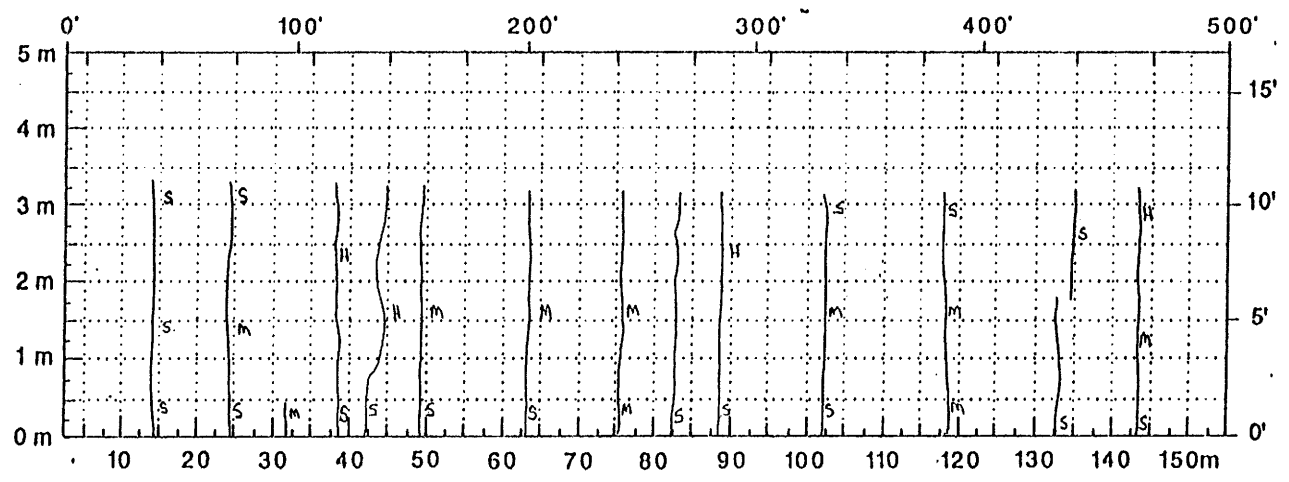


Figure A.37. Location and Details of Section-4 of Houston District.



Comments: Crack Map for Summer

A.40



Comments: Crack Map for Winter

Figure A.38. Crack Map for Section-4 of Houston District.

A.41

TTI MODULUS ANALYSIS SYSTEM (SUMMARY REPORT)													(Version 4.2)			
District:	12												MODULI RANGE(psi)			
County:	102												Minimum	Maximum	Poisson Ratio Values	
Highway/Road:	FM2920		Pavement:	4.00					185,581	185,619	H1: j = 0.35					
			Base:	11.00					500,000	5,000,001	H2: j = 0.25					
			Subbase:	6.00					30,000	600,000	H3: j = 0.25					
			Subgrade:	279.00					42,500		H4: j = 0.35					
Station	Load (lbs)	Measured Deflection (mils):							Calculated Moduli values (ksi):				Absolute Dpth to			
		R1	R2	R3	R4	R5	R6	R7	SURF(E1)	BASE(E2)	SUBB(E3)	SUBG(E4)	ERR/Sens	Bedrock		
1.000	10,847	3.43	2.10	1.62	1.20	0.90	0.69	0.57	186.	3713.8	30.0	64.3	5.30	300.00 *		
2.000	10,863	3.43	2.39	1.88	1.55	1.18	0.98	0.82	186.	5000.0	178.7	42.1	6.57	300.00 *		
3.000	10,815	3.35	2.14	1.65	1.31	0.98	0.69	0.49	186.	4147.9	30.0	59.8	6.58	225.82 *		
4.000	10,839	3.03	1.89	1.58	1.31	1.02	0.77	0.61	186.	5000.0	378.6	51.2	6.71	300.00 *		
5.000	10,719	3.76	2.77	2.31	1.87	1.38	1.06	0.82	186.	4637.3	30.0	37.8	8.56	300.00 *		
6.000	10,775	3.76	2.68	2.23	1.83	1.47	1.22	0.98	186.	5000.0	55.8	35.2	4.86	300.00 *		
7.000	10,687	4.48	3.10	2.65	2.19	1.79	1.43	1.18	186.	4375.1	46.8	28.0	3.17	300.00		
8.000	10,703	4.40	3.02	2.58	2.11	1.71	1.39	1.10	186.	4516.7	33.9	29.7	3.17	300.00		
Mean:		3.70	2.51	2.06	1.67	1.30	1.03	0.82	186.	4548.8	98.0	43.5	5.62	300.00		
Std. Dev:		0.51	0.45	0.44	0.38	0.34	0.30	0.25	0.	464.1	124.0	13.6	1.86	150.15		
Var Coeff(%):		13.77	17.86	21.17	22.89	25.91	29.11	30.84	0.	10.2	100.0	31.2	33.19	50.05		

Figure A.39. FWD Back-Calculation Results for Uncracked Portion of Section-4 of Houston District in Summer.

TTI MODULUS ANALYSIS SYSTEM (SUMMARY REPORT)													(Version 4.2)	
District:	12								MODULI RANGE(psi)					
County:	102								Minimum	Maximum	Poisson Ratio Values			
Highway/Road:	FM2920	Pavement:	4.00						185,581	185,619	H1: j = 0.35			
		Base:	11.00						500,000	5,000,001	H2: j = 0.25			
		Subbase:	6.00						30,000	600,000	H3: j = 0.25			
		Subgrade:	279.00						44,100		H4: j = 0.35			
Station	Load (lbs)	Measured Deflection (mils):							Calculated Moduli values (ksi):				Absolute Dpth to	
		R1	R2	R3	R4	R5	R6	R7	SURF(E1)	BASE(E2)	SUBB(E3)	SUBG(E4)	ERR/Sens	Bedrock
1.000	10,807	3.59	2.01	1.62	1.24	0.94	0.73	0.53	186.	3711.4	30.0	61.8	2.78	252.29 *
2.000	10,719	4.16	2.26	1.81	1.43	1.10	0.82	0.65	186.	2437.2	70.0	50.7	0.47	300.00
3.000	10,759	3.88	2.35	1.88	1.43	1.06	0.82	0.61	186.	3067.4	30.0	53.7	3.45	293.43 *
4.000	10,783	4.97	3.35	2.54	1.95	1.42	1.06	0.82	186.	1702.4	30.0	39.7	3.71	300.00 *
5.000	10,687	4.60	3.02	2.42	1.95	1.47	1.14	0.90	186.	2674.8	30.0	37.5	3.01	300.00 *
6.000	10,687	5.49	3.52	2.92	2.31	1.83	1.47	1.18	186.	1971.0	56.8	29.1	1.33	300.00
Mean:		4.45	2.75	2.20	1.72	1.30	1.01	0.78	186.	2594.0	41.1	45.4	2.46	300.00
Std. Dev:		0.71	0.63	0.50	0.41	0.33	0.28	0.24	0.	733.0	17.7	12.0	1.28	101.82
Var Coeff(%):		15.97	22.83	22.96	24.03	25.48	27.44	30.50	0.	28.3	43.1	26.5	52.14	33.94

Figure A.40. FWD Back-Calculation Results for Cracked Portion of Section-4 of Houston District in Summer.

A.43

TTI MODULUS ANALYSIS SYSTEM (SUMMARY REPORT)														(Version 4.2)	
District:	12									MODULI RANGE(ksi)					
County:	102		Thickness(in)							Minimum	Maximum	Poisson Ratio Values			
Highway/Road:	FN2920		Pavement:	4.00		462,954		463,046		H1: $\mu = 0.35$					
			Base:	11.00		500,000		5,000,001		H2: $\mu = 0.25$					
			Subbase:	6.00		30,000		600,000		H3: $\mu = 0.25$					
			Subgrade:	279.00		45,000				H4: $\mu = 0.35$					
Station	Load (lbs)	Measured Deflection (mils):								Calculated Moduli values (ksi):				Absolute Dpth to	
		R1	R2	R3	R4	R5	R6	R7	SURF(E1)	BASE(E2)	SUBB(E3)	SUBG(E4)	ERR/Sens	Bedrock	
25.000	9.994	2.48	1.65	1.25	0.90	0.73	0.53	0.40	463.	2448.6	53.2	75.8	2.45	300.00	
0.000	9.835	2.81	1.81	1.49	1.06	0.81	0.61	0.46	463.	1963.5	47.0	64.3	1.53	300.00	
54.000	9.879	2.48	1.72	1.45	1.11	0.87	0.65	0.48	463.	3687.5	30.0	63.1	1.57	279.54	
177.000	9.875	2.37	1.61	1.34	1.11	0.84	0.69	0.53	463.	3904.8	154.2	55.8	1.50	300.00	
304.000	9.795	2.96	2.26	1.93	1.56	1.22	0.97	0.73	463.	3540.5	30.0	40.0	2.07	300.00	
362.000	9.863	3.13	2.28	1.94	1.56	1.22	1.00	0.79	463.	3026.6	38.5	39.8	1.11	300.00	
445.000	9.867	3.51	2.69	2.31	1.89	1.49	1.19	0.93	463.	2871.2	30.3	32.5	1.37	300.00	
489.000	9.756	3.30	2.43	2.12	1.75	1.43	1.15	0.92	463.	2834.1	192.2	31.7	0.49	300.00	
Mean:		2.88	2.06	1.73	1.37	1.08	0.85	0.65	463.	3034.6	71.9	50.4	1.51	300.00	
Std. Dev:		0.42	0.41	0.39	0.37	0.30	0.26	0.21	0.	654.3	63.9	16.6	0.59	82.12	
Var Coeff(%):		14.54	19.89	22.84	26.78	27.80	30.47	32.59	0.	21.6	88.8	32.9	38.82	27.37	

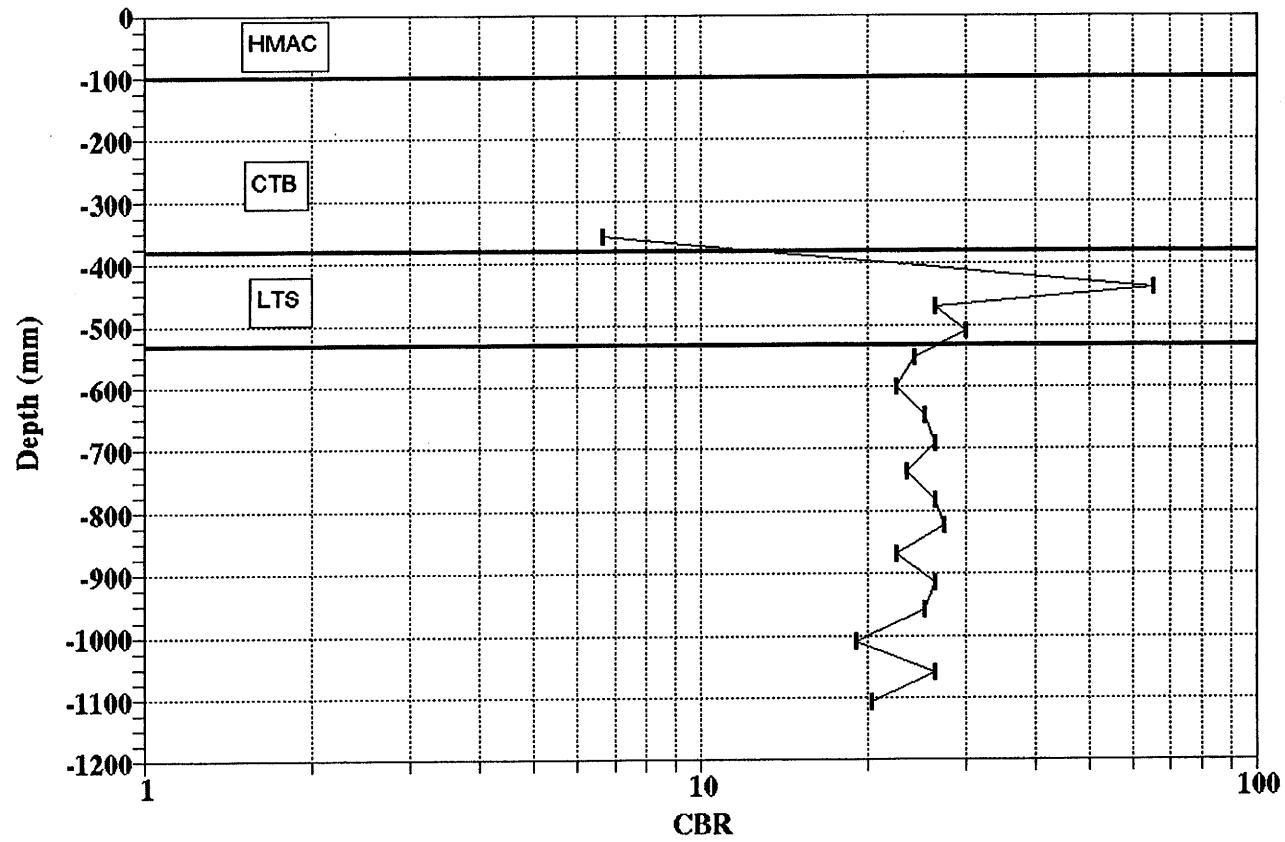
Figure A.41. FWD Back-Calculation Results for Uncracked Portion of Section-4 of Houston District in Winter.

A.44

TTI MODULUS ANALYSIS SYSTEM (SUMMARY REPORT)													(Version 4.2)			
District:	12											MODULI RANGE(psi)				
County:	102											Minimum	Maximum	Poisson Ratio Values		
Highway/Road:	FH2920											Pavement:	4.00	462,954	463,046	H1: u = 0.35
												Base:	11.00	500,000	5,000,001	H2: u = 0.25
												Subbase:	6.00	30,000	600,000	H3: u = 0.25
												Subgrade:	279.00		45,000	H4: u = 0.35
Station	Load (lbs)	Measured Deflection (mils):							Calculated Moduli values (ksi):				Absolute Dpth to Bedrock			
		R1	R2	R3	R4	R5	R6	R7	SURF(E1)	BASE(E2)	SURB(E3)	SURG(E4)	ERR/Sens	Bedrock		
32.000	9,922	3.31	1.80	1.45	1.12	0.85	0.64	0.50	463.	582.3	600.0	58.2	2.00	300.00 *		
80.000	9,930	3.36	1.71	1.37	1.05	0.78	0.60	0.44	463.	636.9	375.3	63.7	2.39	267.39 *		
160.000	9,819	3.37	2.28	1.44	1.13	0.89	0.67	0.52	463.	798.5	124.7	57.5	4.62	300.00		
248.000	9,855	4.46	2.64	1.90	1.48	1.11	0.85	0.65	463.	500.0	120.0	44.5	2.03	300.00 *		
368.000	9,787	4.55	2.61	2.11	1.64	1.26	0.94	0.73	463.	500.0	220.7	38.7	2.46	300.00 *		
470.000	9,787	4.81	2.75	2.24	1.81	1.46	1.17	0.93	463.	500.0	393.7	32.7	3.38	300.00 *		
Mean:		3.98	2.30	1.75	1.37	1.06	0.81	0.63	463.	586.3	305.7	49.2	2.81	300.00		
Std. Dev:		0.70	0.45	0.38	0.32	0.27	0.22	0.18	0.	118.3	186.4	12.4	1.02	76.90		
Var Coeff(%):		17.60	19.58	21.70	23.08	25.14	27.03	28.95	0.	20.2	61.0	25.1	36.15	25.63		

Figure A.42. FWD Back-Calculation Results for Cracked Portion of Section-4 of Houston District in Winter.

HOUSTON DISTRICT FM-2920(EAST) SITE-4



A.45

Figure A.43. Variation of CBR Obtained from DCP Testing for Section-4 of Houston District.

Sample ID	HOU4B	Date of Test	77F	
Height (in)	8.72	Temperature		
	Load lbs.	Def in.	Total Mr	Instant Mr
PEAK 1	452.93	6.269E-05	1149979	1233422
PEAK 2	452.59	6.15E-05	1171249	1223182
PEAK 3	452.47	6.1E-05	1180545	1236869
PEAK 4	453.57	6.072E-05	1188829	1223531
AVERAGE	452.89	6.148E-05	1172650	1229251

Failure Load (lbs) : 15200
 Correction Factor : 1
 Ultimate Stress (psi) : 1209.09

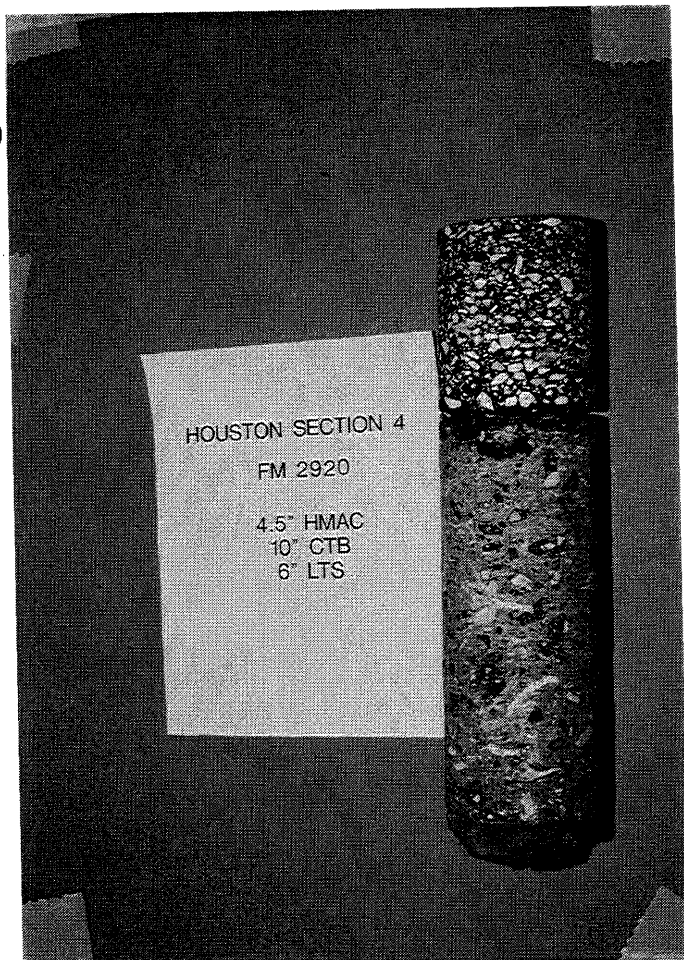


Figure A.44. Results of Laboratory Testing for Cores Obtained from Section-4 of Houston District.

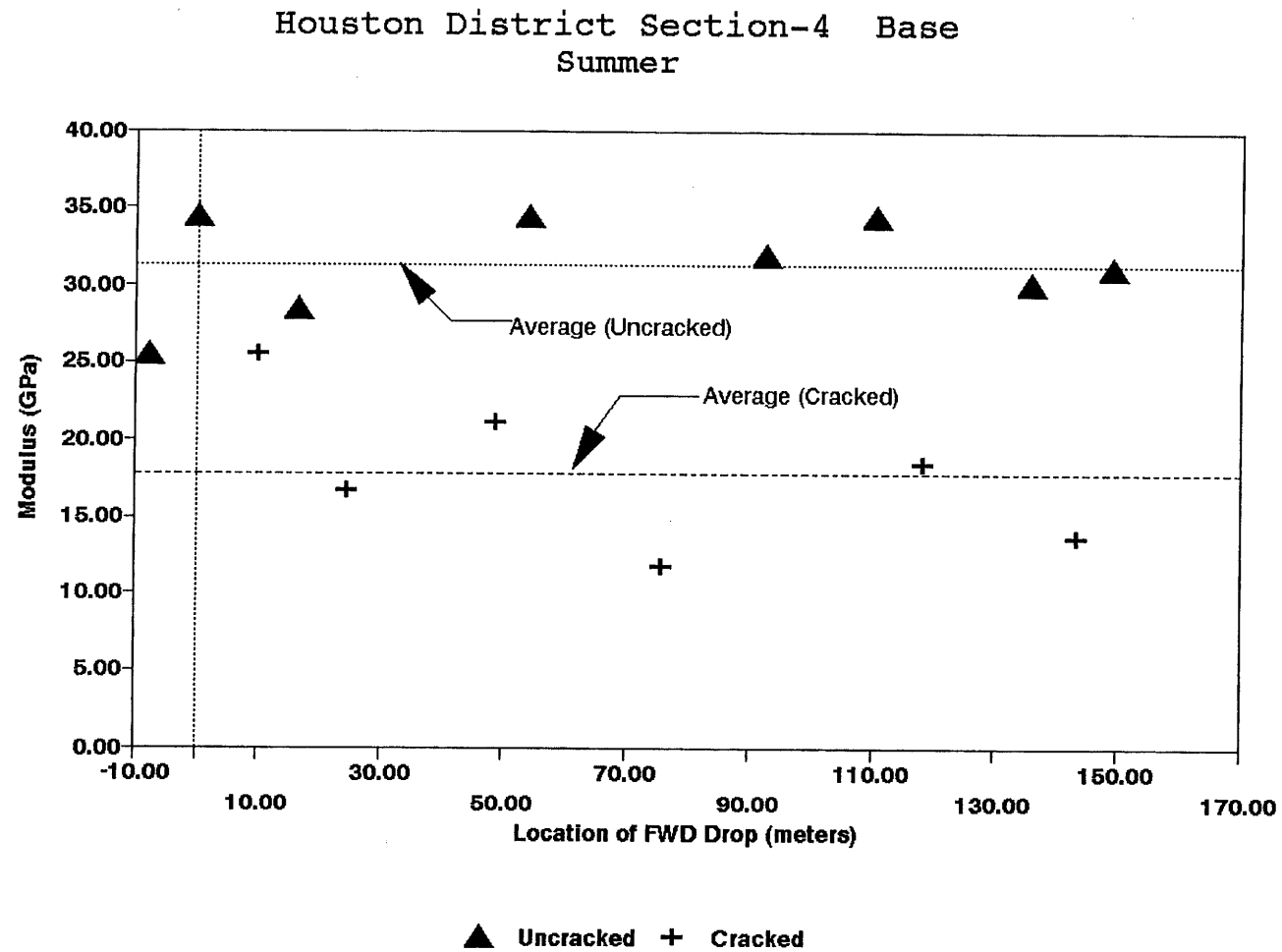
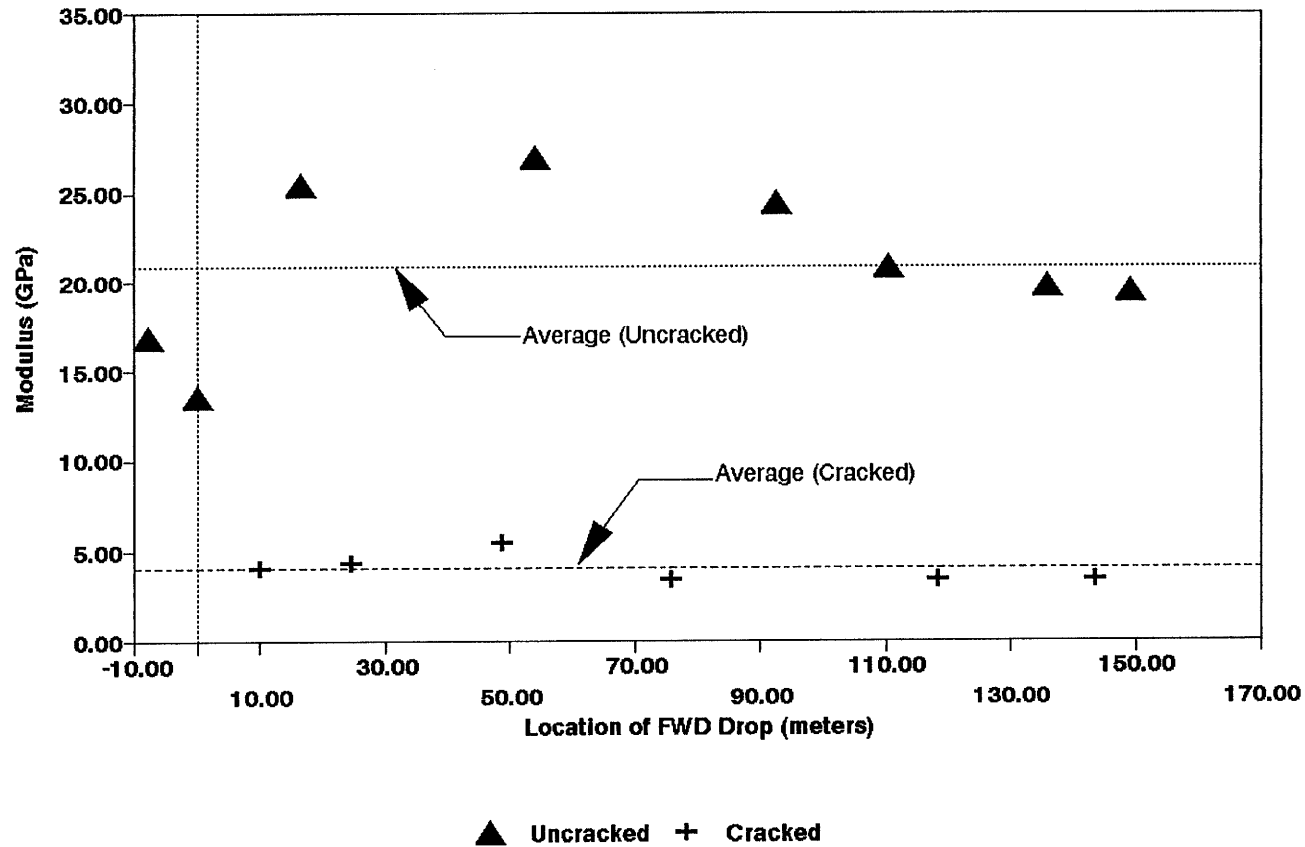


Figure A.45. Variation of Modulus of Stabilized Base within Test Section for Section-4 of Houston District in Summer.

Houston District Section-4 Base
Winter



A.48

Figure A.46. Variation of Modulus of Stabilized Base within Test Section for Section-4 of Houston District in Winter.

A.49

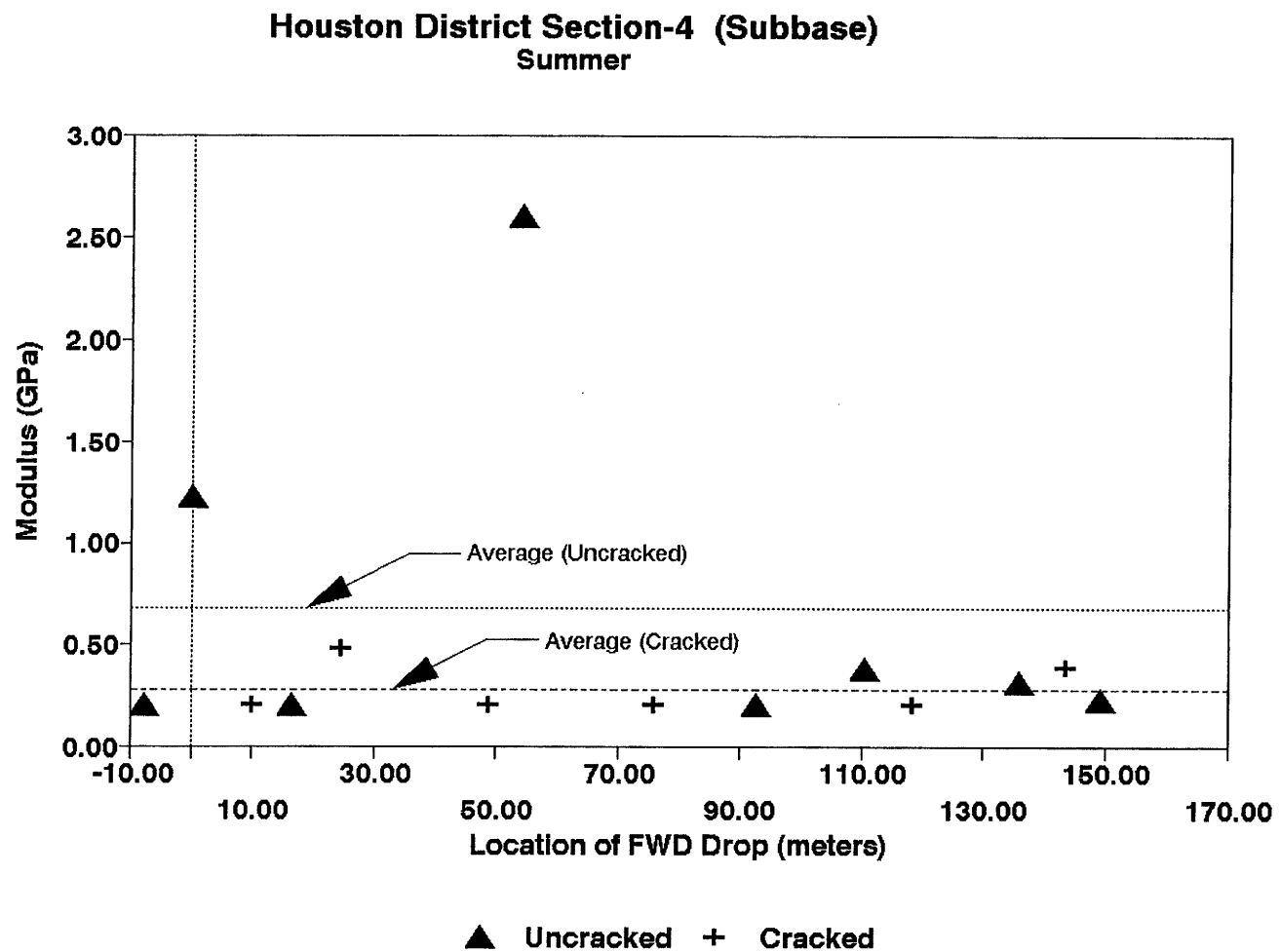


Figure A.47. Variation of Modulus of Stabilized Subbase within Test Section for Section-4 of Houston District in Summer.

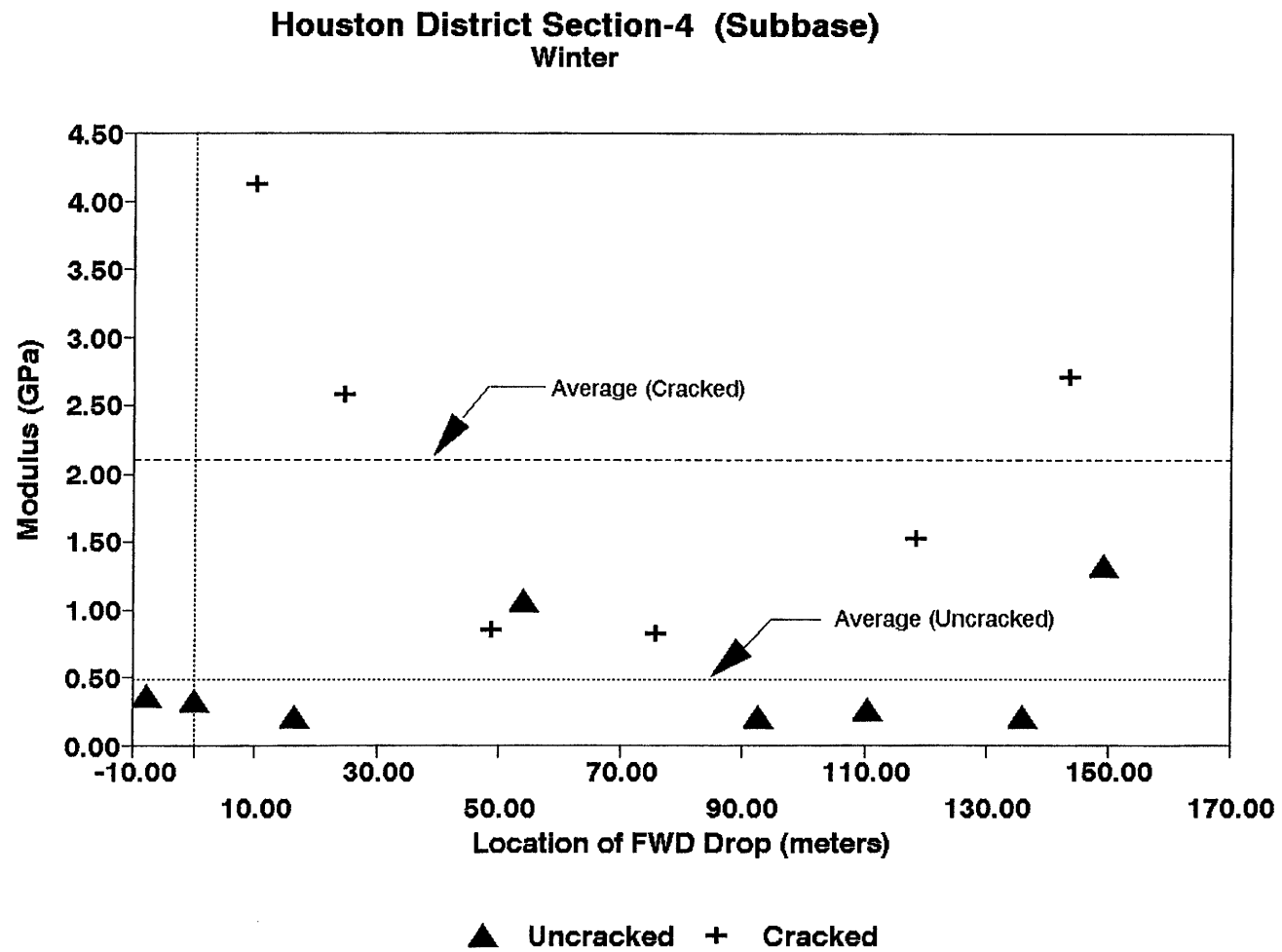


Figure A.48. Variation of Modulus of Stabilized Subbase within Test Section for Section-4 of Houston District in Winter.

Section No.: 5 District: Houston County: Harris Highway: FM-1093
Structure: Asphalt : 76 mm
CTB : 305 mm
LTS : 152 mm
Subgrade

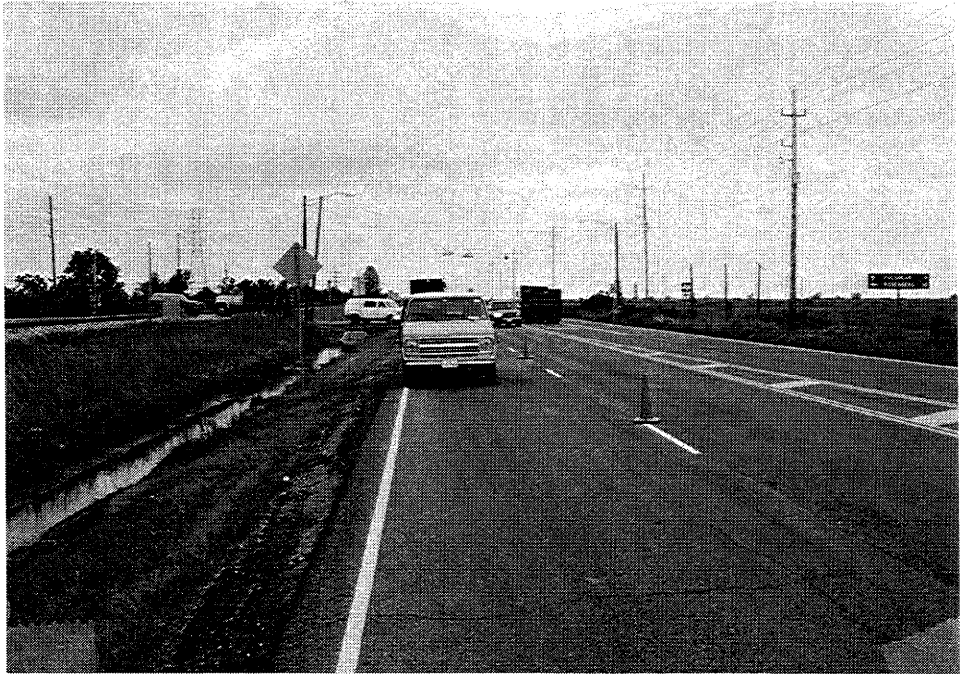
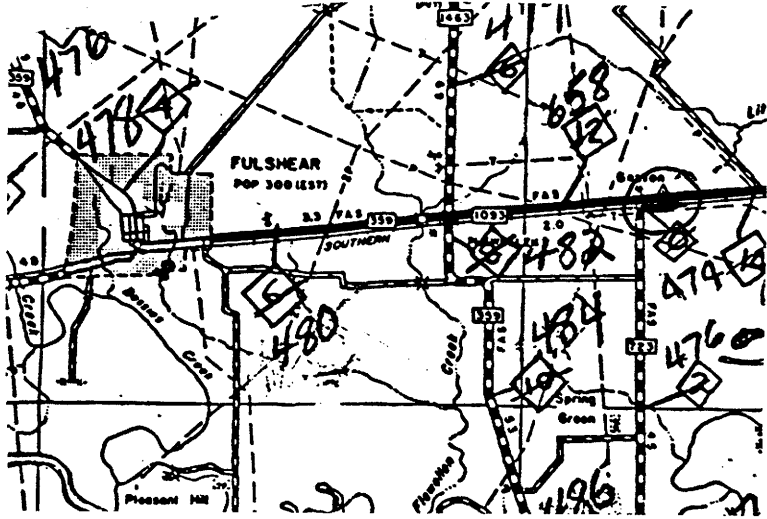
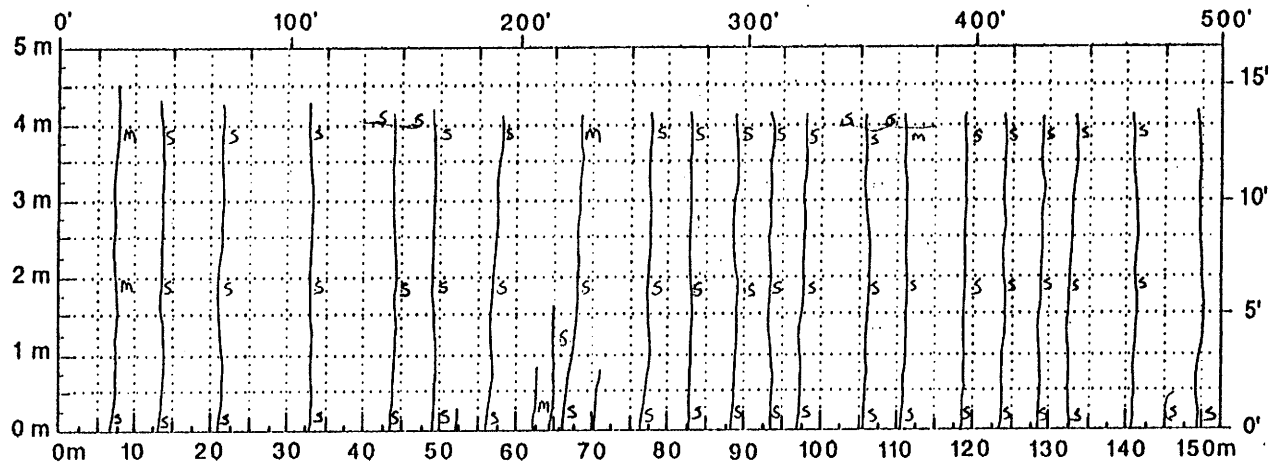
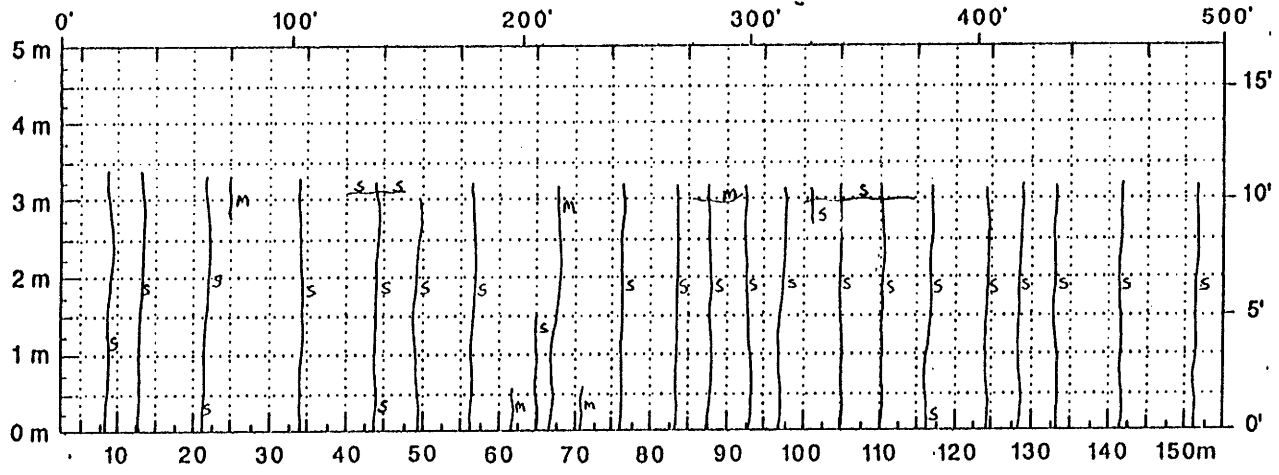


Figure A.49. Location and Details of Section-5 of Houston District.



Comments: Crack Map for Summer

A.52



Comments: Crack Map for Winter

Figure A.50. Crack Map for Section-5 of Houston District.

TTI MODULUS ANALYSIS SYSTEM (SUMMARY REPORT)														(Version 4.2)	
District:	12								MODULI RANGE(psi)						
County:	80								Minimum	Maximum	Poisson Ratio Values				
Highway/Road:	FM1093								591,941	592,059	H1: $\mu = 0.35$				
		Pavement:	3.00					500,000	5,000,001	H2: $\mu = 0.25$					
		Base:	12.00					30,000	600,000	H3: $\mu = 0.25$					
		Subbase:	6.00					20,000		H4: $\mu = 0.35$					
		Subgrade:	279.00												
Station	Load (lbs)	Measured Deflection (mils):							Calculated Moduli values (ksi):				Absolute Dist to Bedrock		
		R1	R2	R3	R4	R5	R6	R7	SURF(E1)	BASE(E2)	SUBB(E3)	SUBG(E4)	ERR/Gens	Bedrock	
1.000	16,303	3.88	3.27	3.00	2.63	2.28	1.92	1.63	592.	5000.0	304.2	31.1	3.22	300.00 *	
2.000	16,071	4.36	3.77	3.38	2.95	2.61	2.24	1.84	592.	5000.0	337.0	25.3	1.80	300.00 †	
3.000	16,135	4.69	4.03	3.58	3.03	2.61	2.16	1.80	592.	4729.0	82.7	26.3	1.68	300.00	
4.000	15,967	5.21	4.49	3.92	3.27	2.73	2.20	1.75	592.	3409.1	36.8	26.6	1.85	300.00	
5.000	15,951	6.06	5.24	4.54	3.78	3.26	2.73	2.20	592.	2874.3	83.4	21.2	1.24	300.00	
6.000	15,919	8.24	6.29	5.19	4.26	3.46	2.81	2.24	592.	760.5	200.0	21.3	0.32	300.00	
7.000	15,919	7.03	6.04	5.38	4.62	3.91	3.22	2.65	592.	2386.2	129.5	17.2	1.08	300.00	
8.000	15,919	5.45	4.53	3.96	3.47	2.97	2.49	2.00	592.	3411.2	209.3	22.6	0.55	300.00	
Mean:		5.61	4.71	4.12	3.50	2.98	2.47	2.01	592.	3446.3	172.9	23.9	1.47	300.00	
Std. Dev:		1.45	1.07	0.85	0.68	0.53	0.43	0.33	0.	1470.7	108.7	4.3	0.91	172.53	
Var Coeff(%):		25.83	22.78	20.66	19.44	17.94	17.24	16.61	0.	42.7	62.9	17.8	61.87	57.51	

Figure A.51. FWD Back-Calculation Results for Uncracked Portion of Section-5 of Houston District in Summer.

TTI MODULUS ANALYSIS SYSTEM (SUMMARY REPORT)														(Version 4.2)	
District:	12														
County:	80														
Highway/Road:	FM1093														
			Thickness(in)						MODULI RANGE(psi)		Poisson Ratio Values				
			Pavement:	3.00					Minimum	Maximum			H1: $\mu = 0.35$		
			Base:	12.00					591,941	592,059			H2: $\mu = 0.25$		
			Subbase:	6.00					500,000	5,000,001			H3: $\mu = 0.25$		
			Subgrade:	279.00					30,000	600,000			H4: $\mu = 0.35$		
										20,000					
Station	Load (lbs)	Measured Deflection (mils):					Calculated Moduli values (ksi):				Absolute Depth to				
		R1	R2	R3	R4	R5	R6	R7	SURF(E1)	BASE(E2)	SUBB(E3)	SUBG(E4)	ERR/Sens	Bedrock	
1.000	15,767	7.72	6.12	4.92	3.90	3.09	2.49	2.00	592.	1014.0	37.3	24.9	1.05	300.00	
2.000	15,863	6.18	5.28	4.31	3.55	2.89	2.32	1.88	592.	1984.8	30.0	26.5	1.38	300.00 †	
3.000	15,767	6.66	5.41	4.38	3.55	2.89	2.28	1.71	592.	1480.1	36.1	27.0	1.03	300.00	
4.000	15,767	8.52	6.79	4.77	3.75	2.97	2.40	1.88	592.	642.0	33.8	26.6	3.57	300.00	
5.000	15,711	8.64	5.62	4.58	3.71	3.01	2.45	2.04	592.	500.0	257.7	24.8	2.46	300.00 †	
6.000	15,791	7.35	6.21	5.00	4.02	3.26	2.65	2.16	592.	1358.2	30.0	23.4	1.59	300.00 †	
7.000	15,735	7.63	6.67	5.50	4.46	3.66	3.02	2.45	592.	1517.8	30.0	20.1	1.80	300.00 †	
8.000	15,863	5.49	4.53	3.88	3.27	2.73	2.32	1.92	592.	2961.4	66.7	25.9	0.92	300.00	
Mean:		7.27	5.83	4.67	3.78	3.06	2.49	2.00	592.	1432.3	65.2	24.9	1.72	300.00	
Std. Dev:		1.10	0.76	0.50	0.36	0.29	0.24	0.22	0.	786.3	78.7	2.3	0.90	174.77	
Var Coeff(%):		15.16	13.08	10.61	9.53	9.38	9.81	11.13	0.	54.9	100.0	9.1	52.21	58.26	

Figure A.52. FWD Back-Calculation Results for Cracked Portion of Section-5 of Houston District in Summer.

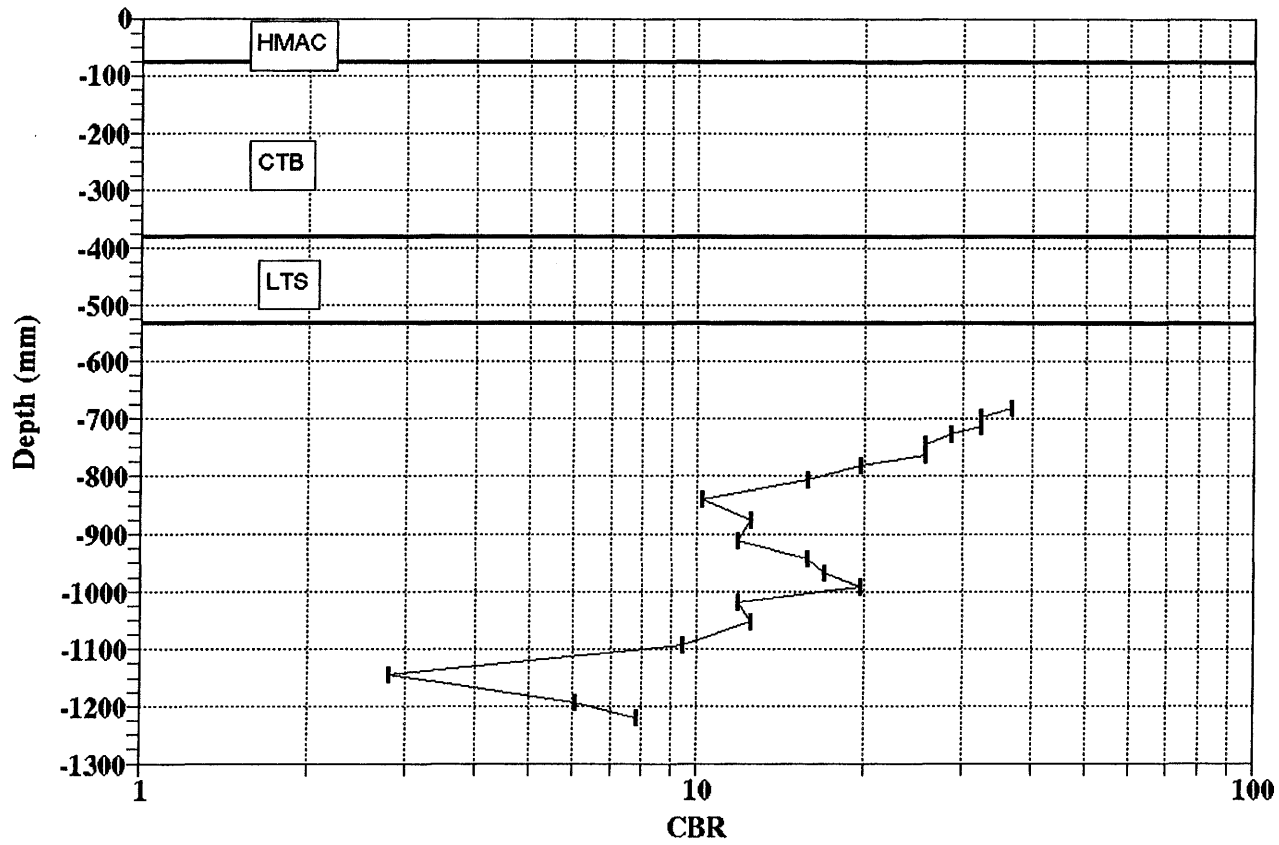
FWD MODULUS ANALYSIS SYSTEM (SUMMARY REPORT)										(Version 4.2)				
District:	12								MODULI RANGE(psi)					
County:	80								Minimum	Maximum	Poisson Ratio Values			
Highway/Road:	FM1093	Pavement:	3.00						499,950	500,050	H1: $\mu = 0.35$			
		Base:	12.00						500,000	5,000,001	H2: $\mu = 0.25$			
		Subbase:	6.00						30,000	600,000	H3: $\mu = 0.25$			
		Subgrade:	279.00						20,000		H4: $\mu = 0.35$			
Station	Load (lbs)	Measured Deflection (mils):							Calculated Moduli values (ksi):				Absolute Dist to Bedrock	
		R1	R2	R3	R4	R5	R6	R7	SURF(E1)	BASE(E2)	SUBB(E3)	SUBG(E4)	ERR/Sens	Bedrock
53.000	10,637	2.67	2.36	2.24	1.94	1.66	1.37	1.17	500.	5000.0	373.3	26.8	4.00	300.00 †
53.000	10,538	2.81	2.41	2.20	1.93	1.70	1.45	1.24	500.	5000.0	373.3	26.1	3.07	300.00 †
96.000	10,419	2.90	2.54	2.38	2.03	1.73	1.48	1.26	500.	5000.0	337.0	24.3	2.90	300.00 †
172.000	10,399	3.33	2.80	2.54	2.18	1.91	1.60	1.32	500.	4674.9	232.0	22.0	1.41	300.00
235.000	10,343	3.72	3.09	2.67	2.23	1.83	1.52	1.22	500.	2721.3	97.2	25.1	1.22	300.00
329.000	10,157	7.18	5.98	4.51	3.39	2.49	1.77	1.39	500.	500.0	30.0	19.1	5.84	255.74 †
395.000	10,157	4.14	3.48	3.11	2.60	2.27	1.85	1.54	500.	2924.6	89.1	19.5	1.41	300.00
446.000	10,216	2.98	2.57	2.42	2.28	1.91	1.61	1.31	500.	5000.0	140.3	22.8	5.03	300.00 †
Mean:		3.72	3.15	2.76	2.32	1.94	1.58	1.31	500.	3852.6	209.0	23.2	3.11	300.00
Std. Dev:		1.48	1.20	0.76	0.48	0.29	0.16	0.12	0.	1661.5	138.6	2.9	1.74	178.20
Var Coeff(%):		39.90	38.13	27.69	20.80	15.18	10.03	8.89	0.	43.1	66.3	12.4	56.09	59.40

Figure A.53. FWD Back-Calculation Results for Uncracked Portion of Section-5 of Houston District in Winter.

FTI MODULUS ANALYSIS SYSTEM (SUMMARY REPORT)													(Version 4.2)	
District:	12								MODULI RANGE(ksi)					
County:	80		Thickness(in)		Minimum	Maximum		Poisson Ratio Values						
Highway/Road:	FM1093		Pavement:	3.00	499,950	500,050		H1: $\mu = 0.35$						
			Base:	12.00	500,000	5,000,001		H2: $\mu = 0.25$						
			Subbase:	6.00	30,000	600,000		H3: $\mu = 0.25$						
			Subgrade:	279.00	20,000		H4: $\mu = 0.35$							
Station	Load (lbs)	Measured Deflection (mils):							Calculated Moduli values (ksi):				Absolute Dist to Bedrock	
		R1	R2	R3	R4	R5	R6	R7	SURF(E1)	BASE(E2)	SUBR(E3)	SUBG(E4)	ERR/Sens	Bedrock
43,000	10,177	5.19	2.85	2.41	1.97	1.57	1.29	1.06	500.	500.0	403.9	31.3	4.27	300.00 †
110,000	10,169	4.98	2.00	1.75	1.48	1.25	1.08	0.92	500.	500.0	600.0	41.9	11.90	300.00 †
142,000	10,137	5.04	2.63	2.27	1.89	1.56	1.27	1.06	500.	500.0	600.0	31.8	5.54	300.00 †
186,000	10,097	5.85	3.91	3.11	2.43	1.92	1.52	1.24	500.	500.0	120.0	25.6	1.54	300.00 †
252,000	10,113	7.38	2.73	2.30	1.93	1.50	1.24	1.08	500.	500.0	47.5	35.9	14.52	300.00 †
348,000	10,057	5.38	3.45	2.88	2.36	1.92	1.57	1.30	500.	500.0	440.6	24.5	1.88	300.00 †
407,000	10,050	6.12	3.89	3.29	2.76	2.19	1.82	1.44	500.	500.0	289.6	21.2	3.11	300.00 †
467,000	10,046	4.61	2.44	2.17	1.81	1.49	1.22	1.01	500.	500.0	600.0	34.1	6.11	300.00 †
Mean:		5.57	2.99	2.52	2.08	1.67	1.38	1.14	500.	500.0	387.7	30.8	6.11	300.00
Std. Dev:		0.88	0.69	0.52	0.41	0.31	0.24	0.17	0.	0.0	218.9	6.7	4.72	191.61
Var Coeff(%):		15.75	23.22	20.70	19.64	18.26	17.47	15.11	0.	0.0	56.5	21.9	77.16	63.87

Figure A.54. FWD Back-Calculation Results for Cracked Portion of Section-5 of Houston District in Winter.

HOUSTON DISTRICT FM-1093(EAST) SITE-5



A.57

Figure A.55. Variation of CBR Obtained from DCP Testing for Section-5 of Houston District.

UNIAXIAL RESILIENT MODULUS

Project 1287 Gage Length (in) 2
 Sample ID HOU51 Date of Test
 Height (in) 5.59 Temperature 77F

	Load lbs.	Def in.	Total Mr	Instant Mr
PEAK 1	494.71	2.541E-05	3098944	3578915
PEAK 2	494.51	2.615E-05	3009925	3205138
PEAK 3	494.31	2.722E-05	2889996	3025851
PEAK 4	494.61	2.6E-05	3027687	3162852
AVERAGE	494.54	2.619E-05	3006638	3243189

Failure Load (lbs) : 33200
 Correction Factor : 0.958
 Ultimate Stress (psi) : 2530

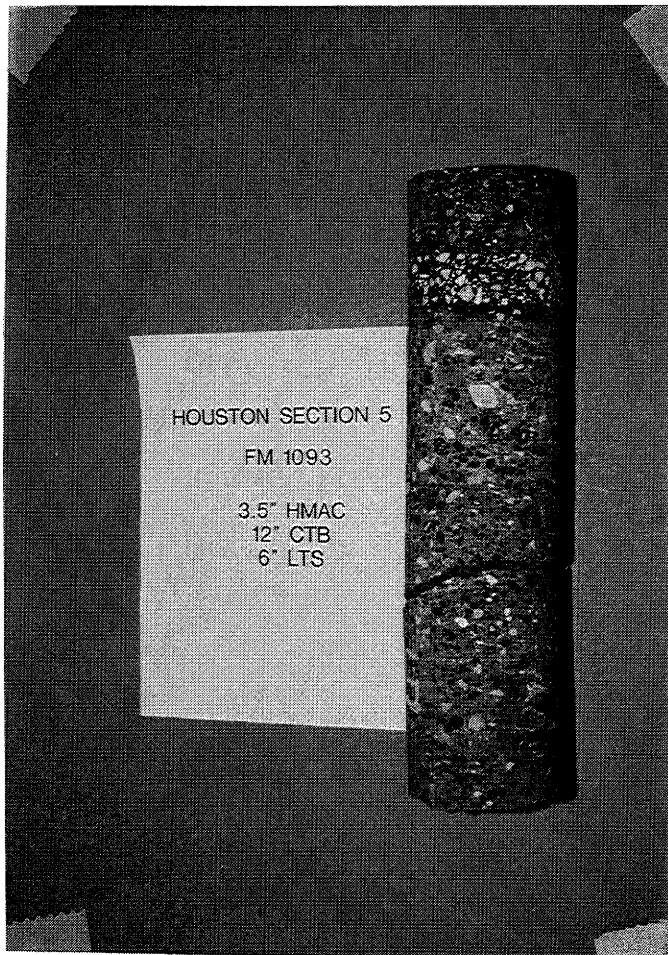


Figure A.56. Results of Laboratory Testing for Cores Obtained from Section-5 of Houston District.

A.59

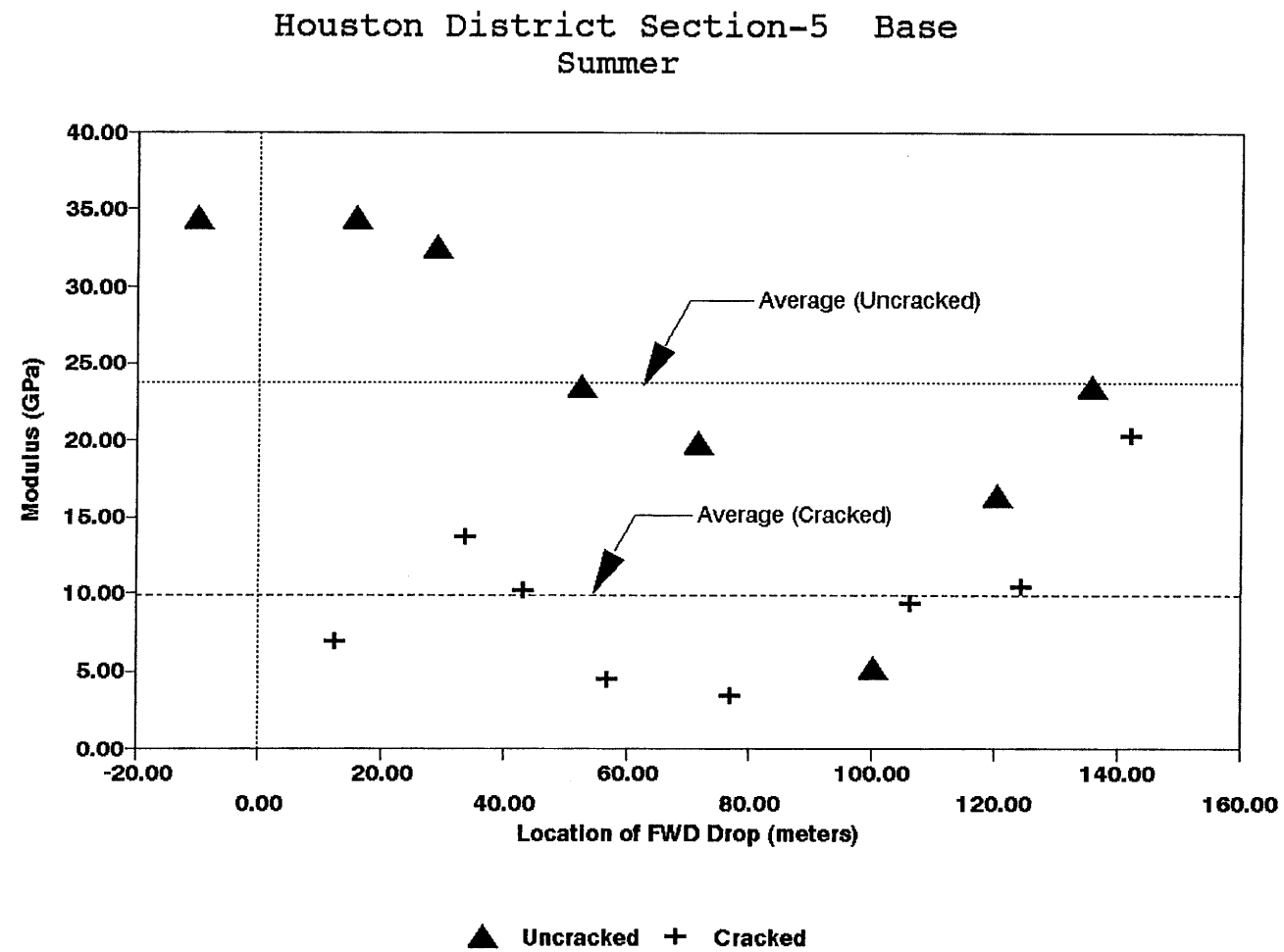


Figure A.57. Variation of Modulus of Stabilized Base within Test Section for Section-5 of Houston District in Summer.

A.60

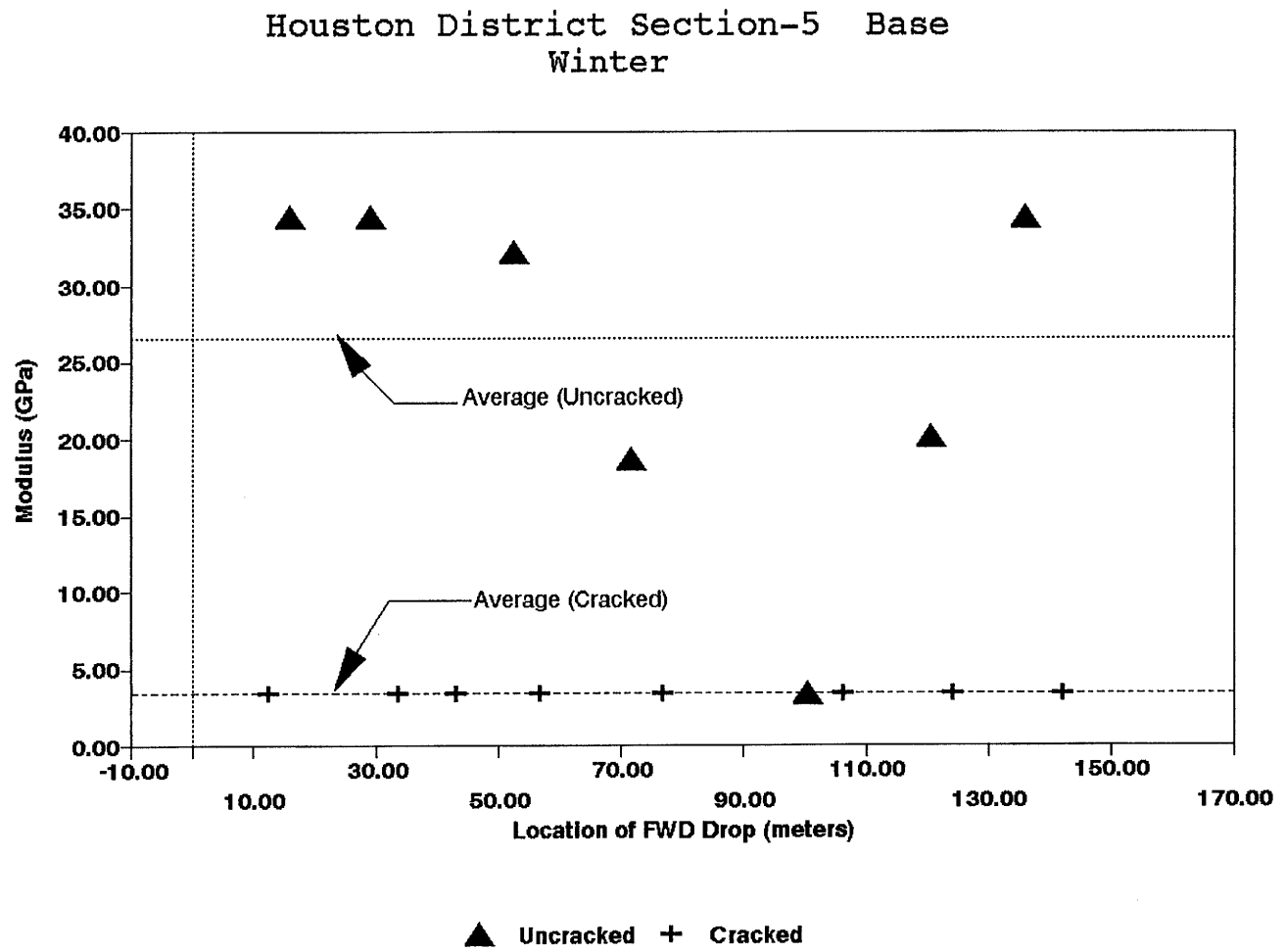


Figure A.58. Variation of Modulus of Stabilized Base within Test Section for Section-5 of Houston District in Winter.

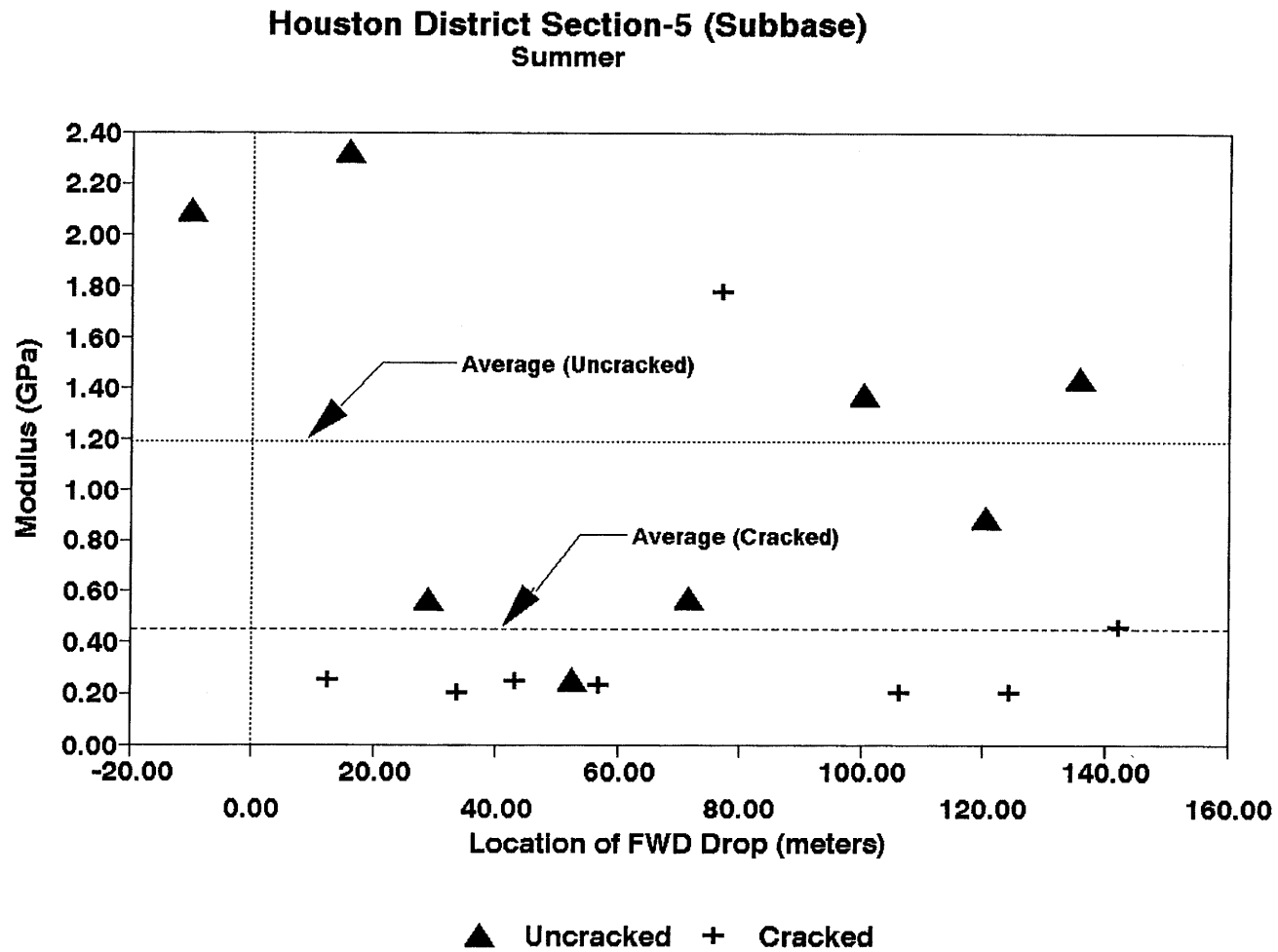


Figure A.59. Variation of Modulus of Stabilized Subbase within Test Section for Section-5 of Houston District in Summer.

A.62

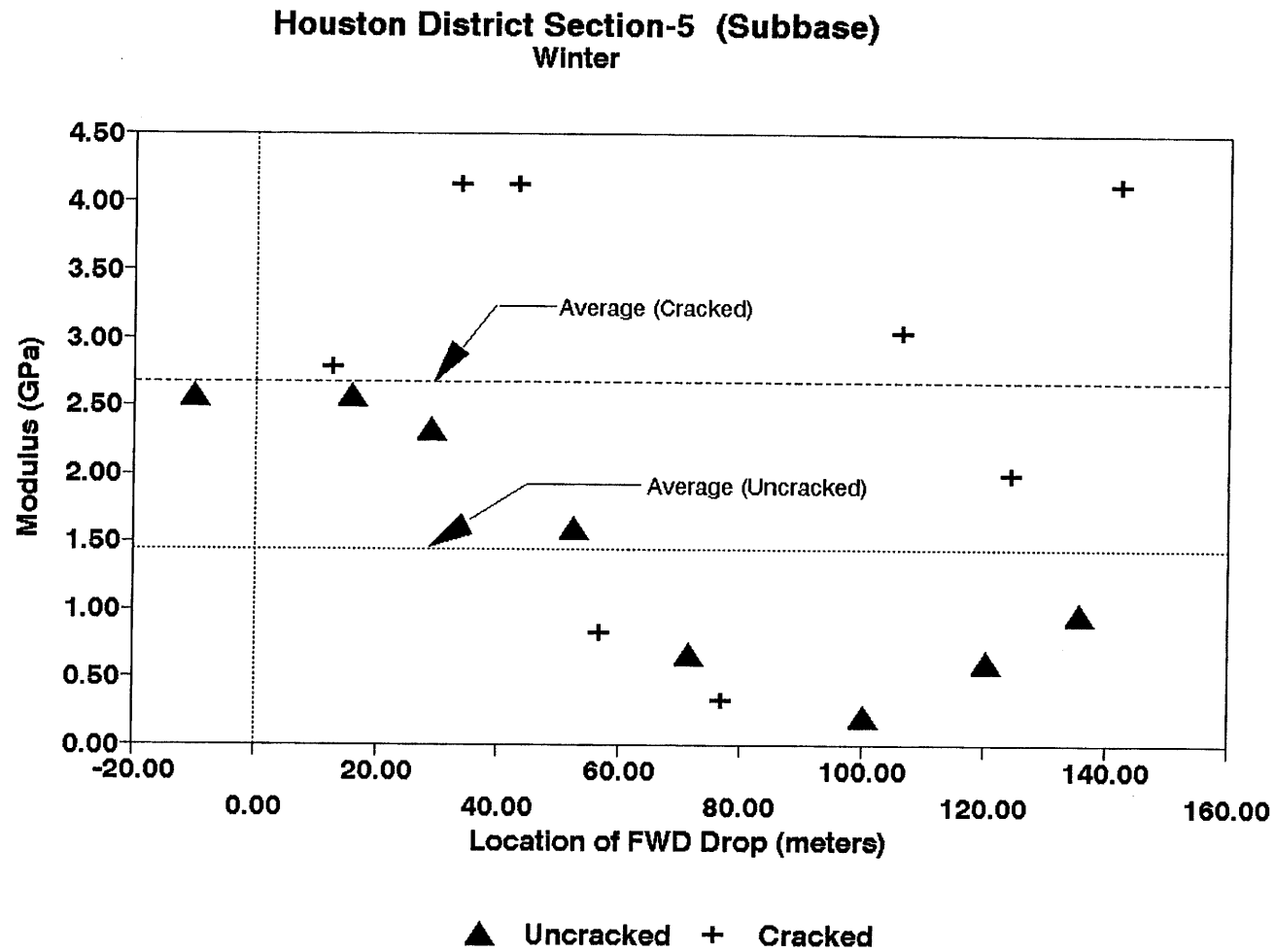


Figure A.60. Variation of Modulus of Stabilized Subbase within Test Section for Section-5 of Houston District in Winter.

Section No.: 6 District: Houston County: Harris Highway: SH-36
Structure: Asphalt : 76 mm
CTB (new) : 152 mm
CTB (old) : 152 mm
LTS : 152 mm
Subgrade

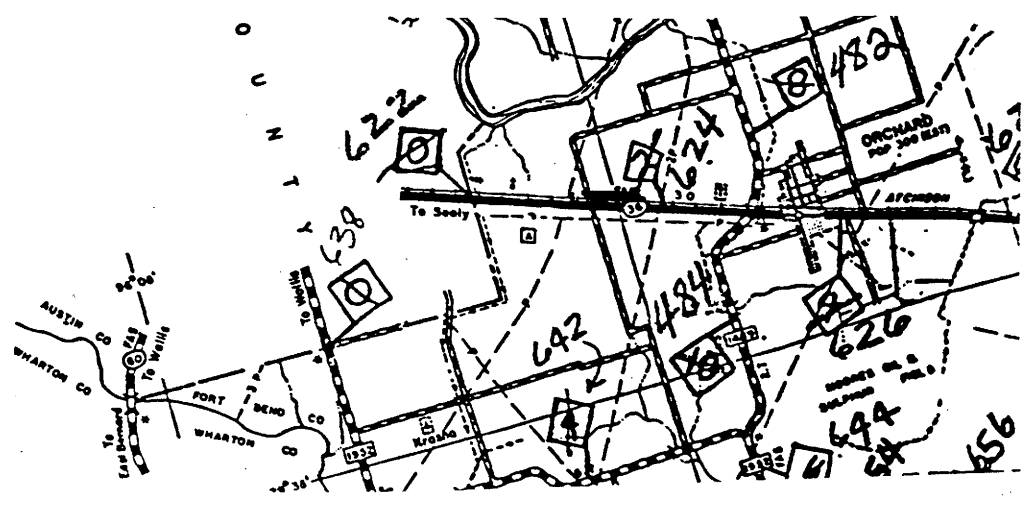
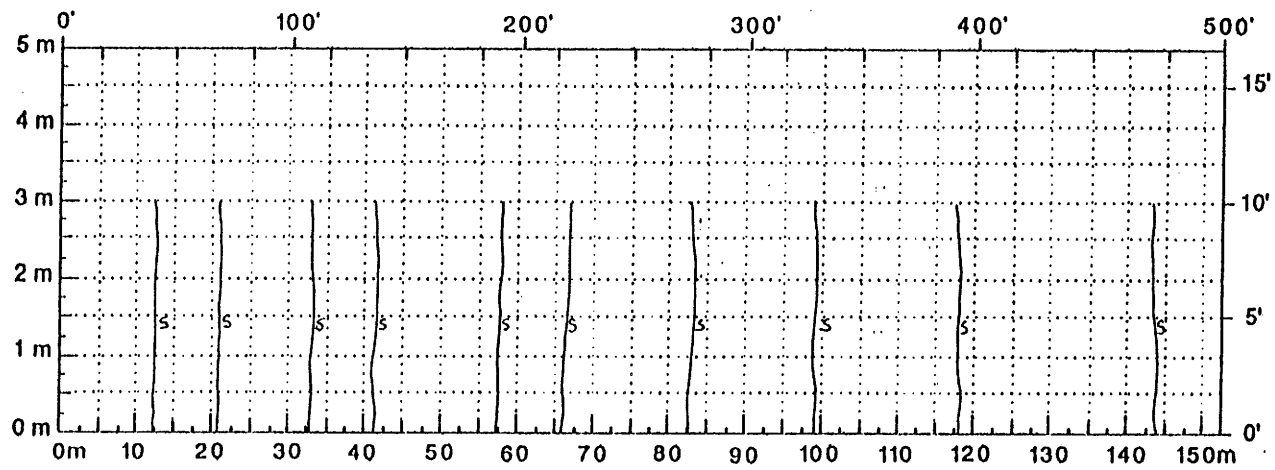
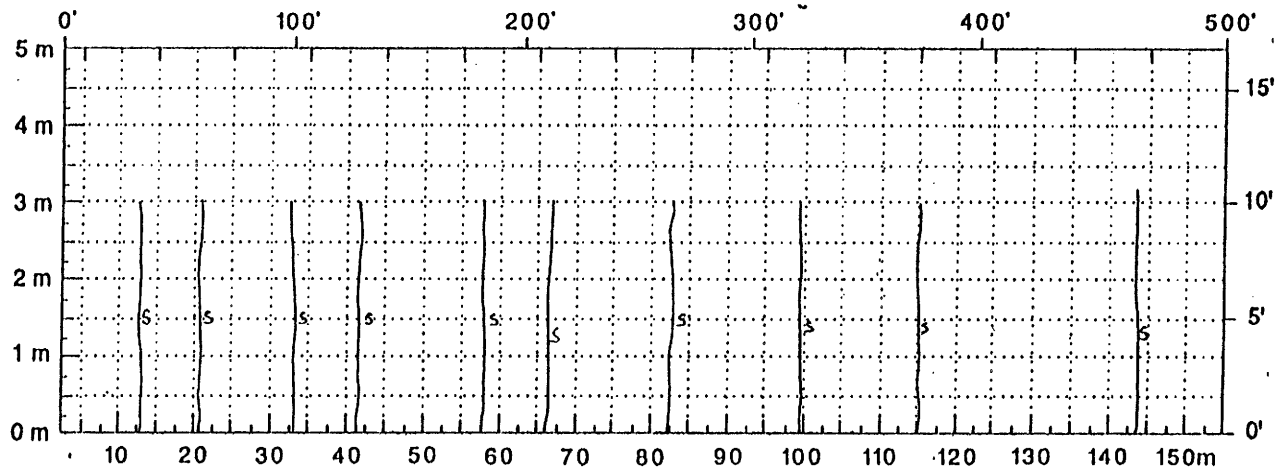


Figure A.61. Location and Details of Section-6 of Houston District.

A.64



Comments: Crack Map for Summer



Comments: Crack Map for Winter

Figure A.62. Crack Map for Section-6 of Houston District.

TTI MODULUS ANALYSIS SYSTEM (SUMMARY REPORT)										(Version 4.2)				
District:	12								MODULI RANGE(psi)					
County:	80								Minimum	Maximum	Poisson Ratio Values			
Highway/Road:	SH0036	Pavement:	3.00						206,979	207,021	H1: J = 0.35			
		Base:	12.00						500,000	5,000,001	H2: J = 0.25			
		Subbase:	6.00						30,000	600,000	H3: J = 0.25			
		Subgrade:	279.00						25,000		H4: J = 0.35			
Station	Load (lbs)	Measured Deflection (mils):							Calculated Moduli values (ksi):				Absolute Dpth to	
		R1	R2	R3	R4	R5	R6	R7	SURF(E1)	BASE(E2)	SUBB(E3)	SUBG(E4)	ERR/Sens	Bedrock
1.000	9,159	3.19	2.64	2.35	2.07	1.79	1.55	1.31	207.	5000.0	337.0	20.2	3.94	300.00 *
2.000	9,039	3.64	2.94	2.65	2.31	1.91	1.63	1.47	207.	4653.2	40.5	19.1	3.55	300.00
3.000	9,199	3.15	2.73	2.42	2.11	1.79	1.59	1.31	207.	5000.0	111.0	21.1	4.95	300.00 *
4.000	9,151	3.11	2.47	2.27	1.99	1.75	1.51	1.31	207.	5000.0	128.8	22.1	3.55	300.00 *
5.000	9,119	3.39	2.73	2.42	2.11	1.83	1.59	1.35	207.	5000.0	307.1	19.1	2.83	300.00 *
6.000	9,119	3.68	2.85	2.58	2.31	1.95	1.67	1.51	207.	3940.7	527.7	17.6	2.46	300.00
7.000	8,999	3.15	2.60	2.31	2.07	1.95	1.63	1.39	207.	5000.0	541.6	18.2	3.59	300.00 *
8.000	9,151	3.96	3.31	2.88	2.55	2.16	1.83	1.59	207.	4263.4	59.1	16.9	3.06	300.00
Mean:		3.41	2.78	2.49	2.19	1.89	1.63	1.41	207.	4732.2	256.6	19.3	3.49	300.00
Std. Dev:		0.32	0.26	0.21	0.19	0.13	0.10	0.11	0.	415.9	202.5	1.8	0.76	85.23
Var Coeff(%):		9.29	9.25	8.27	8.45	7.03	5.95	7.60	0.	8.8	78.9	9.1	21.73	28.41

Figure A.63. FWD Back-Calculation Results for Uncracked Portion of Section-6 of Houston District in Summer..

A.66

TTI MODULUS ANALYSIS SYSTEM (SUMMARY REPORT)														(Version 4.2)	
District:	12														
County:	80														
Highway/Road:	SH0036														
			Thickness(in)		MODULI RANGE(psi)		Poisson Ratio Values								
			Pavement:	3.00	Minimum	Maximum	H1: j = 0.35								
			Base:	12.00	206,979	207,021	H2: j = 0.25								
			Subbase:	6.00	500,000	5,000,001	H3: j = 0.25								
			Subgrade:	279.00	30,000	600,000	H4: j = 0.35								
						20,700									
Station	Load (lbs)	Measured Deflection (mils):							Calculated Moduli values (ksi):				Absolute Dpth to		
		R1	R2	R3	R4	R5	R6	R7	SURF(E1)	BASE(E2)	SUBB(E3)	SUBG(E4)	ERR/Sens	Bedrock	
1.000	9,023	4.12	3.27	2.62	2.23	1.87	1.59	1.39	207.	2616.6	86.3	21.4	2.43	300.00	
2.000	9,071	4.60	3.14	2.50	2.11	1.83	1.63	1.43	207.	1025.6	600.0	22.6	3.68	300.00 *	
3.000	9,055	3.72	2.85	2.50	2.11	1.79	1.51	1.26	207.	3948.4	40.3	21.9	1.62	300.00	
4.000	9,055	5.66	3.10	2.65	2.27	1.91	1.55	1.39	207.	500.0	600.0	23.6	4.85	300.00 *	
5.000	9,015	4.97	3.52	2.96	2.51	2.12	1.83	1.51	207.	1022.1	560.5	18.7	1.43	300.00 *	
6.000	8,983	5.25	4.03	3.08	2.59	2.20	1.96	1.71	207.	1056.0	292.5	18.3	3.93	300.00	
7.000	9,063	4.32	3.40	3.00	2.55	2.12	1.75	1.55	207.	2999.4	41.6	18.5	1.84	300.00	
Mean:		4.66	3.33	2.76	2.34	1.98	1.69	1.46	207.	1881.2	317.3	20.7	2.83	300.00	
Std. Dev:		0.68	0.38	0.25	0.21	0.16	0.16	0.14	0.	1298.9	266.4	2.2	1.33	92.47	
Var Coeff(%):		14.49	11.33	8.96	8.87	8.34	9.72	9.82	0.	69.1	83.9	10.6	46.93	30.82	

Figure A.64. FWD Back-Calculation Results for Cracked Portion of Section-6 of Houston District in Summer..

A.67

TTI MODULUS ANALYSIS SYSTEM (SUMMARY REPORT)													(Version 4.2)	
District:	12												MODULI RANGE(ksi)	
County:	80		Thickness(in)		Minimum		Maximum		Poisson Ratio Values					
Highway/Road:	SH0063		Pavement:	3.00	425,957	426,043	H1: u = 0.35							
			Base:	12.00	500,000	5,000,001	H2: u = 0.25							
			Subbase:	6.00	30,000	600,000	H3: u = 0.25							
			Subgrade:	279.00	20,000		H4: u = 0.35							
Station	Load (lbs)	Measured Deflection (mils):							Calculated Moduli values (ksi):				Absolute Depth to	
		R1	R2	R3	R4	R5	R6	R7	SURF(E1)	BASE(E2)	SUBB(E3)	SUBG(E4)	ERR/Sens	Bedrock
6,000	10,463	3.46	2.93	2.71	2.38	2.12	1.78	1.51	426.	5000.0	212.6	20.0	1.98	300.00 †
25,000	10,359	3.50	2.93	2.69	2.34	2.03	1.72	1.44	426.	5000.0	199.0	20.2	1.57	300.00 †
94,000	10,328	3.17	2.59	2.36	2.10	1.81	1.60	1.31	426.	5000.0	168.4	23.8	2.40	300.00 †
160,000	10,248	3.31	2.67	2.39	2.06	1.88	1.63	1.38	426.	5000.0	323.9	21.9	1.34	300.00 †
236,000	10,137	4.53	3.12	2.70	2.32	1.96	1.68	1.44	426.	1000.1	600.0	23.6	2.84	300.00 †
350,000	10,153	3.49	2.87	2.65	2.35	2.04	1.78	1.52	426.	5000.0	309.5	19.1	0.77	300.00 †
420,000	10,042	3.57	2.77	2.55	2.17	1.95	1.70	1.44	426.	4484.0	246.8	20.8	1.56	300.00
488,000	10,097	4.21	3.28	2.99	2.58	2.21	1.90	1.59	426.	2182.0	560.9	18.7	0.72	300.00 †
Mean:		3.66	2.90	2.63	2.29	2.00	1.72	1.45	426.	4083.3	327.6	21.0	1.65	300.00
Std. Dev:		0.47	0.23	0.20	0.17	0.13	0.10	0.09	0.	1580.4	165.0	1.9	0.74	80.39
Var Coeff(%):		12.77	7.85	7.63	7.44	6.43	5.55	5.97	0.	38.7	50.4	9.2	45.01	26.80

Figure A.65. FWD Back-Calculation Results for Uncracked Portion of Section-6 of Houston District in Winter.

TTI MODULUS ANALYSIS SYSTEM (SUMMARY REPORT)														(Version 4.2)	
District:	12									MODULI RANGE(ksi)		Poisson Ratio Values			
County:	80		(thickness(in))							Minimum	Maximum				
Highway/Road:	SH0063		Pavement:	3.00					425,957	426,043	H1: $\nu = 0.35$				
			Base:	12.00					500,000	5,000,001	H2: $\nu = 0.25$				
			Subbase:	6.00					30,000	600,000	H3: $\nu = 0.25$				
			Subgrade:	279.00					20,000		H4: $\nu = 0.35$				
Station	Load (lbs)	Measured Deflection (mils):							Calculated Moduli values (ksi):				Absolute Dist to Bedrock		
		R1	R2	R3	R4	R5	R6	R7	SURF(E1)	BASE(E2)	SUBB(E3)	SUBG(E4)	ERR/Sens	Bedrock	
42,000	10,149	5.82	3.31	2.83	2.35	1.96	1.65	1.36	426.	500.0	503.0	24.5	5.01	300.00 †	
66,000	10,161	3.47	2.82	2.30	1.95	1.63	1.39	1.17	426.	500.0	535.5	30.5	7.32	300.00 †	
107,000	10,200	4.18	3.21	2.67	2.20	1.74	1.51	1.23	426.	1513.8	202.9	26.4	1.51	300.00	
188,000	9,766	9.06	2.83	2.40	2.07	1.72	1.45	1.22	426.	500.0	43.1	31.9	19.78	300.00 †	
324,000	10,065	6.22	2.88	2.51	2.04	1.85	1.61	1.41	426.	500.0	508.0	27.0	11.34	300.00 †	
378,000	10,022	10.33	4.03	2.95	2.45	2.07	1.81	1.47	426.	500.0	30.0	24.5	16.56	300.00 †	
471,000	10,105	6.72	3.65	2.85	2.35	1.99	1.68	1.39	426.	500.0	130.8	25.7	9.00	300.00 †	
Mean:		6.83	3.25	2.64	2.20	1.85	1.59	1.32	426.	644.8	279.1	27.2	10.07	300.00	
Std. Dev:		2.14	0.46	0.25	0.19	0.16	0.15	0.11	0.	383.2	228.7	2.9	6.40	164.19	
Var Coeff(%):		31.35	14.18	9.36	8.55	8.75	9.15	8.61	0.	59.4	81.9	10.6	63.53	54.73	

Figure A.66. FWD Back-Calculation Results for Cracked Portion of Section-6 of Houston District in Winter.

A.69

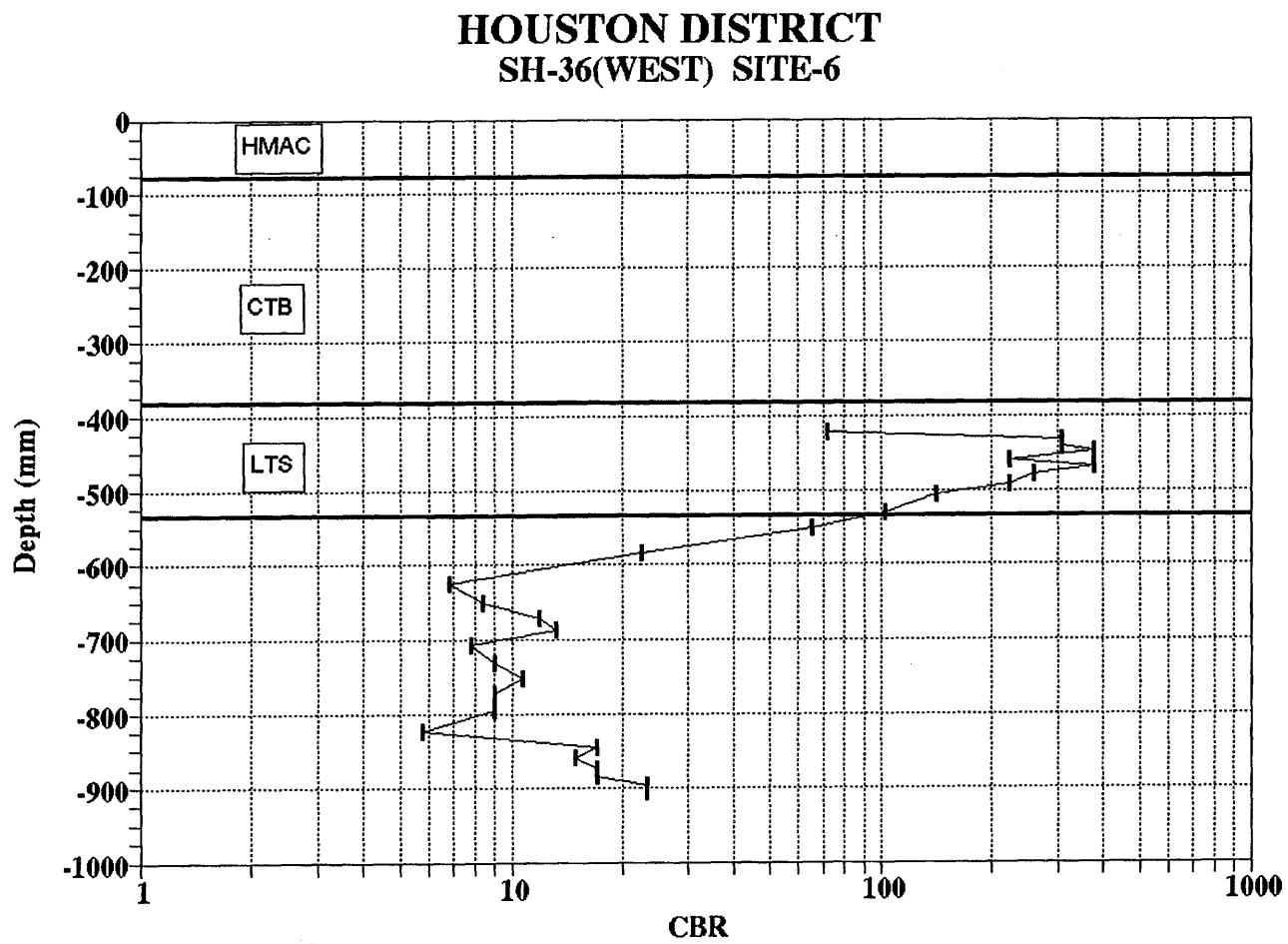


Figure A.67. Variation of CBR Obtained from DCP Testing for Section-6 of Houston District.

UNIAXIAL RESILIENT MODULUS

Project	1287	Gage Length (in)	2
Sample ID	HOU6B	Date of Test	
Height (in)	5.35	Temperature	77F

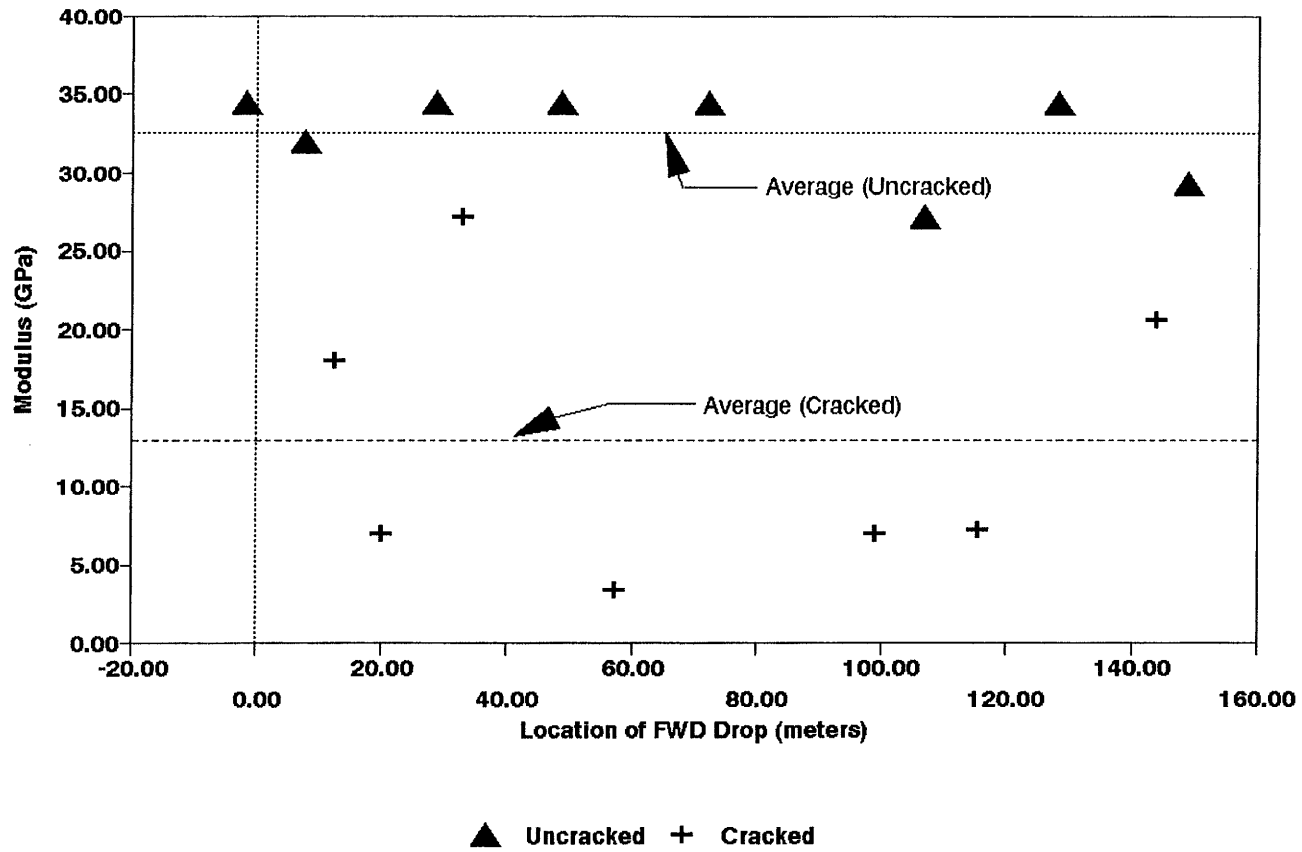
	Load lbs.	Def in.	Total Mr	Instant Mr
PEAK 1	493.67	2.237E-05	3512215	4111198
PEAK 2	493.46	2.226E-05	3528238	3779805
PEAK 3	493.38	2.348E-05	3344064	3642846
PEAK 4	493.49	2.3E-05	3414837	3643667
AVERAGE	493.50	2.278E-05	3449839	3794379

Failure Load (lbs) : 26400
 Correction Factor : 0.95
 Ultimate Stress (psi) : 1995



Figure A.68. Results of Laboratory Testing for Cores Obtained from Section-6 of Houston District.

Houston District Section-6 Base
Summer



A.71

Figure A.69. Variation of Modulus of Stabilized Base within Test Section for Section-6 of Houston District in Summer.

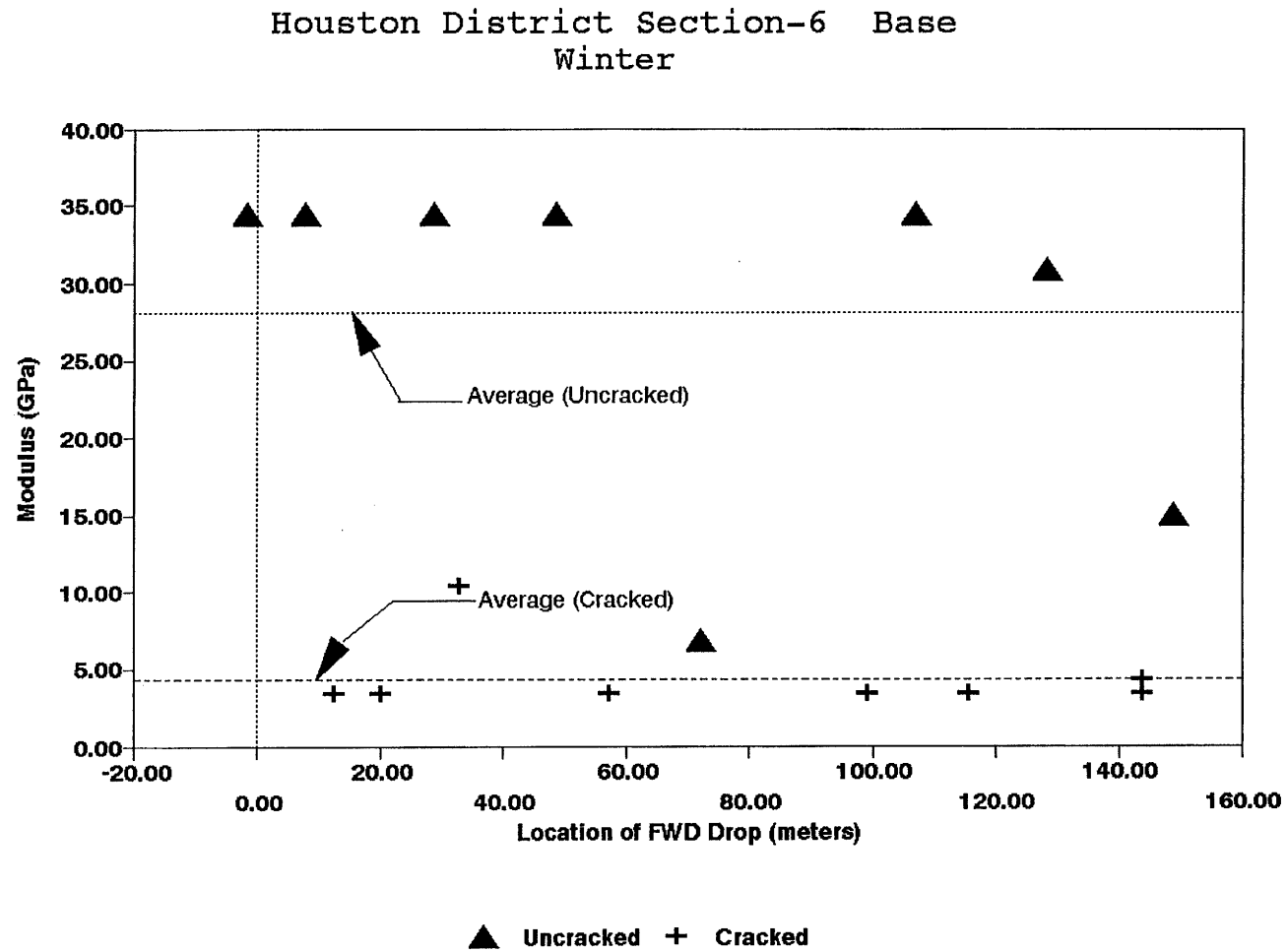


Figure A.70. Variation of Modulus of Stabilized Base within Test Section for Section-6 of Houston District in Winter.

Houston District Section-6 (Subbase) Summer

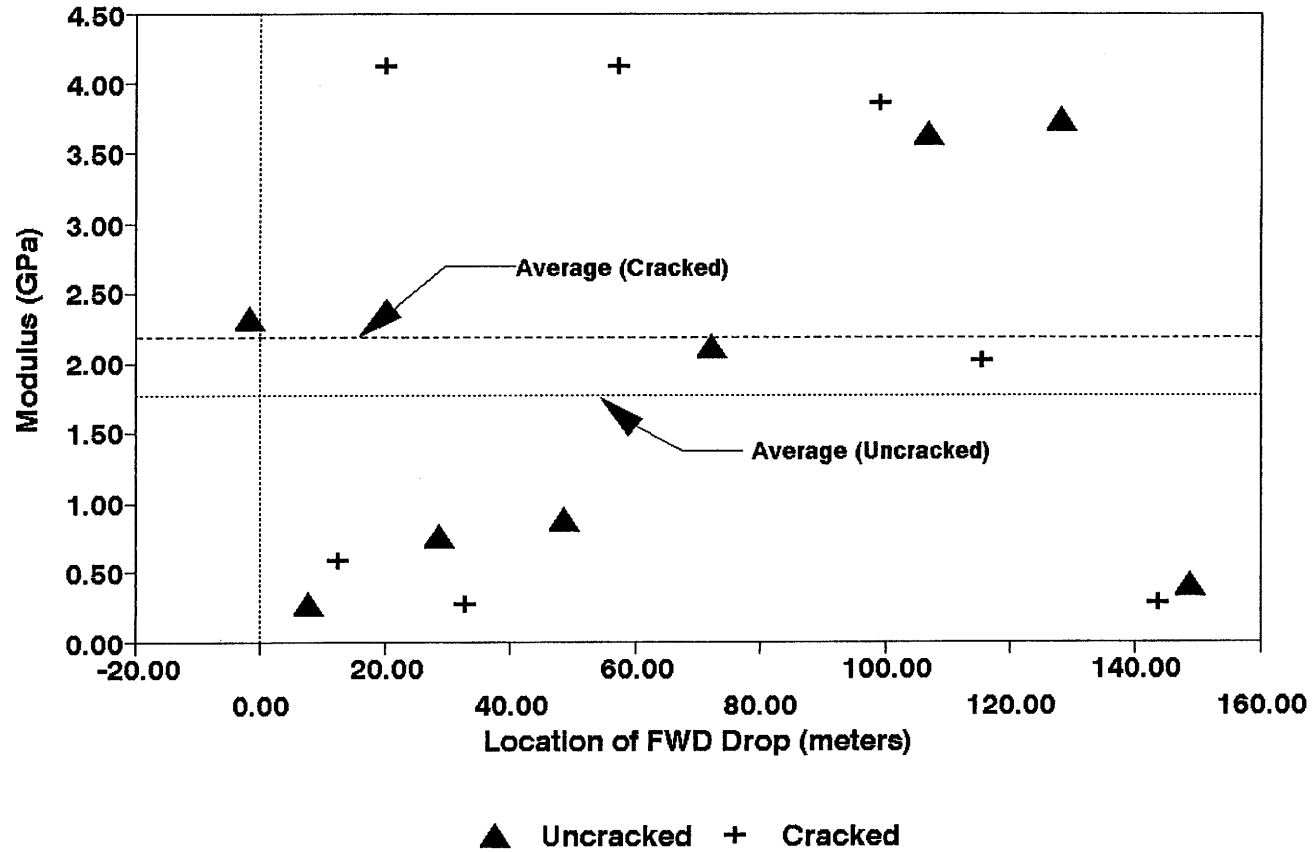


Figure A.71. Variation of Modulus of Stabilized Subbase within Test Section for Section-6 of Houston District in Summer.

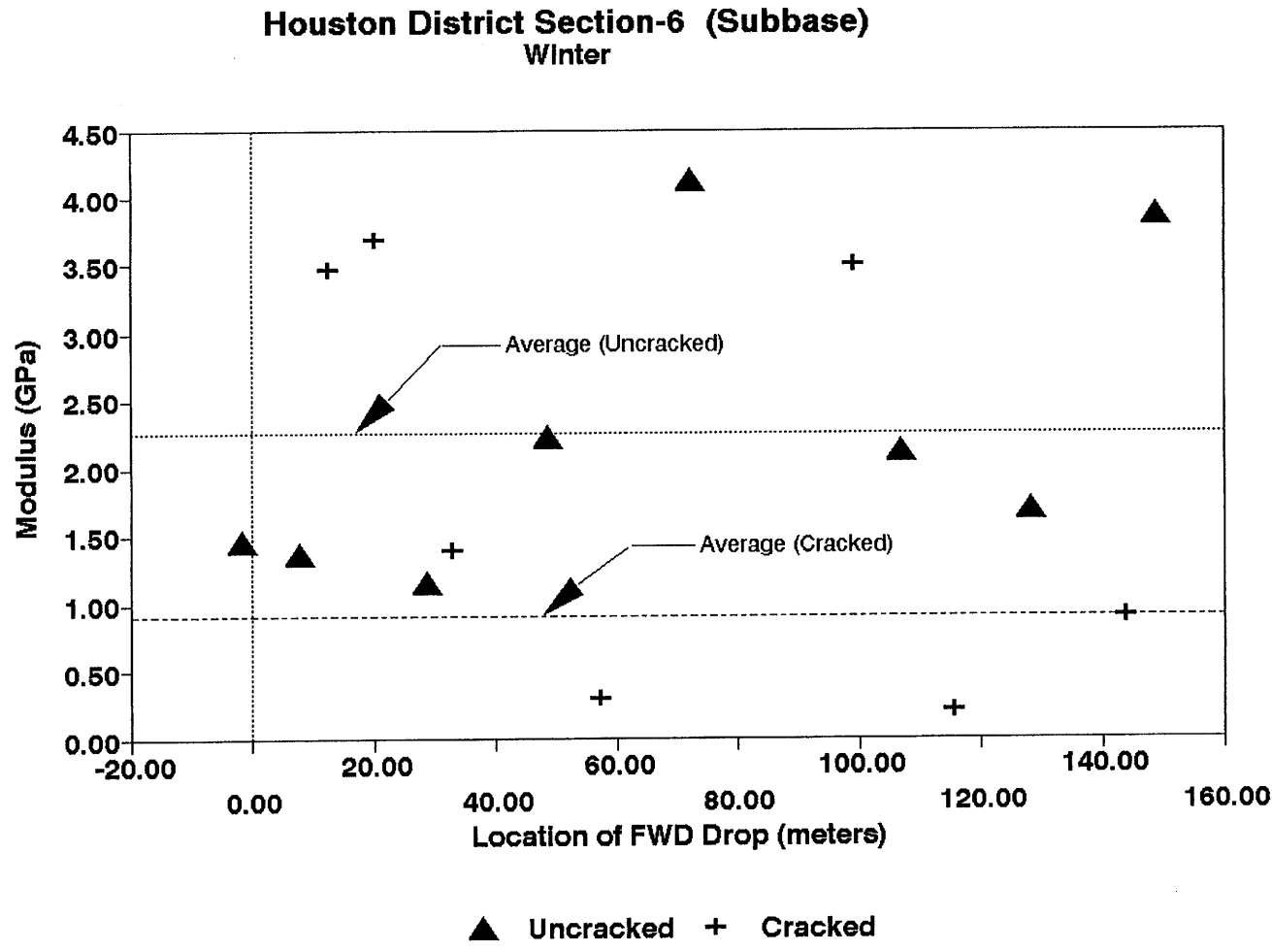


Figure A.72. Variation of Modulus of Stabilized Subbase within Test Section for Section-6 of Houston District in Winter.

Section No.: 7 District: Houston County: Harris Highway: FM-518 (East)
Structure: Asphalt : 89mm
CTB : 406 mm
LTS : 152 mm
Subgrade

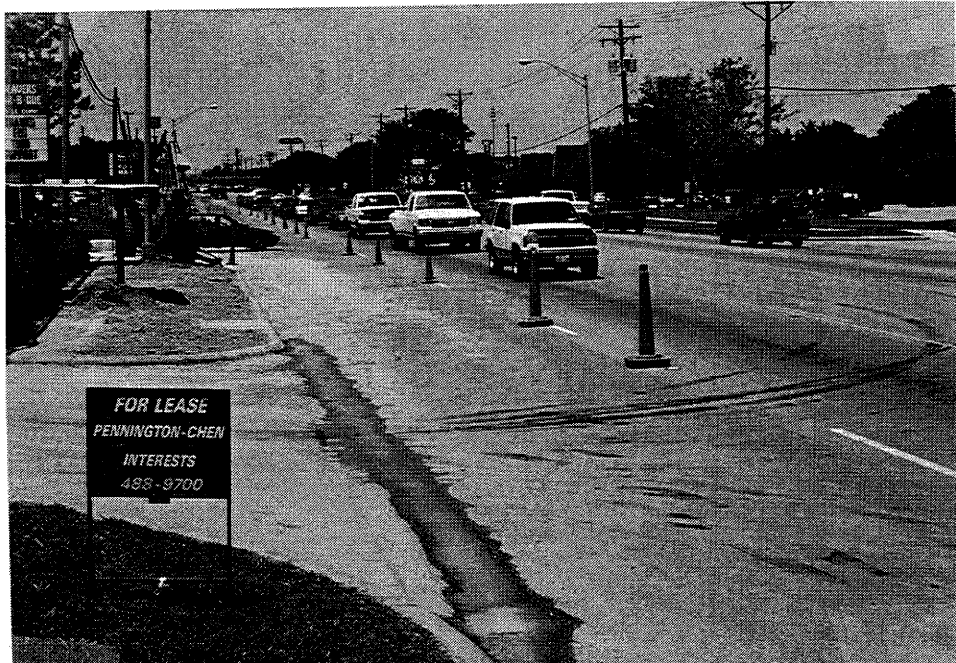
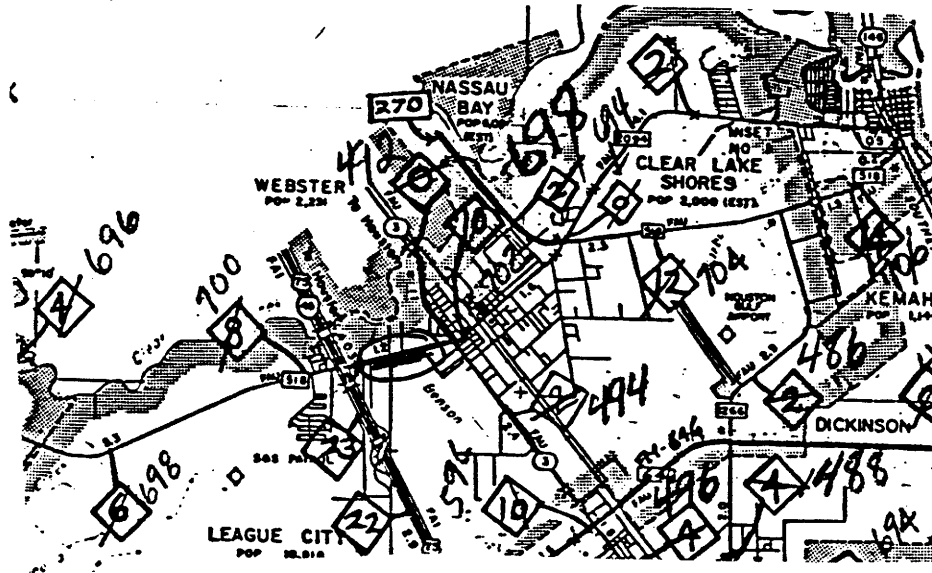
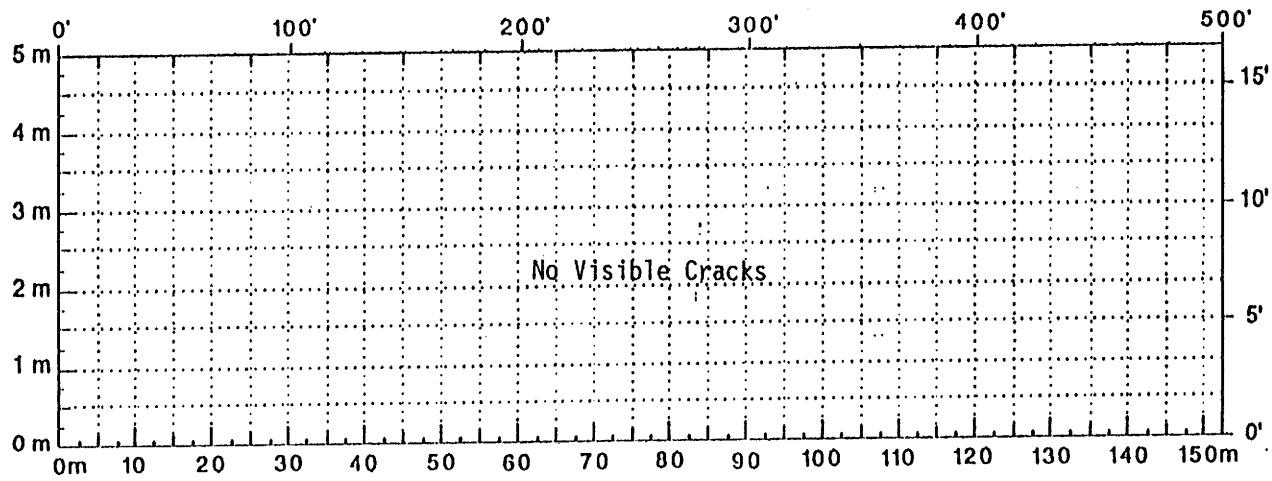
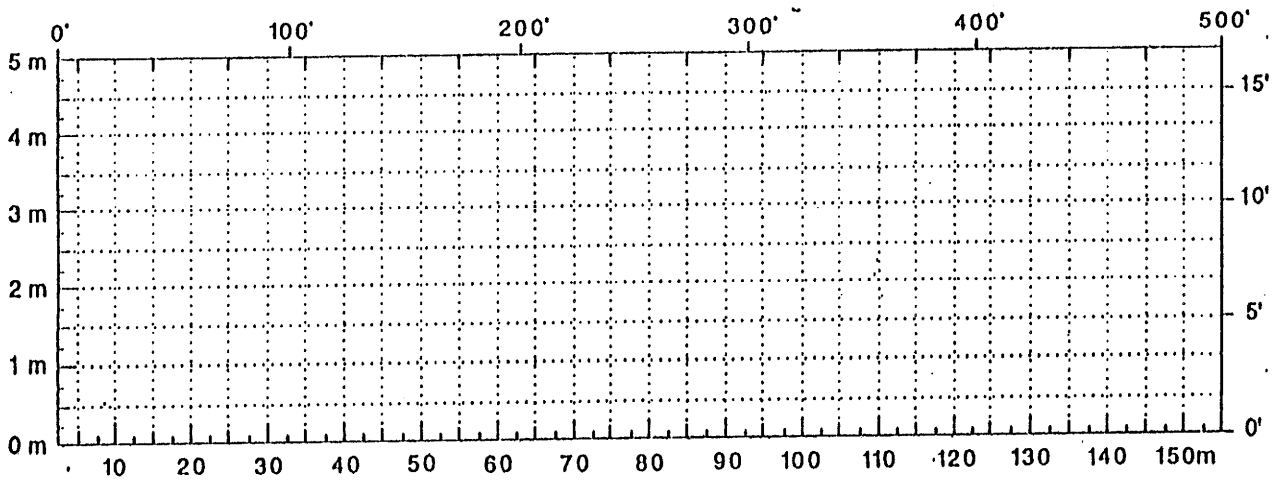


Figure A.73. Location and Details of Section-7 of Houston District.



Comments: Crack Map for Summer



Comments: _____

A.76

Figure A.74. Crack Map for Section-7 of Houston District.

TTI MODULUS ANALYSIS SYSTEM (SUMMARY REPORT)													(Version 4.2)					
District:	12												MODULI RANGE(psi)					
County:	85												Minimum		Maximum		Poisson Ratio Values	
Highway/Road:	FM0518		Pavement:		3.50		212,979		213,021		H1: j = 0.35							
			Base:		16.00		500,000		5,000,001		H2: j = 0.25							
			Subbase:		6.00		30,000		600,000		H3: j = 0.25							
			Subgrade:		274.50		31,900				H4: j = 0.35							
Station	Load (lbs)	Measured Deflection (mils):							Calculated Moduli values (ksi):				Absolute Dpth to					
		R1	R2	R3	R4	R5	R6	R7	SURF(R1)	BASE(R2)	SUBB(R3)	SUBG(R4)	BRR/Sens	Bedrock				
1.000	11,047	4.89	2.60	2.46	2.23	1.99	1.79	1.63	213.	613.8	600.0	37.7	3.39	300.00 *				
2.000	11,023	3.92	2.35	2.23	1.99	1.83	1.67	1.47	213.	1290.8	600.0	35.6	1.91	300.00 *				
3.000	10,991	5.17	3.61	3.27	2.83	2.48	2.08	1.71	213.	761.4	30.0	34.2	2.44	300.00 *				
4.000	11,015	5.78	3.40	3.12	2.71	2.36	2.12	1.92	213.	500.0	246.1	32.5	3.23	300.00 *				
5.000	10,943	6.34	4.65	3.92	3.19	2.52	2.12	1.84	213.	500.0	30.0	32.0	7.35	300.00 *				
6.000	10,967	5.49	3.94	3.69	3.31	2.93	2.53	2.24	213.	840.1	78.3	24.0	1.74	300.00				
7.000	10,919	7.27	5.16	4.00	3.27	2.73	2.28	2.00	213.	500.0	30.0	28.3	9.92	300.00 *				
8.000	10,943	4.52	3.23	2.92	2.55	2.24	2.00	1.71	213.	1042.6	98.6	31.6	3.64	300.00				
Mean:		5.42	3.62	3.20	2.76	2.38	2.07	1.81	213.	756.1	214.1	32.0	4.20	300.00				
Std. Dev:		1.06	0.96	0.65	0.49	0.36	0.27	0.24	0.	290.8	248.5	4.3	2.90	0.00				
Var Coeff(%):		19.48	26.41	20.37	17.71	15.27	12.94	13.20	0.	38.5	100.0	13.4	69.09	0.00				

Figure A.75. FWD Back-Calculation Results for Uncracked Portion of Section-7 of Houston District in Summer.

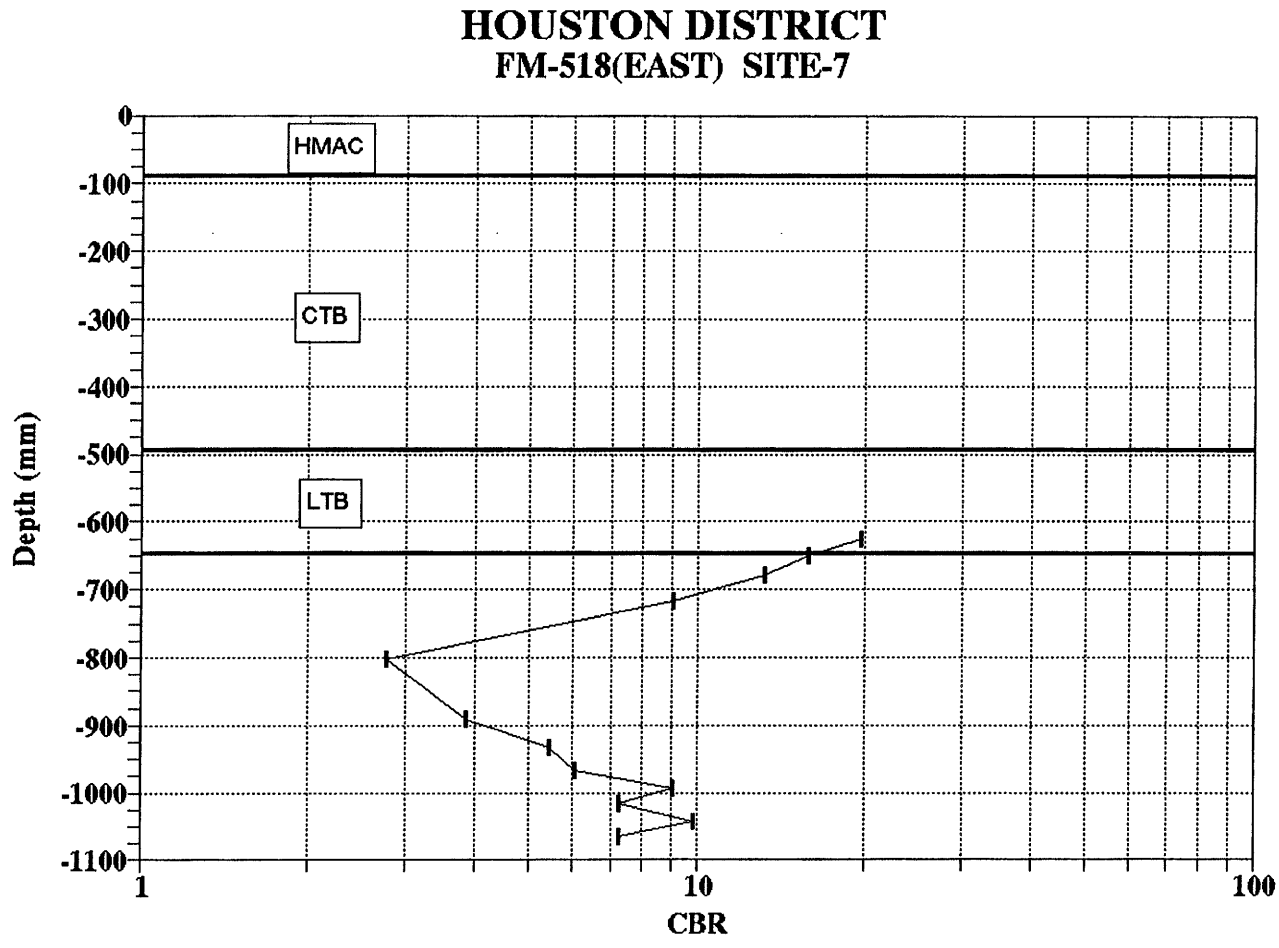


Figure A.76. Variation of CBR Obtained from DCP Testing for Section-7 of Houston District.

UNIAXIAL RESILIENT MODULUS

Project 1287 Gage Length (in) 2
 Sample ID HOU71 Date of Test
 Height (in) 3.94 Temperature 77F

	Load lbs.	Def in.	Total Mr	Instant Mr
PEAK 1	485.34	0.0001941	398015	432876
PEAK 2	485.40	0.0001922	401860	423954
PEAK 3	485.21	0.0001937	398741	414929
PEAK 4	485.33	0.0001911	404175	414292
AVERAGE	485.32	0.0001928	400698	421513

Failure Load (lbs) : 23500
 Correction Factor : 0.908
 Ultimate Stress (psi) : 1697.34

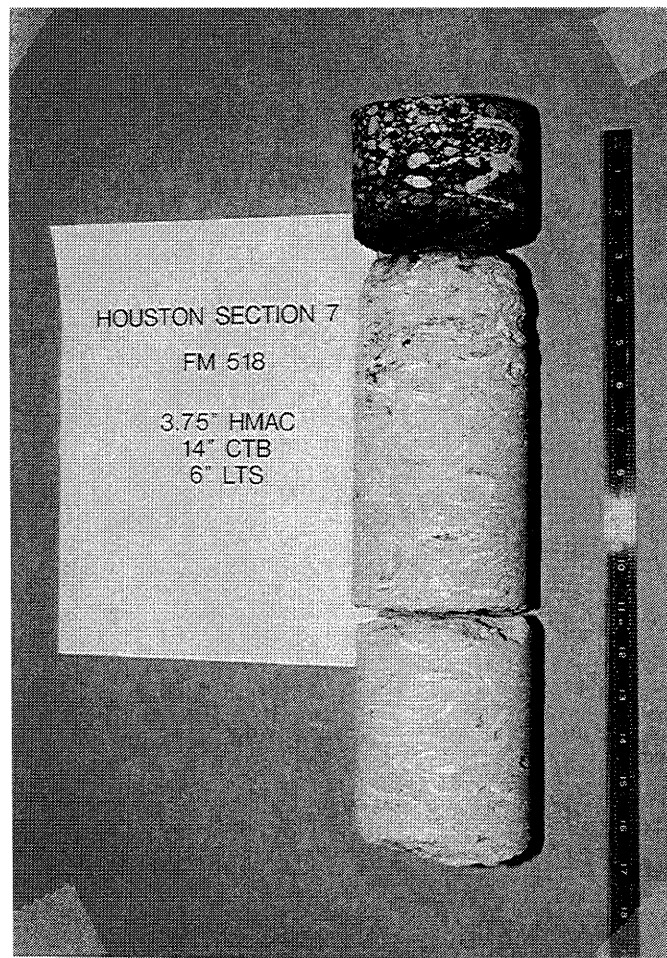


Figure A.77. Results of Laboratory Testing for Cores Obtained from Section-7 of Houston District.

A.80

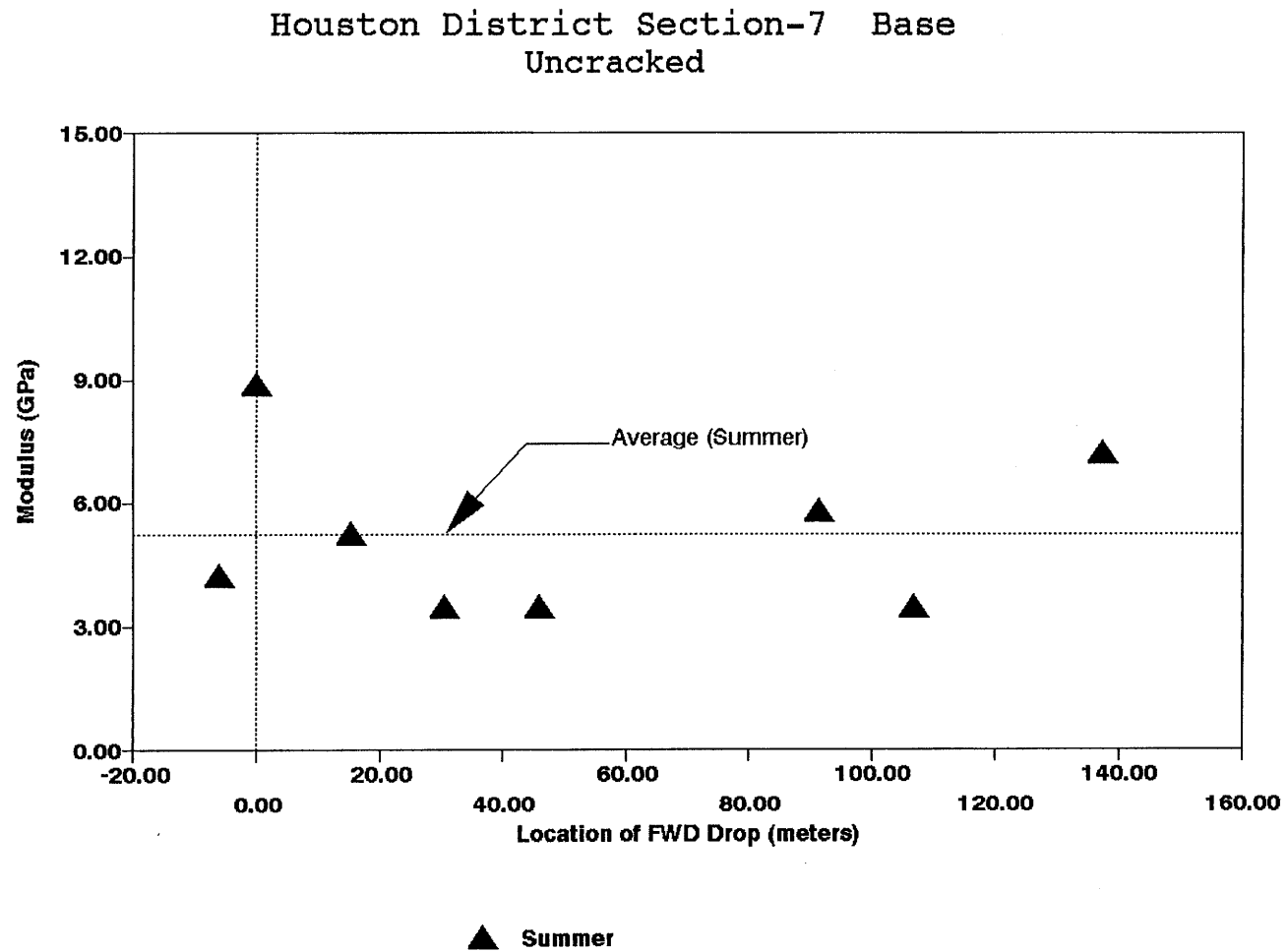


Figure A.78. Variation of Modulus of Stabilized Base within Test Section for Section-7 of Houston District in Summer.

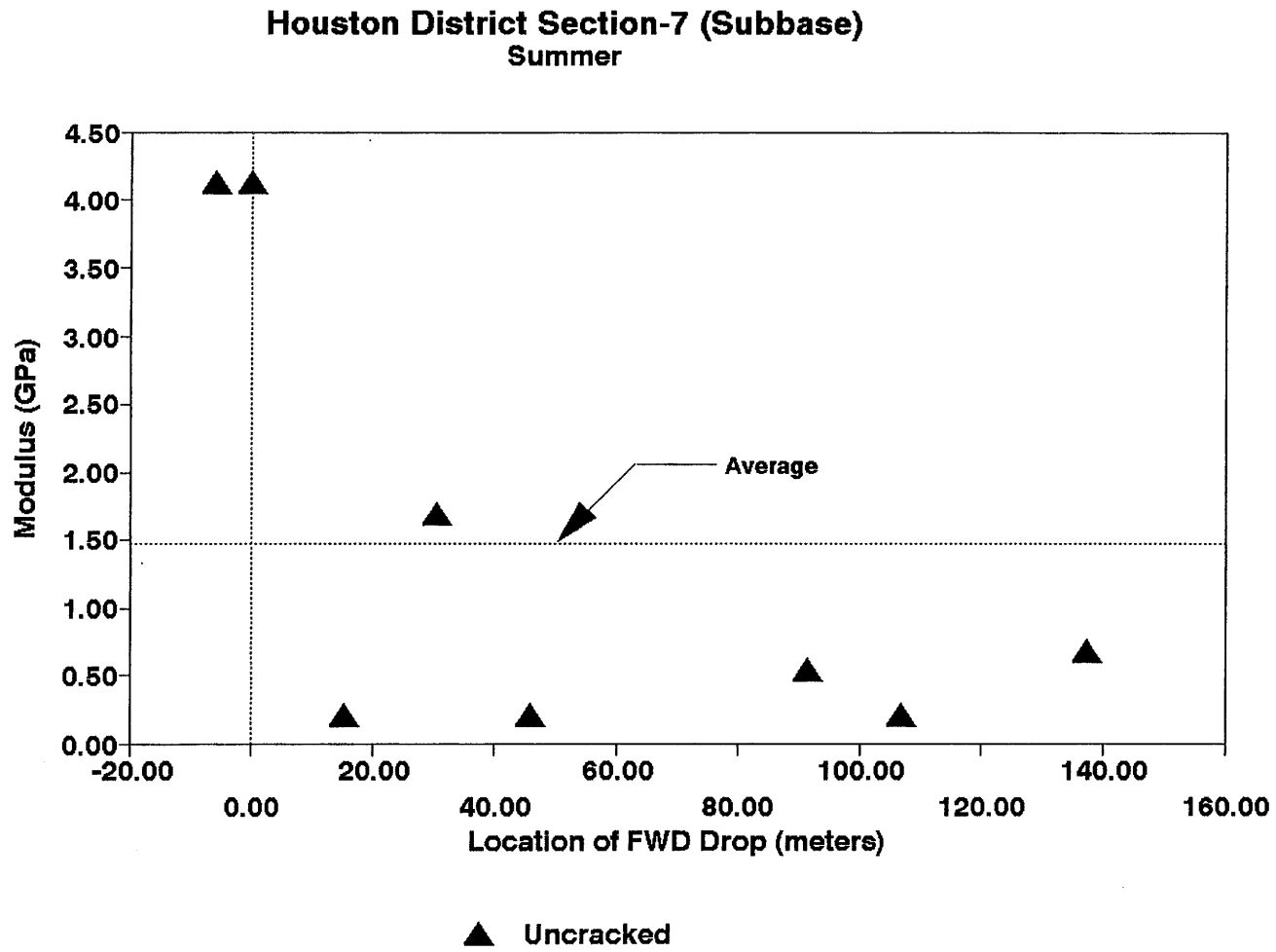


Figure A.79. Variation of Modulus of Stabilized Subbase within Test Section for Section-7 of Houston District in Summer.

Section No.: 1 District: Bryan County: Walker Highway: FM-3478
Structure: Asphalt : 38 mm
Flex base : 203 mm
CTS : 152 mm
Subgrade

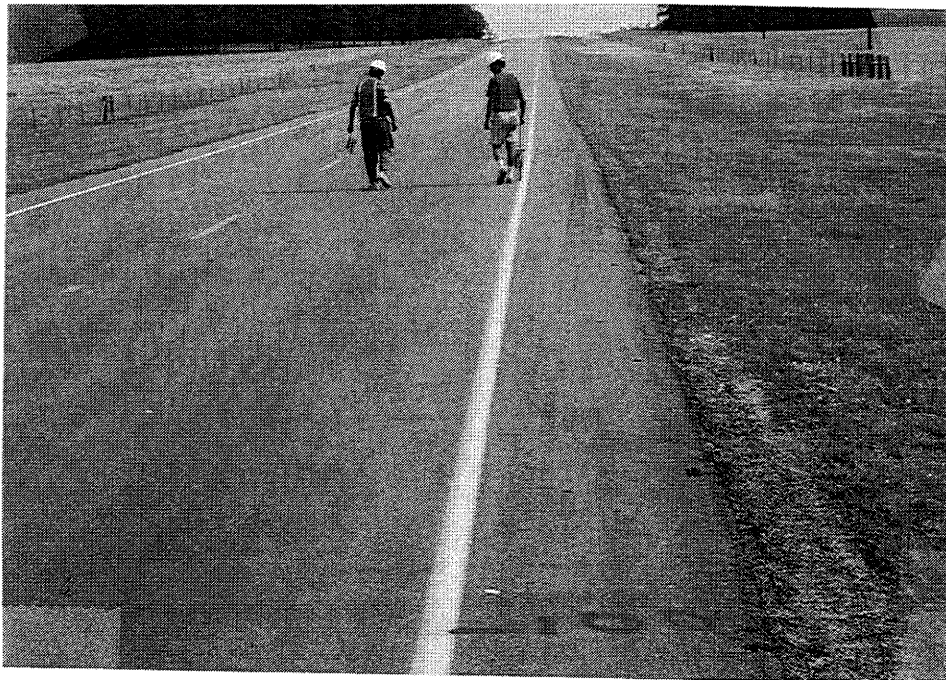
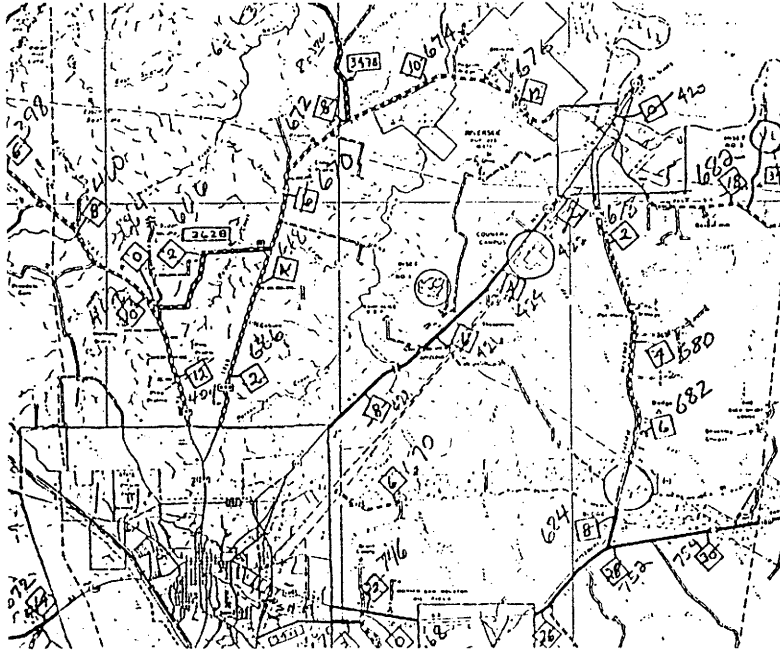
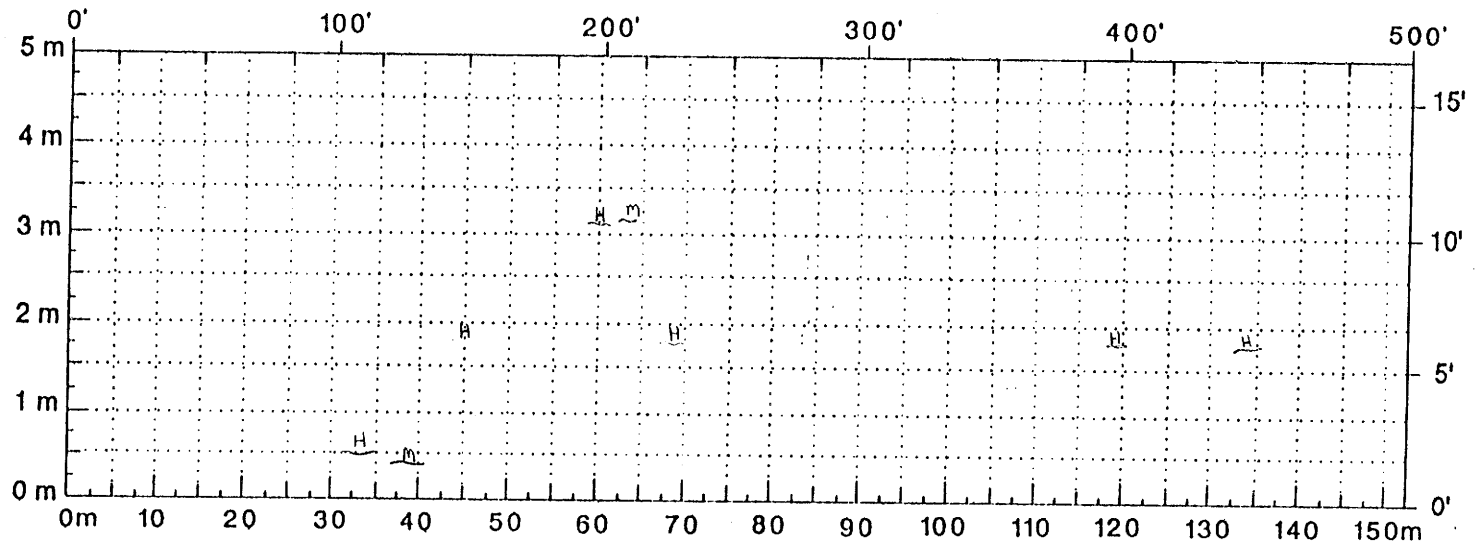


Figure A.80. Location and Details of Section-1 of Bryan District.

A.83



Comments: _____

Figure A.81. Crack Map for Section-1 of Bryan District.

TTI MODULUS ANALYSIS SYSTEM (SUMMARY REPORT)

(Version 4.2)

District:	0		MODULI RANGE(ksi)										
	County:	347	Thickness(in)							Minimum	Maximum	Poisson Ratio Values	
Highway/Road:			Pavement:	1.50	404,960	405,040	H1: u = 0.35						
			Base:	8.00	20,000	400,000	H2: u = 0.35						
			Subbase:	6.00	10,000	300,000	H3: u = 0.25						
			Subgrade:	124.10	20,000		H4: u = 0.35						
Station	Load (lbs)	Measured Deflection (mils):							Calculated Moduli values (ksi):				Absolute Dpth to ERR/Sens Bedrock
		R1	R2	R3	R4	R5	R6	R7	SURF(E1)	BASE(E2)	SUBB(E3)	SURB(E4)	
0.000	15,694	30.76	15.99	9.17	6.47	4.59	3.45	2.74	405.	65.5	99.5	13.0	5.13 300.00
0.005	15,977	19.56	11.59	8.36	6.38	4.91	3.67	2.92	405.	157.7	306.0	12.3	5.72 300.00 *
0.010	15,802	16.49	9.57	7.20	5.61	4.24	3.19	2.42	405.	209.5	300.0	14.4	6.89 258.40 *
0.015	15,889	16.71	10.22	7.58	5.74	4.24	3.13	2.35	405.	207.9	300.0	13.9	4.07 245.11 *
0.020	15,901	20.15	12.02	8.24	5.83	4.05	2.86	2.10	405.	139.6	186.2	14.4	1.08 204.91
0.025	15,814	19.40	11.61	7.98	5.40	3.78	2.66	1.99	405.	152.7	150.7	15.4	1.07 202.01
0.030	15,679	23.04	13.52	8.04	5.21	3.70	2.76	2.10	405.	121.0	74.0	15.7	4.61 280.05
0.035	15,643	27.47	16.02	8.83	5.53	3.87	2.74	2.22	405.	106.8	35.1	14.8	5.32 215.75
0.040	15,647	24.63	14.02	9.02	6.33	4.59	3.41	2.61	405.	95.9	163.2	12.8	3.79 289.78
0.045	15,663	38.44	20.33	8.74	4.81	3.18	2.33	1.91	405.	65.0	10.0	17.4	7.86 112.84 *
0.050	15,587	36.12	16.68	8.52	5.22	3.49	2.61	2.01	405.	53.2	30.4	15.6	4.29 205.81
0.055	15,520	28.06	15.94	9.21	6.24	4.49	3.43	2.71	405.	85.5	77.1	13.0	5.66 300.00
0.060	15,480	43.30	23.26	11.02	7.00	5.14	3.93	3.04	405.	50.3	22.4	11.2	9.53 300.00
0.000	15,238	57.45	28.73	12.04	7.09	5.08	3.86	3.09	405.	33.7	10.0	10.6	9.81 104.07 *
0.005	15,305	58.66	31.23	13.22	7.83	5.54	3.99	3.09	405.	34.8	10.0	9.7	9.02 112.08 *
0.004	15,222	53.70	26.19	11.11	6.76	4.96	3.74	2.76	405.	34.8	12.5	11.2	10.05 111.34
0.000	15,269	53.06	29.02	12.90	7.20	4.89	3.47	2.72	405.	41.4	10.0	10.5	6.97 126.67 *
0.000	15,083	73.46	43.12	18.74	8.68	5.63	4.20	3.30	405.	23.7	10.0	7.4	12.04 75.06 *
0.000	15,083	63.72	36.07	16.11	8.81	5.82	4.24	3.28	405.	31.4	10.0	8.2	7.25 118.04 *
0.000	15,317	41.78	23.43	11.65	7.09	4.90	3.63	2.80	405.	61.2	15.7	11.2	7.28 245.57
0.000	15,087	68.58	36.96	15.18	8.06	5.53	4.09	3.13	405.	25.0	10.0	8.5	8.31 96.41 *
0.000	15,079	75.67	43.61	17.28	7.76	4.97	3.68	2.85	405.	20.1	10.0	8.2	13.98 71.01 *
0.000	15,301	66.89	36.14	12.30	5.07	3.59	2.93	2.37	405.	22.1	10.0	11.6	14.56 57.74 *
0.000	15,091	69.25	38.18	14.19	5.88	3.93	3.06	2.48	405.	21.5	10.0	10.2	14.51 63.94 *
0.000	14,864	82.78	49.83	20.88	8.04	4.43	3.33	2.96	405.	20.0	10.0	7.3	26.69 64.18 *
Mean:		44.37	24.53	11.50	6.56	4.54	3.38	2.64	405.	75.2	75.1	11.9	8.22 139.61
Std. Dev:		21.40	12.07	3.77	1.16	0.72	0.54	0.42	0.	58.7	99.7	2.8	5.33 82.90
Var Coeff(%):		48.23	49.20	32.79	17.69	15.96	15.87	16.01	0.	78.1	100.0	23.7	64.79 59.38

Figure A.82. FWD Back-Callulation Results for Uncracked Portion of Section-1 of Bryan District

A.85

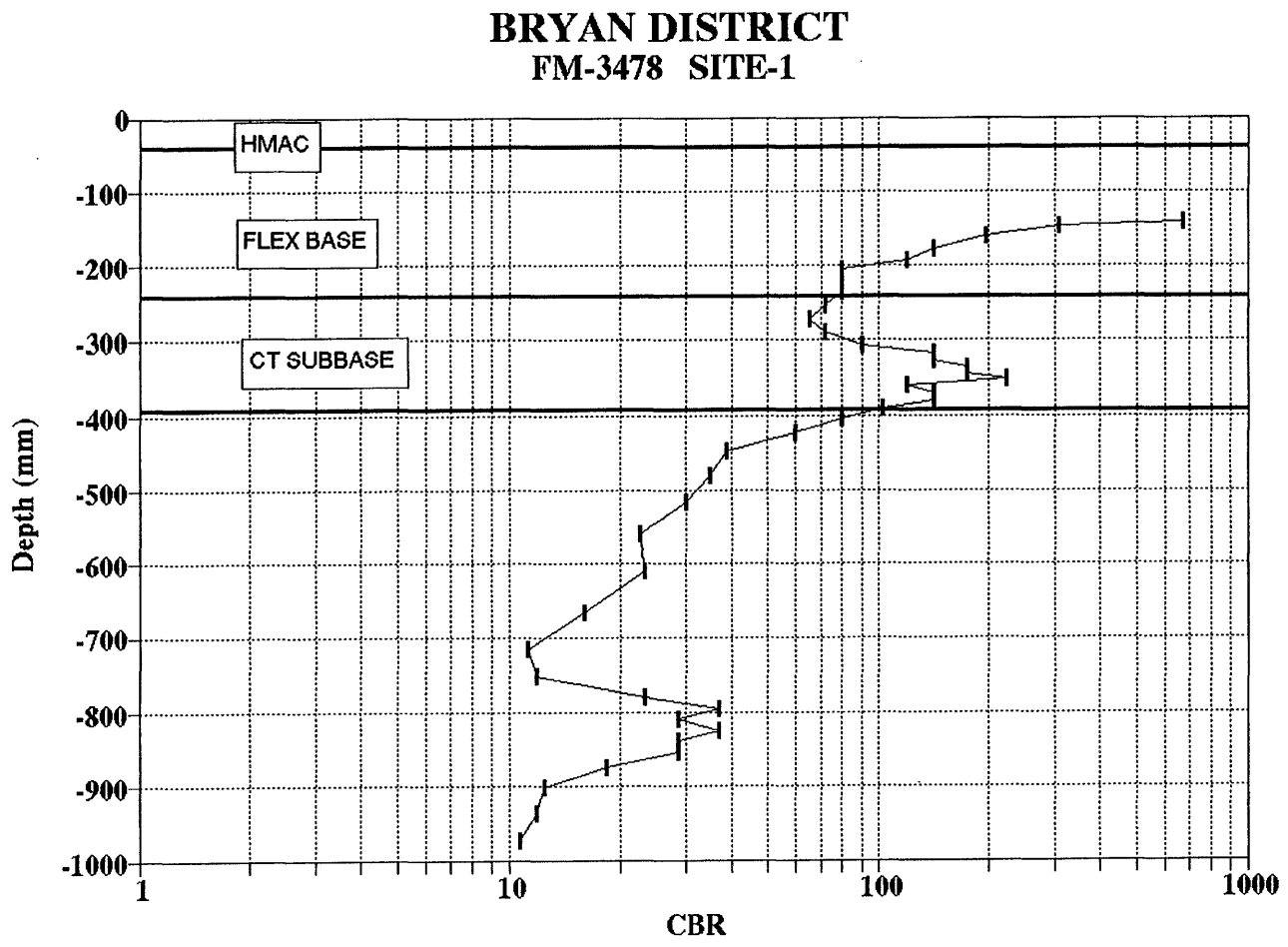


Figure A.83. Variation of CBR Obtained from DCP Testing for Section-1 of Bryan District.

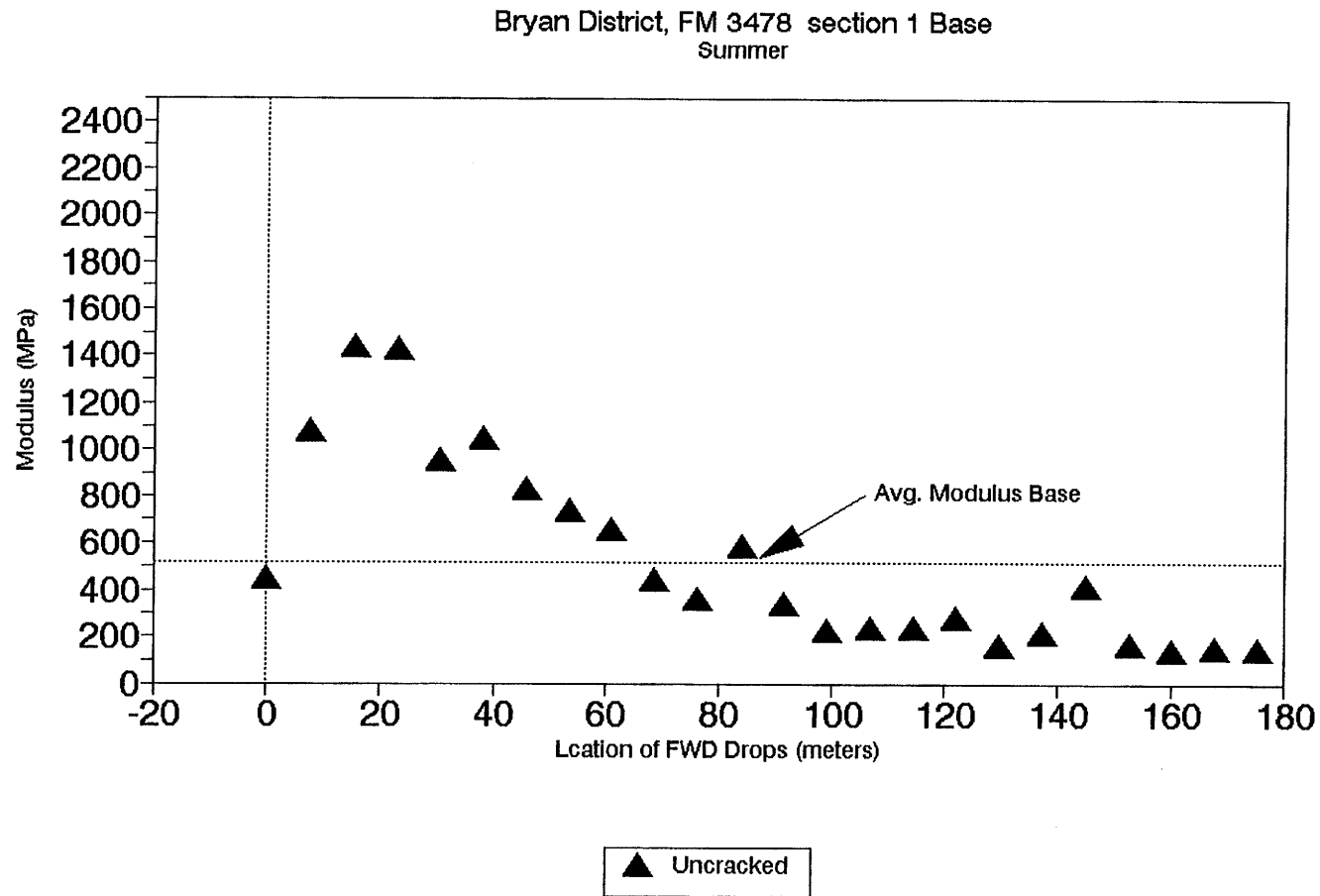


Figure A.84. Variation of Modulus of Stabilized Base within Test Section for Section-1 of Bryan District.

A.87

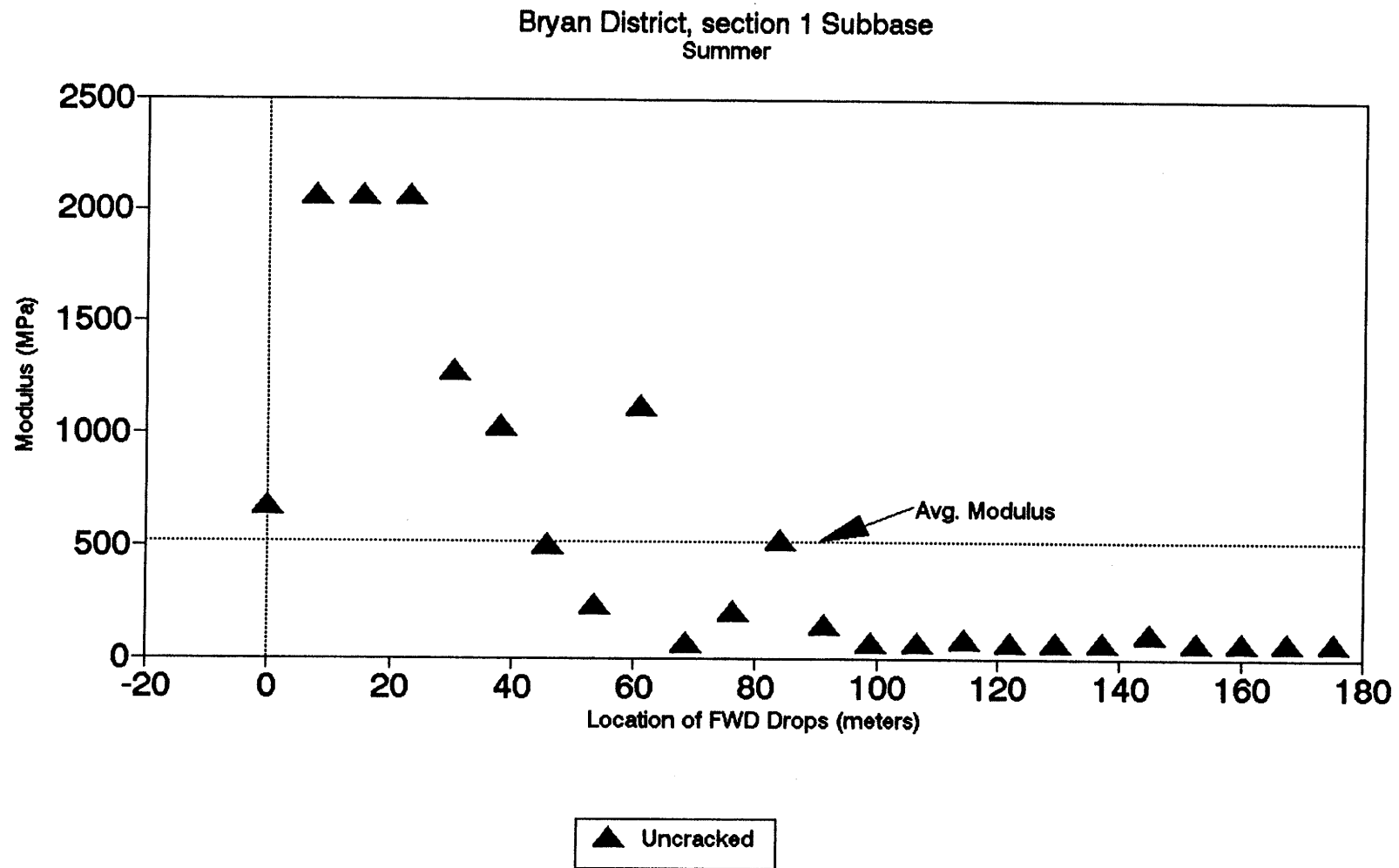


Figure A.85. Variation of Modulus of Stabilized Subbase within Test Section for Section-1 of Bryan District.

Section No.: 2 District: Bryan County: Walker Highway: FM-3478
Structure: Asphalt : 19mm
CLS : 178 mm
LTS : 152 mm
Subgrade

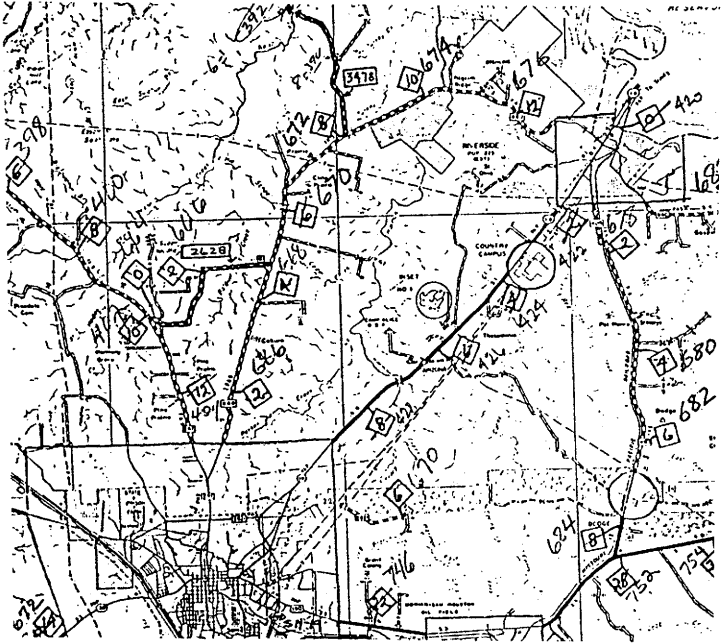
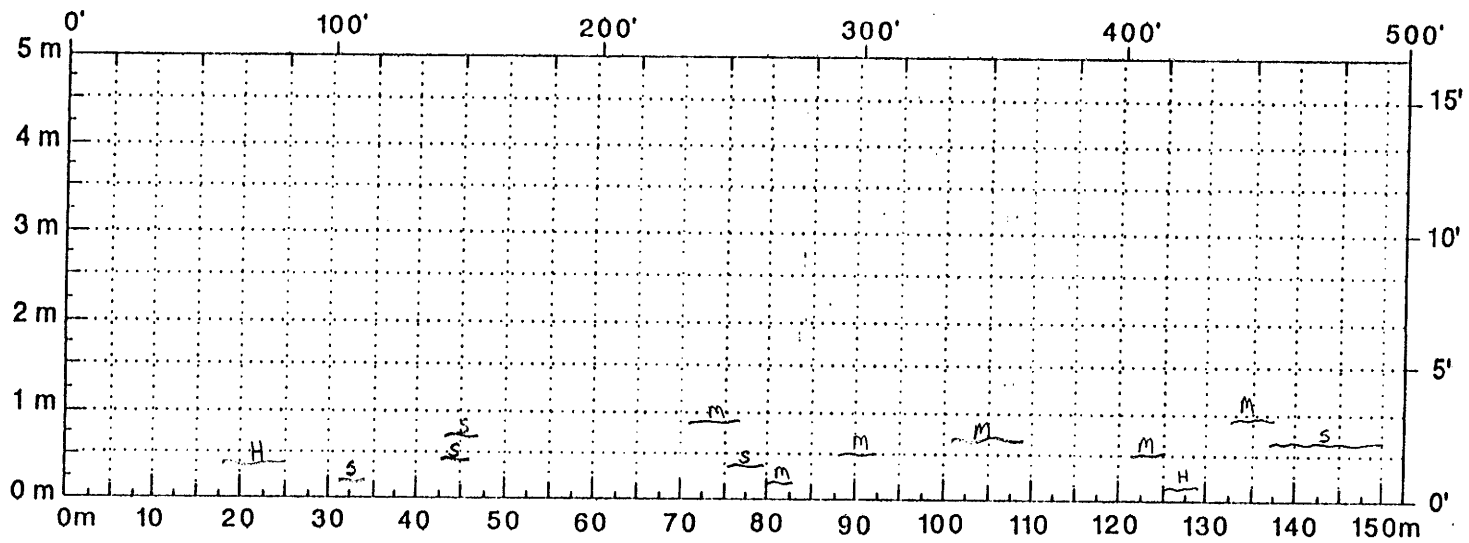


Figure A.86. Location and Details of Section-2 of Bryan District.

A.89



Comments: _____

Figure A.87. Crack Map for Section-2 of Bryan District.

TTI MODULUS ANALYSIS SYSTEM (SUMMARY REPORT)

(Version 4.2)

District:	County:	Highway/Road:	Thickness(in)	MODULI RANGE(psi)		Poisson Ratio Values	
				Minimum	Maximum	H1: u =	H2: u =
0	347		Pavement: 0.80	337,166	337,234	H1: u = 0.35	
			Base: 7.00	20,000	400,000	H2: u = 0.35	
			Subbase: 6.00	10,000	300,000	H3: u = 0.25	
			Subgrade: 72.90		10,000	H4: u = 0.35	

Station	Load (lbs)	Measured Deflection (mils):							Calculated Moduli values (ksi):				Absolute Dpth to	
		R1	R2	R3	R4	R5	R6	R7	SURF(E1)	BASE(E2)	SUBB(E3)	SUBG(E4)	ERR/Sens	Bedrock
0.000	10,061	23.16	11.02	5.75	3.07	2.11	1.63	1.28	337.	57.8	77.3	12.2	10.07	99.24
0.000	10,189	23.42	9.68	4.71	2.89	1.86	1.45	1.14	337.	47.2	97.1	14.2	10.11	157.40
25.000	9,370	36.26	16.59	6.54	3.45	2.27	1.62	1.14	337.	36.1	16.7	9.8	13.31	77.14
50.000	9,513	29.74	13.36	5.17	2.80	1.91	1.39	1.09	337.	42.8	22.1	12.4	14.53	71.10
75.000	9,752	19.14	8.94	4.66	2.43	1.50	1.12	0.88	337.	69.9	69.7	15.6	6.10	90.22
100.000	9,219	74.19	33.04	9.81	4.39	3.03	2.53	1.83	337.	20.0	10.0	5.5	27.05	57.34 †
125.000	9,152	75.08	37.47	13.16	6.35	4.44	3.33	2.87	337.	20.0	10.0	4.3	18.55	62.73 †
150.000	9,291	42.70	23.22	9.02	4.35	2.87	1.93	1.44	337.	38.4	10.0	7.4	13.57	75.92 †
175.000	9,601	30.11	15.94	7.07	3.59	2.47	1.80	1.43	337.	55.0	23.1	9.5	12.68	85.97
200.000	9,144	59.94	34.01	12.52	5.74	3.74	2.67	2.08	337.	22.2	10.0	5.1	14.04	68.36 †
225.000	9,334	29.12	13.12	6.01	3.60	2.57	2.05	1.73	337.	39.4	53.8	9.8	14.21	203.60
250.000	9,700	23.85	12.40	6.29	3.77	3.05	2.15	1.76	337.	54.9	111.7	9.5	13.82	204.97
275.000	9,386	27.91	12.94	5.68	3.61	2.56	2.13	1.71	337.	42.2	57.2	10.1	15.44	141.97
300.000	9,374	27.44	10.39	4.83	2.94	2.18	1.77	1.49	337.	33.2	82.5	12.4	15.41	230.58
325.000	9,386	30.19	15.53	7.36	4.17	3.10	2.35	2.06	337.	47.7	39.0	8.3	13.57	136.86
350.000	9,295	32.94	15.12	6.51	3.41	2.36	1.74	1.39	337.	38.6	24.2	9.7	13.04	94.16
375.000	9,199	33.95	15.00	6.31	3.50	2.46	2.06	1.62	337.	34.2	27.6	9.4	14.94	105.98
400.000	9,168	50.58	20.56	5.52	3.09	2.33	1.84	1.44	337.	20.6	10.0	10.0	22.07	59.02 †
425.000	9,029	41.09	16.29	4.58	2.84	2.04	1.64	1.30	337.	25.9	11.8	11.8	21.07	55.74 †
450.000	9,346	30.79	17.11	8.30	4.21	2.70	1.90	1.45	337.	61.0	19.5	8.1	8.92	87.30
475.000	9,223	35.33	17.76	7.48	4.03	2.75	1.97	1.59	337.	41.3	18.9	8.4	13.00	106.32
500.000	9,227	42.40	22.54	8.20	3.74	2.43	1.61	1.33	337.	35.0	10.0	8.1	13.74	63.52 †
0.000	9,211	47.02	23.51	7.57	3.54	2.43	1.89	1.50	337.	26.7	10.0	8.2	17.41	55.56 †
Mean:		37.67	18.07	7.09	3.72	2.57	1.94	1.55	337.	39.6	35.7	9.6	14.64	86.67
Std. Dev:		15.12	7.80	2.30	0.91	0.63	0.47	0.41	0.	13.8	31.7	2.7	4.46	32.17
Var Coeff(%):		40.15	43.20	32.47	24.38	24.46	24.11	26.64	0.	35.0	88.6	28.6	30.45	37.12

A.90

Figure A.88. FWD Back-Calculation Results for Uncracked Portion of Section-2 of Bryan District.

**BRYAN DISTRICT
FM-3478 SITE-2 (Station-0)**

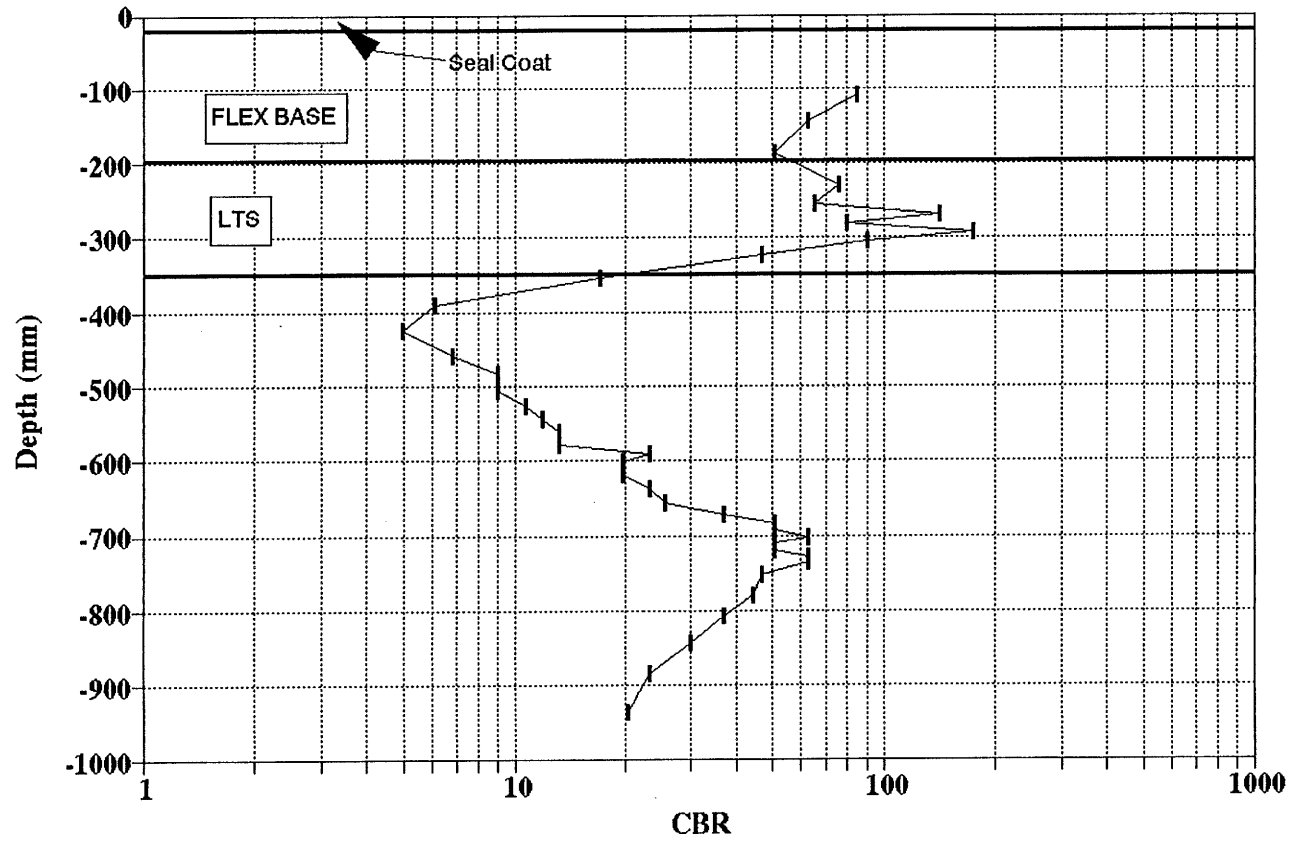
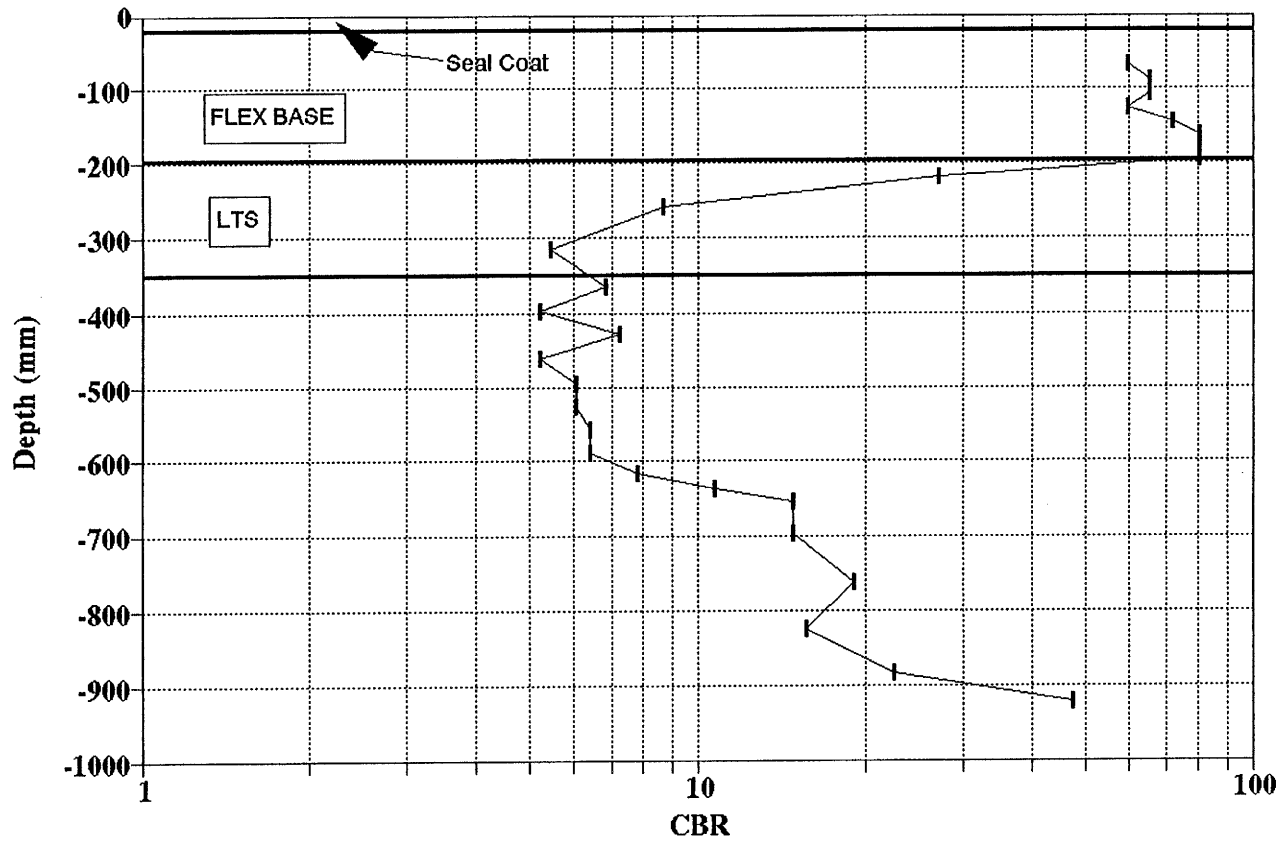


Figure A.89. Variation of CBR Obtained from DCP Testing for Section-2 (at station 0') of Bryan District.

BRYAN DISTRICT
FM-3478 SITE-2 (Station at 125'-0")



A.92

Figure A.90. Variation of CBR Obtained from DCP Testing for Section-2 (at Station 125') of Bryan District.

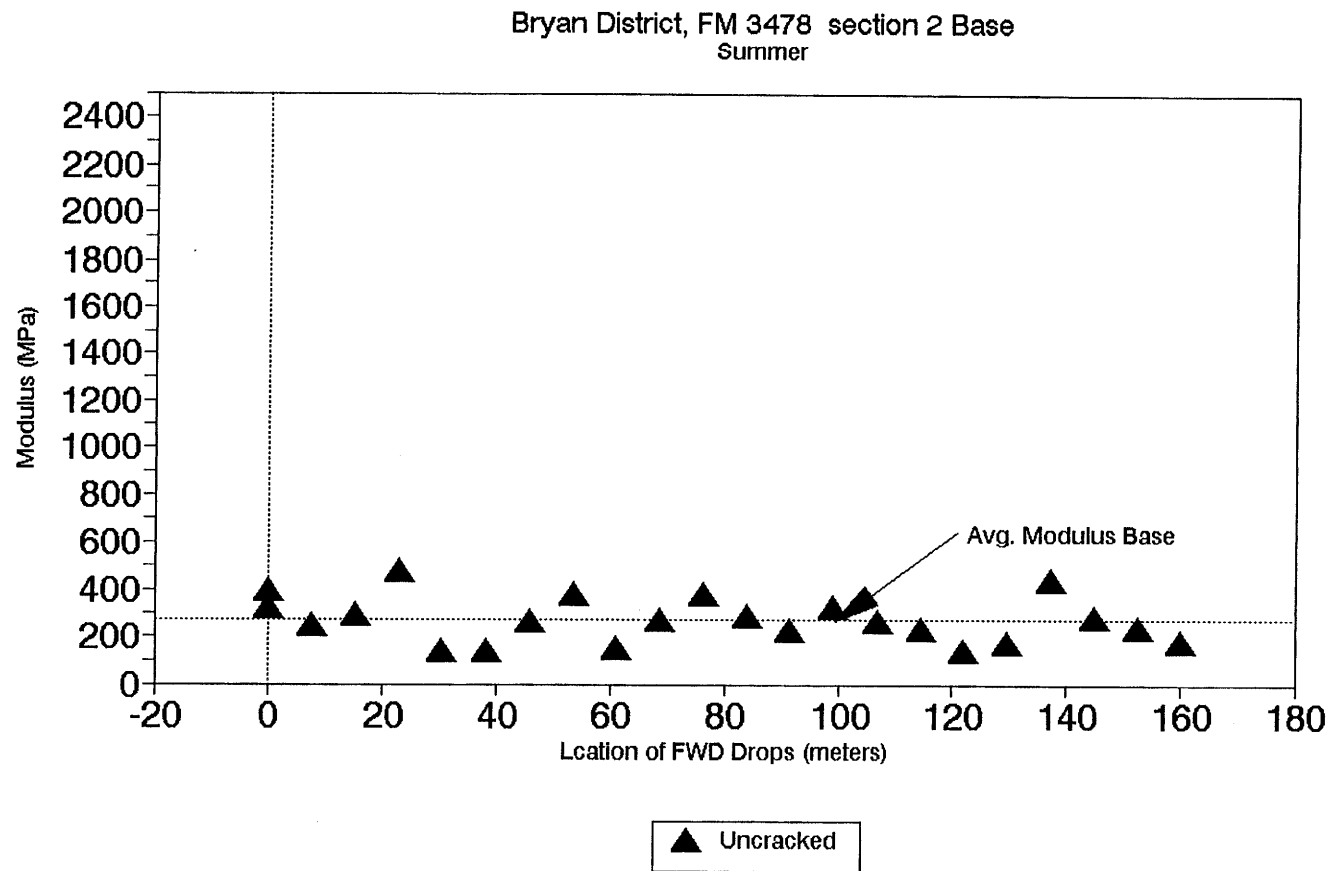


Figure A.91. Variation of Modulus of Stabilized Base within Test Section for Section-2 of Bryan District.

A.94

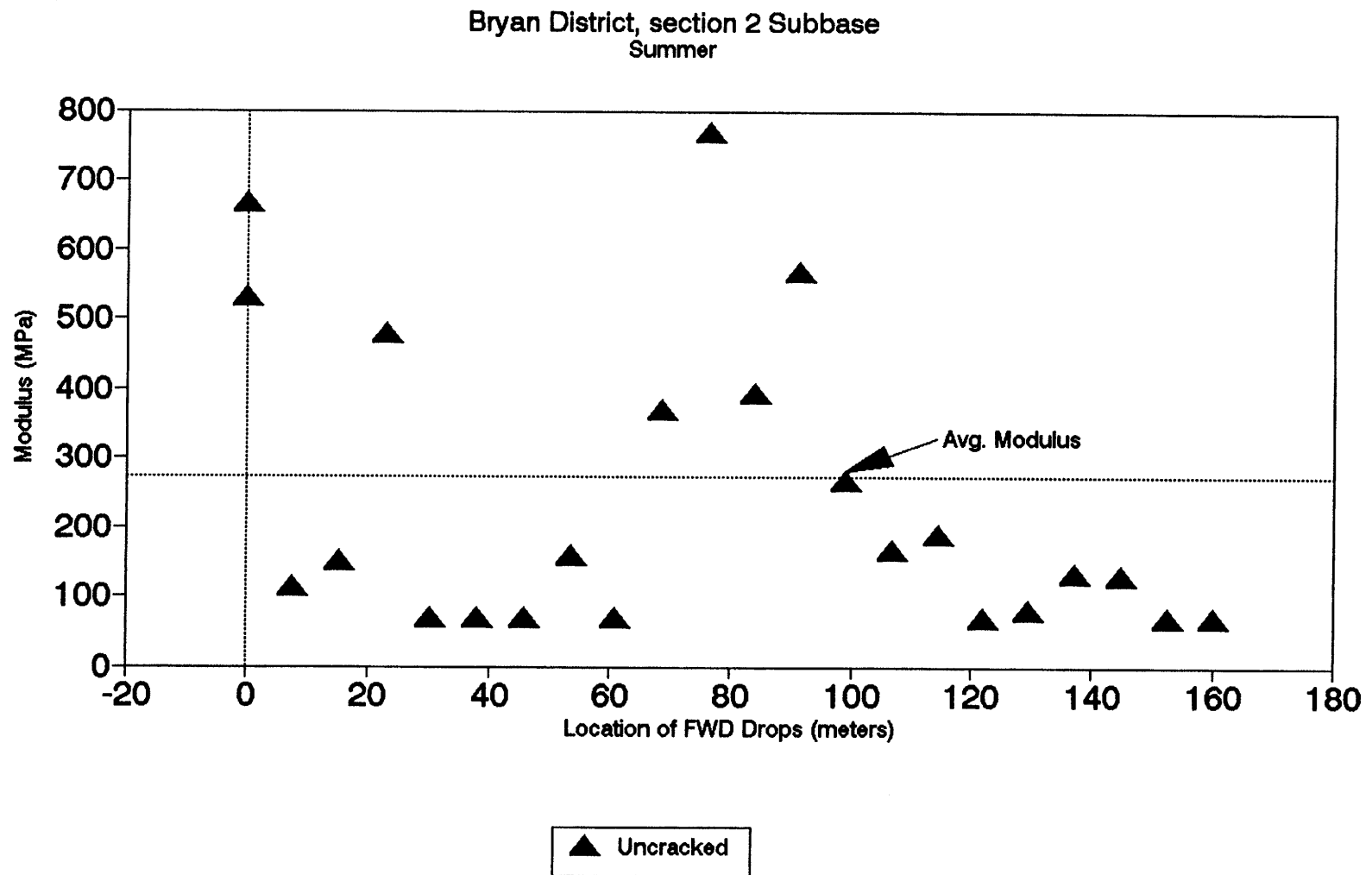


Figure A.92. Variation of Modulus of Stabilized Subbase within Test Section for Section-2 of Bryan District.

Section No.: 3 District: Bryan County: Brazos Highway: US 190
Structure: Asphalt : 102 mm
CTB : 457 mm
Subgrade

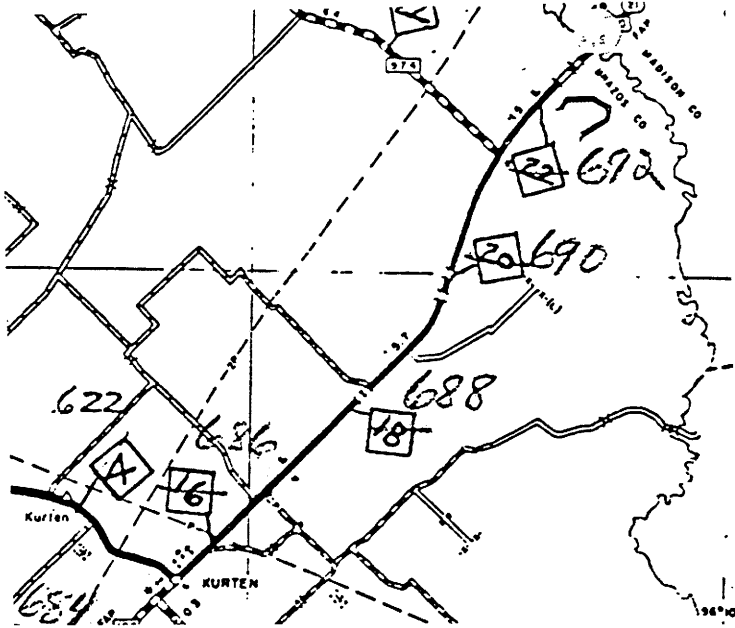
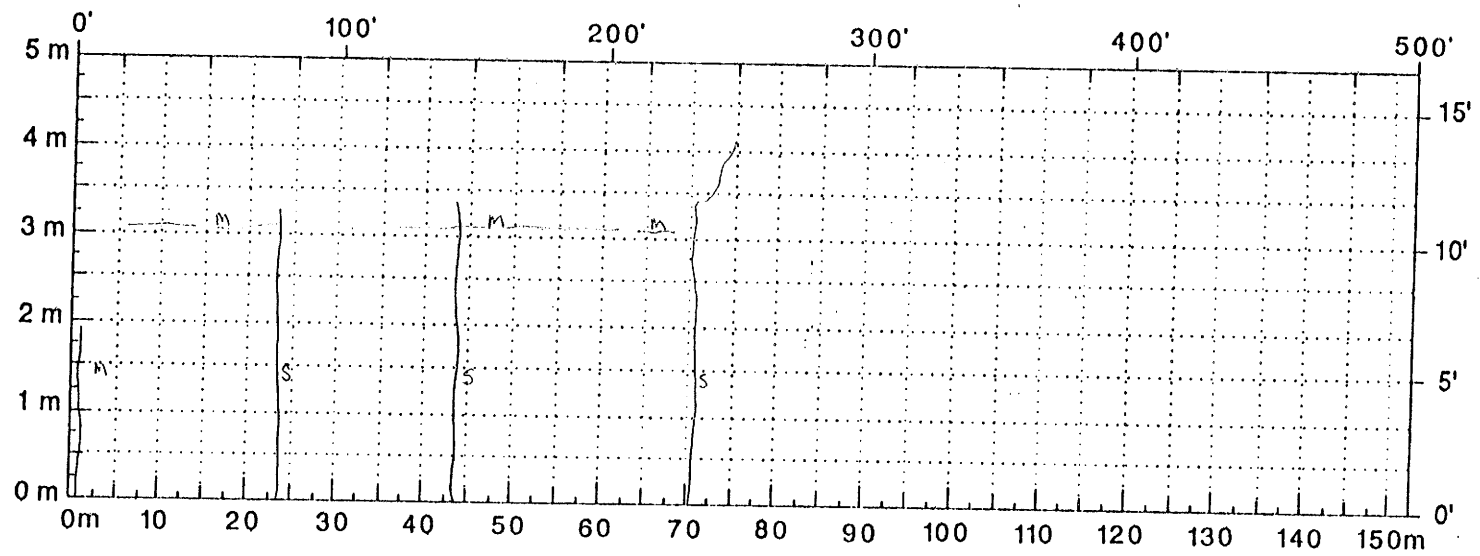


Figure A.93. Location and Details of Section-3 of Bryan District.

A.96



Comments: _____

Figure A.94. Crack Map for Section-3 of Bryan District.

TTI MODULUS ANALYSIS SYSTEM (SUMMARY REPORT)

(Version 4.2)

District:	0	MODULI RANGE(ksi)		Poisson Ratio Values	
County:	190	Minimum	Maximum	H1: $\mu = 0.35$	
Highway/Road:		168,383	168,417	H2: $\mu = 0.25$	
		500,000	5,000,001	H3: $\mu = 0.25$	
		0	0	H4: $\mu = 0.35$	
		20,000			

Station	Load (lbs)	Measured Deflection (mils):							Calculated Moduli values (ksi):				Absolute Dpth to	
		R1	R2	R3	R4	R5	R6	R7	SURF(E1)	BASE(E2)	SUBB(E3)	SUBG(E4)	ERR/Sens	Bedrock
0.000	15,694	10.22	6.35	4.70	3.44	2.61	1.96	1.64	168.	500.0	0.0	26.2	9.74	300.00 #
10.000	15,583	10.54	6.61	4.89	3.69	2.81	2.17	1.72	168.	500.0	0.0	24.0	8.66	300.00 #
29.000	15,782	6.51	4.42	3.76	3.04	2.49	1.99	1.60	168.	1523.6	0.0	26.8	6.74	300.00
39.000	15,687	6.44	4.19	3.58	2.90	2.43	2.00	1.66	168.	1623.7	0.0	27.2	5.36	300.00
62.000	15,655	6.47	4.00	3.54	3.01	2.52	2.11	1.75	168.	1903.8	0.0	25.3	3.74	300.00
76.000	15,718	5.28	3.75	3.40	2.90	2.50	2.12	1.80	168.	4253.1	0.0	19.5	7.82	300.00
95.000	15,687	5.89	3.73	3.38	2.89	2.51	2.10	1.81	168.	2937.7	0.0	22.8	4.48	300.00
106.000	15,492	5.12	4.20	3.69	3.11	2.63	2.17	1.81	168.	4040.6	0.0	17.8	11.15	300.00
117.000	15,671	5.21	4.00	3.54	3.00	2.56	2.20	1.86	168.	4285.7	0.0	18.3	9.26	300.00
137.000	15,679	4.54	3.48	3.20	2.71	2.35	2.09	1.80	168.	5000.0	0.0	20.3	9.27	300.00 #
151.000	15,694	4.49	2.98	2.87	2.41	2.15	1.87	1.59	168.	5000.0	0.0	24.7	7.08	300.00 #
168.000	15,687	4.89	3.04	2.80	2.45	2.16	1.89	1.63	168.	5000.0	0.0	23.7	5.03	300.00 #
187.000	15,643	4.37	2.76	2.55	2.24	2.00	1.77	1.54	168.	5000.0	0.0	28.1	7.09	300.00 #
200.000	15,671	3.78	2.58	2.40	2.11	1.87	1.67	1.48	168.	5000.0	0.0	32.9	12.44	300.00 #
211.000	15,694	4.38	2.66	2.49	2.22	1.97	1.76	1.55	168.	5000.0	0.0	28.6	6.19	300.00 #
227.000	15,754	4.59	3.05	2.78	2.50	2.24	1.94	1.69	168.	5000.0	0.0	23.9	6.44	300.00 #
263.000	15,706	5.02	3.36	3.11	2.70	2.39	2.05	1.77	168.	5000.0	0.0	20.2	6.32	300.00 #
Mean:		5.75	3.83	3.33	2.78	2.36	1.99	1.69	168.	3621.6	0.0	24.1	7.46	300.00
Std. Dev:		1.92	1.15	0.70	0.43	0.26	0.16	0.11	0.	1723.3	0.0	4.0	2.36	107.65
Var Coeff(%):		33.33	29.99	20.97	15.48	11.03	7.91	6.69	0.	47.6	0.0	16.8	31.71	35.85

A.97

Figure A.95. FWD Back-Calculation Results for Uncracked Portion of Section-3 of Bryan District.

ITI MODULUS ANALYSIS SYSTEM (SUMMARY REPORT)														(Version 4.2)	
District:	0													MODULI RANGE(psi)	
County:	190			Thickness(in)					Minimum		Maximum		Poisson Ratio Values		
Highway/Road:				Pavement:		4.00		168,383		168,417		H1: $\mu = 0.35$			
				Base:		18.00		500,000		5,000,001		H2: $\mu = 0.25$			
				Subbase:		0.00		0		0		H3: $\mu = 0.25$			
				Subgrade:		278.00				20,000		H4: $\mu = 0.35$			
Station	Load (lbs)	Measured Deflection (mils):					Calculated Moduli values (ksi):						Absolute Dist to Bedrock		
		R1	R2	R3	R4	R5	R6	R7	SURF(E1)	BASE(E2)	SUBB(E3)	SUBG(E4)	ERR/Sens	Bedrock	
1,000	15,496	10.42	5.61	4.55	3.58	2.82	2.20	1.76	168.	500.0	0.0	25.5	3.85	300.00 †	
36,000	15,611	7.21	4.17	3.55	2.94	2.44	2.05	1.71	168.	1165.6	0.0	28.7	1.76	300.00	
69,000	15,623	5.05	3.65	3.29	2.81	2.39	2.06	1.74	168.	4616.0	0.0	19.8	8.65	300.00	
142,000	15,663	5.01	2.91	2.71	2.31	2.04	1.85	1.59	168.	5000.0	0.0	25.0	4.18	300.00 †	
226,000	15,726	5.83	3.25	3.04	2.74	2.20	1.90	1.59	168.	2883.8	0.0	26.9	3.79	300.00	
Mean:		6.70	3.92	3.43	2.88	2.38	2.01	1.68	168.	2833.1	0.0	25.2	4.45	300.00	
Std. Dev:		2.26	1.06	0.70	0.46	0.29	0.14	0.08	0.	2006.3	0.0	3.3	2.54	74.76	
Var Coeff(%):		33.71	26.95	20.41	15.96	12.36	6.94	4.90	0.	70.8	0.0	13.2	57.03	24.92	

Figure A.96. FWD Back-Calculation Results for Cracked Portion of Section-3 of Bryan District.

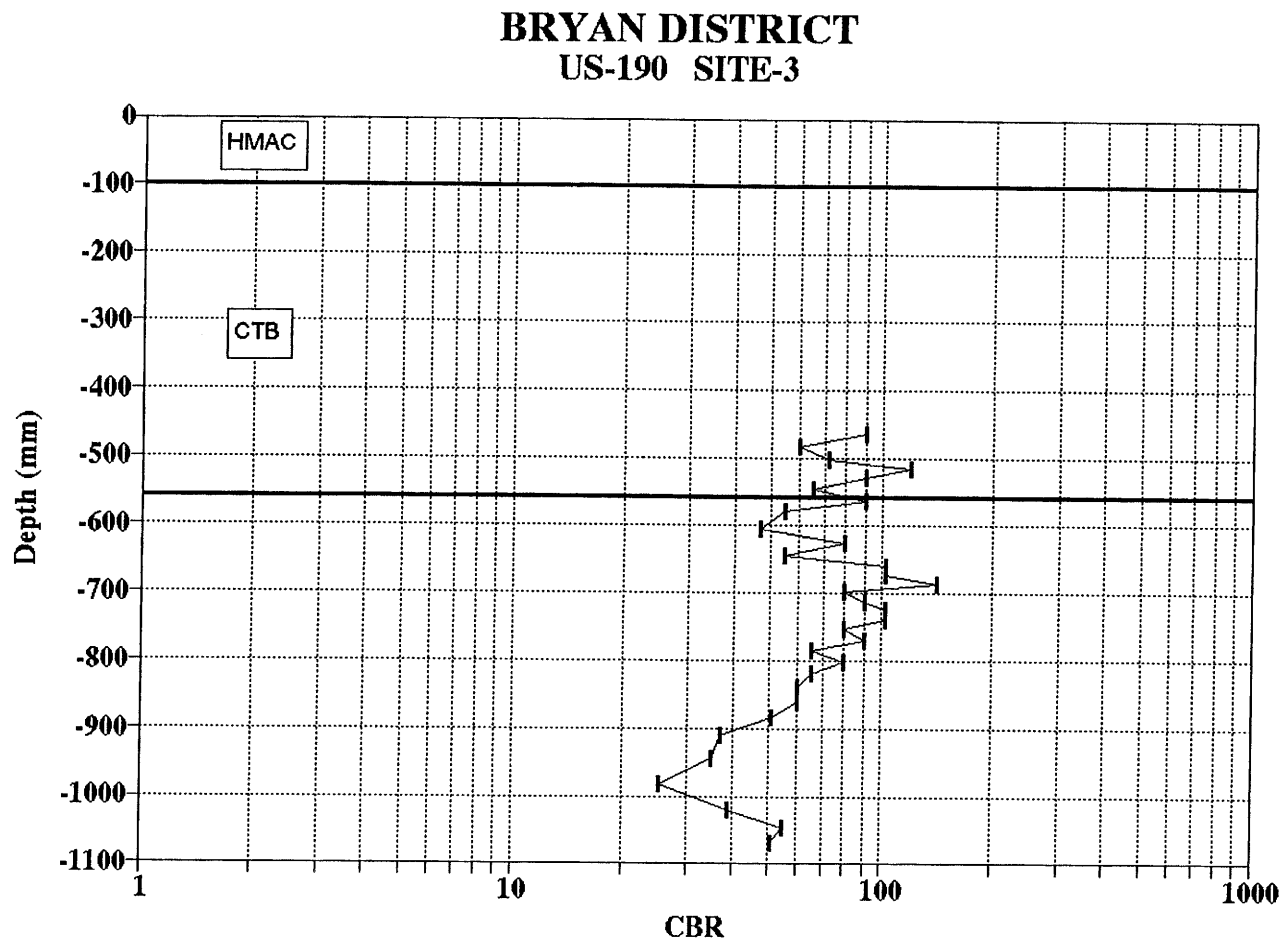


Figure A.97. Variation of CBR Obtained from DCP Testing for Section-3 of Bryan District.

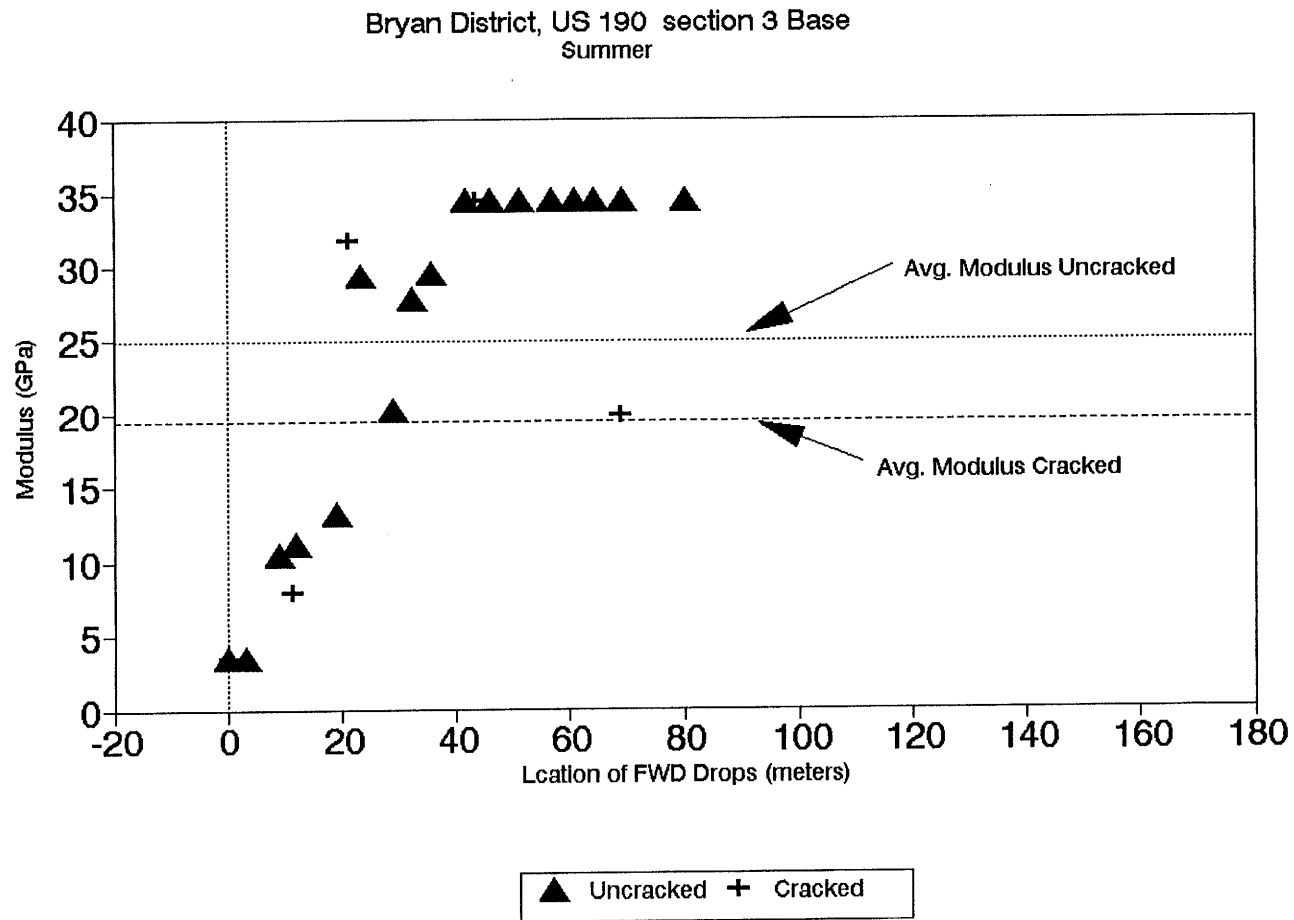


Figure A.98. Variation of Modulus of Stabilized Base within Test Section for Section-3 of Bryan District.

Section No.: 4 District: Bryan County: Brazos Highway: FM-1179
Structure: Asphalt : 51 mm
Flex Base : 279 mm
LTS : 203 mm
Subgrade

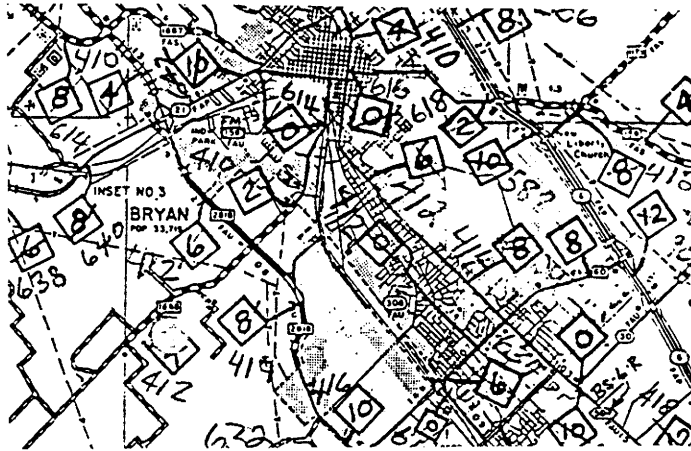
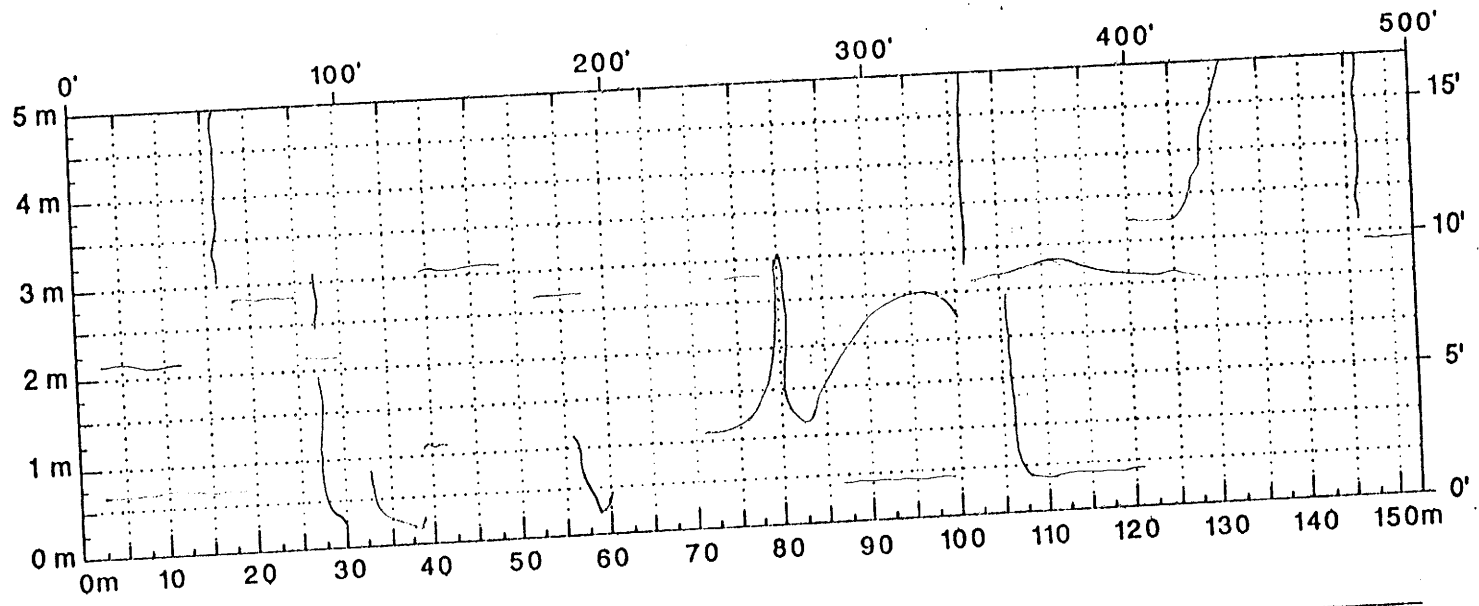


Figure A.99. Location and Details of Section-4 of Bryan District.

A.102



Comments: All Cracks are sealed

Figure A.100. Crack Map for Section-4 of Bryan District.

TTI MODULUS ANALYSIS SYSTEM (SUMMARY REPORT)

(Version 4.2)

District: 11	MODULI RANGE(psi)	
County: 79	Thickness(in)	Minimum Maximum
Highway/Road:	Pavement: 2.00	303,370 303,430
	Base: 11.00	20,000 400,000
	Subbase: 8.00	10,000 300,000
	Subgrade: 216.30	20,000
		Poisson Ratio Values
		H1: u = 0.35
		H2: u = 0.35
		H3: u = 0.25
		H4: u = 0.35

Station	Load (lbs)	Measured Deflection (mils):							Calculated Moduli values (ksi):				Absolute Dpth to	
		R1	R2	R3	R4	R5	R6	R7	SURF(E1)	BASE(E2)	SUBB(E3)	SUBG(E4)	ERR/Sens	Bedrock
0.000	15,222	37.78	19.26	8.62	5.19	3.59	2.67	2.17	303.	45.3	10.0	19.9	4.59	171.32 †
25.000	15,258	44.59	24.52	10.73	5.46	3.28	2.43	1.98	303.	33.2	10.0	17.8	12.35	86.13 †
51.000	15,424	33.15	16.30	7.06	4.17	2.81	2.11	1.69	303.	53.2	10.4	26.3	5.36	125.46
76.000	15,301	37.35	20.26	9.57	5.87	3.94	2.94	2.35	303.	48.7	10.0	17.6	4.20	216.11 †
111.000	15,377	29.22	13.77	6.36	4.28	3.00	2.31	1.90	303.	59.1	17.2	24.8	4.00	231.87
125.000	15,460	30.55	15.17	8.09	5.57	3.84	2.80	2.19	303.	63.1	17.1	19.0	2.24	256.78
150.000	15,480	26.29	13.15	7.72	5.33	3.69	2.71	2.12	303.	77.5	25.2	19.7	1.25	266.60
175.000	15,293	27.31	14.79	8.83	5.97	4.28	2.97	2.33	303.	83.0	18.9	17.3	1.39	189.16
200.000	15,234	24.26	12.94	7.88	5.21	3.49	2.56	2.02	303.	96.9	17.9	20.6	0.74	204.46
225.000	15,091	23.76	11.89	6.93	4.62	3.06	2.31	1.85	303.	87.6	20.5	23.0	1.06	186.04
275.000	15,512	23.92	11.21	7.10	5.37	3.85	3.02	2.43	303.	72.0	95.4	18.4	2.46	300.00
300.000	15,412	23.57	11.92	7.18	5.30	3.86	2.95	2.38	303.	82.7	52.9	18.7	2.61	300.00
325.000	15,369	23.60	10.93	6.54	4.85	3.46	2.66	2.11	303.	72.9	65.5	20.3	2.77	300.00
351.000	15,361	22.77	10.28	6.54	5.00	3.65	2.75	2.16	303.	71.1	123.9	19.4	2.01	300.00
375.000	15,428	23.65	11.96	7.22	5.19	3.67	2.83	2.18	303.	85.2	41.2	19.6	2.36	300.00
400.000	14,975	49.15	31.33	17.89	11.07	6.89	4.80	3.67	303.	39.1	10.0	8.7	8.92	148.79 †
425.000	15,218	28.96	14.13	7.69	5.23	3.69	2.87	2.37	303.	64.6	19.7	19.3	2.74	300.00
450.000	15,277	35.45	16.97	8.33	5.38	3.73	2.92	2.43	303.	48.9	13.3	19.1	3.38	278.47
475.000	15,484	27.81	13.43	6.89	4.93	3.55	2.71	2.30	303.	66.6	21.7	21.1	4.42	300.00
500.000	15,134	21.22	10.65	6.37	4.89	3.64	2.85	2.35	303.	87.6	78.0	19.8	3.53	300.00
Mean:		29.72	15.24	8.18	5.44	3.75	2.81	2.25	303.	66.9	33.9	19.5	3.62	237.31
Std. Dev:		7.68	5.23	2.55	1.40	0.81	0.53	0.39	0.	17.9	32.6	3.4	2.76	110.78
Var Coeff(%):		25.84	34.34	31.17	25.69	21.73	18.89	17.44	0.	26.8	95.9	17.5	76.31	46.68

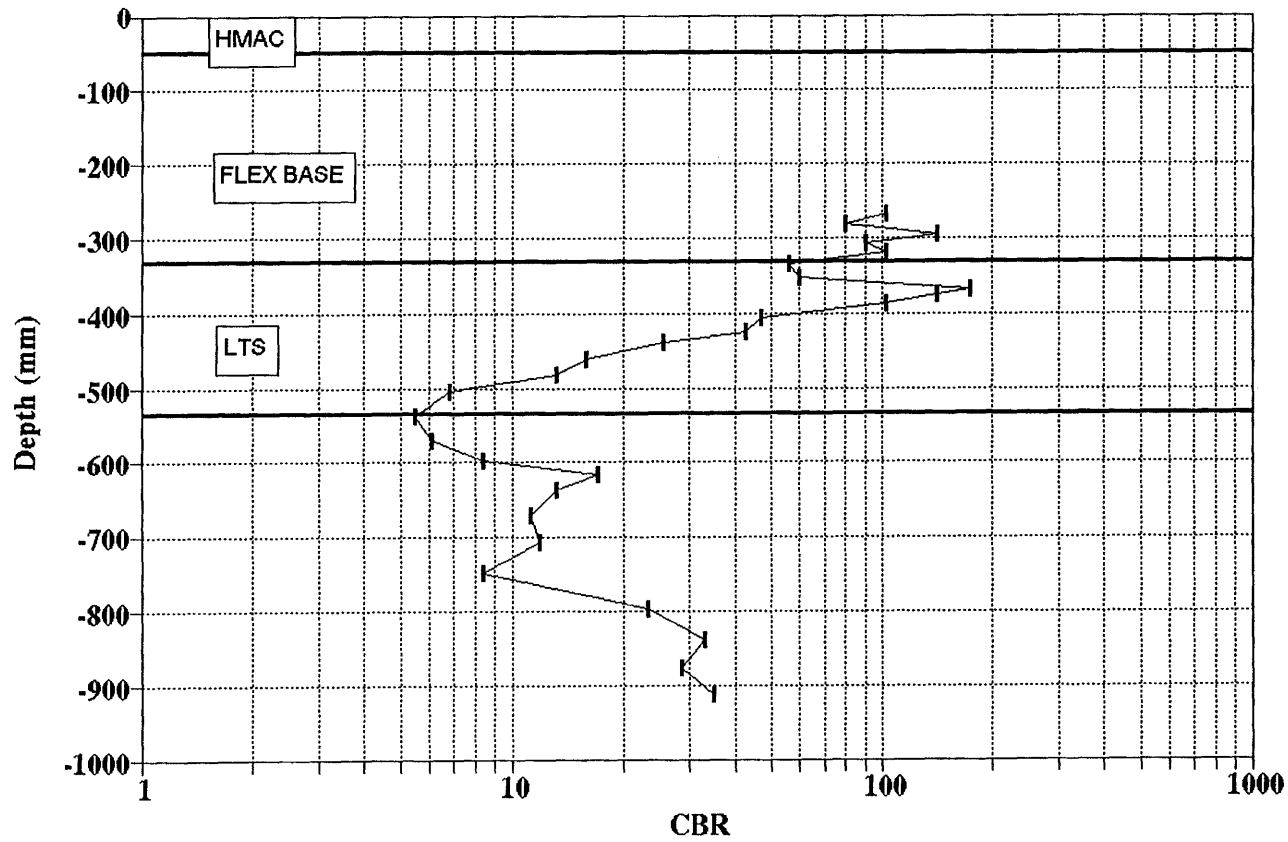
A.103

Figure A.101. FWD Back-Calculation Results for Uncracked Portion of Section-4 of Bryan District.

TTI MODULUS ANALYSIS SYSTEM (SUMMARY REPORT)														(Version 4.2)	
District:	11									MODULI RANGE(ksi)					
County:	79									Minimum	Maximum	Poisson Ratio Values			
Highway/Road:			Pavement:	2.00					303,370	303,430	H1: u = 0.35				
			Base:	11.00					20,000	400,000	H2: u = 0.35				
			Subbase:	8.00					10,000	300,000	H3: u = 0.25				
			Subgrade:	220.30					20,000		H4: u = 0.35				
Station	Load (lbs)	Measured Deflection (mils):							Calculated Moduli values (ksi):				Absolute Dpth to		
		R1	R2	R3	R4	R5	R6	R7	SURF(E1)	BASE(E2)	SUBB(E3)	SURG(E4)	ERR/Sens	Bedrock	
324.000	15,214	34.19	16.93	7.63	4.79	3.37	2.48	2.04	303.	51.5	10.9	22.3	5.04	180.74	
340.000	15,265	29.93	14.34	6.96	4.67	3.28	2.39	1.86	303.	59.6	15.6	22.8	3.10	300.00	
425.000	15,075	28.32	15.49	9.64	6.67	4.43	3.21	2.46	303.	83.0	16.5	15.9	1.12	194.26	
493.000	15,158	26.06	13.50	8.39	5.71	3.83	2.89	2.35	303.	83.1	22.5	18.3	1.22	206.73	
577.000	15,524	21.63	9.54	6.09	4.78	3.56	2.77	2.22	303.	72.2	199.8	20.3	2.90	300.00	
Mean:		28.03	13.96	7.74	5.32	3.69	2.75	2.19	303.	69.9	53.1	19.9	2.68	241.40	
Std. Dev:		4.65	2.79	1.36	0.86	0.46	0.33	0.24	0.	14.1	82.1	2.9	1.61	74.77	
Var Coeff(%):		16.59	19.96	17.54	16.18	12.51	11.99	10.99	0.	20.1	100.0	14.4	60.16	30.97	

Figure A.102. FWD Back-Calculation Results for Cracked Portion of Section-4 of Bryan District.

**BRYAN DISTRICT
FM-1179 SITE-4**



A.105

Figure A.103. Variation of CBR Obtained from DCP Testing for Section-4 of Bryan District.

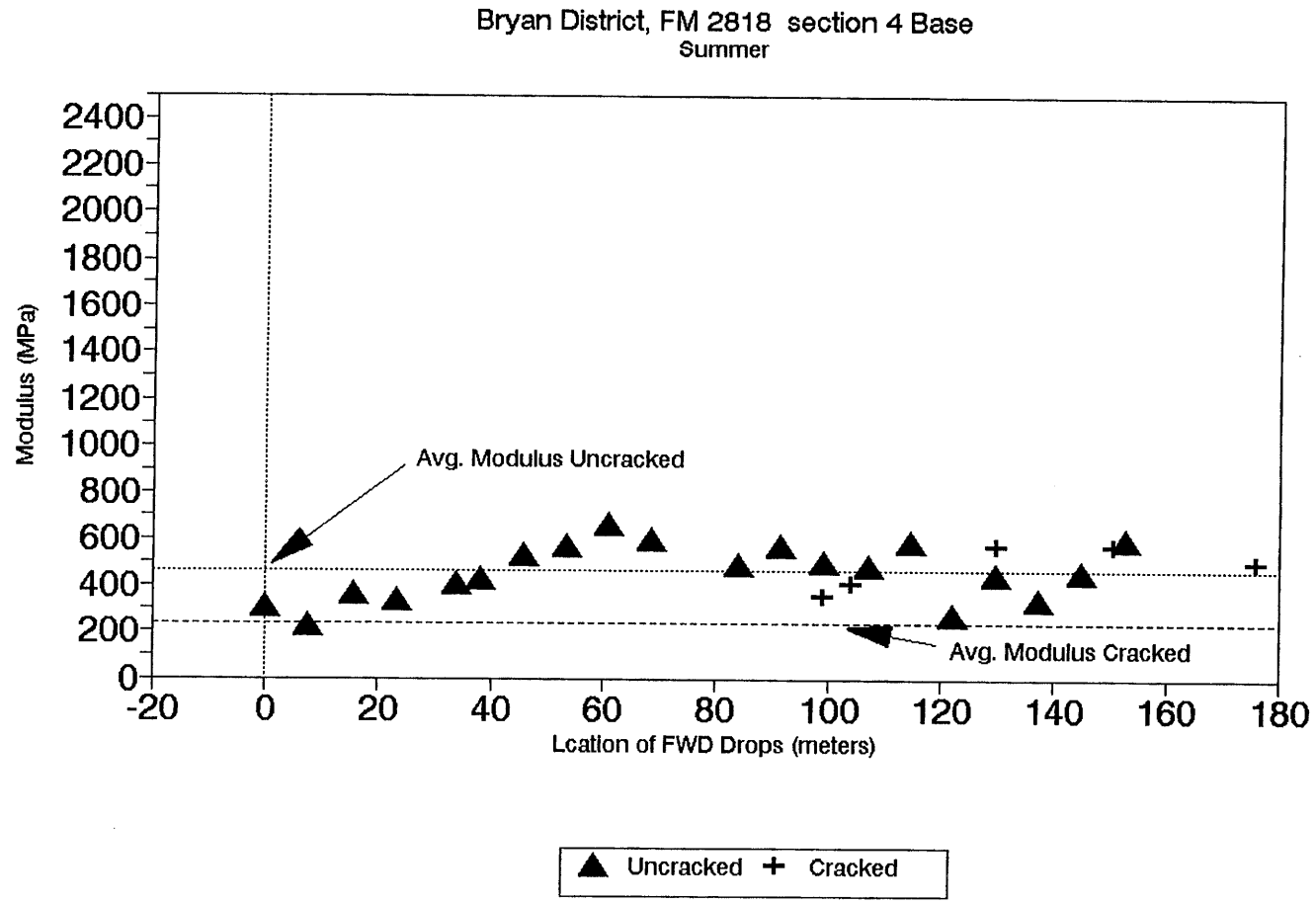


Figure A.104. Variation of Modulus of Stabilized Base within Test Section for Section-3 of Bryan District.

A.107

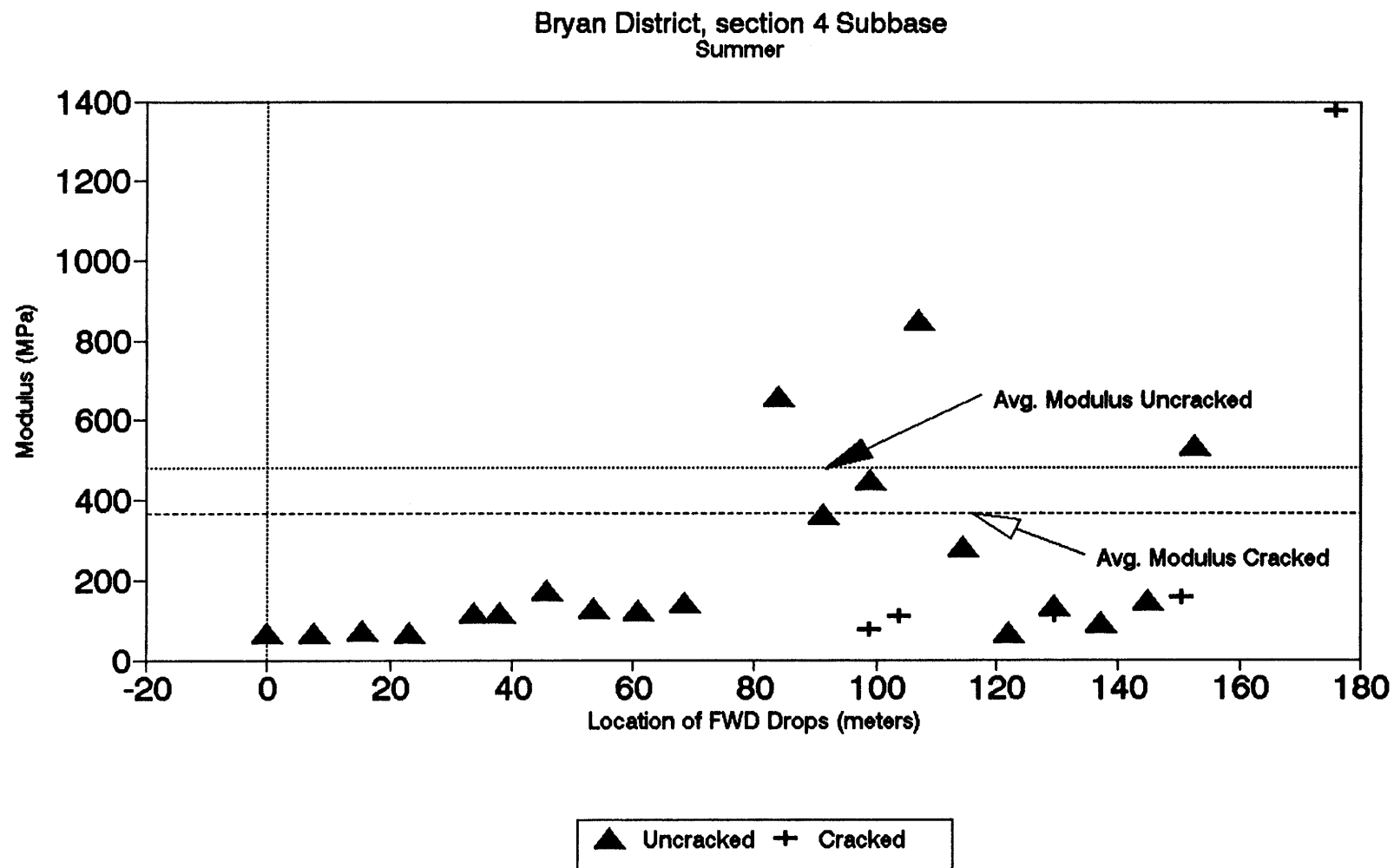


Figure A.105. Variation of Modulus of Stabilized Subbase within Test Section for Section-4 of Bryan District.

Section No.: 5 District: Bryan County: Brazos Highway: FM-2818
Structure: Asphalt : 51 mm
Flex base : 254 mm
LTS : 203 mm
Subgrade

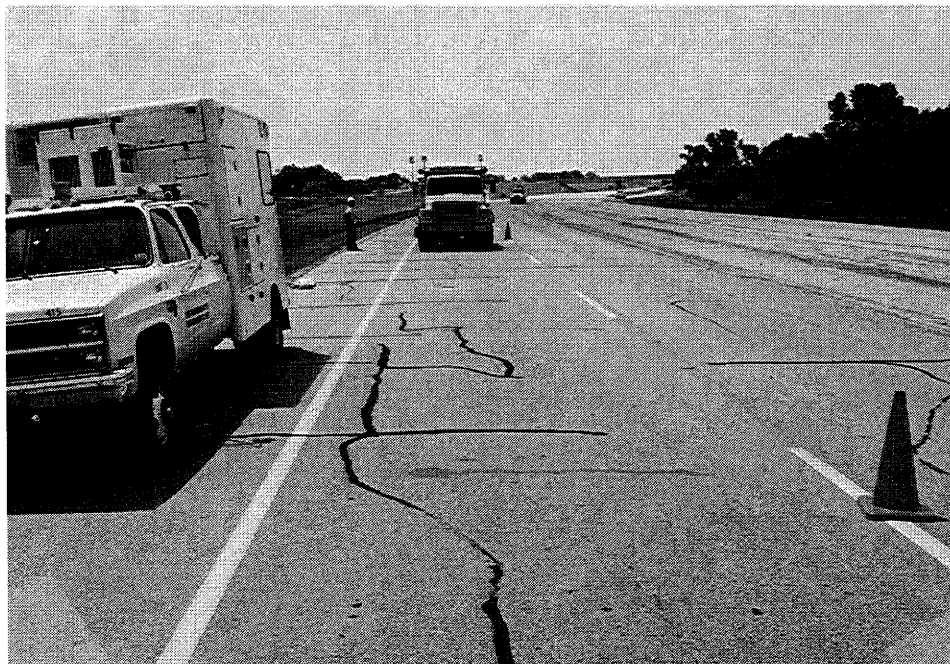
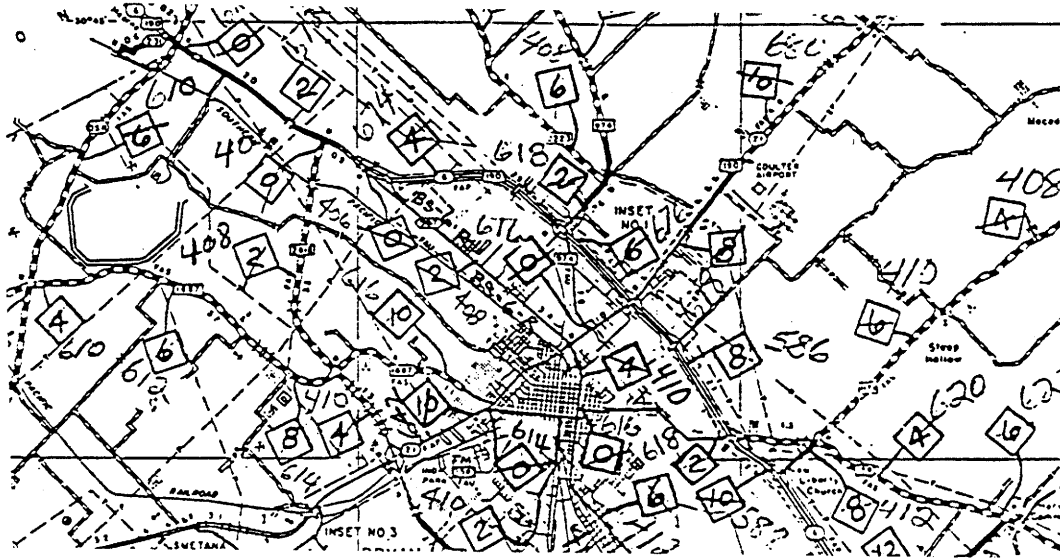
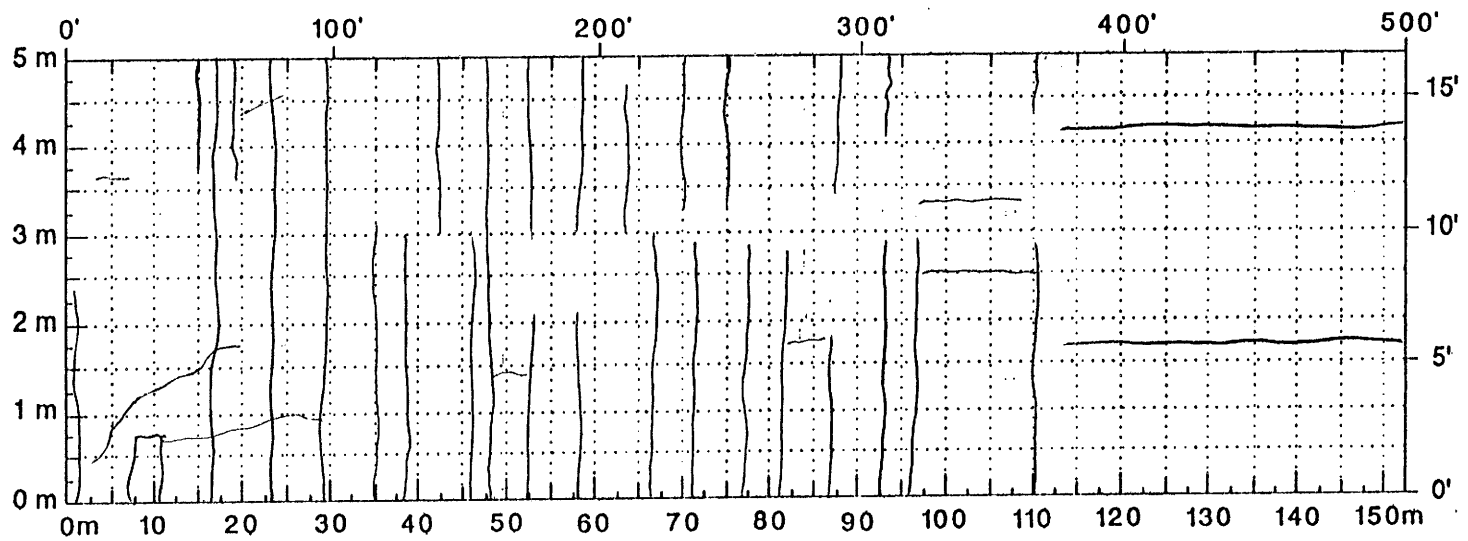


Figure A.106. Location and Details of Section-5 of Bryan District.

A.109



Comments: All Cracks are sealed

Figure A.107. Crack Map for Section-5 of Bryan District.

TTI MODULUS ANALYSIS SYSTEM (SUMMARY REPORT)

(Version 4.2)

District:	0	MODULI RANGE(psi)	
County:	281	Minimum	Maximum
Highway/Road:		Poisson Ratio Values	
	Pavement:	2.00	226,077 226,123
	Base:	10.00	20,000 400,000
	Subbase:	8.00	10,000 300,000
	Subgrade:	280.00	20,000

Station	Load (lbs)	Measured Deflection (mils):							Calculated Moduli values (ksi):				Absolute Dist to Bedrock	
		R1	R2	R3	R4	R5	R6	R7	SURF(E1)	BASE(E2)	SUBB(E3)	SUBG(E4)	ERR/Sens	Bedrock
0.000	15,337	23.17	13.05	10.15	8.21	6.52	5.11	4.11	226.	95.1	266.6	11.7	0.69	300.00
16.000	15,317	23.23	13.47	10.67	8.56	6.83	5.24	4.18	226.	102.8	220.5	11.1	0.96	300.00
89.000	15,206	18.09	10.69	8.85	7.33	5.94	4.74	3.86	226.	153.4	300.0	12.5	2.07	300.00 *
113.000	15,353	17.98	11.28	9.38	7.78	6.22	4.98	4.00	226.	170.8	300.0	11.5	1.05	300.00 *
132.000	15,182	19.42	11.57	9.43	7.63	6.13	4.83	3.85	226.	132.2	300.0	12.0	0.93	300.00 *
159.000	15,305	19.04	11.76	9.52	7.75	6.18	4.87	3.90	226.	146.4	272.5	11.8	0.72	300.00
193.000	15,261	22.07	12.96	9.92	7.76	6.09	4.83	3.84	226.	110.3	180.7	12.3	0.53	300.00
214.000	15,210	23.25	13.96	10.53	8.24	6.59	5.08	4.06	226.	109.6	143.5	11.4	0.81	300.00
238.000	15,146	24.03	14.63	11.25	8.70	6.81	5.32	4.25	226.	111.2	120.7	10.8	0.46	300.00
303.000	15,178	22.57	13.01	9.81	7.66	5.83	4.43	3.46	226.	108.6	128.9	13.0	0.49	300.00
345.000	15,277	22.59	12.74	9.21	6.86	5.15	3.78	2.93	226.	110.6	80.4	15.1	0.51	268.34
416.000	15,333	20.53	11.98	7.87	5.37	3.76	2.70	2.08	226.	154.0	25.6	20.8	0.57	229.84
494.000	15,250	25.00	12.65	7.33	4.64	3.24	2.49	2.03	226.	92.2	19.4	23.9	0.54	294.29
Mean:		21.61	12.60	9.53	7.42	5.79	4.49	3.58	226.	122.9	181.4	13.7	0.79	300.00
Std. Dev:		2.33	1.11	1.08	1.19	1.11	0.93	0.76	0.	25.5	103.2	4.1	0.43	55.47
Var Coeff(%):		10.80	8.81	11.36	16.01	19.24	20.70	21.19	0.	20.7	56.9	29.6	54.35	18.49

A.110

Figure A.108. FWD Back-Calculation Results for Uncracked Portion of Section-5 of Bryan District.

ITI MODULUS ANALYSIS SYSTEM (SUMMARY REPORT)

(Version 4.2)

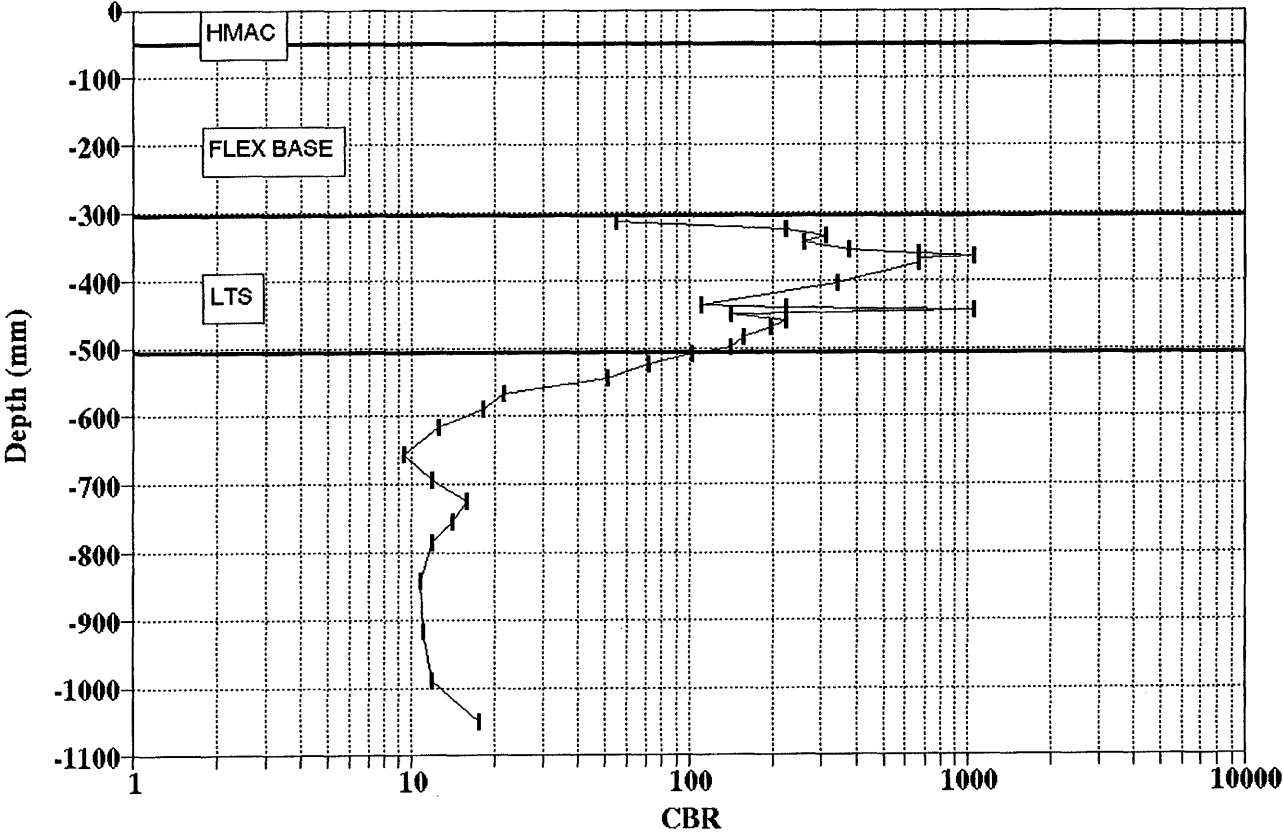
District: 0					MODULI RANGE(psi)			
County: 281					Minimum	Maximum	Poisson Ratio Values	
Highway/Road:	Pavement:	Thickness(in)					H1: u = 0.35	
	Base:	2.00		226,077	226,123		H2: u = 0.35	
	Subbase:	10.00		20,000	400,000		H3: u = 0.25	
	Subgrade:	8.00		10,000	300,000		H4: u = 0.35	
		280.00			20,000			

Station	Load (lbs)	Measured Deflection (mils):							Calculated Moduli values (ksi):				Absolute Dpth to	
		R1	R2	R3	R4	R5	R6	R7	SURF(E1)	BASE(E2)	SUBB(E3)	SURG(E4)	ERR/Sens	Bedrock
628.000	15,293	21.02	12.65	9.54	7.73	6.12	4.81	3.82	226.	121.0	200.4	12.3	0.81	300.00
76.000	15,337	20.53	11.81	9.32	7.63	6.25	4.89	3.97	226.	117.3	300.0	12.3	1.29	300.00 †
100.000	15,373	19.55	11.61	9.31	7.61	6.16	4.88	3.91	226.	132.5	300.0	12.1	0.90	300.00 †
117.000	15,305	20.44	11.62	9.45	7.83	6.37	4.89	3.94	226.	120.1	300.0	12.1	2.06	300.00 †
142.000	15,285	22.08	12.78	10.14	8.16	6.38	4.96	3.93	226.	108.8	227.2	11.7	0.85	300.00
194.000	15,174	22.10	13.35	10.14	8.17	6.62	5.00	4.05	226.	116.2	176.4	11.4	1.06	300.00
221.000	15,277	22.62	13.89	10.64	8.49	6.64	5.16	4.09	226.	120.3	147.3	11.2	0.28	300.00
306.000	15,226	24.25	13.90	9.97	7.55	5.59	4.20	3.24	226.	105.1	70.7	13.6	0.47	300.00
320.000	15,182	24.30	13.49	9.65	7.21	5.32	4.04	3.06	226.	97.9	75.0	14.3	0.63	267.54
365.000	15,218	22.51	12.12	8.36	6.05	4.35	3.08	2.34	226.	107.8	54.6	17.7	1.23	208.27
460.000	15,345	21.42	11.55	6.92	4.37	3.03	2.25	1.84	226.	127.6	19.3	26.3	0.57	272.87
Mean:		21.89	12.62	9.40	7.35	5.71	4.38	3.47	226.	115.9	170.1	14.1	0.92	300.00
Std. Dev:		1.51	0.93	1.01	1.17	1.12	0.93	0.77	0.	10.2	105.1	4.4	0.49	61.62
Var Coeff(%):		6.89	7.37	10.79	15.98	19.53	21.25	22.08	0.	8.8	61.8	31.5	52.88	20.54

A.111

Figure A.109. FWD Back-Calculation Results for Cracked Portion of Section-5 of Bryan District.

**BRYAN DISTRICT
FM-2818 SITE-5 (Final)**



A.112

Figure A.110. Variation of CBR Obtained from DCP Testing for Section-5 of Bryan District.

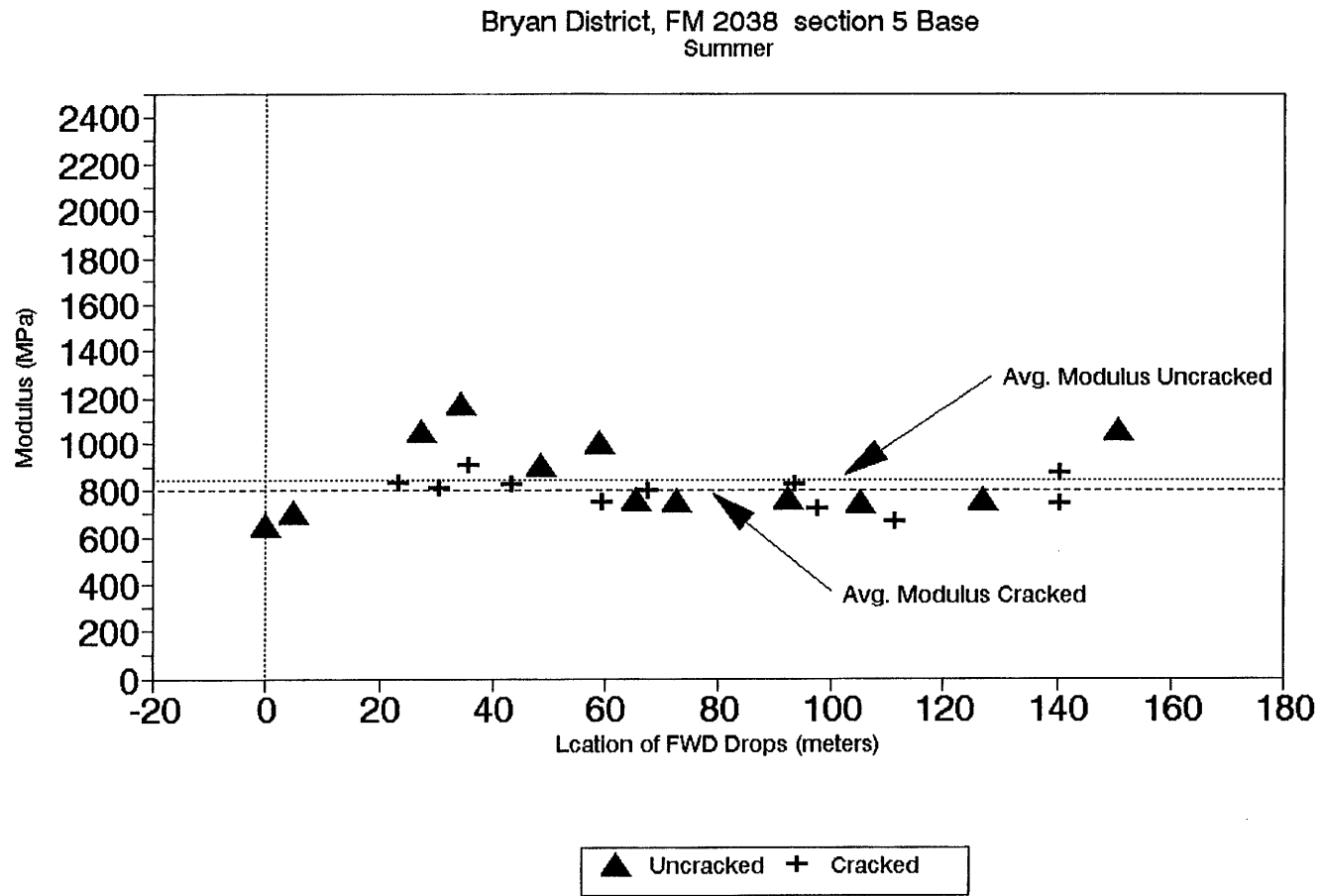


Figure A.111. Variation of Modulus of Stabilized Base within Test Section for Section-5 of Bryan District.

A.114

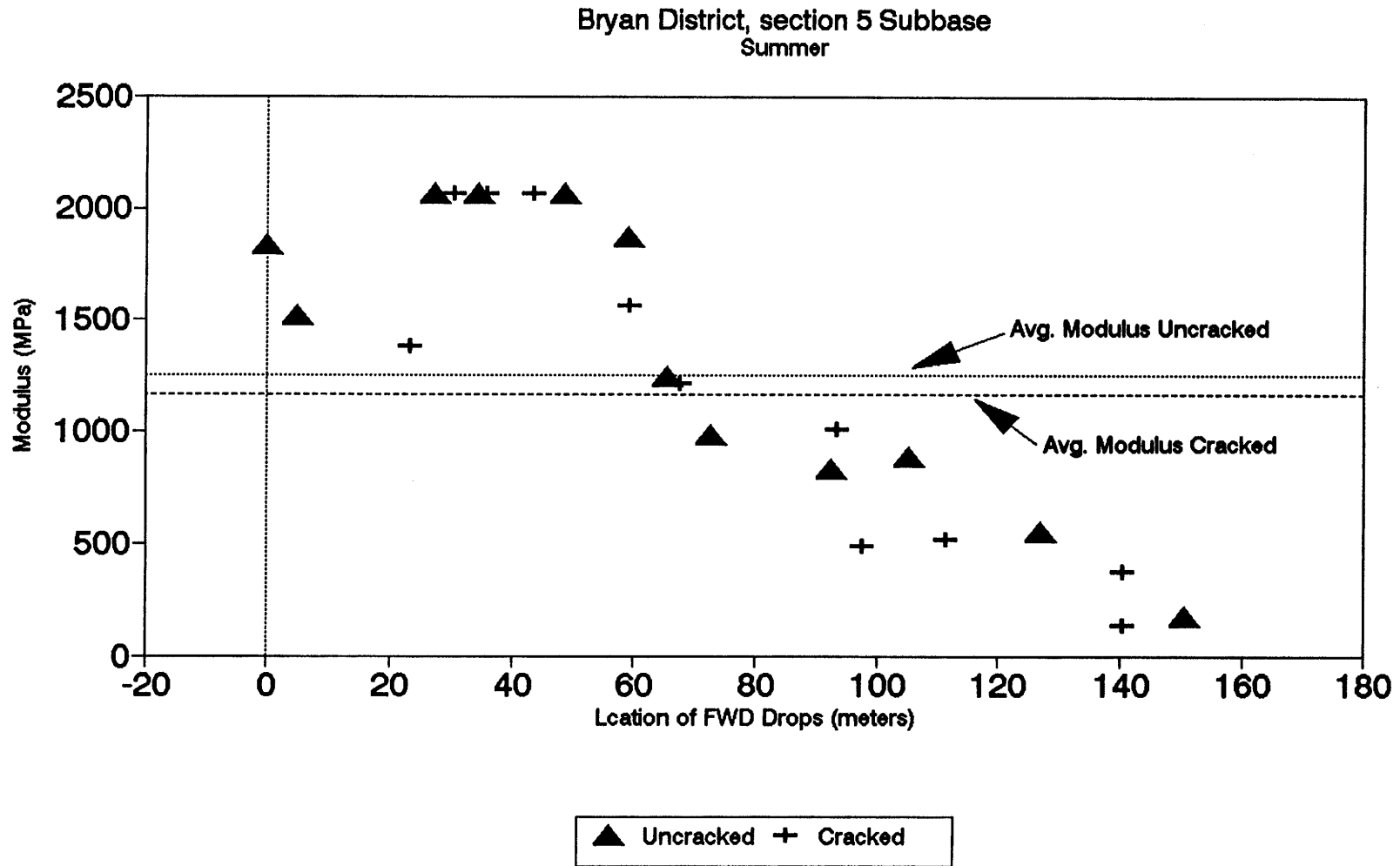


Figure A.112. Variation of Modulus of Stabilized Subbase within Test Section for Section-5 of Bryan District.

Section No.: 6 District: Bryan County: Brazos Highway: FM-2038
Structure: Seal Coat : 13 mm
CTS : 203 mm
Subgrade

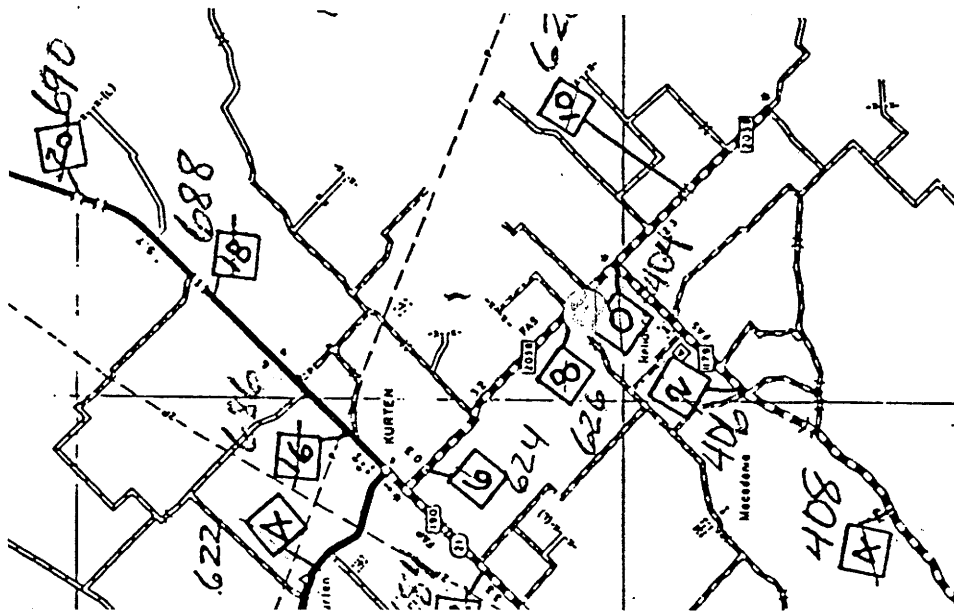
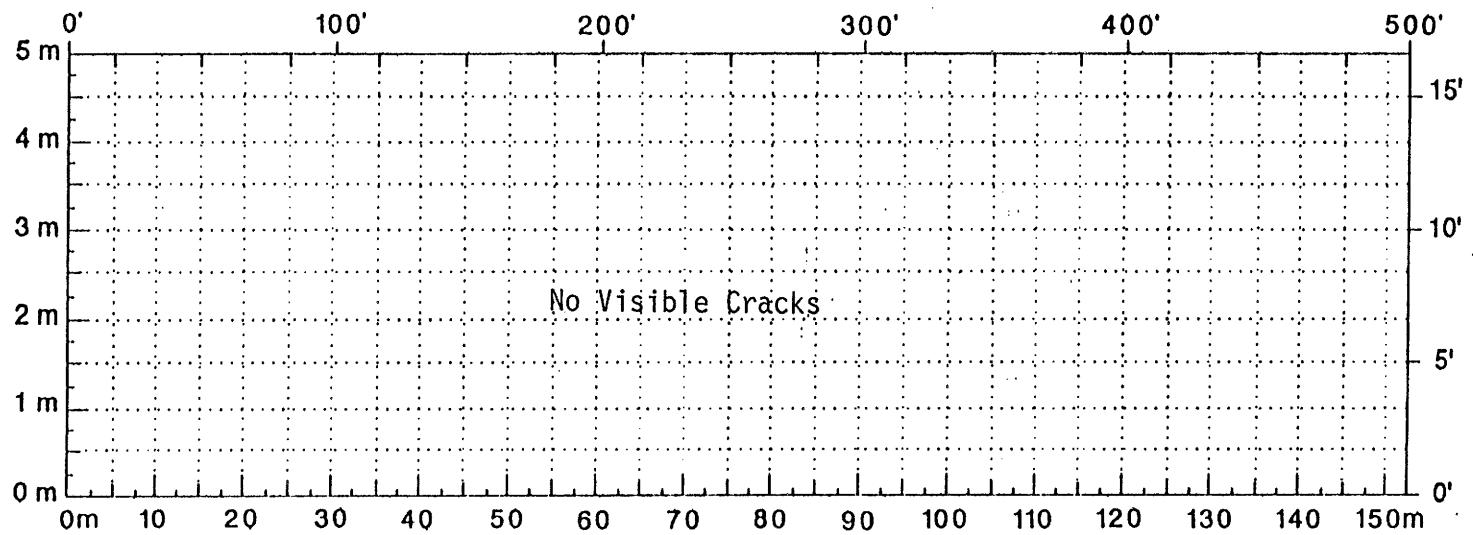


Figure A.113. Location and Details of Section-6 of Bryan District.

A.116



Comments: No Visible Cracks

Figure A.114. Crack Map for Section-6 of Bryan District.

TTI MODULUS ANALYSIS SYSTEM (SUMMARY REPORT)

(Version 4.2)

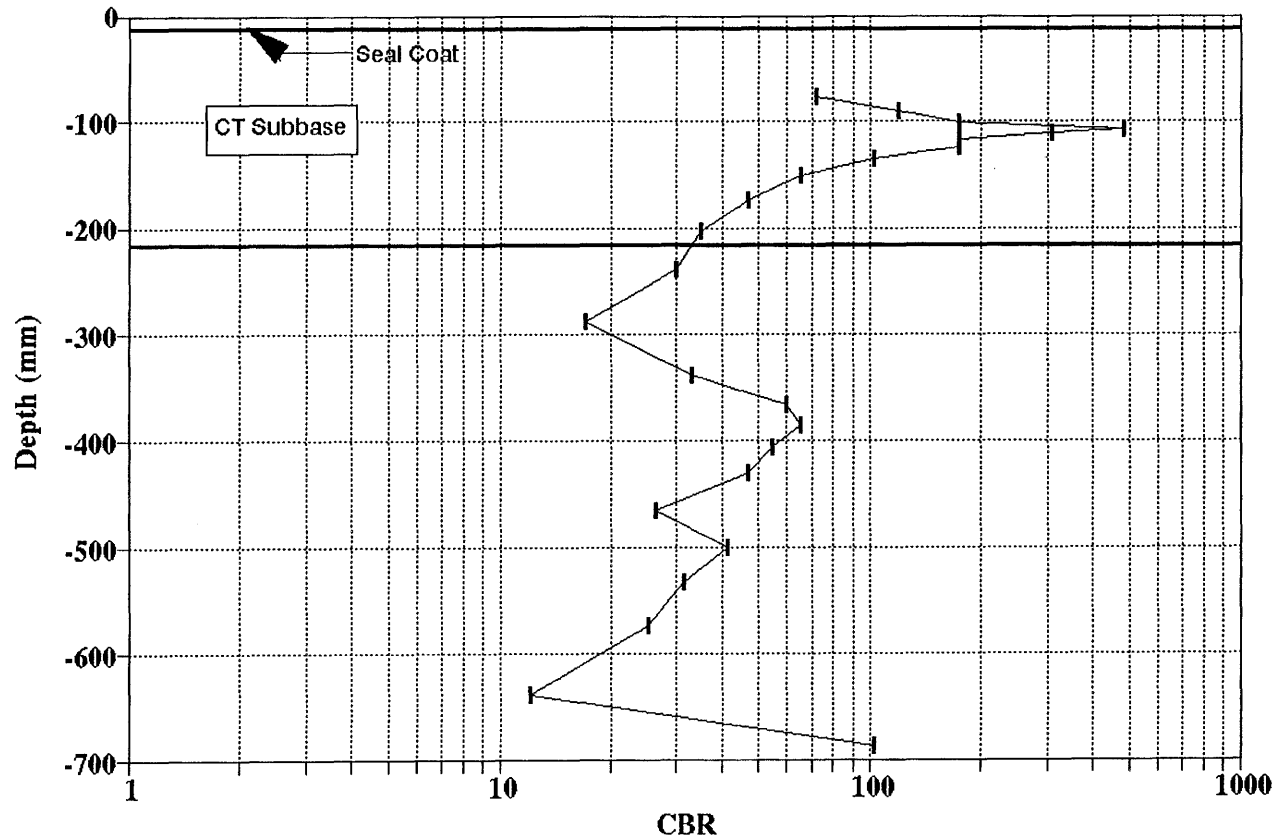
District:	0	MODULI RANGE(ksi)		Poisson Ratio Values	
County:	203	Thickness(in)	Minimum	Maximum	H1: u = 0.35
Highway/Road:		Pavement:	161,084	161,116	H2: u = 0.25
		Base:	10,000	300,000	H3: u = 0.25
		Subbase:	0	0	H4: u = 0.35
		Subgrade:	97.80	7,500	

Station	Load (lbs)	Measured Deflection (mils):							Calculated Moduli values (ksi):				Absolute Dpth to	
		R1	R2	R3	R4	R5	R6	R7	SURF(E1)	BASE(E2)	SUBB(E3)	SUBG(E4)	ERR/Sens	Bedrock
6911.000	14,880	53.32	34.80	17.94	9.56	5.94	3.98	3.09	161.	95.9	0.0	7.4	4.55	107.42
0.000	14,288	54.13	37.64	18.50	9.91	5.57	3.57	2.74	161.	87.9	0.0	6.9	5.08	108.86
26.000	14,364	46.92	34.38	18.23	8.96	4.89	3.31	3.03	161.	112.6	0.0	7.6	7.96	84.41
50.000	14,284	45.15	31.67	17.50	9.20	6.63	3.64	2.90	161.	140.3	0.0	7.3	4.96	102.24
80.000	14,368	40.67	30.31	17.25	8.89	5.07	3.52	2.97	161.	160.0	0.0	7.9	5.89	95.22
102.000	14,447	37.06	26.93	15.20	8.75	5.08	3.54	2.85	161.	195.7	0.0	8.5	4.04	113.45
126.000	14,336	36.70	27.56	16.91	9.69	5.45	3.35	2.63	161.	221.0	0.0	7.8	3.87	105.84
150.000	14,411	30.53	22.51	13.90	8.20	4.83	3.32	2.51	161.	297.2	0.0	9.1	2.75	116.72
175.000	14,193	56.34	33.41	16.45	8.22	4.99	3.48	2.79	161.	66.5	0.0	7.9	3.59	86.71
200.000	14,570	30.22	24.19	15.61	9.23	5.65	3.73	2.65	161.	300.0	0.0	8.4	4.19	136.86 †
226.000	14,535	32.92	19.91	10.32	5.48	3.33	2.34	2.02	161.	140.8	0.0	13.2	2.96	99.00
250.000	14,574	35.42	26.91	15.77	8.78	5.24	3.66	2.86	161.	228.5	0.0	8.3	4.65	125.70
275.000	14,511	44.87	32.82	19.26	10.85	6.31	4.08	2.86	161.	164.6	0.0	6.8	2.85	119.17
300.000	14,646	32.80	26.10	16.28	9.59	5.69	3.76	2.86	161.	300.0	0.0	7.9	3.34	122.12 †
325.000	14,511	42.21	28.75	17.35	9.75	5.83	4.03	3.09	161.	173.2	0.0	7.6	2.66	128.63
351.000	14,149	65.09	40.91	20.79	10.41	5.86	4.13	3.28	161.	62.1	0.0	6.2	4.88	90.65
375.000	13,998	69.15	44.52	23.62	12.41	7.14	5.09	3.96	161.	66.7	0.0	5.3	5.00	108.95
400.000	14,264	51.10	35.58	20.29	11.33	6.58	4.17	3.09	161.	123.7	0.0	6.4	2.22	120.63
425.000	14,213	68.50	41.18	20.24	10.76	5.42	3.68	2.93	161.	53.8	0.0	6.4	4.15	89.70
450.000	14,121	80.20	44.01	16.63	7.79	4.78	3.85	3.30	161.	30.8	0.0	7.1	10.71	71.41
475.000	14,074	72.46	38.59	16.00	8.89	6.07	4.73	3.74	161.	39.4	0.0	7.2	11.41	102.76
500.000	13,955	96.11	49.95	18.94	10.03	7.54	5.49	4.45	161.	25.3	0.0	5.8	14.46	72.31
525.000	14,101	74.24	48.57	21.87	11.45	7.31	5.00	3.76	161.	52.7	0.0	5.4	8.27	105.41
Mean:		52.00	33.97	17.60	9.48	5.70	3.89	3.06	161.	136.5	0.0	7.5	5.41	106.29
Std. Dev:		18.05	8.24	2.79	1.43	0.95	0.68	0.52	0.	87.4	0.0	1.6	3.13	18.83
Var Coeff(%):		34.70	24.26	15.87	15.10	16.64	17.53	16.97	0.	64.0	0.0	21.0	57.80	17.72

A.117

Figure A.115. FWD Back-Calculation Results for Uncracked Portion of Section-6 of Bryan District.

**BRYAN DISTRICT
FM-2038 SITE-6 (Final)**



A.118

Figure A.116. Variation of CBR Obtained from DCP Testing for Section-6 of Bryan District.

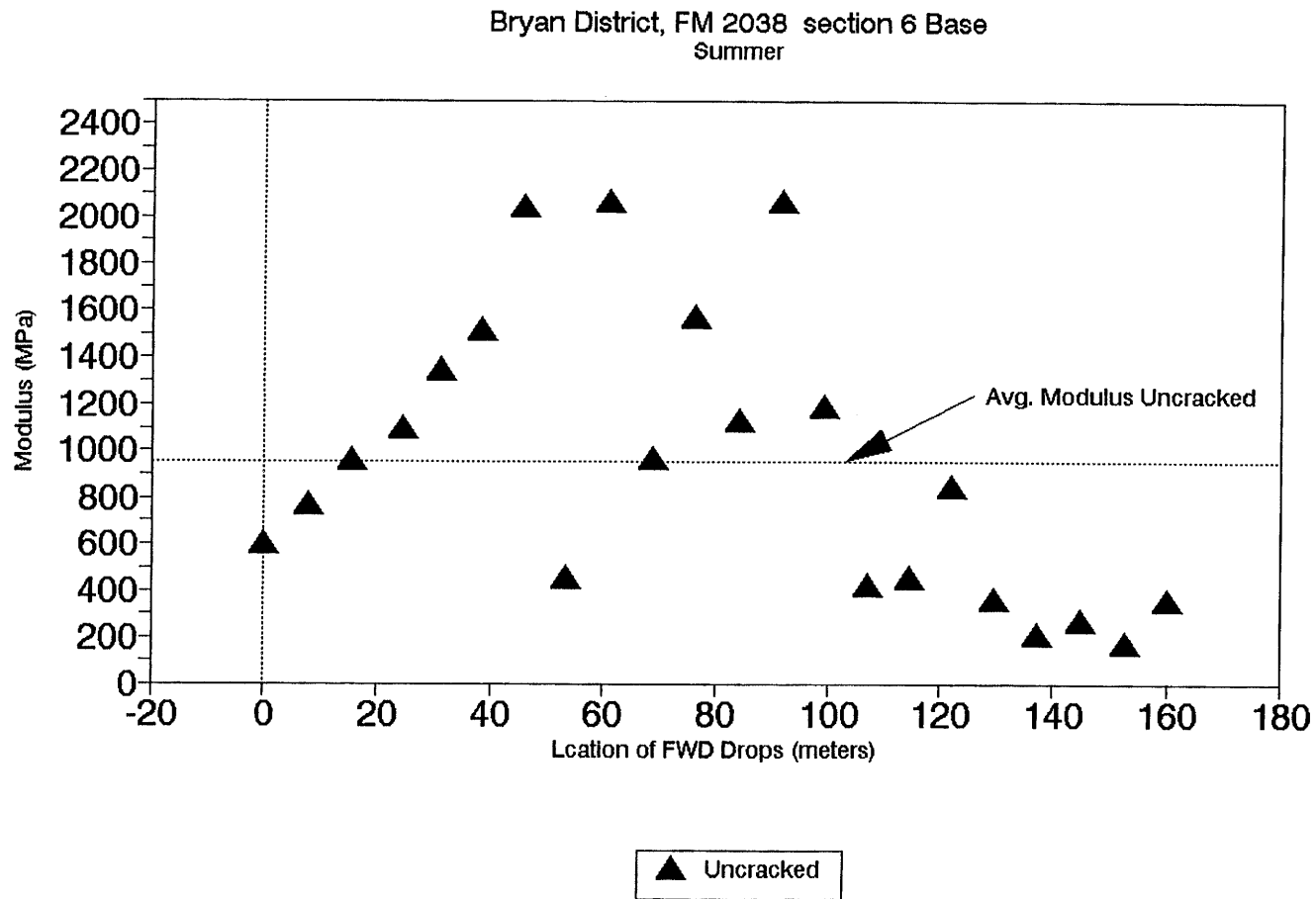


Figure A.117. Variation of Modulus of Stabilized Base within Test Section for Section-6 of Bryan District.

Section No.: 1 District: Atlanta County: Bowie Highway: FM-2516
Structure: Asphalt : 70 mm
LTB : 254 mm
Subgrade

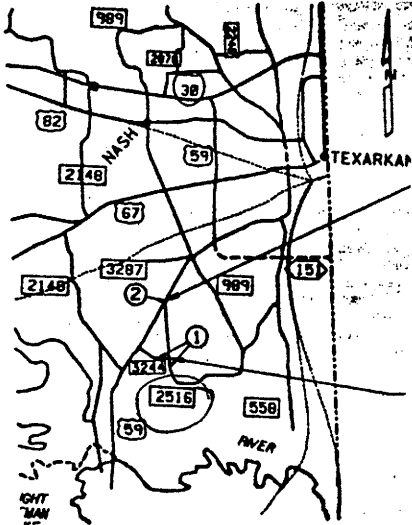
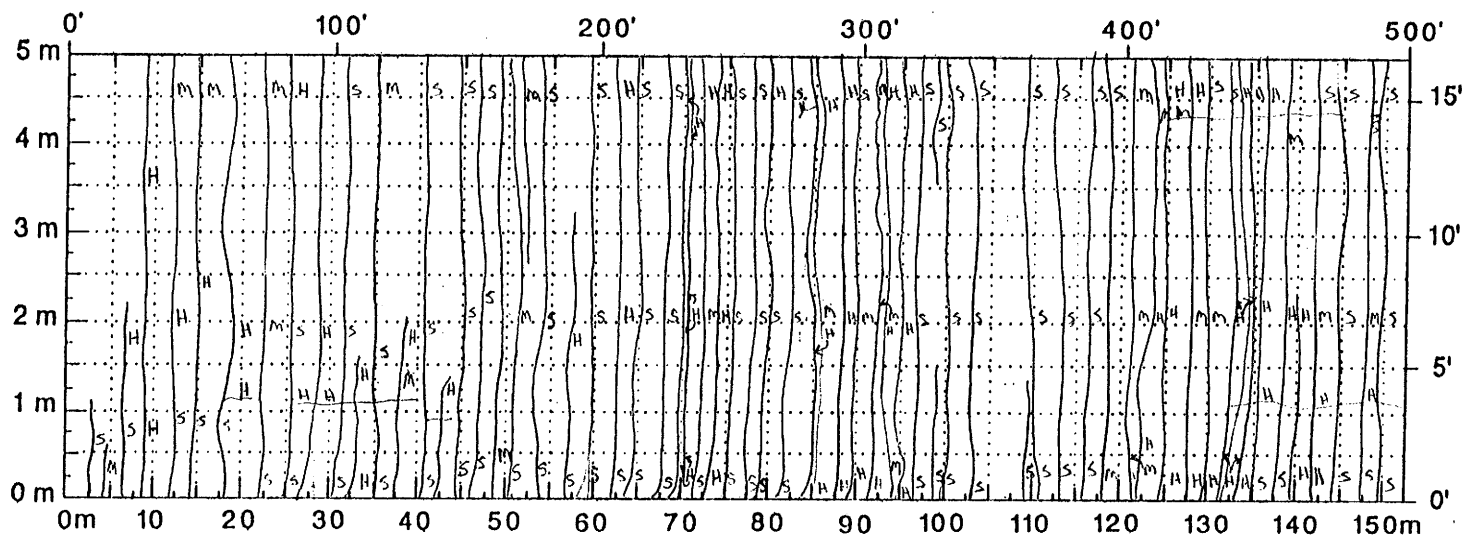


Figure A.118. Location and Details of Section-1 of Atlanta District.

A.121



Comments: _____

Figure A.119. Crack Map for Section-1 of Atlanta District.

TTI MODULUS ANALYSIS SYSTEM (SUMMARY REPORT)

(Version 4.2)

District: 19		MODULI RANGE(psi)		
County: 19		Minimum	Maximum	Poisson Ratio Values
Highway/Road: FM2516	Pavement: 2.80	591,941	592,059	H1: j = 0.35
	Base: 10.00	200,000	2,000,000	H2: j = 0.25
	Subbase: 0.00	0	0	H3: j = 0.25
	Subgrade: 287.20		20,000	H4: j = 0.35

Station	Load (lbs)	Measured Deflection (mils):							Calculated Moduli values (ksi):				Absolute Dpth to ERR/Sens Bedrock
		R1	R2	R3	R4	R5	R6	R7	SURF(E1)	BASE(E2)	SUBB(E3)	SUBG(E4)	
0.000	12,895	8.43	7.53	6.16	4.77	3.71	2.90	2.28	592.	1252.3	0.0	16.9	2.43 300.00
39.000	12,495	8.63	7.41	5.79	4.52	3.48	2.77	2.32	592.	977.3	0.0	17.7	1.57 300.00
85.000	12,423	7.41	6.79	5.50	4.24	3.32	2.56	2.07	592.	1432.0	0.0	18.3	3.10 300.00
135.000	12,295	8.96	7.61	6.33	4.93	3.94	3.15	2.44	592.	1145.8	0.0	15.3	1.13 300.00
194.000	12,271	7.86	7.00	5.41	4.08	3.13	2.44	1.95	592.	1002.8	0.0	19.2	2.85 300.00
237.000	12,127	7.04	6.09	5.29	4.24	3.29	2.56	2.07	592.	1805.8	0.0	18.1	1.97 300.00 †
271.000	12,039	7.29	6.09	5.00	3.87	3.01	2.35	1.91	592.	1270.0	0.0	19.8	0.94 300.00
320.000	12,079	7.98	6.63	5.54	4.36	3.48	2.69	1.87	592.	1281.3	0.0	17.3	0.54 206.27
357.000	12,055	8.47	7.49	6.12	4.65	3.48	2.60	1.91	592.	928.6	0.0	16.9	3.77 268.63
386.000	12,039	7.74	6.79	5.58	4.36	3.32	2.48	1.71	592.	1179.7	0.0	17.9	2.94 200.11
422.000	12,071	6.52	5.72	4.91	3.91	3.09	2.48	1.95	592.	1933.5	0.0	19.3	1.64 300.00 †
462.000	11,967	7.94	7.00	5.79	4.52	3.48	2.65	1.99	592.	1204.5	0.0	16.8	2.57 300.00
Mean:		7.86	6.85	5.62	4.37	3.39	2.64	2.04	592.	1284.5	0.0	17.8	2.12 300.00
Std. Dev:		0.71	0.62	0.44	0.33	0.26	0.22	0.21	0.	309.4	0.0	1.3	0.98 173.56
Var Coeff(%):		9.03	9.13	7.90	7.48	7.74	8.38	10.33	0.	24.1	0.0	7.1	46.42 57.85

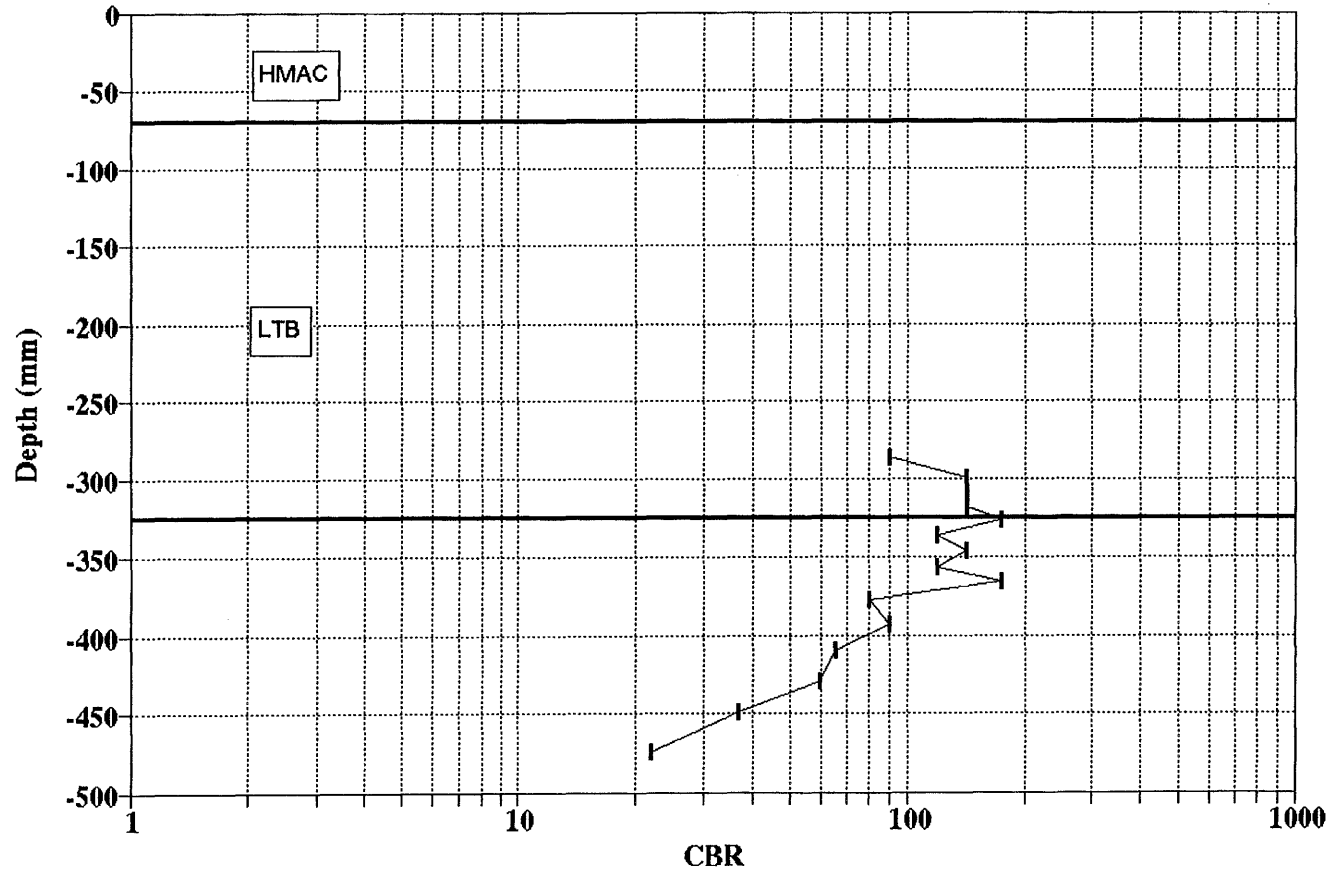
A.122

Figure A.120. FWD Back-Calculation Results for Uncracked Portion of Section-1 of Atlanta District.

FWD MODULUS ANALYSIS SYSTEM (SUMMARY REPORT)													(Version 4.2)	
District:	19								MODULI RANGE(psi)					
County:	19		Thickness(in)						Minimum	Maximum	Poisson Ratio Values			
Highway/Road:	FM2516		Pavement:	2.80				591.941	592.059	H1: $\mu = 0.35$				
			Base:	10.00				200,000	2,000,000	H2: $\mu = 0.25$				
			Subbase:	0.00				0	0	H3: $\mu = 0.25$				
			Subgrade:	287.20				20,000		H4: $\mu = 0.35$				
Station	Load (lbs)	Measured Deflection (mils):							Calculated Moduli values (ksi):				Absolute Dpth to	
		R1	R2	R3	R4	R5	R6	R7	SURF(E1)	BASE(E2)	SUBB(E3)	SUBG(E4)	ERR/Sens	Bedrock
22.000	11,911	9.49	7.16	5.54	4.08	3.29	2.56	2.15	592.	581.3	0.0	18.9	2.68	300.00
46.000	11,999	8.67	7.53	5.50	4.24	3.29	2.65	2.15	592.	779.3	0.0	18.1	3.13	300.00
99.000	11,983	9.45	7.33	5.75	4.32	3.25	2.56	2.03	592.	603.0	0.0	18.5	0.96	300.00
207.000	11,839	10.83	7.94	5.91	4.16	3.13	2.44	2.03	592.	345.7	0.0	19.1	1.69	300.00
265.000	11,847	8.31	6.09	4.66	3.55	2.71	2.10	1.75	592.	643.8	0.0	22.7	2.13	300.00
314.000	11,743	9.57	6.34	4.91	3.75	3.01	2.39	1.95	592.	499.0	0.0	21.1	6.03	300.00
370.000	11,679	9.77	7.20	5.58	4.08	3.05	2.31	1.83	592.	453.7	0.0	19.5	0.86	300.00
414.000	11,647	8.35	6.09	5.04	3.95	3.13	2.48	1.99	592.	892.1	0.0	19.1	3.29	300.00
Mean:		9.31	6.96	5.36	4.02	3.11	2.44	1.98	592.	599.7	0.0	19.6	2.60	300.00
Std. Dev:		0.84	0.70	0.44	0.26	0.19	0.17	0.14	0.	175.7	0.0	1.5	1.66	69.97
Var Coeff(%):		9.06	10.04	8.19	6.41	6.19	7.10	7.10	0.	29.3	0.0	7.7	63.93	23.32

Figure A.121. FWD Back-Calculation Results for Cracked Portion of Section-1 of Atlanta District.

ATLANTA DISTRICT
FM-2516 SITE-1



A.124

Figure A.122. Variation of CBR Obtained from DCP Testing for Section-1 of Atlanta District.

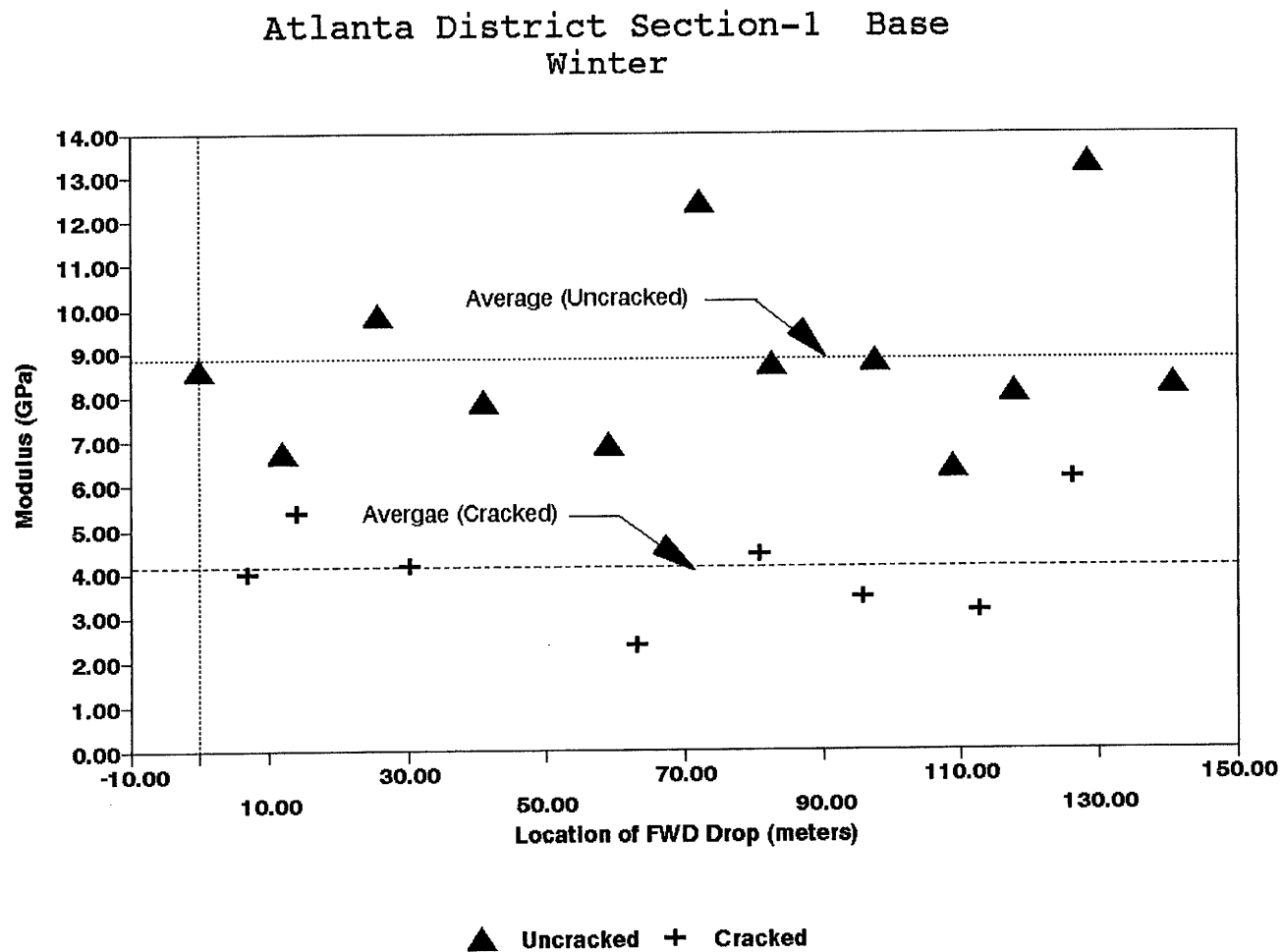


Figure A.123. Variation of Modulus of Stabilized Base within Test Section for Section-1 of Atlanta District.

Section No.: 2 District: Atlanta County: Bowie Highway: SH-8
Structure: Asphalt : 44 mm
LFA Base : 254 mm
Select Mat'l : 300 mm
Subgrade

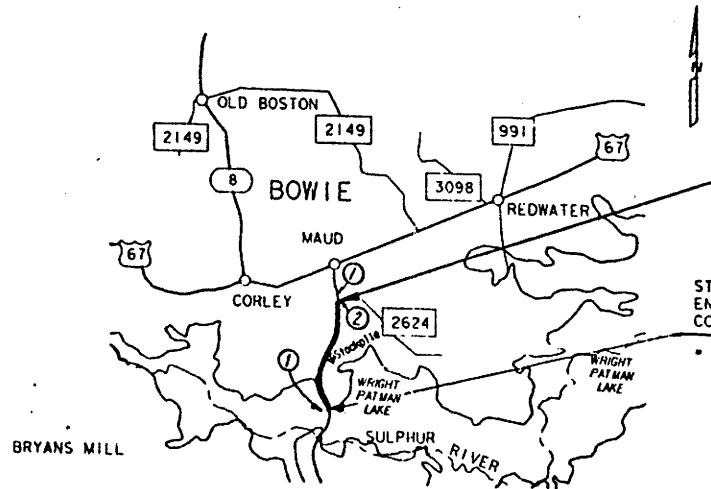
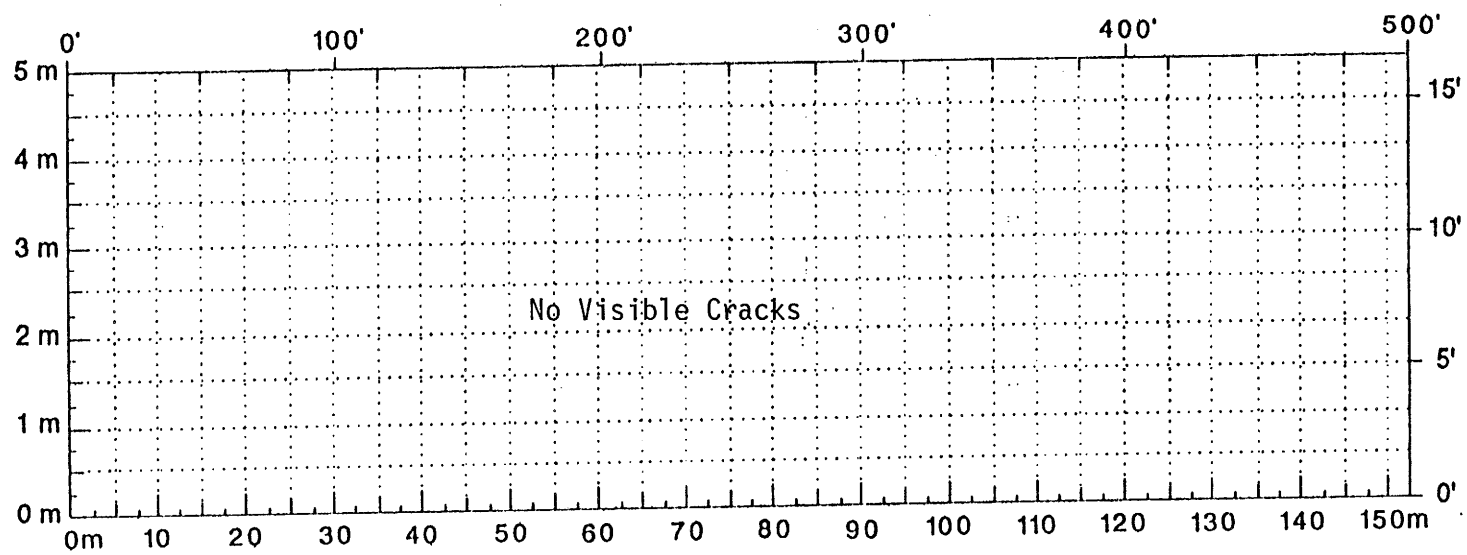


Figure A.124. Location and Details of Section-2 of Atlanta District.

A.127



Comments: No Visible Cracks

Figure A.125. Crack Map for Section-2 of Atlanta District.

TTI MODULUS ANALYSIS SYSTEM (SUMMARY REPORT)

(Version 4.2)

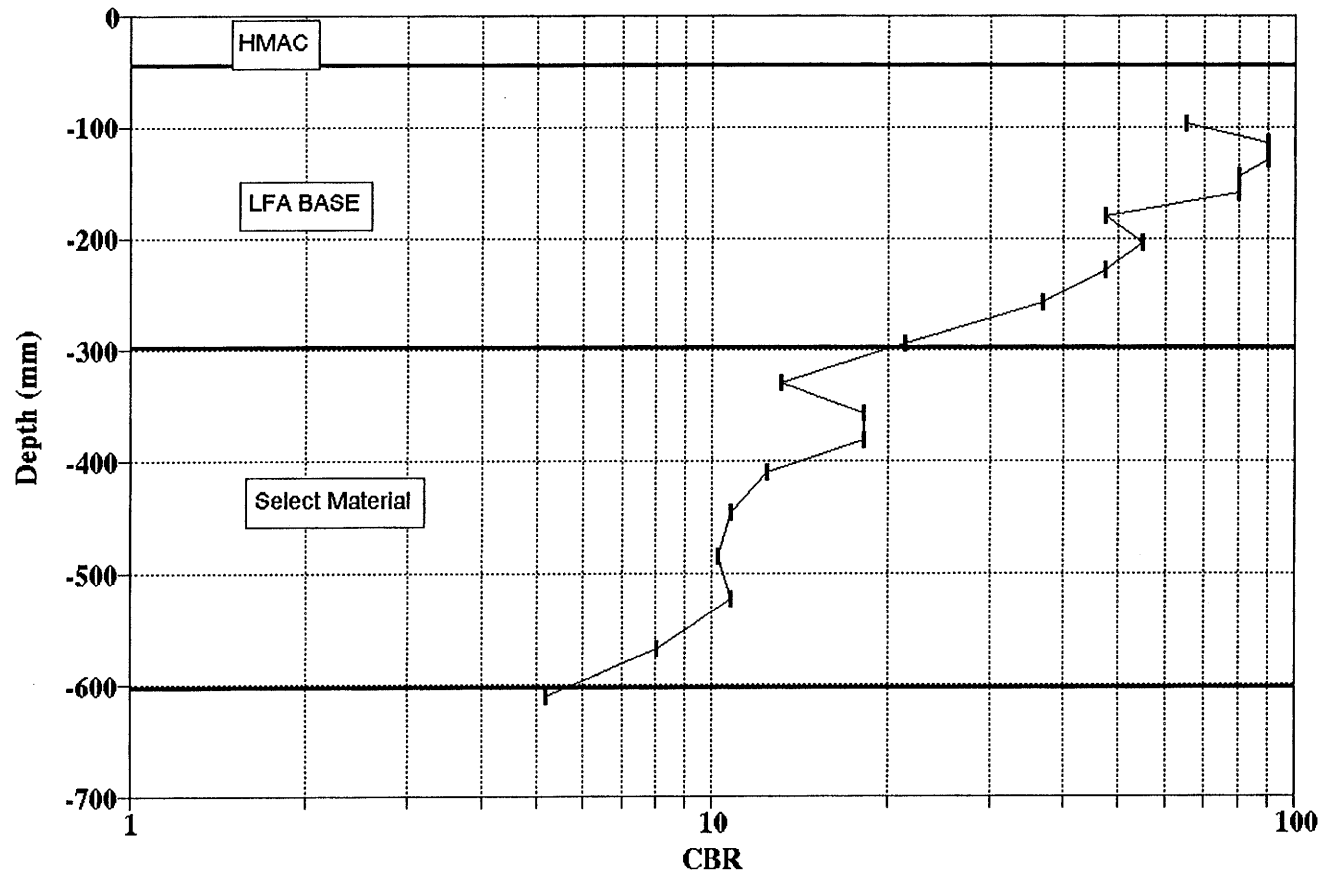
District: 19	MODULI RANGE(psi)	
County: 19	Thickness(in)	Minimum Maximum
Highway/Road: SH0008	Pavement: 1.80	867,513 867,687
	Base: 10.00	5,000 400,000
	Subbase: 12.00	5,000 300,000
	Subgrade: 74.00	10,000
		Poisson Ratio Values
		H1: J = 0.35
		H2: J = 0.25
		H3: J = 0.35
		H4: J = 0.35

Station	Load (lbs)	Measured Deflection (mils):							Calculated Moduli values (ksi):				Absolute Dpth to	
		R1	R2	R3	R4	R5	R6	R7	SURF(E1)	BASE(E2)	SUBB(E3)	SUBG(E4)	ERR/Sens	Bedrock
0.000	11,711	39.38	19.67	8.79	4.61	3.32	2.52	2.03	868.	23.2	15.8	8.9	7.55	112.94
16.000	11,503	39.54	19.47	8.58	4.65	3.09	2.31	1.91	868.	22.5	14.6	9.3	6.88	108.05
49.000	11,639	40.76	19.26	8.20	4.28	2.90	2.27	1.91	868.	20.2	16.4	9.9	7.67	93.09
82.000	11,527	55.34	24.04	9.29	4.56	2.98	2.35	2.03	868.	10.8	16.7	9.0	6.89	73.16
115.000	11,495	53.91	25.40	9.29	4.48	3.13	2.48	2.15	868.	12.0	13.2	9.0	9.66	63.46
150.000	11,431	63.08	28.24	9.49	4.28	3.09	2.69	2.32	868.	8.1	15.6	8.8	10.31	56.97
178.000	11,487	49.60	15.02	6.79	4.65	3.29	2.52	1.99	868.	9.8	248.0	8.3	5.74	186.78 †
217.000	11,519	49.64	23.67	9.83	5.14	3.56	2.77	2.44	868.	14.5	15.5	8.0	7.57	95.46
248.000	11,335	42.06	22.35	9.78	5.26	3.44	2.69	2.24	868.	22.4	10.8	8.2	8.43	106.31
283.000	11,383	42.92	24.94	11.24	5.58	3.79	3.02	2.60	868.	25.4	7.7	7.7	10.15	83.55
313.000	11,407	52.45	27.04	10.87	5.54	3.86	3.15	2.72	868.	14.2	11.6	7.3	9.77	86.43
346.000	11,359	36.49	21.77	10.24	5.42	3.79	3.02	2.56	868.	33.8	9.1	8.1	10.50	100.33
379.000	11,407	36.04	22.27	10.99	5.71	3.86	3.15	2.64	868.	38.0	7.9	7.9	10.14	94.78
413.000	11,367	44.96	23.34	10.37	5.71	4.06	3.28	2.76	868.	18.4	14.9	7.0	8.56	119.22
444.000	11,263	38.89	16.71	8.24	5.18	3.79	3.02	2.52	868.	16.7	62.9	7.0	4.96	300.00
481.000	11,103	56.60	29.84	14.24	7.50	4.83	3.78	3.21	868.	14.5	9.1	5.5	6.61	103.77
510.000	11,295	49.07	24.49	10.74	5.99	4.25	3.32	2.76	868.	15.0	16.6	6.6	7.43	128.32
Mean:		46.51	22.80	9.82	5.22	3.59	2.84	2.40	868.	18.8	29.8	8.0	8.17	97.79
Std. Dev:		7.93	3.93	1.64	0.80	0.51	0.42	0.37	0.	8.2	57.6	1.1	1.70	32.23
Var Coeff(%):		17.05	17.22	16.68	15.24	14.28	14.78	15.36	0.	43.5	100.0	13.6	20.81	32.96

A.128

Figure A.126. FWD Back-Calculation Results for Uncracked Portion of Section-2 of Atlanta District.

ATLANTA DISTRICT
SH-8 SITE-2



A.129

Figure A.127. Variation of CBR Obtained from DCP Testing for Section-2 of Atlanta District.

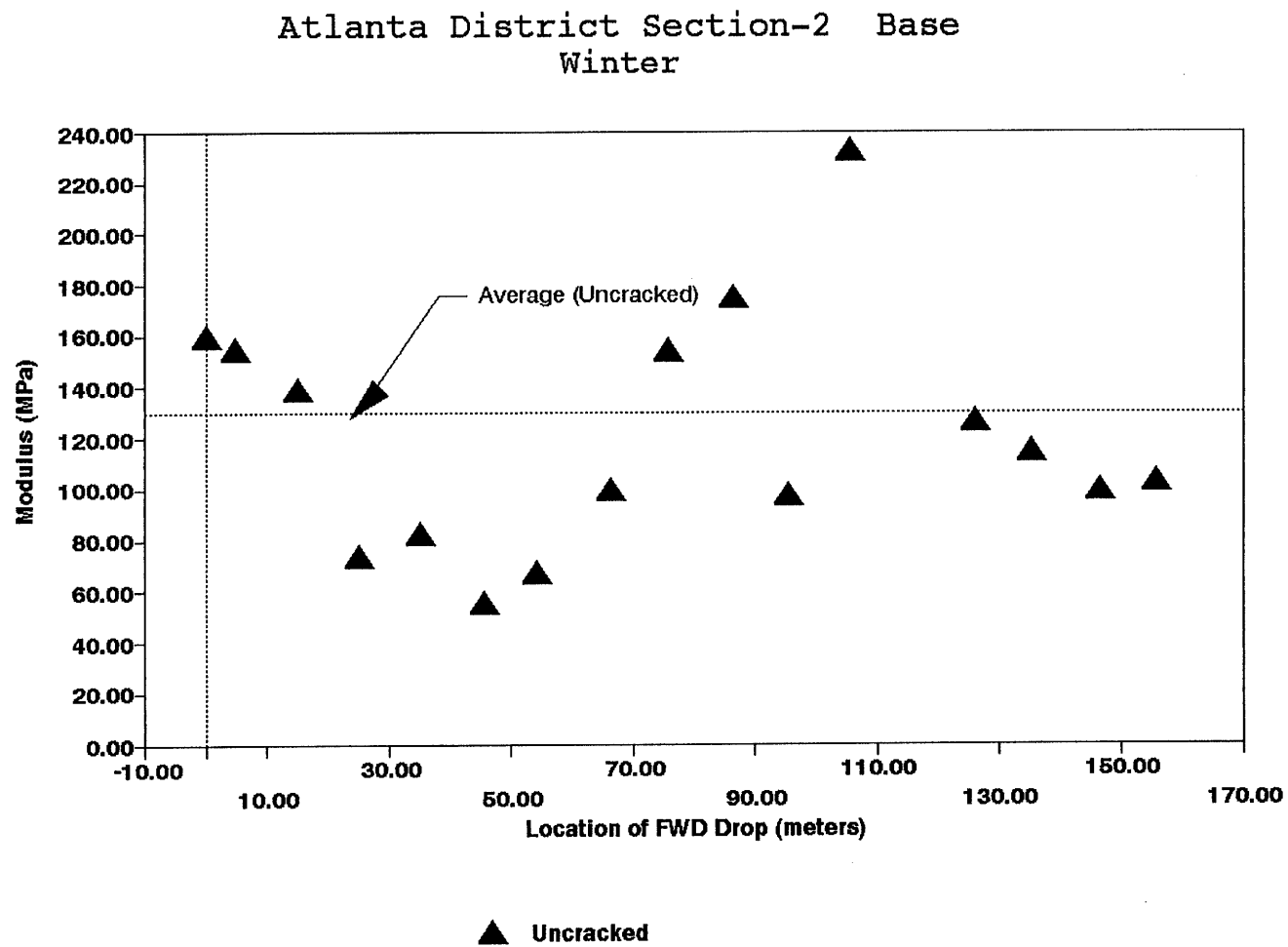


Figure A.128. Variation of Modulus of Stabilized Base within Test Section for Section-2 of Atlanta District.

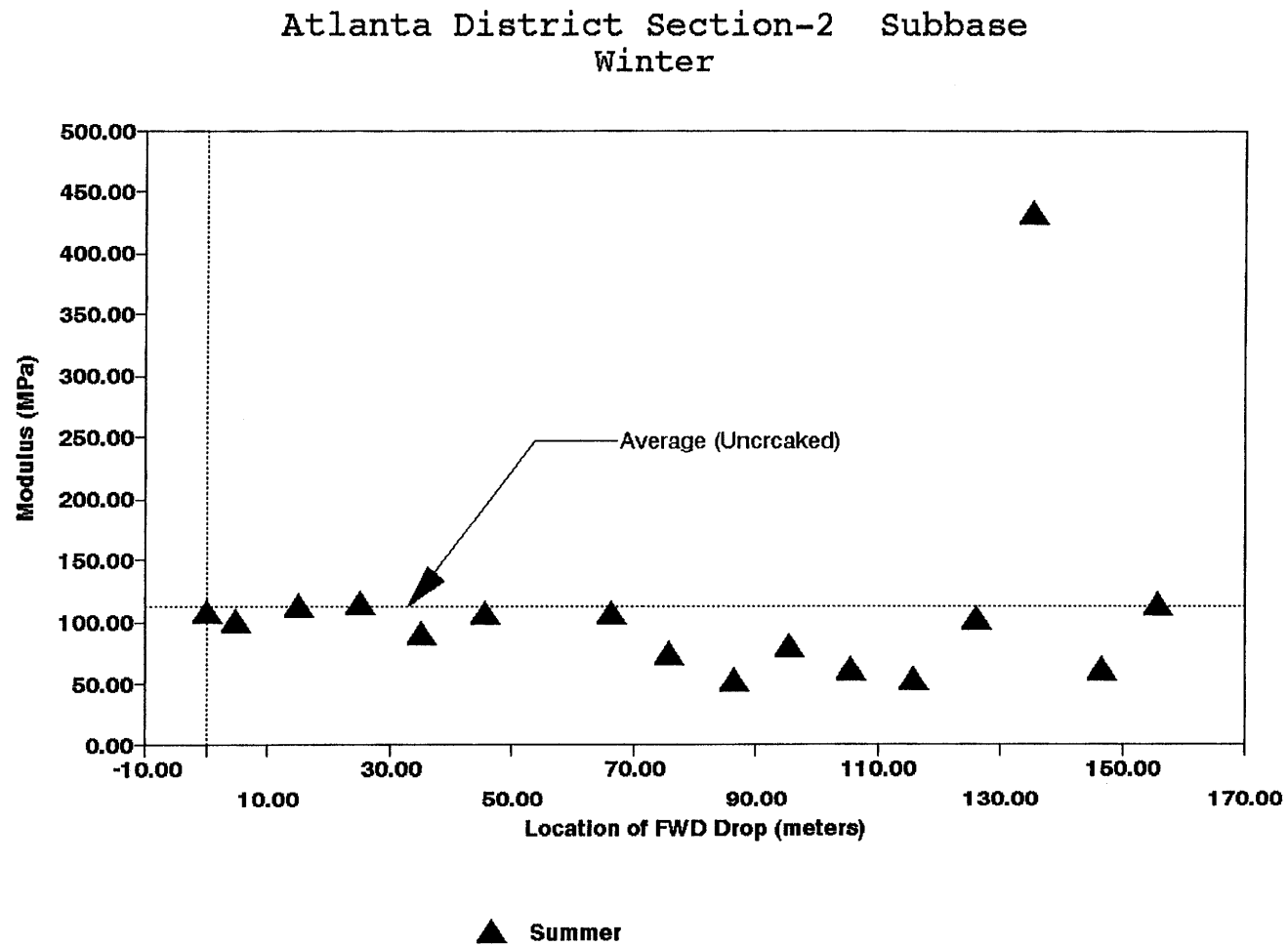


Figure A.129. Variation of Modulus of Stabilized Subbase within Test Section for Section-2 of Atlanta District.

Section No.: 3 District: Atlanta County: Cass Highway: SH-8
Structure: Asphalt : 70 mm
LFA Base : 254 mm
Subgrade

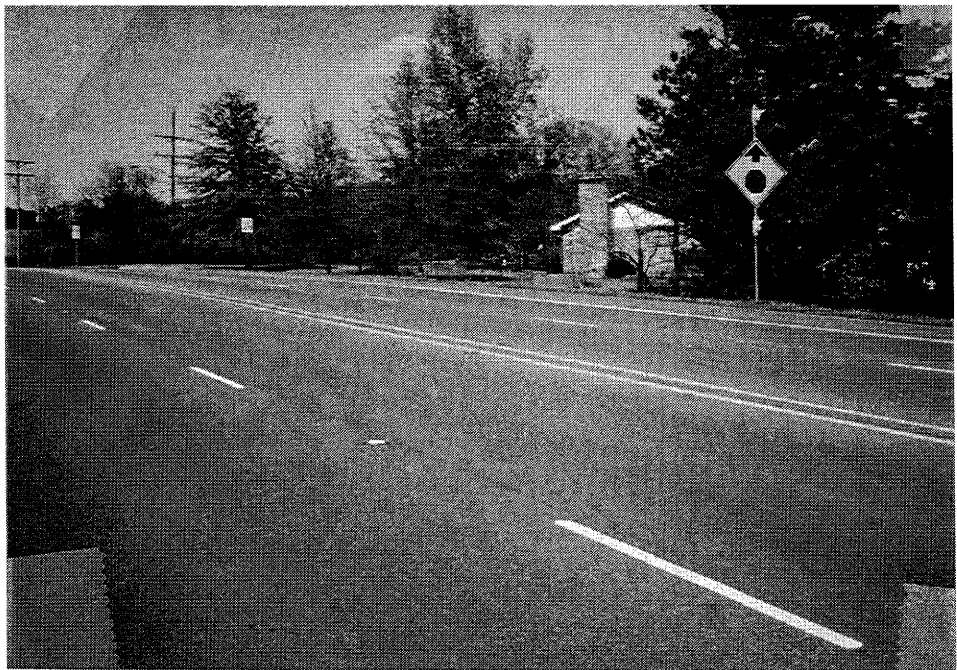
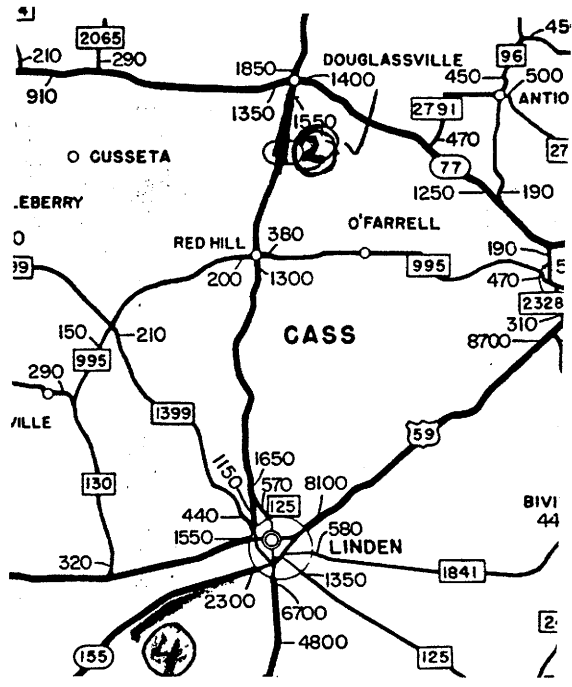
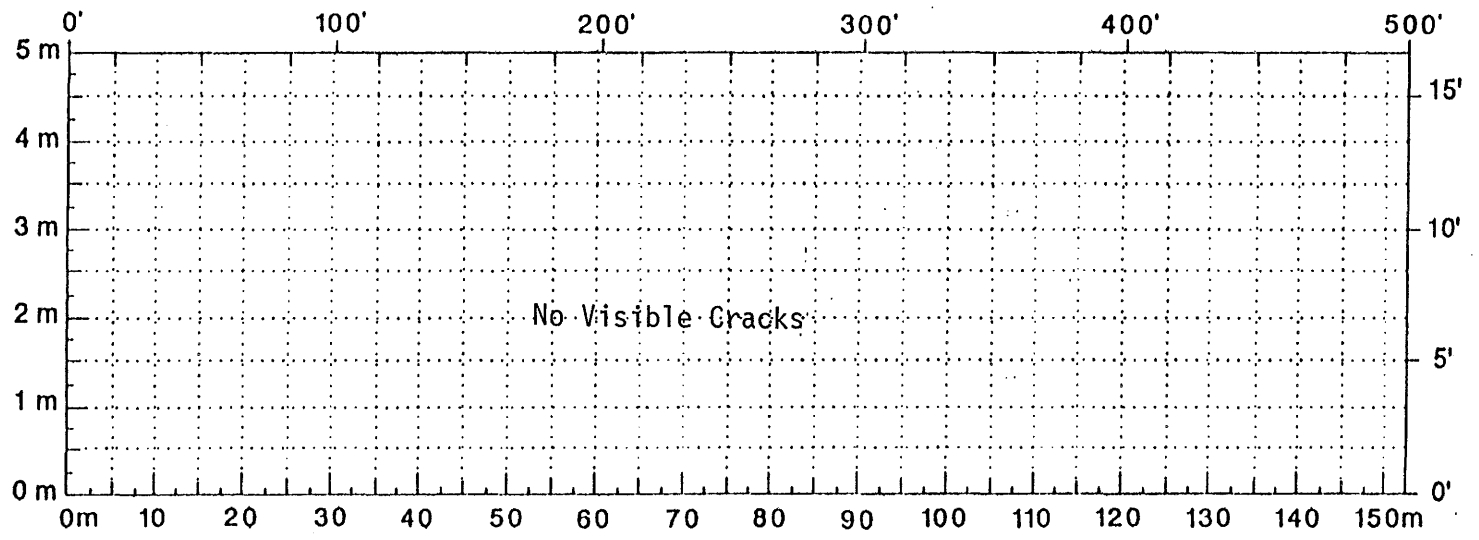


Figure A.130. Location and Details of Section-3 of Atlanta District.

A.133



Comments: No Visible Cracks

Figure A.131. Crack Map for Section-3 of Atlanta District.

TTI MODULUS ANALYSIS SYSTEM (SUMMARY REPORT)

(Version 4.2)

District: 19									MODULI RANGE(psi)					
County: 34									Minimum	Maximum	Poisson Ratio Values			
Highway/Road: SH0008		Thickness(in)									H1: J = 0.35	H2: J = 0.25	H3: J = 0.25	H4: J = 0.35
		Pavement:	2.80						614,938	615,062				
		Base:	10.00						20,000	400,000				
		Subbase:	0.00						0	0				
		Subgrade:	76.20						20,000					
Station	Load (lbs)	Measured Deflection (mils):							Calculated Moduli values (ksi):				Absolute Dpth to Bedrock	
		R1	R2	R3	R4	R5	R6	R7	SURF(E1)	BASE(E2)	SUBB(E3)	SUBG(E4)	ERR/Sens	Bedrock
0.000	11,367	38.85	20.74	8.45	4.12	2.55	1.97	1.67	615.	20.0	0.0	9.6	11.38	82.13 †
36.000	11,359	36.12	19.43	8.04	4.12	2.71	2.06	1.67	615.	20.0	0.0	10.2	11.24	93.53 †
67.000	11,407	39.25	20.37	8.24	3.99	2.55	2.02	1.71	615.	20.0	0.0	9.8	12.18	80.93 †
105.000	11,351	38.89	21.90	8.70	4.16	2.67	2.06	1.75	615.	20.0	0.0	9.2	12.26	78.66 †
133.000	11,327	37.30	21.03	8.58	4.20	2.71	2.06	1.75	615.	20.0	0.0	9.5	10.79	82.84 †
165.000	11,295	37.83	21.20	8.66	4.12	2.59	2.02	1.67	615.	20.0	0.0	9.4	11.20	77.96 †
198.000	11,319	36.49	21.61	9.24	4.61	2.86	2.23	1.83	615.	20.1	0.0	9.1	9.58	86.73
232.000	11,287	40.23	23.50	9.70	4.69	2.86	2.14	1.83	615.	20.0	0.0	8.3	11.51	80.38 †
264.000	11,215	40.64	23.54	9.87	4.69	2.94	2.27	1.75	615.	20.0	0.0	8.1	12.17	77.59 †
297.000	11,215	42.88	23.87	9.37	4.61	2.86	2.23	1.87	615.	20.0	0.0	8.1	14.94	80.49 †
331.000	11,231	40.68	22.35	9.12	4.40	2.78	2.14	1.75	615.	20.0	0.0	8.6	12.77	80.09 †
364.000	11,207	39.46	20.42	8.54	4.40	2.86	2.18	1.79	615.	20.0	0.0	9.1	11.69	94.92 †
397.000	11,239	29.44	16.88	8.24	4.73	3.17	2.35	1.87	615.	35.1	0.0	9.4	10.03	155.63
429.000	11,151	28.83	16.26	8.41	5.30	3.79	2.86	2.24	615.	43.8	0.0	8.5	12.96	300.00
463.000	11,071	36.16	20.25	9.45	5.09	3.29	2.39	1.95	615.	22.8	0.0	8.4	8.91	111.25
495.000	11,111	33.84	17.62	7.66	4.24	2.78	2.06	1.71	615.	22.5	0.0	10.2	11.15	125.99
Mean:		37.31	20.69	8.77	4.47	2.87	2.19	1.80	615.	22.8	0.0	9.1	11.55	89.03
Std. Dev:		3.87	2.27	0.63	0.37	0.32	0.22	0.14	0.	6.8	0.0	0.7	1.42	23.54
Var Coeff(%):		10.38	10.96	7.16	8.39	11.04	9.89	7.92	0.	29.7	0.0	7.7	12.33	26.44

A.134

Figure A.132. FWD Back-Calculation Results for Uncracked Portion Section-3 of Atlanta District.

A.135

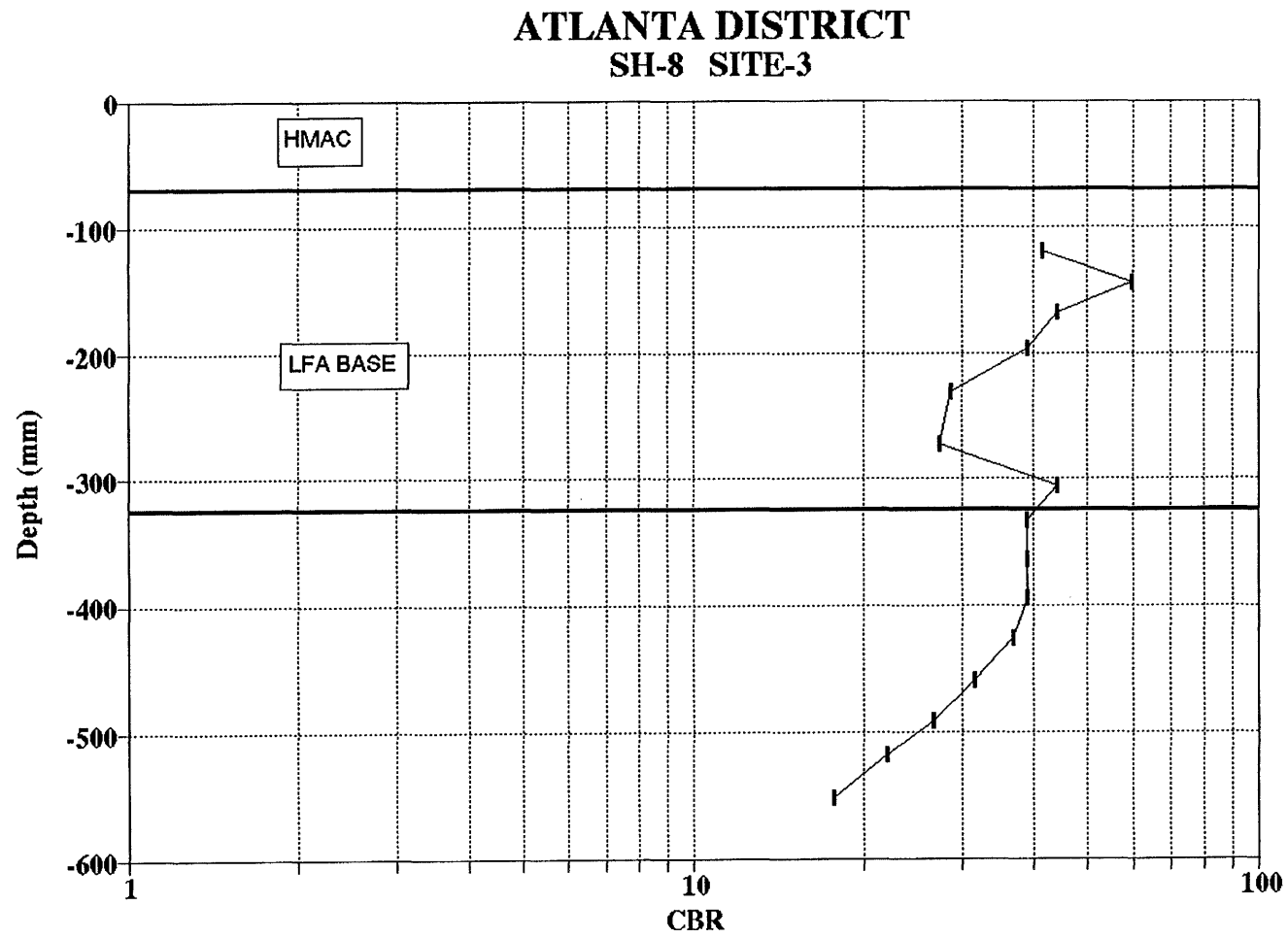
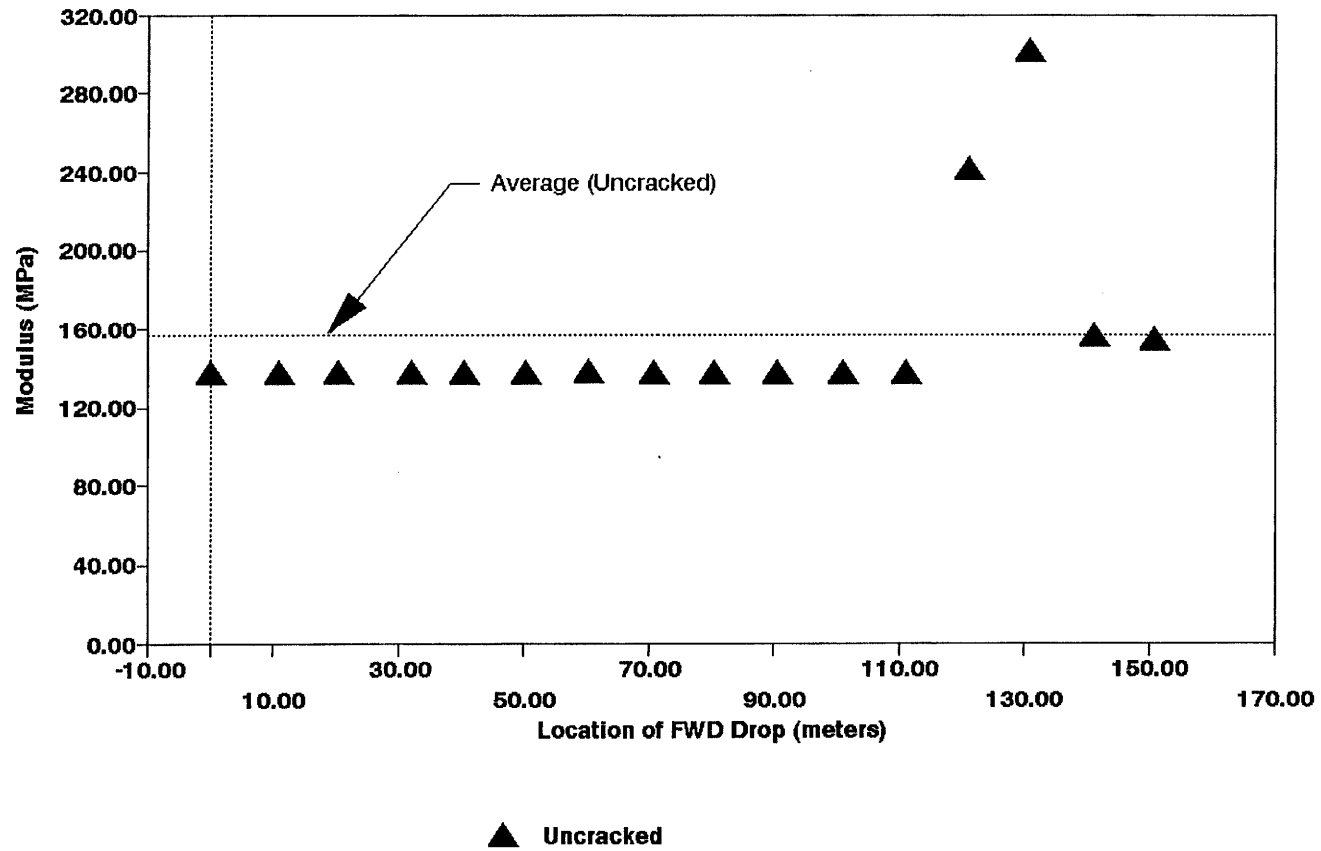


Figure A.133. Variation of CBR Obtained from DCP Testing for Section-3 of Atlanta District.

Atlanta District Section-3 Base
Winter



A.136

Figure A.134. Variation of Modulus of Stabilized Base within Test Section for Section-3 of Atlanta District.

Section No.: 4 District: Atlanta County: Cass Highway: SH-77
Structure: Asphalt : 51 mm
LFA Base : 254 mm
Subgrade

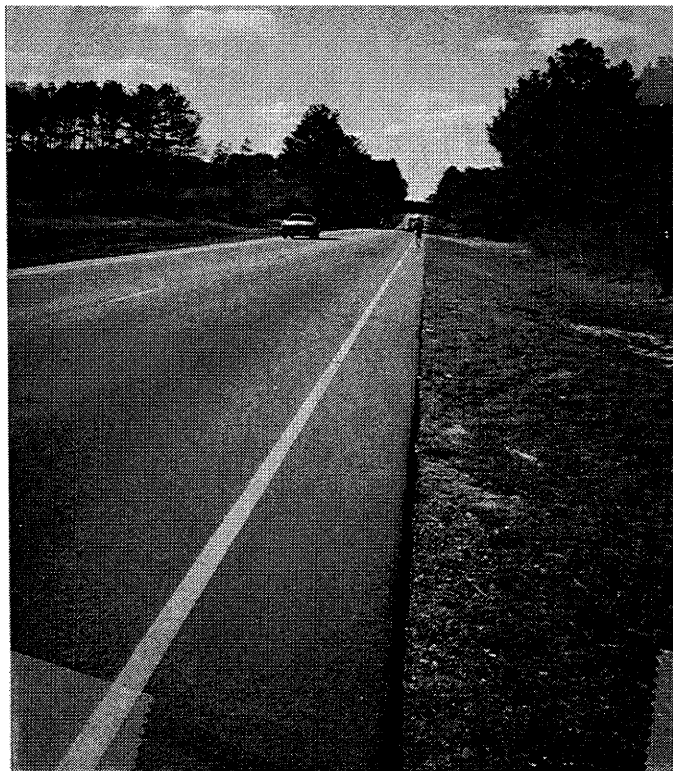
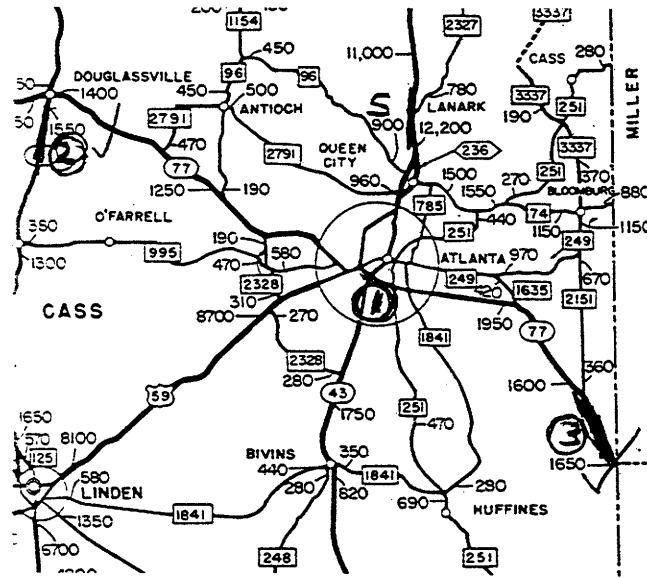
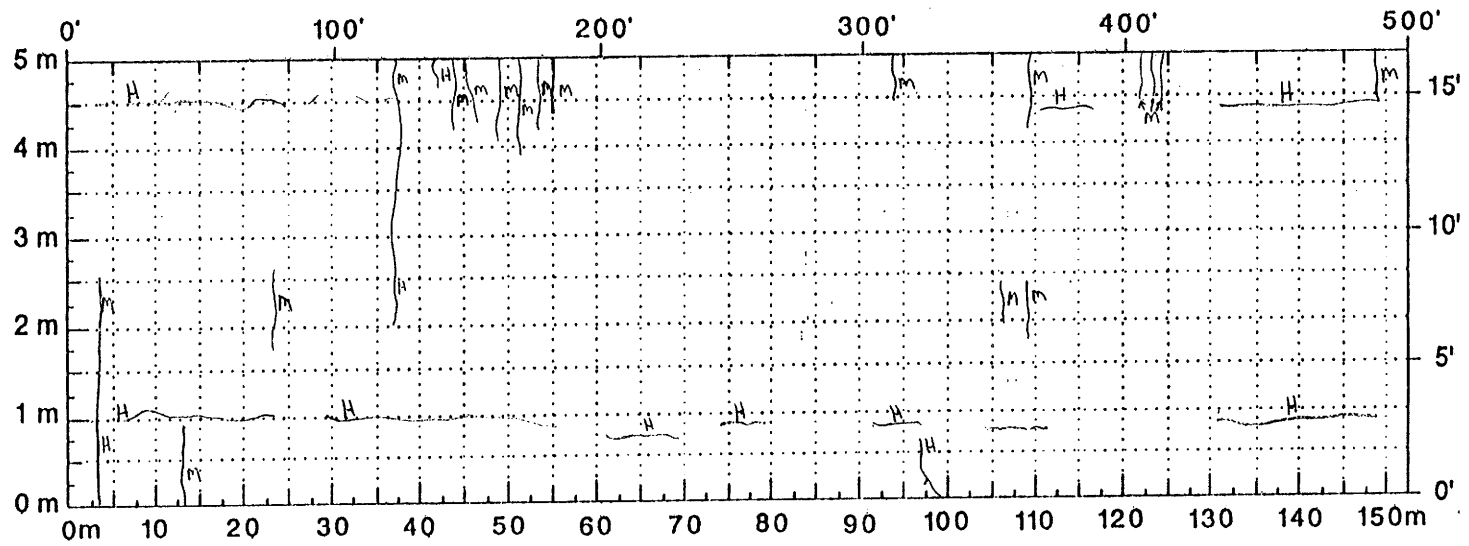


Figure A.135. Location and Details of Section-4 of Atlanta District.

A.138



Comments: _____

Figure A.136. Crack Map for Section-4 of Atlanta District.

TTI MODULUS ANALYSIS SYSTEM (SUMMARY REPORT)

(Version 4.2)

District: 19	MODULI RANGE(psi)		Poisson Ratio Values	
County: 34	Minimum	Maximum	H1: J = 0.35	
Highway/Road: SH0077	835,316	835,484	H2: J = 0.25	
Pavement: 2.00	20,000	400,000	H3: J = 0.25	
Base: 10.00	0	0	H4: J = 0.35	
Subbase: 0.00	10,000			
Subgrade: 105.40				

Station	Load (lbs)	Measured Deflection (mils):							Calculated Moduli values (ksi):				Absolute Dpth to	
		R1	R2	R3	R4	R5	R6	R7	SURF(E1)	BASE(E2)	SUBB(E3)	SUBG(E4)	ERR/Sens	Bedrock
0.000	11,879	13.52	10.58	7.00	4.28	2.63	1.64	1.18	835.	211.3	0.0	14.1	7.29	128.55
35.000	11,527	23.86	14.69	8.20	4.40	2.55	1.68	1.30	835.	59.4	0.0	12.5	6.80	103.13
80.000	11,663	18.89	13.09	8.08	4.56	2.59	1.64	1.18	835.	99.9	0.0	12.7	8.58	102.20
125.000	11,599	22.84	14.94	9.74	5.71	3.21	1.93	1.38	835.	80.8	0.0	10.5	7.34	100.98
164.000	11,495	26.02	16.13	9.16	5.09	3.05	2.02	1.54	835.	56.7	0.0	10.9	4.81	122.03
197.000	11,759	24.76	15.52	9.33	5.18	2.94	1.89	1.38	835.	64.4	0.0	11.3	6.63	103.55
232.000	11,567	18.41	13.83	9.20	5.42	3.21	2.02	1.50	835.	126.3	0.0	10.7	8.32	116.15
265.000	11,559	14.13	11.77	7.87	4.73	2.90	1.81	1.34	835.	202.2	0.0	12.3	9.31	129.38
300.000	11,583	14.01	10.87	7.24	4.44	2.59	1.60	1.14	835.	188.9	0.0	13.5	8.31	107.88
334.000	11,615	13.68	10.74	7.04	4.12	2.47	1.60	1.22	835.	190.6	0.0	14.1	8.68	118.05
364.000	11,519	15.31	12.14	7.83	4.56	2.74	1.72	1.26	835.	159.6	0.0	12.6	9.49	120.31
397.000	11,527	16.13	12.27	7.66	4.40	2.63	1.64	1.26	835.	136.4	0.0	12.8	9.24	118.07
431.000	11,527	15.72	12.35	8.70	5.26	3.29	2.14	1.58	835.	185.1	0.0	10.9	7.08	142.79
462.000	11,543	14.17	10.91	7.62	4.65	2.86	1.89	1.38	835.	206.6	0.0	12.5	6.41	130.39
496.000	11,559	12.01	9.96	7.12	4.65	2.94	1.89	1.38	835.	310.7	0.0	12.6	6.14	139.48
Mean:		17.56	12.65	8.12	4.76	2.84	1.81	1.33	835.	151.9	0.0	12.3	7.63	117.45
Std. Dev:		4.64	1.96	0.91	0.46	0.27	0.18	0.13	0.	71.8	0.0	1.2	1.35	12.81
Var Coeff(%):		26.44	15.52	11.15	9.69	9.36	9.70	10.00	0.	47.3	0.0	9.6	17.74	10.91

A.139

Figure A.137. FWD Back-Calculation Results for Uncracked Portion Section-4 of Atlanta District.

ATLANTA DISTRICT
SH-77 SITE-4 Station @ 0'

A.140

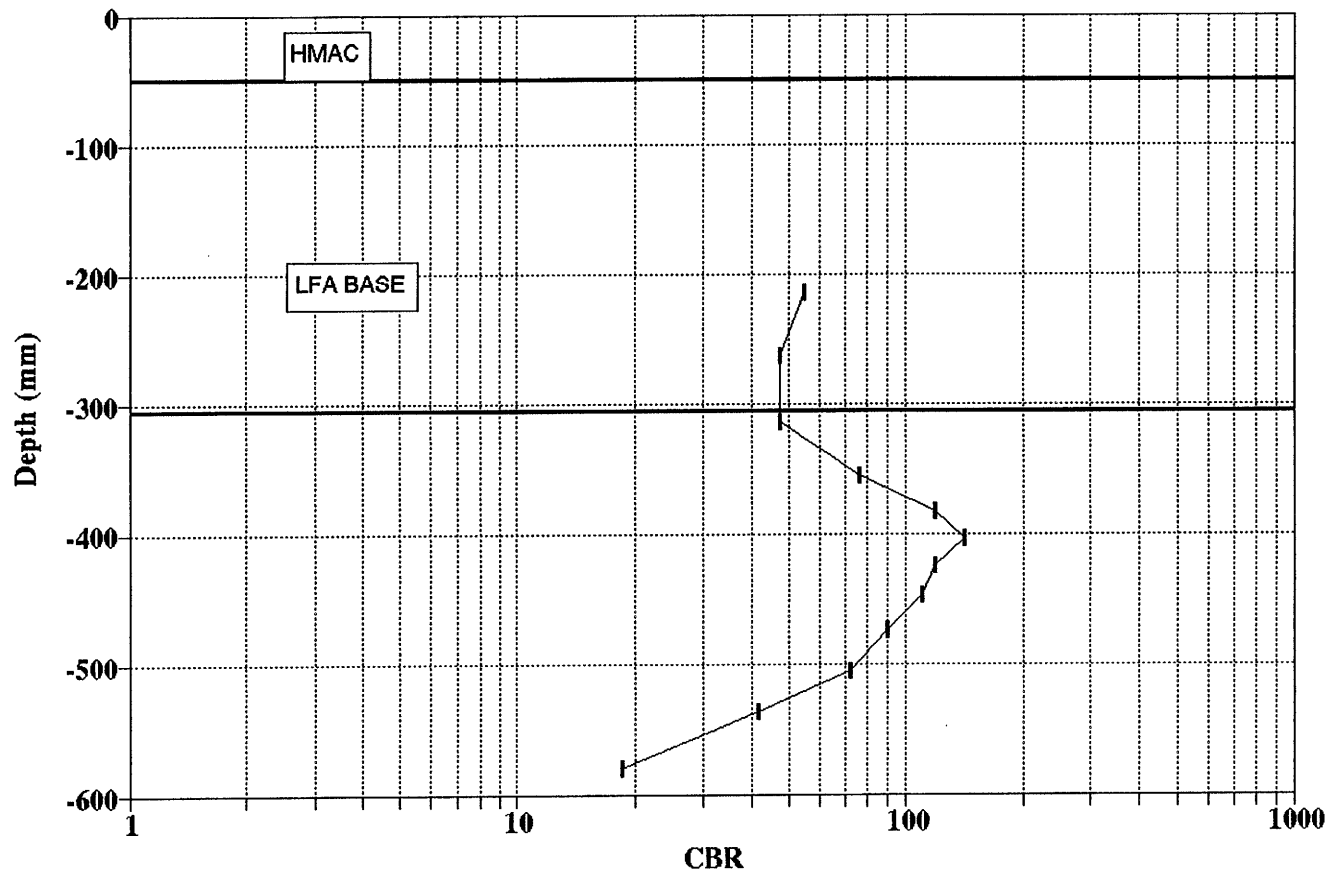
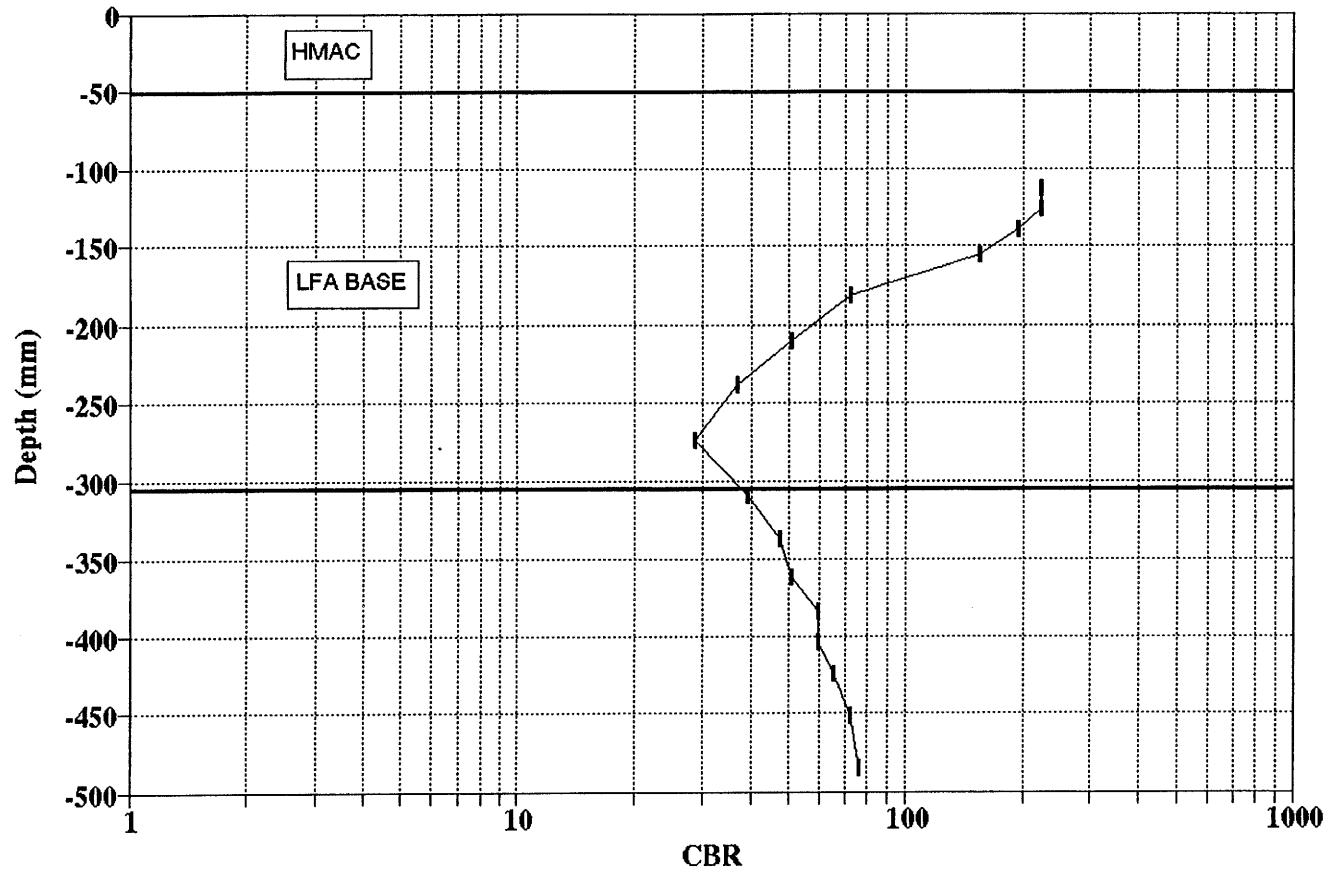


Figure A.138. Variation of CBR Obtained from DCP Testing (at Station 0') for Section-4 of Atlanta District.

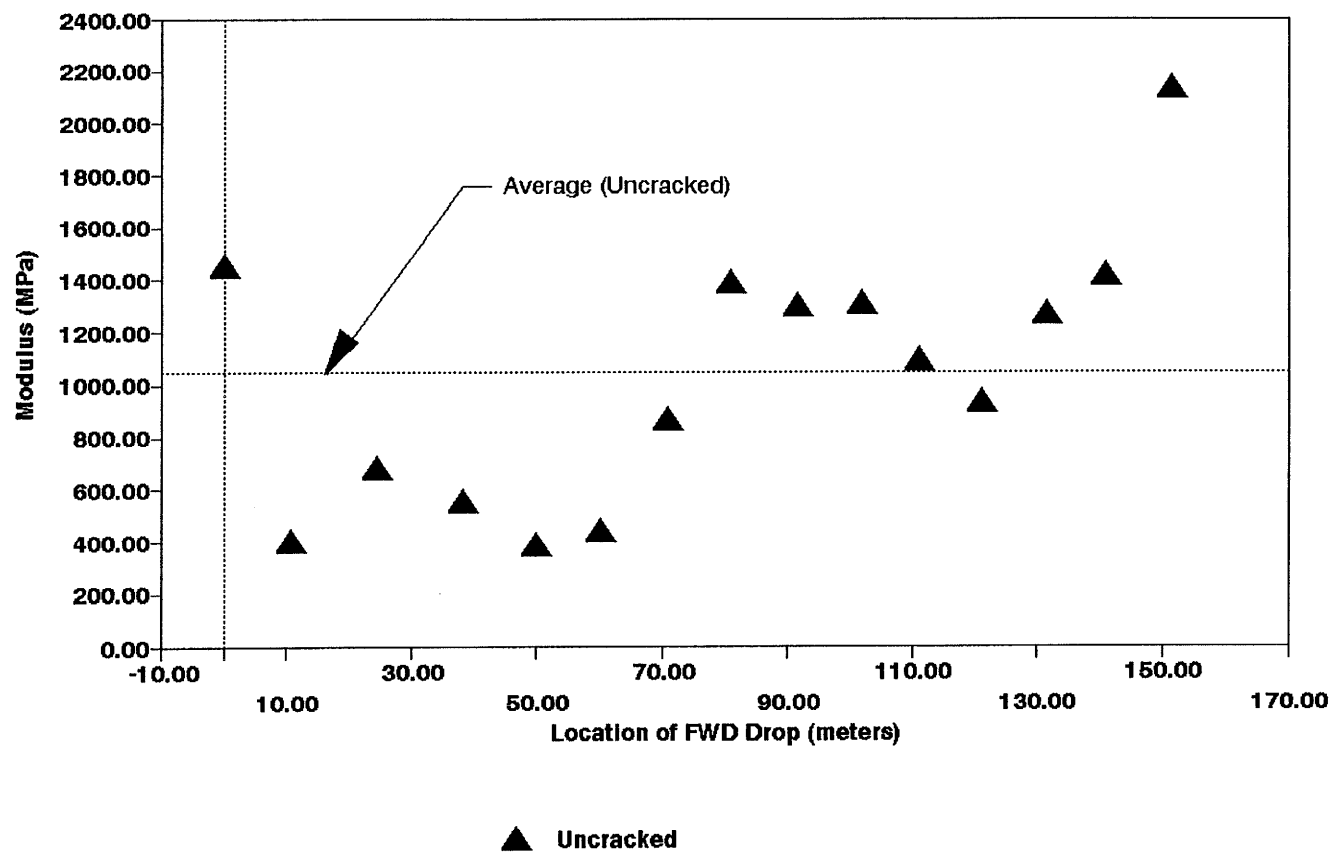
ATLANTA DISTRICT
SH-77 SITE-4 Trial-2 Station @ 30'



A.141

Figure A.139. Variation of CBR Obtained from DCP Testing (at Station 30') for Section-4 of Atlanta District.

Atlanta District Section-4 Base
Winter



A.142

Figure A.140. Variation of Modulus of Stabilized Base within Test Section for Section-4 of Atlanta District.

Section No.: 5 District: Atlanta County: Harrison Highway: US-59
Structure: Asphalt : 267 mm
LFA Base : 406 mm
Subgrade

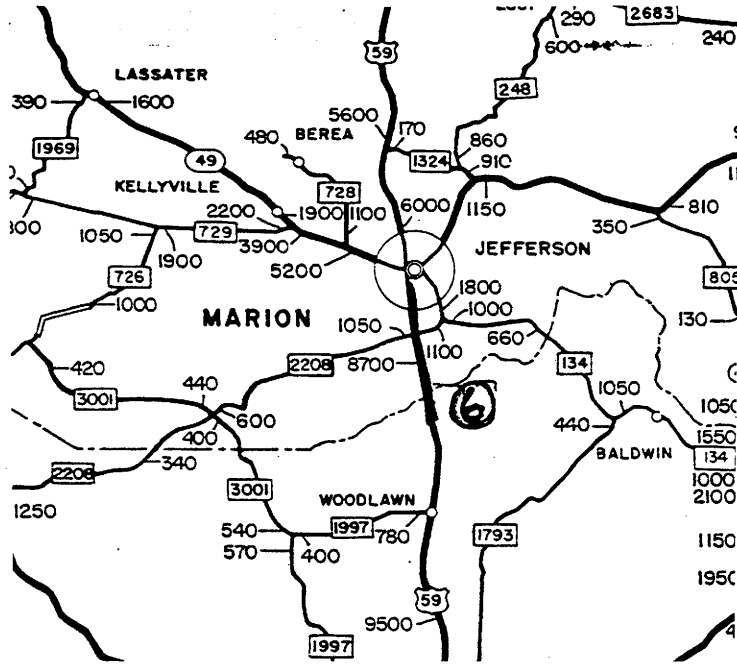


Figure A.141. Location and Details of Section-5 of Atlanta District.

A.144

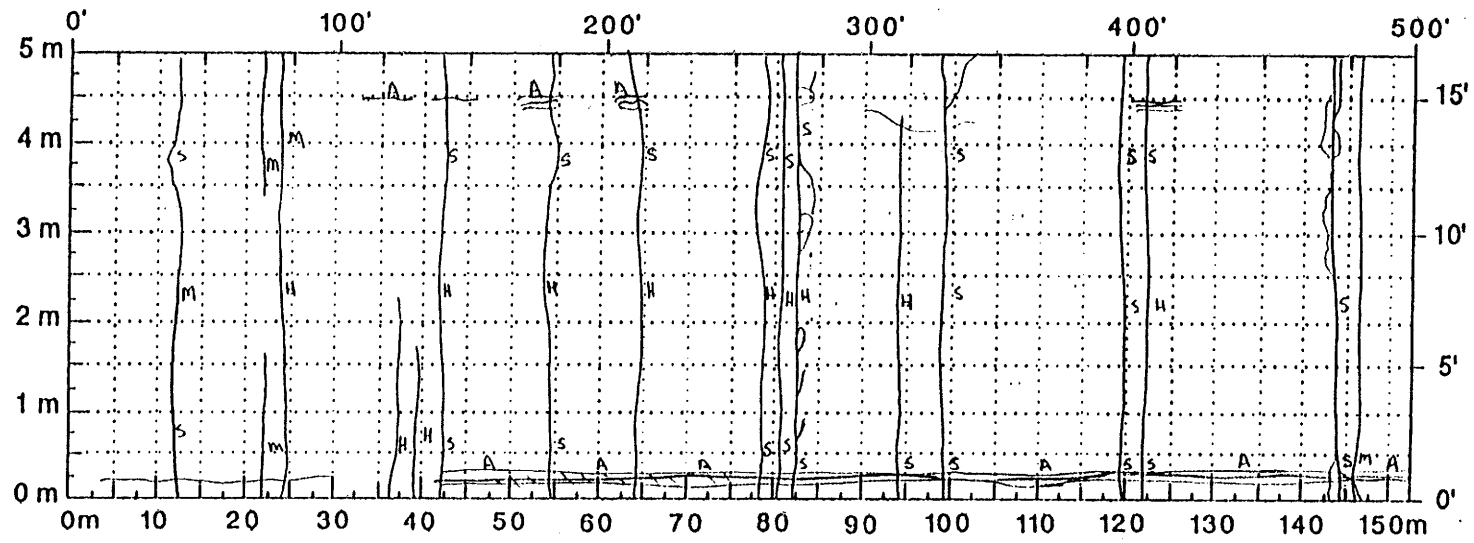


Figure A.142. Crack Map for Section-5 of Atlanta District.

TTI MODULUS ANALYSIS SYSTEM (SUMMARY REPORT)

(Version 5.0)

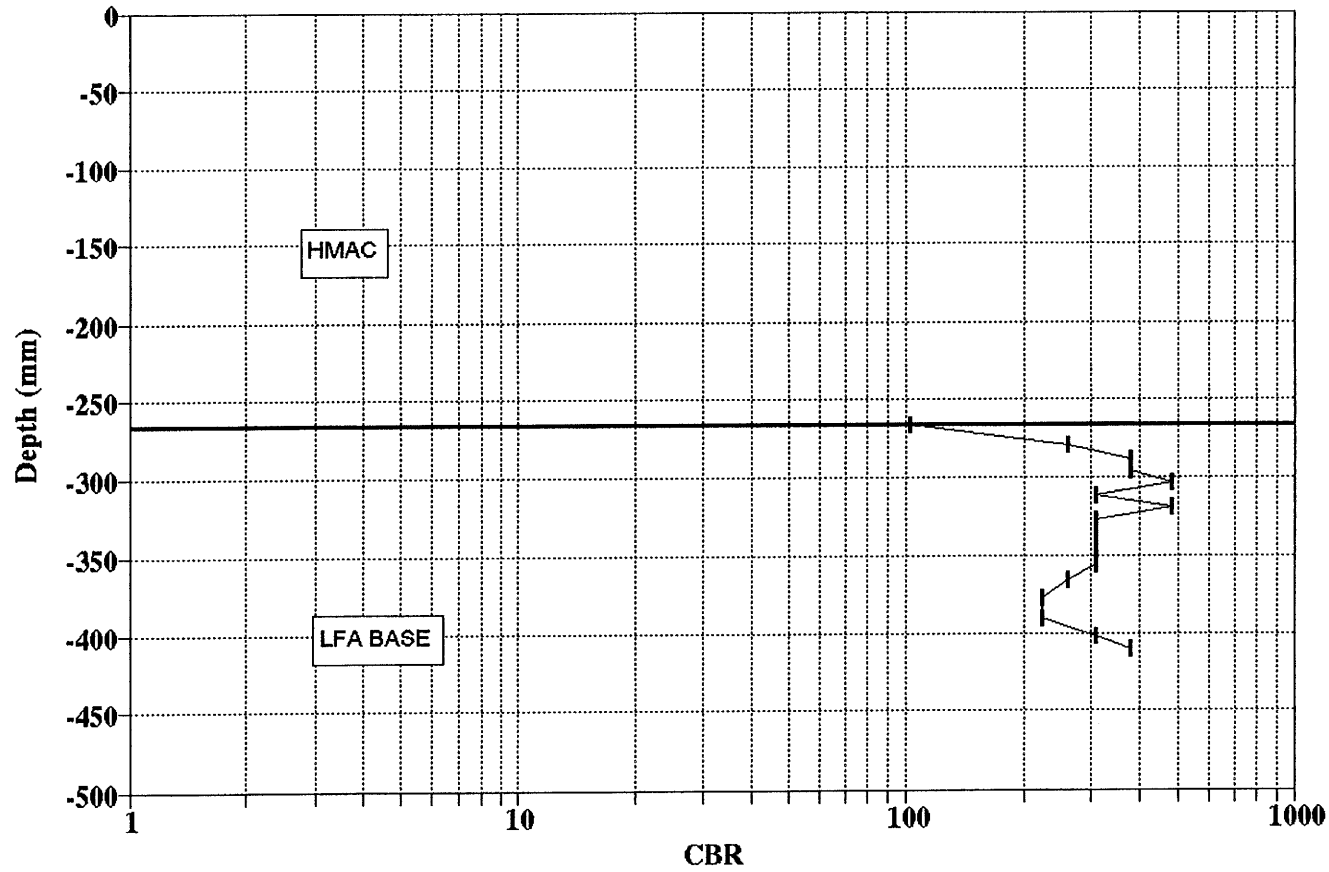
District:	19	MODULI RANGE(psi)		Poisson Ratio Values	
County:	183	Thickness(in)	Minimum	Maximum	H1: % = 0.35
Highway/Road:	US0059	Pavement:	400,000	800,000	H2: % = 0.25
		Base:	50,000	1,000,000	H3: % = 0.25
		Subbase:	0	0	H4: % = 0.40
		Subgrade:	273.50	25,000	

Station	Load (lbs)	Measured Deflection (mils):							Calculated Moduli values (ksi):				Absolute Dpth to	
		R1	R2	R3	R4	R5	R6	R7	SURF(E1)	BASE(E2)	SUBB(E3)	SUBG(E4)	ERR/Sens	Bedrock
0.000	12,135	4.72	2.88	2.50	2.16	1.97	1.68	1.46	466.	1000.0	0.0	24.2	1.84	300.00 *
25.000	11,975	4.56	2.80	2.46	2.16	1.93	1.68	1.46	493.	1000.0	0.0	24.0	1.84	300.00 *
50.000	11,911	4.97	3.25	2.83	2.49	2.20	1.89	1.63	474.	945.6	0.0	19.9	0.42	300.00
75.000	11,647	5.74	3.79	3.00	2.57	2.24	1.93	1.71	427.	453.3	0.0	21.2	2.06	300.00
100.000	11,655	5.78	3.62	3.08	2.65	2.32	2.02	1.75	400.	618.8	0.0	19.6	1.32	300.00 *
126.000	11,639	5.01	2.96	2.58	2.28	2.01	1.76	1.54	400.	1000.0	0.0	22.4	1.57	300.00 *
151.000	12,031	4.89	3.00	2.58	2.16	1.93	1.68	1.46	432.	918.4	0.0	24.4	1.29	300.00
176.000	12,023	6.15	4.36	3.41	2.89	2.51	2.18	1.91	507.	324.4	0.0	19.3	2.26	300.00
200.000	12,279	6.96	5.27	4.62	3.91	3.32	2.77	2.36	664.	251.1	0.0	13.6	0.89	300.00
226.000	11,671	5.17	3.70	3.41	2.98	2.63	2.27	2.03	577.	806.7	0.0	14.5	0.81	300.00
250.000	11,527	6.03	4.40	3.87	3.10	2.67	2.31	2.03	615.	285.8	0.0	16.3	1.67	300.00
275.000	11,287	6.76	4.73	3.79	3.18	2.74	2.35	2.03	431.	275.4	0.0	16.6	1.51	300.00
300.000	11,191	5.50	3.29	2.87	2.49	2.16	1.93	1.67	400.	696.8	0.0	19.9	2.24	300.00 *
326.000	11,351	7.74	5.14	4.21	3.46	2.90	2.44	2.07	400.	196.2	0.0	16.3	1.25	300.00 *
351.000	11,495	6.72	4.40	3.71	3.18	2.71	2.27	1.95	400.	354.0	0.0	17.0	0.68	300.00 *
378.000	11,559	5.90	3.62	3.12	2.77	2.43	2.10	1.87	400.	658.8	0.0	18.3	1.94	300.00 *
400.000	11,591	5.62	3.46	3.04	2.69	2.40	2.10	1.83	400.	885.7	0.0	17.8	1.74	300.00 *
425.000	12,191	4.97	3.58	3.16	2.85	2.51	2.18	1.91	606.	919.9	0.0	15.9	0.32	300.00
450.000	12,119	4.64	3.13	2.79	2.45	2.13	1.89	1.67	563.	1000.0	0.0	19.8	0.66	300.00 *
475.000	11,967	6.92	4.28	3.25	2.69	2.36	2.06	1.79	400.	258.7	0.0	22.0	4.03	300.00 *
501.000	12,791	4.72	3.21	3.08	2.77	2.43	2.14	1.83	724.	1000.0	0.0	17.0	2.03	300.00 *
Mean:		5.69	3.76	3.21	2.76	2.40	2.08	1.81	485.	659.5	0.0	19.0	1.54	300.00
Std. Dev:		0.91	0.74	0.57	0.45	0.35	0.28	0.23	101.	312.2	0.0	3.1	0.82	0.00
Var Coeff(%):		16.03	19.60	17.78	16.15	14.53	13.32	12.89	21.	47.3	0.0	16.5	53.32	0.00

A.145

Figure A.143. FWD Back-Calculation Results for Uncracked Section-5 of Atlanta District.

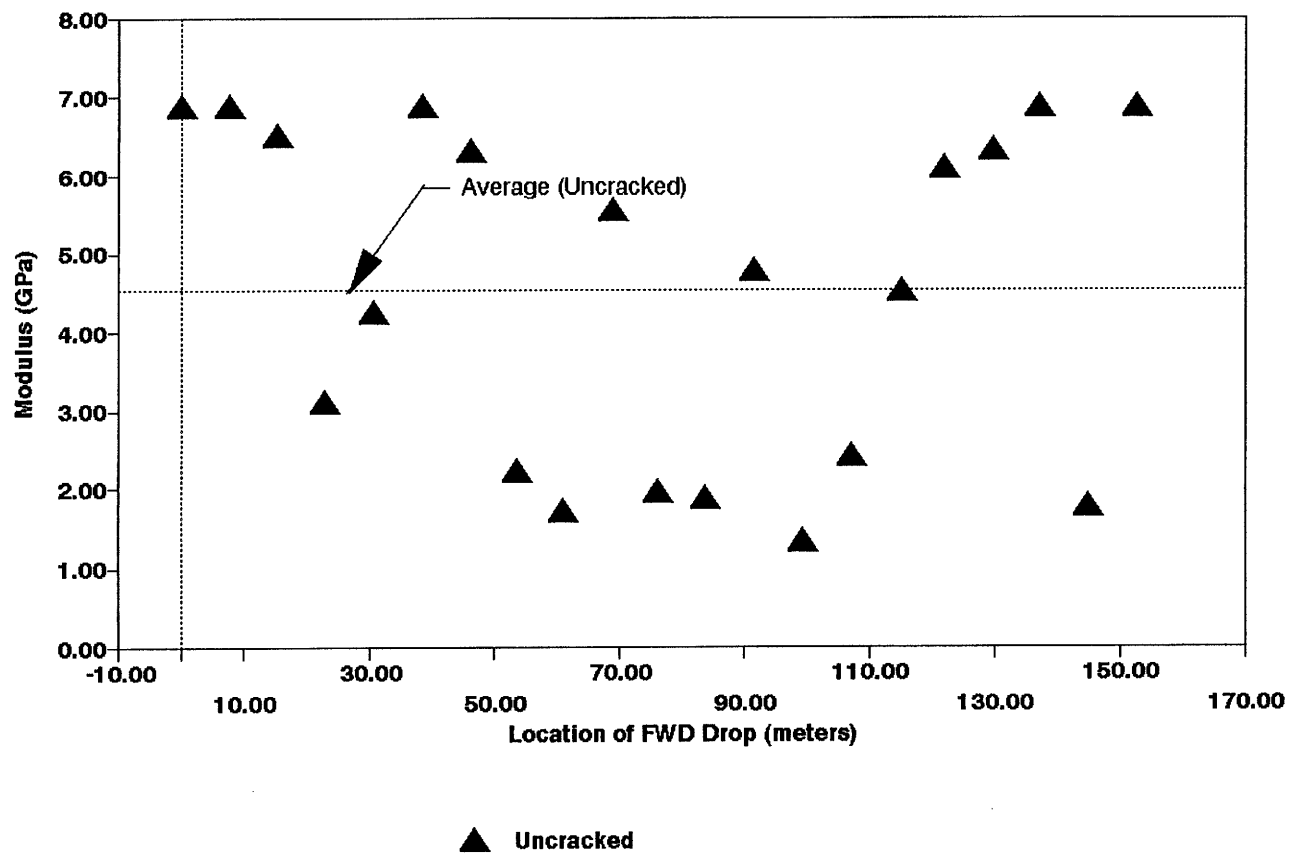
**ATLANTA DISTRICT
US-59 SITE-5**



A.146

Figure A.144. Variation of CBR Obtained from DCP Testing for Section-5 of Atlanta District.

Atlanta District Section-5 Base
Winter



A.147

Figure A.145. Variation of Modulus of Stabilized Base within Test Section for Section-5 of Atlanta District.

Section No.: 6 District: Atlanta County: Panola Highway: Loop 436
 Structure: Seal Coat : 12 mm
Flex Base : 305 mm
LFA : 305 mm
Subgrade

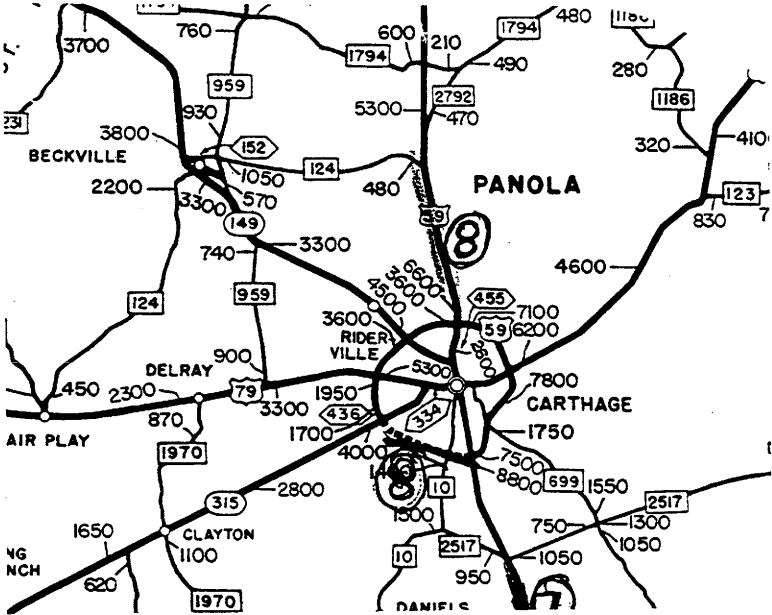


Figure A.146. Location and Details of Section-6 of Atlanta District.

A.149

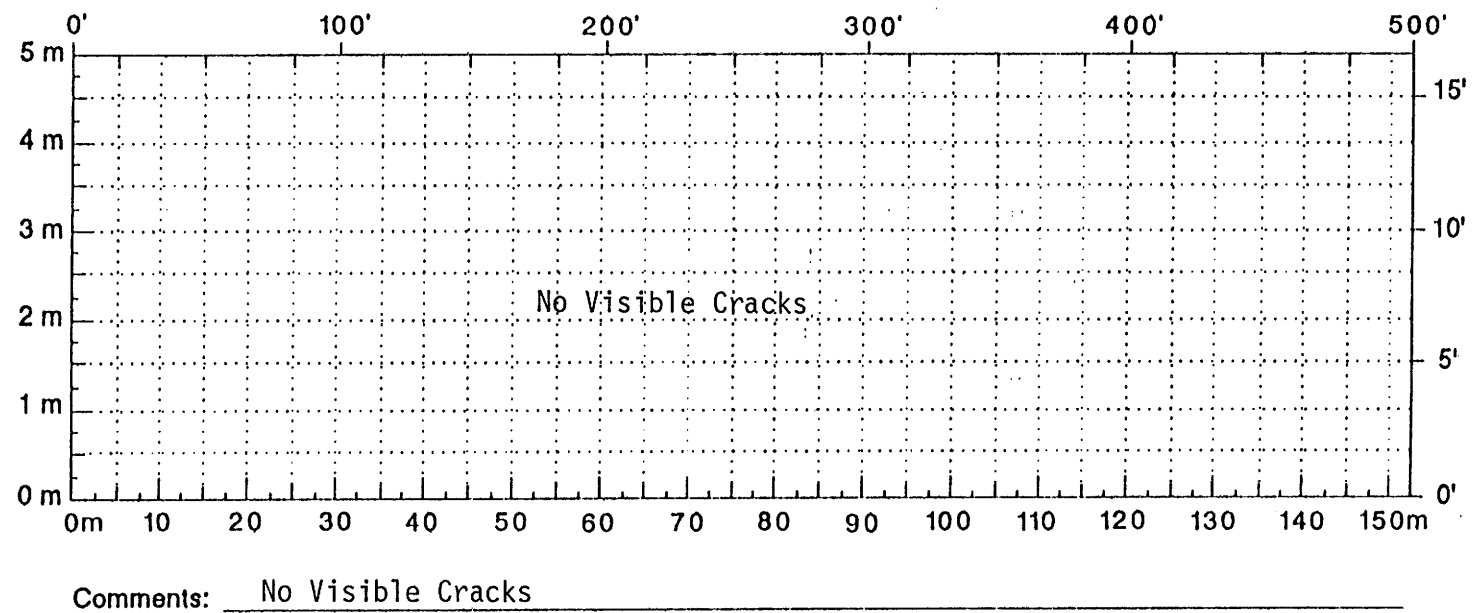


Figure A.147. Crack Map for Section-6 of Atlanta District.

A.150

TTI MODULUS ANALYSIS SYSTEM (SUMMARY REPORT)													(Version 5.0)	
District: 19									MODULI RANGE(psi)		Poisson Ratio Values			
County: 183									Minimum	Maximum	H1: % = 0.35			
Highway/Road: LP0436									20,000	100,000	H2: % = 0.30			
									40,000	1,000,000	H3: % = 0.25			
									25,000		H4: % = 0.40			
									Calculated Moduli values (ksi):				Absolute Dpth to	
Station	Load (lbs)	Measured Deflection (mils):							SURF(E1)	BASE(E2)	SUBB(E3)	SUBG(E4)	ERR/Sens	Bedrock
		R1	R2	R3	R4	R5	R6	R7						
146.000	11,279	23.25	6.79	3.54	2.57	1.86	1.47	1.22	500.	45.9	80.6	27.0	5.06	300.00
203.000	11,247	24.15	6.38	3.25	2.28	1.70	1.30	1.14	500.	41.6	89.0	29.5	4.75	300.00
252.000	11,239	20.20	5.97	3.21	2.28	1.74	1.26	1.06	500.	52.9	105.5	28.8	4.21	231.04
304.000	11,735	19.67	5.47	3.04	2.36	1.82	1.26	1.10	500.	52.1	366.5	27.0	3.36	300.00
360.000	11,391	20.60	5.56	3.00	2.32	1.89	1.51	1.22	500.	46.8	474.9	25.6	6.06	300.00
404.000	11,343	25.12	6.91	3.41	2.85	2.43	1.97	1.75	500.	37.6	433.9	21.9	8.32	300.00
450.000	11,503	22.60	6.01	3.46	2.89	2.40	1.97	1.71	500.	43.0	622.2	21.0	5.92	300.00
500.000	11,095	22.03	5.47	3.12	2.61	2.13	1.76	1.54	500.	41.7	691.4	22.5	5.55	300.00
Mean:		22.20	6.07	3.25	2.52	2.00	1.56	1.34	500.	45.2	358.0	25.4	5.40	300.00
Std. Dev:		1.95	0.57	0.20	0.25	0.29	0.30	0.28	0.	5.3	243.1	3.2	1.48	37.48
Var Coeff(%):		8.78	9.47	6.13	9.92	14.46	19.27	20.87	0.	11.7	67.9	12.8	27.43	12.49

Figure A.148. FWD Back-Calculation Results for Uncracked Section-6 of Atlanta District.

A.151

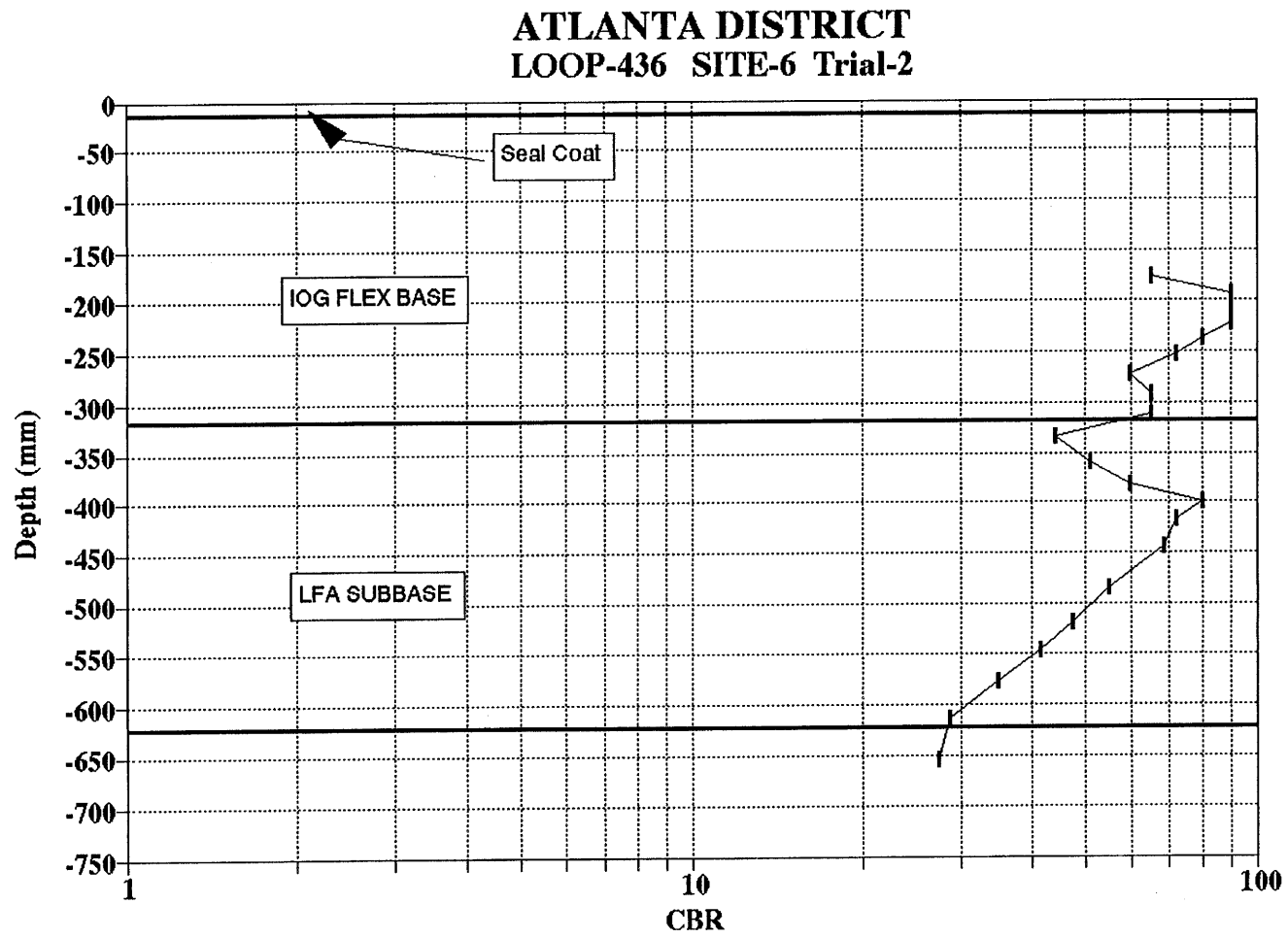


Figure A.149. Variation of CBR Obtained from DCP Testing for Section-6 of Atlanta District.

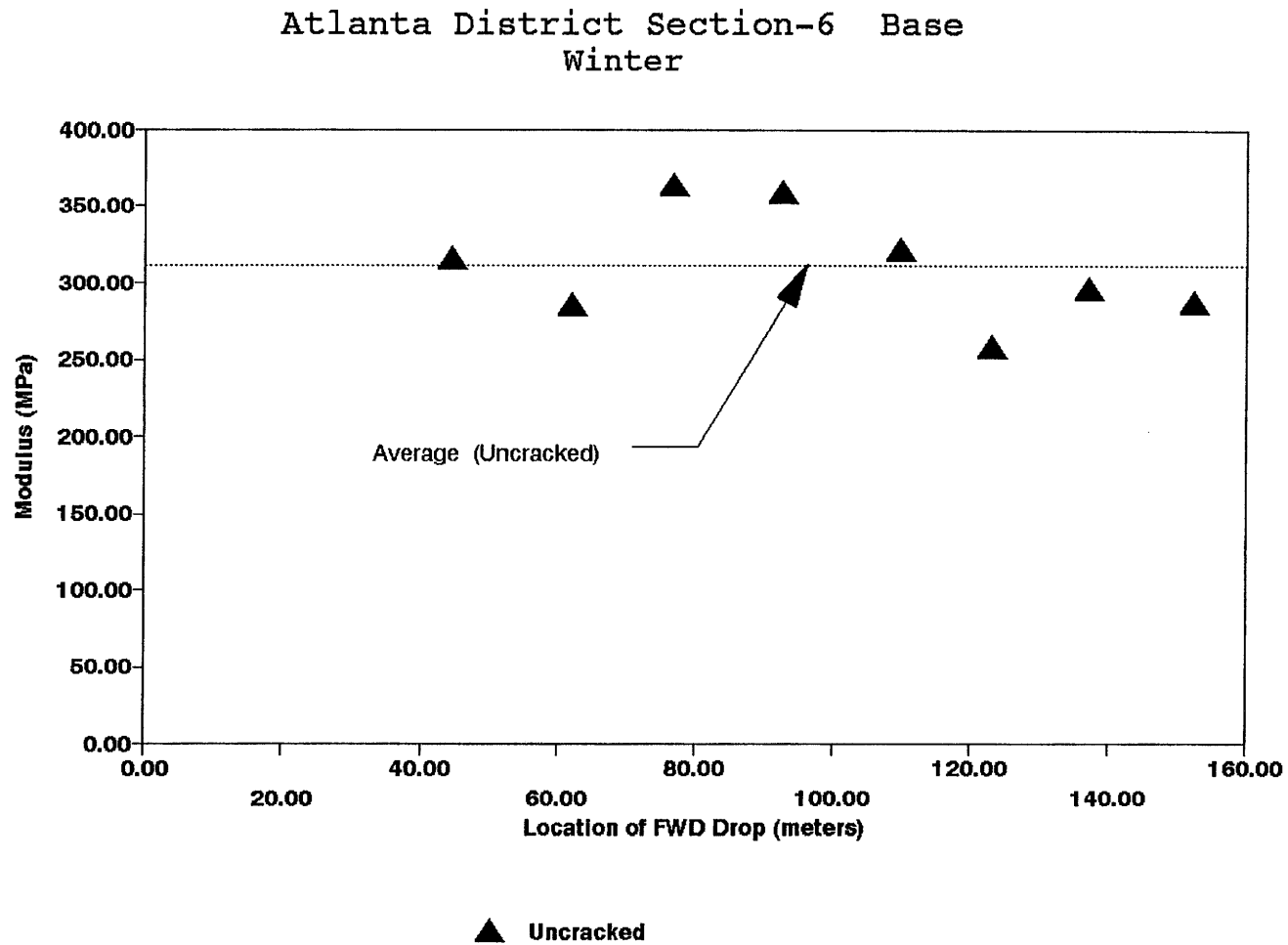
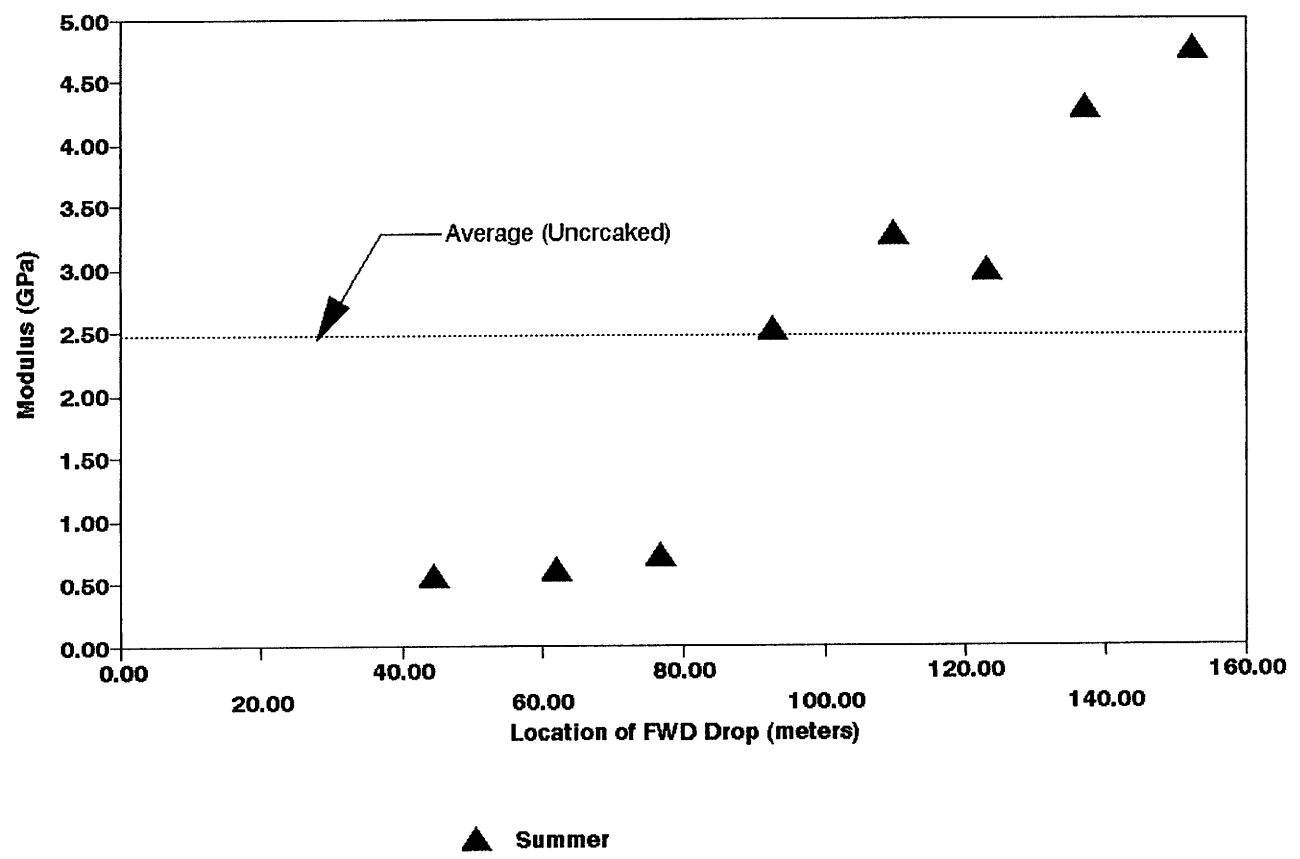


Figure A.150. Variation of Modulus of Stabilized Base within Test Section for Section-6 of Atlanta District.

Atlanta District Section-6 Subbase
Winter



A.153

Figure A.151. Variation of Modulus of Stabilized Subbase within Test Section for Section-6 of Atlanta District.

Section No.: 7 District: Atlanta County: Panola Highway: Loop 436
 Structure: Seal Coat : 12 mm
Flex Base : 305 mm
LFA subbase : 305 mm
Subgrade

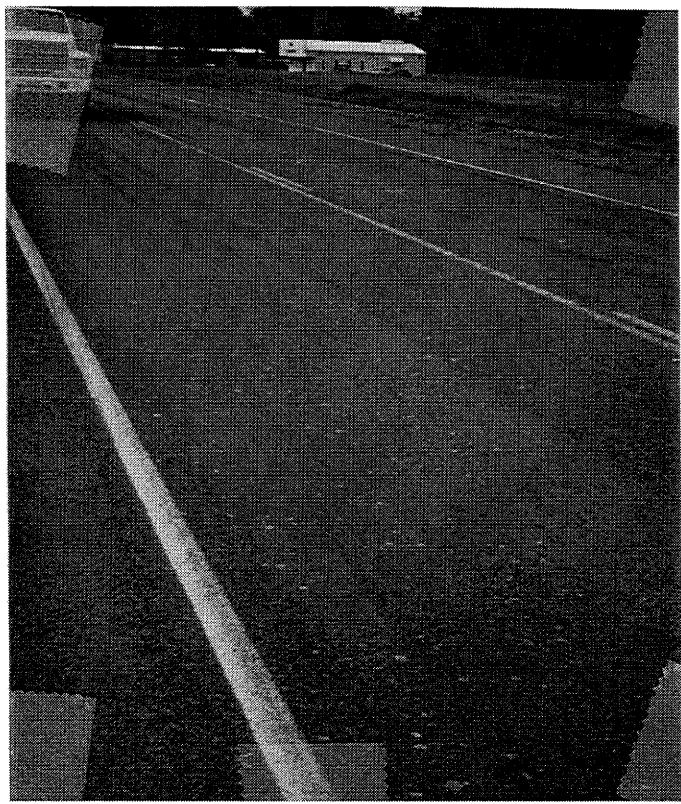
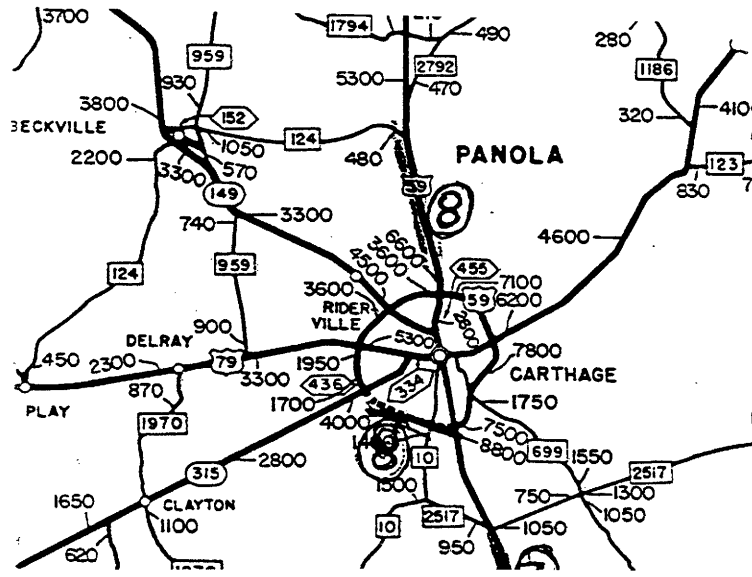


Figure A.152. Location and Details of Section-7 of Atlanta District.

A.155

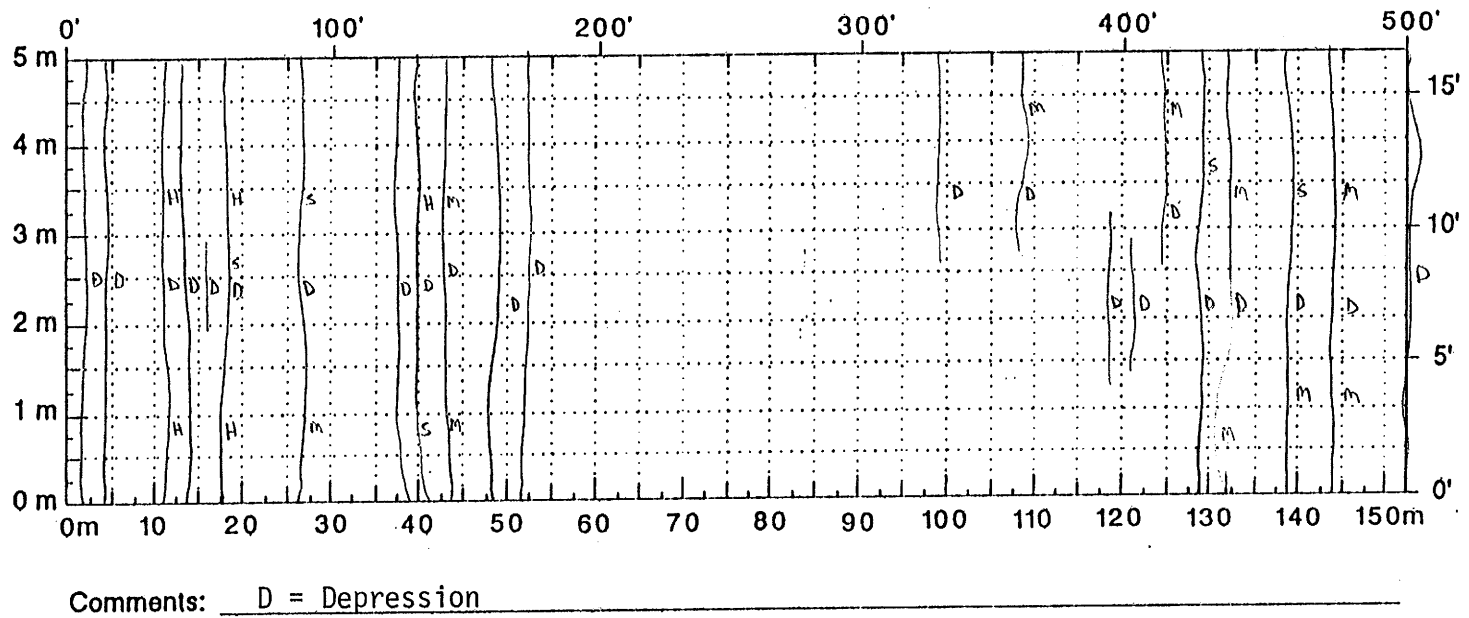


Figure A.153. Crack Map for Section-7 of Atlanta District.

TTI MODULUS ANALYSIS SYSTEM (SUMMARY REPORT)													(Version 5.0)	
District:	19												MODULI RANGE(psi)	
County:	183								Minimum		Maximum		Poisson Ratio Values	
Highway/Road:	LP0436		Pavement:		0.50		499,950		500,050		H1: % = 0.35			
			Base:		12.00		20,000		100,000		H2: % = 0.30			
			Subbase:		12.00		40,000		1,000,000		H3: % = 0.25			
			Subgrade:		275.50		25,000				H4: % = 0.40			
Station	Load (lbs)	Measured Deflection (mils):							Calculated Moduli values (ksi):				Absolute Dpth to	
		R1	R2	R3	R4	R5	R6	R7	SURF(E1)	BASE(E2)	SUBB(E3)	SUBG(E4)	ERR/Sens	Bedrock
697.000	11,439	15.47	5.47	3.71	2.93	2.32	1.85	1.54	500.	67.6	502.3	17.4	3.49	300.00
751.000	11,455	19.42	6.71	4.16	3.51	2.67	2.06	1.67	500.	54.2	352.3	17.6	3.53	300.00
772.000	11,175	14.46	5.43	3.91	3.18	2.55	2.02	1.67	500.	71.7	522.5	14.3	3.36	300.00
808.000	11,903	16.98	5.14	3.62	3.06	2.51	1.89	1.58	500.	60.4	846.9	16.0	4.78	300.00
845.000	12,047	16.21	4.94	3.50	2.89	2.36	1.89	1.58	500.	64.4	833.8	16.6	5.70	300.00
906.000	11,215	17.67	6.17	3.50	3.06	2.47	2.02	1.71	500.	57.2	466.4	18.1	6.85	300.00
966.000	11,159	20.89	5.14	3.21	2.85	2.43	2.02	1.79	500.	44.7	914.9	19.1	7.48	300.00
Mean:		17.30	5.57	3.66	3.07	2.47	1.96	1.65	500.	60.0	634.1	17.0	5.03	300.00
Std. Dev:		2.24	0.64	0.31	0.23	0.12	0.08	0.09	0.	9.0	224.1	1.6	1.70	27.36
Var Coeff(%):		12.97	11.48	8.43	7.36	4.79	4.29	5.30	0.	15.1	35.3	9.2	33.75	9.12

Figure A.154. FWD Back-Calculation Results for Uncracked Portion of Section-7 of Atlanta District.

A.157

FWD MODULUS ANALYSIS SYSTEM (SUMMARY REPORT)														(Version 4.2)		
District:	19											MODULI RANGE(psi)				
County:	183								Thickness(in)	Minimum	Maximum	Poisson Ratio Values				
Highway/Road:	LP0436								Pavement:	0.50	591,941	592,059	H1: $\mu = 0.35$			
									Base:	12.00	20,000	400,000	H2: $\mu = 0.35$			
									Subbase:	12.00	10,000	1,000,000	H3: $\mu = 0.25$			
									Subgrade:	275.50	25,000		H4: $\mu = 0.35$			
Station	Load (lbs)	Measured Deflection (mils):							Calculated Moduli values (ksi):				Absolute Dpth to Bedrock			
		R1	R2	R3	R4	R5	R6	R7	SURF(E1)	BASE(E2)	SUBB(E3)	SUBG(E4)	ERR/Sens	Bedrock		
1082.000	11,127	21.95	6.54	4.21	3.38	2.71	2.18	1.83	592.	43.5	407.5	18.5	3.89	300.00		
1148.000	12,967	18.12	6.79	3.91	3.26	2.71	2.18	1.87	592.	66.2	374.5	20.2	7.39	300.00		
1165.000	12,439	21.05	5.56	3.66	3.26	2.82	2.23	1.91	592.	49.0	782.1	19.4	5.61	300.00		
Mean:		20.37	6.30	3.93	3.30	2.75	2.20	1.87	592.	52.9	521.4	19.3	5.63	300.00		
Std. Dev:		2.00	0.65	0.28	0.07	0.06	0.03	0.04	0.	11.8	226.4	0.9	1.75	0.00		
Var Coeff(%):		9.83	10.32	7.01	2.10	2.31	1.31	2.14	0.	22.4	43.4	4.4	31.11	0.00		

Figure A.155. FWD Back-Calculation Results for Cracked Portion of Section-7 of Atlanta District.

ATLANTA DISTRICT LOOP-436 SITE-7

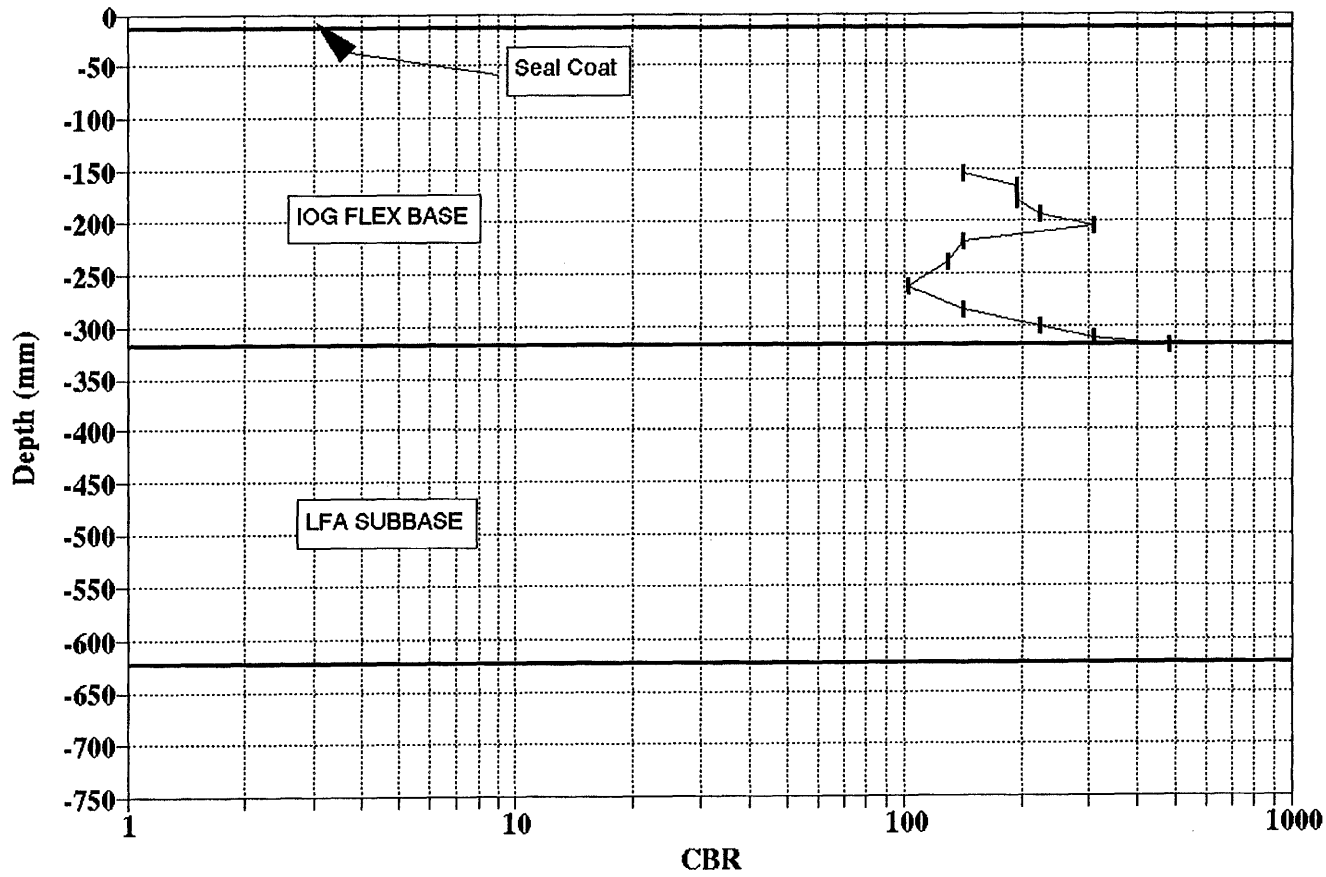
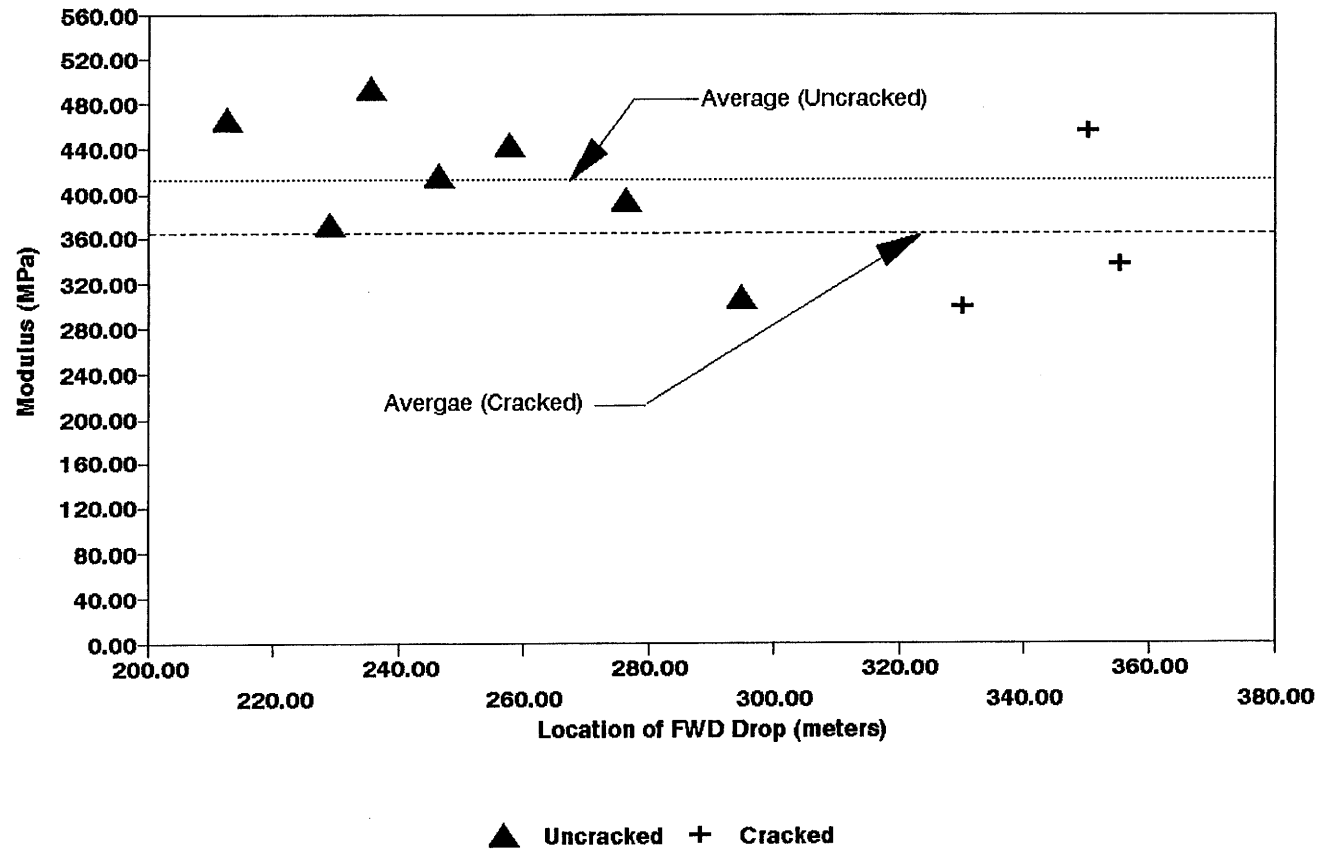


Figure A.156. Variation of CBR Obtained from DCP Testing for Section-7 of Atlanta District.

Atlanta District Section-7 Base
Winter



A.159

Figure A.157. Variation of Modulus of Stabilized Base within Test Section for Section-7 of Atlanta District.

A.160

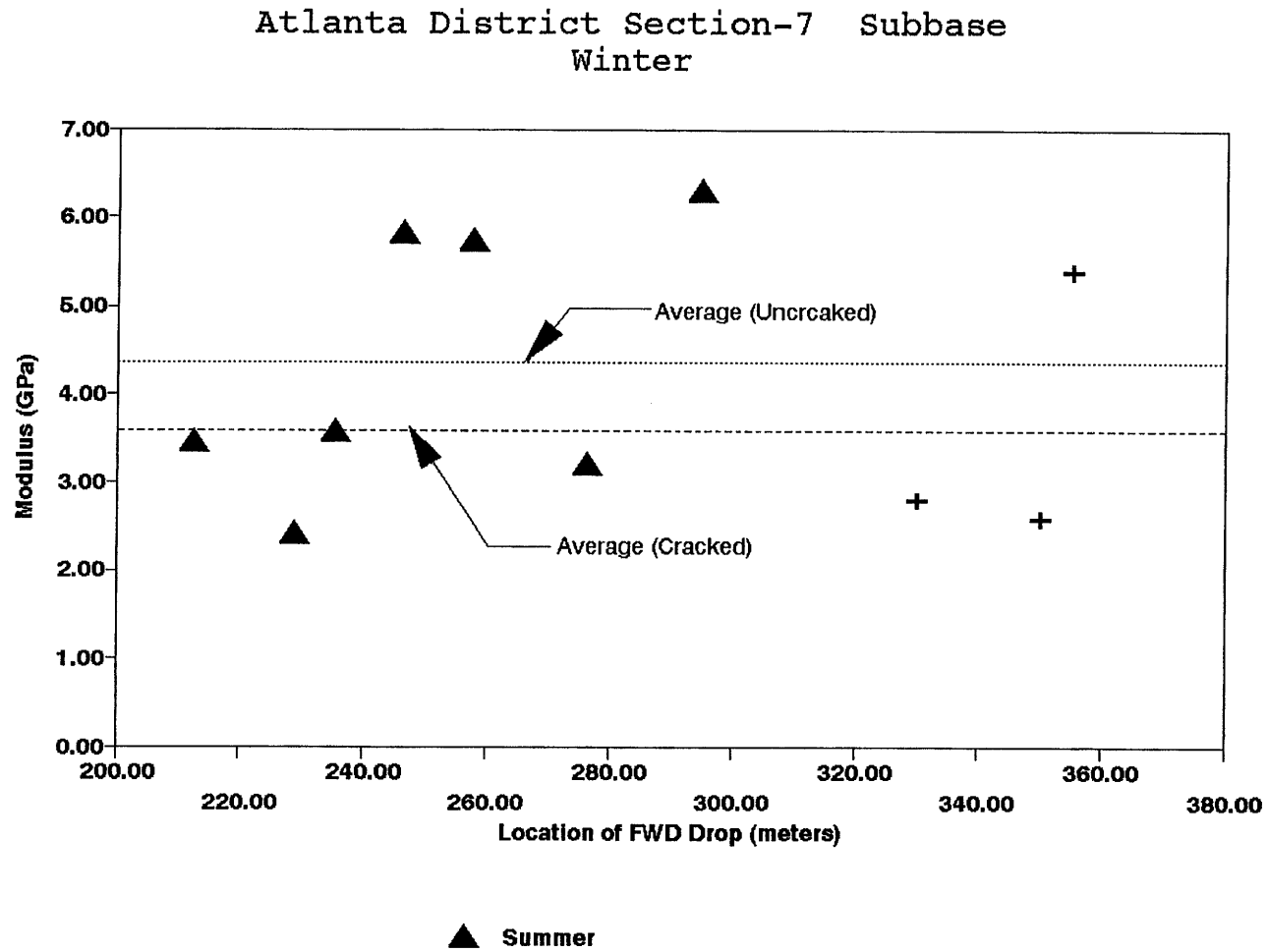


Figure A.158. Variation of Modulus of Stabilized Subbase within Test Section for Section-7 of Atlanta District.

Section No.: 8 District: Atlanta County: Cass Highway: SH - 8
 Structure: Asphalt : 51 mm
LFA Base : 254 mm
Subgrade

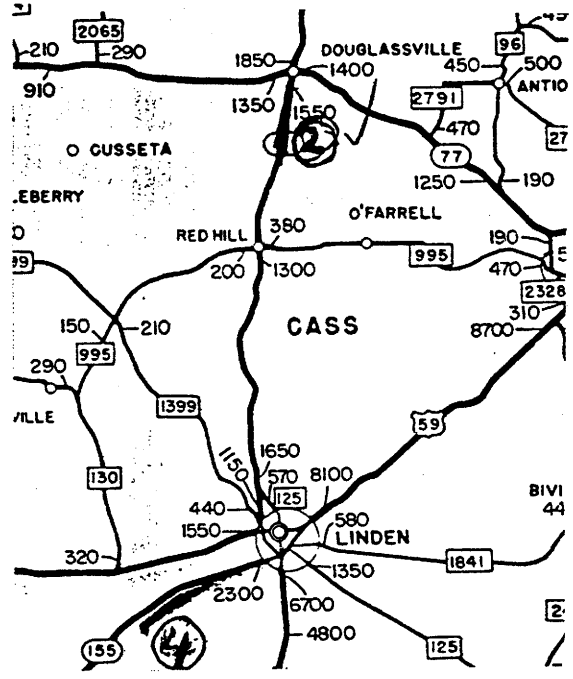


Figure A.159. Location and Details of Section-8 of Atlanta District.

A.162

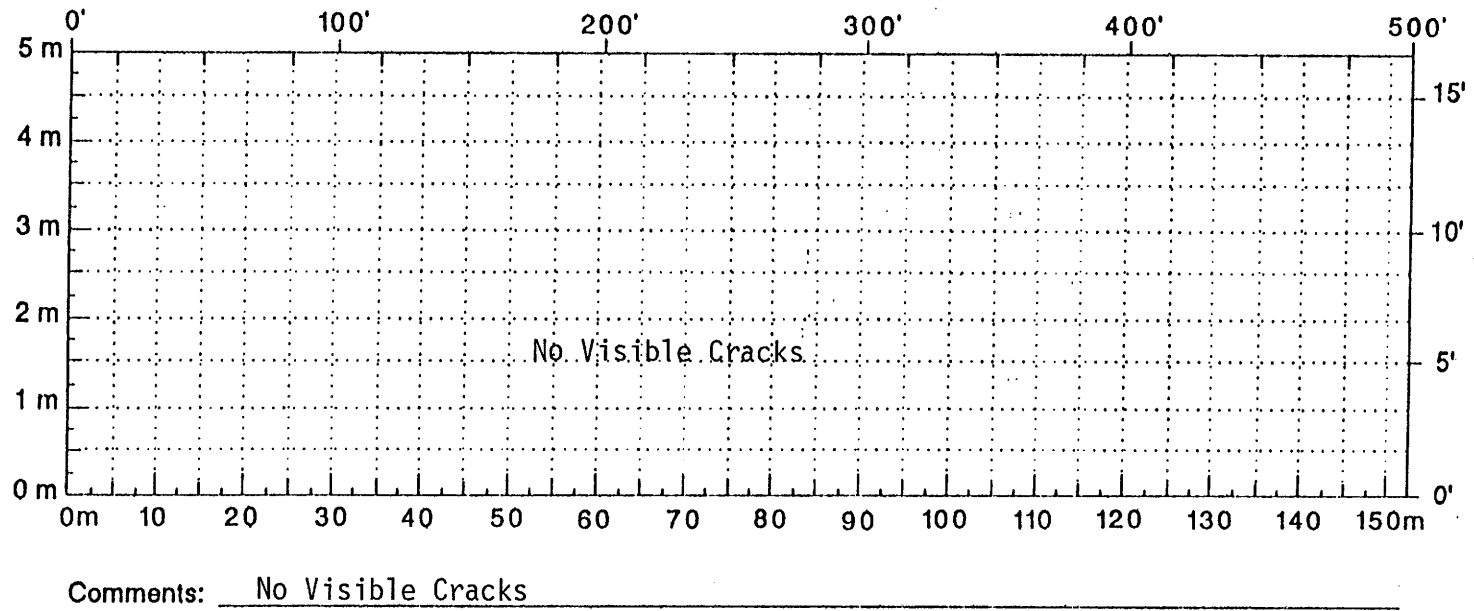


Figure A.160. Crack map for Section-8 of Atlanta District.

A.163

TTI MODULUS ANALYSIS SYSTEM (SUMMARY REPORT)														(Version 4.2)	
District:	19														
County:	34														
Highway/Road:	SH0008														
			Thickness(in)						MODULI RANGE(psi)		Poisson Ratio Values				
			Pavement:	2.00				Minimum	Maximum			H1:	$\nu = 0.35$		
			Base:	10.00				20,000	400,000			H2:	$\nu = 0.25$		
			Subbase:	0.00				0	0			H3:	$\nu = 0.25$		
			Subgrade:	83.20					25,000			H4:	$\nu = 0.35$		
Station	Load (lbs)	Measured Deflection (mils):							Calculated Moduli values (ksi):				Absolute Dist to		
		R1	R2	R3	R4	R5	R6	R7	SURF(E1)	BASE(E2)	SUBB(E3)	SUBG(E4)	ERR/Sens	Bedrock	
751.000	12,279	21.99	13.95	7.95	4.48	2.63	1.68	1.22	1294.	75.8	0.0	11.8	3.74	111.35	
801.000	12,175	15.03	10.00	6.08	3.51	2.05	1.30	0.98	1294.	135.8	0.0	15.1	3.77	107.25	
863.000	12,023	21.66	13.34	6.83	3.63	2.16	1.43	1.10	1294.	63.3	0.0	13.6	5.52	97.50	
913.000	12,111	15.84	9.96	5.33	2.77	1.55	0.92	0.65	1294.	95.2	0.0	18.4	7.04	88.84	
955.000	12,039	18.32	10.82	5.66	2.93	1.66	1.01	0.77	1294.	74.2	0.0	17.1	4.99	88.08	
1001.000	11,927	16.65	10.62	5.41	2.69	1.43	0.88	0.65	1294.	81.1	0.0	18.2	9.63	78.83	
1057.000	11,911	14.94	9.63	5.25	2.77	1.58	1.05	0.77	1294.	107.7	0.0	17.9	6.46	93.43	
1101.000	11,791	17.59	10.41	5.50	2.93	1.66	1.05	0.77	1294.	78.8	0.0	17.0	4.45	97.07	
1152.000	11,879	13.11	8.27	4.46	2.32	1.28	0.80	0.65	1294.	118.9	0.0	21.6	6.89	88.41	
1203.000	11,911	11.97	7.12	3.50	1.83	1.12	0.76	0.61	1294.	123.1	0.0	26.3	7.00	89.00	
1250.000	11,663	18.98	10.54	5.08	2.85	1.82	1.26	0.98	1294.	66.6	0.0	16.9	7.20	122.26	
Mean:		16.92	10.42	5.55	2.97	1.72	1.10	0.83	1294.	92.8	0.0	17.6	6.06	95.17	
Std. Dev:		3.20	1.94	1.16	0.70	0.43	0.28	0.21	0.	24.9	0.0	3.9	1.77	11.09	
Var Coeff(%):		18.93	18.63	20.91	23.55	24.87	25.79	24.82	0.	26.8	0.0	22.0	29.22	11.65	

Figure A.161. FWD Back-Calculation Results for Uncracked Portion of Section-8A of Atlanta District.

TTI MODULUS ANALYSIS SYSTEM (SUMMARY REPORT)														(Version 4.2)	
District:	19														
County:	34														
Highway/Road:	SH0008														
			Pavement: 2.00							MODULI RANGE(psi)		Poisson Ratio Values			
			Base: 10.00							Minimum	Maximum	H1: $\mu = 0.35$			
			Subbase: 0.00							20,000	400,000	H2: $\mu = 0.25$			
			Subgrade: 95.40							0	0	H3: $\mu = 0.25$			
										25,000		H4: $\mu = 0.35$			
Station	Load (lbs)	Measured Deflection (mils):							Calculated Moduli values (ksi):				Absolute Dpth to ERR/Sens Bedrock		
		R1	R2	R3	R4	R5	R6	R7	SURF(E1)	BASE(E2)	SUBB(E3)	SUBG(E4)			
4751.000	11,575	15.31	10.37	6.58	4.48	2.94	1.97	1.42	1294.	162.5	0.0	12.2	2.09	159.85	
4809.000	11,537	8.71	7.16	5.45	3.79	2.63	1.89	1.38	1294.	400.0	0.0	15.2	7.58	214.21 *	
4852.000	11,535	11.77	9.06	5.62	3.22	2.13	1.55	1.22	1294.	206.8	0.0	15.5	7.15	139.66	
4902.000	11,215	35.35	19.92	9.87	5.38	3.13	2.06	1.54	1294.	25.8	0.0	9.5	2.59	112.48	
4953.000	11,191	41.45	22.76	10.87	5.91	3.79	2.65	2.03	1294.	20.4	0.0	8.4	4.89	113.21	
5001.000	11,199	37.99	21.28	9.37	4.52	2.71	1.93	1.50	1294.	20.0	0.0	10.2	5.98	77.06 *	
5052.000	11,167	43.20	20.83	8.08	3.95	2.43	1.85	1.54	1294.	20.0	0.0	10.4	13.10	73.45 *	
5100.000	11,247	29.20	17.74	8.99	4.85	3.05	2.23	1.79	1294.	38.0	0.0	10.1	5.85	106.74	
5151.000	11,327	27.32	16.05	7.58	3.91	2.43	1.75	1.38	1294.	36.1	0.0	12.2	6.31	89.26	
5200.000	11,143	36.32	18.81	7.74	3.87	2.51	1.89	1.54	1294.	20.0	0.0	11.7	6.97	82.14 *	
5250.000	11,383	21.01	14.08	8.24	4.85	3.01	2.14	1.67	1294.	81.2	0.0	10.7	4.67	137.69	
Mean:		27.97	16.19	8.04	4.43	2.80	1.99	1.55	1294.	93.7	0.0	11.5	6.11	107.42	
Std. Dev:		12.17	5.33	1.70	0.78	0.45	0.28	0.22	0.	120.1	0.0	2.2	2.92	31.86	
Var Coeff(%):		43.53	32.95	21.22	17.69	16.23	14.29	14.30	0.	100.0	0.0	19.6	47.79	29.66	

Figure A.163. FWD Back-Calculation Results for Uncracked Portion of Section-8C of Atlanta District.

FWD MODULUS ANALYSIS SYSTEM (SUMMARY REPORT)													(Version 4.2)	
District:	19								MODULI RANGE (psi)		Poisson Ratio Values			
County:	34								Minimum	Maximum				
Highway/Road:	SH000B								1,293,570	1,293,830	H1: $\mu = 0.35$			
		Pavement:	2.00					20,000	400,000	H2: $\mu = 0.25$				
		Base:	10.00					0	0	H3: $\mu = 0.25$				
		Subbase:	0.00							H4: $\mu = 0.35$				
		Subgrade:	99.70					25,000						

Station	Load (lbs)	Measured Deflection (mils):							Calculated Moduli values (ksi):				Absolute Depth to	
		R1	R2	R3	R4	R5	R6	R7	SURF(E1)	BASE(E2)	SUBB(E3)	SURG(E4)	ERR/Sens	Bedrock
6752.000	11,399	24.60	14.82	7.45	4.03	2.55	1.81	1.46	1294.	47.0	0.0	12.6	5.44	105.81
6800.000	11,399	22.60	15.15	8.58	4.89	3.05	2.23	1.83	1294.	68.6	0.0	10.7	5.76	141.26
6850.000	11,335	28.02	18.15	9.29	4.97	3.09	2.31	1.91	1294.	42.2	0.0	10.1	7.04	103.41
6904.000	11,383	23.33	15.72	6.54	4.69	3.01	2.27	1.87	1294.	62.1	0.0	10.8	7.11	114.87
6954.000	11,239	29.40	17.95	9.16	4.93	3.05	2.23	1.79	1294.	37.2	0.0	10.2	5.71	105.91
7019.000	11,399	26.14	17.16	9.12	4.93	3.09	2.31	1.91	1294.	49.8	0.0	10.3	6.97	107.67
7051.000	11,367	24.19	16.13	8.33	4.52	2.94	2.23	1.87	1294.	55.0	0.0	11.0	7.64	108.42
7101.000	11,271	28.46	16.51	7.99	4.24	2.74	2.14	1.87	1294.	35.5	0.0	11.5	6.77	98.74
7152.000	11,319	21.62	13.71	7.00	3.91	2.67	2.10	1.83	1294.	62.9	0.0	12.7	7.97	122.78
7200.000	11,239	24.19	15.11	7.54	4.36	2.98	2.27	1.79	1294.	53.1	0.0	11.5	7.94	153.52
7250.000	11,239	28.26	17.00	8.16	4.52	3.13	2.44	1.99	1294.	38.7	0.0	10.8	8.56	119.45
Mean:		25.53	16.13	8.29	4.54	2.94	2.21	1.83	1294.	50.2	0.0	11.1	6.99	111.73
Std. Dev:		2.66	1.38	0.75	0.38	0.19	0.15	0.14	0.	11.3	0.0	0.9	1.02	13.66
Var Coeff(%):		10.42	8.57	9.06	8.27	6.61	7.26	7.40	0.	22.4	0.0	8.1	14.57	12.23

Figure A.164. FWD Back-Calculation Results for Uncracked Portion of Section-8D of Atlanta District.

A.167

TTI MODULUS ANALYSIS SYSTEM (SUMMARY REPORT)													(Version 4.2)	
District:	19								MODULI RANGE (psi)			Poisson Ratio Values		
County:	34	Thickness (in)							Minimum	Maximum				
Highway/Road:	SH0008	Pavement:	2.00					1,293,570	1,293,830	H1: u = 0.35				
		Base:	10.00					20,000	400,000	H2: u = 0.25				
		Subbase:	0.00					0	0	H3: u = 0.25				
		Subgrade:	69.10					25,000		H4: u = 0.35				
Station	Load (lbs)	Measured Deflection (mils):							Calculated Moduli values (ksi):				Absolute Dpth to	
		R1	R2	R3	R4	R5	R6	R7	SURF(E1)	BASE(E2)	SUBB(E3)	SUBG(E4)	ERR/Sens	Bedrock
8753.000	11,151	38.15	24.20	13.12	7.34	4.44	3.02	2.28	1294.	35.0	0.0	5.7	5.74	134.31
8801.000	11,103	39.66	25.60	13.78	7.62	4.68	3.15	2.32	1294.	33.1	0.0	5.4	5.95	128.36
8857.000	11,023	41.82	27.54	15.07	8.40	5.14	3.49	2.56	1294.	32.0	0.0	4.8	5.92	137.07
8906.000	11,095	36.04	24.12	13.66	7.91	4.87	3.28	2.44	1294.	43.0	0.0	5.2	5.33	145.02
8951.000	11,143	34.73	24.04	13.87	7.99	4.95	3.36	2.52	1294.	47.5	0.0	5.2	5.55	149.98
9003.000	11,335	25.65	14.57	6.29	2.73	1.47	0.97	0.77	1294.	34.3	0.0	13.6	9.62	64.07
9054.000	11,439	18.08	10.66	4.91	2.16	1.04	0.67	0.53	1294.	59.0	0.0	17.9	10.41	64.18
9101.000	11,303	18.49	9.55	3.54	1.34	0.73	0.59	0.53	1294.	42.7	0.0	24.3	15.22	56.71
9151.000	11,383	16.53	8.73	3.37	1.39	0.85	0.63	0.53	1294.	55.0	0.0	24.4	12.52	59.62
9201.000	11,391	19.63	11.07	4.50	1.83	0.97	0.67	0.53	1294.	45.3	0.0	19.3	12.48	59.59
9250.000	11,399	17.43	9.18	3.58	1.43	0.77	0.55	0.49	1294.	49.6	0.0	24.0	12.77	58.40
Mean:		27.84	17.21	8.70	4.56	2.72	1.85	1.41	1294.	43.3	0.0	13.6	5.23	81.12
Std. Dev:		10.23	7.77	5.06	3.19	2.02	1.36	0.98	0.	9.1	0.0	8.6	3.66	30.96
Var Coeff(%):		36.76	45.13	58.20	69.93	74.43	73.21	69.37	0.	21.0	0.0	63.2	39.67	38.17

Figure A.165. FWD Back-Calculation Results for Uncracked Portion of Section-8E of Atlanta District.

FWD MODULUS ANALYSIS SYSTEM (SUMMARY REPORT)														(Version 4.2)		
District:	19									MODULI RANGE(psi)						
County:	34			Thickness(in)						Minimum	Maximum	Poisson Ratio Values				
Highway/Road:	SH000B			Pavement:	2.00			1,293,570		1,293,830		H1: $\mu = 0.35$				
				Base:	10.00			20,000		400,000		H2: $\mu = 0.25$				
				Subbase:	0.00			0		0		H3: $\mu = 0.25$				
				Subgrade:	69.70					13,500		H4: $\mu = 0.35$				
Station	Load (lbs)	Measured Deflection (mils):							Calculated Moduli values (ksi):				Absolute Dpth to			
		R1	R2	R3	R4	R5	R6	R7	SURF(E1)	BASE(E2)	SUBB(E3)	SUBG(E4)	ERR/Sens	Bedrock		
10751.000	10,967	25.90	13.21	5.29	2.53	1.62	1.22	1.06	1294.	31.7	0.0	14.4	11.80	72.88		
10803.000	11,247	23.90	11.65	4.79	2.49	1.66	1.30	1.06	1294.	38.7	0.0	15.6	13.27	88.76		
10854.000	11,263	22.15	11.57	5.25	2.69	1.74	1.34	1.14	1294.	47.8	0.0	14.7	11.17	85.39		
10900.000	11,239	25.57	13.75	6.70	3.38	2.01	1.43	1.14	1294.	42.0	0.0	11.9	7.11	83.08		
10951.000	11,247	27.28	14.12	6.25	2.98	1.82	1.34	1.18	1294.	33.5	0.0	12.8	8.93	73.05		
11002.000	11,247	24.43	12.97	5.75	2.89	1.82	1.39	1.22	1294.	40.6	0.0	13.5	10.52	81.46		
11051.000	11,295	15.35	9.14	4.95	2.65	1.82	1.43	1.18	1294.	109.8	0.0	15.1	10.63	98.55		
11103.000	11,287	21.62	11.69	5.20	2.61	1.74	1.34	1.14	1294.	49.6	0.0	14.8	12.29	80.73		
11152.000	11,263	20.32	11.57	5.37	2.73	1.74	1.34	1.14	1294.	58.3	0.0	14.4	10.91	83.63		
11202.000	11,239	9.65	7.37	5.16	3.42	2.32	1.68	1.30	1294.	373.7	0.0	12.5	4.15	223.15 *		
11250.000	11,127	30.87	19.14	9.37	4.48	2.51	1.72	1.54	1294.	33.8	0.0	8.7	8.54	75.79		
Mean:		22.46	12.38	5.83	2.99	1.89	1.41	1.19	1294.	78.1	0.0	13.5	9.94	81.71		
Std. Dev:		5.84	2.99	1.30	0.59	0.28	0.15	0.13	0.	100.5	0.0	2.0	2.61	17.31		
Var Coeff(%):		26.02	24.16	22.39	19.66	14.88	10.93	11.25	0.	100.0	0.0	14.5	26.22	21.18		

Figure A.166. FWD Back-Calculation Results for Uncracked Portion of Section-8F of Atlanta District.

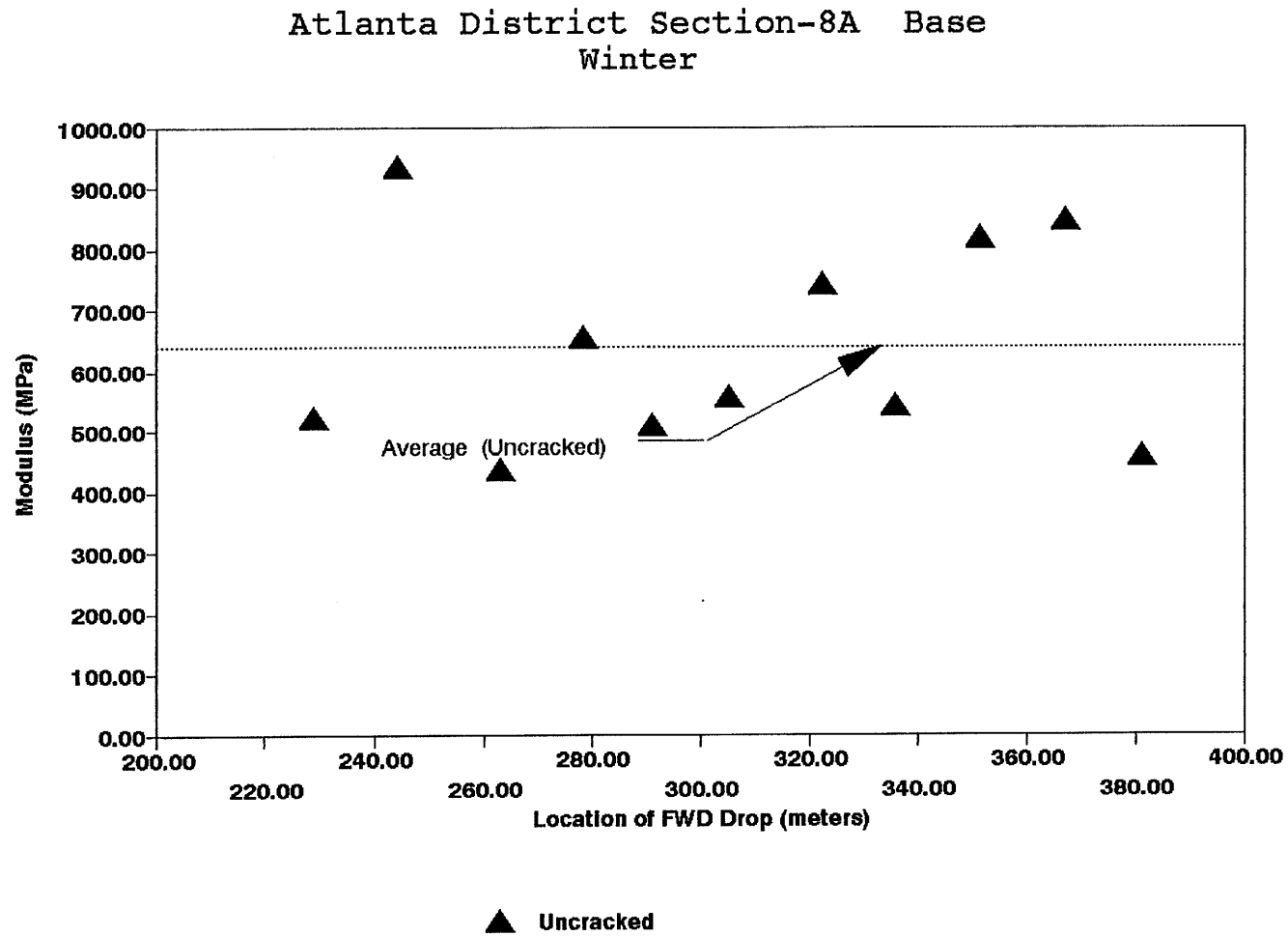


Figure A.167. Variation of Modulus of Stabilized Base within Test Section for Section-8A of Atlanta District.

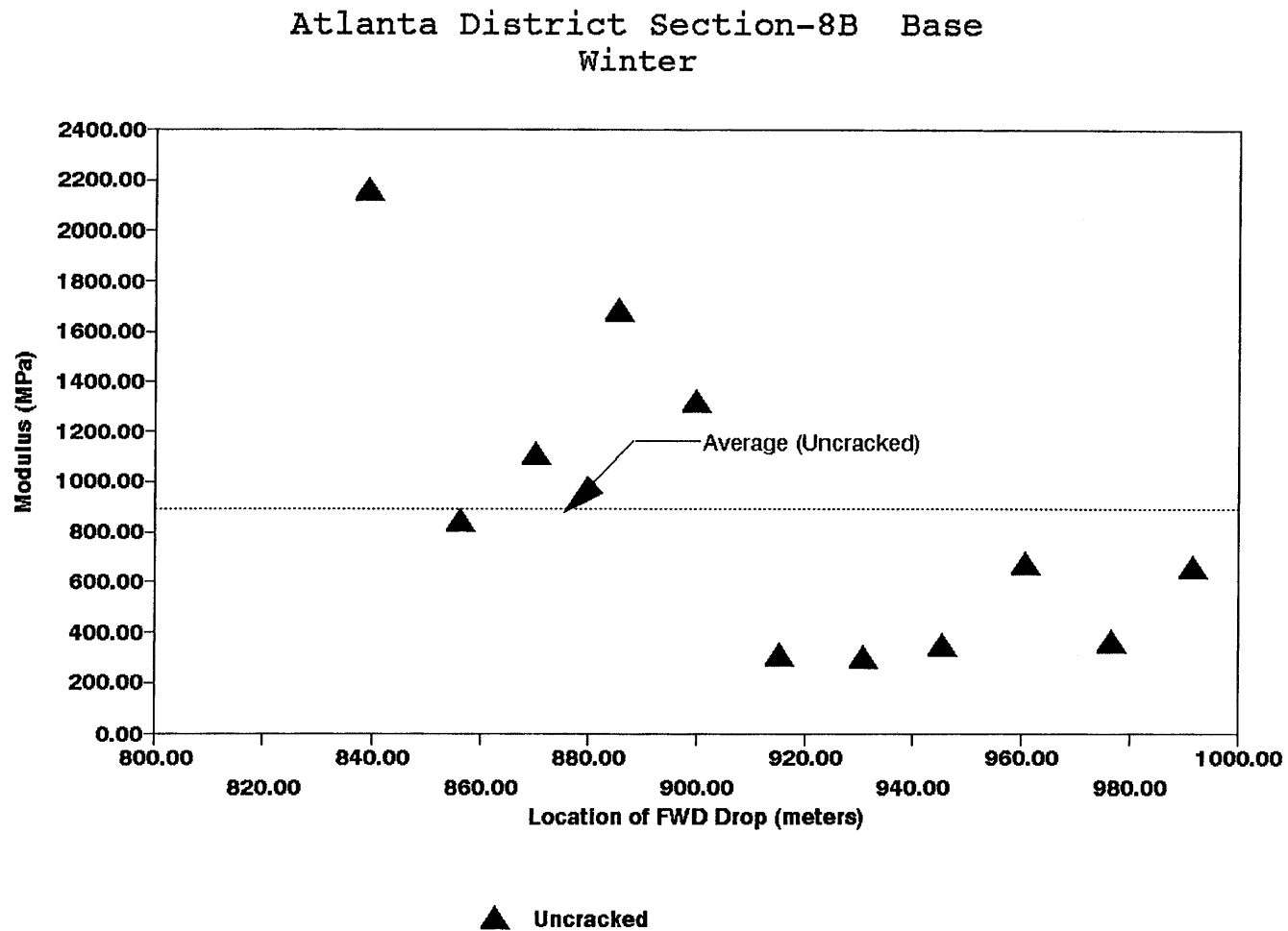
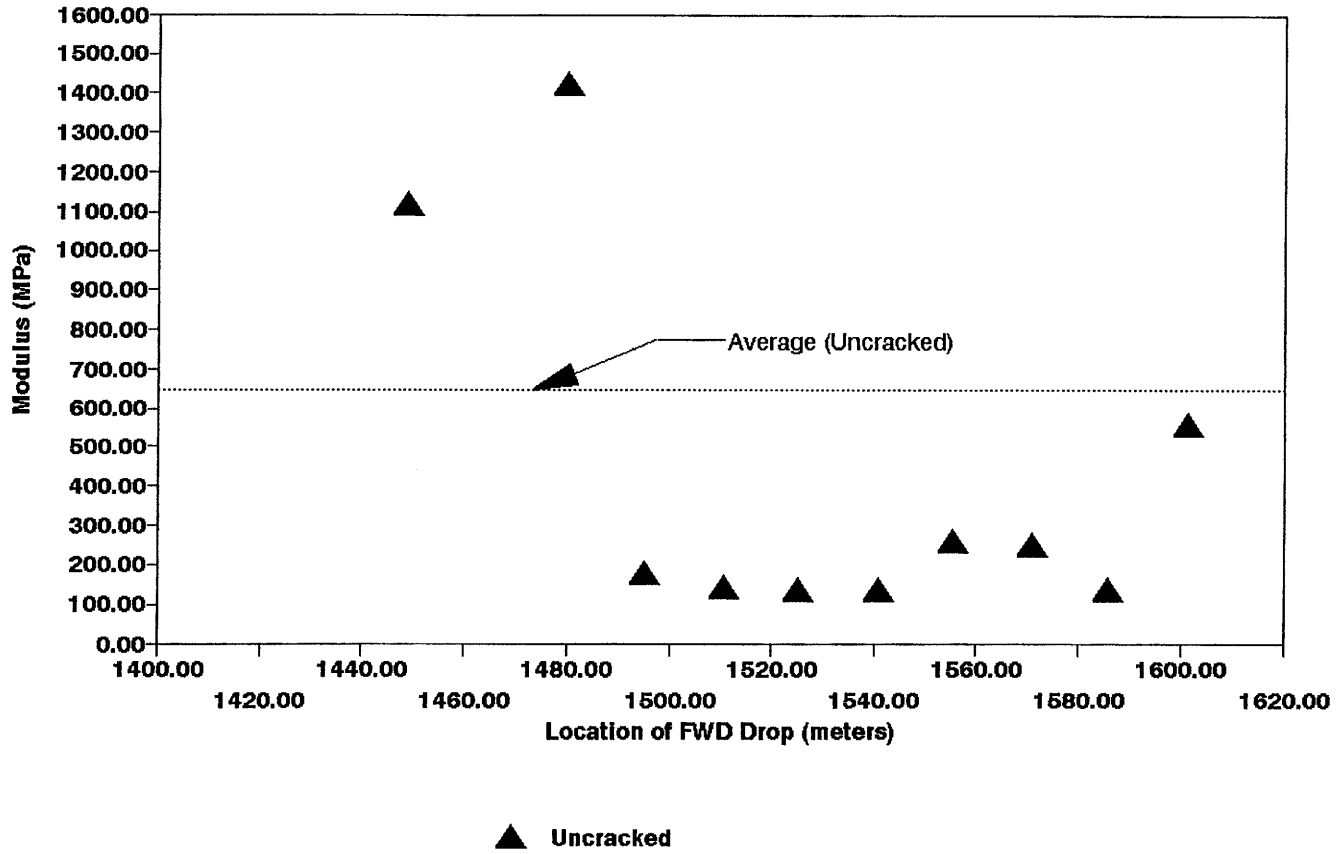


Figure A.168. Variation of Modulus of Stabilized Base within Test Section for Section-8B of Atlanta District.

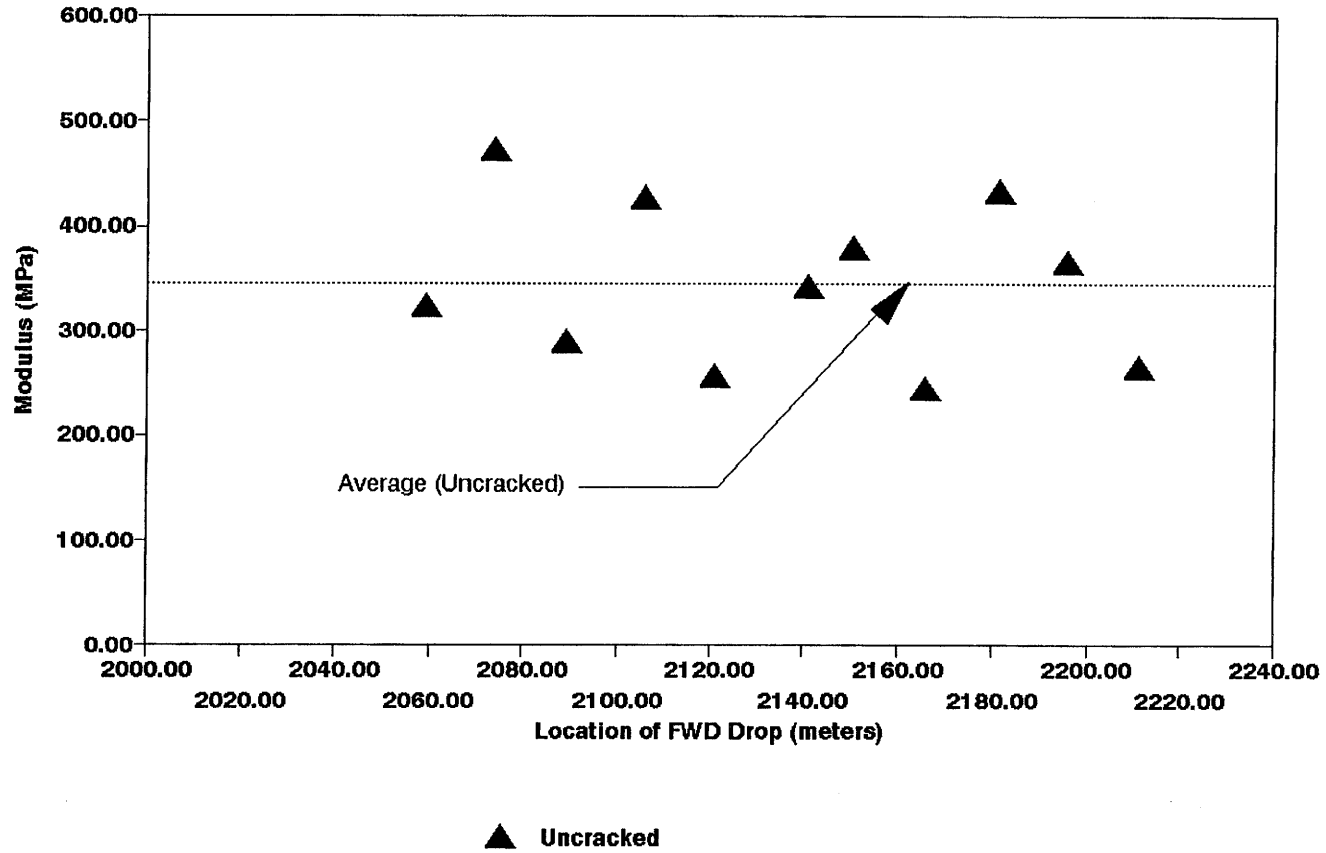
Atlanta District Section-8C Base
Winter



A.171

Figure A.169. Variation of Modulus of Stabilized Base within Test Section for Section-8C of Atlanta District.

Atlanta District Section-8D Base
Winter



A.172

Figure A.170. Variation of Modulus of Stabilized Base within Test Section for Section-8D of Atlanta District.

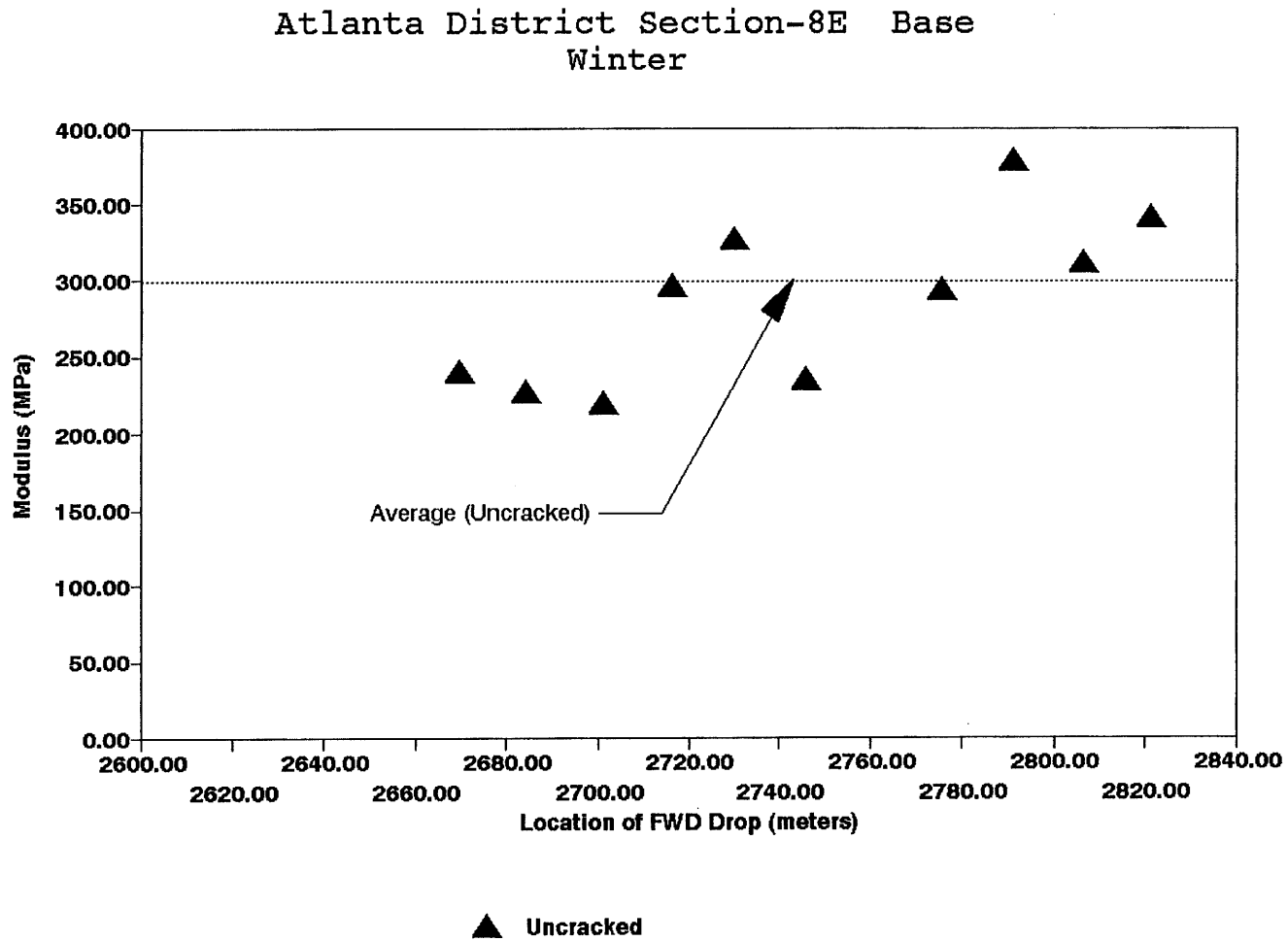


Figure A.171. Variation of Modulus of Stabilized Base within Test Section for Section-8E of Atlanta District.

Atlanta District Section-8F Base
Winter

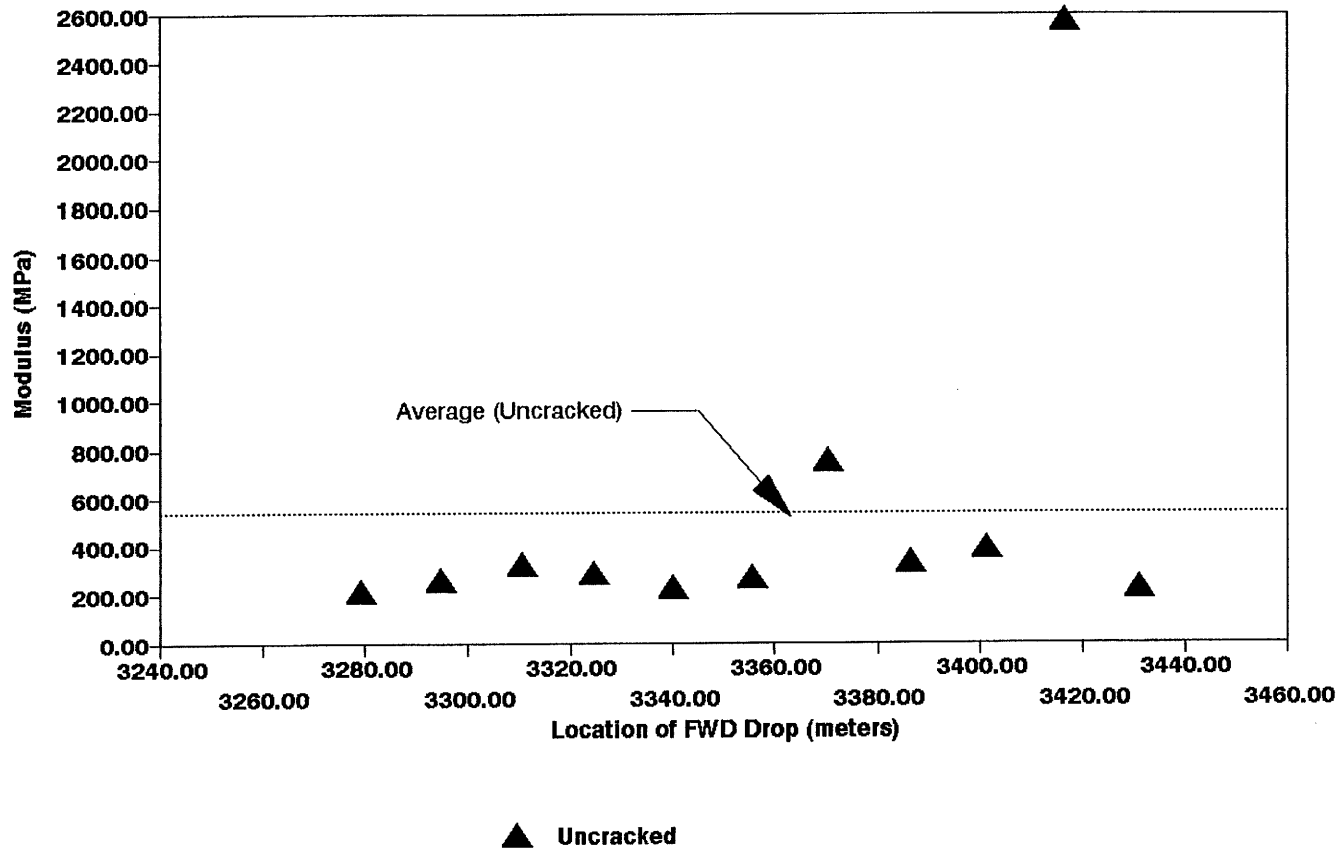


Figure A.172. Variation of Modulus of Stabilized Base within Test Section for Section-8F of Atlanta District.

Section No.: 9 District: Atlanta County: Cass Highway: SH-155

Structure: Asphalt : 64 mm

LTB : 202 mm

Flex. Subbase : 76 mm

Subgrade

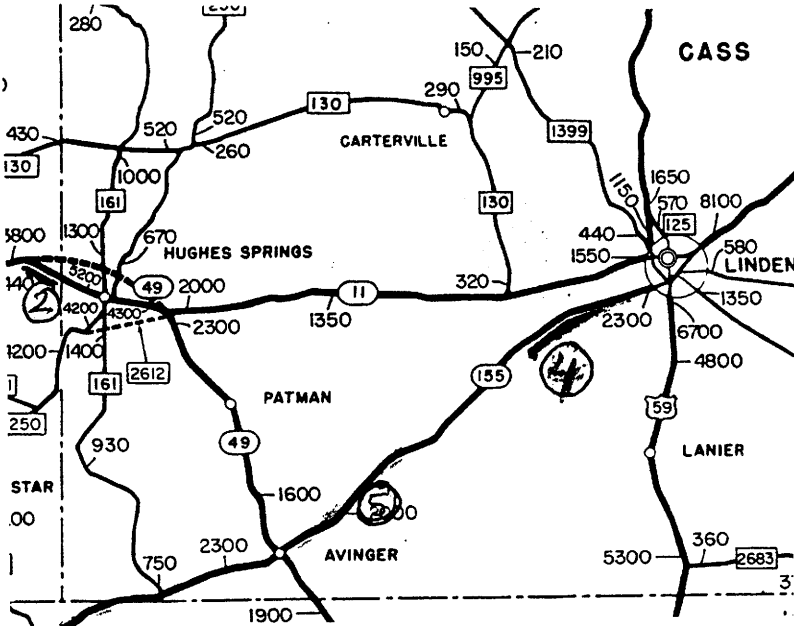
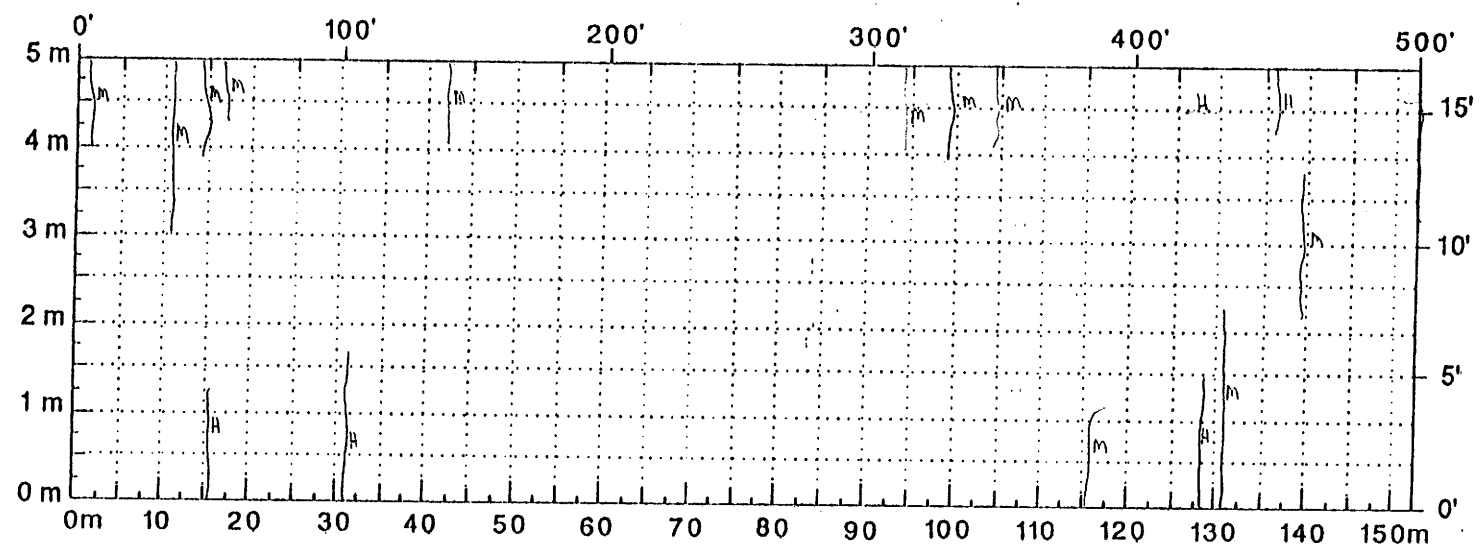


Figure A.173. Location and Details of Section-9 of Atlanta District.

A.176



Comments: _____

Figure A.174. Crack Map for Section-9 of Atlanta District.

TTI MODULUS ANALYSIS SYSTEM (SUMMARY REPORT)

(Version 4.2)

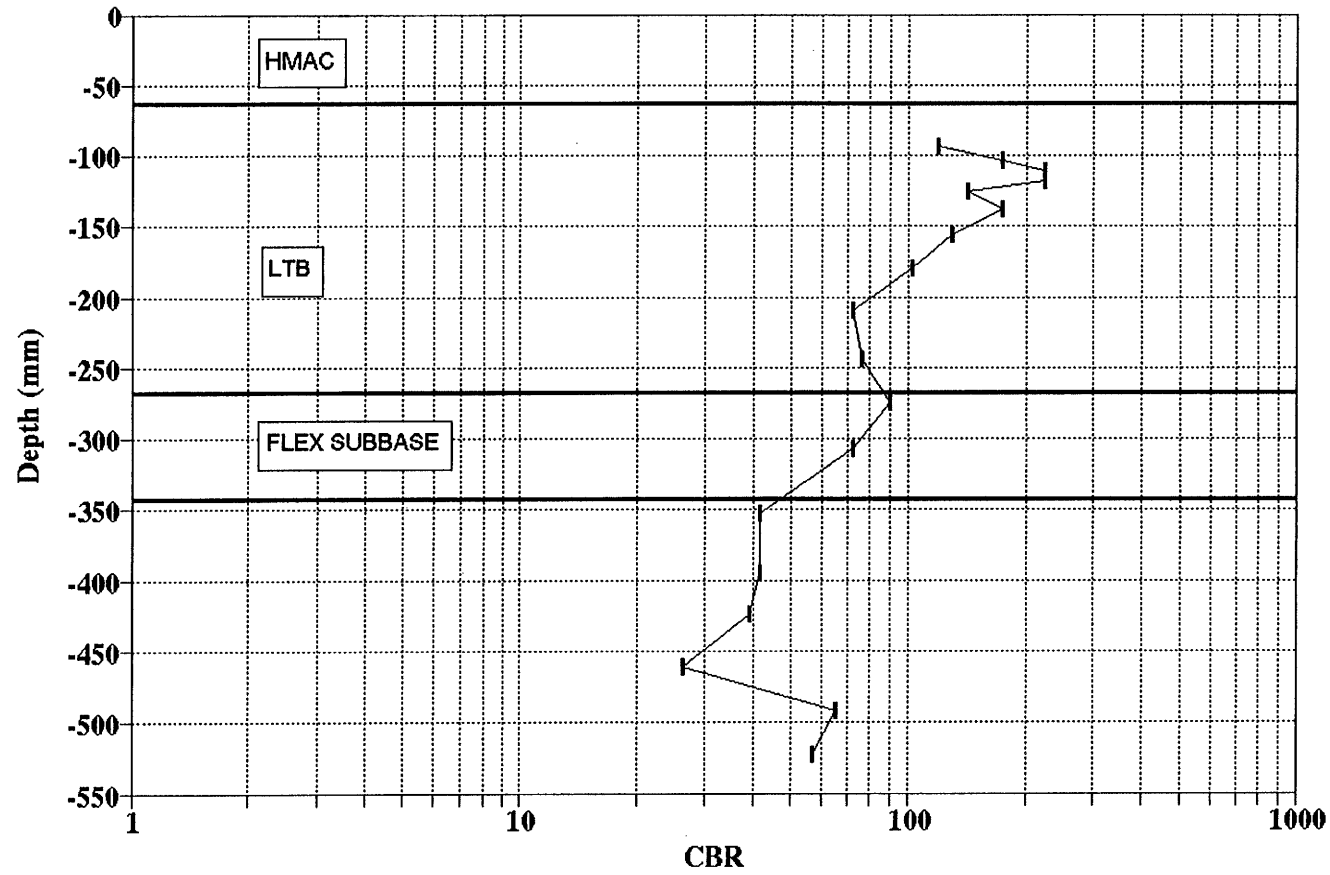
District: 19		MODULI RANGE(ksi)		
County: 34	(thickness(in))	Minimum	Maximum	Poisson Ratio Values
Highway/Road: SH0155	Pavement: 2.50	970,503	970,697	H1: $\mu = 0.35$
	Base: 8.00	20,000	400,000	H2: $\mu = 0.25$
	Subbase: 3.00	10,000	300,000	H3: $\mu = 0.35$
	Subgrade: 178.70		25,000	H4: $\mu = 0.35$

Station	Load (lbs)	Measured Deflection (mils):							Calculated Moduli values (ksi):				Absolute Depth to ERR/Sens Bedrock
		R1	R2	R3	R4	R5	R6	R7	SURF(E1)	BASE(E2)	SURB(E3)	SURB(E4)	
0.000	11,415	25.94	13.34	6.25	3.34	2.16	1.64	1.38	971.	31.0	11.3	19.3	2.14 109.00
33.000	11,351	23.78	12.18	5.62	2.93	1.93	1.51	1.30	971.	35.0	11.0	21.5	2.81 99.89
68.000	11,487	14.58	8.31	5.16	3.14	2.13	1.60	1.34	971.	96.0	68.7	21.7	2.32 266.02
101.000	11,479	18.00	9.75	4.75	2.61	1.82	1.39	1.18	971.	62.7	13.9	24.8	3.48 123.61
135.000	11,439	13.76	6.87	3.91	2.20	1.51	1.18	0.98	971.	76.3	68.5	29.5	3.60 140.74
166.000	11,439	12.70	7.49	4.62	2.93	1.97	1.43	1.16	971.	127.0	64.0	23.8	0.95 245.73
201.000	11,375	16.17	9.84	5.75	3.42	2.20	1.51	1.18	971.	110.3	10.0	21.1	0.72 178.42 *
234.000	11,367	21.17	12.14	6.45	3.83	2.55	1.85	1.50	971.	56.7	14.8	17.5	1.31 204.30
272.000	11,399	19.42	11.81	7.37	4.61	3.01	2.02	1.46	971.	90.9	13.6	19.6	1.37 182.48
301.000	11,431	13.44	9.14	6.16	3.99	2.59	1.81	1.38	971.	222.8	10.0	18.7	0.93 189.36 *
338.000	11,327	13.72	9.01	6.33	4.16	2.90	2.06	1.58	971.	166.3	69.8	16.5	1.21 252.76
366.000	11,303	12.54	9.63	7.04	4.81	3.21	2.23	1.63	971.	351.3	10.0	15.2	2.36 218.93 *
401.000	11,503	10.38	8.89	6.79	4.81	3.40	2.44	1.83	971.	400.0	86.8	14.9	3.76 274.33 *
434.000	11,463	10.75	9.06	6.95	4.97	3.56	2.52	1.91	971.	400.0	86.8	14.1	2.84 247.49 *
467.000	11,255	14.46	10.54	7.79	5.54	3.83	2.73	2.07	971.	255.6	35.8	12.5	1.15 259.07
500.000	11,295	14.70	11.11	8.12	5.50	3.86	2.69	1.99	971.	283.3	10.0	12.9	1.25 222.53 *
Mean:		15.97	9.94	6.19	3.92	2.66	1.91	1.49	971.	172.8	36.6	18.7	2.01 192.26
Std. Dev:		4.52	1.79	1.18	1.04	0.75	0.49	0.32	0.	128.9	31.2	4.7	1.04 68.31
Var Coeff(%):		28.31	18.04	18.99	26.47	28.16	25.63	21.45	0.	74.6	85.3	25.3	51.97 35.53

A.177

Figure A.175. FWD Back-Calculation Results for Uncracked Portion of Section-9 of Atlanta District.

ATLANTA DISTRICT
SH-155 SITE-9



A.178

Figure A.176. Variation of CBR Obtained from DCP Testing for Section-9 of Atlanta District.

Atlanta District Section-9 Base
Winter

A.179

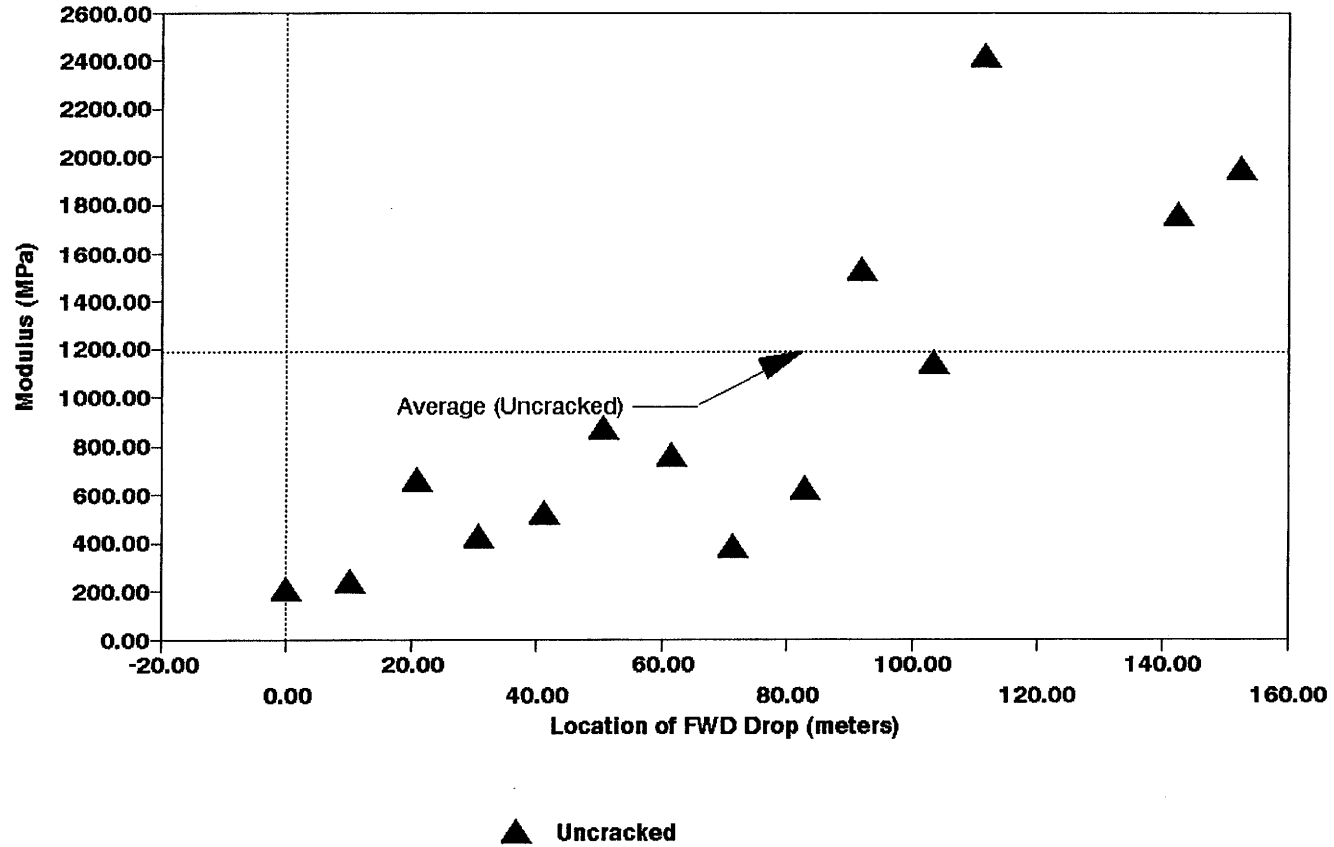


Figure A.177. Variation of Modulus of Stabilized Base within Test Section for Section-9 of Atlanta District.

A.180

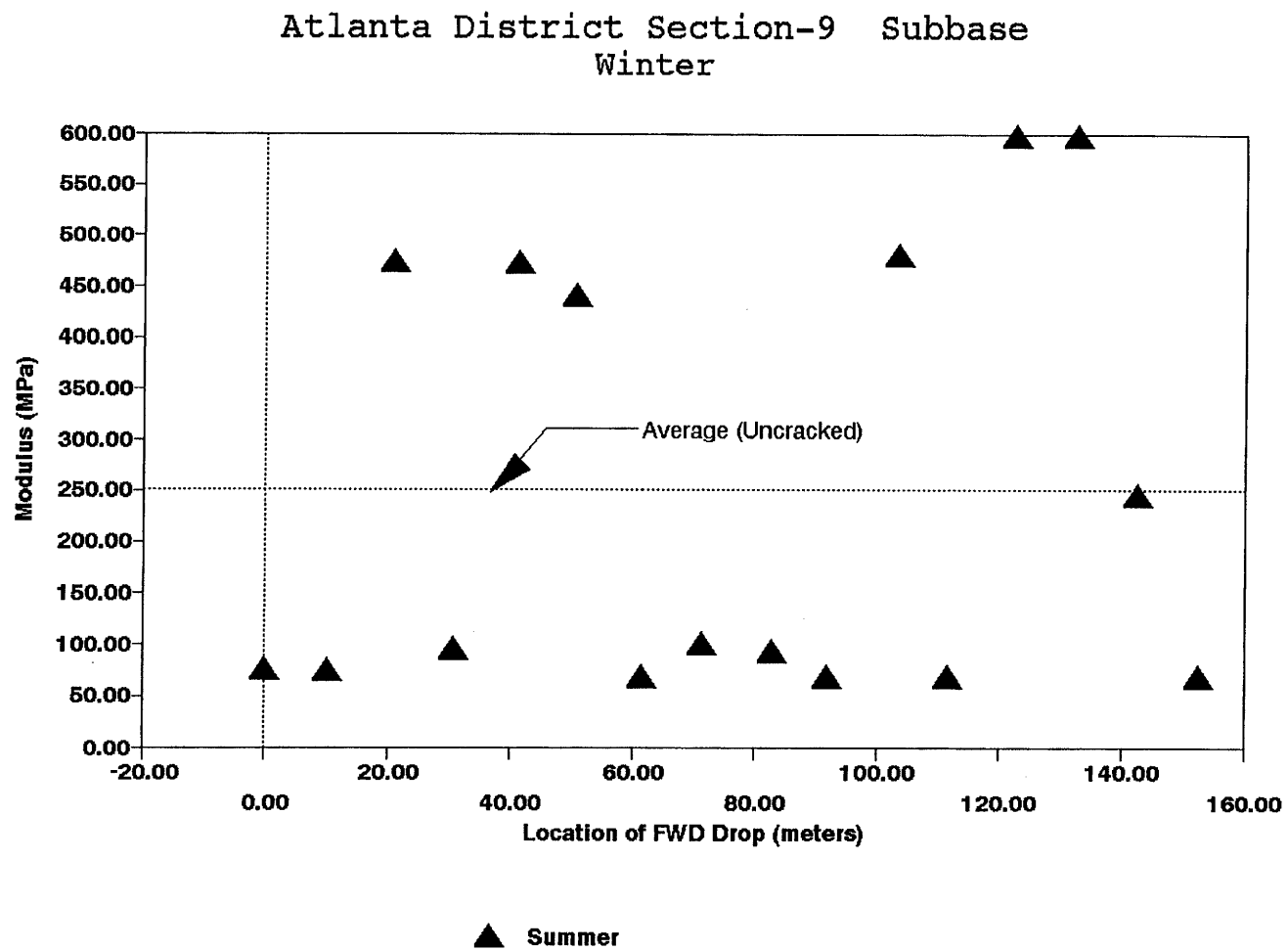


Figure A.178. Variation of Modulus of Stabilized Subbase within Test Section for Section-9 of Atlanta District.

Section No.: 10 District: Atlanta County: Cass Highway: SH-155
Structure: Seal Coat : 12 mm
LFA Base : 254 mm
Subgrade

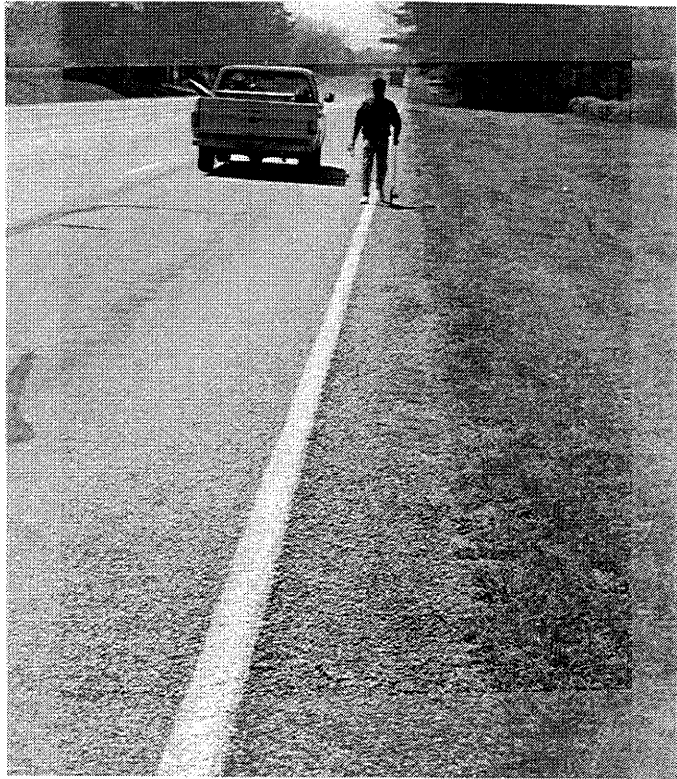
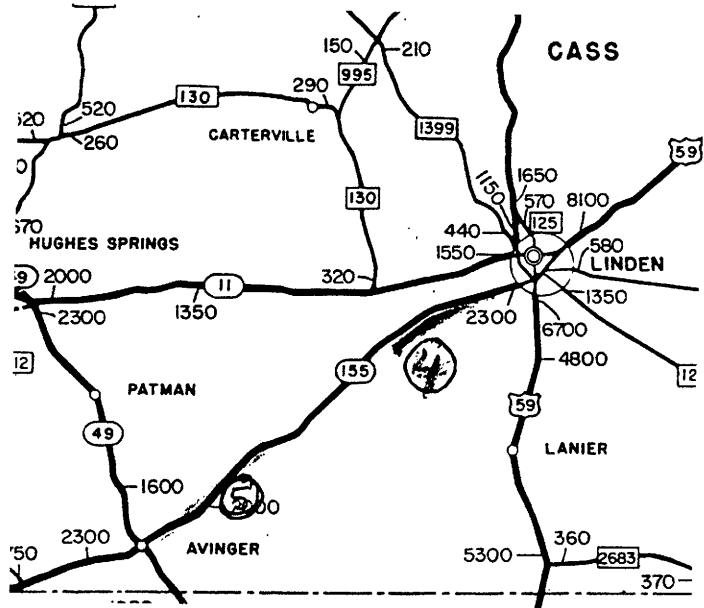


Figure A.179. Location and Details of Section-10 of Atlanta District.

A.182

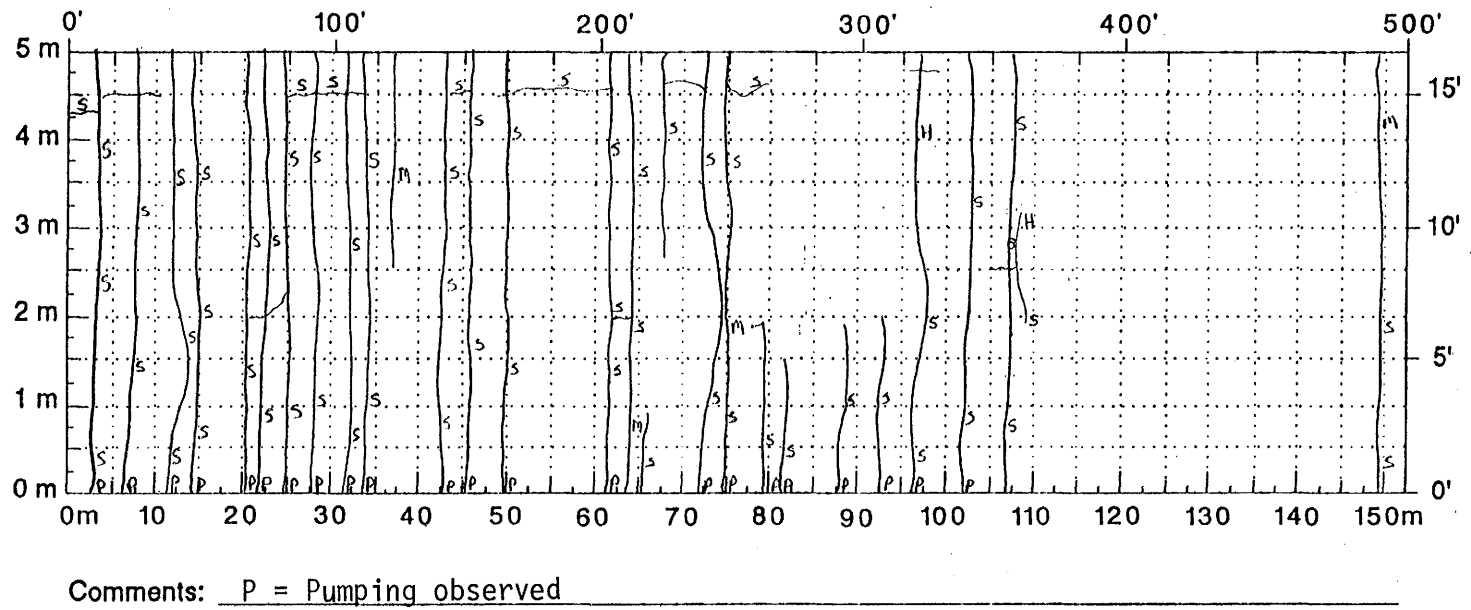


Figure A.180. Crack Map for Section-10 of Atlanta District.

TTI MODULUS ANALYSIS SYSTEM (SUMMARY REPORT)														(Version 5.0)	
District:	19			MODULI RANGE(psi)											
County:	34			Thickness(in)		Minimum		Maximum		Poisson Ratio Values					
Highway/Road:	SH0155			Pavement:	0.50	400,000	800,000	H1: % = 0.35							
				Base:	10.00	20,000	2,000,000	H2: % = 0.25							
				Subbase:	0.00	0	0	H3: % = 0.35							
				Subgrade:	104.30	19,000		H4: % = 0.40							
Station	Load (lbs)	Measured Deflection (mil δ):							Calculated Moduli values (ksi):				Absolute Dpth to		
		R1	R2	R3	R4	R5	R6	R7	SURF(E1)	BASE(E2)	SUBB(E3)	SUBG(E4)	ERR/Sens	Bedrock	
0.000	14,183	6.60	5.72	4.54	3.14	2.20	1.43	0.93	800.	1973.6	0.0	20.1	2.59	138.10 *	
34.000	13,415	8.39	7.29	6.00	3.26	2.43	1.60	0.93	620.	1158.8	0.0	17.6	6.29	104.82	
86.000	14,863	7.17	6.17	4.75	3.42	2.40	1.64	1.06	800.	1993.7	0.0	19.1	1.24	139.97 *	
142.000	14,159	10.55	9.10	7.08	5.01	3.36	2.10	1.18	800.	1108.4	0.0	13.2	3.35	115.69 *	
179.000	14,711	8.31	7.20	5.29	3.46	2.09	1.01	0.73	800.	998.4	0.0	23.0	10.76	86.76 *	
221.000	14,591	7.21	6.09	4.58	3.18	2.20	1.47	0.98	800.	1685.0	0.0	21.0	1.55	150.85 *	
270.000	12,623	9.12	7.49	5.45	3.59	2.16	1.22	0.73	800.	764.6	0.0	18.6	6.56	103.00 *	
334.000	12,655	8.51	7.29	5.25	3.42	2.09	1.22	0.77	800.	857.5	0.0	19.0	6.57	108.52 *	
Mean:		8.23	7.04	5.37	3.56	2.37	1.46	0.91	778.	1317.5	0.0	18.9	4.86	114.86	
Std. Dev:		1.26	1.07	0.85	0.61	0.42	0.33	0.16	64.	494.4	0.0	2.8	3.25	20.23	
Var Coeff(%):		15.30	15.18	15.82	17.00	17.81	22.85	17.81	8.	37.5	0.0	15.0	66.92	17.61	

Figure A.181. FWD Back-Calculation Results for Uncracked Portion of Section-10 of Atlanta District.

TTI MODULUS ANALYSIS SYSTEM (SUMMARY REPORT)

(Version 4.2)

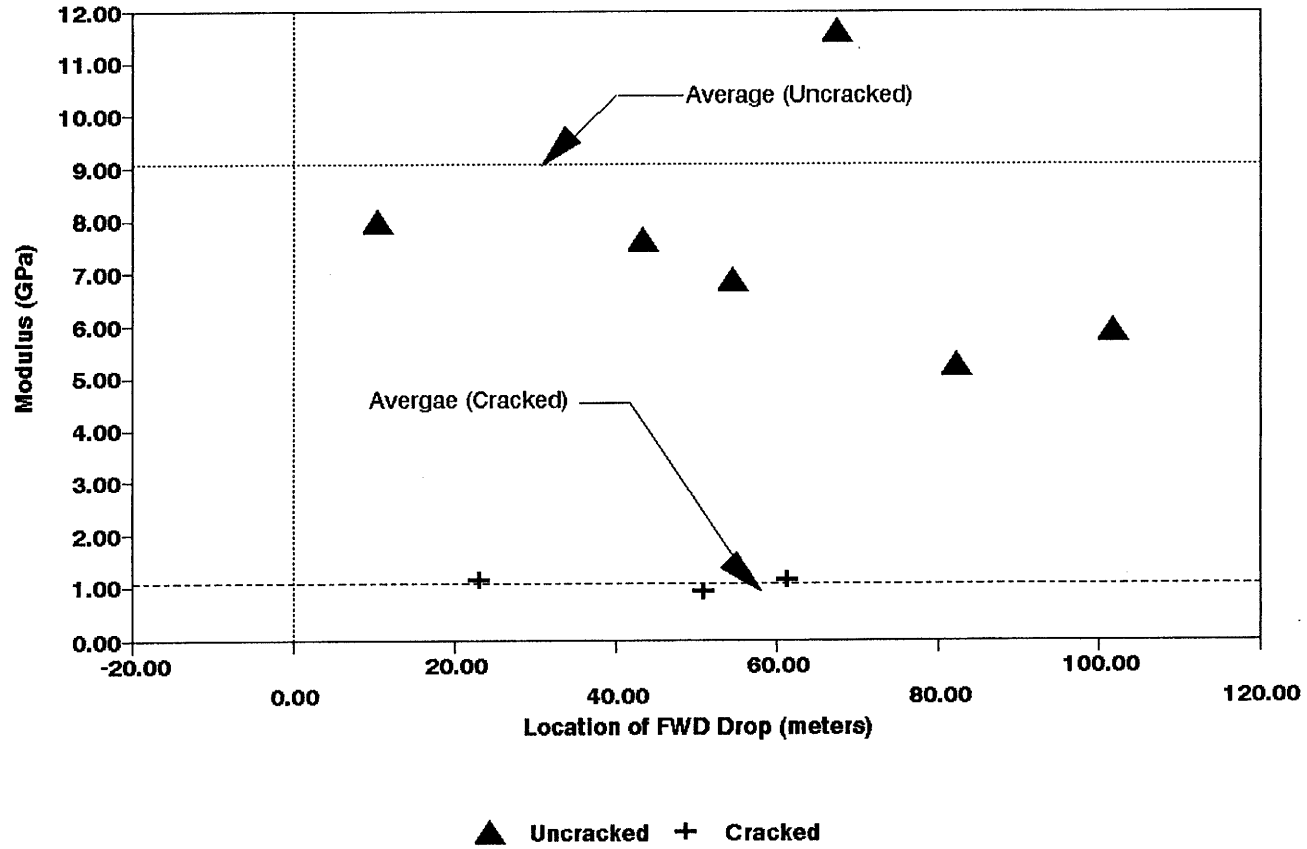
District: 1		MODULI RANGE(psi)		
County: 1	Thickness(in)	Minimum	Maximum	Poisson Ratio Values
Highway/Road: SH155	Pavement: 0.50	970,903	971,097	H1: J = 0.35
	Base: 10.00	20,000	400,000	H2: J = 0.25
	Subbase: 0.00	0	0	H3: J = 0.30
	Subgrade: 71.30	25,000		H4: J = 0.35

Station	Load (lbs)	Measured Deflection (mils):							Calculated Moduli values (ksi):				Absolute Dpth to	
		R1	R2	R3	R4	R5	R6	R7	SURF(E1)	BASE(E2)	SUBB(E3)	SUBG(E4)	ERR/Sens	Bedrock
1.000	8,566	13.40	9.59	5.75	2.93	1.47	0.84	0.57	971.	165.4	0.0	11.3	8.30	82.16
1.000	8,710	15.07	10.87	6.04	2.89	1.51	0.92	0.69	971.	135.6	0.0	11.1	10.06	74.65
1.000	8,614	13.23	8.40	5.12	2.81	1.51	0.80	0.53	971.	167.9	0.0	12.4	2.73	89.97
Mean:		13.90	9.62	5.64	2.88	1.50	0.85	0.60	971.	156.3	0.0	11.6	7.03	81.78
Std. Dev:		1.02	1.24	0.47	0.06	0.02	0.06	0.08	0.	18.0	0.0	0.7	3.83	6.24
Var Coeff(%):		7.32	12.84	8.34	2.12	1.54	7.16	13.96	0.	11.5	0.0	6.1	54.39	7.63

A.184

Figure A.182. FWD Back-Calculation Results for Cracked Portion of Section-10 of Atlanta District.

Atlanta District Section-10 Base
Winter



A.185

Figure A.183. Variation of Modulus of Stabilized Base within Test Section for Section-9 of Atlanta District.

Section No.: 11 District: Atlanta County: Cass Highway: SH-77
Structure: Asphalt : 57 mm
LTB : 254 mm
Subgrade

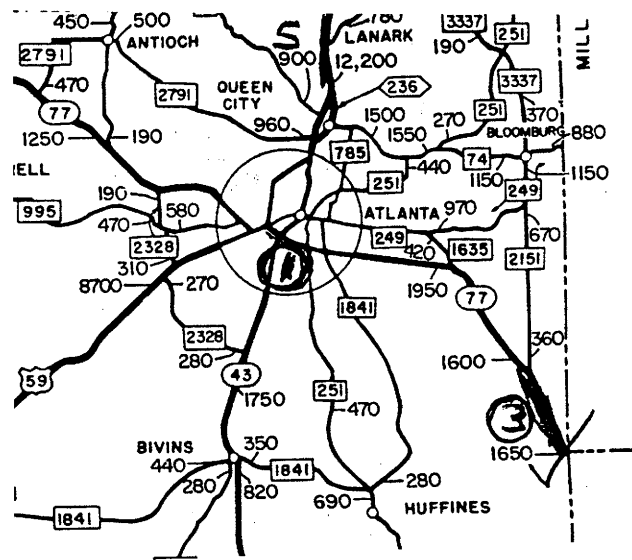
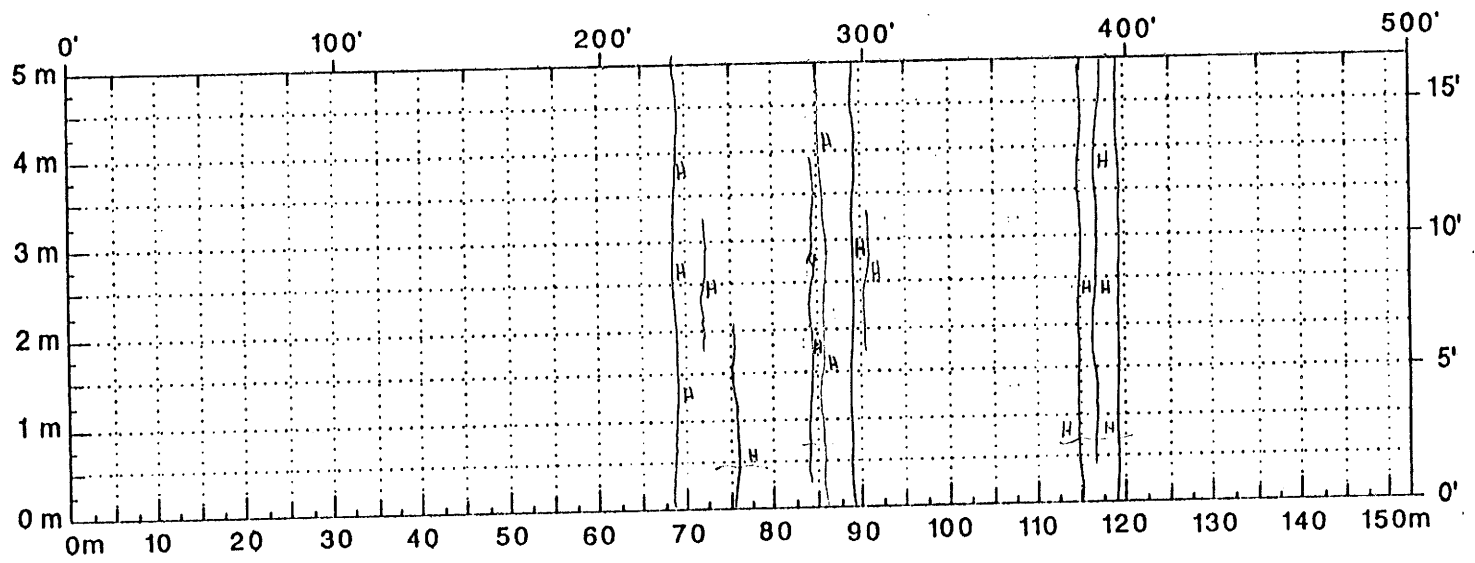


Figure A.184. Location and Details of Section-11 of Atlanta District.

A.187



Comments: _____

Figure A.185. Crack Map for Section-11 of Atlanta District.

TTI MODULUS ANALYSIS SYSTEM (SUMMARY REPORT)													(Version 4.2)	
District:	19								MODULI RANGE(ksi)					
County:	34		Thickness(in)						Minimum	Maximum	Poisson Ratio Values			
Highway/Road:	SH0077		Pavement:	2.30		900,710		900,890		H1: $\mu = 0.35$				
			Base:	10.00		20,000		400,000		H2: $\mu = 0.25$				
			Subbase:	0.00		0		0		H3: $\mu = 0.25$				
			Subgrade:	147.50		25,000				H4: $\mu = 0.35$				
Station	Load (lbs)	Measured Deflection (mils):							Calculated Moduli values (ksi):				Absolute Dpth to	
		R1	R2	R3	R4	R5	R6	R7	SURF(E1)	BASE(E2)	SUBB(E3)	SUBG(E4)	ERR/Sens	Bedrock
0.000	11,383	17.18	10.04	5.70	3.42	2.32	1.72	1.42	901.	80.6	0.0	18.3	3.08	226.94
33.000	11,431	15.88	10.13	6.20	3.71	2.47	1.81	1.46	901.	105.0	0.0	17.1	3.73	221.55
67.000	11,415	21.22	11.61	6.54	3.79	2.51	1.85	1.50	901.	55.4	0.0	16.4	2.63	168.60
100.000	11,335	26.31	12.88	6.29	3.71	2.51	1.81	1.46	901.	33.1	0.0	16.6	3.26	191.93
133.000	11,375	25.00	12.88	6.33	3.71	2.40	1.72	1.38	901.	36.4	0.0	16.7	1.51	182.37
168.000	11,319	21.17	12.35	6.58	3.71	2.40	1.72	1.38	901.	52.6	0.0	16.3	3.97	140.99
201.000	11,327	16.90	10.50	5.95	3.34	2.09	1.47	1.18	901.	77.8	0.0	18.6	6.29	138.11
234.000	11,407	10.02	7.45	5.20	3.26	2.13	1.51	1.14	901.	267.4	0.0	19.7	5.16	198.19
268.000	11,295	13.19	9.47	6.33	3.95	2.55	1.64	1.22	901.	161.5	0.0	16.5	6.13	156.79
300.000	11,367	10.18	8.40	5.58	3.34	2.05	1.30	0.98	901.	233.8	0.0	19.5	11.28	143.01
333.000	11,359	9.24	7.00	4.54	2.65	1.74	1.22	0.93	901.	250.1	0.0	23.5	7.44	179.92
369.000	11,327	10.75	7.66	5.20	3.26	2.05	1.30	0.93	901.	209.3	0.0	20.4	6.48	150.65
401.000	11,319	14.25	9.14	5.91	3.59	2.16	1.34	0.98	901.	117.7	0.0	18.8	7.01	132.51
435.000	11,327	11.20	8.11	5.12	2.81	1.78	1.13	0.98	901.	162.6	0.0	22.3	10.54	123.67
470.000	11,367	15.19	8.81	5.12	2.98	1.82	1.22	0.85	901.	87.8	0.0	21.7	4.98	139.81
509.000	11,327	10.67	7.74	5.20	3.26	2.01	1.39	1.06	901.	214.8	0.0	20.2	6.14	145.84
Mean:		15.52	9.64	5.74	3.41	2.19	1.51	1.18	901.	134.1	0.0	18.9	5.60	159.79
Std. Dev:		5.45	1.96	0.62	0.37	0.27	0.24	0.23	0.	80.3	0.0	2.3	2.68	27.64
Var Coeff(%):		35.12	20.32	10.78	10.80	12.45	16.14	19.21	0.	59.9	0.0	12.1	47.88	17.30

Figure A.186. FWD Back-Calculation Results for Cracked Portion of Section-11 of Atlanta District.

A.189

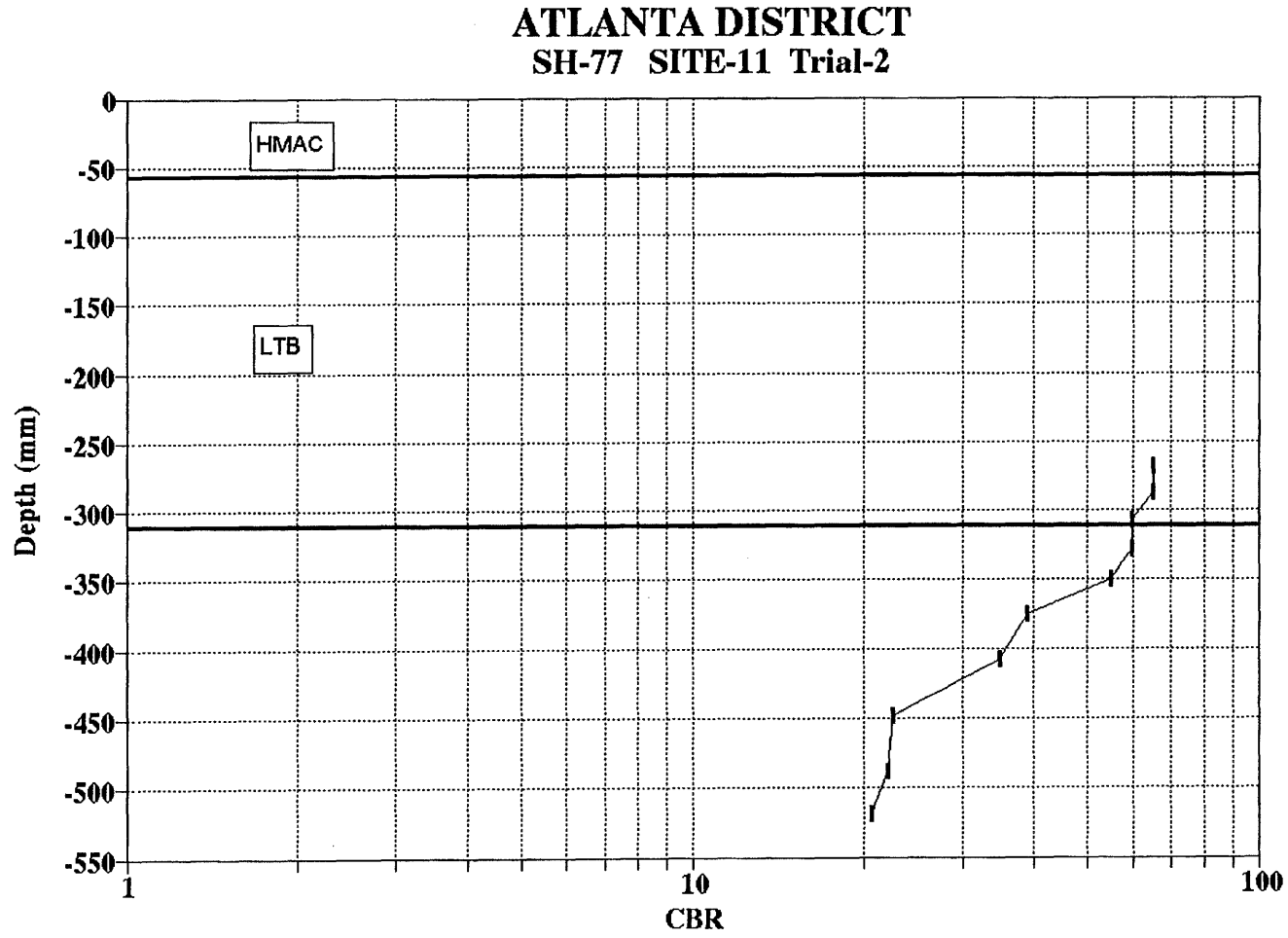


Figure A.187. Variation of CBR Obtained from DCP Testing for Section-11 of Atlanta District.

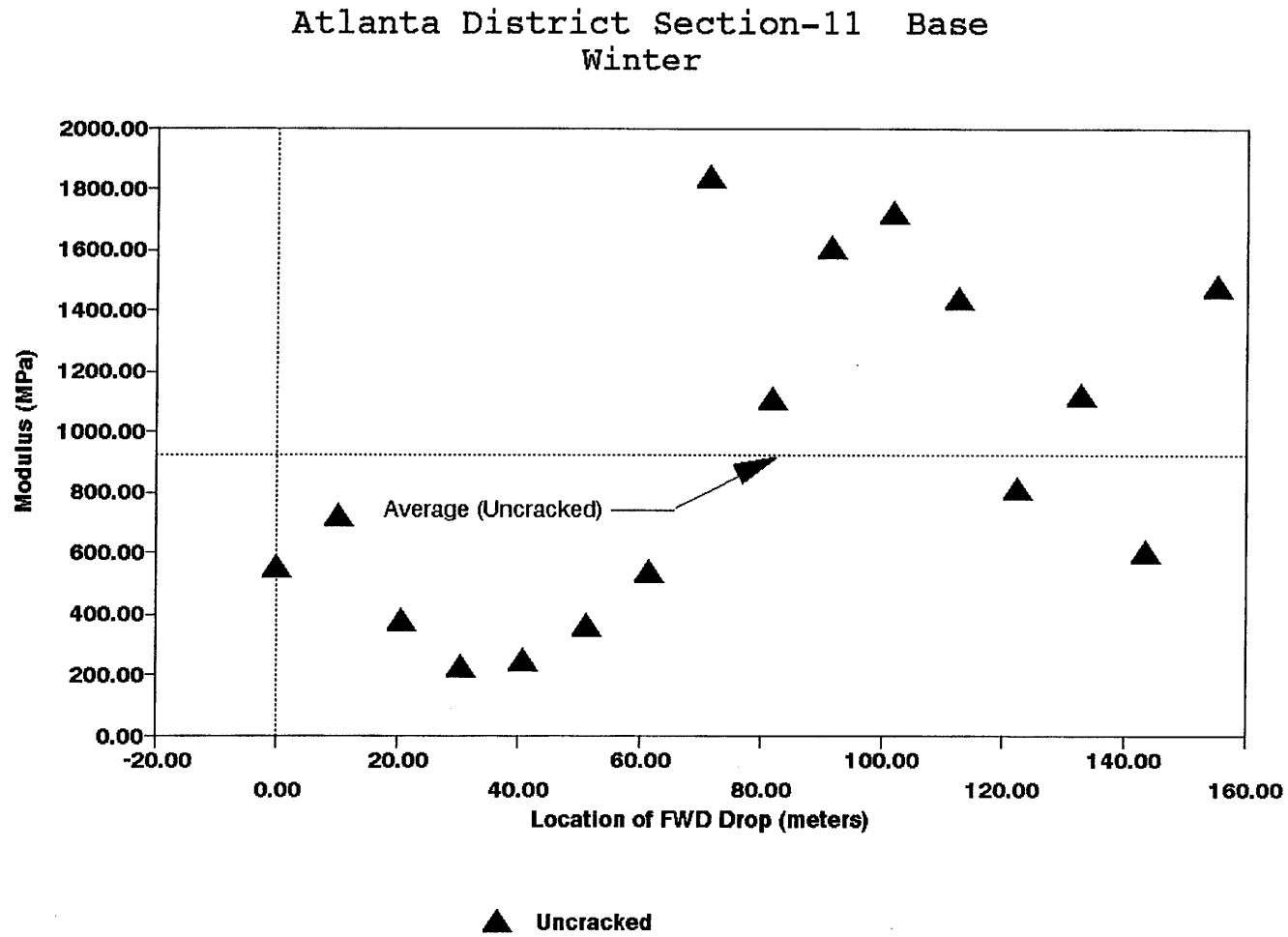


Figure A.188. Variation of Modulus of Stabilized Base within Test Section for Section-11 of Atlanta District.

Section No.: 1 District: Fort Worth County: Parker Highway: SH-199
Structure: Asphalt : 51 mm
Flex Base : 254 mm
LTS : 153 mm
Subgrade

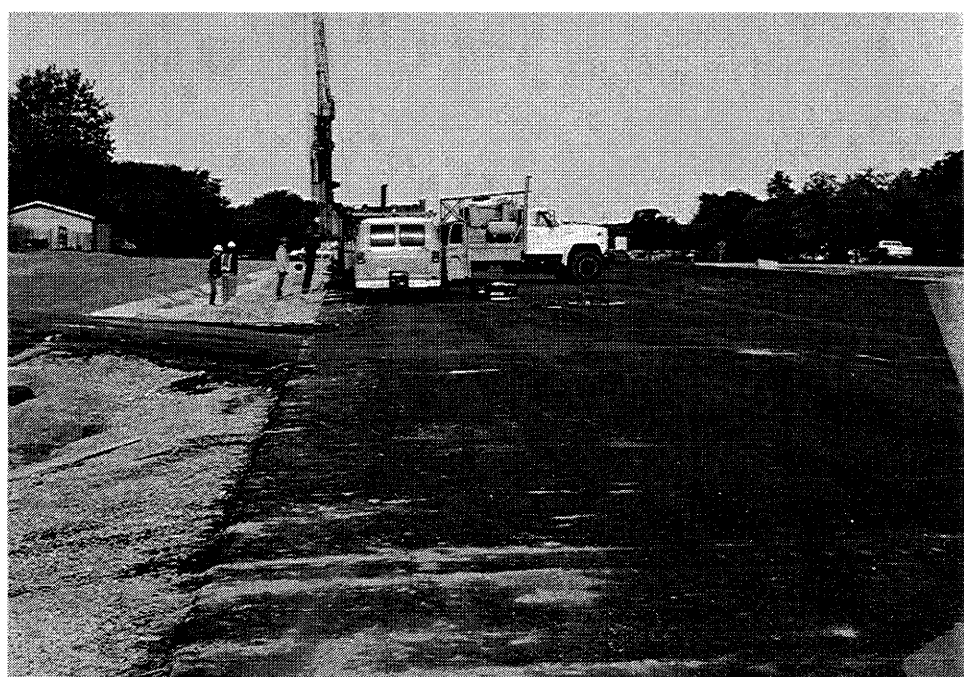
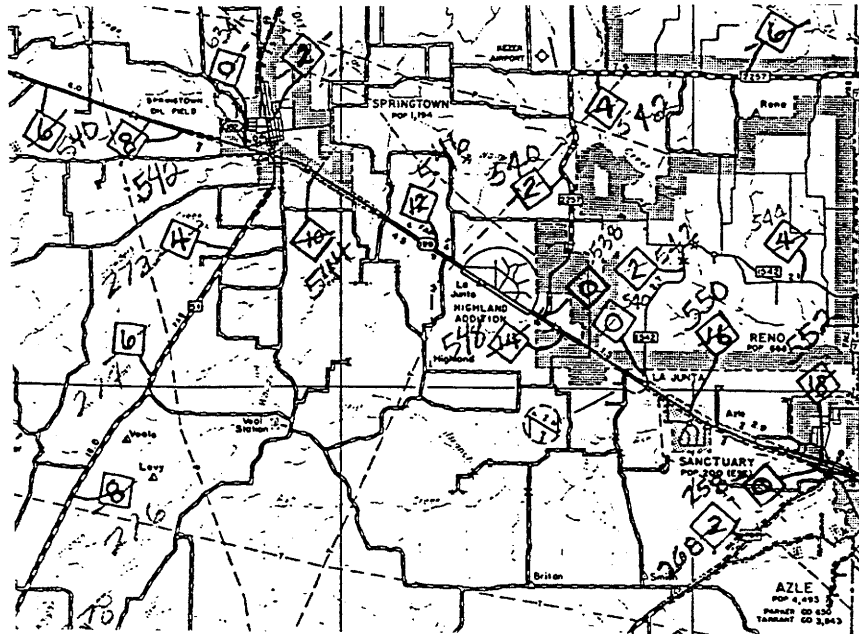
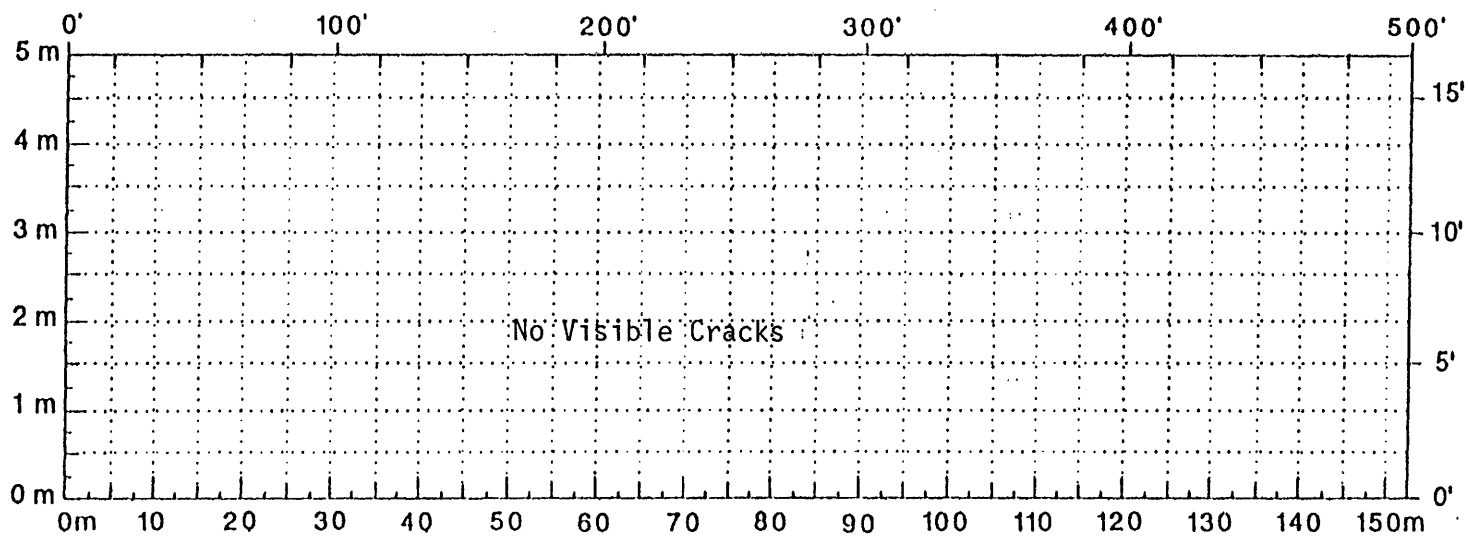


Figure A.189. Location and Details of Section-1 of Fort Worth District.

A.192



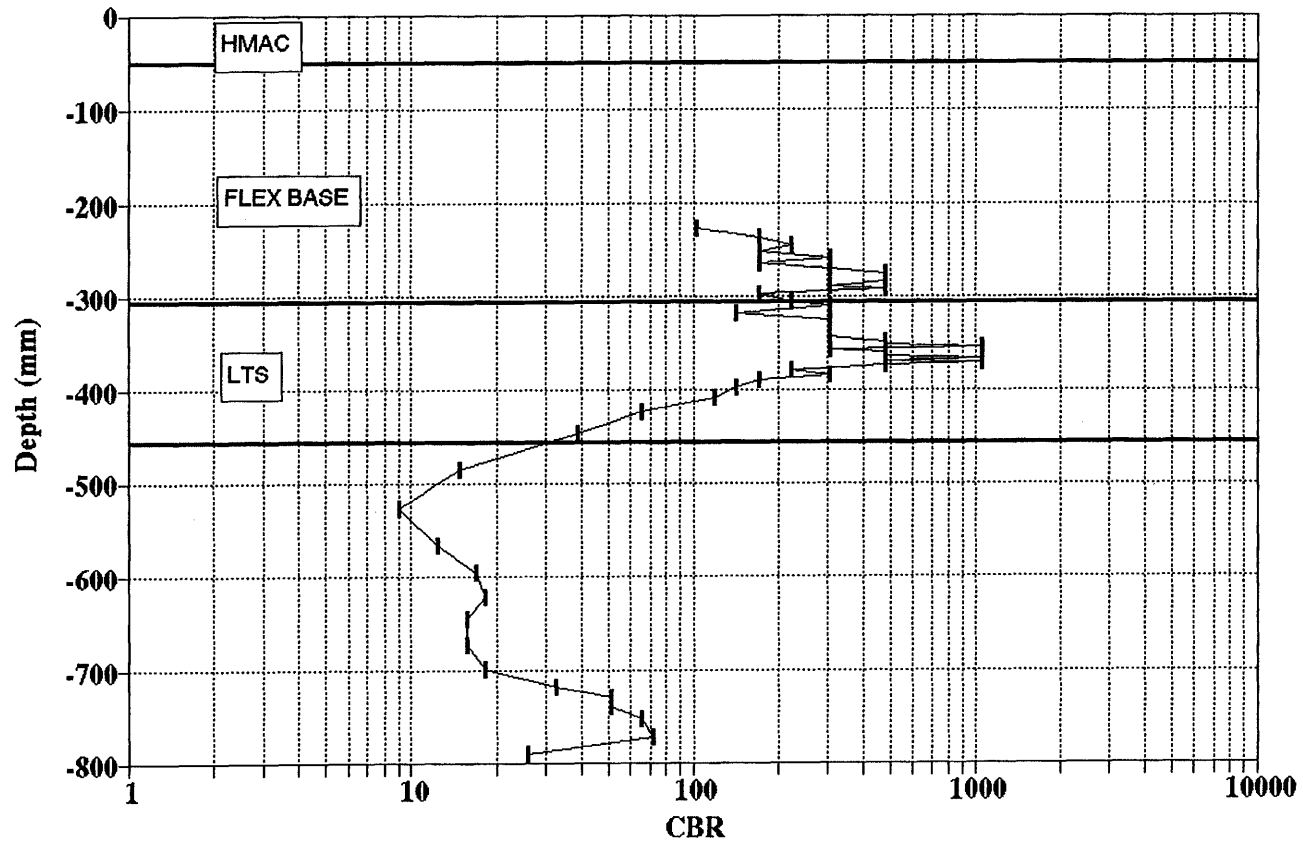
Comments: No Visible Cracks

Figure A.190. Crack Map for Section-1 of Ft. Worth District.

TTI MODULUS ANALYSIS SYSTEM (SUMMARY REPORT)													(Version 4.2)	
District:	2													
County:	184													
Highway/Road:	SH0199													
			Thickness(in)		MODULI RANGE(psi)		Poisson Ratio Values							
			Pavement:	2.00	Minimum	1,206,280	Maximum	1,206,520	H1: u = 0.35					
			Base:	10.00		20,000		400,000	H2: u = 0.35					
			Subbase:	6.00		10,000		300,000	H3: u = 0.25					
			Subgrade:	282.00				20,000	H4: u = 0.35					
Station	Load (lbs)	Measured Deflection (mils):							Calculated Moduli values (ksi):				Absolute Dpth to	
		R1	R2	R3	R4	R5	R6	R7	SURF(E1)	BASE(E2)	SUBB(E3)	SUBG(E4)	ERR/Sens	Bedrock
0.000	16,747	24.25	13.74	7.83	5.15	3.75	3.01	2.45	1206.	85.4	24.2	21.3	2.96	300.00
28.000	16,723	25.91	14.61	8.39	5.43	3.74	2.81	2.19	1206.	83.9	15.2	21.5	1.13	258.63
50.000	16,680	22.69	12.09	6.63	4.33	3.28	2.65	2.09	1206.	78.5	35.8	24.2	3.67	300.00
75.000	16,600	25.37	13.39	6.73	3.97	2.89	2.22	1.74	1206.	69.9	15.9	27.4	3.52	169.59
100.000	16,461	24.64	14.24	7.84	4.69	3.13	2.42	1.94	1206.	91.2	10.0	25.7	2.83	193.68 †
127.000	16,358	25.69	15.09	8.42	4.92	3.21	2.47	1.90	1206.	84.4	10.0	24.0	3.34	160.95 †
150.000	16,433	19.83	11.00	6.71	4.27	3.04	2.41	1.91	1206.	110.8	27.0	25.6	2.23	300.00
175.000	16,155	27.98	16.06	8.81	5.23	3.47	2.66	2.06	1206.	72.1	10.0	21.9	2.72	183.87 †
200.000	16,485	17.56	9.52	5.99	4.09	2.96	2.33	1.76	1206.	116.0	62.1	26.4	1.33	300.00
226.000	16,354	21.33	11.12	6.04	3.81	2.78	2.12	1.58	1206.	85.2	25.7	27.9	2.10	300.00
250.000	16,354	20.78	11.06	6.02	3.74	2.61	2.10	1.48	1206.	93.3	21.1	29.3	2.96	273.89
276.000	16,247	23.46	12.79	7.11	4.60	3.31	2.54	1.88	1206.	80.9	22.6	23.3	1.96	300.00
300.000	16,255	19.66	10.62	6.31	4.15	3.01	2.31	1.79	1206.	100.7	35.6	25.8	1.34	300.00
326.000	16,298	19.11	10.43	6.54	4.67	3.48	2.83	2.18	1206.	96.5	93.7	22.3	2.20	300.00
350.000	16,135	24.27	14.09	8.34	5.40	3.76	2.94	2.29	1206.	91.0	16.5	20.5	1.90	287.70
375.000	16,112	23.83	12.41	7.35	4.99	3.57	2.69	2.02	1206.	71.7	38.8	21.2	0.23	250.72
400.000	16,155	19.76	10.97	6.59	4.48	3.25	2.51	1.98	1206.	102.1	40.0	23.8	1.49	300.00
425.000	16,048	19.85	11.24	6.90	4.68	3.36	2.65	2.04	1206.	106.4	37.1	22.7	1.68	300.00
450.000	16,167	19.22	10.63	6.41	4.24	3.22	2.65	2.04	1206.	100.7	52.3	24.0	3.18	300.00
475.000	16,044	19.76	11.25	7.32	5.30	3.86	3.07	2.35	1206.	101.8	76.2	19.7	1.18	300.00
500.000	16,024	19.31	10.52	6.33	4.39	3.40	2.86	2.09	1206.	90.0	87.2	22.5	3.72	300.00
Mean:		22.11	12.23	7.08	4.60	3.29	2.58	1.99	1206.	91.1	36.0	23.9	2.27	300.00
Std. Dev:		2.90	1.82	0.88	0.52	0.34	0.28	0.24	0.	12.9	25.0	2.6	0.97	99.71
Var Coeff(%):		13.14	14.89	12.39	11.29	10.30	10.82	12.06	0.	14.1	69.4	10.8	42.60	33.24

Figure A.191. FWD Back-Calculation Results for Uncracked Portion of Section-1 of Ft. Worth District.

FORT WORTH DISTRICT
SH-199 SITE-1



A.194

Figure A.192. Variation of CBR Obtained from DCP Testing for Section-1 of Fort Worth District.

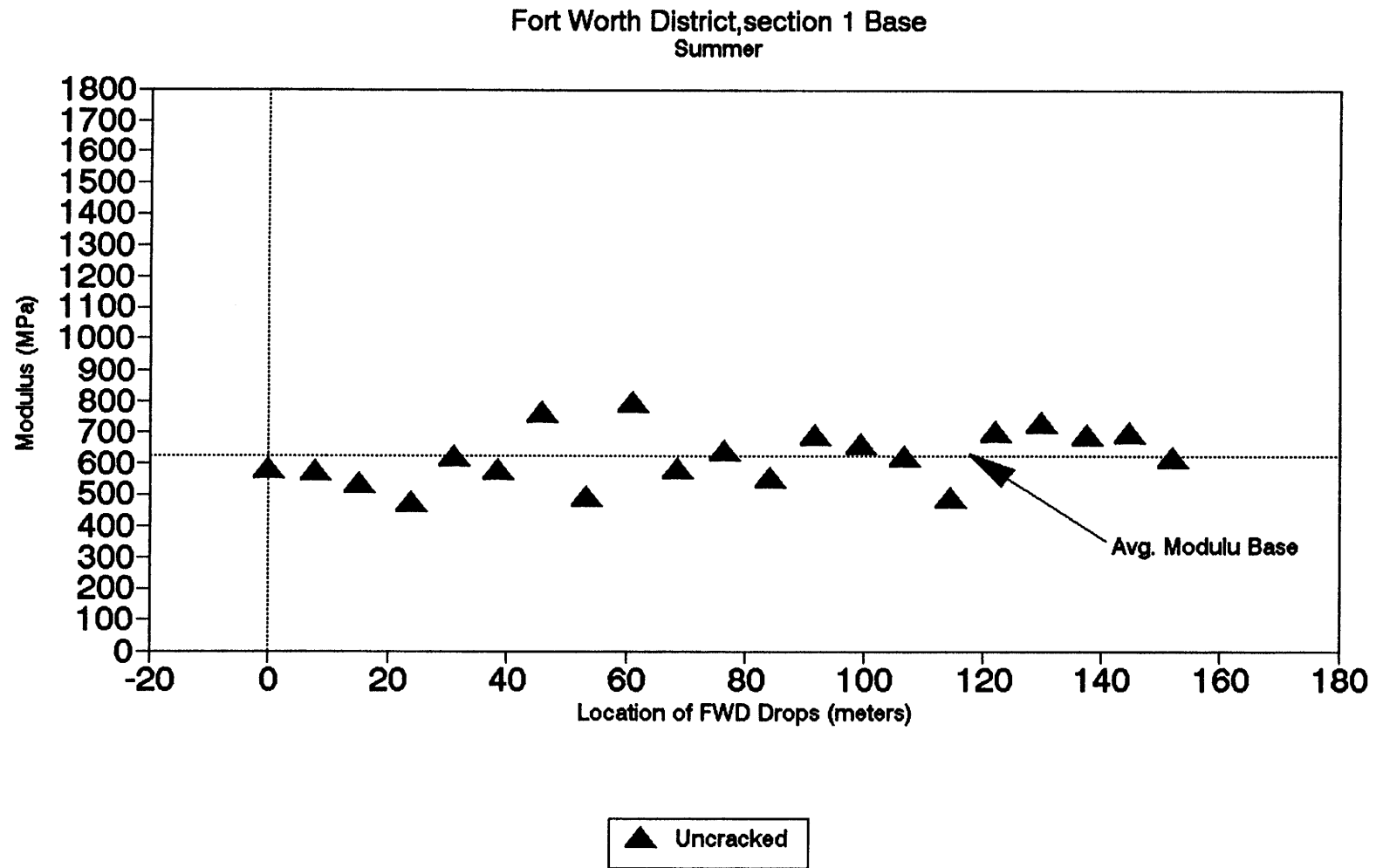


Figure A.193. Variation of Modulus of Stabilized Base within Test Section for Section-1 of Fort Worth District.

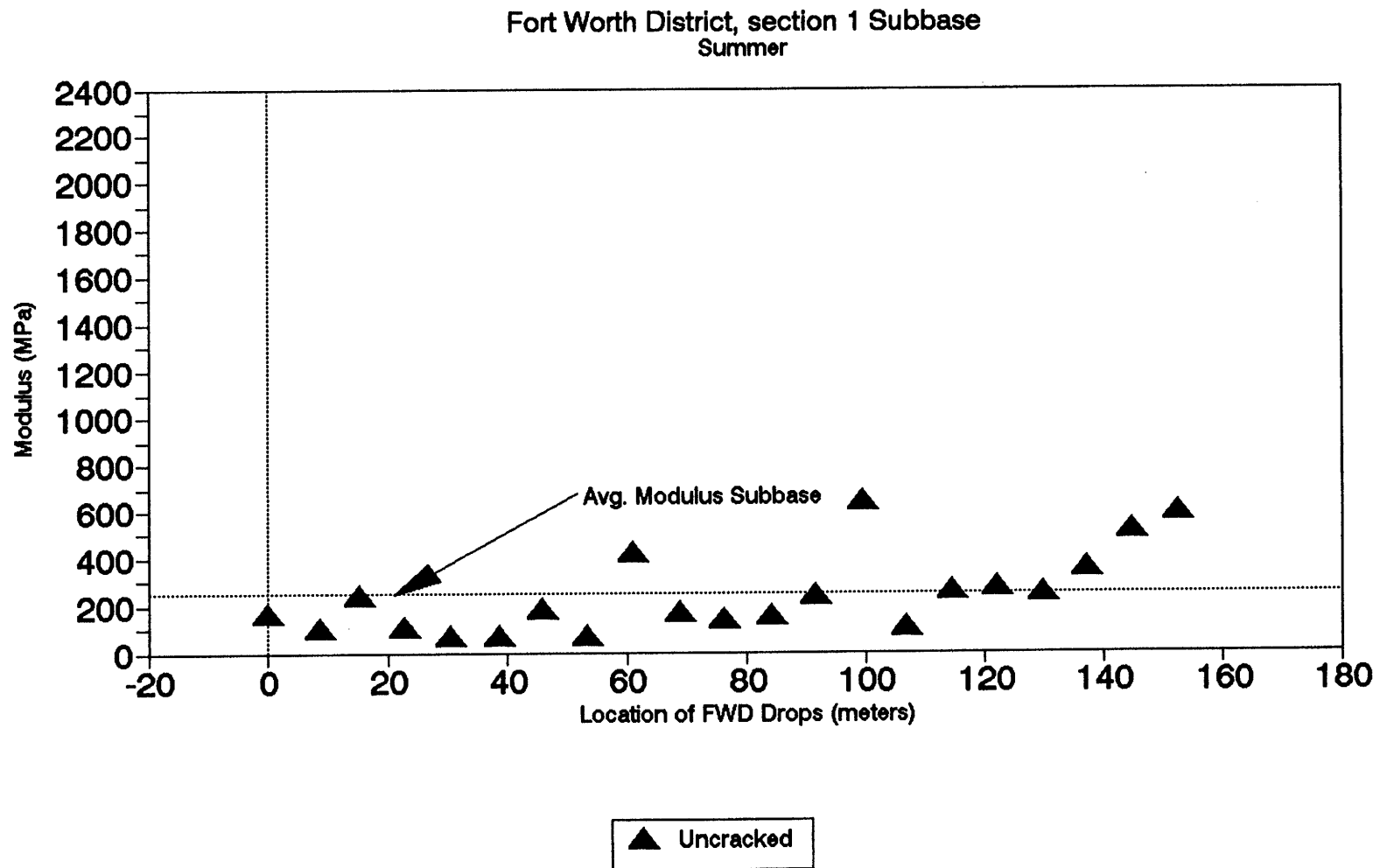


Figure A.194. Variation of Modulus of Stabilized Subbase within Test Section for Section-1 of Fort Worth District.

Section No.: 2 District: Fort Worth County: Tarrant Highway: FM-1709
Structure: Asphalt : 102 mm
Flex Base : 152 mm
LTS : 152 mm
Subgrade

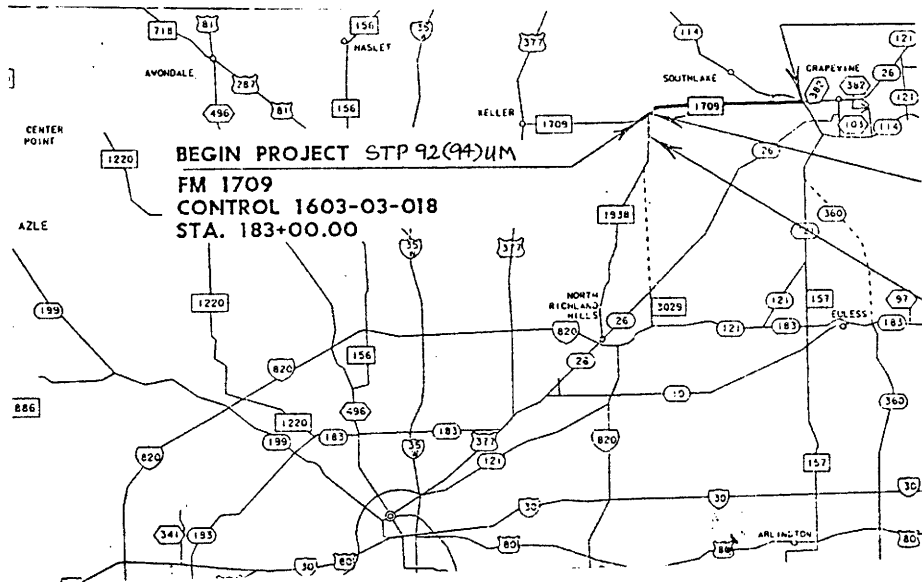


Figure A.195. Location and Details of Section-2 of Fort Worth District.

A.198

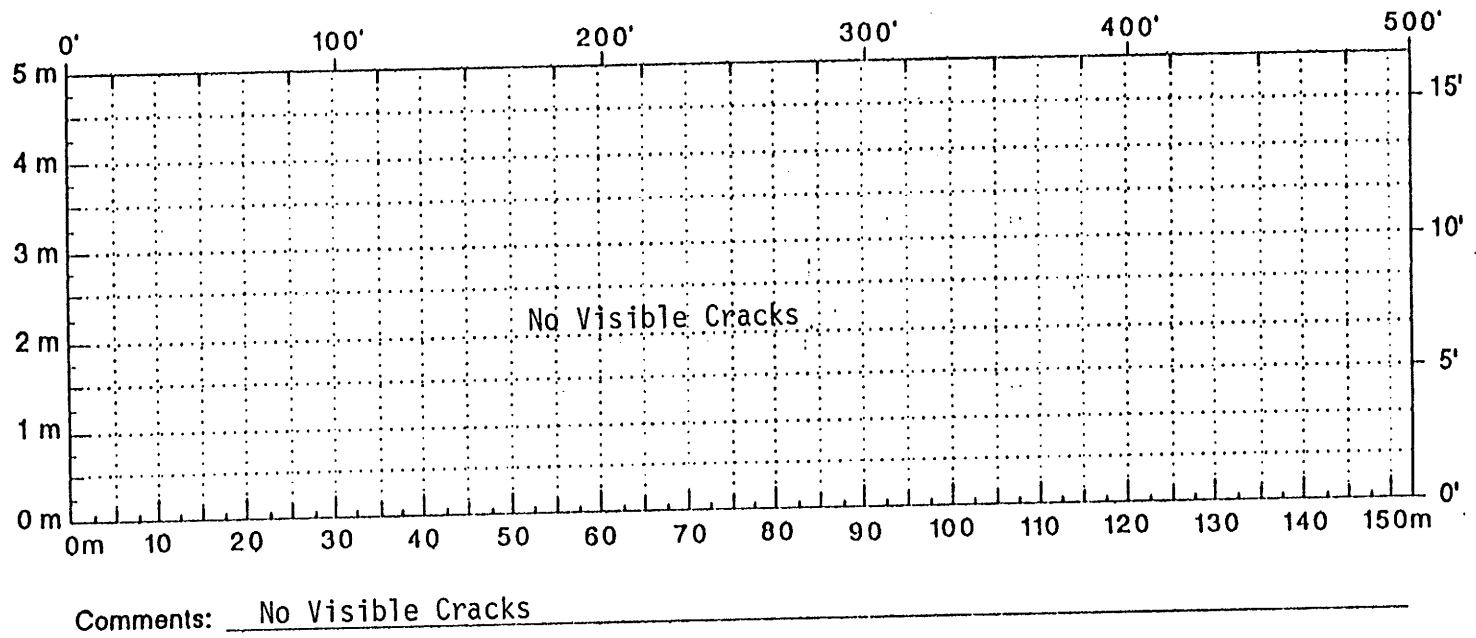


Figure A.196. Crack Map for Section-2 of Ft. Worth District.

TTI MODULUS ANALYSIS SYSTEM (SUMMARY REPORT)													(Version 4.2)			
District:	2												MODULI RANGE(psi)			
County:	220												Minimum	Maximum	Poisson Ratio Values	
Highway/Road:	FM1709		Pavement:	4.00					835,316	835,484	R1: u = 0.35					
			Base:	6.00					20,000	400,000	R2: u = 0.35					
			Subbase:	6.00					10,000	300,000	R3: u = 0.25					
			Subgrade:	284.00					20,000		R4: u = 0.35					
Station	Load (lbs)	Measured Deflection (mils):							Calculated Moduli values (ksi):				Absolute Dpth to			
		R1	R2	R3	R4	R5	R6	R7	SURF(E1)	BASE(E2)	SUBB(E3)	SUBG(E4)	ERR/Sens	Bedrock		
0.000	16,175	32.38	22.78	13.64	8.43	5.73	4.24	3.25	835.	49.2	11.2	13.2	1.06	265.31		
29.000	16,263	28.00	18.19	10.01	6.09	4.18	3.21	2.30	835.	33.4	21.9	17.5	1.33	260.84		
50.000	16,183	19.14	12.63	7.63	5.08	3.67	2.80	2.13	835.	79.3	54.3	20.7	1.33	300.00		
80.000	16,044	18.56	11.39	6.71	4.53	3.33	2.69	2.11	835.	42.4	186.0	22.3	1.97	300.00		
100.000	16,203	17.16	10.61	6.39	4.20	3.06	2.46	1.82	835.	66.6	96.2	24.5	1.97	300.00		
125.000	16,175	17.03	10.08	5.61	3.57	2.62	2.02	1.56	835.	56.3	77.8	28.8	1.61	300.00		
151.000	16,024	16.94	9.51	5.23	3.43	2.49	1.98	1.52	835.	36.6	242.5	29.7	1.41	300.00		
176.000	16,187	12.67	7.56	4.65	3.22	2.41	1.88	1.39	835.	92.5	228.2	32.1	1.55	278.39		
200.000	15,814	25.48	15.12	7.63	4.45	3.15	2.33	1.78	835.	21.7	40.5	21.7	2.97	176.48 *		
225.000	15,929	15.93	9.87	5.46	3.49	2.37	1.90	1.40	835.	97.6	37.2	30.5	2.18	268.77		
251.000	15,873	15.90	8.65	4.87	3.35	2.54	2.02	1.52	835.	42.3	300.0	30.2	3.10	300.00 *		
Mean:		19.93	12.40	7.08	4.53	3.23	2.50	1.89	835.	56.2	117.8	24.7	1.86	300.00		
Std. Dev:		6.03	4.59	2.68	1.56	1.01	0.72	0.55	0.	24.9	102.3	6.1	0.67	137.51		
Var Coeff(%):		30.25	37.01	37.88	34.46	31.25	28.71	29.06	0.	44.3	86.9	24.8	35.93	45.84		

Figure A.197. FWD Back-Calculation Results for Uncracked Portion of Section-2 of Ft. Worth District.

**FORT WORTH DISTRICT
FM-1709 SITE-2 (Trial-1)**

A.200

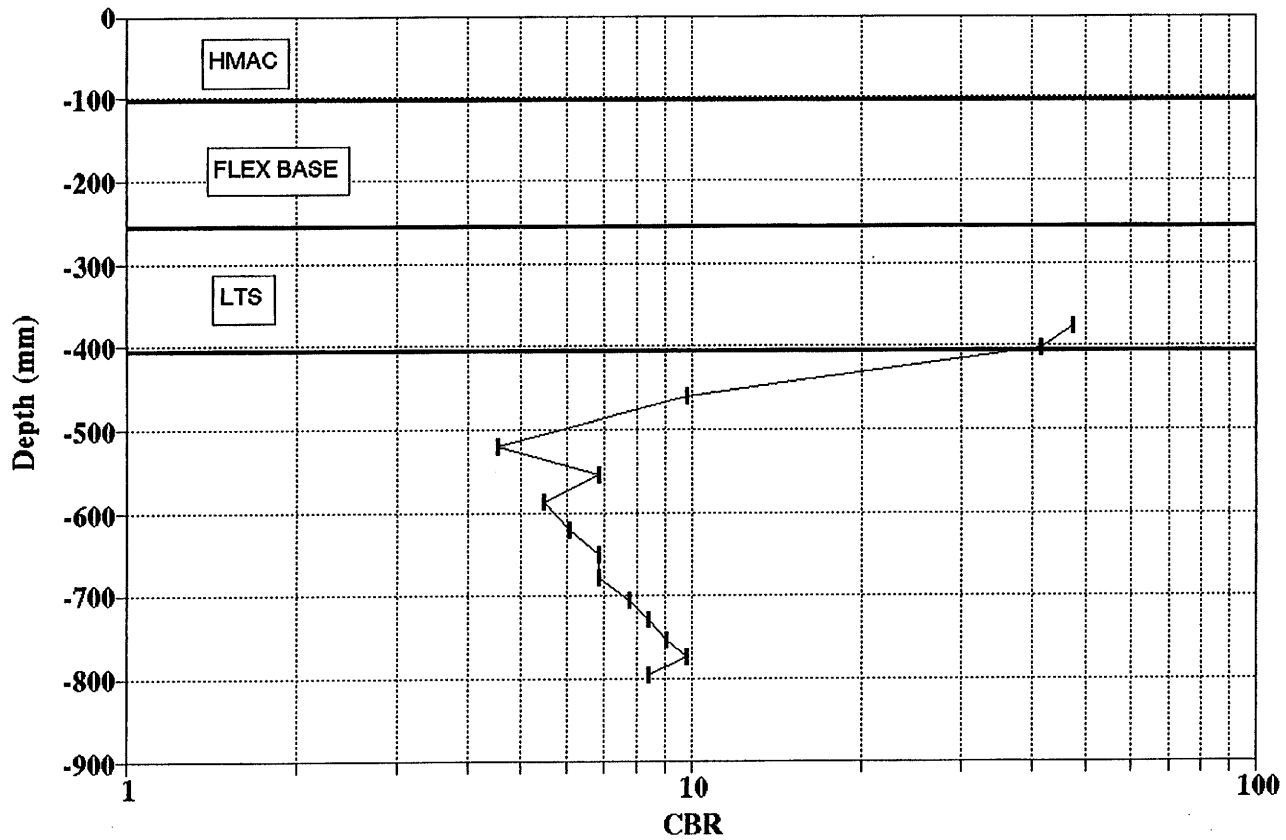


Figure A.198. Variation of CBR Obtained from DCP Testing for Section-2 of Fort Worth District.

A.201

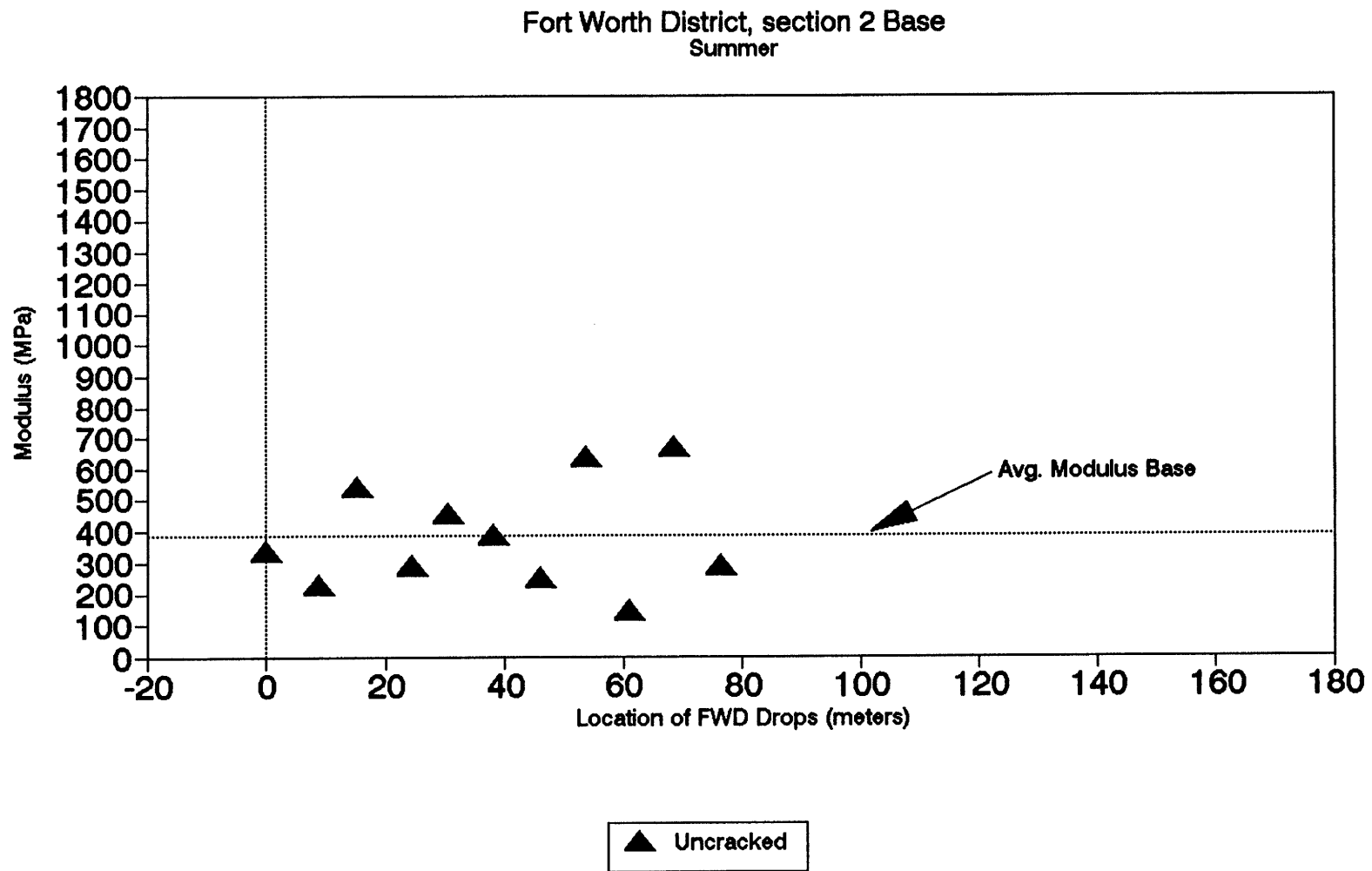


Figure A.199. Variation of Modulus of Stabilized Base within Test Section for Section-2 of Fort Worth District.

A.202

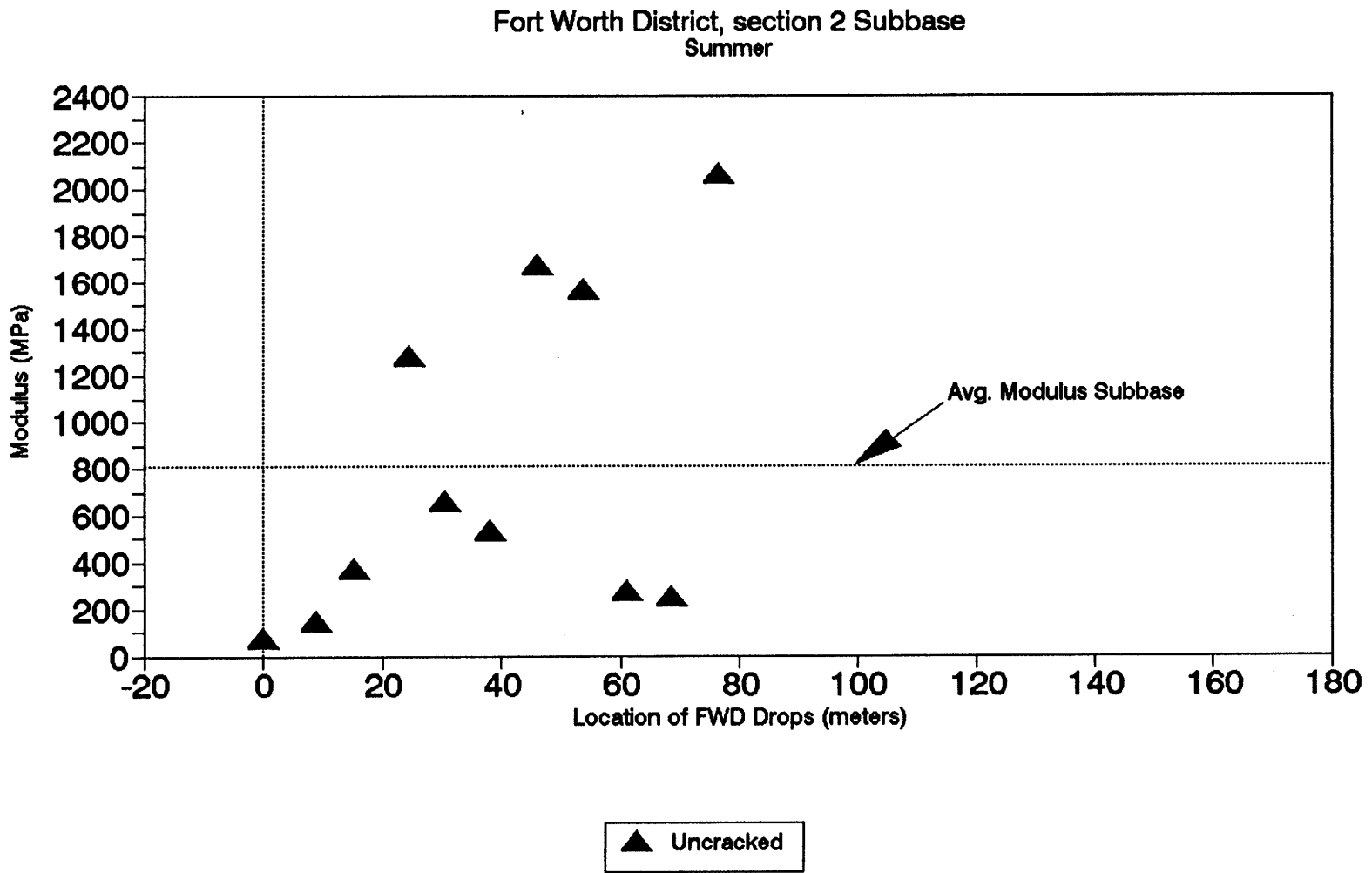


Figure A.200. Variation of Modulus of Stabilized Subbase within Test Section for Section-2 of Fort Worth District.

Section No.: 3 District: Fort Worth County: Tarrant Highway: SH-121
Structure: Asphalt : 38 mm
Flex Base : 279 mm
LTS : 203 mm
Subgrade

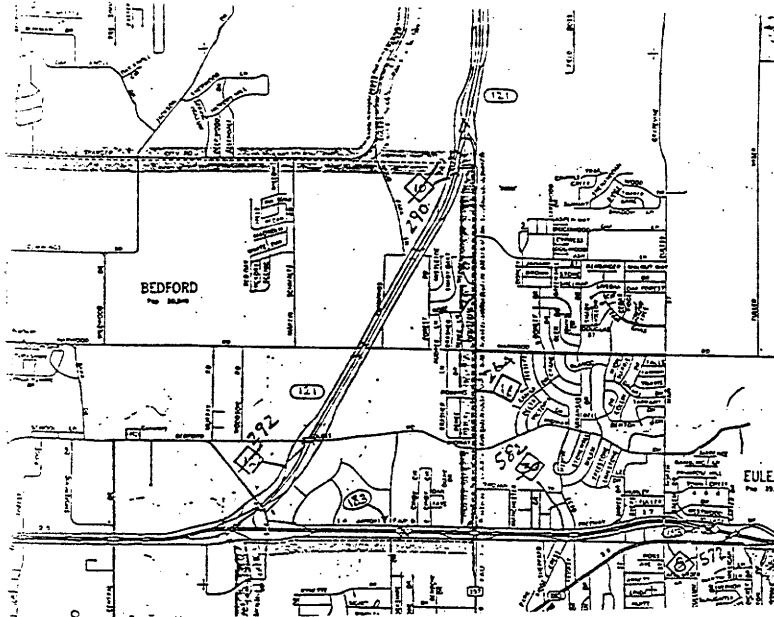
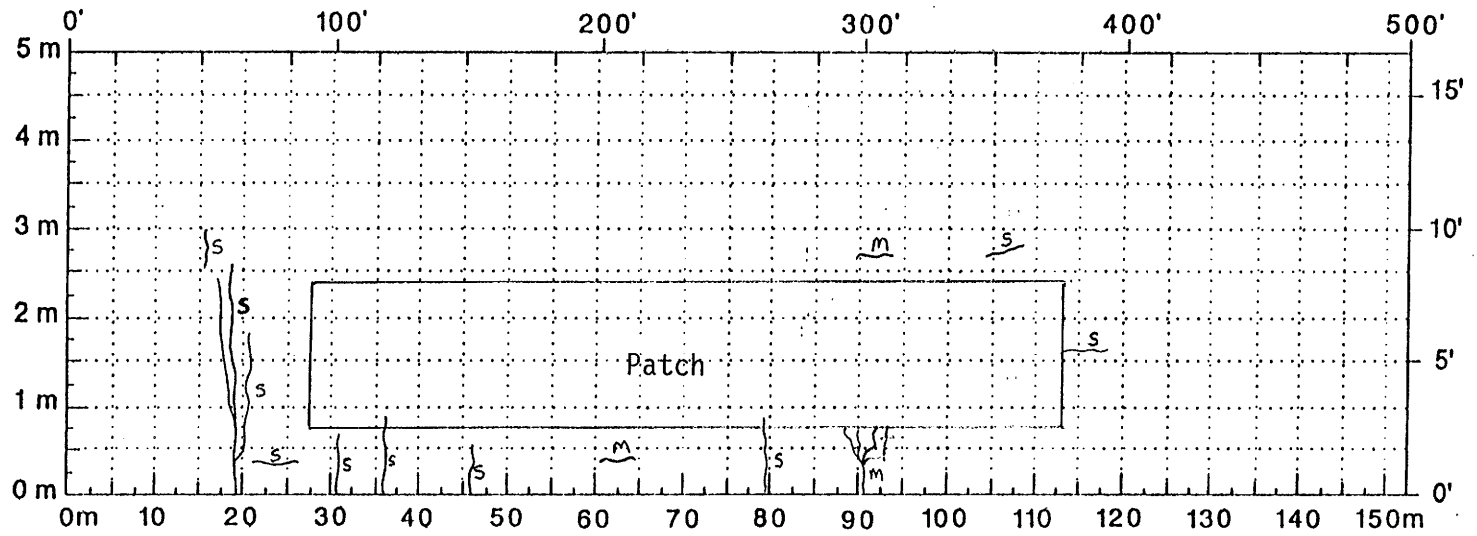


Figure A.201. Location and Details of Section-3 of Fort Worth District.

A.204



Comments: _____

Figure A.202. Crack Map for Section-3 of Ft. Worth District.

A.205

TTI MODULUS ANALYSIS SYSTEM (SUMMARY REPORT)													(Version 4.2)			
District:	2												MODULI RANGE(ksi)			
County:	220												Minimum	Maximum	Poisson Ratio Values	
Highway/Road:	SH0121		Pavement:	1.50					639,136	639,264	H1: $\mu = 0.35$					
			Base:	11.00					20,000	400,000	H2: $\mu = 0.35$					
			Subbase:	8.00					10,000	300,000	H3: $\mu = 0.25$					
			Subgrade:	279.50					25,000		H4: $\mu = 0.35$					
Station	Load (lbs)	Measured Deflection (mils):							Calculated Moduli values (ksi):				Absolute Dpth to Bedrock			
		R1	R2	R3	R4	R5	R6	R7	SURF(E1)	BASE(E2)	SUBB(E3)	SUBG(E4)	ERR/Sens	Bedrock		
0.000	16,719	12.75	5.45	3.65	2.72	2.15	1.72	1.41	639.	141.7	300.0	40.2	1.37	300.00 †		
51.000	16,322	13.55	6.17	3.88	2.88	2.24	1.78	1.48	639.	138.5	175.7	37.4	2.03	300.00		
100.000	16,211	20.41	8.67	4.72	3.00	2.21	1.85	1.35	639.	89.9	36.3	36.7	1.44	300.00		
153.000	16,120	18.54	9.39	4.50	3.02	2.20	1.67	1.27	639.	113.9	24.6	37.8	5.39	300.00		
200.000	16,358	16.75	7.70	4.07	2.70	2.05	1.54	1.17	639.	118.8	41.8	40.5	3.36	300.00		
251.000	16,576	17.29	8.85	4.88	3.11	2.28	1.69	1.22	639.	137.7	28.0	37.6	2.99	300.00		
300.000	16,358	17.00	7.16	3.35	2.35	1.68	1.38	1.15	639.	102.9	52.2	48.1	4.91	256.62		
362.000	16,092	13.07	5.93	3.74	2.68	1.99	1.57	1.26	639.	147.2	126.8	40.3	0.72	300.00		
401.000	16,139	13.34	6.34	3.75	2.76	1.88	1.54	0.98	639.	155.2	81.2	41.4	2.39	217.60		
457.000	15,937	13.00	6.32	4.03	2.82	2.06	1.59	1.22	639.	165.0	89.9	38.7	0.34	272.95		
500.000	16,008	10.05	4.96	3.24	2.44	2.02	1.62	1.24	639.	201.8	300.0	42.5	3.48	263.42 †		
Mean:		15.07	6.99	3.98	2.77	2.07	1.61	1.25	639.	137.5	114.2	40.1	2.58	300.00		
Std. Dev:		3.10	1.47	0.53	0.23	0.18	0.11	0.13	0.	31.1	102.6	3.2	1.63	58.65		
Var Coeff(%):		20.58	21.08	13.32	8.44	8.56	6.71	10.74	0.	22.6	89.8	8.0	63.01	19.55		

Figure A.203. FWD Back-Calculation Results for Uncracked Portion of Section-3 of Ft. Worth District.

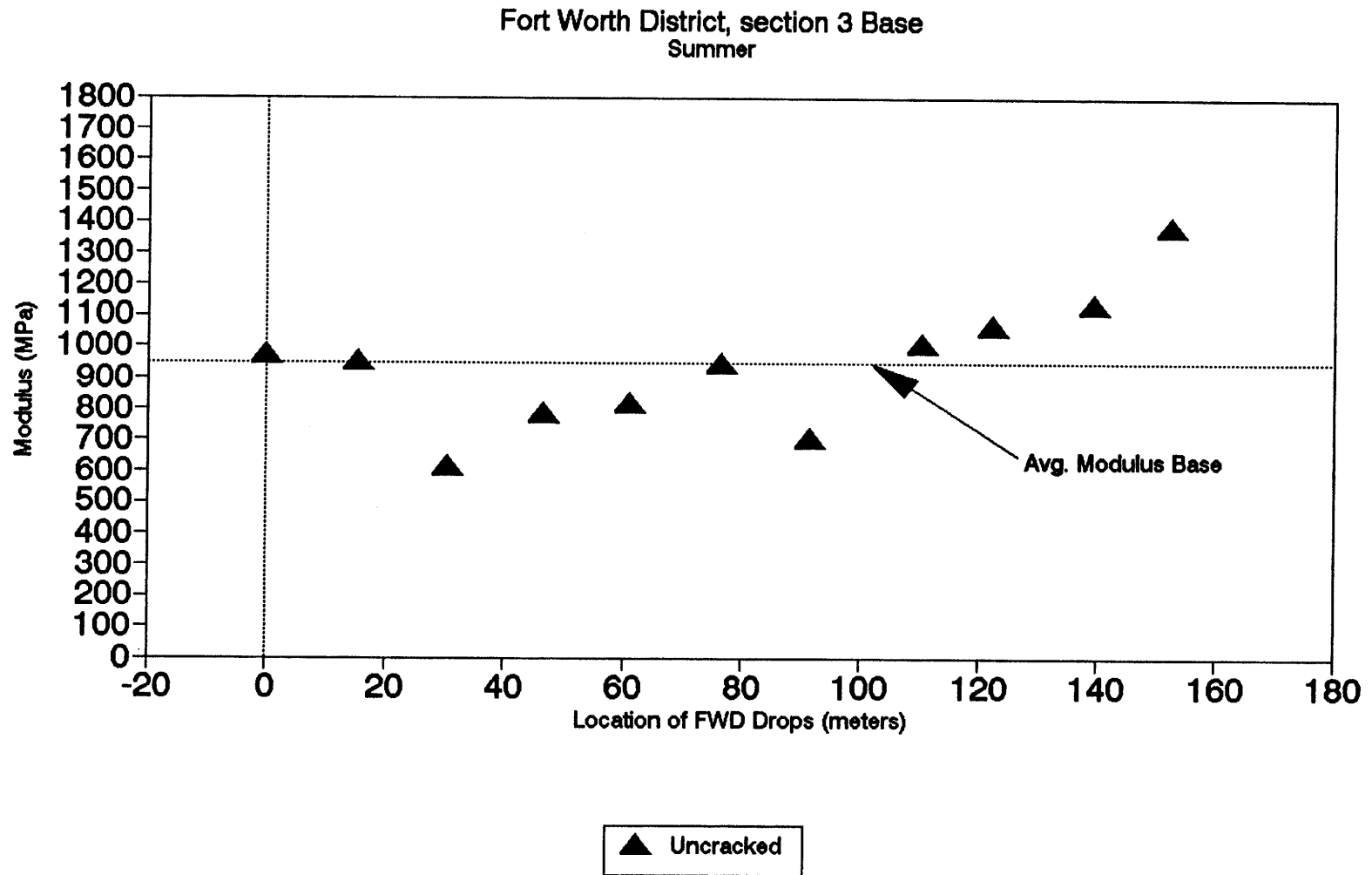


Figure A.204. Variation of Modulus of Stabilized Base within Test Section for Section-3 of Fort Worth District.

A.207

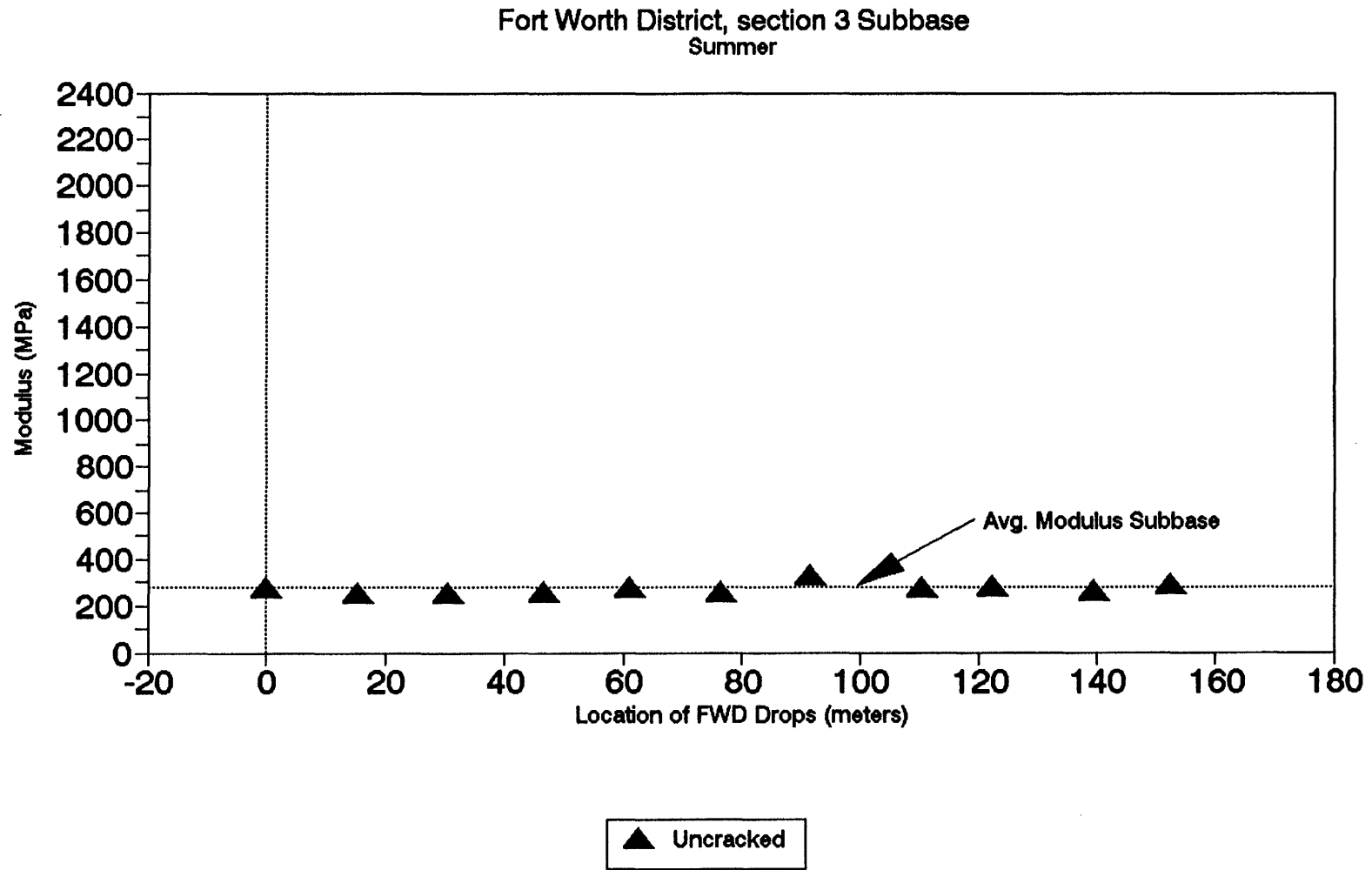


Figure A.205. Variation of Modulus of Stabilized Subbase within Test Section for Section-3 of Fort Worth District.

Section No.: 4 District: Fort Worth County: Tarrant Highway: US-287
Structure: Asphalt : 229 mm
LTS : 152 mm
Subgrade

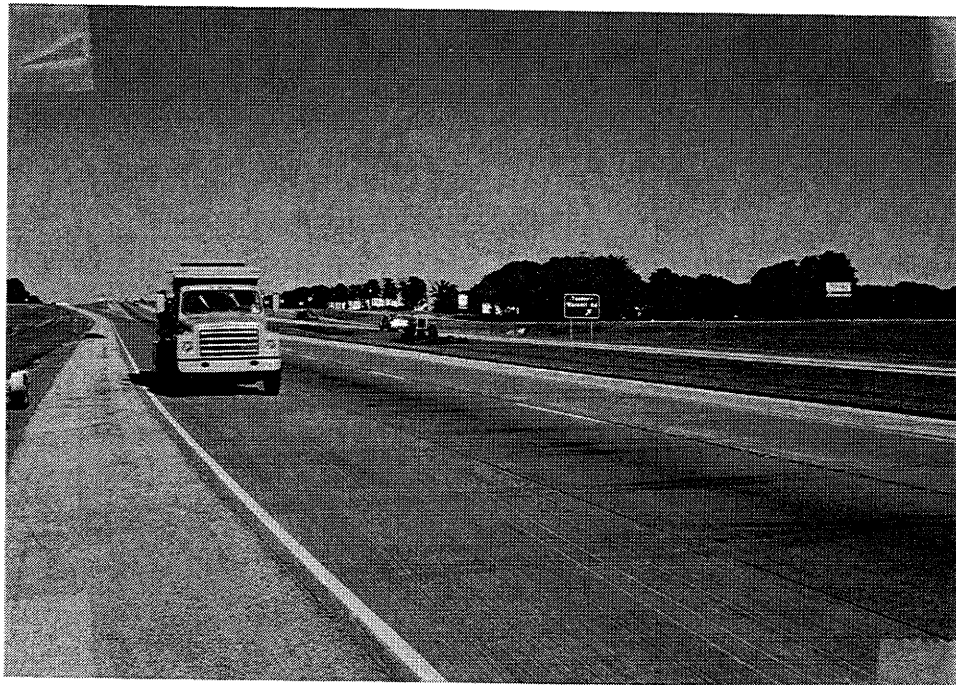
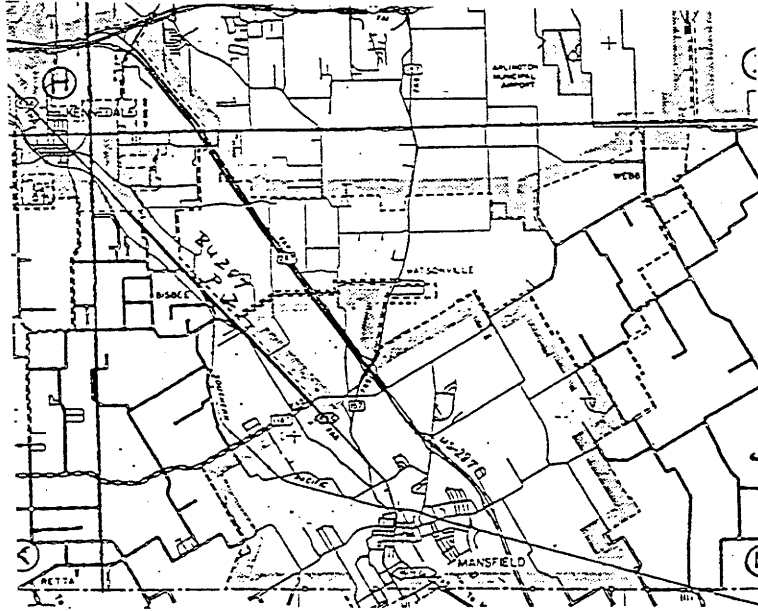
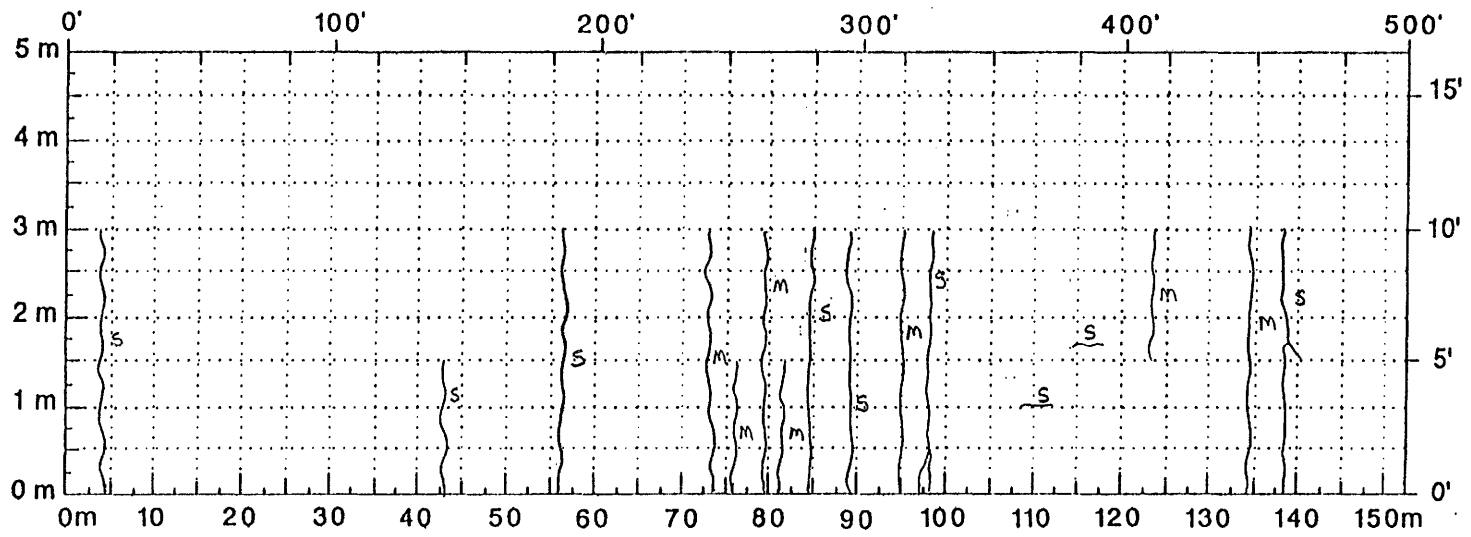


Figure A.206. Location and Details of Section-4 of Fort Worth District.

A.209



Comments: _____

Figure A.207. Crack Map for Section-4 of Ft. Worth District.

FTI MODULUS ANALYSIS SYSTEM (SUMMARY REPORT)

(Version 4.2)

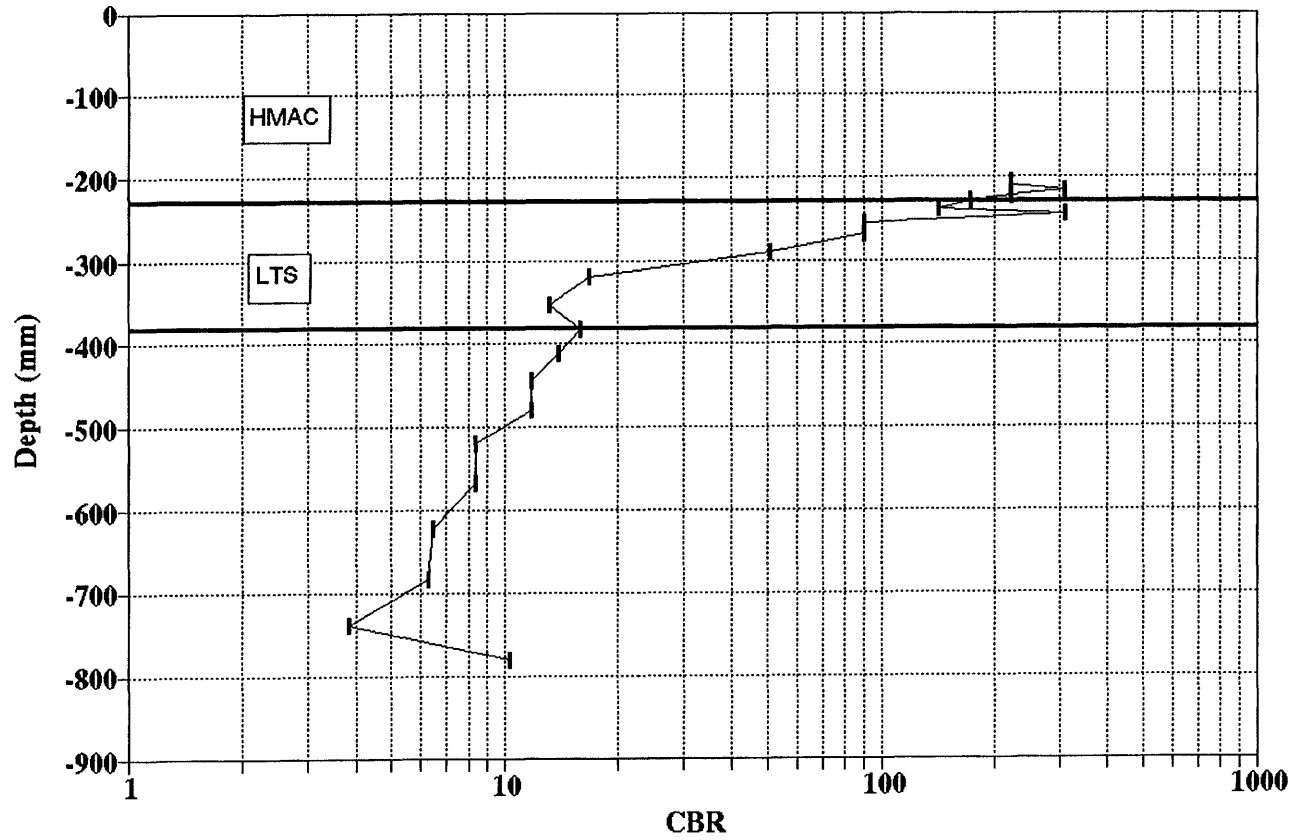
District: 2		MODULI RANGE(ksi)		
County: 220	Thickness(in)	Minimum	Maximum	Poisson Ratio Values
Highway/Road:US0287	Pavement: 9.00	935,107	935,294	H1: u = 0.35
	Base: 6.00	20,000	400,000	H2: u = 0.35
	Subbase: 0.00	0	0	H3: u = 0.25
	Subgrade: 144.60		20,000	H4: u = 0.35

Station	Load (lbs)	Measured Deflection (mils):							Calculated Moduli values (ksi):				Absolute Dist to Bedrock	
		R1	R2	R3	R4	R5	R6	R7	SURF(E1)	BASE(E2)	SUBB(E3)	SUBG(E4)	ERR/Sens	Bedrock
0.000	17,871	13.48	10.61	7.50	5.24	4.10	3.04	2.24	935.	96.8	0.0	18.2	4.22	119.98
25.000	17,037	15.73	10.80	7.00	4.74	3.39	2.63	1.96	935.	20.3	0.0	20.3	7.92	170.49 †
50.000	17,172	10.68	8.19	5.74	4.13	3.13	2.35	1.82	935.	175.7	0.0	22.5	3.69	136.74
75.000	17,144	10.62	7.88	5.57	4.12	3.21	2.55	1.83	935.	241.2	0.0	21.9	5.11	100.51
101.000	17,411	11.31	8.24	5.84	4.28	3.36	2.67	1.93	935.	205.2	0.0	21.4	5.82	103.92
126.000	17,049	11.15	8.79	6.42	4.65	3.50	2.74	2.11	935.	212.7	0.0	19.5	3.11	137.58
150.000	16,914	12.16	8.85	5.98	4.19	3.32	2.78	2.16	935.	99.7	0.0	21.2	7.77	300.00
175.000	16,858	14.08	9.98	7.13	4.84	3.86	3.37	2.53	935.	66.4	0.0	18.1	8.58	300.00
202.000	17,137	12.56	9.52	6.91	5.26	4.10	3.21	2.57	935.	204.9	0.0	17.1	4.46	168.28
225.000	16,715	13.02	9.74	7.29	5.50	4.26	3.47	2.65	935.	194.9	0.0	15.7	4.75	133.16
258.000	16,493	14.04	10.78	7.87	5.78	4.48	3.44	2.69	935.	103.9	0.0	15.1	4.22	158.65
278.000	16,370	14.92	11.02	8.15	5.85	4.41	3.69	2.74	935.	71.7	0.0	14.9	5.96	300.00
303.000	16,739	24.98	10.85	8.09	5.89	4.50	3.94	2.76	935.	20.0	0.0	15.0	17.99	300.00 †
Mean:		13.75	9.63	6.88	4.96	3.82	3.07	2.31	935.	131.8	0.0	18.5	6.43	159.62
Std. Dev:		3.74	1.14	0.90	0.67	0.52	0.49	0.36	0.	76.9	0.0	2.8	3.87	58.03
Var Coeff(%):		27.22	11.83	13.13	13.52	13.52	15.98	15.67	0.	58.4	0.0	15.1	60.18	36.36

A.210

Figure A.208. FWD Back-Calculation Results for Uncracked Portion of Section-4 of Ft. Worth District.

FORT WORTH DISTRICT
US-287 SITE-4



A.211

Figure A.209. Variation of CBR Obtained from DCP Testing for Section-4 of Fort Worth District.

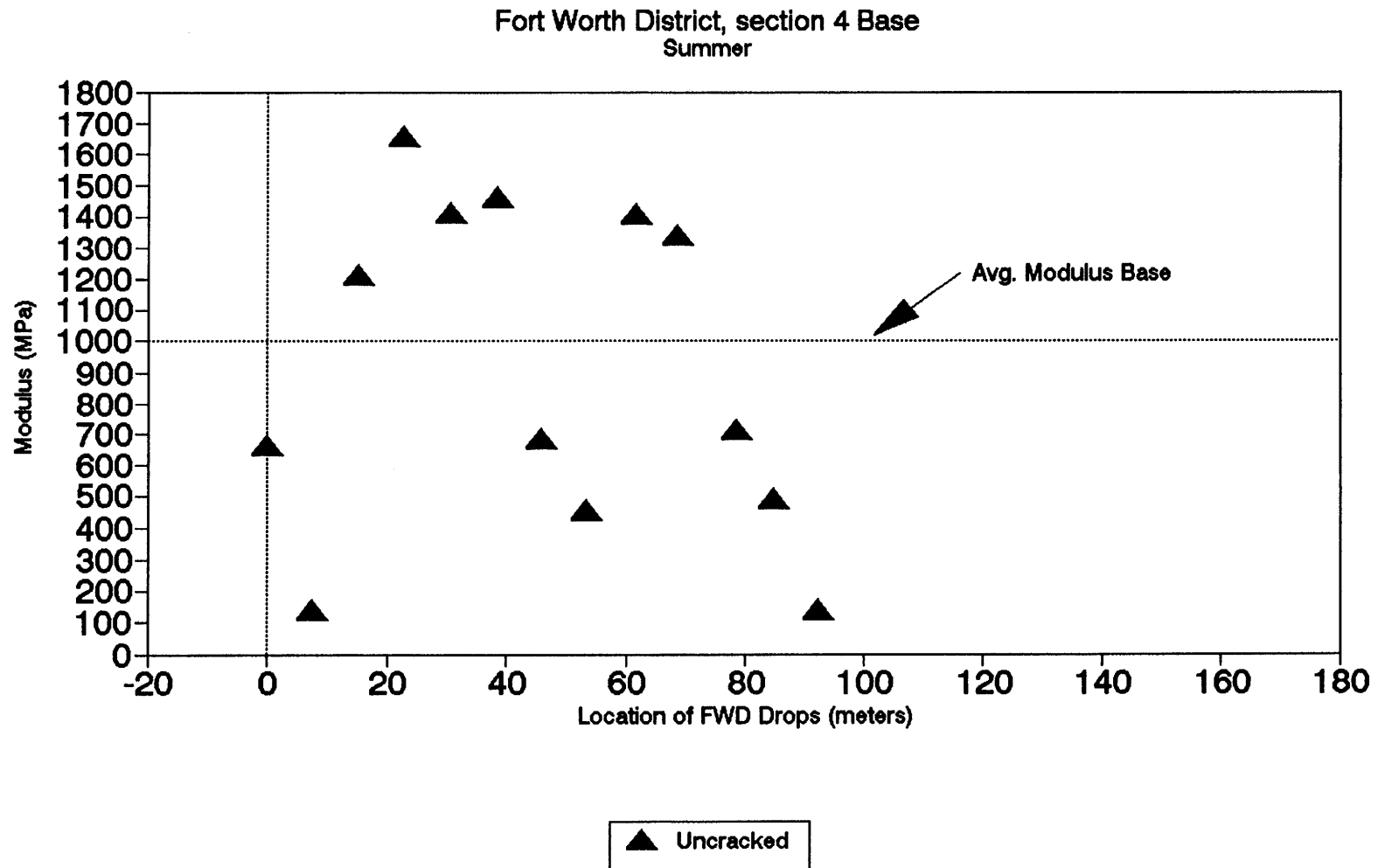


Figure A.210. Variation of Modulus of Stabilized Base within Test Section for Section-4 of Fort Worth District.

Section No.: 5 District: Fort Worth County: Tarrant Highway: US-287
Structure: Asphalt : 25 mm
Flex Base : 279 mm
LTS : 203 mm
Subgrade

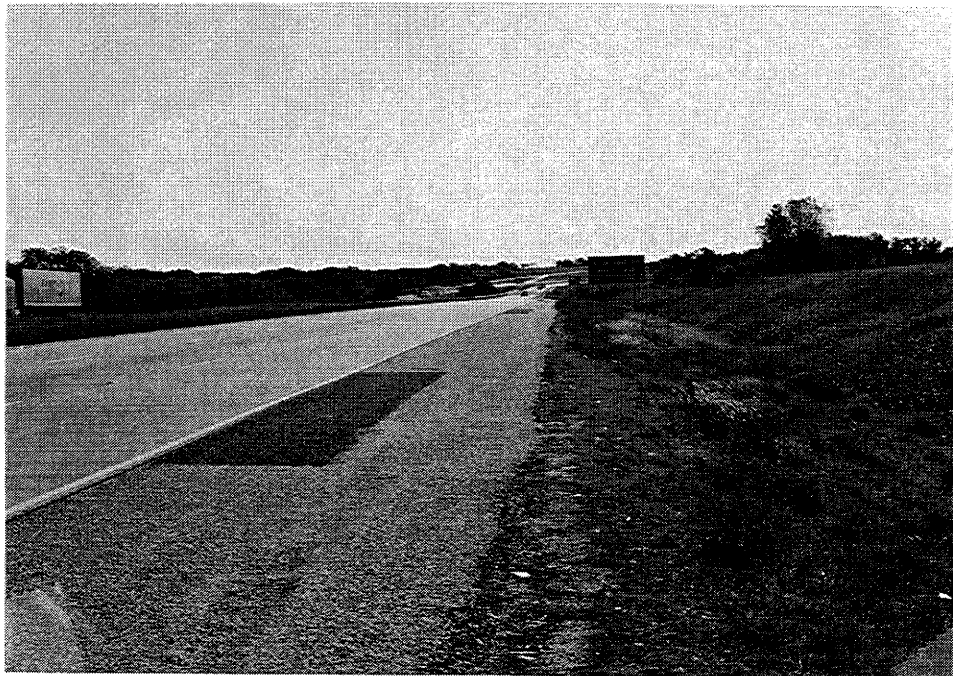
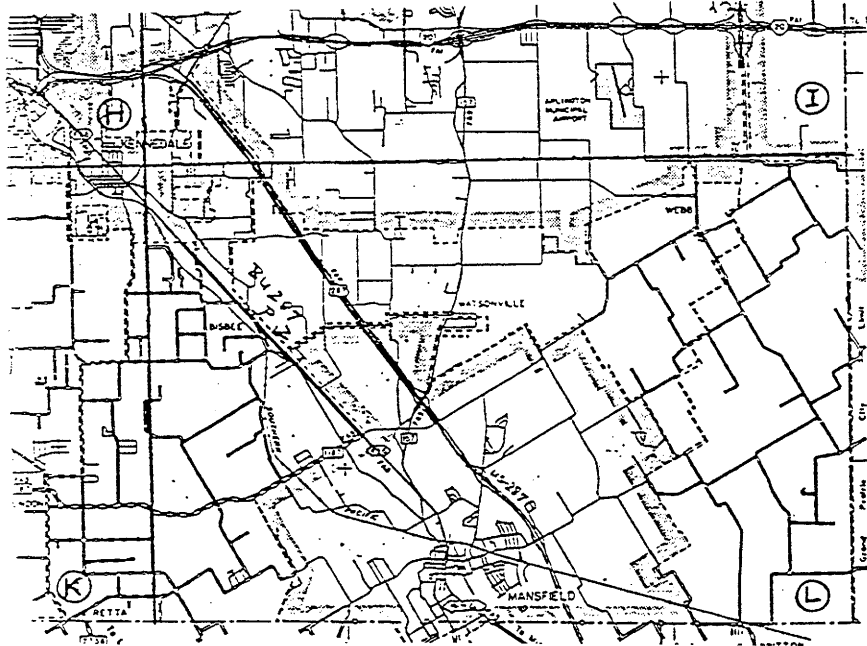
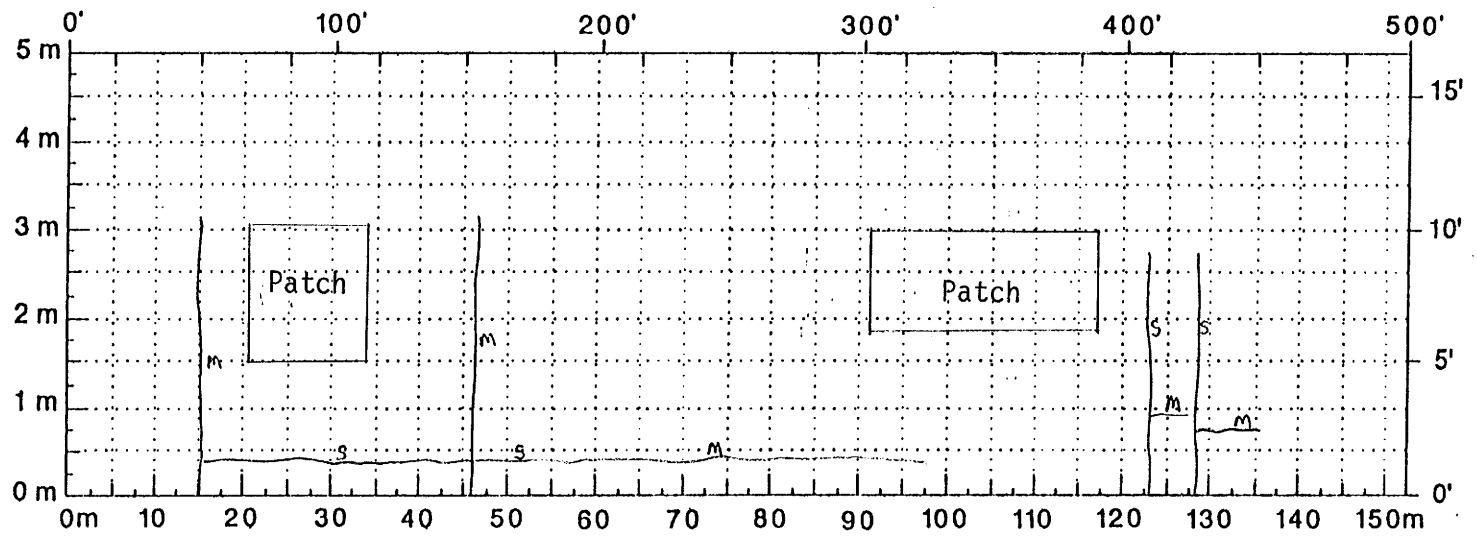


Figure A.211. Location and Details of Section-5 of Fort Worth District.

A.214



Comments: _____

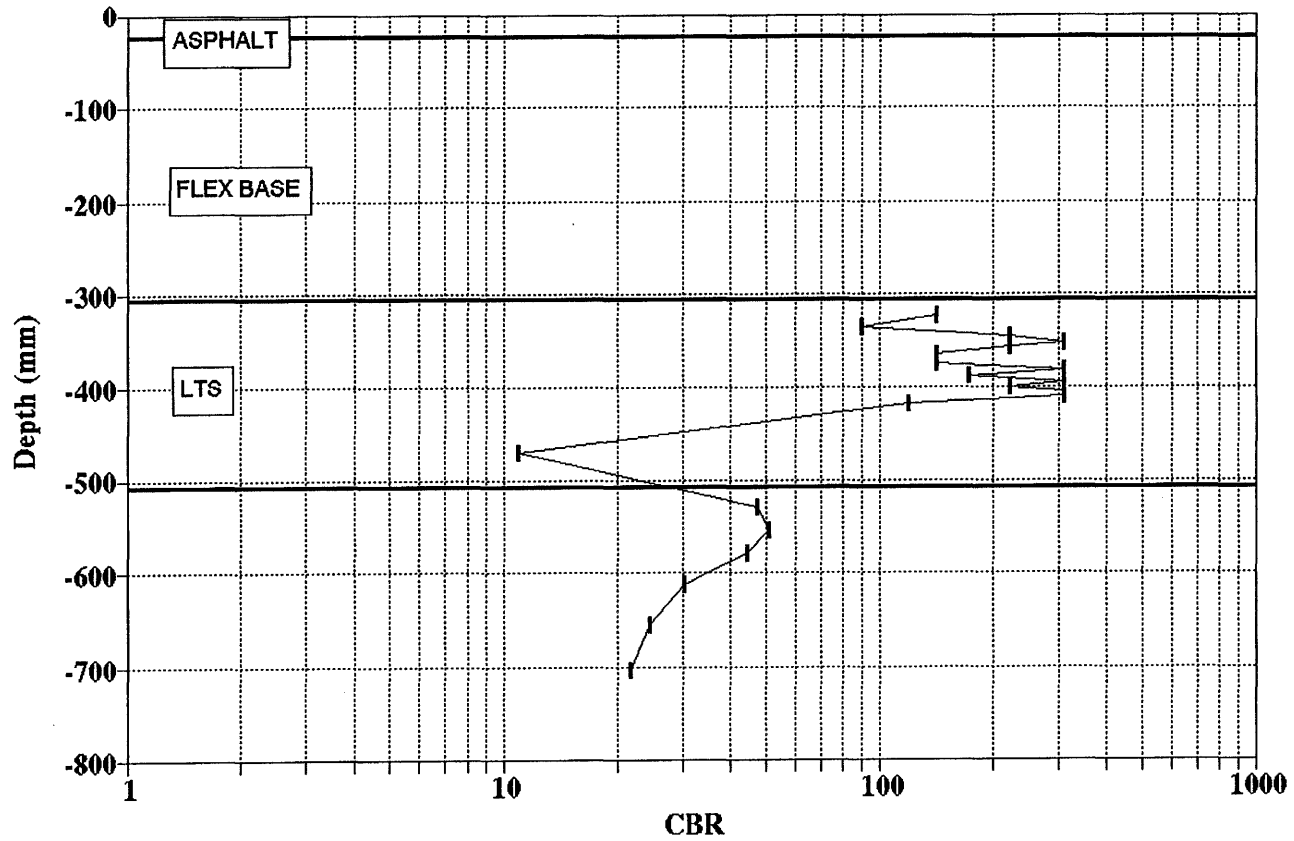
Figure A.212. Crack Map for Section-5 of Ft. Worth District.

A.215

TTI MODULUS ANALYSIS SYSTEM (SUMMARY REPORT)													(Version 4.2)	
District:	2								MODULI RANGE(psi)					
County:	220		Thickness(in)						Minimum	Maximum	Poisson Ratio Values			
Highway/Road:	2S0287		Pavement:	1.00		745,125		745,275		H1: $\nu = 0.35$				
			Base:	11.00		20,000		400,000		H2: $\nu = 0.35$				
			Subbase:	8.00		10,000		300,000		H3: $\nu = 0.25$				
			Subgrade:	272.40		25,000				H4: $\nu = 0.35$				
Station	Load (lbs)	Measured Deflection (mils):						Calculated Moduli values (ksi):				Absolute Dpth to Bedrock		
		R1	R2	R3	R4	R5	R6	R7	SURF(E1)	BASE(E2)	SUBB(E3)	SUBG(E4)	ERR/Sens	Bedrock
0.000	16,962	17.69	6.59	5.04	3.86	3.00	2.35	1.78	745.	101.8	300.0	30.1	4.19	250.25 †
25.000	16,835	18.70	7.26	5.33	4.04	2.98	2.57	1.66	745.	94.4	300.0	27.9	2.70	300.00 †
50.000	16,612	21.20	9.77	6.84	5.24	3.48	2.52	1.96	745.	100.6	93.3	23.7	4.22	183.95
75.000	16,402	26.96	11.15	6.78	4.43	3.32	2.41	1.68	745.	70.8	40.5	24.8	1.26	300.00
101.000	16,473	21.46	9.14	6.07	4.17	3.02	2.49	2.02	745.	89.2	90.5	26.3	1.87	300.00
125.000	16,604	19.80	9.21	6.50	4.61	3.36	2.49	1.91	745.	108.7	101.1	25.1	1.94	280.65
150.000	16,318	23.56	10.66	6.58	4.63	3.39	2.46	2.00	745.	88.2	48.1	24.6	1.18	240.32
176.000	16,135	25.99	10.13	6.72	4.52	3.34	2.48	1.92	745.	86.6	72.5	23.7	1.63	290.34
201.000	16,235	23.59	9.77	6.63	4.67	3.40	2.57	1.94	745.	77.4	90.6	23.6	1.48	254.19
225.000	16,159	28.30	10.17	6.02	4.25	3.32	2.61	1.91	745.	55.4	97.3	25.1	2.56	212.31
251.000	16,088	24.83	9.19	5.72	4.05	2.85	2.37	1.85	745.	65.7	94.3	27.1	1.68	297.86
281.000	16,155	25.13	10.81	5.75	3.91	2.81	2.16	1.72	745.	78.6	29.0	28.9	1.93	300.00
300.000	16,207	26.81	11.19	6.98	4.72	3.34	2.55	2.05	745.	70.5	43.7	23.4	1.01	300.00
325.000	16,127	29.06	12.07	7.46	5.04	3.59	2.75	2.20	745.	64.1	40.0	21.7	0.70	300.00
349.000	16,231	14.65	9.22	6.33	4.78	3.64	4.06	1.89	745.	202.3	156.5	20.2	7.93	99.02
375.000	16,151	26.02	12.56	8.42	5.93	4.32	3.27	2.57	745.	85.3	48.9	19.0	1.08	300.00
400.000	15,845	38.59	17.28	9.70	6.09	4.39	3.46	2.78	745.	51.7	15.6	17.6	1.87	300.00
425.000	16,000	30.50	16.37	9.95	5.94	4.07	3.01	2.36	745.	90.5	10.0	20.8	2.15	196.41 †
450.000	15,957	30.40	13.13	8.15	5.21	3.72	2.88	2.40	745.	64.8	28.1	20.8	1.53	300.00
475.000	15,957	27.06	11.51	6.96	4.76	3.64	2.78	2.16	745.	68.0	48.3	22.0	1.59	300.00
500.000	15,913	29.16	13.94	8.41	5.38	3.98	3.16	2.61	745.	74.3	25.4	20.0	2.06	300.00
Mean:		25.21	11.01	6.97	4.77	3.47	2.73	2.07	745.	84.2	84.5	23.6	2.22	292.46
Std. Dev:		5.29	2.61	1.31	0.66	0.44	0.45	0.31	0.	31.2	80.1	3.3	1.59	129.11
Var Coeff(%):		20.98	23.74	18.80	13.90	12.73	16.31	15.24	0.	37.0	94.9	14.0	71.51	44.15

Figure A.213. FWD Back-Calculation Results for Uncracked Portion of Section-5 of Ft. Worth District.

**FORT WORTH DISTRICT
US-287 SITE-5**



A.216

Figure A.214. Variation of CBR Obtained from DCP Testing for Section-5 at Station-1 of Fort Worth District.

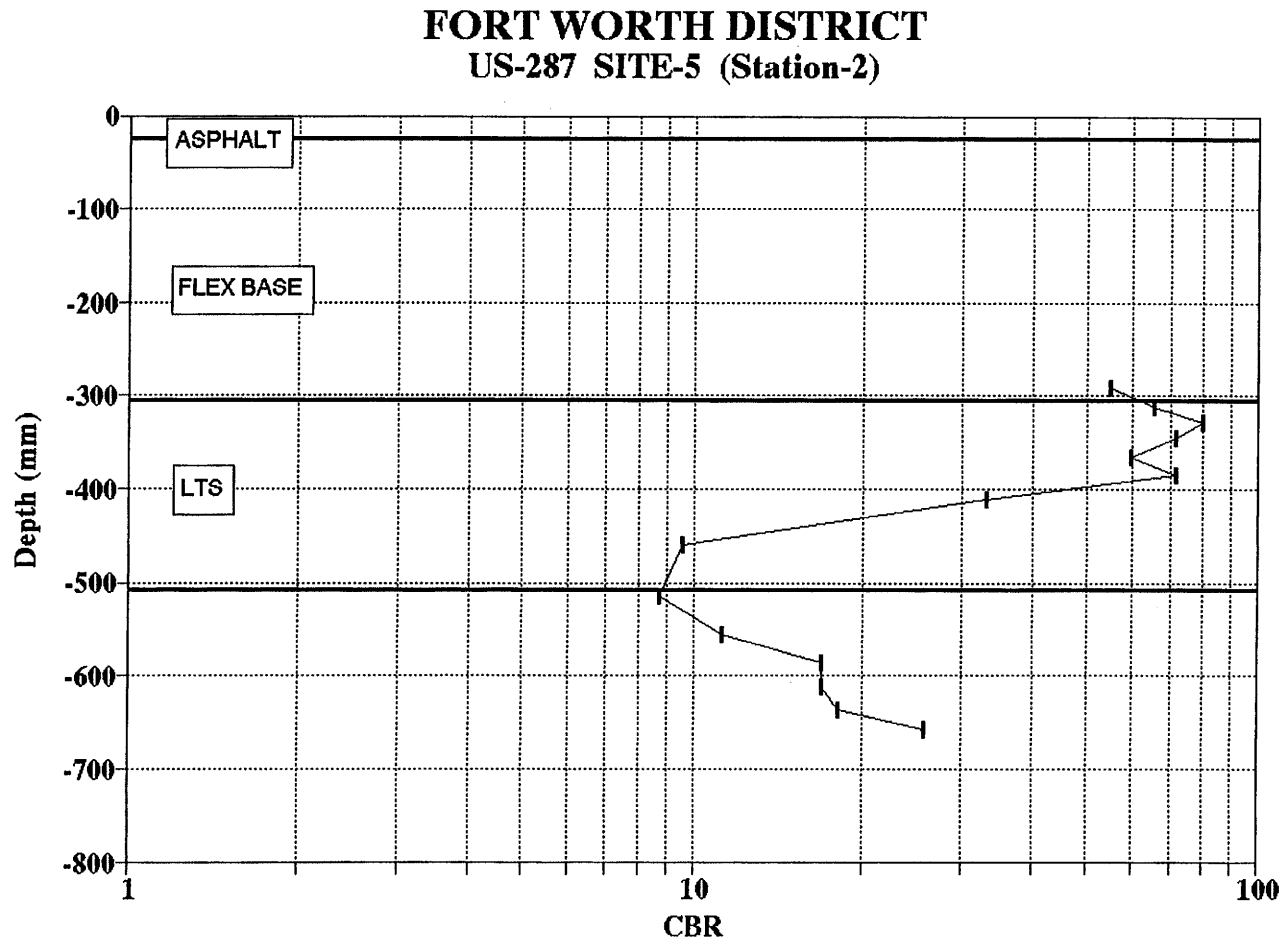


Figure A.215. Variation of CBR Obtained from DCP Testing for Section-5 at Station-2 of Fort Worth District.

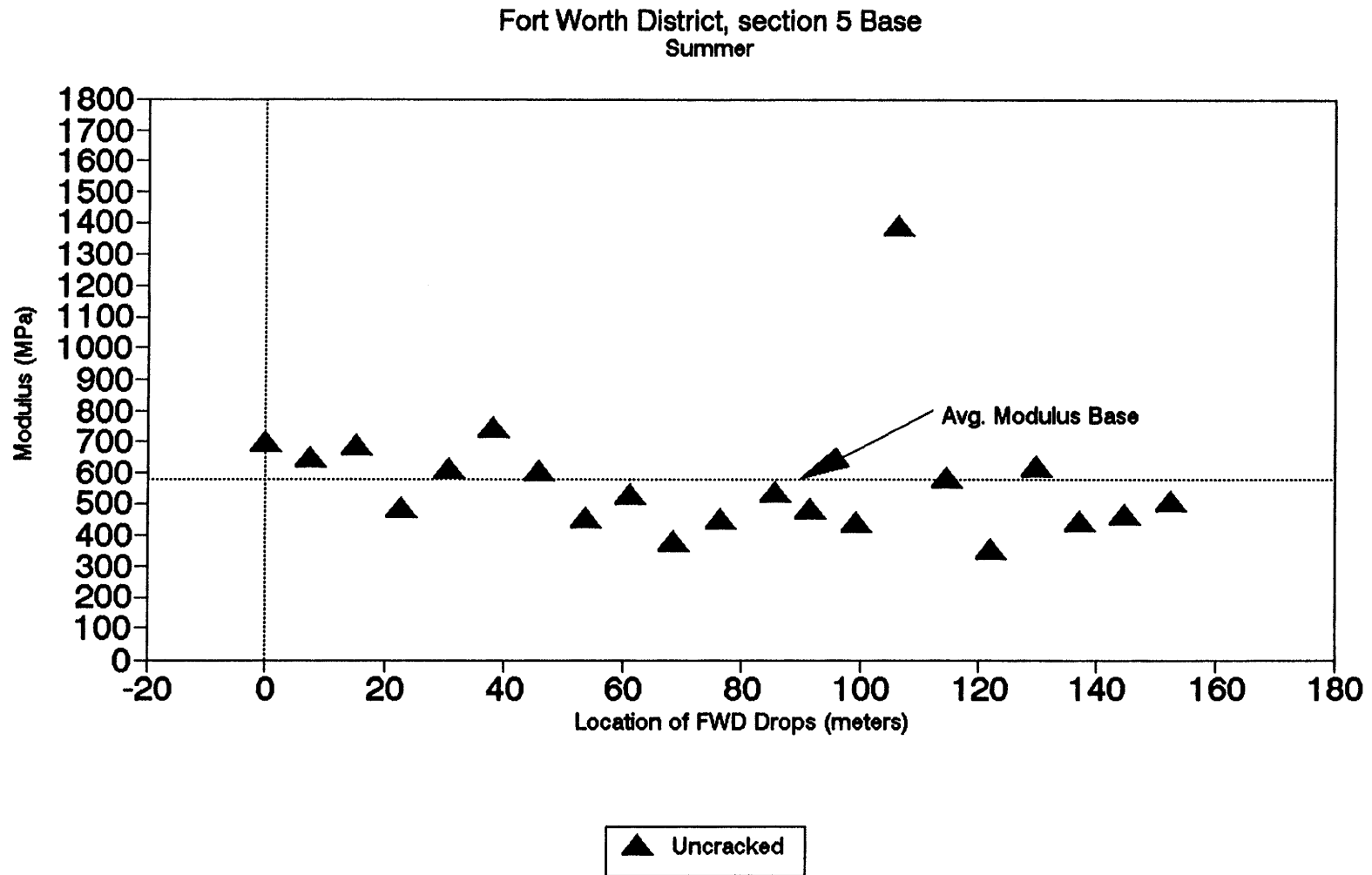


Figure A.216. Variation of Modulus of Stabilized Base within Test Section for Section-5 of Fort Worth District.

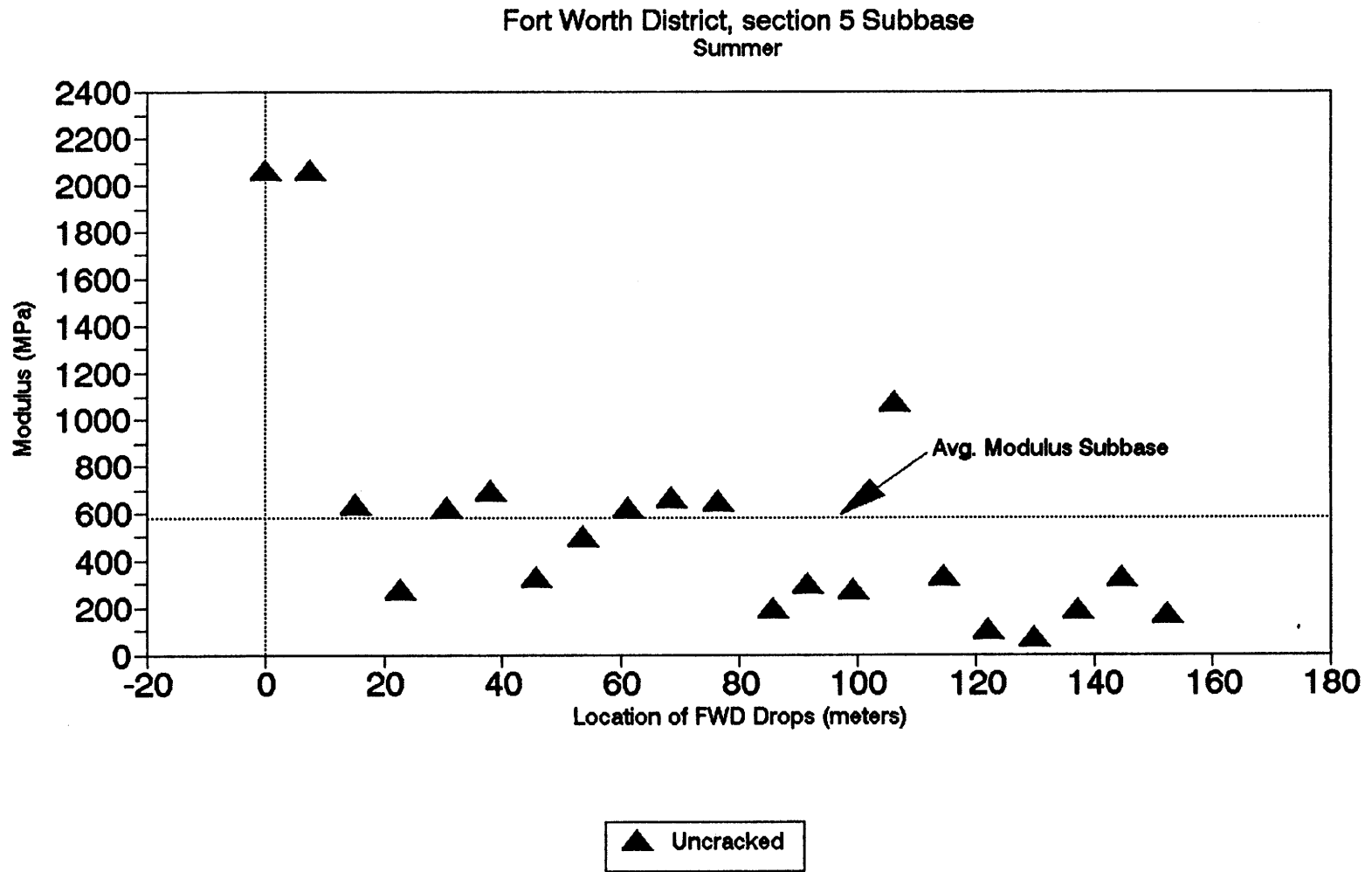


Figure A.217. Variation of Modulus of Stabilized Subbase within Test Section for Section-5 of Fort Worth District.

Section No.: 6 District: Fort Worth County: Johnson Highway: US-287
Structure: Asphalt : 25 mm
Flex Base : 279 mm
LTS : 356 mm
Subgrade

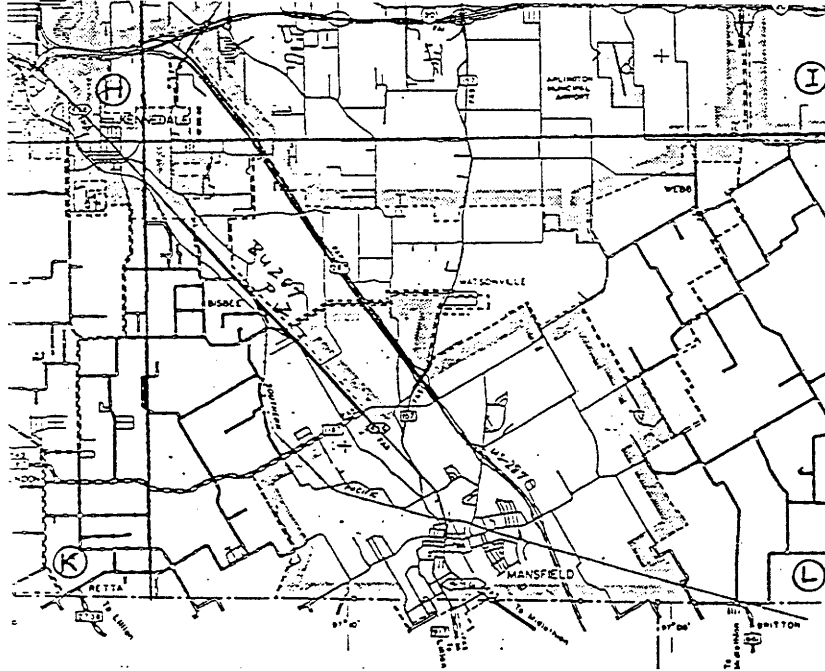


Figure A.218. Location and Details of Section-6 of Fort Worth District.

A.221

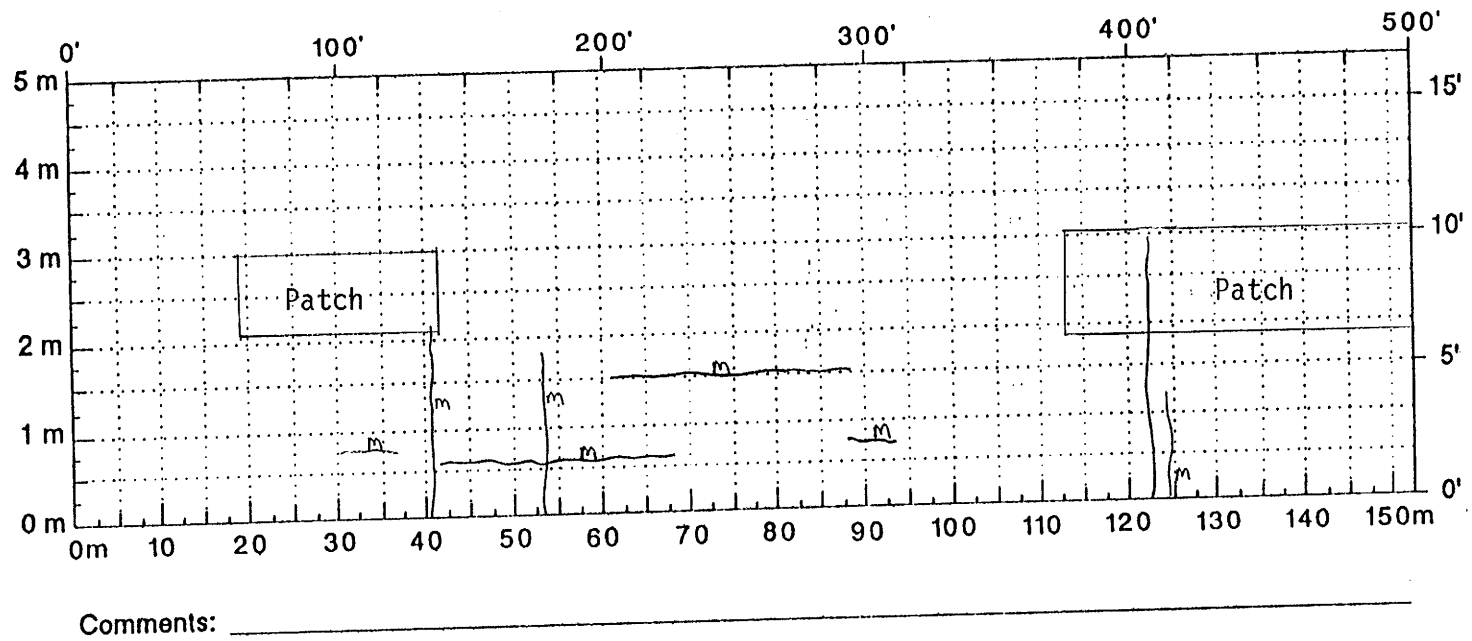


Figure A.219. Crack Map for Section-6 of Ft. Worth District.

TTI MODULUS ANALYSIS SYSTEM (SUMMARY REPORT)

(Version 4.2)

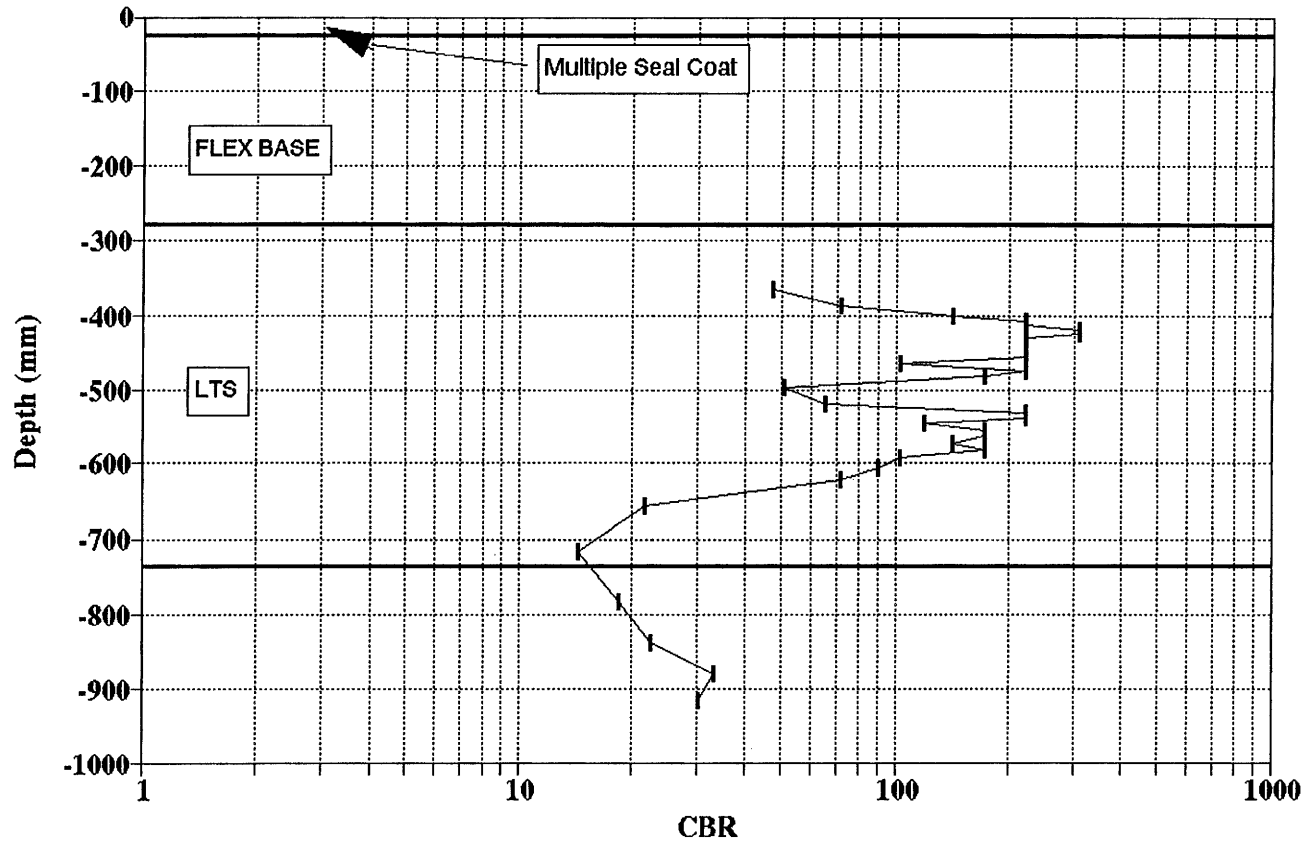
District: 2	MODULI RANGE(psi)			Poisson Ratio Values	
County: 127	Thickness(in)	Minimum	Maximum	H1: u = 0.35	
Highway/Road:US0287	Pavement: 1.00	591,741	591,859	H2: u = 0.35	
	Base: 11.00	20,000	400,000	H3: u = 0.25	
	Subbase: 14.00	10,000	300,000	H4: u = 0.35	
	Subgrade: 274.00	20,000			

Station	Load (lbs)	Measured Deflection (mils):							Calculated Moduli values (ksi):				Absolute Dpth to	
		R1	R2	R3	R4	R5	R6	R7	SURF(E1)	BASE(E2)	SUBB(E3)	SURG(E4)	ERR/Sens	Bedrock
0.000	16,290	20.60	8.67	6.29	5.22	4.17	3.43	2.67	592.	84.3	209.6	18.9	1.34	298.26
26.000	16,104	22.00	8.37	6.27	5.21	4.21	3.42	2.72	592.	70.5	281.3	18.3	0.60	300.00
50.000	16,104	19.77	8.20	6.16	5.00	4.17	3.30	2.87	592.	85.4	252.3	19.0	0.75	300.00
78.000	16,044	22.24	9.24	6.68	5.48	4.46	3.46	2.72	592.	76.5	174.8	17.9	0.59	300.00
102.000	16,060	22.03	9.70	6.69	5.67	4.65	3.99	3.15	592.	78.8	192.9	16.7	3.18	300.00
126.000	15,782	23.12	9.39	6.56	5.26	4.33	3.52	2.93	592.	70.3	157.2	18.0	1.94	300.00
150.000	15,706	22.65	8.57	6.30	5.06	4.14	3.41	2.81	592.	66.8	222.2	18.3	1.05	300.00
175.000	15,683	24.22	9.87	6.35	5.28	4.33	3.50	2.87	592.	65.9	131.5	18.1	3.10	300.00
200.000	15,897	26.80	9.37	5.72	4.98	4.08	3.35	2.75	592.	52.5	175.1	19.2	3.76	300.00
225.000	15,953	25.06	8.36	5.42	4.94	4.16	3.37	2.54	592.	54.3	300.0	18.8	3.76	300.00 #
251.000	15,770	25.63	9.63	6.54	5.45	4.47	3.61	2.95	592.	58.3	171.0	17.2	1.95	300.00
276.000	15,484	26.45	9.11	5.41	4.68	4.02	3.11	2.80	592.	51.7	165.5	20.0	4.60	300.00
301.000	15,623	27.78	9.19	5.44	4.79	3.89	3.16	2.57	592.	48.7	171.6	20.3	4.07	300.00
326.000	15,468	29.94	9.17	5.84	5.06	4.18	3.32	2.68	592.	42.8	223.0	18.8	2.65	300.00
350.000	15,440	22.04	9.13	6.02	4.87	3.89	3.15	2.43	592.	74.2	122.5	19.6	2.11	282.57
375.000	15,544	22.11	9.49	6.55	5.00	4.05	3.20	2.60	592.	79.1	104.4	19.1	1.34	300.00
400.000	15,671	20.08	9.73	7.02	5.52	4.35	3.42	2.66	592.	101.5	104.0	17.6	0.29	300.00
425.000	15,627	22.65	10.36	6.85	5.43	4.30	3.43	2.63	592.	82.5	87.6	18.1	1.90	274.88
451.000	15,687	21.90	9.67	6.90	5.50	4.38	3.53	2.89	592.	81.6	129.5	17.5	0.85	300.00
475.000	15,810	27.19	11.15	7.29	5.84	4.63	3.62	2.95	592.	61.5	88.0	17.0	1.40	300.00
499.000	15,341	25.75	10.83	7.17	5.56	4.53	3.60	2.63	592.	64.5	88.2	16.9	2.07	209.96
Mean:		23.81	9.39	6.36	5.23	4.26	3.42	2.75	592.	69.1	169.2	18.4	2.06	300.00
Std. Dev:		2.75	0.76	0.56	0.31	0.22	0.20	0.17	0.	14.6	62.5	1.0	1.27	48.86
Var Coeff(%):		11.57	8.13	8.83	5.93	5.09	5.77	6.17	0.	21.2	37.0	5.4	61.59	16.29

A.222

Figure A.220. FWD Back-Calculation Results for Uncracked Portion of Section-6 of Ft. Worth District.

FORT WORTH DISTRICT US-287 SITE-6



A.223

Figure A.221. Variation of CBR Obtained from DCP Testing for Section-6 of Fort Worth District.

A.224

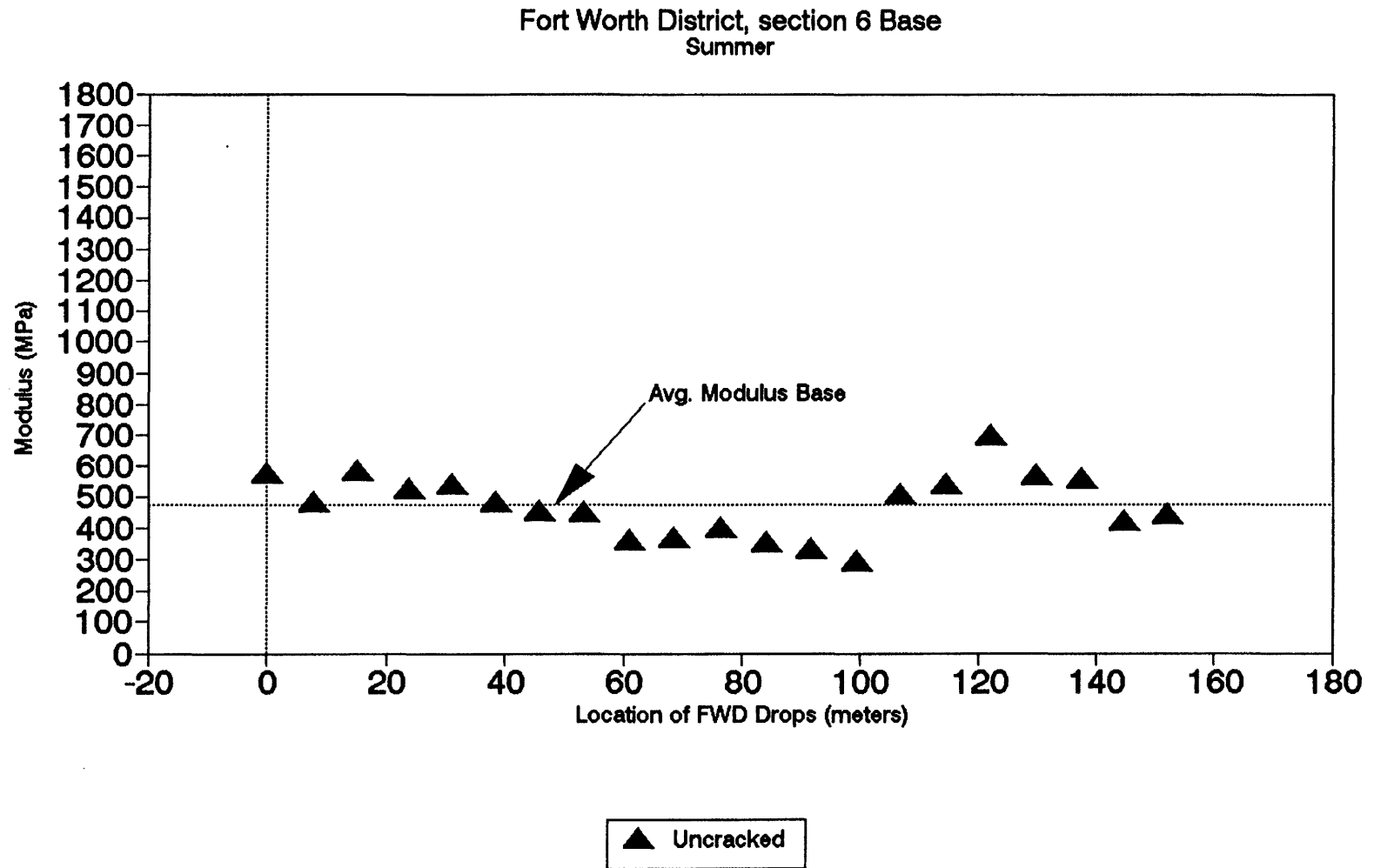


Figure A.222. Variation of Modulus of Stabilized Base within Test Section for Section-6 of Fort Worth District.

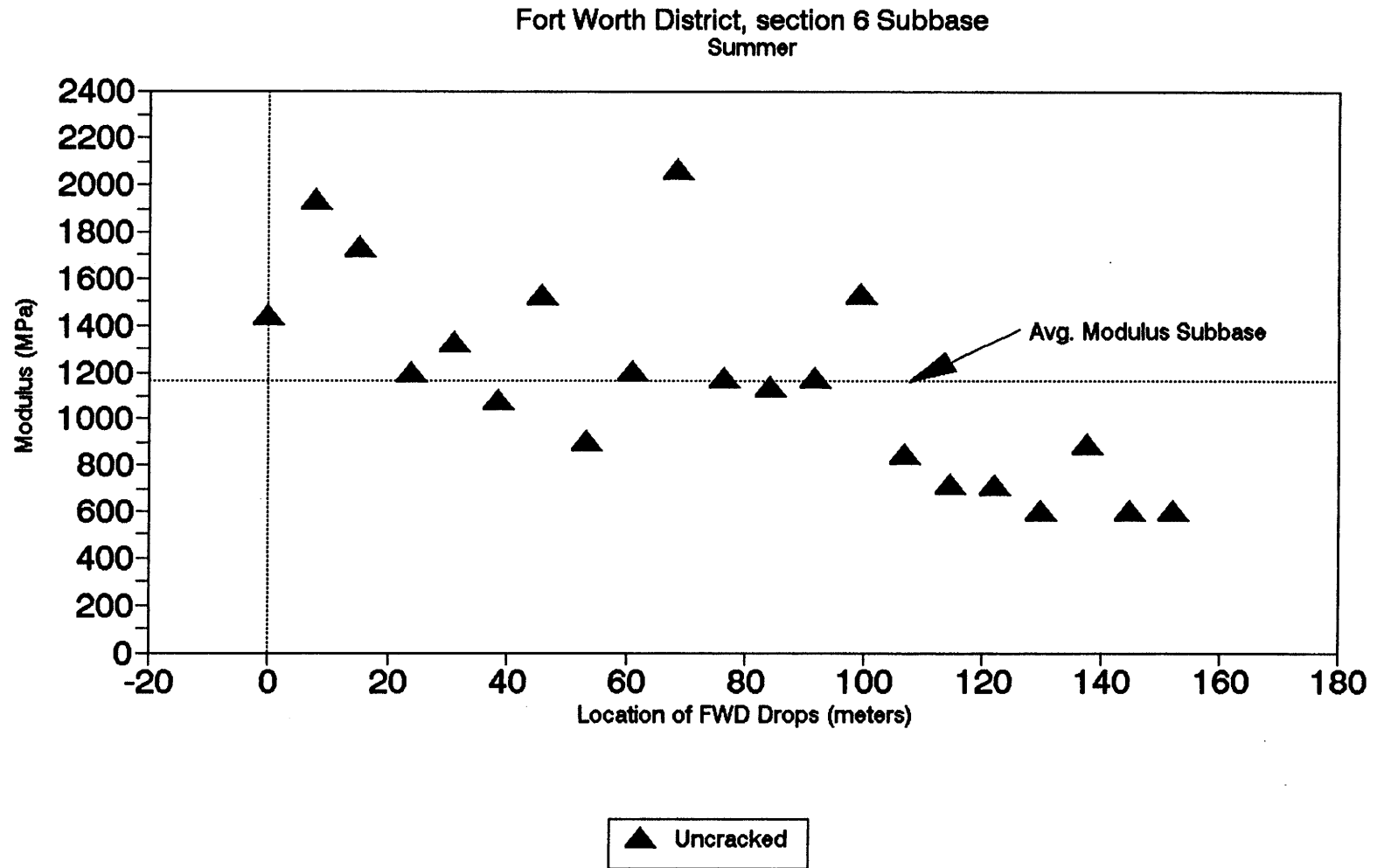


Figure A.223. Variation of Modulus of Stabilized Subbase within Test Section for Section-6 of Fort Worth District.